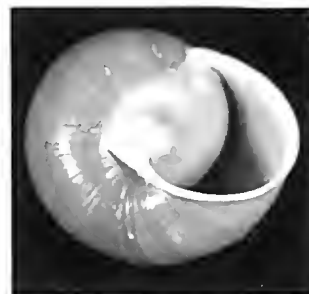
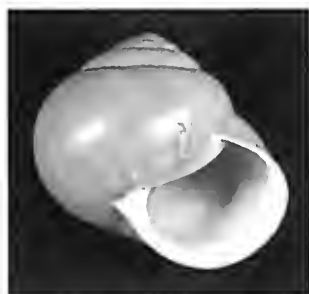


# Memoirs

of the Queensland Museum | **Nature**



ISSN 0079-8835  
Brisbane | 30 June 2016

**59**



# Memoirs of the Queensland Museum | **Nature**

Volume 59



**Minister:** The Honourable Anastacia Palaszczuk MP Premier and Minister for the Arts

**CEO & Director:** S. Miller, BSc (Hons), PhD, FGS, F Min Soc, FAIMM, FAGS

**Editor in Chief:** J.N.A. Hooper, PhD

**Managing Editor:** S.M. Verschoore

**Subject Editors:** J.M. Healy PhD DSc, C.L. Lambkin PhD, A.C. Rozefelds PhD.



**Queensland  
Government**

© The State of Queensland, Queensland Museum 2016  
PO Box 3300, South Brisbane Qld 4101, Australia  
Phone 61 3840 7555  
Fax 61 7 3846 1226  
[www.qm.qld.gov.au](http://www.qm.qld.gov.au)

National Library of Australia card number  
ISSN 0079-8835 (Print)  
ISSN 2204-1478 (Online)

**COVER:**

Design & layout by Sarah Verschoore  
Images: *Pallidelix simonhudsoni* sp. nov. by John Stanisic

**NOTE**

Papers published in this volume and in all previous volumes of the *Memoirs of the Queensland Museum* may be reproduced for scientific research, individual study or other educational purposes. Properly acknowledged quotations may be made but queries regarding the republication of any papers should be addressed to the director. Copies of the journal can be purchased from the Queensland Museum Shop.

A Guide to Authors is available from the Queensland Museum website:  
[www.qm.qld.gov.au/About+Us/Publications/Memoirs+of+the+Queensland+Museum](http://www.qm.qld.gov.au/About+Us/Publications/Memoirs+of+the+Queensland+Museum)

A Queensland Government Project  
Typeset at the Queensland Museum  
Printed by Ellipsis Media  
Building O3 Campus Services  
University of Southern Queensland,  
Backer Street, Toowoomba Qld 4350



# Range extension of the Short-beaked Echidna *Tachyglossus aculeatus* (Monotremata: Tachyglossidae) and the Northern Brown Bandicoot *Isoodon macrourus* (Marsupialia: Peramelidae) in Queensland: Mua (Moa Island), Torres Strait

Garrick HITCHCOCK

Simon D. CONATY

David G. FELL

Greg GORDON

Mark S. INGRAM

Terry M. REIS

David J. STANTON

John N. WIGNESS

Corresponding author: Hitchcock, G., School of Culture, History and Language, The Australian National University, ACT 0200, Australia, Email: garrick.hitchcock@anu.edu.au

<http://dx.doi.org/10.17082/j.2204-1478.59.2014.2013-06>

LSID urn:lsid:zoobank.org:pub:93929C37-A355-A96A-A666-DAFD097C558B

Citation: Hitchcock, G., Conaty, S.D., Fell, D.G., Gordon, G., Ingram, M.S., Reis, T.M., Stanton, D.J. & Wigness, J.N. 2014: Range extension of the Short-beaked Echidna *Tachyglossus aculeatus* (Monotremata: Tachyglossidae) and the Northern Brown Bandicoot *Isoodon macrourus* (Marsupialia: Peramelidae) in Queensland: Mua (Moa Island), Torres Strait. *Memoirs of the Queensland Museum – Nature* 59: 1–7. Brisbane. ISSN 2204-1478 (Online edition) ISSN 0079-8835 (Print edition). Accepted: 14 November 2013. First published online: 7 November 2014.

## ABSTRACT

Until recently there have been no confirmed records of medium-sized native terrestrial mammals from the Torres Strait Islands, far north Queensland. The Short-beaked Echidna (*Tachyglossus aculeatus* Shaw, 1792) and the Northern Brown Bandicoot (*Isoodon macrourus* Gould, 1842) are reported here occurring on Mua (Moa Island). This is the most northerly known occurrence of these species in Australia; both also occur in New Guinea. □ *Echidna*, *Bandicoot*, *Torres Strait Islands*, *refugial fauna*, *translocation*, *dispersal*.

The mammal assemblage of Torres Strait is not well documented, with little research having been undertaken (Cameron *et al.* 1978:193; Ingram 2008:619; Lavery *et al.* 2012:180; McNiven & Hitchcock 2004:107; Strahan 1995:444). The largest native terrestrial mammals known to occur on the islands are the introduced Dingo (*Canis lupus dingo*), which

was once widespread in the region (McNiven & Hitchcock 2004:120–122), and unidentified wallabies on Albany Island (Warham 1962:102) and Agile Wallabies (*Macropus agilis*) on Friday Island (Cameron *et al.* 1978:193) in southwest Torres Strait, close to Cape York Peninsula. There are no confirmed records of medium-sized mammals in the literature, although

the presence of echidnas and bandicoots on several islands has been reported previously by Torres Strait Islanders and others: echidnas on Mua (Moa Island) (Brooke Nicholls 1919:24; Brooke Nicholls & Dunbabin 1920; McNiven & Hitchcock 2004:107,109) and Horn Island (McNiven & Hitchcock 2004:109); and bandicoots on Mua (Bosun 2008:17; Manas 2001:5, 2007:19; Tennant 1959:154), Badu Island (Garnett & Jackes 1983:40) and Torres Strait (island not specified) (Leonard *et al.* 1995:592). Our report on a specimen of *Tachyglossus aculeatus* from Mua in the Australian Museum, Sydney (AMS), and collection of two specimens of *Isodon macrourus* on Mua, in 2011 and 2013, confirms their occurrence in Torres Strait.

## MUA

Mua (also known as Moa Island) (10°11'S, 142°16'E) is located approximately midway between Australia and New Guinea and is the second-largest island in Torres Strait. It is a rocky, lightly vegetated continental island of about 17 km diameter, with an area of around 172 km<sup>2</sup>. Mua features low-lying sandy plains bordered by granite hills and ridges on its eastern side. The vegetation and flora are the most diverse in the Torres Strait region with 22 broad vegetation groups and some 700 native species known. Major vegetation groups are *Eucalypt*- and *Corymbia*-dominant open forests and woodlands, *Welchiodendron*-dominant closed to open forests and woodlands, *Melaleuca*-dominant shrublands and woodlands, evergreen and semi-deciduous vine forests and thickets, grasslands and mangroves. It is also home to the largest freshwater creek among the islands of the region, Koey Kussa ('Big Creek') (3D Environmental 2013; Stanton *et al.* 2008; Wannan 2008). There are two Torres Strait Islander communities on the island: Kubin and St Pauls, which had populations of 163 and 258 respectively as at the 2011 census (Australian Bureau of Statistics 2012). The majority of the Mualgal, the traditional owners of the island, reside at the former settlement.

## METHODS, COLLECTIONS & IDENTIFICATION

A visit to Mua was made between 20–25 March 2011 to assist in the development of a plan for managing the biodiversity and cultural values on the island for the Torres Strait Regional Authority (TSRA) (3D Environmental 2013). As part of this research, an inventory was made of the known terrestrial vertebrate fauna of the island. This involved review of previous literature and museum records, discussions with local community members, and limited field investigations (observation, including spotlighting) in collaboration with the Mua Lagalgau Rangers (a team of local Indigenous Rangers, part of the TSRA's Land and Sea Ranger Program).

**Echidna.** A review of museum specimens in Australia identified a preserved specimen (flat skin) of a juvenile *Tachyglossus aculeatus* from Mua in the Australian Museum Mammalogy Collection (registration number M.4594), which was presented by Albert Sherbourne Le Soeuf, then Curator of the Taronga Zoological Park and registered into the collection on 28 June 1929. There is no other information associated with the specimen (Patricia Egan & Sandy Ingleby pers. comm. 2012). Le Soeuf also presented two specimens of Water Rat (*Hydromys chrysogaster*) from Mua (M.4558–9) to the AMS in April of that year (Troughton 1935:255).

**Bandicoots.** A partial male specimen was collected on 22 March 2011 by the survey team on the road between Kubin and St Pauls, at 10°12'26.1"S, 142°16'36.1"E (WGS84 datum). It had most likely been killed by a vehicle. The vegetation in this locality is low woodland dominated by *Melaleuca* and *Asteromyrtus* with a groundcover of sedges. Both the upper and lower jaws were located, but only cranial fragments remained. The pelvis, tail and some fur and tissue were also collected. This material was forwarded to the Queensland Museum (QM) (registration number QM JM19620).

A second, complete male specimen was subsequently obtained by TSRA staff on 18 July 2013 (Fig. 1). This animal was also

roadkill. It was collected within hours of death, frozen and subsequently transferred to the QM (registration number QM JM20021). The collection location was 10°10'55.7"S, 142°18'26.5"E, which is 3 km west of the St Pauls community.

The Mua specimens were examined by one of us (GG) and compared with a sample of up to 25 specimens of Southern Brown Bandicoot (*Isoodon obesulus peninsulae*) and 91 *I. macrourus* from north Queensland. The full range of measurements was not available on all specimens. Both specimens were identified as *I. macrourus* based on the length of the upper molar row, which exceeded 13.75 mm in length, a diagnostic criterion for *I. macrourus* in Queensland (Van Dyck *et al.* 2013:297-298). Both specimens had a molar row > 15.5 mm in length. The molar row of *I. o. peninsulae* and *I. auratus* is less than 13.75 mm.

*Other observations of bandicoots.* In addition to the roadkill specimens, five adults and two juveniles were also observed over the course of three nights of spotlighting (22-24 March 2011) in the community of St Pauls and along the road between St Pauls and Kubin. Based on location it is likely that all observations were of different individuals. One of the juveniles was being consumed by a cat on the St Pauls-Kubin road. One adult animal was observed in St Pauls in close proximity to houses. This limited

field investigation suggests that the species is common on the island.

## DISCUSSION

The AMS and QM specimens represent the most northerly known occurrence of *Tachyglossus aculeatus* and *Isoodon macrourus* in Australia. The species occur on the adjoining mainlands: *T. aculeatus* is widespread in Australia, including continental islands, and is also found in southern, southeast and northeast New Guinea, while *I. macrourus* is found in north and eastern Australia, including Cape York Peninsula, and southern and southeast New Guinea (Augee 2008; Flannery 1995a; Gordon 2008). *Isoodon* are not known from any of the other islands off the New Guinea coast (Flannery 1995b), and this is also the case with *Tachyglossus*, save an unconfirmed record from Salawati, eastern Indonesia, a Magnesian land-bridge island connected to New Guinea during the Pleistocene (Flannery 1995b:54; Menzies 2011:21). Both species are abundant in the Trans-Fly region of New Guinea immediately adjacent to the Torres Strait Islands (Hitchcock pers. obs.; Waithman 1979). Torres Strait was formed by rising sea levels in the early Holocene that inundated the Arafura Plain, the low-lying land bridge connecting Australia and New Guinea, with final separation of the mainlands

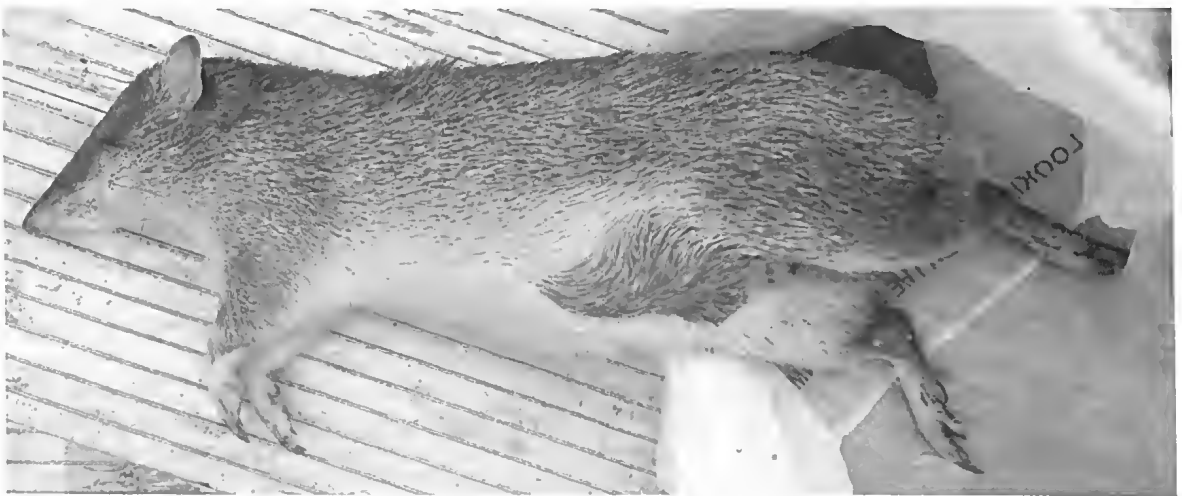


FIG. 1. *Isoodon macrourus* collected on Mua on 18 July 2013 (photo: Mark Ingram).

occurring 9000–8000 years ago (Barham 1999; Jennings 1972; McNiven 2011; Woodroffe *et al.* 2000). The echidna and bandicoot populations on Mua are most likely refugial ones, although it is also possible that they were translocated there by Torres Strait Islanders or Papuans in the past (Ingram 2008:620–621; see also Flannery 1995a:68–69; Heinsohn & Hope 2006:89; McNiven 2008:454–455; McNiven & Hitchcock 2004:117–121). To date, echidna or bandicoot remains have not been recovered from any archaeological excavations in the region (McNiven & Hitchcock 2004:109; McNiven pers. comm. 2013).

*Tachyglossus aculeatus* has been previously reported on Mua by local people, who state that they are still found on the island, though in small numbers, and were formerly hunted for food (Lillian Bosun pers. comm. 2011; McNiven & Hitchcock 2004:107, 109). Most recently, one of the Mualgal Rangers has reported encountering a dead animal on the edge of closed forest, on the outskirts of the St Pauls community (Guyai Uiduldam pers. comm. 2012). In the local Kala Lagaw Ya language (also known as Western-Central Torres Strait Language), the word for echidna is 'Kuyk' (which can also mean 'head', 'lump', 'knob' or 'base of a tree trunk'), although it is most commonly referred to as 'porcupine'. In November 1919, naturalist E. Brooke Nicholls and ornithologist W.R. McLennan visited the island (see Campbell 1920). On 9 November, Brooke Nicholls noted that 'the only mammals we have heard of are a large rat and the echidna' (Brooke Nicholls 1919:24; Brooke Nicholls & Dunbabin 1920). There is no mention of them encountering either animal. The presence of echidnas has also been reported on Horn Island, although no confirmed records yet exist (McNiven & Hitchcock 2004:109). Dogs, cats and pigs – all of which are present on Mua – are known to predate on echidnas, particularly burrow young (Augee *et al.* 2006:120; Griffiths 1989:429).

In Kala Lagaw Ya the word for bandicoot is 'Makas', which is also the generic name for rodents, however it is more commonly referred to by its English name. It is possible that when local people mentioned or described a 'large rat' to Brooke Nicholls (1919:24; Brooke Nicholls

& Dunbabin 1920), they were referring to the bandicoot. While they were hunted in the past at Kubin and St Pauls for consumption, using fire and/or dogs (Bosun 2008:17; Manas 2001:5, 2007:19; McNiven & Hitchcock 2004:109, 143; Tennant 1959:154), local people state that this has not occurred for several decades. The biggest threat to the Northern Brown Bandicoot on Mua at present is almost certainly predation by domestic and feral dogs and cats.

Bandicoots are also said to occur on neighbouring Badu Island (10°7'S, 142°9'E) (Garnett & Jackes 1983:40; McNiven & Hitchcock 2004:134). Badu is around 11 km in diameter with an area of 100 km<sup>2</sup>, and is separated from Mua by a shallow, narrow (<3 km wide) channel. Garnett and Jackes (1983:54) state that 'within living memory the bandicoot, *Peraueles uasuta*, has been introduced'. The basis for this identification and putative origin of the species is not clear.

It is interesting to note that a 1936 newspaper article (Lux 1936:2) suggested a recent origin (or re-establishment) of bandicoots in Torres Strait:

A hitherto unknown pest in the guise of the bandicoot has made a mysterious appearance in the Torres Strait Islands. How it made the 40-mile journey over water constitutes the mystery, but his presence is established by the resultant havoc amongst the native yam, taro and mainioca [*sic*] gardens. The menace is very real, as the islanders, due to their repugnance for anything furred as a diet – as opposed to his mainland brethren – has no inducement to hunt the pest as food, and thus keep down its numbers.

Several years earlier, the Anglican missionary at St Pauls, Mua, noted that 'the gardens have not been so successful, owing to an invasion of bandicoots' (Home Secretary's Department, 1932:13). Of course, the possibility exists that this writer either misinterpreted a population increase of the species as an introduction, or was simply wrong, perhaps only noting bandicoots after the commencement of mission gardening

efforts in the mid-1920s (see Schomberg 1996: 26, 79).

Nonetheless, consideration must be given to Torres Strait Islanders, or other people, being responsible for the introduction of the species to Torres Strait. The Rev. J.W. Schomberg is known to have imported a single Emu (*Dromaius novaehollandiae*) and three Common Brushtail Possums (*Trichosurus vulpecula*) to Mua in the 1920s (Schomberg n.d.:219-220; Schomberg 1996: 41). The possibility that bandicoots reached the islands by chance dispersal, by rafting, must also be considered. Large logs commonly wash ashore on the Torres Strait islands from New Guinea rivers, including the Fly River, during the annual wet season. In 1981, Pernetta and Hyndman (1982:108) collected a live specimen of *I. macrourus* from a tree floating down the middle Fly.

English anthropologist Alfred Cort Haddon considered that there was no true terrestrial hunting in Torres Strait, on account of the deficient mammal fauna of the islands, which he thought to be restricted to dogs, rats, mice and bats (Haddon 1912a:137, 1912b:152, 1912c:230; 1912d:358). It is now clear that on Mua at least, bandicoots are common and were formerly hunted, as were echidnas. Questions remain, however, about the antiquity of the presence of bandicoots on the island.

Further survey work is required to ascertain the origin and status of echidnas and bandicoots on Mua and the bandicoots reported on nearby Badu. Knowledge of the mammals of these and other islands in Torres Strait will also be critical for the development of land management practices and species conservation in the region (Torres Strait NRM Reference Group 2005; 3D Environmental 2013).

#### ACKNOWLEDGEMENTS

We wish to thank the Mualgal (Torres Strait Islanders) Corporation for granting permission to conduct surveys on Mua, and the Mua Lagalgau Rangers (Senior Ranger John Wigness and Rangers Erimiah Manas and Guyai Uiduldam) and Tony O'Keefe (formerly TSRA)

for their assistance in the field in 2011. Special thanks to Mua elders Fr John Manas and Mrs Lillian Bosun for sharing their reminiscences of echidnas and bandicoots on the island. Thanks also to staff of the TSRA Land and Sea Management Unit for collecting and arranging for the transportation of the second specimen to the QM. We would also like to thank Sandy Ingleby (Mammalogy, AMS) and Patricia Egan (Archives & Records, AMS) for additional information on the echidna specimen, Heather Janetzki and Jessica Worthington Wilmer (Natural Environments Program, QM) for preparing tissue samples, David Hyndman for alerting us to his collection of a bandicoot on the Fly River, and Chris Rodwell (Northern Australia Quarantine Strategy, Department of Agriculture, Fisheries and Forestry, Cairns) for arranging quarantine permits. Insightful comments on an earlier draft of this paper by Steven Hamilton, Robin Hide, Ian McNiven, James Menzies, Damian Miley and Michael Sale are acknowledged and appreciated.

#### LITERATURE CITED

- 3D Environmental. 2013. Profile for management of the habitats and related ecological and cultural resource values of Mua Island. Unpubl. report to Torres Strait Regional Authority. January 2013.
- Augee, M.L. 2008. Short-beaked Echidna, *Tachyglossus aculeatus*. Pp. 37-39. In, Van Dyck, S. & Strahan, R. (eds) *The mammals of Australia*. 3rd ed. (Reed New Holland: Sydney).
- Augee, M.L., Gooden, B. & Musser, A. 2006. *Echidna: extraordinary egg-laying mammal*. (CSIRO Publishing: Collingwood, Vic.).
- Australian Bureau of Statistics. 2012. 2011 census data. (Australian Bureau of Statistics: Canberra). Available from: <http://abs.gov.au>
- Barham, A.J. 1999. The local environmental impact of prehistoric populations on Saibai Island, northern Torres Strait, Australia: enigmatic evidence from Holocene swamp lithostratigraphic records. *Quaternary International* 59(1): 71-105. [http://dx.doi.org/10.1016/S1040-6182\(98\)00073-1](http://dx.doi.org/10.1016/S1040-6182(98)00073-1)
- Bosun, L.L. 2008. Affidavit of Lena Lillian Bosun. 26 September 2008. Torres Strait Regional Seas Native Title Claim, Q6040 of 2001. (Native Title Office, Torres Strait Regional Authority: Thursday Island). (Unpubl.).
- Brooke Nicholls, E. 1919. The islands of Torres Straits. Box 1, MLMSS 235, Nicholls Brooke Papers.

- (Mitchell Library, State Library of New South Wales: Sydney).
- Brooke Nicholls, E. & Dunbabin, T. 1920. In tropic seas. Islands of Torres Straits. *The Argus*, 6 March, p. 8.
- Cameron, E., Cogger, H. & Heatwole, H. 1978. A natural laboratory. *Australian Natural History* 19(6): 190-197.
- Campbell, A.J. 1920. Notes on additions to the "H.L. White Collection". *Emu* 20(2): 49-66. <http://dx.doi.org/10.1071/MU920049>
- Flannery, T. 1995a. *Mammals of New Guinea*. Rev. ed. (Reed Books: Chatswood).
- Flannery, T. 1995b. *Mammals of the South-West Pacific & Moluccan Islands*. (Reed Books: Chatswood).
- Garnett, S.T. & Jackes, B.R. 1983. Vegetation of Badu Island, Torres Strait. *Queensland Naturalist* 24: 40-52.
- Gordon, G. 2008. Northern Brown Bandicoot, *Isodon macrourus*. Pp. 178-180. In, Van Dyck, S. & Strahan, R. (eds) *The mammals of Australia*. 3rd ed. (Reed New Holland: Sydney).
- Griffiths, M. 1989. Tachyglossidae. Pp. 407-435. In, Walton, D.W. & Richardson, B.J. (eds) *Fauna of Australia, volume 1B: Mammalia*. (Australian Government Publishing Service: Canberra).
- Haddon, A.C. 1912a. Food and its preparation and narcotics. Pp. 130-143. In, Haddon, A.C. (ed.) *Reports of the Cambridge anthropological expedition to Torres Straits, volume 4: arts and crafts*. (Cambridge University Press: Cambridge).
- 1912b. Hunting and fishing. Pp. 152-171. In, Haddon, A.C. (ed.) *Reports of the Cambridge anthropological expedition to Torres Straits, volume 4: arts and crafts*. (Cambridge University Press: Cambridge).
- 1912c. Science. Pp. 218-237. In, Haddon, A.C. (ed.) *Reports of the Cambridge anthropological expedition to Torres Straits, volume 4: arts and crafts*. (Cambridge University Press: Cambridge).
- 1912d. Decorative, pictorial and glyptic art. Pp. 342-393. In, Haddon, A.C. (ed.) *Reports of the Cambridge anthropological expedition to Torres Straits, volume 4: arts and crafts*. (Cambridge University Press: Cambridge).
- Heinsohn, T. & Hope, G. 2006. The Torresian connections: zoogeography of New Guinea. Pp. 71-93. In, Merrick, J.R., Archer, M., Hickey, G.M. & Lee, M.S.Y. (eds) *Evolution and biogeography of Australian vertebrates*. (Auscipub: Oatlands).
- Home Secretary's Department. 1932. Report upon the Operations of the Sub-Departments of Aborigines, Dunwich Benevolent Asylum, Inebriates Institution (Dunwich), Jubilee Sanatorium for Consumptives (Dalby), Westwood Sanatorium, Home for Epileptics (Willowburn), Prisons, Queensland Industrial Institution for the Blind, Diamantina Hospital for Chronic Diseases (South Brisbane), and Eventide Home (Charters Towers). (Government Printer: Brisbane).
- Ingram, G. 2008. The terrestrial vertebrates of Mua, western Torres Strait. *Memoirs of the Queensland Museum, Cultural Heritage Series* 4(2): 619-628.
- Jennings, J.N. 1972. Some attributes of Torres Strait. Pp. 29-38. In, Walker, D. (ed.) *Bridge and barrier: the natural and cultural history of Torres Strait*. (Australian National University: Canberra).
- Lavery, T.H., Watson, J.W. & Leung, L.K.-P. 2012. Terrestrial vertebrate richness of the inhabited Torres Strait Islands, Australia. *Australian Journal of Zoology* 60(3): 180-191. <http://dx.doi.org/10.1071/ZO12043>
- Leonard, D., Beilin, R. & Moran, M. 1995. Which way kaikai blo umi? Food and nutrition in the Torres Strait. *Australian Journal of Public Health* 19(6): 589-595. <http://dx.doi.org/10.1111/j.1753-6405.1995.tb00463.x>
- Lux. 1936. Australian explorer. *The Queenslander*, 16 April, p. 2.
- Manas, J.H. 2001. Yellub a ngau unai. P. 51. In, Kubin Community Council (ed.) *Gelani ngazu kazi - dugong my son*. (Kubin Community Council: Mua Island).
2007. Affidavit of John Henry Manas. 6 September 2007. Torres Strait Regional Seas Native Title Claim, Q6040 of 2001. (Native Title Office, Torres Strait Regional Authority: Thursday Island). (Unpubl.).
- McNiven, I.J. 2008. Inclusions, exclusions and transitions: Torres Strait Islander constructed landscapes over the past 4000 years, northeast Australia. *The Holocene* 8(3): 449-462. <http://dx.doi.org/10.1177/0959683607087934>
2011. Torres Strait Islanders: the 9000-year history of a maritime people. Pp. 210-219. In, *The Torres Strait Islands*. (Queensland Art Gallery / Gallery of Modern Art: Brisbane).
- McNiven, I.J. & Hitchcock, G. 2004. Torres Strait Islander marine subsistence specialization and terrestrial animal translocation. *Memoirs of the Queensland Museum, Cultural Heritage Series* 3(1): 105-162.
- Menzies, J. 2011. *A handbook of New Guinea's marsupials and monotremes*. 2nd ed. (University of Papua New Guinea Press/Masalai Press: Oakland, CA).
- Pernetta, J.C. & Hyndman, D.C. 1982. Working paper 13: ethnozoology of the Ok Tedi drainage. Pp. 73-207. In, Maunsell & Partners Pty Ltd. (ed.) *Ok Tedi environmental study, volume 5: population and resource use; ethnobiology*. Unpubl. report to Ok Tedi Mining Limited, Port Moresby.
- Schomberg, N. (comp.). n.d. Photographs: Badu - Poid - St. Pauls - Moa Island; taken by the Rev. J.W.

- Schomberg 1921-1935. Copy held at Queensland Museum, Brisbane. (Unpubl.)
1996. Angels in paradise: true stories and incidents of the Torres Straits from August 1921 to February 1936. Unpubl. manuscript held in John Oxley Museum, Brisbane; Queensland Museum, Brisbane; Australian Institute of Aboriginal and Torres Strait Islander Studies, Canberra; and National Museum of Australia, Canberra.
- Stanton, D.J., Fell, D.G. & Gooding, D.O. 2008. Vegetation communities and regional ecosystems of the Torres Strait Islands, Queensland, Australia. Unpubl. report to Torres Strait Regional Authority. (3D Environmental: Brisbane). Available from: [http://tsra.gov.au/media/65261/3d-torresstrait-report-finalversion\\_1nov2008.pdf](http://tsra.gov.au/media/65261/3d-torresstrait-report-finalversion_1nov2008.pdf)
- Strahan, R. (ed.) 1995. *The mammals of Australia*. 2nd ed. (Reed New Holland: Sydney).
- Tennant, K. 1959. *Speak you so gently*. (V. Gollancz: London).
- Torres Strait NRM Reference Group. 2005. Land and sea management strategy for Torres Strait. (Bessen Consulting Services: Fremantle). (Unpubl.).
- Troughton, E.L.G. 1935. Five new rats of the genera *Hydromys* and *Melomys* from northern Australia. *Records of the Australian Museum* 19(4): 251-258. <http://dx.doi.org/10.3853/j.0067-1975.19.1935.701>
- Van Dyck, S., Gynther, I. & Baker, A. (eds) 2013. *Field companion to the mammals of Australia*. (Reed New Holland: Sydney).
- Waithman, J. 1979. A report on a collection of mammals from southwest Papua, 1972-1973. *The Australian Zoologist* 20(2): 313-326.
- Wannan, B. 2008. Terrestrial vegetation of Gelam's homeland, Mua. *Memoirs of the Queensland Museum, Cultural Heritage Series* 4(2): 605-613.
- Warham, J. 1962. Bird islands within the Great Barrier Reef and Torres Strait. *Emu* 62(2): 99-111.
- Woodroffe, C.D., Kennedy, D.M., Hopley, D., Rasmussen, C.E. & Smithers, S.G. 2000. Holocene reef growth in Torres Strait. *Marine Geology* 170(3-4): 331-346. [http://dx.doi.org/10.1016/S0025-3227\(00\)00094-3](http://dx.doi.org/10.1016/S0025-3227(00)00094-3)



# New records of blind snakes resembling the robust blind snake *Anilius ligatus* (Peters 1879), on Cape York Peninsula.

*Memoirs of the Queensland Museum - Nature* 59: 8. 2014. Blind snakes are extremely secretive with numerous Australian species known from few specimens or localities (Vanderduys 2013). Two recent records of blind snakes morphologically resembling *Anilius ligatus* (until recently *Ramphotyphlops ligatus*; Hedges *et al.* 2014) occur much further north than previously recognised, 330 km and 525 km north, respectively, of the nearest records (Atlas of Living Australia 2013; fig. 1). The first (QMJ92808) 184 mm SVL, 8 mm tail length, (including spinose tip) was collected on the 8th of June 2010 at 13°39.09'S; 142°47.78'E in a funnel trap, during a survey of Oyala Thumotang (Mungkan Kandju) National Park. The trap site was located within tall open *Eucalyptus tetrodonta* woodland, with a *Melaleuca viridiflora* subcanopy on grey sandy soil. *Corymbia confertiflora*, *C. stockeri* and *Erythrophleum chlorostachys* were also common in the tree layer. There was a thick ground cover dominated by *Heteropogon triticeus* and *Sarga plumosum*. The area is mapped as being 50% Regional Ecosystem (RE) 3.5.7 x 2a: "*Eucalyptus tetrodonta* woodland on sand plains", mixed with other REs (Queensland Herbarium 2013) and our data conform to this description. The second specimen (QMJ93151) was collected in a pitfall bucket on the 27th of May 2013 at 12°03.22'S; 142°03.27'E during fauna surveys approximately 70 km north of Weipa, on the western side of Cape York Peninsula. The trap site was located within tall open forest dominated by *Eucalyptus tetrodonta* on hard soils consisting of dry orange loam with bauxite. *Erythrophleum chlorostachys* and *Corymbia nesophila* were also present in the tree layer, while the ground layer was dominated by *Eulalia mackinlayi*, *Heteropogon triticeus*, *Sarga*

*plumosum* and *Schellhammeria multiflora*. The area is mapped as Regional Ecosystem 3.5.2: "*Eucalyptus tetrodonta* and *Corymbia nesophila* tall woodland on deeply weathered plateaus and remnants" (Queensland Herbarium 2013) and the site conforms well to this description. Based on available identification keys in Cogger (2000) and Wilson (2005) both specimens are clearly morphologically *A. ligatus* as currently understood. Examination of the specimens by Dr Andrew Amey (Queensland Museum) confirmed this. However, recent genetic work on specimens from nearly 2000 km (south) and over 700 km (west; straight line, across the Gulf of Carpentaria) from our Cape York Peninsula specimens (fig. 1) has shown that *A. ligatus* is both paraphyletic and polyphyletic indicating the presence of cryptic species (Marin *et al.* 2013). The genetic affiliation of the Cape York Peninsula specimens requires further investigation. The nominal *A. ligatus* taxa presented in Marin *et al.* (2013), the disjunct distributions of many reptilian taxa, and similar distribution of non-reptilian taxa across the Carpentaria Barrier (e.g. Kikkawa 1969; Blacket *et al.* 2001), suggests that many species currently recognised as occurring across the monsoonal tropics may be rich in cryptic taxa, providing a fertile ground for further taxonomic studies.

## Literature cited

- Australian Living Atlas. 2013. Atlas of Living Australia. Search under "*Ramphotyphlops ligatus*", "*Typhlops ligatus*" and all species listed. Data downloaded July 2013. <http://www.ala.org.au/>
- Blacket, M.J., Adams, M., Cooper, S.B.J., Krajewski, C. & Westerman, M. 2001. Systematics and Evolution of the Dasyurid Marsupial Genus *Sminthopsis*: I. The Macroura Species Group. *Journal of Mammalian Evolution*, 8(2): 149-170. <http://dx.doi.org/10.1023/A:1011322031747>
- Cogger, H.G. 2000. *Reptiles and Amphibians of Australia*. (Reed New Holland: Sydney).
- Hedges, S.B., Marion, A.B., Lipp, K.M., Marin, J., & Vidal, N. 2014. A taxonomic framework for typhlopoid snakes from the Caribbean and other regions (Reptilia, Squamata). *Caribbean Herpetology* 49: 1-61.
- Kikkawa, J. & Pearse, K. 1969. Geographical distribution of land birds in Australia - A numerical analysis. *Australian Journal of Zoology* 17: 821-840. <http://dx.doi.org/10.1071/ZO9690821>
- Marin, J., Donnellan, S.C., Hedges, S.B., Doughty, P., Hutchinson, M.N., Cruaud, C. & Vidal, N. 2013. Tracing the history and biogeography of the Australian blindsnake radiation. *Journal of Biogeography* 40: 928-937. <http://dx.doi.org/10.1111/jbi.12045>
- Queensland Herbarium. 2013. Regional Ecosystem Description Database (REDD). Version 6.1 (February 2013) (Queensland Department of Science, Information Technology, Innovation and the Arts: Brisbane).
- Vanderduys, E.P. 2013. Additional information on *Ramphotyphlops aspiina* Couper, Covacevich & Wilson 1998, A poorly known blind snake from the Mitchell Grass Downs of Queensland. *Memoirs of the Queensland Museum - Nature* 56: 71-76.
- Wilson, S. 2005. *A Field Guide to Reptiles of Queensland*. (Reed New Holland: Sydney).

Angus McNab and Mark Sanders, EcoSmart Ecology, 48 Streeton Parade, Everton Park, Queensland, Australia, 4053. Eric Vanderduys, CSIRO Ecosystem Sciences, ATSIP PMB PO, Aitkenvale, Queensland, Australia 4814.

First published online: 7 November 2014 – <http://dx.doi.org/10.17082/j.2204-1478.59.2014.2014-1>  
 LSID: urn:lsid:zoobank.org:pub:ODA30508-42FB-4C3C-B68F-C77123CFACC2

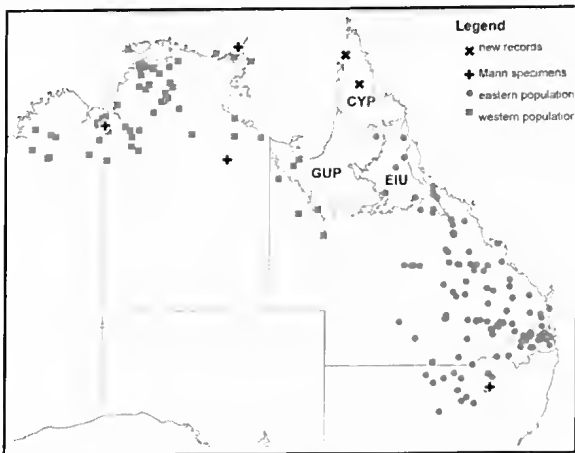


FIG. 1. Known records of *Anilius ligatus* in proximity to individuals collected on Cape York, Queensland (new records x). Four genetically tested specimens are marked (+). Relevant Bioregional boundaries are shown: CYP = Cape York Peninsula, EIU = Einasleigh Uplands, GUP = Gulf Plains. Data collected from Atlas of Living Australia, Atlas of NSW Wildlife and Marin *et al.* (2013).



**CONFIRMATION OF THE PRESENCE OF THE SPOTTED-TAILED QUOLL, *DASYURUS MACULATUS* (DASYURIDAE, MARSUPIALIA) FROM THE LATE PLEISTOCENE KING CREEK CATCHMENT, DARLING DOWNS, SOUTHEASTERN QUEENSLAND, AUSTRALIA.**

*Memoirs of the Queensland Museum – Nature* 59: 9–10. 2014. Quolls (*Dasyurus* spp.) are a rare component of Pleistocene deposits of the eastern Darling Downs. Molnar & Kurz (1997) listed *Dasyurus* sp. from four localities in the King Creek catchment (Queensland Museum Locality (QML) 100, QML796, QML913 and Pilton). Price & Webb (2006) recorded the eastern quoll (*Dasyurus viverrinus*) from QML796, while Price & Sobbe (2005) recorded a quoll from QML1396 that is morphometrically similar to, but showing some morphological difference from the spotted-tailed quoll (*Dasyurus maculatus*). Here we report a new specimen from QML796 that confirms the presence of *D. maculatus* in the late Pleistocene King Creek catchment.

**Family DASYURIDAE Goldfuss, 1820**

**Genus *Dasyurus* Geoffroy, 1796**

***Dasyurus maculatus* Kerr, 1792**

**Material.** Queensland Museum Fossil (QMF) 57026, an isolated unworn right  $M_1$  from QML796 (bulk sediment derived from stratigraphic units A4/A7 as per Price & Webb 2006) (Fig. 1).

**Description.** QMF57026 is sub-oval in occlusal outline, with the buccal margin more bulbous than the lingual, measuring 7.01 mm (crown maximum length)  $\times$  3.89 mm (crown maximum width). The tallest cusp, the protoconid is placed medially on the buccal margin, while the second tallest cusp, the paraconid is positioned antero-lingually from the protoconid. The metaconid is placed lingually from the protoconid and is approximately equal in height to the paraconid. The hypoconid, entoconid and hypoconulid are lower in height than the other three cusps and form a basin like structure on the posterior of the tooth crown.

**Remarks.** The position of the cusps on the tooth crown and relatively large size confirms QMF57026 as a species of *Dasyurus*. It is morphologically and morphometrically similar to extant *D. maculatus* (QMJ16744) in the Queensland Museum collections and is assigned to this species. Measurements of lower fourth molars ( $M_1$ ) of combined extant, sub-fossil and late Pleistocene Australian mainland populations of *D. maculatus* are in the range of 6–7.3 mm (crown max. length)  $\times$  3.3–4 mm (crown max. width) (Marshall & Hope 1973) while similar measurements for extant *D. viverrinus* are in the range 5–6 mm  $\times$  2.4–3.1 mm (Bartholomai 1971). This places QMF57026 near the upper end of measurements for *D. maculatus* and well above the measurements for *D. viverrinus* further supporting its assignment to *D. maculatus*.

The specimen shows little evidence of stream abrasion hence it is unlikely to have been reworked from an upstream deposit. Unit A7 has an optically stimulated luminescence (OSL) age of  $122 \pm 22$  ka while unit A4 has an OSL age of  $107 \pm 18$  ka (Price *et al.* 2011), thus indicating the presence of the species in the late Pleistocene Darling Downs ecosystem. *Dasyurus viverrinus* is also recorded at QML796 during the above mentioned age range (Price & Webb 2006) indicating that both *D. maculatus* and *D. viverrinus* occurred sympatrically in the late Pleistocene King Creek ecosystem. A similar sympatric occurrence of spotted-tailed and eastern quolls is recorded during the late Pleistocene at Capricorn Caves (Cramb *et al.* 2009). Modern *D. maculatus*, the most arboreal of the extant quolls, occur in a range of habitats including wet and dry sclerophyll forests and vine thickets. The presence of *D. maculatus* may provide additional support for the existence of such

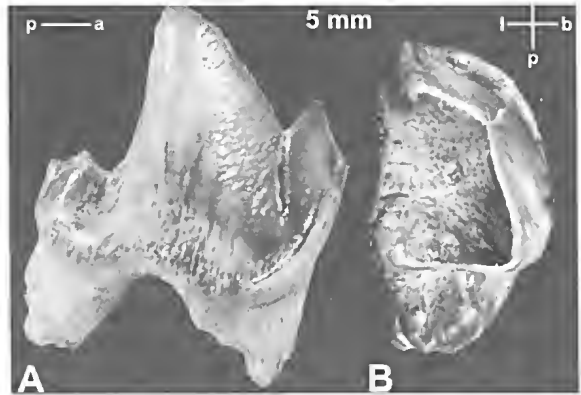


FIG. 1. QMF57026; Right  $M_1$ , *Dasyurus maculatus* from QML796. A, Lateral view of buccal surface; B, Occlusal view of tooth crown. Abbreviations: a, anterior; b, buccal; l, lingual; p, posterior.

palaeo-habitats in the Pleistocene King Creek catchment (e.g. Price & Sobbe 2005). The sympatric occurrences of spotted-tailed and eastern quolls in the historic period are known only from more temperate climates of southeastern mainland Australia and Tasmania (Belcher *et al.* 2008; Jones 2008). A similar climate regime may have also been a key factor that allowed both taxa to occur sympatrically on the Pleistocene Darling Downs. In contrast, the modern eastern Darling Downs occurs in the sub-tropical climate belt and retains a population of *D. maculatus*, while *D. viverrinus* is locally extinct. The timing of this extinction is uncertain but is likely to have occurred prior to European occupation as there are no historic records of *D. viverrinus* on the Darling Downs.

**Acknowledgements**

Trevor Sutton is thanked for his continued support in fossil collection. Heather Janetzki provided access to comparative specimens in the Queensland Museum collection. We thank Robin Beck and an anonymous reviewer for constructive comment on an earlier draft of this manuscript. This research is supported in part by ARC Discovery grants DP0881279, DE120101533, DP120101752.

**Literature Cited**

- Bartholomai, A. 1971. *Dasyurus daumalli*, a new species of fossil marsupial (Dasyuridae) in the upper Cainozoic deposits of Queensland. *Memoirs of the Queensland Museum* 16(1): 19–26.
- Belcher, C., Burnett, S. & Jones, M. 2008. Spotted-tail Quoll. Pp. 60–62. In: Van Dyck, S., Strahan, R. (eds) *The Mammals of Australia* (3rd edition). (Reed New Holland: Sydney).
- Cramb, J., Hocknull, S. & Webb, G.E. 2009. High diversity Pleistocene rainforest dasyurid assemblages with implications for the radiation of the Dasyuridae. *Austral Ecology* 34: 663–669. <http://dx.doi.org/10.1111/j.1442-9993.2009.01972.x>
- Jones, M. 2008. Eastern Quoll. Pp. 62–64. In: Van Dyck, S. & Strahan, R. (eds) *The Mammals of Australia* (3rd edition). (Reed New Holland: Sydney).
- Marshall, L.G. & Hope, J.H. 1973. A revaluation of *Dasyurus bowlingi* Spencer & Kershaw 1910 (Marsupialia, Dasyuridae) from King Island, Bass Strait. *Proceedings of the Royal Society of Victoria* 85(2): 225–236.
- Molnar, R.E. & Kurz, C. 1997. The distribution of Pleistocene vertebrates on the eastern Darling Downs based on the Queensland Museum collections. *Proceedings of the Linnæan Society of New South Wales* 117: 107–133.
- Price, G.J. & Sobbe, I.H. 2005. Pleistocene palaeoecology and environmental change on the Darling Downs, southeastern Queensland, Australia. *Memoirs of the Queensland Museum* 51(1): 171–201.

- Price, G.J. & Webb, G.E. 2006. Late Pleistocene sedimentology, taphonomy and megafauna extinction on the Darling Downs, southeastern Queensland. *Australian Journal of Earth Sciences* 53: 947–970.
- Price, G.J., Webb, G.E., Zhao, J.-x., Feng, Y.-x., Murray, A.S., Cooke, B.N., Hocknull, S.A. & Sobbe, I.H. 2011. Dating megafaunal extinction on the Pleistocene Darling Downs, eastern Australia: the promise and pitfalls of dating as a test of extinction hypotheses. *Quaternary Science Reviews* 30: 899–914. <http://dx.doi.org/10.1016/j.quascirev.2011.01.011>
- Ian H. SOBBE<sup>1</sup> & Gilbert J. PRICE<sup>2, 1</sup>, Geosciences, Natural Environments Program, Queensland Museum, PO Box 3300, South Brisbane Qld 4010; 2, School of Earth Sciences, The University of Queensland, St. Lucia Qld 4072.
- First published online: 7 November 2014 – <http://dx.doi.org/10.17082/j.2204-1478.59.2014.2013-5>
- LSID: urn:lsid:zoobank.org:pub:DF0BB935-8957-460F-B7E3-B12607669C1E

# Five new species of soil burrowing cockroaches from Queensland (Blattodea: Blaberidae: Geoscaphinae)

H.A. ROSE

Faculty of Agriculture and Environment, University of Sydney, NSW 2006. Corresponding author: harley.rose@sydney.edu.au

J.A. WALKER

Commonwealth Department of Agriculture, Box 96, Cairns International Airport, Cairns, Qld 4870

J.R. WOODWARD

School of Botany, University of Melbourne, Vic 3010

<http://dx.doi.org/10.17082/j.2204-1478.59.2014.2014-02>

LSID urn:lsid:zoobank.org:pub:F837EAC9-D3C6-42E4-84F6-3CB4B1583510

Citation: Rose, H.A., Walker, J.A. & Woodward, J.R. 2014: Five new species of soil burrowing cockroaches from Queensland (Blattodea: Blaberidae: Geoscaphinae). *Memoirs of the Queensland Museum – Nature* 59: 11–23. Brisbane. ISSN 2204-1478 (Online), ISSN 0079-8835 (Print). Accepted: 30 October 2014. First published online: 23 December 2014.

## ABSTRACT

Five new species of soil burrowing Geoscaphinae are described from Queensland: *Macropanesthia intermorpha*, *M. lineopunctata*, *M. mutica*, *M. spuritegmina*, and *Neogeoscapheus hanni*. Redescriptions of subfamilies Panesthiinae and Geoscaphinae are given, and a key to the genera of Geoscaphinae and keys to species of *Macropanesthia* and *Neogeoscapheus* are provided. □ *Blattodea*, *Blaberidae*, *Geoscaphinae*, *Panesthiinae*, *Australian ground burrowing cockroaches*

Within the cockroach family Blaberidae, the subfamily Geoscaphinae is an Australian endemic group of cockroaches living in permanent burrows in sandy or loamy soils; their diet is dry leaves. The subfamily Panesthiinae occurs in India, Tibet, China, Japan, South East Asia, the island of New Guinea, Indonesia, Australia and some Pacific islands; most feed on rotting wood and two species are known to feed on dry leaves. The two subfamilies have close genetic affinities (Maekawa *et al.*, 2003). Morphologically, the two subfamilies are very similar and the taxonomic division is based on two characters. The first is related to the absence of wings or tegmina in Geoscaphinae, and their presence or absence in Panesthiinae. Those *Panesthia* lacking wings or tegmina were differentiated from Geoscaphinae using the second character which relates to the laterocaudal angle of tergite 7. Roth (1977) differentiated Australian

*Panesthia* from Geoscaphinae mainly on the basis of the laterocaudal angle of tergite 7: in Panesthiinae, if such a process is produced, it is directed caudally and not upwards, whereas in Geoscaphinae this process is 'directed laterally or obliquely, and slightly or strongly dorsad'. This character was no longer useful in 1994 when Walker *et al.* described new species of Geoscaphinae, one of which had laterocaudal angles of tergite 7 produced acutely and directed ventrocaudally.

In this paper we describe five new species of Geoscaphinae, one with processes at the laterocaudal angle of tergite 7 only very weakly produced, and we have therefore modified the descriptions of Australian Panesthiinae and Geoscaphinae to accommodate all known species. Herein are four new species of *Macropanesthia* from central and northern

Queensland and one new *Neogeoscapheus* from northern Queensland, bringing the total number of Geoscapheinae to 24.

Keys to *Macropanesthia* and *Neogeoscapheus* from Walker *et al.* (1994) have been modified. These are for adult specimens only, but may also be effective when applied to some late instar nymphs.

Measurements are in millimetres and scale bars represent 5 mm. In descriptions of males, measurements of the holotype are given and those of paratypes are in brackets. Measurements of females refer to paratypes. Numbers of paratypes measured are in brackets. Terminology used for male genital phallomeres is that of McKittrick (1964) and Roth (1977).

#### Abbreviations Used

**Collectors.** ACK, A.C. Kotze; GBM, G.B. Monteith; HAR, H.A. Rose; JAW, J.A. Walker; JRW, J.R. Woodward.

**Museums and Collections.** ANIC, Australian National Insect Collection, Canberra; DAFF, Queensland Department of Agriculture, Fisheries and Forestry, Brisbane; QM, Queensland Museum, Brisbane; USIC, University of Sydney Insect Collection, Sydney; JAWPC, James Walker private collection, Cairns.

#### SYSTEMATICS

(Blattodea: Blaberoidea, Blaberidae,  
Geoscapheinae, Panesthiinae)

The higher-level classification of Blattodea is undergoing re-assessment due to the assignment to this order of the termites (epifamily Termitoidae) (Inward *et al.*, 2007; Beccaloni & Eggleton, 2011; 2013). Within the Blaberidae there are several subfamilies one of which is Panesthiinae, the characteristics of which were described by Roth (1977). At that time members of Panesthiinae consisted of both wood feeding and soil burrowing cockroaches; however, differences between these two groups were considered by Rugg and Rose (1984) to warrant subfamily status, so Geoscapheinae was erected to accommodate the soil burrowing cockroaches. Descriptions of these

two subfamilies were subsequently modified by Walker *et al.* (1994). We now make further modifications to the subfamily descriptions, by deleting reference to T7, to account for the new species described herein.

#### Subfamily Panesthiinae

Living in rotting logs and feeding on wood, or living under rocks and feeding on dry leaves; robust, well sclerotised and having strong tibial spines; front femora with tibial spines modified for digging; wings or tegmina usually present (though may be vestigial or reduced through damage); ocellar spots usually present; anterior pronotal tubercles usually present in males; usually with a full complement of male blaberid genital phallomeres; oothecal membrane present.

#### Subfamily Geoscapheinae

Living in permanent burrows in soil and feeding on dry plant material, predominantly leaves; robust, well sclerotised and having strong tibial spines; front femora with tibial spines modified for digging; apterous; ocellar spots absent; anterior pronotal tubercles present or absent; always with a loss of one, or more, male blaberid genital phallomeres; oothecal membrane present or absent.

#### KEY TO THE GENERA OF GEOSCAPHEINAE

1. Posterior margin of tergite 6 without spines or tubercles exclusive of the laterocaudal angle, but may be thickened and weakly undulate or with a raised ridge. . . . . 2
  - Posterior margin of tergite 6 with one or more raised spines or tubercles exclusive of the laterocaudal angle. . . . . 3
2. Laterocaudal angle of tergite 6 produced into a dorsally curved spine . *Geoscapheus* Tepper
  - Laterocaudal angle of tergite 6 not produced into a large spine . . *Macropanesthia* Saussure
3. Posterior margin of tergite 6 thickened laterally and with several erect rounded tubercles arising from the thickened margin . . . . . *Parapanesthia* Roth

- Posterior margin of tergite 6 with one or more acute spines or broadly rounded tubercles arising sublaterally... *Neogeoscapheus* Roth

#### KEY TO SPECIES OF *MACROPANESTHIA*

1. Thoracic nota coloured uniformly (ferruginous, dark brown or black) ..... 2
  - Thoracic nota with a distinct lateral marginal yellow, or cream to orange band ..... *kraussiana* (Saussure)
  - Mesonotum and metanotum dark brown to black and with submarginal smoky yellow to orange patches laterally ..... *spuritegmina* sp. nov.
2. Anterolateral corners of tergites 6 and 7 (and often 5) with deep pits ..... 3
  - Anterolateral corners of tergites without such pits ..... 4
3. Posterior margin of supraanal plate smooth, lateral corners (posterior to cerci) rounded ..... *mackerrasae* Roth
  - Posterior margin of supraanal plate crenulate, lateral corners (posterior to cerci) produced into acute spines .... *kinkuna* Walker *et al.*
4. Cerci apically bulbous, dorsal surface covered with short dense setae ..... 5
  - Cerci subrectangular and usually concave dorsally either side of a basal medial ridge, dorsal surface glabrous or sparsely setose.. 8
5. Laterocaudal angle of tergite 7 produced into a sharp spine and directed dorsally . 6
  - Laterocaudal angle of tergite 7 produced acutely and directed ventrocaudally ..... *rothi* Walker *et al.*
6. Tergites smooth or weakly and sparsely punctate ..... 7
  - Tergites having a row of deep punctations on the anterior margin (Fig. 2) ..... *lineopunctata* sp. nov.
7. Pronotal length less than 15 mm; total insect length less than 55 mm; males with weakly developed pronotal-disc tubercles ..... *heppleorum* Walker *et al.*

- Pronotal length greater than 15 mm; total insect length usually greater than 60 mm; males with clearly developed pronotal-disc tubercles ..... *rhinoceros* Saussure

8. Tergite 4 strongly punctate medially ..... *intermorpha* sp. nov.
  - Tergite 4 smooth or very finely punctate medially ..... 9
9. Lateral margin of sternite 7 projecting beyond the lateral margin of tergite 7 and visible dorsally (Fig. 5) .... *mutica* sp. nov.
  - Lateral margin of sternite 7 not projecting beyond the lateral margin of tergite 7 and not visible dorsally ..... 10
10. Posterior margin of tergite 6 with a broadly rounded peak 3-5 mm from lateral margin ..... *lithgowae* Walker *et al.*
  - Posterior margin of tergite 6 thickened laterally ..... 11
11. Pronotal width less than 18 mm; total insect length up to (but usually less than) 40 mm; pronotum of male with weak medial posteromarginal tubercles ..... *saxicola* Walker *et al.*
  - Pronotal width greater than 19 mm; total insect length 40-60 mm (usually greater than 45 mm); pronotum of male with strong medial posteromarginal tubercles ..... *monteithi* Roth

#### KEY TO SPECIES OF *NEOGEOSCAPHEUS*

1. Laterocaudal angle of tergite 6 produced into a large spine directed laterodorsally; lateral margin of sternite 7 projecting beyond lateral margin of tergite 7 when viewed dorsally (Fig. 9) .... *hanni* sp. nov.
  - Laterocaudal angle of tergite 6 not produced into a large spine; lateral margin of sternite 7 not projecting beyond lateral margin of tergite 7 when viewed dorsally.. 2
2. Posterior margin of tergite 6 with one or more large spines exclusive of the laterocaudal angle ..... 3
  - Posterior margin of tergite 6 with a sublateral rounded tubercle on each side ..... *hirsutus* (Shaw)

3. Tergite 6 with laterocaudal angle produced into a small spine directed ventrocaudally, anterolateral corner with a deep pit ..... *dalmsi* Roth
- Tergite 6 without laterocaudal angle produced into a spine and anterolateral pit absent ..... *barbarae* Walker *et al.*

***Macropanesthia intermorpha* sp. nov.**

(Fig. 1)

**Etymology.** From the possession of some morphological features similar to those of *M. rhinoceros*, *M. heppleorum* and *G. dilatatus*.

**Material Examined.** (North Central Queensland)

**Holotype.** QM: ♂, QMT189900, 19°56'13"S 144°16'04"E, Poison Creek, 101 km NNE of Hughenden, 850 m, dug up, 19.iv.1995, HAR, JAW, JRW.

**Paratypes.** ANIC 1♂, 1♀, 19°57'S 144°18'E, Poison Creek via Kennedy Development Rd, 142 km S of The Lynd, dug up, 15.x.1994, JRW. QM: 1♂, QMT189901, 1♀, QMT189902, same data as holotype.

**Other Material.** JAWPC: 1♂, 1♀, same data as holotype; 3♀, S19.9370° E144.2677°, Poison Ck via Kennedy Development Rd, 850 m, dug up, 20.iii.2004, HAR, JAW, JRW. QM: 1♂, 19°57'S 144°18'E, Poison Creek, via Kennedy Development Rd, 142 km S of The Lynd, dug up, 15.x.1994, JRW; 1♂ nymph, 1♀ nymph, 19°57'S 144°18'E, Poison Creek via Kennedy Development Rd, 142 km S of The Lynd, dug up, 31.iii.1997, ACK, HAR, JRW; 1♂, 1♀, S19.9370° E144.2677°, Poison Ck via Kennedy Development Rd, 850 m, dug up, 20.iii.2004, HAR, JAW, JRW. USIC: 1♀, same data as holotype; 1♀, S19.9483° E144.2754°, nr Poison Creek, 99 km N of Hughenden, dug up, 16.ix.2012, HAR, JRW.

**DESCRIPTION**

**Male. Colour.** Head ferruginous, genae, clypeus and labrum dark brown to black; pronotum ferruginous laterally and posteriorly, dark red brown to black medially and anteriorly; meso- and metanotum ferruginous; legs ferruginous, tibial spines black apically; tergite 1 ferruginous; T2-4 ferruginous medially, dark red brown to black laterally; T5-7 and supraanal plate dark red brown to black; sternites ferruginous medially, dark brown to black laterally; subgenital plate and cerci dark red brown; dorsal and ventral surfaces shiny.

**Measurements.** Total length, 54.4 (50.2 - 55.2); pronotal length × width, 14.8 × 21.8 (14.8 - 15.1 × 22.0 - 22.5) (n = 2).

**Head.** Hidden beneath pronotum, finely punctate, frons slightly wrinkled.

**Thorax.** Pronotum densely and weakly punctate laterally, finely punctate posteriorly, anterior margin thickened and raised, disc anteriorly weakly striate and granulose, depressed medially with two oblique anterior grooves; meso- and metanotum finely and sparsely punctate; anteroventral margin of front femur with 3, rarely 2 or 4, large spines basally, posterior margin with a small distal spine.

**Abdomen.** Tergite 1 finely and sparsely punctate; T2-3 weakly punctate medially, strongly punctate laterally; T4-7 strongly punctate, posterior margin of T5 and 6 thickened laterally, laterocaudal angle of T7 produced into an acute laterally directed spine; supraanal plate strongly punctate, posterior margin entire, and laterocaudal angles weakly produced and broadly rounded; sternites weakly punctate medially, strongly punctate laterally, posterior margin of S7 shallowly concave exposing the subgenital plate, lateral margin produced anteriorly forming an obtuse angle often visible dorsally; subgenital plate finely punctate; cerci bulbous, densely setose ventrally, dorsal surface convex and setose, dorsal basal medial ridge weak or absent; genitalia reduced, L2d absent, L2vm present, L1 very weakly developed and only partially sclerotised, R2 ranging from a membranous cone with only the tip sclerotised, to a short weakly sclerotised curved spur.

**Female.** Differs from male as follows: pronotum less developed, disc less depressed, anterior margin not thickened and not raised; posterior margin of sternite 7 entire; subgenital plate absent.

**Measurements.** Total length, 54.1 - 55.0; pronotal length × width, 12.9 - 13.6 × 20.6 - 22.3 (n = 2).

**Nymph.** Similar to adults but without adult pronotal characters; colour, pale tan to brown for early instars, ferruginous to dark brown in later instars; abdominal punctations weaker, becoming stronger in later instars.

**Material Examined.** (Central Queensland)

**Holotype.** QM: ♂, QMT189884, 23°33'27"S 145°43'09"E, 42 km WNW of Jericho, 335 m, dug up, 23.iii.1999, ACK, HAR, JRW.

**Paratypes.** ANIC: 1♂, 1♀, 'Busthinia' 23°33'S 145°43'E, 45 km E of Barcaldine, dug up, 2.iv.1997, ACK, HAR, JRW. QM: 1♂, QMT189885, 1♀, QMT189886, same data as holotype; 1♂, QMT189887, 1♀, QMT189888, 22°24'30'S 145°30'00'E, 68 km NE of Aramac, 320 m, dug up, 14.iii.2006 HAR, JRW.

**Other Material.** JAWPC: 1♀, 3♂ nymphs, 22°24'30'S 145°30'00'E, 68 km NE of Aramac, 320 m, dug up, 14.iii.2006, HAR, JRW; 1♂, 1♀, 1♂ nymph, 23°34'26'S 145°37'41'E, 51 km WNW of Jericho, dug up, 2.v.2000, HAR, JRW; 1♂, 'Busthinia Station' 23°33'S 145°43'E, 41.5 km WNW of Jericho, walking on ground surface, 12.xi.1998, JAW, JRW. QM: 2♂ nymphs, 3♀ nymphs, 'Busthinia' 23°33'S 145°43'E, 45 km E of Barcaldine, dug up, 2.iv.1997, ACK, HAR, JRW. USIC: 1♂, 1♀, 23°00'02'S 145°43'36'E, 49 km ESE of Aramac, dug up, 15.iii.2006, HAR, JRW.

**Description. Male.** *Colour.* Head ferruginous, genae, clypeus, mandibles and labrum dark brown to black, maxillary and labial palps dark brown to black, antennae ferruginous, dark brown basally; pronotum ferruginous to dark brown; meso- and metanotum ferruginous; tergites and supraanal plate ferruginous to dark brown; legs ferruginous, coxae and femora ferruginous, dark brown apically, tibiae dark brown to black, tibial spines black, tarsi ferruginous; sternites ferruginous medially, dark brown to black laterally; supraanal plate dark brown to black; cerci ferruginous to brown; dorsal and ventral surfaces shiny.

**Measurements.** Total length, 58.2 (56.2 - 57.3); pronotal length × width, 16.1 × 24.2 (16.0 - 17.0 × 22.8 - 23.0) (n = 3).

**Head.** Hidden beneath pronotum, weakly and sparsely punctate, frons slightly depressed.

**Thorax.** Pronotum weakly punctate posteriorly and laterally, granulose anteriorly, disc depressed medially with two oblique anterior grooves, anterior margin thickened and raised medially; meso- and metanotum weakly and finely punctate; front femur with 2 or 3, rarely 1 or 4, large spines basally and a small spine distally on the anteroventral margin, posteroventral margin with a small distal spine.

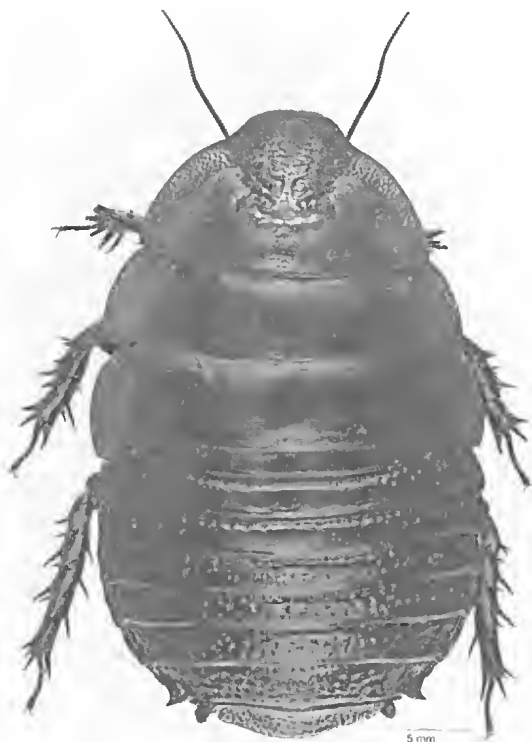


FIG. 1. *Macropanesthia intermorpha* sp. nov., paratype, QMT189901, dorsal view.

**Distribution and remarks.** This species is known only from areas within a few km north and south of Poison Creek on the Kennedy Development road, 101 km NNE of Hughenden. It is found in coarse sandy soil with diverse flora consisting mainly of eucalypts and *Callitris*. On the north eastern bank of Poison Creek adjacent to the road, *M. intermorpha* is sympatric with *M. rhinoceros*. The morphology of *M. intermorpha* superficially resembles certain features found within two genera. The thorax is similar to that of *M. rhinoceros* and *M. heppleorum*, including the absence of male pronotal tubercles in the latter, whilst its abdominal punctations resemble those of some northern populations of *G. dilatatus*.

***Macropanesthia lineopunctata* sp. nov.**  
(Fig. 2)

**Etymology.** From a distinctive line of punctations on each tergite.

**Abdomen.** Tergite 1 weakly, finely and sparsely punctate; T2-6 weakly and finely punctate medially, with a few broad strong punctations laterally, anterior margin with a row of large deep anteriorly directed punctations (Fig. 2); T7 with fine weak punctations and a few broad weak punctations medially, strong broad punctations laterally, laterocaudal angle produced into a strong acute spine directed slightly dorsocaudally; supraanal plate with both strong broad punctations and weak fine punctations, laterocaudal angles produced into blunt obtuse spines, posterior margin usually with ventrally directed crenulation medially; sternites finely and weakly punctate medially, strongly and broadly punctate laterally, posterior margin of S7 shallowly concave exposing subgenital plate; subgenital plate finely and weakly punctate; cerci bulbous and densely setose; genitalia reduced and variable, L2d absent, L2vm present, L1 ranging from weakly developed and very weakly sclerotised to absent, R2 weakly sclerotised and ranging from a small curved spine to a small hook.

**Female.** Differs from male as follows: pronotum less developed, disc less depressed, anterior margin not thickened and raised; posterior margin of sternite 7 entire; subgenital plate absent.

**Measurements.** Total length, 55.0 - 55.5; pronotal length  $\times$  width, 14.1 - 14.2  $\times$  22.1 - 22.5 (n = 3).

**Nymph.** Similar to adults but without adult pronotal characters; colour, pale tan to brown for early instars, ferruginous to dark brown in later instars; abdominal punctations weaker, becoming stronger in later instars.

**Distribution and Remarks.** Initially, *M. lineopunctata* was known only from a dense population at its type locality in central Queensland. Further collections have shown it to be widespread to the north and west of this collection site. It is found mostly in coarse sandy soil. The flora consists of a diverse savannah woodland with eucalypts and *Callitris* being dominant.

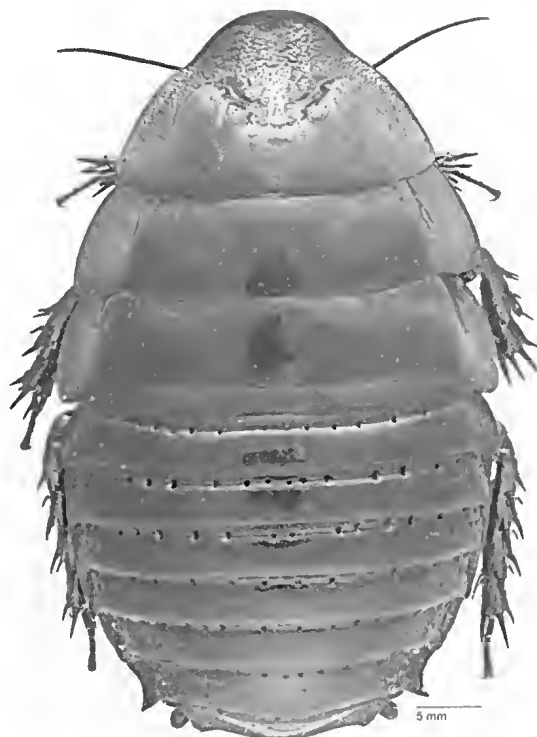


FIG. 2. *Macropanesthia lineopunctata* sp. nov., holotype, dorsal view.

*Macropanesthia mutica* sp. nov.  
(Figs 3-5)

**Etymology.** From *muticus*, alluding to the lack of processes where such usually occur. All other Geoscapheinae possess spines on tergites 6 and or 7.

**Material Examined.** (North East Queensland)

**Holotype.** QM: ♂, QMT189893, 17°01'14"S 145°36'00"E, 19 km ESE of Mareeba, 765 m, dug up, 29.ix.1992 HAR, JAW.

**Paratypes.** ANIC: 1♂, 1♀, same data as holotype. QM: 1♂, QMT189894, 1♀, QMT189895, same data at holotype; 1♂, QMT189896, 1♀, QMT189897, 17°06'05"S 145°33'01"E, 8.8 km W of Mount Edith, 890 m, dug up, 13.vi.2011 J.A.Cullen, JAW; 1♂, QMT189898, 16°57'08"S 145°35'53"E, 19 km ENE of Mareeba, 640 m, dug up, 16.ii.2002 J.A.Cullen, HAR, JAW; 1♀, QMT189899, 16°57'08"S 145°35'53"E, 19 km ENE of Mareeba, 640 m, dug up, 18.xi.2006 J.A.Cullen, HAR, JAW, JRW.



**Other Material.** JAWPC: 1♂, 2♀, same data as holotype; 1♂, 1♀, S17.01577° E145.61620°, Lambs Head Track, 1023 m, dug up, 3.vii.2011, JAW, J.A.Cullen; 1♀, 1♂ nymph, 2♀ nymphs, S17.01609° E145.62889° Lambs Head Track, 1186 m, dug up, 3.vii.2011, JAW, J.A.Cullen; 1♂, S17.027° E145.606°, Pandanus Creek, 695 m, dug up, 16.ii.2002, J.A.Cullen, HAR, JAW. DAFF, Brisbane: 1♂, Clohesy R. State Forest Reserve, on ground, 10.iv.1972, S. Dansey, J.H.B; 2♂, Upper Clohesy R, in soil under rainforest 18.iv.1975, J.H.Barrett; QM: 2♂, 2♀, same data as holotype; 1♀, Lambs Head Track, via Davies Ck Road, 10.xii.1989, 800-900 m, GBM, Thompson, Janetzki; 1♂, S17.027° E145.606°, Pandanus Creek, 695 m, dug up, 5.x.1994, JRW; 1♂, 1♀, S17.02103° E145.60834°, Lambs Head Track, 846 m, on ground surface, viii 2003, JAW, J.A.Cullen, N.J.Cullen, K.L.Anderson, R.Anderson; 3♀, 2♂ nymphs, 5♀ nymphs, S17.01610° E145.62553°, Lambs Head Track, 1145 m, dug up, 31.v.2009, J.A.Cullen, JAW; 1♂, S17.027° E145.606°, Pandanus Creek, 695 m, dug up, 9.xi.1994, HAR, JRW; 1♂, S17.03786° E145.57837°, Mount Turtle, 915 m, dug up, 29.iii.2009, D.Foreman, J.A.Cullen, JAW; 1♂ nymph, S17.09642° E145.55154°, 8.7 km W of Mount Edith, 1015 m, dug up, 13.vi.2011 J.A.Cullen, JAW. USIC: 1♂, 1♀, 1♂ nymph, 1♀ nymph, same data as holotype; 2♀, 5♂ nymphs, 2♀ nymphs, S16.9521° E145.5982°, Clohesy River, 640 m dug up, 16.ii.2002 J.A.Cullen, HAR, JAW; 2♂, 2♀ nymphs, 16°57'08"S 145°35'53"E, 19 km ENE of Mareeba, 640 m, dug up, 18.xi.2006 J.A.Cullen, HAR, JAW, JRW.

**Description. Male.** *Colour.* Head ferruginous, clypeus light tan to orange, mandibles dark brown to black; pronotum ferruginous to dark brown, anterior margin dark brown to black medially, disc dark brown to black posteriorly; meso- and metanotum ferruginous to dark brown; legs ferruginous, tibial spines dark brown to black apically; tergites 1-6 ferruginous to dark brown, often darker laterally; T7 and supraanal plate dark brown to black; cerci dark brown to black; sternite 2 dark brown to black laterally; S3-6 ferruginous medially, dark brown to black laterally; S7 dark brown to black, ferruginous anteromedially; subgenital plate dark brown to black; dorsal surface matt, ventral surface somewhat shiny.

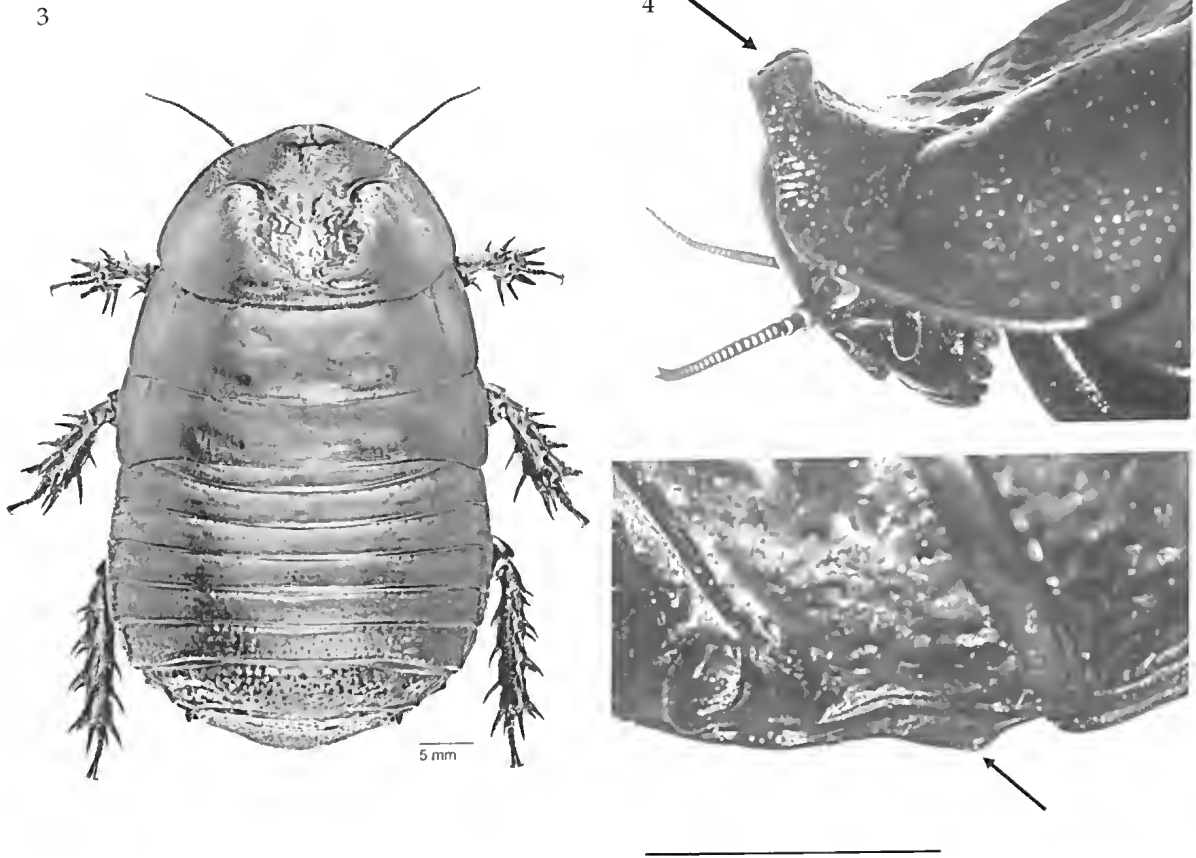
**Measurements.** Total length, 57.2 (56.4 - 58.0); pronotal length × width, 17.5 × 26.9 (16.3 - 17.1 × 24.9 - 25.4) (n = 4).

**Head.** Hidden by pronotum, slightly depressed above clypeus, finely and weakly punctate.

**Thorax.** Pronotum convex, punctate laterally with weak punctations posterolaterally, anterior margin thickened and raised medially forming two partly fused blunt tubercles (Fig. 4), weakly striate 3-4 mm posterior to marginal tubercles, disc widely depressed from 4-5 mm from marginal tubercles to 2-3 mm from posterior margin, and thickened medially, depressed disc floor weakly roughened, anterior portion of disc with a pair of oblique posteriorly curved grooves, terminating 2-3 mm from anterolateral margin; meso- and metanotum sparsely and very weakly punctate, having fine irregular grooves; anteroventral margin of front femur with 2 or 3, rarely 1 or 4, large spines basally, a very small spine distally, and posterior margin with a large distal spine.

**Abdomen.** Tergites 1-6 weakly and sparsely punctate medially, with punctations becoming stronger and denser laterally; posterior margin of T6 slightly thickened laterally forming a weakly crenulate ridge; T7 with large shallow punctations, and the laterocaudal angle produced into a small rounded spine directed laterocaudally to slightly ventrocaudally; supraanal plate with large punctations, convex posteriorly, posterior margin entire, and laterocaudal angles weakly produced and broadly rounded; sternite 2 densely punctate laterally; S3-6 very weakly and sparsely punctate medially and densely punctate laterally; S7 very weakly and sparsely punctate anteromedially, weakly punctate laterally and posteriorly, posterior margin concavely truncated exposing subgenital plate, and lateral margin produced anteriorly, forming an obtuse angle visible dorsally (Fig. 5); subgenital plate weakly punctate; cerci broadly triangular, tapering to a broadly rounded tip, dorsal surface weakly punctate and sparsely setose apically and with a smooth medial ridge basally, ventral surface densely setose; genitalia reduced, L2d absent, L2vm present, L1 present but not strongly sclerotised, R2 ranging from a curved sclerotised spur to a weakly curved sclerotised hook.

**Female.** Differs from male as follows: pronotum less developed, disc less depressed, posterior margin not thickened, anterior margin only



FIGS 3-5. *Macropanesthia mutica* sp. nov., holotype: 3, dorsal view; 4, pronotum, lateral view; 5, lateral margin of sternite 7.

slightly thickened and without tubercles; posterior margin of S7 entire; subgenital plate absent; abdomen relatively wider than male giving a pear shaped outline.

**Measurements.** Total length, 52.9 - 59.2; pronotal length  $\times$  width, 15.0 - 16.1  $\times$  23.0 - 25.4 (n = 4).

**Nymph.** Similar to adults but without adult pronotal characters; colour, pale tan to brown for early instars, ferruginous to dark brown in later instars; abdominal punctations weaker, becoming stronger in later instars.

**Distribution and Remarks.** Known from the northern and western flanks of the Lamb Range in north Queensland, from near Clohesy River

to near to Lake Tinaroo. Sites are semi-open eucalypt and sheoak forests, and at Pandanus Creek, rainforest. Ground surface specimens were first collected by foresters working in Clohesy State Forest in the 1970s and the authors have since dug up specimens close to these original collection sites. A specimen has also been collected by JAW close to the summit of Lambs Head. This species does not fit any of the original generic descriptions for soil burrowing cockroaches (Roth 1977; Walker *et al.* 1994), however it clearly belongs within the subfamily Geoscaphaeinae. In the opinion of the authors, the existing genera may not reflect phylogeny, and thus at this present time the erection of a new genus to accommodate *M.*

*mutica* would not be appropriate. Accordingly, the current key to the genera of Geoscapheinae (Walker *et al.*, 1994) has been altered by deleting the reference to the laterocaudangle of T7, and this species keys to *Macropanesthia*.

*Macropanesthia spuritegmia* sp. nov.  
(Fig. 6)

**Etymology.** Reference to the coloured lateral patches on meso- and metanota; from a short distance away, these patches superficially resemble tegmina.

**Material Examined.** (Central Queensland)

**Holotype.** QM: ♂, QMT189889, 23°33'51"S 145°50'00"E, 30 km WNW of Jericho, 335 m, dug up, 12.xi.1998, JAW, JRW.

**Paratypes.** ANIC: 1♀, same data as holotype; 1♂, 23°33'53"S 145°48'39"E, 32 km WNW of Jericho, dug up, 23.iii.1999, ACK, HAR, JRW. QM: 1♂, QMT189890, 1♀, QMT189891, same data as holotype; 1♀, QMT189892, 23°34'03"S 145°51'49"E, 27 km WNW of Jericho, 335 m, dug up, 21.v.2008 HAR, JAW.

**Other Material.** JAWPC: 1♀, 1♂ nymph, same data as holotype; 2♀, 3♀ nymphs, 23°33'52"S 145°48'42"E, 32 km WNW of Jericho, dug up, 22.iii.2004, HAR, JRW; 1♂ 23°34'03"S 145°51'49"E, 27 km WNW of Jericho, 335 m, dug up, 21.v.2008, HAR, JAW. USIC: 2♂, 1♂ nymph, 3♀ nymphs, S23.5675° E145.8636°, 27 km WNW of Jericho, dug up, 17.ix.2012, HAR, JRW.

**Description. Male. Colour.** Head black, clypeus dark brown with a pale brown medial band and often pale brown laterally, antennae black, mandibles black basally and distally but brown medially; pronotum black; meso- and metanotum black, submarginal smoky yellowish to orange patches anterolaterally extending nearly to laterocaudal angles (Fig. 6), anterolateral patch larger on mesonotum than metanotum; tergite 1 black; T2-7 ferruginous to dark red brown anteromarginally, black posteromarginally and laterally; supraanal plate dark red brown to black; legs black; sternites dark red brown anteriorly tending to black posteriorly; subgenital plate black; cerci black; dorsal and ventral surfaces shiny.

**Measurements.** Total length, 39.4 (36.8 - 37.1); pronotal length × width, 10.6 × 17.2 (10.0 × 15.0 - 15.2) (n = 2).

**Head.** Finely punctate, hidden beneath pronotum.

**Thorax.** Pronotum broadly and weakly punctate lateromarginally, finely punctate posteromedially, anterior margin thickened and raised medially, disc depressed and granular to anterior margin and with two weak oblique anterior grooves; meso- and metanotum finely and sparsely punctate; anteroventral margin of front femur with 2 or 3, rarely 4, large spines basally, posterior margin with a large distal spine.

**Abdomen.** Tergite 1 smooth; T2-7 finely and sparsely punctate with punctations becoming dense and stronger laterally; laterocaudal angle of T7 produced into a small acute spine directed ventrocaudally; supraanal plate coarsely and weakly punctate, posterior margin with ventrally directed small acute crenulations medially, laterocaudal angles weakly developed; sternites weakly punctate medially, densely and weakly punctate laterally; posterior margin of S7 weakly concave exposing subgenital plate; subgenital plate weakly punctate; cerci acutely triangular, tapering to a finely rounded point, densely setose ventrally, dorsal surface glabrous and with a weak rounded ridge basally; genitalia much reduced, L2vm present, L2d, L1 and R2 absent.

**Female.** Differs from male as follows: pronotum less developed, disc less depressed, posterior margin not thickened, anterior margin not thickened and not raised; posterior margin of sternite 7 entire; subgenital plate absent; generally larger and wider.

**Measurements.** Total length, 36.4 - 42.3; pronotal length × width, 10.3 - 10.9 × 17.1 - 18.7 (n = 3).

**Nymph.** Similar to adults but without adult pronotal characters; colour, smoky dark brown; abdominal punctations weaker, becoming stronger in later instars; smoky yellowish to orange patches on meso- and metanota not as defined as in adults.

**Distribution and Remarks.** Known only from a localised area adjoining the Capricorn Highway, east of Alice River for 6 km, in sandy soil where *Callitris* dominates. Despite extensive efforts, no further populations have been found. Some specimens have pronota with weak smoky yellowish to orange patches posterolaterally.

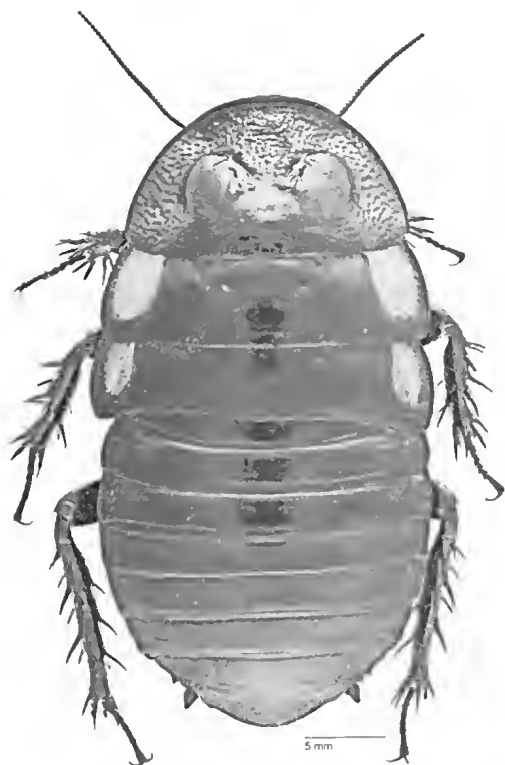


FIG. 6. *Macropoanesthia spuriteguina* sp. nov., holotype, dorsal view.

*Neogeoscapheus hamni* sp. nov.  
(Figs 7-9)

**Etymology.** After the Hann Tableland, where it was first discovered.

**Material Examined.** (North East Queensland)

**Holotype.** QM: ♂, QMT189879, 16°47'47"S 145°10'56"E, Hann Tableland, 20 km SW of Mount Molloy, 520 m, dug up, 10.ii.1996, GBM, HAR, JAW, JRW.

**Paratypes.** ANIC: 1♂, 1♀, same data as holotype. QM: 1♀, QMT189880, same data as holotype; 1♂, QMT189881, 16°48'S 145°10'E, Hann Tableland, 20 km SW of Mount Molloy, dug up, 8.xii.1995, GBM; 1♂, QMT189882, 16°39'10"S 145°15'36"E, 8 km WNW of Mount Molloy, 500 m, dug up, 14.xii.2003, J.A.Cullen, JAW; 1♂, QMT189883, 16°57'14"S 145°13'54'E, 'Glen Russell', 22 km WNW of Mareeba, 575 m, dug up, 17.ii.2002, J.A.Cullen, GBM, HAR, JAW.

**Other Material.** JAWPC: 5♀, 1♂ nymph, 16°57'14"S 145°13'54'E, 'Glen Russell', 22 km WNW of Mareeba, 575 m, dug up, 17.ii.2002, J.A.Cullen, GBM, HAR, JAW; 1♂, S16.6527° E145.2601°, Bowerbird Ck, 8 km WNW of

Mt Molloy, 495 m, dug up, 17.x.2006, N.Lo, JAW; 1♂, 2♀, 5♂ nymphs, 1♀ nymph, S16.6527° E145.2601°, Bowerbird Ck, 8 km WNW of Mt Molloy, 495 m, dug up, 4.v.2008, J.A.Cullen, JAW; 1♂, 2♀, 5♂ nymphs, 3♀ nymphs, S16.6642° E145.2995°, 3.5 km WNW of Mt Molloy, 425 m, dug up, 26.iii.2004, HAR, JAW, JRW; 1♀, 2♀ nymphs, S16.6648° E145.2989°, Sandy Creek, NW of Mt Molloy, 445 m, dug up, 24.x.2010, JAW. DAFF, Brisbane: 1♂, Hann Tableland via Mt Molloy, 14.xii.1995 GBM; 1♂, N base of Hann Tableland, 500 m, 10.ii.1996, GBM. QM: 1♂, 2♀, 1♂ nymph, 1♀ nymph, same data as holotype; 1♂, 1♀ nymph, S16.63885° E145.24513°, Luster Ck, 9.5 km WNW of Mt Molloy, 425 m, dug up, 9.viii.2009, J.A.Cullen, JAW; 1♀, S16.63455° E145.24861°, Luster Ck, 9.5 km WNW of Mt Molloy, 505 m, dug up, 9.viii.2009, J.A.Cullen, JAW; 1♂, 2♀, 3♀ nymphs, 16°39'10"S 145°15'36'E, 8 km WNW of Mount Molloy, 500 m, dug up, 14.xii.2003, J.A.Cullen, JAW; 1♀, S16.6551° E145.2950°, 4.4 km NW of Mt Molloy, 584 m, dug up, 2.vii.2008, JAW. USIC: 2♂, 1♀, 1♂ nymph, 16°56'56"S 145°13'25'E, 'Glen Russell', Hann Tableland, 33 km SSW of Mount Molloy, 580 m, dug up, 25.xi.2008 HAR, JRW; 1♀, 1♂ nymph, S16.6527° E145.2601°, Bowerbird Ck, 8 km WNW of Mt Molloy, 495 m, dug up, 26.iii.2004, HAR, JAW, JRW; 1♂, 1♀ nymph, S16.6590° E145.2630°, 7.5 km WNW of Mt Molloy, 520 m, dug up, 26.iii.2004 HAR, JAW, JRW; 1♀, S16.6642° E145.2995°, 3.5 km WNW of Mt Molloy, 425 m, dug up, 10.v.2003, JAW; 1♂, 1♀, S16.6642° E145.2995°, 3.5 km WNW of Mt Molloy, 425 m, dug up, 21.xi.2008, HAR, JAW.

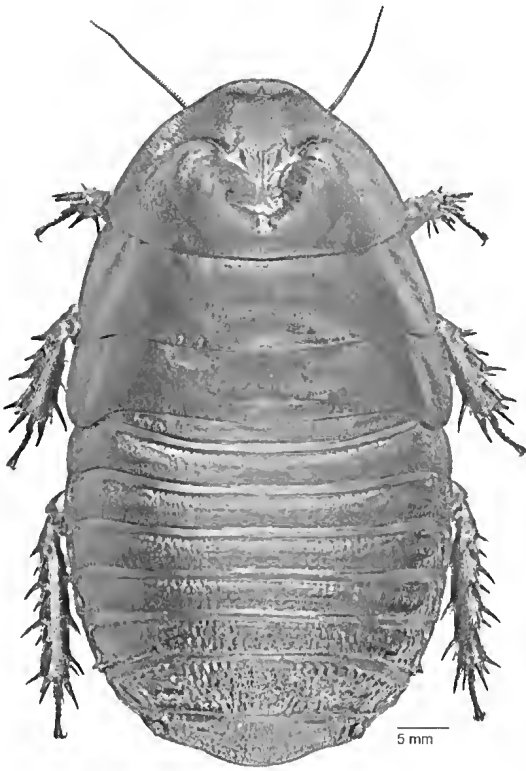
**Description. Male. Colour.** Head ferruginous, clypeus often paler, genae and basal half of labrum dark brown to black; thoracic nota ferruginous, usually paler laterally, dark brown to black medially; legs ferruginous, tibial spines and tarsi dark brown to black; abdominal tergites ferruginous anteriorly, dark brown to black posteriorly; supraanal plate dark brown to black; sternite 2-6 ferruginous medially, dark brown to black laterally; subgenital plate ferruginous, lateral and posterior margins dark brown to black; cerci ferruginous to dark brown; dorsal surface matt, ventral surface somewhat shiny.

**Measurements.** Total length, 64.9 (60.1 - 61.9); pronotal length × width, 18.6 × 28.1 (17.0 - 17.8 × 25.4 - 28.0) (n = 4).

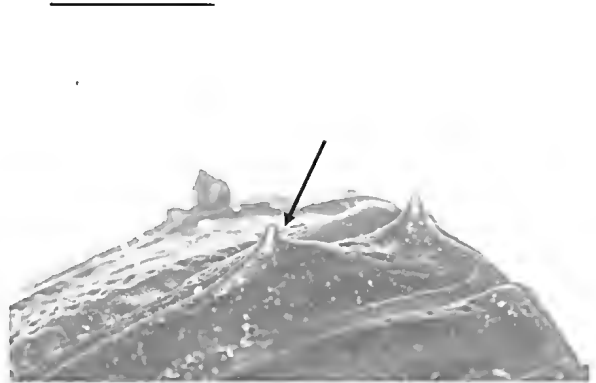
**Head.** Hidden beneath pronotum, finely and weakly punctate, frons weakly striate.

**Thorax.** Pronotum convex, finely punctate laterally, anterior margin raised medially with two slightly recurved submarginally fused tubercles, disc weakly striate posterior to

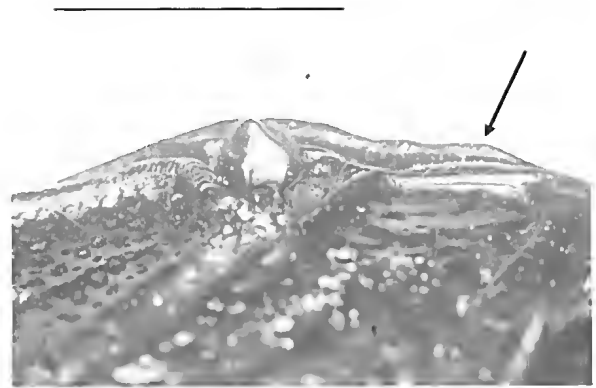
7



8



9



FIGS 7-9. *Neogeoscapheus hamni* sp. nov., holotype: 7, dorsal view; 8, tergite 6, dorsal view; 9, lateral margin of sternite 7.

submarginal tubercles, depressed medially with a median groove and two oblique anterior grooves, lateral margins raised forming four broad rounded tubercles; meso- and metanotum finely and weakly punctate, with weak tegminal depressions, fine irregular sculpturing medially; anteroventral margin of front femur with 2 to 4, usually 3, large spines basally, posterior margin with a large distal spine.

**Abdomen.** Tergites 1-6 finely punctate with punctations stronger laterally; T6 with pronounced punctations medially, the laterocaudal angle produced into an acute laterodorsally directed spine, posterior margin with a similar acute spine 4-6 mm from the lateral margin (Fig. 8); T7 strongly punctate, the anterior margin with a row of strong submarginal punctations, the

posterior margin thickened where it meets a very weakly developed laterocaudal angle; supraanal plate strongly and coarsely punctate, lateral and posterior margins thickened and finely punctate; sternites smooth and shiny medially, weakly and densely punctate posterolaterally; S7 smooth anteromedially, weakly punctate marginally, lateral margins produced beyond T7 and visible dorsally (Fig. 9), the posterior margin concavely truncated exposing a finely punctate subgenital plate; cerci broadly triangular, tapering to a broadly rounded apex, dorsal surface glabrous and concave either side of a rounded basal median ridge; genitalia reduced, L2d absent, L2vm present, L1 present but weakly developed and not strongly sclerotised, R2 a well sclerotised curved spine.

**Female.** Differs from male as follows: pronotum less developed, disc less depressed, posterior margin not thickened, anterior margin only slightly thickened and not produced into two tubercles; posterior margin of sternite 7 entire; subgenital plate absent.

**Measurements.** Total length, 60.8 - 63.6; pronotal length  $\times$  width, 16.2 - 17.0  $\times$  24.8 - 26.1 ( $n = 2$ ).

**Nymph.** Similar to adults but without adult pronotal characters; colour, pale tan to brown for early instars, ferruginous to dark brown in later instars; abdominal punctations weaker, becoming stronger in later instars.

**Distribution and Remarks.** This species is known from north Queensland from two elevated areas separated by the upper Mitchell River. The first collections were made at the northern edge of the Hann Tableland, and two further populations were discovered at the south western base of the tableland on 'Glen Russell'. Subsequently, a number of smaller populations have also been discovered on the western slopes of the Carbine Tableland. All sites have sandy granitic soils with eucalypt dominated vegetation. Specimens from the Carbine Tableland exhibit considerable variation in the development of spines on the posterior margin of T6. Some specimens possess a single spine on each side whilst others have two or three and of varying size. This is in contrast with populations to the west, associated with the Hann Tableland, where all specimens possess only single spines. The other three species of *Neogeoscapheus* found in central and south east Queensland are considerably smaller than *N. hauni*.

## DISCUSSION

The Geoscapheinae is a well defined group with regard to their biology. All 24 species are found in Queensland, with five also occurring in other states. While most species have fairly limited ranges, five are widely distributed (*M. rhinoceros*, *M. heppleorum*, *M. kraussianna*, *G. dilalalus*, *G. robustus*); the latter three species are found west of the Great Dividing Range. Some species occur as sympatric populations. We believe that discovery of further new species of

geoscapheines unlikely, although recognition of new species from within existing collections may result from more detailed examination.

Walker *et al.* (1994) suggested that genera within Geoscapheinae may not reflect phylogeny and that further studies of intergeneric relationships were required. Later studies on isozymes by Humphrey *et al.* (1998), on male genitalia and oothecal membranes, Walker and Rose (1998), and molecular techniques by Maekawa *et al.* (2003), have also suggested the generic classification is not well supported. We are undertaking further studies to clarify and review phylogenetic relationships within and between Australian Panesthiinae and Geoscapheinae.

## ACKNOWLEDGEMENTS

We appreciate the valuable assistance of A.C. Kotze and G.B. Monteith. Habitus images were provided by Geoff Thompson and for which we are most grateful. Insightful comments by a reviewer of the manuscript were very helpful.

## LITERATURE CITED

- Beccaloni, G. W. & Eggleton, P. 2011. Order Blattodea Brunner von Wattenwyl, 1882. In Zhang, Z.-Q. (ed.). Animal biodiversity: an outline of higher-level classification and survey of taxonomic richness. *Zootaxa* **3148**: 199-200.
2013. Order Blattodea. *Zootaxa* **3703**: 46-48.
- Humphrey, M., Colgan, D.J. & Rose, H.A. 1998. Electrophoretic studies of cockroaches of the Australian endemic subfamily Geoscapheinae. *Zoological Journal of the Linnean Society* **124**: 209-234.
- Inward, D., Beccaloni, G.W. & Eggleton, P. 2007. Death of an order: a comprehensive molecular phylogenetic study confirms that termites are eusocial cockroaches. *Biology Letters* **3**: 331-335.
- Maekawa, K., Lo, N., Rose, H.A. & Matsumoto, T. 2003. The evolution of soil-burrowing cockroaches (Blattaria: Blaberidae) from wood-burrowing ancestors following an invasion of the latter from Asia into Australia. *Proceedings of the Royal Society London B* **270**: 1301-1307.
- McKittrick, F.A. 1964. Evolutionary studies of cockroaches. *Cornell University Agricultural Experiment Station Memoirs* **389**: 1-197.

## Five new species of soil burrowing cockroaches

- Roth, L.M. 1977. A taxonomic revision of the Panesthiinae of the world. I. The Panesthiinae of Australia (Dictyoptera: Blattaria: Blaberidae). *Australian Journal of Zoology* Supplementary Series **48**: 1-112.
- Rugg, D. & Rose, H.A. 1984. The taxonomic significance of reproductive behaviour in some Australian cockroaches (Blattodea: Blaberidae). *Journal of the Australian Entomological Society* **23**:118.
- Walker, J.A., Rugg, D. & Rose, H.A. 1994. Nine new species of Geoscaphinae (Blattodea: Blaberidae) from Australia. *Memoirs of the Queensland Museum* **35**: 263-284.
- Walker, J.A. & Rose, H.A. 1998. Oothecal structure and male genitalia of the Geoscaphinae and some Australian *Panesthia* (Blattodea: Blaberidae). *Australian Journal of Entomology* **37**: 23-26.





## IN MEMORIUM

### Richard ‘Dinosaur Dick’ Suter (1935–2013)



FIG. 1. Dick Suter (sitting) with Tom and Sharon Hurley showing the plesiosaur skeleton that Dick had prepared.

Richard (Dinosaur Dick) Suter was born in December 1935 in Melbourne but first arrived in Boulia, Western Queensland in 1953. He loved the country, the flora & fauna, the people and the rest of his life he was either associated with the place, or lived there.

Interviewed by the ABC journalist, Leonie Lyons, in 2008 he said: *"I spent about 26 years in the district before I cleared off down to Sydney to get away from the heat and the flies... and then started coming back out here in 1984 for my health."*

He, and his brothers, John and Bill spent a large portion of their lives in many different but complimentary pursuits around Boulia. Dick had many career changes and he worked on many local stations, undertook contract fencing, was a land owner and sheep farmer,

semi-professional fisherman, museum curator and fossil discoverer.

Dick had contact with the Queensland Museum (QM) from the early 1960's; but it was his brother, John, who got him interested in fossil hunting. He was also fully aware that the fossil faunas of the Toolebuc Formation in Western Queensland had hardly been touched. Dick and John made a significant collection with the intention that it be put on display in Boulia but the local council, at that time, could not supply a venue for it. As a result, for several years, the collection was on display in John's shed in Sydney. It was donated to the South Australian Museum in 2007.

Dick also continued to collect, and this new collection, 'Boulia Collection' went on display

at the town's Stone House museum in 1998. At the same time, Dick met Tom and Sharon Hurley who realised that John and Dick had hit upon a successful prospecting strategy for finding large vertebrate fossils. Early collectors had assumed, incorrectly, that what was lying on the surface was all that was to be found. Dick discovered that further digging may reveal additional parts of the skeleton still encased in limestone, more deeply buried in the soil. Tom and Sharon also brought new ideas, quad bikes, GPS's, and mechanised digging which resulted in new and significant discoveries in the Boulia region.

Some of the fossils that were found and donated or were named after the team, include *Bouliachelys suteri*, (Suter's Boulia turtle). Two large cartilaginous fish, a 3 m swordfish like fish (*Australopachycormus hurleyi* Kear 2007). Another new species, found by Dick, is currently being studied by Dr Alan Bartholomai as this is being written. Isopod crustaceans (*Brunnaega tomhurleyi* Wilson & Kear 2011) were also described from a fossil fish skull. Other fossils sent to QM and other museums include 2 other swordfish specimens, a shark skull complete with skin, teeth and vertebrae, a chimaeroid tooth plate, what looks like sardines in a layer 10 deep, an ankylosaur dinosaur and two pterosaur bones. In the 'Boulia collection' at the Stone House Museum are 2 relatively complete ichthyosaur skulls, 2 large plesiosaurs, sharks, fish, ammonites, a kronosaur, vertebrae of a sauropod dinosaur, trees, shells and more. While not all were found by Dick he did help facilitate the discovery and collection of fossils from the district.

Dick volunteered his time at the museum and became the long-term curator until his untimely end in June 2013, aged 77 years. The 'Boulia collection' was gifted to QM and is now part of the state collection. Dick didn't just volunteer at the museum, he spent many hours weeding the burrs from the median strip of Boulia's main street and other public areas and involved himself in many community projects. He was passionate about the local community, supporting local events and the flying doctor.

He received multiple Volunteer and Australia Day awards. In 2007 he was recognised for his contribution in the Queensland Tidy Towns Awards with the Queensland Outstanding Individual award.

Dick was a true and reliable friend. He stood for fairness, honesty and respect. He valued friendship and had a good sense of humour. In the past 15 years, Dick became famous as 'Dinosaur Dick' but not just for his fossil exploits. He shared yarns with the tourists at the Stone House Museum on a wide variety of subjects. Stories included growing up with a dad who was a circus lion tamer, of fishing, fighting, fencing, fossils, shooting, horses, motorbikes, sheep, feral pigs and cats. Dick with his stories was certainly one of the museum's attractions and a well-known mining identity described him as "*the most interesting man he had ever met and his main form of propulsion was his mouth!*" Dick will be remembered perhaps, most of all, for his story telling, and the African proverb "*that when an old man dies, a library burns down*" seems particularly appropriate. If he wasn't a legend from all of his exploits then the chance discovery of a truly unbelievable plesiosaur in May 2012 and preparing it in just 9 months on his own certainly qualifies him (Fig. 1.).

Dinosaur Dick described his fossil collecting years as the best years of his life. What a lucky man that his best years were at the end of a long and full life.

### Names created to honour Dick Suter

Fossil sea turtle

*Bouliachelys suteri* Kear & Lee 2006

### Author citations for Honorifics

Kear, B.P. & Lee, M.S. 2006. A primitive protostegid from Australia and early sea turtle evolution. *Biology Letters* 2:116-119

### Tom & Sharon Hurley

<http://dx.doi.org/10.17082/j.2204-1478.59.2015.2014-17>

First published online 21 January 2015.

# Numerical analysis of the inter-relationships of some extinct and extant taxa of Araucariaceae

H. Trevor CLIFFORD

Mary E. DETTMANN

Scott A. HOCKNULL

Ancient Environments Program, Queensland Museum, Hendra Facility, 122 Gerler Rd, Hendra, Qld 4011 Australia. Email: scott.hocknull@qm.qld.gov.au

<http://dx.doi.org/10.17082/j.2204-1478.59.2015.2013-04>

LSID urn:lsid:zoobank.org:pub:1A1AF2E1-951D-4366-8C0A-1D8E8A23A2CD

Citation: Clifford, H.T., Dettmann, M.E. & Hocknull, S.A. 2015. Numerical analysis of the inter-relationships of some extinct and extant taxa of Araucariaceae. *Memoirs of the Queensland Museum – Nature* 59: 27–38. Brisbane, ISSN 2204-1478 (Online), ISSN 0079-8835 (Print). Accepted: 20 October 2014. First published online: 20 February 2015.

## ABSTRACT

The inter-relationships between extant and selected extinct taxa of Araucariaceae were explored using thirty morphological and anatomical characters. The sample of Araucariaceae included all three extant genera of the family with three extinct species of *Araucaria* and the fossil genera *Emwadea* and *Wairarapaia*. The data were analysed using phenetic and cladistic methodology which revealed there was close agreement between the two when applied to extant taxa but not to extant plus extinct taxa. All analyses recognised that the araucarioid taxa with embedded seeds formed a group separate from the agathoid taxa whose seeds at maturity separate from the seed-scale. However, whereas the parsimony (cladistic) analyses failed to distinguish clades within *Araucaria* the phenetic analyses recognised four Sections within the genus and placed the three fossil species of *Araucaria* in Sect. *Eutacta*. The fossil genera *Emwadea* and *Wairarapaia* united with *Agathis* and *Wollemia*. □ *Araucariaceae*, *Wollemia*, *Emwadea*, *Wairarapaia*, seed-cones, phylogeny.

The description of *Emwadea microcarpa* Dettmann *et al.* (2012) based on permineralised seed-cones with preserved anatomy, from the mid-Cretaceous (late Albian) of western Queensland, adds to the data base of confirmed araucarian remains worldwide and supports the widely held view that during the Mesozoic and early Tertiary the family was more diverse than at present (Hill 1990; Cantrill 1992; Stockey 1994; Stockey *et al.* 1994; Pole 1995; Chambers *et al.* 1998; Hill & Brodribb 1999; Cantrill & Raine 2006; Dettmann *et al.* 2012)

Whilst the araucarian affinities of many well preserved fossil seed-cones is not in doubt, their relationships with each other and with extant

taxa has not been explored, until recently, by quantitative phenetic or cladistic analyses (Escapa & Catalano 2013). The extant Araucariaceae are represented by three genera *Araucaria*, *Agathis* and *Wollemia* (Farjon 2010), whose relationships have not been unambiguously established by cladistic studies based on gene sequencing data (Gilmore & Hill 1997; Stephanovic *et al.* 1998; Setoguchi *et al.* 1998; Codrington *et al.* 2002; Rai *et al.* 2008). Furthermore, these cladistic studies do not strongly support either the widely accepted four Sections into which extant *Araucaria* species were grouped by Wilde & Eames (1952) or the two Section grouping espoused by Laubenfels (1988). For example, whereas according to Setoguchi *et al.* (1998) Sect. *Arancaria* is the

sister group to the clade Sects *Bunya* and *Intermedia* according to Gilmore & Hill (1997) it is the sister group to Sect. *Eutacta*.

Such disparity may be a consequence of the current Sections being based on morphological and anatomical data derived from extant taxa and so do not take into account the structure of Mesozoic seed-cones that may share characters with more than one extant Section of *Arancaria* (Stockey 1994; Stockey *et al.* 1994; Ohsawa *et al.* 1995).

In view of the uncertainty of the interrelationship within Araucariaceae it was decided to investigate relationships between the three extant genera and five fossil taxa of the family incorporating morphological and anatomical data for all extant taxa and those fossils for which adequate descriptions are available. Both phenetic and cladistic analyses were undertaken.

## MATERIAL AND METHODS

Fourteen taxa, of which nine are extant, were selected for study. They were the genera *Pinus*, *Podocarpus*, *Phyllocladus*, *Agathis* and *Wollemia* together with the four currently accepted Sections of extant *Arancaria* (Wilde & Eames 1955). Following Farjon (2010) no subgeneric ranks were recognised within *Agathis*. The five fossil taxa, namely *Euvadea microcarpa* Dettmann, Clifford & Peters, *Wairarapaia wildenlallii* Cantrill & Raine, *Araucaria mirabilis* (Spegazzini) Windhausen, *A. nipponensis* Stockey, H. Nishida & M. Nishida and *A. vulgaris* (Stopes & Fujii) Ohsawa, H. Nishida & M. Nishida were chosen because the anatomical details of their ovule/seed-cones are available.

Since the development of the seed-cones of most araucarian taxa has not been studied the homologies of their characters could not be determined directly. Instead, it was necessary to choose a theoretical model against which to make comparisons. The model accepted was that proposed by Florin (1944) as it provides a suitable framework for this purpose, notwithstanding it is predicated on the structure of mature cones. Allowance therefore has to be made for the considerable changes in

structure that may occur following pollination (Tomlinson & Takaso 2002). For example, the ovules of young seed-cones of extant conifers are often initially orthotropous but are later inverted.

Here it has been accepted that the ovules derive from an axillary complex which is subtended by a scale, and that each ovule is sessile or terminal on a more or less developed axis terminating in a pair of bracts fused marginally to form an integument around the nucellus. The axis may or may not bear lateral appendages below the integumentary bracts. If present, these appendages may generate secondary axes. Such a modular construction of the cone is supported by the recent studies of developmental genetics reviewed by Mathews & Kramer (2012).

Although all ovules are postulated to arise directly from the axils of bracts or from axillary complexes, due to the activity of intercalary meristems at the complex or bract bases, they may appear to arise from the adaxial surface of the bract rather than its subtending axis.

The interpretation of the bract-ovule complex can be resolved only through a study of its ontogeny. Although the pattern of vascular traces in the mature complexes may reflect their ontogeny, this assumption cannot be justified *a priori* because primordia, at least those of ovules, may develop from almost any tissue and generate their own vascular tissues (Bouman in Johri 1984). Furthermore, the formation of adventitious buds on wound callus tissues and the development of ovules from single epidermal cells, both of which may become vascularized (Romberger *et al.* 1993), suggests that the arrangement of the vascular tissues may not always be phylogenetically informative.

However, the situation is much less clear with the interpretation of the 'ligule' which is restricted to araucarian seed scale where the ovule is always inverted. Although generally accepted as arising from the ovule stalk it has recently been reinterpreted as an extension of the chalaza (Dettmann *et al.* 2012) or a stigma (Krassilov & Barinova 2014). To distinguish between these hypotheses the development of the ligule must be determined, but as cautioned by Tomlinson & Takaso (2002, p. 1251), 'If part-for-part

equivalence is assumed, one has to invoke both heterochrony (i.e. changes in developmental timing among parts) and heterotopy (i.e. spatial transference of characters), but only with considerable manipulation of the original model.' Due to such developmental flexibility, 'plants become so transformed by meristematic involution that to expect to be able to identify all structures of a putative ancestor is unrealistic.' (Tomlinson & Takaso 2002, p. 1272). An example of heterochrony such as that postulated by Tomlinson & Takaso (2002) is the reversal of the sepaline and petaline whorls in *Xyris* and other monocot flowers with a double perianth (Remizowa *et al.* 2012).

The seeds of many conifer species are accompanied by accessory structures variously described as teeth (*Cryptomeria*), appendages (*Cunninghamia*), arils (*Taxus* and *Phyllocladus*) or 'ligules' (*Araucaria*). As these structures, with the possible exception of the ligule, arise from immediately below the integuments they are accepted as homologous.

The difficulty of interpreting characters is furthermore compounded by the lack of a definite sister group for the conifers (Taylor *et al.* 2009, pp. 870-871) which, in the literature, has led to conflicting reports of character states. The two following examples illustrate the problem.

The cotyledon numbers of *Araucaria* species are given as 4 by Kindel (2001), 2-4 by Laubenfels (1988) or in 2 free and 2 fused and 2 fused pairs, with 4 free, or 4 fused into 2 pairs at the base. (Farjon 2010, p. 185). A similar diversity of ovule number per ovuliferous scale has also been reported for the genus. Whereas *Araucaria* species usually bear only one ovule per scale, both 2 and 3 ovules have been reported (Wilde & Eames 1955; Mitra 1927). Numbers of ovules in excess of 1 per scale may be teratological malformations and so may be ignored if not regarded as atavistic.

Because the best preserved fossil taxa are represented by ovuliferous cones these provided most of the characters studied. For each of the 14 taxa included in the analysis information, where available, was collated for 30 characters, of which at least one was known for each fossil

taxon. This stricture was introduced so as to ensure the fossil and extant taxa are not *ab initio* members of unrelated taxa. The characters and their states are given in Appendix 1 and the taxa together with their character scores are listed in Appendix 2.

Due to the paucity of character states available for the fossil taxa evidence of structure within the data matrix was investigated using only simple phenetic and phylogenetic methods. The former were based upon a Similarity Index (S.I.) defined as the percentage of characters shared by two taxa and so varies from zero when they share no character states to 100% when they are identical.

Two types of phenetic analyses were undertaken. One analysis constructed a Constellation Diagram in which those taxa with arbitrarily high similarity values were linked to each other; the other was the formation of a dendrogram using a simple distance measure and group average as the clustering strategy (Swofford & OLSEN 1990). This clustering strategy tends to preserve the spatial interrelationships of the taxa with a minimum of distortion because it uses all distances available at each step in the development of the dendrogram and the distances depend upon all characters.

In contrast every step of the cladistic analyses was based on parsimony settings within the software program PAUP 4.0.8. (Swofford 2003) which forms a dendrogram whose ultimate branches imply relationships between taxa but more accurately, as stressed by Farjon (2010, p. 1035), the interrelationships that are generated from analysis of the selected characters.

Characters assumed to be phylogenetically informative were scored in MacClade 4 (Maddison & Maddison 2005), and subject to two tree generating analyses. One was based on phenetic (UPGM) and the other on cladistics principles using parsimony settings within the software program PAUP 4.0.8 (Swofford 2003). Each analysis was undertaken first with extant taxa only, then repeated with the addition of the extinct taxa.

Where required character states were polarised by setting *Pinus* as the outgroup taxon, with all ingroup taxa monophyletic. All character states were unordered and unweighted, consisting of up to three character states. Each analysis used the Tree Bisection and analysis bootstraps were calculated from 1000 replicates where only values of exceeding 50% were recorded.

## RESULTS

Pair-wise comparisons of all taxa as measured by the S.I. are given in Table 1. These values varied from 23% (*Pinus* – *Arancaria*, Sect. *Arancaria*) to 94% (*A. mirabilis* – *A. vulgaris* and *A. mirabilis* – *A. nipponensis*). Choosing an arbitrary value of 75% the Constellation Diagram was drawn which linked all taxa with this or a higher score (Fig. 1). At this level of similarity four groups of taxa emerged of which one included only *Pinus*. In another *Phyllocladus* was linked to *Podocarpus*. The remaining taxa had either embedded or stalked seeds. The former were all the members

of *Arancaria* and were linked to one another through *A. mirabilis*, an extinct taxon, the latter comprised four genera inter-linked through *Wairarapaia*, another extinct taxon (Fig. 1).

On subjecting the nine extant taxa to a group average clustering program (UPGMA) a dendrogram with four major branches emerged (Fig. 2). Their terminal taxa were as follows: *Pinus*; *Podocarpus* and *Phyllocladus*; *Araucaria* (all Sects); *Agathis* and *Wollemia*. The four Sections of *Arancaria* were united into two pairs, namely Sects *Entacta* plus *Intermedia* and Sects *Arancaria* plus *Bunya*.

When the UPGMA analysis was repeated with the addition of five extra, less well-described, extinct araucarian taxa *Arancaria* again separated into two groups one of which included all the fossil species plus the Section *Entacta* and the other included the Sections *Intermedia*, *Araucaria* and *Bunya*. The agathoid genera again formed a close-knit group but with *Wollemia* linked to *Wairarapaia* instead of to *Agathis* (Fig. 3).

Table 1. Indices of Similarity below and the numbers of characters used in their calculation above the diagonal. *Ar.* abbreviation of *Arancaria*.

Taxon	Similarity Index \ Number of Comparisons													
<i>Pinus</i>	X	30	29	30	30	33	27	30	27	26	19	21	21	21
<i>Ar. Sect. Entacta</i>	33	X	29	30	30	30	28	30	27	26	10	22	21	20
<i>Ar. Sect. Intermedia</i>	38	19	X	29	19	29	27	29	25	25	19	22	21	19
<i>Ar. Sect. Araucaria</i>	23	73	90	X	30	30	28	30	27	26	20	24	21	20
<i>Ar. Sect. Bunya</i>	27	63	76	83	X	30	28	30	27	26	20	22	21	30
<i>Agathis</i>	57	53	59	50	67	X	27	30	26	26	20	22	21	21
<i>Wollemia</i>	41	61	70	56	61	78	X	27	25	23	19	20	18	19
<i>Podocarpus</i>	73	35	38	23	23	47	39	X	26	26	20	22	20	21
<i>Phyllocladus</i>	66	37	44	26	22	54	52	88	X	24	20	19	19	21
<i>Euvadea</i>	38	62	56	50	38	73	70	38	54	X	19	21	20	19
<i>Wairarapaia</i>	49	74	74	65	60	80	84	40	55	79	X	15	16	15
<i>Ar. vulgaris</i>	38	86	64	68	73	41	60	18	37	57	67	X	16	15
<i>Ar. nipponensis</i>	43	71	67	67	71	48	61	30	37	60	63	88	X	15
<i>Ar. mirabilis</i>	43	80	79	80	90	43	63	24	24	47	67	93	93	X

Parsimony analysis (PAUP) of the data for extant taxa generated a cladogram which was in most respects similar to the dendrogram generated by group average clustering (UPGMA). The genera *Podocarpus* and *Phyllocladus* constituted a single clade whilst the four Sections of *Araucaria* were resolved into three clades with the Sects *Araucaria* and *Bunya* sharing a common ancestor (Fig. 4)

Repeating the parsimony analysis with the addition of the five fossil taxa resulted in the loss of much of the structure present evident in Fig. 4. As before *Podocarpus* and *Phyllocladus* formed a clade with strong bootstrap support. However, although there was still strong bootstrap support for recognising the Araucariaceae and *Araucaria* as monophyletic there was no bootstrap support above 50% for

recognising Sections within the genus. Nor was there any strong support for recognising separate clades amongst the agathoid genera all of which shared a common ancestor (Fig. 5).

That different tree topologies were generated is not surprising given the considerable morphological difference exhibited by taxa in characters other than those of the ovuliferous-cone which were here emphasised because of the decision to restrict the data to characters that were available for at least one fossil taxon. For example, had seedlings been considered those of *Araucaria*, *Agathis* and *Wollemia* are quite different. Whereas the first plumular leaves of *Wollemia nobilis* are opposite decussate cataphylls with an abrupt transition to adult-like foliage (Offord *et al.* 1999) those of *Agathis* spp. are a mixture of alternately arranged

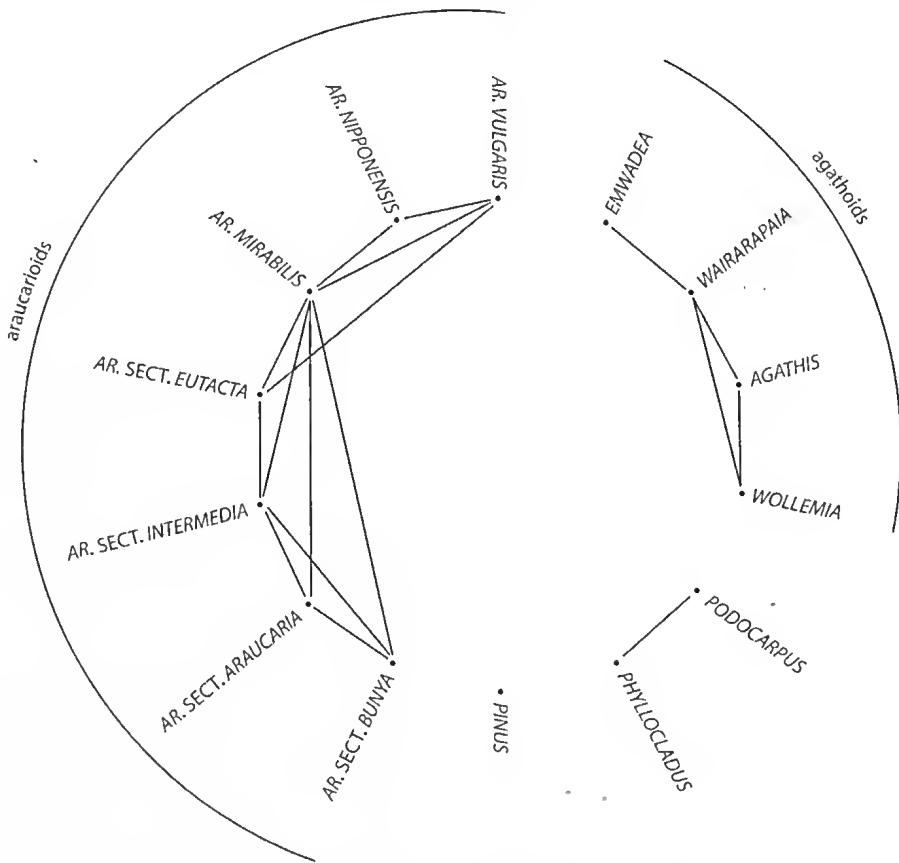


FIG. 1. Constellation Diagram in which those taxa with pair-wise Similarity Index values of 75% or more linked with straight lines. Ar. Abbreviation of *Araucaria*.

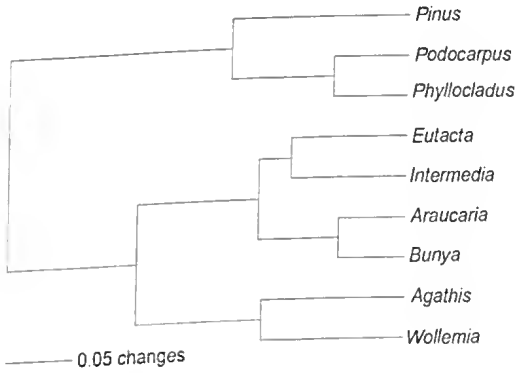


FIG. 2. Relationships of extant taxa expressed as a dendrogram generated by a UPGMA analysis of data in Appendix 2.

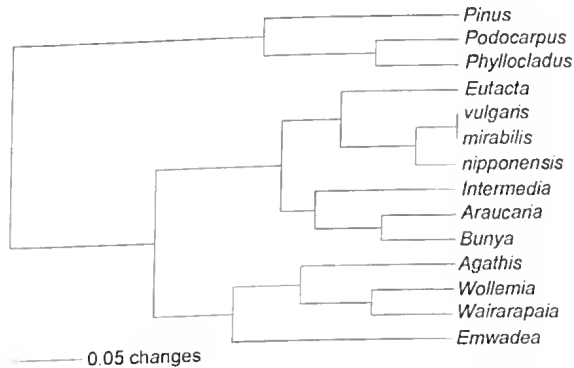


FIG. 3. Relationships of extant and fossil taxa expressed as dendrogram generated by a UPGMA analysis of the data in Appendix 2.

leaves, similar in shape to, but smaller than those of the adult plant. In contrast the initial plumular leaves of *Araucaria* spp. have needle-shaped leaves.

## GENERAL DISCUSSION

Though the above analyses produced different results they share much in common in that *Phyllocladus* and *Podocarpus* are consistently associated and separated from the *Araucariaceae* whose taxa always divide into two groups the araucarioid with sessile seeds and the other the agathoid with seeds that,

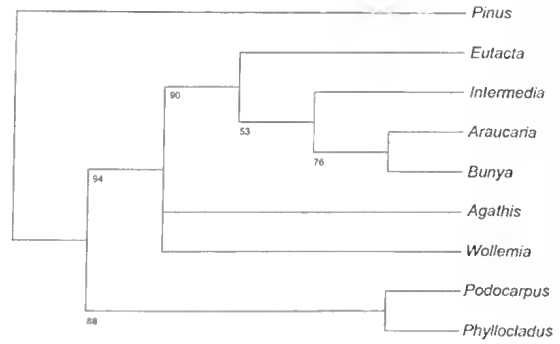


FIG. 4. Relationships of extant taxa expressed as a cladogram generated by the parsimony program PAUP employing data of Appendix 2. Numbers represent bootstrap values returned greater than 50%.

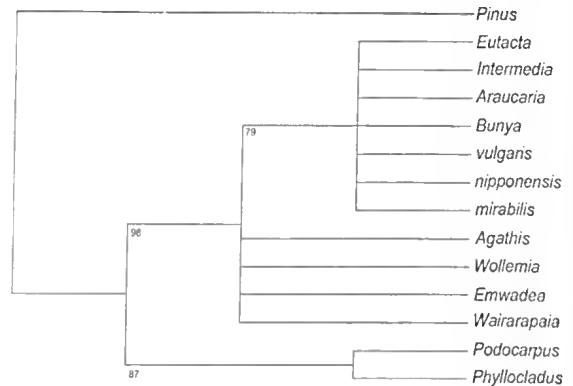


FIG. 5. Relationships of extant and fossil taxa expressed as a cladogram generated by the parsimony program PAUP employing data from appendix 2. Numbers represent bootstrap values returned greater than 50%.

at maturity, separate from their subtending scales. Within these two clades the taxa are aligned somewhat differently in the above and published analyses.

Furthermore, the agathoid genera, *Agathis* and *Wollemia*, behaved less consistently than did the araucarioid taxa. In six of the eleven cladistic analyses available *Agathis* and *Wollemia* are in different clades (Setoguchi *et al.* 1988; Codrington *et al.* 2002; Stephanović *et al.* 1998; Biffin *et al.* 2010; Escapa & Catalano 2013; herein Figs 4 & 5), and in five the same clade (Kunzmann 2007; Leslie *et al.* 2012; Liu *et al.*



al. 2009; Rai *et al.* 2008; Gilmour & Hill 1997). The reasons for this disparity are not clear. They may reflect that the analyses are not based on the same taxa, and characters, or that the analyses are based on different amounts of data. As shown by Liu *et al.* (2009) parsimony analyses undertaken on the basis of single gene sequences favoured the tree topology ((*Agathis*, *Wollemia*) *Araucaria*), but on statistical grounds neither ((*Agathis*, *Araucaria*) *Wollemia*) nor ((*Araucaria*, *Wollemia*) *Agathis*) could be rejected when the analyses were based on the sequences of eight genes.

Although the parsimony analyses, which involved both extinct and extant taxa, detected no clades within *Araucaria* those based solely on extant taxa recognised the presence of two clades. One was Sect. *Entacta* and the other clade resolved into three subclades, corresponding with the currently recognised Sections in the genus (Fig. 4). Therefore, as proposed by Axsmith *et al.* (2008) and Leslie *et al.* (2012), Sect. *Entacta* is the oldest of those recognised in the genus.

This conclusion is supported by the result of the group average clustering analysis (UPGMA) which assigned all three of the extinct species of *Araucaria* to the Sect. *Entacta*. Two of these species, *A. nipponensis* (Setoguchi *et al.* 1988) and *A. vulgaris* (Ohsawa *et al.* 1995) had been reported as sharing seed-cone characters with members of the Sect. *Entacta*. The third *A. mirabilis*, has hitherto been closely allied with *A. bidwillii*, an extant species and sole representative of *Araucaria* Sect. *Bunya* (Calder 1953; Stockey 1978). Both these authors, writing before cladistics methodology became widely accepted, laid great stress on 'the separate origins of the bract and ovulate-scale vascular supplies which seem to ally *A. mirabilis* with this species,' (Stockey 1975, p. 865, referring to *A. bidwillii*). Nonetheless, their support was not fully forthcoming in that the vasculature only 'seemed' to ally *A. mirabilis* and *A. bidwillii*. Furthermore, 20 years later Stockey *et al.* (1994, p. 813) noted the double cone-scale trace, 'is exceedingly difficult to interpret in fossil cones,' thereby casting doubt

on the reliability of the origin of the vascular trace as a taxonomic character.

Attempts to fix the absolute age of the crown groups Sects *Entacta* and *Bunya*, using sequencing data and the fossil record have produced conflicting results. Axsmith *et al.* (2008) concluded that the araucarian crown group arose in the Late Triassic with the crown groups for the Sects *Entacta* and *Bunya* arising in the Middle and Late Jurassic respectively. That is their relative ages were in the same order as that postulated by the cladistic analyses. Using similar data Biffin *et al.* (2010) and Leslie *et al.* (2012) concluded the araucarian crown group was much younger and developed in the Middle Jurassic. According to the former authors the crown group of Sect. *Bunya* arose in the mid Cretaceous and Sect. *Entacta* in the early Paleogene a reversal in the order of appearance to that proposed by Axsmith *et al.* (2008). In contrast, Leslie *et al.* (2012) agreed with the relative ages of Sects *Entacta* and *Bunya*, as proposed by Axsmith *et al.* (2008), but postulated that they arose towards the end of the Paleogene and the beginning of the Neogene respectively.

To resolve these differences much more work is required to encompass the diversity existing amongst extant taxa and the discovery of fossil specimens of mature ovuliferous cones with attached foliage. The emended description of *Araucaria vulgaris* by Ohsawa *et al.* (1995), incorporating foliage characters, led to the recognition of new Section (*Yezonia*) of *Araucaria* and further Sections may be required to accommodate the diversity predicted to exist amongst Jurassic and Cretaceous araucarians known presently only from ovuliferous cones (Stockey 1994; Stockey *et al.* 1992, 1994).

Furthermore, since the double origin of the vascular strands to the ovuliferous cone scale complex of *A. bidwillii* depends largely on the single elegant study of Eames (1913) it needs independent confirmation. In their treatment of the taxonomy of the conifers Pilger & Melchior (1954) provide a diagrammatic longitudinal section of a seed-cone scale of *A. bidwillii* which shows the origin of the vascular strand as single but branching close to the stele. The lack of

certainly of the double origin of the ovuliferous cone vascular strands casts doubt on its value as a diagnostic character.

The failure of the cladistic analyses to recognise clades in the combined sample of extant and fossil taxa suggest that the data are inadequate or that the Sections of *Araucaria* are in need of recircumscription taking into account fossil material. As Axsmith *et al.* (2008, p. 7) pointed out 'it is likely that phylogenetic studies based only on extant taxa underestimate the true complexity, as the fossil record indicated high levels of extinct diversity, including completely extinct Sections'.

The emergence in the parsimony analyses of four possible new clades of seed shedding Araucariaceae, (*Agathis*, *Wollemia*, *Enuvadea* and *Wairarapaia*) and the recognition that the extinct species assigned to *Araucaria* do not form a single clade support the view that in Jurassic and Cretaceous times there were species whose seed-cones differed from those of all extant species. Furthermore, the parsimony analyses involving both extant and extinct taxa offer no conclusive evidence of possible phylogenetic relationships within the Araucariaceae other than that agathoid and araucarioid taxa constitute separate sister clades and that the agathoid is the older of the two clades (Fig. 5).

Until data are available from ovuliferous cones with fully developed seeds and attached foliage any formal classification of the family incorporating extinct taxa must be regarded as tentative. As noted by Bigwood and Hill (1985) the three species they allotted to the foliage form genus *Araucarioides* could not be assigned, with confidence, to either *Agathis* or *Araucaria* as there are few differences in leaf and cuticle morphology between these genera (Burrows & Bullock 1999). Therefore, the foliage of some species of *Araucarioides* may belong to other araucarian genera including the extant *Wollemia* or the fossil *Wairarapaia* and *Enuvadea*, for which foliage characters are presently limited. The Section (*Perpendicularis*) of *Araucaria* proposed by Pole (1995), based solely on cuticle characters, is questionable.

Given the plethora of cladistic and phenetic analytical techniques available (Felsenstein 2004) the choice of characters and taxa included in the analysis will determine the phylogenetic relationships that are generated. Therefore, it is not surprising, that studies on the araucarians using different data sets, and taxa, have produced differing although not always inconsistent results. Although recourse to genomic data may be helpful as noted by Soltis *et al.* (2004), referring to extant taxa, even complete genomic data by themselves are not a panacea for phylogenetic reconstructions. Therefore, although it is unfortunate that genomic data are unlikely to become available for Paleozoic conifers and Cretaceous araucarians this lack of data is not a major problem when combining genomic and morphological data. Instead it is the inadequate fossil record. In particular there is a lack of specimens with foliage connected to ovuliferous cones.

## ACKNOWLEDGEMENTS

The authors thank Ross McKinnon, Curator of the Brisbane Botanic Gardens for providing living material; Gordon Guymer, for allowing us access to the Queensland Herbarium Library; Andrew Rozefelds, Ancient Environments Section, Queensland Museum for providing living plant material and offering helpful comments on an early draft of the manuscript; Bryan Simon, Queensland Herbarium for advice on nomenclatural problems.

## LITERATURE CITED

- Axsmith, B.J., Escapa, I.H. & Huber, P. 2008. An araucarian bract-scale complex from the lower Jurassic of Massachusetts: Implications for estimating phylogenetic and stratigraphic congruence in Araucariaceae. *Palaontologica Electronica* PE11.3.13A: 1–9.
- Bigwood, A.J. & Hill, R.S. 1985. Tertiary araucarian macrofossils from Tasmania. *Australian Journal of Botany* 33: 645–656.
- Biffin, E., Hill, R.S. & Lowe A.T. 2010. Did Kauri (*Agathis*: Araucariaceae) survive the Oligocene drowning of New Zealand? *Systematic Botany* 59(5): 594–602.

- Bouman, F. 1984. The Ovule. pp. 123–57. In Johri, B.M. (ed.). *Embryology of the Angiosperms*. Springer-Verlag, Berlin.
- Burrows, G.E. & Bullock S. 1999. Leaf anatomy of Wollemi pine (*Wollemia nobilis*), Araucariaceae. *Australian Journal of Botany* 47: 795–806.
- Calder, M.G. 1953. A coniferous petrified forest in Patagonia. *Bulletin of the British Museum (Nat. Hist.) Geology* 2: 99–138.
- Cantrill, D.J. 1992. Araucarian foliage from the Lower Cretaceous of southern Australia. *International Journal of Plant Science* 153: 622–645.
- Cantrill, D.J. & Raine, J.I. 2006. *Wairarapaia mildenhallii* gen. et sp. nov. a new araucarian cone related to *Wollemia* from the Cretaceous of New Zealand. *International Journal of Plant Science* 16: 1259–1269.
- Chambers, T.C., Drinnen, A.N. & McLoughlin, S. 1998. Some morphological features of Wollemi pine (*Wollemia nobilis*: Araucariaceae) and their comparison to Cretaceous plant fossils. *International Journal of Plant Science* 159: 160–171.
- Codrington, T.A., Scott, L.J., Scott, K.D., Graham, G.C., Rossetto, M., Ryan, M., Whiffin, T., Henry, R.J. & Hill, K. 2002. Unresolved phylogenetic position of *Wollemia*, *Araucaria* and *Agathis*. pp. 69–73. In Wilcox, M. & Bielecki, R. (eds) *International Araucariaceae Symposium*. Auckland, New Zealand.
- Dettmann, M.E., Clifford, H.T. & Peters, M. 2012. *Emvadea microcarpa* gen. et sp. nov. – anatomically preserved araucarian seed cones from the Winton Formation (late Albian), western Queensland, Australia. *Alcheringa* 36: 217–237.
- Eames, A.J. 1913. The morphology of *Agathis australis*. *Annals of Botany* 27: 1–38.
- Escapa, I.H. & Catalano, S.A. 2013. Phylogenetic analysis of Araucariaceae: integrating molecules, morphology, and fossils. *International Journal of Plant Science* 174: 1153–1170.
- Farjon, A. 2010. *A Handbook of the World's Conifers*. Brill, Leiden-Boston.
- Felsenstein, J. 2004. *Inferring Phylogenies*. Sinauer Associates, Sunderland, Mass.
- Florin, R. 1944. Die Koniferen des Oberkarbon und des unteren Perms. Heft 7. *Palaeontographica* 85 Abt. B.: 457–64.
- Gilmore, S. & Hill, K.D. 1997. Relationships of the Wollemi pine (*Wollemia nobilis*) and a molecular phylogeny of the Araucariaceae. *Telopea* 7: 275–291.
- Hill, R.S. 1990. *Araucaria* (Araucariaceae) Species from Australian Tertiary Sediments – a micromorphological study. *Australian Systematic Botany* 3: 203–220.
- Hill, R.S. & Brodribb, T.J. 1999. Turner Review No.2: Southern conifers in time and space. *Australian Journal of Botany* 47: 639–696.
- Holloway, J.T. 1937. Ovule anatomy and development and embryology in *Phyllocladus alpinus* (Hook.) and *P. glaucus* (Carr.). *Transactions of the Royal Society of New Zealand* 67: 149–165.
- Kindel, K.-H. 2001. Die Gattung *Araucaria*. *Mitteilungen der Deutsche Dendrologische Gesellschaft* 86: 191–218.
- Krassilov, V. & Barinova, S. 2014. Carpel-fruit in a coniferous genus *Araucaria* and the enigma of the angiosperm origin. *Journal of Plant Sciences* 2(5): 159–166.
- Kunzmann, L. 2007. Araucariaceae (Pinopsida) Aspects in palaeobiogeography, paleodiversity in the Mesozoic. *Zoologischer Anzeiger* 246: 257–277.
- Laubenfels, D.J. de 1988. Coniferales In: *Flora Malesiana ser.1*, 10: 337–453. Kluwer, Academic Publishers Dordrecht.
- Leslie, A.B., Beaulieu, J.M., Rai, H.S., Crane, P.R., Donoghue, M.J. & Mathews, S. 2012. Hemisphere-scale differences in conifer evolutionary dynamics. *Proceedings National Academy of Science* 100: 16217–16221.
- Liu, N., Zhu, Y., Wei, Z.-X., Chen, J., Wang, Q.-B., Jian, S.-G., Zhou, D.-W., Shi, J., Yang, Y. & Zhong, Y. 2009. Phylogenetic relationships and divergence times of the family Araucariaceae based on DNA sequences of eight genes. *Chinese Science Bulletin* 54: 2648–2655.
- Maddison, D.R. & Maddison, W.P. 2005. *MacClade 4: Analysis of phylogeny and character evolution*. Version 4.08a. <http://macclade.org>.
- Mathews, S. & Kramer, E.M. 2012. The evolution of reproductive structures in seed plants are-examination based on insights from developmental genetics. *New Phytologist* 194: 910–923.
- Mitra, A.K. 1927. On the occurrence of two ovules on araucarian cone-scales. *Annals of Botany* (N.S.) 41: 461–471.
- Offord, C.A., Porter, C.L., Meagher, P.F. & Errington, G. 1999. Sexual reproduction and early plant growth of the Wollemi Pine (*Wollemia nobilis*), a rare and threatened Australian conifer. *Annals of Botany* 84: 1–9.
- Ohsawa, T., Nishida, H. & Nishida, M. 1995. *Yezonia*, a new Section of *Araucaria* (Araucariaceae) based on permineralised vegetative and reproductive organs of *A. vulgaris* comb. nov. from the upper Cretaceous of Hokkaido, Japan. *Journal of Plant Research* 108: 25–39.
- Page, C.N. 1990. Gymnosperms: Coniferophytina (Conifers and Ginkgoales). pp. 279–361. In Kubitzki, K. & Green, P.S. (eds) *The families and*

- genera of vascular plants. Vol. 1, Pteridophytes and Gymnosperms. Koeltz, Koenigstein.
- Pilger, R. & Melchior, H. 1954. Gymnospermae. In A. Engler's, *Syllabus der Pflanzen-Familien*. Band 1. Abteilung xvi. Berlin-Nikolassee. Gebrüder Bornträger.
- Pole, M. 1995. Late Cretaceous macrofloras of Eastern Otago, New Zealand, Gymnosperms. *Australian Systematic Botany* 8: 1067–1106.
- Rai, H.S., Reeves, P.A., Peakall, R., Olmstead, R.G., & Graham, S.W. 2008. Inference of higher order conifer relationships from a multi-locus plastid data set. *Botany* 86: 658–669.
- Remizowa, M.V., Kuznetsov, A.N., Kunetsova, P.S., Rudall, P.J., Nuraliev, M.S. & Soksoff, D.D. 2012. Flower development and vasculature in *Xyris grandis* (Xyridaceae, Poales); a case study for examining petal diversity in monocot flowers with a double perianth. *Botanical Journal of the Linnean Society* 169: 93–111.
- Romberger, J.A., Hejnowicz, Z. & Hill, J.F. 1993. *Plant structure: function and development. A treatise on anatomy and vegetative development, with special reference to Woody Plants*. Springer-Verlag, Berlin.
- Rouane, M.L., Gondran, M. & Woltz, P.H. 1988. Heterocotyle et évolution cotylédonaire chez les Podocarpaceae. *Gaussonia* 4: 7–15.
- Rouane, M.-L. & Woltz, P.H. 1980. Intérêt évolution des Araucariacées. *Bulletin de la Société de Histoire Naturelle de Toulouse* 116: 120–136.
- Setoguchi, H., Ohsawa, T.A., Pintaud, J.-C., Joffré, T. & Vaillon, J.M. 1998. Phylogenetic relationships within Araucariaceae based on rbcL gene sequences. *American Journal of Botany* 85: 1507–1516.
- Soltis, D.E., Albert, V.A., Savolainen, V., Hilu, K., Qui, Y.-L., Chase, M.A., Farris, J.S., Stephanović, S., Rice, D.A., Palmer, J.D. & Soltis, P.S. 2004. Genome-scale data, angiosperm relationships, and 'ending congruence': a cautionary tale in phylogenetics. *Trends in Plant Science* 9: 477–483.
- Stephanović, S., Jager, M., Deutsch, J., Broutin, M. & Masselot, M. 1998. Phylogenetic relationships of conifers inferred from partial 28S rRNA gene sequences. *American Journal of Botany* 85: 688–697.
- Stockey, R.A. 1975. Seeds and embryos of *Araucaria mirabilis*. *American Journal of Botany* 62: 856–858.
1978. Reproductive biology of Cerro Cuadrado fossil conifers: Ontogeny and reproductive strategies in *Araucaria mirabilis* (Spegazzini) Windhausen. *Palaentographica Abt.* 166B: 1–15.
1978. On the structure and evolutionary relationships of the Cerro Cuadrado fossil conifer seedlings. *Journal of the Linnean Society Botany* 76: 167–176.
1982. The Araucariaceae: An evolutionary perspective. *Review of Palaeobotany and Palynology* 37: 133–154.
1994. Mesozoic Araucariaceae: morphology and systematic relationships. *International Plant Research* 107: 493–502.
- Stockey, R.A., Nishida, H. & Nishida, M. 1992. Upper Cretaceous araucarian cones from Hokkaido: *Araucaria nihongii* sp. nov. *Review of Palaeobotany and Palynology* 72: 27–40.
1994. Upper Cretaceous araucarian cones from Hokkaido and Saghalien: *Araucaria nipponensis* sp. nov. *International Journal of Plant Science* 155: 806–815.
- Swofford, D.L. 2003. PAUP\*. *Phylogenetic Analysis Using Parsimony (\*and Other Methods)*. Version 4. Sinauer Associates, Sunderland, Massachusetts.
- Taylor, T.N., Taylor, E.L. & Krings, M. 2009. *Paleobotany: The Biology and Evolution of Fossil Plants*. Academic Press, New York.
- Tomlinson, P.B. & Takaso, T. 2002. Seed cone structure in conifers in relation to development pollination: a biological response. *Canadian Journal of Botany* 80: 1250–1273.
- Wilde, M.H. & Eames, A.J. 1952. The ovule and seed of *Araucaria bidwillii* with discussion of the taxonomy of the genus. III. Taxonomy. *Annals of Botany (N.S.)* 16: 27–47.
1955. The ovule and 'seed' of *Araucaria bidwillii* with discussion of the taxonomy of the genus. III. Anatomy of ovulate scales. *Annals of Botany (N.S.)* 47: 343–349.

## APPENDIX 1

Character states according to original authors or as subsequently recorded. The principal authors consulted were the following and the numbers in brackets after each are the characters involved; Dettmann *et al.* 2012 (11, 17); Farjon 2010 (27); Holloway 1937 (28); Wilde & Eames 1952 (29); Stockey 1975 (19, 24); Stockey 1982 (25); Rouane *et al.* 1988, Rouane & Woltz 1980 (24)

### Leaf anatomy

1. Compartmented cells: present 0, absent 1.
2. Nerve number at maximum leaf width: single 0, two or more 1.
3. Adult foliage: epi- 0, hypo- 1, amphistomatic 2.

### Vegetative morphology

4. Adult leaf attachment: decurrent 0, petiolate 1.
5. Lamina shape: flat 0, awl-shaped and beaked 1, cylindrical 2.
6. Apophysis: present 0, absent or inconspicuous 1.
7. Leaf disposition with respect to axis: appressed 0, spreading 1.

### Ovuliferous cone

8. Bract-scale at maturity: separating from cone axis 0, retained on cone axis 1.
9. Bract-scale length at maturity: longer than ovuliferous complex 0, shorter than ovuliferous complex 1.
10. Ovules per bract-scale: one 0, two or more 1.
11. Vasculature of ovuliferous complex: arising within cone axis 0, arising within bract-scale 1.
12. Fertile bracts per ovuliferous cone: 20 or less 0, 21 or more 1.
13. Apex of bract-scale: acute 0, apiculate 1, obtuse 2.
14. Apex of bract-scale: deciduous 0, not deciduous 1.
15. Ovuliferous complex at maturity: succulent 0, not succulent 1.
16. Ovuliferous cone: terminal 0, axillary 1.

17. Vascular strands to cone-scale complex: one 0, two 1.

18. Bract-scale base: auriculate 0, non auriculate 1
19. Cotyledon length as a fraction of embryo length: less half 0, more than half 1.

### Ovule and seed anatomy

20. Ovules at maturity: free of bract 0, embedded in bract 1.
21. Ovule integument: winged laterally 0, not winged laterally 1.
22. Ovule accessory structures: more or less fused to bract-scale 0, separate from bract-scale 1.
23. Nucellus: stipitate 0, non-stipitate 1.
24. Cotyledon numbers: two 0, three or more 1.

### Seeds and seedlings

25. Hypocotyl: fleshy 0, not fleshy.
26. Cotyledon vein number: one or two 0, three or more 1.
27. Seed shape in transverse section: laterally compressed 0, dorsally compressed 1, not compressed 2.
28. Mesotesta anatomy: simple sclereids 0, branched cylindrical sclereids 1, parenchyma 2.
29. Cotyledon petioles of seedlings: long 0, short 1.
30. Seed length: less than 30mm 0, 30mm or more 1.

## APPENDIX 2

Appendix 2. Taxa and their character states as defined in Table 1. *Ar.* abbreviation of *Araucaria*.

Character states	1	2	3	4	5	6	7	8	9	10	11	12	13	14	15	16	17	18	19	20	21	22	23	24	25	26	27	28	29
<i>Pinus</i>	1	0	0/2	1	2	1	1	1	1	1	0	1	0	1	1	0	1	1	1	0	1	1	1	1	1	0	1	1	0
<i>Ar. Sect. Entacta</i>	0	1	2	0	1	0	0	0	0	0	1	1	1	0	1	0	1	1	1	1	1	0	0	0/1	1	1	1	0	1
<i>Ar. Sect. Internedea</i>	0	1	2	0	0	0	1	0	0	0	1	1	1	1	1	1	0	1	?	1	1	0	0	0	1	1	1	2	1
<i>Ar. Sect. Araucaria</i>	0	1	2	0	0	0	1	0	0	0	1	1	1	0	1	1	0	1	1	1	1	0	0	0	0	1	1	0	1
<i>Ar. Sect. Bunya</i>	0	1	2	0	0	0	1	0	0	0/1	0	1	1	1	1	1	1	1	1	1	1	0	0	0	0	1	1/2	0	1
<i>Agallia</i>	1	1	2	1	0	1	1	0	0	0	1	1	2	1	1	0	0	0	0	0	0	1	0	0	1	1	1	1	0
<i>Wollenia</i>	0	1	2	0	0	1	1	0	0	0	0	1	1	1	1	0	1	0	1	0	0	1	?	0	1	1	1	?	1
<i>Podocarpus</i>	1	0	1/2	1	0	1	1	1	1	0	0	0	0	1	0	1	0	1	0	0	1	1	1	1	1	0	2	1	0
<i>Phyllocladus</i>	1	?	?	0	0	1	?	1	1	0	0	0	0	1	0	0	0	1	0	0	1	1	1	1	1	0	1	1	0
<i>Entedea</i>	0	?	0	0	1	1	0	1	0	0	1	1	2	1	1	0	0	1	0	0	0	1	0	0	?	?	1	0	?
<i>Wairarapaia</i>	?	1	?	0	0	?	?	?	0	0	1	1	1	?	1	0	?	1	1	0	0	1	0	0	?	?	?	1	?
<i>Ar. vulgaris</i>	?	1	1	0	1	0	0	0	0	0	0	1	1	0	1	0	1	1	?	?	1	0	0	?	?	?	1	0	?
<i>Ar. nipponensis</i>	?	?	?	0	1	?	0	0	0	0	0	1	?	1	1	0	?	?	1	1	1	0	0	0	?	?	2	0	?
<i>Ar. mirabilis</i>	?	?	?	?	?	?	?	?	0	0	0	1	1	?	1	?	1	1	1	1	1	0	0	0	0	1	1/2	0	?

# Spatial gradient in the distribution of whaler sharks (Carcharhinidae) in Moreton Bay, southeastern Queensland

**TAYLOR, S.M.**

Western Australian Fisheries and Marine Research Laboratories, PO Box 20, North Beach, WA 6920, Australia. Email: Steve.Taylor@fish.wa.gov.au

**JOHNSON, J.W.**

Queensland Museum, PO Box 3300, South Brisbane, QLD 4101

**BENNETT, M.B.**

School of Biomedical Sciences, the University of Queensland, St Lucia, QLD 4072, Australia

<http://dx.doi.org/10.17082/j.2204-1478.59.2015.2014-08>

LSID urn:lsid:zoobank.org:pub:3EB860B0-70CF-4CEA-BD45-A1195AC0CD78

Citation: Taylor, S.M., Johnson, J.W. & Bennett, M.B. 2015. Spatial gradient in the distribution of whaler sharks (Carcharhinidae) in Moreton Bay, southeastern Queensland. *Memoirs of the Queensland Museum – Nature* 59: 39–53. Brisbane. ISSN 2204-1478 (Online), ISSN 0079-8835 (Print). Accepted: 15 September 2014. First published online: 31 March 2015.

## ABSTRACT

Experimental gillnetting and setlining provided a detailed account of shark and ray composition at three shallow water sites in Moreton Bay between 2004 and 2007 (n=350 elasmobranchs). The species composition of elasmobranchs significantly differed between sites and shark abundance was highest at the western site (St Helena Island, Waterloo Bay). Juvenile Dusky (*Carcharhinus obscurus*) and Pigeye Sharks (*C. amboinensis*) were more abundant at the western site and appear to be rare in the eastern bay. Approximately 8% of the 206 tagged sharks were recaptured, 60% within two kilometres from their release position, with time at liberty ranging from four to 402 days. The results suggest that the documented east-west gradient in teleost diversity in Moreton Bay also extends to the Carcharhinidae. Further research is recommended to determine whether the diversity patterns observed from the three sites are broadly representative of each of these regions. Setlining and rod and line fishing for sharks in a deeper part of the bay between 1978 and 1992 (n=440 elasmobranchs) revealed a different species composition. The Spottail Shark (*C. sorrah*) and the Spinner Shark (*C. brevipinna*) comprised 50% and 39% of the catch in this deeper site, respectively, but were rarely caught in shallow regions of the bay, suggesting that the species composition is also partitioned by depth. Western fringes of the bay have been heavily modified by anthropogenic activities and the importance of this area to juvenile whaler sharks needs to be considered. Future sampling at the same fixed locations may provide the opportunity to examine whether recent re-zoning of the Marine Bay Marine Park in 2009, or other factors such as changes in commercial or recreational fishing, have influenced the species composition and abundance of sharks. □ whaler sharks, abundance, nursery area.

Sharks play an important role in shaping marine ecosystems in coastal waters (Cortés 1999) and their populations often support commercial and recreational fisheries that provide economic and social benefits to humans (Walker 1998). Many species of sharks use coastal waters as nursery areas which appear to offer new-born (hereon in referred to as neonates) and juvenile sharks protection from larger sharks and an abundance of prey items (Heupel *et al.* 2007). Proximity to land means that the negative effects of human population growth, such as habitat degradation and loss, pollution, and overfishing can compromise shark populations in some coastal areas (Knip *et al.* 2010). An understanding of shark abundance and species assemblages in coastal waters is therefore of particular importance.

Moreton Bay is a large, semi-enclosed subtropical bay covering an area of approximately 1600 km<sup>2</sup>. The bay is bounded by the rapidly expanding Brisbane region of the mainland, to the west, and three sand islands, Moreton, North and South Stradbroke Islands, to the east (Johnson 2010). The environmental conditions vary throughout the bay, with predominantly 'estuarine' conditions (low salinity, high turbidity) in western parts and 'marine conditions' (high salinity, low turbidity) in the eastern bay (Davie & Hooper 1998). The variety of habitats support a diverse teleost and elasmobranch (sharks and rays) fauna, with over 1,190 fish species reported in the bay and adjacent shelf waters to 200 m depth (Johnson 2010). Research on elasmobranchs in the bay area has increased significantly over the last decade, which has resulted in the documentation of many aspects of the biology and ecology of numerous species. Topics have included species inventories (Johnson 1999, 2010; Kyne *et al.* 2005), growth and aging (Huveneers *et al.* 2013), general shark biology and ecology (Kyne *et al.* 2011; Dudgeon *et al.* 2013), sensory biology (Schluessel *et al.* 2008; Harahush *et al.* 2009) and parasitology (Cutmore *et al.* 2010, 2011). In respect to whaler sharks (Carcharhinidae), 14 species have been reported in the bay (Johnson 2010). Although the population structures, diets, habitat occupancy and movement patterns have been

described for some species (Taylor & Bennett 2008, 2013; Werry *et al.* 2011, 2012), there is little information on spatial relationships among the multiple species within the bay.

Site-specific information on the distribution and abundance of the majority of sharks, and their relationship to the different environmental conditions that occur within the bay are poorly understood for most species. Here, we examined whether the species composition and abundance of whaler sharks differed at three shallow locations (eastern site, central site and western site) in the central region of Moreton Bay, prior to re-zoning of the Moreton Bay Marine Park (MBMP) in 2009. Under this re-zoning plan, there are now nine types of designated areas within the MBMP, four of which relate to recreational and commercial fishing. These are Marine national parks (green zones), Conservation parks (yellow zones), Habitat protection (dark blue zones), and General use areas (light blue zones) (State of Queensland, 2010). We also explored whether the shark fauna differed between shallower and deeper parts of the bay and provide information on the movement and recapture rate of tagged sharks.

## MATERIALS AND METHODS

**Gillnetting and setlining 2004–2007.** Three fixed sites in central regions of Moreton Bay were chosen for the shallow water sites (Figure 1). The western location was adjacent to St Helena Island, Waterloo Bay (27°24'S 153°12'E), the central location was Horseshoe Bay, Peel Island (27°30'S 153°22'E) and the eastern location was Deanbilla Bay, North Stradbroke Island (27°31'S 153°24.46'E). The western site comprised an area with mud/sand substrate and variable seagrass cover dominated by *Zostera capricorni*. This site is characterised by turbid, estuarine waters in fairly close proximity to the Brisbane River mouth and the Port of Brisbane and has input from sewage and rainfall outflow which drain into the area from the predominantly urban catchment (Dennison & Abal 1999). The eastern site was a mangrove-fringed bay adjacent to oyster leases and the central site was a sandy bay. In comparison



to the western site, both of these areas are in relatively pristine condition, representing good ecological health and water quality.

A pilot study was conducted between May and October 2004 to examine the feasibility of using gillnets and setlines to capture juvenile sharks for an ongoing postgraduate study on sharks (Taylor 2008). Sampling was conducted at various times of the day and different states of the tide. These fishing methods were successful and subsequent intensive sampling occurred between October 2004 and May 2007. The bottom-set gillnet and bottom-set setline were deployed from a 5 m research vessel. The gillnet (100 m long, 2 m drop and 8.9 cm mesh size) was anchored at both ends and set in shallow water, typically around 2 m deep. The set line contained 30 hooks (baited with Sea Mullet *Mugil cephalus*) equally spaced along a 400 m length of 4 mm braided rope which was fished in close proximity to the net (typically 2–5 m depth). Gangions were 2 m long and consisted of a shark clip attached to 1 m of braided nylon cord that connected to 1 m of multi-strand stainless steel wire and a size 10/0 stainless steel hook. The setline was not used at the central site due to the large number of recreational boats. Nets and lines were typically set one hour before dawn and fished for four hours, although changing weather conditions sometimes resulted in shorter sets. Nets were checked every 30 minutes and all animals were carefully removed from the net and released whenever possible. Hooks were checked every two hours and empty hooks were re-baited with Sea Mullet.

All sharks were measured to the nearest cm (total length, TL) and those assessed to be in a good condition at the time of capture were tagged in the dorsal musculature at the base of the first dorsal fin. Sharks smaller than 150 cm TL were brought onboard the boat and tagged with a plastic-tipped dart tag (type PDA, Hallprint, South Australia) while sharks larger than 150 cm TL were tagged with a stainless steel-tipped dart tag (type SSG, Hallprint, South Australia). Prior to tagging these larger sharks, a rope-noose was looped around the shark's caudal fin and attached to the stern

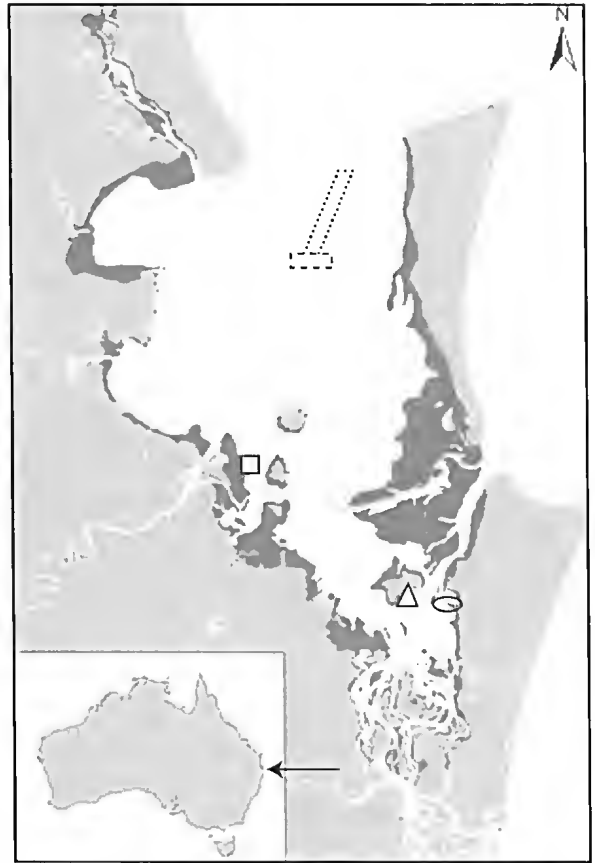


FIG. 1. Map of Moreton Bay indicating the sites where fishing was conducted. Black square = adjacent to St Helena Island, black triangle = Horseshoe Bay, Peel Island, black circle = Deanbilla Bay, North Stradbroke Island. Sampling at these sites was conducted between 2004 and 2007. Black box with small dotted lines = Pearl Channel, black box with large dotted lines = southern end of Pearl Channel to south of Central Banks. Sampling at these sites was conducted between 1978 and 1992. Dark grey shaded areas indicate waters  $\leq 3$  m in depth. Offset map and arrow indicates the bay's location on the east coast of Australia.

of the boat. To ensure the safe release of the sharks, whenever possible all handling and tagging time was limited to less than 3 minutes. Although every effort was made to tag and release sharks, some sharks were already dead upon gear retrieval. These sharks were taken back to the University for ongoing dietary and reproductive studies (Taylor 2008). Some

specimens were also lodged at the Queensland Museum.

#### Rod and line fishing and setlining 1978–1992.

Rod and line fishing and setlining for sharks were conducted at a deeper water site in the north of Moreton Bay. Rod and line fishing was conducted at the Pearl Channel (between 27°12'S 153°13'E & 27°06'S 153°18'E) opportunistically according to weather conditions. Fishing occurred between October and April, mostly at a depth of 10–20 m, and from dawn to around 11am. Three rods and overhead/spinning reels with 18–27 kg monofilament line, each with 30 cm of single strand wire and ganged 5/0 hooks were baited with whole pilchards (*Clupeidae*), or small Striped Barracuda (*Sphyraena obtusata*). One of the lines was fished loosely on the sea bed while the others fished in mid-water. During fishing, the boat drifted with the wind/current and was repositioned to the channel as necessary.

Setlining was conducted from the southern end of Pearl Channel to south of Central Banks (approx. between 27°12'S 153°13'E & 27°12'S 153°15'E). Fishing was conducted occasionally between November and April, mostly at a depth of 10–20 m, from dawn to 9 or 10am. The setline consisted of a 150 m section of mainline (6 mm braided rope) with 25 litre plastic drum floats at each end, placed parallel with the current and anchored at both ends. Twenty-four droppers were evenly spaced approximately 6 m apart and consisted of 0.75 m of 3 mm braided cord connected to a shark clip and 1 m of braided stainless steel wire. Each dropper had 2 ganged 9/0 hooks that were baited alternatively with half or whole Striped Barracuda, Sea Mullet, or large squid. Baits were generally suspended off the sea bed.

During all field work, separation of the closely related Common Blacktip Shark (*C. limbatus*) and the Australian Blacktip Shark (*C. tilstoni*) in the field was impractical, as the most useful diagnostic feature (counts of precaudal vertebrae) generally could not be taken. However, several specimens that were retained and dissected had precaudal vertebrae counts consistent with the Common Blacktip Shark (94–

98). Vertebral counts taken from another study (n=88 sharks) revealed that 100% of neonates from Moreton Bay were Common Blacktip Sharks, although one juvenile Australian Blacktip specimen was recorded (Harry *et al.* 2012). Our material is provisionally listed as the Common Blacktip Shark. Further research is recommended to determine whether the Australian Blacktip is resident in the area, and if so, its community interrelationships with the Common Blacktip Shark. A single ray, tentatively identified as a manta ray was caught and subsequently released from the gillnet. This animal was not identified to species level because it was caught before dawn and a concerted effort was made to release it as soon as possible. Both the Giant Manta Ray (*Manta birostris*) and, more commonly, the Reef Manta Ray (*Manta alfredi*) have been reported in southeastern Queensland and as such this individual is tentatively listed as *Manta* sp. It is possible, however, that this animal may have been a Japanese Devil Ray (*Mobula japanica*) which has been reported within the MBMP.

#### STATISTICAL ANALYSIS

Statistical analysis was restricted to the gillnet data. Catch data were collated as the number of elasmobranchs for each species caught during each fishing event. For those few occasions when an event was greater than or less than four hours, the catch was standardised to a four hour event. Multivariate analyses to identify spatial patterns in the species assemblage was conducted using PRIMER 6.0 (Clarke & Gorley 2006). Before analysis, data were square root transformed and similarity matrices were constructed using the Bray-Curtis similarity coefficient (Clarke & Warwick 2001). Ordination of the numerical abundance data from each fishing session was carried out using non-metric multidimensional scaling (MDS). A one-way analysis of similarities (ANOSIM) was used to examine changes in the elasmobranch composition between sites. Similarity percentages (SIMPER) were used to determine which elasmobranchs characterised the assemblage at each site.

TABLE 1. Fishing effort by gear type in central regions of Moreton Bay between October 2004 and May 2007

Season	St Helena		Horseshoe Bay		Deanbilla Bay	
	Gillnet hrs	Setline hrs	Gillnet hrs	Gillnet hrs	Setline hrs	
Spring (Sep–Nov)	20.0	29.7	12.0	17.0	15.8	
Summer (Dec–Feb)	24.6	42.3	15.0	20.9	18.8	
Autumn (Mar–May)	20.8	39.2	12.0	28.9	22.5	
Winter (Jun–Aug)	13.8	14.1	20.0	20.0	15.8	
Total hrs-1	79.2	125.3	59.0	86.8	72.9	

## RESULTS

**Sampling effort 2004–2007.** In total, 423 hours of gillnet and setline fishing was conducted at the three central sites between October 2004 and May 2007. Effort was fairly evenly spread among seasons and sites although overall fishing effort was slightly higher at St Helena (Table 1). Sampling effort for shark fishing between 1978 and 1992 was not routinely collected.

**Catch by location and season.** A total of 350 elasmobranchs from 12 families were caught between 2004 and 2007 (Table 2) and 440 elasmobranchs from four families between 1978 and 1992 (Table 4). In terms of abundance and diversity, *Carcharhinidae* dominated the numerical catch accounting for 68% of all elasmobranchs caught at the shallow sites and 86% of all elasmobranchs at the deeper site. Overall, the Australian Sharpnose Shark (*Rhizoprionodon taylori*), the Grey Carpetshark (*Chiloscyllium punctatum*) and the Pigeye Shark (*Carcharhinus amboinensis*) were the most abundant species at the shallow, central sites (Table 2, Figure 2). The Pigeye Shark, Nervous Shark (*C. cautus*) and Dusky Shark (*C. obscurus*) were fairly common in setline catches at St Helena, yet none of these species were caught at Deanbilla Bay and Horseshoe Bay. The catch rate of elasmobranchs at the shallow water sites was lowest in winter when only 23 elasmobranchs were caught (Table 3). The Australian Sharpnose Shark was the most abundant elasmobranch during spring, summer

and autumn when it accounted for 23.9%, 32.8% and 36.2% of the numerical catch.

The MDS ordination showed that the St Helena data formed a cluster while the Deanbilla Bay and Horseshoe Bay data points were more widely dispersed (Figure 3). Analysis of similarities revealed that the elasmobranch catch from gillnets was significantly different between shallow water sites (global  $r = 0.2$ ,  $P < 0.001$ ). A significant difference in the elasmobranch composition occurred between St Helena and Deanbilla Bay (Global  $r = 0.3$ ,  $P < 0.001$ ) and St Helena and Horseshoe Bay (Global  $r = 0.1$ ,  $P < 0.04$ ). SIMPER revealed that the gillnet catch at St Helena was characterised by the Australian Sharpnose Shark, Eastern Shovelnose Ray (*Aptychotrema rostrata*) and the Australian Weasel Shark (*H. australiensis*) which accounted for 16.4 (56.7%), 5.0 (17.1%) and 4.0 (13.9%) of the average within-group similarity of 28.9. The gillnet catch at Horseshoe Bay was characterised by the Eastern Shovelnose Ray, the Australian Sharpnose Shark and the Common Blacktip which accounted for 2.4 (34.7%), 2.2 (31.7%) and 1.1 (16.1%) of the average within-group similarity of 6.9. The catch data at Deanbilla Bay was characterised by the Scalloped Hammerhead Shark (*Sphyrna lewini*), the Grey Carpetshark and the Common Blacktip which accounted for 7.6 (51.6%), 5.1 (34.5%) and 0.7 (4.7%) of the average within-group similarity of 14.7.

The species composition at the deeper site was dominated by the Spottail Shark (*C. sorrah*) and Spinner Shark (*C. brevipinna*), both of which

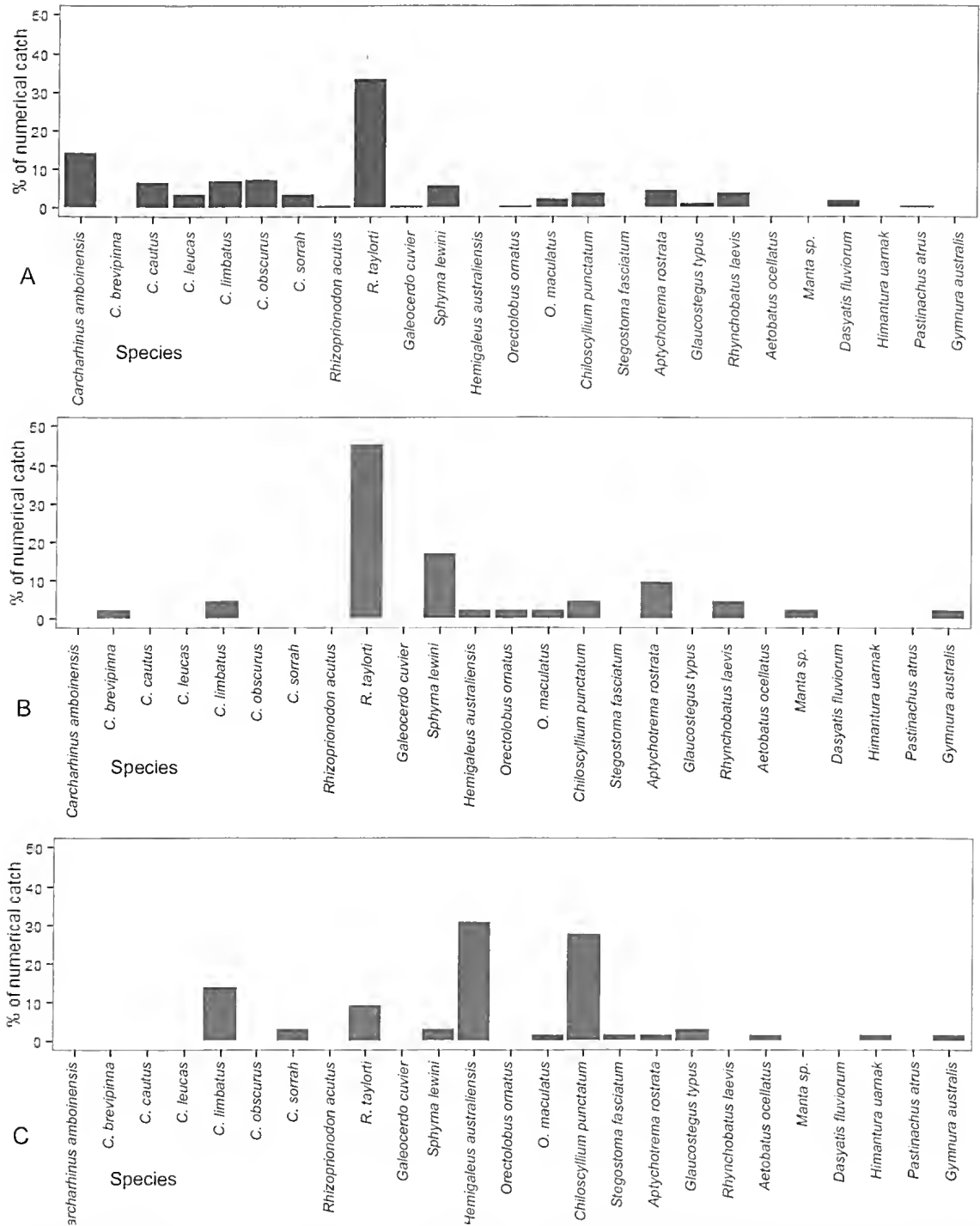


FIG. 2. Numerical catch of elasmobranchs in Moreton Bay at (A) St Helena Island, (B) Horseshoe Bay, Peel Island and (C) Deanbilla Bay, North Stradbroke Island. Sampling at these sites was conducted between 2004 and 2007 (n=350 elasmobranchs).

# Whaler sharks in Moreton Bay

TABLE 2. The number of elasmobranchs caught by gillnet and setline at shallow, central sites in Moreton Bay, between October 2004 and May 2007.

Species	St Helena		Horseshoe Bay	Deanbilla Bay	
	Gillnet	Setline	Gillnet	Gillnet	Setline
<b>Carcharhinidae</b>					
<i>Carcharhinus amboinensis</i>	3	31	0	0	0
<i>C. brevipinna</i>	0	0	1	0	0
<i>C. cautus</i>	0	16	0	0	0
<i>C. leucas</i>	0	8	0	0	0
<i>C. limbatus</i>	11	6	2	9	0
<i>C. obscurus</i>	7	11	0	0	0
<i>C. sorrah</i>	1	7	0	0	2
<i>Rhizoprionodon acutus</i>	1	0	0	0	0
<i>R. taylori</i>	81	0	19	5	1
<i>Galeocerdo cuvier</i>	0	1	0	0	0
<b>Sphyrnidae</b>					
<i>Sphyrna lewini</i>	0	0	1	19	1
<b>Hemigaleidae</b>					
<i>Hemigaleus australiensis</i>	14	0	7	2	0
<b>Orectolobidae</b>					
<i>Orectolobus ornatus</i>	0	1	1	0	0
<i>O. maculatus</i>	0	6	1	0	1
<b>Hemiscylliidae</b>					
<i>Chiloscyllium punctatum</i>	9	0	2	18	0
<b>Stegastomidae</b>					
<i>Stegostoma fasciatum</i>	0	0	0	0	1
<b>Rhinobatidae</b>					
<i>Aptychotrema rostrata</i>	11	0	4	1	0
<i>Glaucostegus typus</i>	0	3	0	0	2
<b>Rhynchobatidae</b>					
<i>Rhynchobatus laevis</i>	1	8	2	0	0
<b>Myliobatidae</b>					
<i>Aetobatus ocellatus</i>	0	0	0	1	0
<b>Mobulidae</b>					
<i>Manta sp.</i>	0	0	1	0	0
<b>Dasyatidae</b>					
<i>Dasyatis fluviorum</i>	0	5	0	0	0
<i>Himantura uarnak</i>	0	0	0	0	1
<i>Pastinachus atrus</i>	0	1	0	0	0
<b>Gymnuridae</b>					
<i>Gymnura australis</i>	0	0	1	0	1
<b>Total numbers</b>	<b>139</b>	<b>104</b>	<b>42</b>	<b>55</b>	<b>10</b>

TABLE 3 The seasonal catch of elasmobranchs at shallow, central sites in Moreton Bay between October 2004 and May 2007 using a gillnet and setline. Spring = September–November, summer = December–February, autumn = March–May, winter = June–August.

Species	Season			
	Spring	Summer	Autumn	Winter
<b>Carcharhinidae</b>				
<i>Carcharhinus amboinensis</i>	19	5	10	0
<i>C. brevipinna</i>	0	1	0	0
<i>C. cautus</i>	3	4	9	0
<i>C. leucas</i>	1	7	0	0
<i>C. limbatus</i>	8	12	7	1
<i>C. obscurus</i>	2	0	11	5
<i>C. sorrah</i>	5	5	0	0
<i>Rhizoprionodon acutus</i>	1	0	0	0
<i>R. taylori</i>	22	39	42	3
<i>Galeocerdo cuvier</i>	0	1	0	0
<b>Sphyrnidae</b>				
<i>Sphyrna lewini</i>	1	10	10	0
<b>Hemigaleidae</b>				
<i>Hemigaleus australiensis</i>	9	11	3	0
<b>Orectolobidae</b>				
<i>Orectolobus ornatus</i>	1	0	0	1
<i>O. maculatus</i>	0	0	2	6
<b>Hemiscylliidae</b>				
<i>Chiloscyllium punctatum</i>	9	6	9	5
<b>Stegastomidae</b>				
<i>Stegostoma fasciatum</i>	0	1	0	0
<b>Rhinobatidae</b>				
<i>Aptychotrema rostrata</i>	3	8	4	1
<i>Glaucostegus typus</i>	0	0	4	1
<b>Rhynchobatidae</b>				
<i>Rhynchobatus laevis</i>	2	6	3	0
<b>Myliobatidae</b>				
<i>Aetobatus ocellatus</i>	1	0	0	0
<b>Mobulidae</b>				
<i>Manta sp.</i>	1	0	0	0
<b>Dasyatidae</b>				
<i>Dasyatis fluviorum</i>	3	0	2	0
<i>Himantura uaruak</i>	1	0	0	0
<i>Pastinachus atrus</i>	0	1	0	0
<b>Gymnuridae</b>				
<i>Gymnura australis</i>	1	1	0	0
<b>Total numbers</b>	<b>93</b>	<b>118</b>	<b>116</b>	<b>23</b>

3D Stress: 0.15

## DISCUSSION

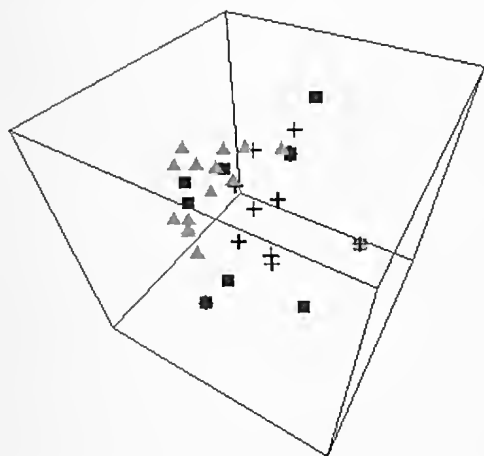


FIG. 3. Multidimensional scaling of the Bray–Curtis similarity matrices derived from the elasmobranch catch in gillnets at three sites in central region of Moreton Bay between 2004 and 2007. Stress value is shown in the top-right corner. Grey triangles = St Helena, black crosses = Horseshoe Bay, Peel Island, black squares = Deanbilla Bay, North Stradbroke Island.

were rarely caught at the shallower sites (Table 4). The Scalloped Hammerhead Shark also appeared to be fairly common at the deeper site. Most species of carcharhinid and sphyrnid sharks caught at the deeper site were larger than at the shallower sites (Table 5).

**Tagging.** Between May 2004 and May 2007, 206 carcharhiniform sharks were tagged, most of which were neonates and juveniles. In total, 8% were recaptured (Table 6) with recapture rates highest for the Common Blacktip Shark (19%), Dusky Shark (11%) and Spottail Shark (9%). Of the recaptured sharks, 87% were caught within 10 km of their respective release position and 60% were recaptured within 2 km from their original capture location. A Pigeye Shark was recaptured in the exact same location over a year later (time at liberty 402 days). Time at liberty ranged from four to 402 days and 44% of sharks were recaptured within 50 days. Recaptured sharks were caught by recreational fishers (38%), in commercial gillnets (50%), in crab pots (6%) and by the setline used in this study (6%).

**Shark abundance and species composition.** The species assemblages that characterised the three shallow-water sites were markedly different. The Australian Sharpnose Shark dominated the gillnet catch at St Helena and Horseshoe Bay, Peel Island, and was present at Deanbilla Bay, off North Stradbroke Island. This small species of shark reaches a maximum size of approximately 67 cm TL (Last & Stevens 2009) and appeared to be particularly susceptible to gillnets, with only a single specimen caught on setlines. Catches of multiple individuals in a single gillnet suggested conspecific association, although it is unknown whether the association is limited to particular cohorts, related to mating activities, or reflects normal foraging behaviour. Variation in both the species present and their relative abundance at the three sample locations highlights local-scale (<25 km) differences in distributions of elasmobranch species within Moreton Bay. While the drivers of the distributions of sharks and rays within the bay are unknown, it is likely that many species are influenced by the 'east-west' gradients in salinity and turbidity that have been documented to influence teleost community structure (Davie & Hooper 1998). Further sampling at more sites within western, central and eastern fringes of the Bay would help confirm whether the shark abundance and diversity patterns observed from the sites are broadly representative of each of these regions. It must be noted that the selectivity of the fishing gear used in the current study led to the capture of sharks between 39 cm and 204 cm TL. Previous research has documented the abundance of several batoids, such as the Bluespotted Maskray (*Neotrygon kuhlii*), the Brown Whipray (*Himantura toshi*), and the Common Stingaree (*Trygonoptera testacea*) (Johnson 2010; Pierce *et al.* 2011), which were largely absent from this study due to their small size and the selectivity of the fishing gear used. Furthermore, during the experimental fishing in deeper regions of the bay (10–20 m in depth), baits were generally fished off the sea-bed, selecting against benthic dwelling elasmobranchs. However, the sampling approach outlined in this

TABLE 4. The number and percent contribution of elasmobranchs caught by setline and rod and line fishing in shallow and deeper regions of Moreton Bay. Sampling conducted at shallow water sites between 2004 and 2007 and at deeper sites between 1978 and 1992.

Species	Shallow water setlining (<5 m depth, St Helena and Deanbilla Bay)		Deeper water setlining (10–20 m depth, Pearl Channel to Central Banks)		Deeper water rod and line fishing (10–20 m depth, Pearl Channel)	
	N	%	N	%	N	%
<b>Carcharhinidae</b>						
<i>Carcharhinus amboinensis</i>	31	27.2	0	0	0	0
<i>C. brevipinna</i>	0	0.0	59	32.4	71	27.5
<i>C. cautus</i>	16	14.0	0	0	0	0
<i>C. leucas</i>	8	7.0	0	0	5	1.9
<i>C. limbatus</i>	6	5.3	14	7.7	15	5.8
<i>C. obscurus</i>	11	9.6	0	0	0	0
<i>C. sorrah</i>	9	7.9	101	55.5	121	46.9
<i>Rhizoprionodon acutus</i>	0	0.0	0	0	9	3.5
<i>R. taylori</i>	1	0.9	0	0	0	0
<i>Galeocerdo cuvier</i>	1	0.9	0	0	0	0
<b>Sphyrnidae</b>						
<i>Sphyrna lewini</i>	1	0.9	8	4.4	34	13.2
<b>Orectolobidae</b>						
<i>Orectolobus ornatus</i>	1	0.9	0	0	0	0
<i>O. maculatus</i>	7	6.1	0	0	0	0
<b>Hemiscylliidae</b>						
<i>Chiloscyllium punctatum</i>	0	0	0	0	1	0.4
<b>Stegastomidae</b>						
<i>Stegostoma fasciatum</i>	1	0.9	0	0	0	0
<b>Rhinobatidae</b>						
<i>Glaucostegus typus</i>	5	4.4	0	0	0	0
<b>Rhynchobatidae</b>						
<i>Rhynchobatus laevis</i>	8	7.0	0	0	0	0
<b>Rhinopteridae</b>						
<i>Rhinoptera neglecta</i>	0	0	0	0	2	0.8
<b>Dasyatidae</b>						
<i>Dasyatis fluviorum</i>	5	4.4	0	0	0	0
<i>Himantura uarnak</i>	1	0.9	0	0	0	0
<i>Pastinachus atris</i>	1	0.9	0	0	0	0
<b>Gymnuridae</b>						
<i>Gymnura australis</i>	1	0.9	0	0	0	0
<b>Total numbers</b>	<b>114</b>		<b>182</b>		<b>258</b>	



## Whaler sharks in Moreton Bay

TABLE 5. The size (TL, cm) of Carcharhinidae and Sphyrnidae sharks caught in shallow and deeper regions of Moreton Bay. Sampling conducted at shallow water sites between 2004 and 2007 and at deeper sites between 1978 and 1992.

Species	Size range (TL, cm)		
	Shallow water (gillnet and setlining, St Helena, Horseshoe Bay and Deanbilla Bay)	Deeper water setlining (10–20 m depth, Pearl Channel to Central Banks)	Deeper water rod and line fishing (10–20 m depth, Pearl Channel)
<b>Carcharhinidae</b>			
<i>Carcharhinus amboinensis</i>	72–164	-	-
<i>C. brevipinna</i>	69	~100–210	76–230
<i>C. cautus</i>	81–149	-	-
<i>C. leucas</i>	168–202	-	150–210
<i>C. limbatus</i>	70–114	~100–150	90–166
<i>C. obscurus</i>	91–136	-	-
<i>C. sorrah</i>	71–123	~90–150	65–150
<i>Rhizoprionodon acutus</i>	89	-	73–85
<i>R. taylori</i>	39–75	-	-
<i>Galeocerdo cuvier</i>	204	-	-
<b>Sphyrnidae</b>			
<i>Sphyrna lewini</i>	43–84	~100–160	~65–300

TABLE 6. The number of sharks tagged in Moreton Bay, the number recaptured and the average distance travelled.

Species	Number tagged	Number recaptured	% recaptured	Average distance travelled in km (standard deviation)
<i>Carcharhinus amboinensis</i>	34	1	2.9	0
<i>C. brevipinna</i>	1	0	0	-
<i>C. cautus</i>	6	0	0	-
<i>C. leucas</i>	9	0	0	-
<i>C. limbatus</i>	26	5	19.2	1.0 (1.0)
<i>C. obscurus</i>	65	7	10.8	4.9 (4.3)
<i>C. sorrah</i>	11	1	9.1	15
<i>Rhizoprionodon taylori</i>	31	1	3.2	0
<i>S. lewini</i>	13	1	7.7	0
<i>Hemigaleus australiensis</i>	10	0	0	-
<b>Total number</b>	<b>206</b>	<b>16</b>	<b>7.8</b>	

study is likely to provide an accurate representation of the whaler shark fauna.

The Spottail Shark and Spinner Shark were particularly abundant at the deeper site, and yet these sharks were rarely caught in the shallow regions. Although experimental fishing at the deeper and shallow sites were conducted during two different time periods, it is unlikely that this time factor was responsible for the different species composition. It is also extremely unlikely that seasonal migrations to and from the shallow and deeper sites were responsible for the different species composition because both sharks were rare in all four seasons at the shallow sites. It has been suggested previously that the Spottail Shark prefers deeper water (Stevens *et al.* 2000), which may account for its relatively low abundance in shallower nearshore waters of Moreton Bay. This observation and our results suggest that there is some degree of species-separation by depth within Moreton Bay.

The observation that most of the sharks caught in the shallow-water sites were either neonate or juvenile (Taylor & Bennett 2013), provides support for the existence of nursery areas (*sensu* Heupel *et al.* 2007) for several species of Carcharhinidae within the bay. In contrast, most of the sharks caught at the deeper site were relatively large, with many in excess of 200 cm TL. Why these individuals appear to prefer the deeper areas of the bay is uncertain, although the presence of commercial crab and prawn fisheries may influence their distributions. Groups of sharks are often seen to follow working trawlers to feed on bycatch that escapes the net, or is discarded during the sorting process. In the years subsequent to when sampling was carried out, there has been a significant reduction in the number of prawn trawling licenses and consequently effort from trawl boats in the area. Hence a regular food resource from escaped and dumped bycatch has been greatly reduced. The implementation of bycatch reduction technology also continues to lessen the amount of discards from existing trawl operators (Courtney *et al.* 2006). Trawling activity would likely have acted to concentrate sharks in particular areas of the bay and its

reduction may have led to significant changes in the abundance, species composition and spatial distribution of sharks within the area.

There may also have been flow-on effects to shark populations from changes in other fisheries in the region. In the 1970s and 80s, seasonally from October to April, vast shoals of Spotted Mackerel (*Scomberomorus munroi*) were prevalent around the channels and banks of northern Moreton Bay (J. Johnson *pers. obs.*). Our catch data indicated that carcharhinid sharks were most common in the bay during the same months. Pilot studies conducted in this area between May and September resulted in the capture of such low numbers of sharks that sampling during this period was discontinued. From the late 1980s high speed ring-netting techniques started to be employed by commercial fishers in Moreton Bay specifically to target Spotted Mackerel. Escalating commercial catches together with a largely unrestricted recreational take, depleted the mackerel stock to the point that concerns were raised about the sustainability of the fishery (Begg *et al.* 2005). From December 2002 to April 2003 a ban on targeted netting of Spotted Mackerel and a reduced commercial quota was phased in by the Queensland Government, along with lower recreational bag limits and increased minimum size regulations. Despite these measures, anecdotal evidence suggests size and structure of the Spotted Mackerel population entering south-east Queensland waters have still not nearly recovered to levels approaching that prior to the period when ring-netting was practiced. Recreational catches of 30 or more large Spotted Mackerel per fishing session per boat were regularly achievable by competent anglers in Moreton Bay throughout the 1970s and 1980s. Notwithstanding current bag limits, that has generally been impossible in this area for many years. A reduction in this important food resource has probably had a significant influence on the historical abundance and composition of shark populations in the area. Recent stock status reports (e.g. State of Queensland, 2013) indicate that the Spotted Mackerel population on the east coast is sustainably fished and

predominantly comprises young fish (mainly within the one to four year old age groups).

The overall recapture rate of sharks in this study was fairly high (8%) which likely reflects the large amount of recreational and commercial fishing effort that occurs within Moreton Bay, rather than small population sizes. Recreational fishing effort in the Moreton Bay catchment was estimated to be 337,111 fisher days (77, 634 standard error) between October 2010 and September 2011 (Taylor *et al.* 2012). Although sharks are targeted by a small number of recreational fishers in the bay, the majority of sharks caught by recreational fishers are released alive (Taylor *et al.* 2012). Furthermore, current regulations prohibit the harvest of sharks 1.5 m TL or larger and there is an in possession limit of one shark per person (State of Queensland, 2012). The largest source of fishing mortality of whaler sharks in Moreton Bay occurs in the East Coast Inshore Fin Fish Fishery (ECIFFF) (State of Queensland, 2011). A small number of commercial fishers in Moreton Bay have targeted sharks opportunistically using gillnets for over 40 years. In 2011/12 439t of shark quota was taken in the ECIFFF, 423t of which was taken using monofilament gillnets (State of Queensland, 2013). The stock status for many species of sharks in Queensland is uncertain (State of Queensland, 2011) and the lack of long-term species-specific catch data and the high diversity in the catch composition make it difficult to assess whether population sizes have been affected by commercial fishing. The Department of Agriculture, Fisheries and Forestry is currently collecting and assessing critical information for determining the population status of sharks harvested in Queensland (State of Queensland, 2012).

Most tagged sharks were caught in close proximity to their original capture location and all the Dusky Shark and Pigeys Shark recaptures occurred within western fringes of the bay. Anecdotal reports from a commercial shark fisher with over 40 years' experience in Moreton Bay (John Page, *pers comm*) suggest that juvenile Dusky Sharks and Pigeys Sharks are not caught in the eastern side of the Bay. Furthermore, a 23 hour active track of a neonate

Dusky Shark (99 cm TL) caught in Waterloo Bay in March 2006 also revealed localised movements (Taylor 2008). During the day, this shark was restricted to water less than 2 m in depth while at night the shark ventured into slightly deeper water from 2–5 m in depth but remaining within the 'estuarine waters' of Waterloo Bay. More data are clearly needed, although the results from experimental fishing, tagging, acoustic tracking and anecdotal reports from a commercial fisher all suggest that neonate and juvenile Dusky Sharks have a restricted range in western fringes of the Bay.

**Management implications.** The re-zoning of the Moreton Bay Marine Park in 2009 increased the amount of protection from all forms of fishing (green zones) from 0.5% to 16% of the total area. The impacts of this increased protection on the shark fauna is currently unknown; however, the results of future sampling using comparable gear could be compared to that outlined in this study to assess whether the species abundance and composition has changed due to levels of protection, or other identified anthropogenic factors. Neonate and juvenile sharks are abundant in western fringes of Moreton Bay and while occupying these shallow waters may have been an effective evolutionary strategy, these areas are increasingly becoming affected as the human population in southeast Queensland continues to rise. Within Moreton Bay, urbanisation, sand dredging, construction of canal estates and the extension of the Brisbane airport and the Port of Brisbane may have reduced the availability of suitable habitat for sharks in Moreton Bay. Future research should investigate the importance of these nearshore habitats to shark populations throughout Queensland's waters. This would help ensure that shark populations continue to play an important role in Queensland's inshore ecosystems.

## ACKNOWLEDGEMENTS

We are extremely grateful for the fishing advice provided by John Page. The primary author would like to thank the many volunteers who assisted in field work, particularly Dr Scott

Cutmore, Dr Simon Pierce, Joanna Stead, Dr Tracey Scott-Holland, Sebastian Pardo, John Combs, Dr Adrian Gutteridge, Dr Lindsay Marshall and Dr Chris Rohner. We would also like to thank Kevin Townsend from the Moreton Bay Research Station for maintaining the research boat used in the study. The Primary Investigator's research was supported by the William Edwards Trust UK, a University of Queensland (UQ) Confirmation Scholarship and a Queensland Smart State Award. We thank Dr Wayne Sumpton (Department of Agriculture, Fisheries and Forestry) for his assistance throughout the project. We also wish to thank the Moreton Bay Research Station, Sea World Research and Rescue Foundation and the Tangalooma Wild Dolphin Resort for research support. Sampling was conducted under Queensland General Fisheries Permit PRM03951I and 55543. All procedures were approved by the UQ Animal Ethics Committee. We thank Dr John Healy and two anonymous reviewers for their insightful comments.

#### LITERATURE CITED

- Begg, G.A., O'Neill, M.F., Cadrin, S.X. & Bergenius, M.A.J. 2005. Stock assessment of the Australian east coast spotted mackerel fishery. CRC Reef Research Centre Technical Report No. 58, CRC Reef Research Centre, Townsville, Australia.
- Clarke, K.R. & Gorley, R.N. 2006. PRIMER v6: User manual/tutorial. PRIMER-E, Plymouth.
- Clarke, K.R., & Warwick, R.N. 2001. Change in marine communities: an approach to statistical analysis and interpretation, 2nd edition. PRIMER-E: Plymouth.
- Cortes, E. 1999. Standardized diet compositions and trophic levels of sharks. *ICES Journal of Marine Science* 56:707-717 (<http://dx.doi.org/10.1006/jmsc.1999.0489>).
- Courtney, A.J., Tonks, M.L., Campbell, M.J., Roy, D.P., Gaddes, S.W., Kyne, P.M., & O'Neill, M.F. 2006. Quantifying the effects of bycatch reduction devices in Queensland's (Australia) shallow water eastern king prawn (*Penaeus plebejus*) trawl fishery. *Fisheries Research* 80: 136-147 (<http://dx.doi.org/10.1016/j.fishres.2006.05.005>).
- Cutmore, S.C., Bennett, M.B. & Cribb, T.H. 2010. A new tetraphyllidean genus and species, *Caulopatara pageri* n.g., n.sp. (Tetraphyllidea: Phyllobothriidae), from the grey carpet shark *Chiloscyllium punctatum* Muller and Henle (Orectolobiformes: Hemiscyllidae). *Systematic Parasitology* 77:13-21 (<http://dx.doi.org/10.1007/s11230-010-9252-0>).
- Cutmore, S.C., Theiss, S.M., Bennett, M.B. & Cribb, T.H. 2011. *Hemipristicolo gunterae* gen. n., sp. n. (Cestoda: Tetraphyllidea: Phyllobothriidae) from the snaggletooth shark, *Hemipristis elongata* (Carchariiformes: Hemigaleidae), from Moreton Bay, Australia. *Folia Parasitologica* 58:187-196 (<http://dx.doi.org/10.14411/fp.2011.019>).
- Department of Agriculture Fisheries and Forestry 2013. *Stock status of Queensland's fisheries resources* 2012, pp 120.
- Davie, P.J.F. & Hooper, J.N.A. 1998. Patterns of biodiversity in marine invertebrate and fish communities of Moreton Bay. Pp 331-346. In I.R. Tibbets Hall, N.J., Dennison, W.C., (ed) *Moreton Bay and catchment*. (School of Marine Science, the University of Queensland: Brisbane).
- Dennison, W.C., & Abal, E.G. 1999. Moreton Bay study - a scientific basis for the healthy waterways campaign. Page 245. South East Queensland Regional Water Quality Management Strategy.
- Dudgeon, C.L., Lanyon, J.M. & Semmens, J.M. 2013. Seasonality and site fidelity of the zebra shark, *Stegostoma fasciatum*, in southeast Queensland, Australia. *Animal Behaviour* 85:471-481 (<http://dx.doi.org/10.1016/j.anbehav.2012.12.013>). Elsevier Ltd.
- Harahush, B.K., Hart, N.S., Green, K. & Collin, S.P. 2009. Retinal neurogenesis and ontogenetic changes in the visual system of the brown banded bamboo shark, *Chiloscyllium punctatum* (hemiscyllidae, elasmobranchii). *Journal of Comparative Neurology* 513:83-97 (<http://dx.doi.org/10.1002/cne.21953>).
- Harry, A.V., Morgan, J.A.T., Ovenden, J.R., Tobin, A.J., Welch, D.J. & Simpfendorfer, C.A. 2012. Comparison of the reproductive ecology of two sympatric Blacktip Sharks (*Carcharhinus limbatus* and *Carcharhinus tilstoni*) off north-eastern Australia with species identification inferred from vertebral counts. *Journal of Fish Biology* 81:1225-1233 (<http://dx.doi.org/10.1111/j.1095-8649.2012.03400.x>).
- Heupel, M.R., Carlson, J.K. & Simpfendorfer, C.A. 2007. Shark nursery areas: concepts, definition, characterization and assumptions. *Marine Ecology-Progress Series* 337:287-297 (<http://dx.doi.org/10.3354/meps337287>).
- Huveneers, C., Stead, J., Bennett, M.B., Lee, K.A. & Harcourt, R.G. 2013. Age and growth determination of three sympatric wobbegong sharks: How reliable is growth band periodicity in Orectolobidae? *Fisheries Research* 147:413-425. Elsevier B.V. (<http://dx.doi.org/10.1016/j.fishres.2013.03.014>).

- Johnson, J.W. 1999. Annotated checklist of the fishes of Moreton Bay, Queensland, Australia. *Memoirs of the Queensland Museum* 43(2):709–762.
- Johnson, J.W. 2010. Fishes of the Moreton Bay Marine Park and adjacent continental shelf waters, Queensland, Australia. *Memoirs of Queensland Museum* 54(3):299–353.
- Knip, D.M., Heupel, M.R. & Simpfendorfer, C.A. 2010. Sharks in nearshore environments: models, importance, and consequences. *Marine Ecology-Progress Series* 402:1–11(<http://dx.doi.org/10.3354/meps08498>).
- Kyne, P.M., Compagno, L.J.V, Stead, J. & Bennett, M.B. 2011. Distribution, habitat and biology of a rare and threatened eastern Australian endemic shark: Colclough's shark, *Brachaelurus colcloughi* Ogilby, 1908. *Marine and Freshwater Research* 62:540–547 (<http://dx.doi.org/10.1071/MF10160>).
- Kyne, P.M., Johnson, J.W., Courtney, A.J. & Bennett, M.B. 2005. New biogeographical information on Queensland chondrichthyans. *Memoirs of the Queensland Museum* 50:321–327.
- Last, P.R. & Stevens, J.D. 2009. Sharks and Rays of Australia. CSIRO Publishing, pp 656.
- Pierce, S.J., Scott-Holland, T.B. & Bennett, M.B. 2011. Community composition of elasmobranch fishes utilizing intertidal sand flats in Moreton Bay, Queensland, Australia. *Pacific Science* 65:235–247 (<http://dx.doi.org/10.2984/65.2.235>).
- Schluessel, V., Bennett, M.B., Bleckmann, H.H., Blomberg, S. & Collin, S.P. 2008. Morphometric and ultrastructural comparison of the olfactory system in elasmobranchs: the significance of structure-function relationships based on phylogeny and ecology. *Journal of Morphology* 269:1365–1386 (<http://dx.doi.org/10.1002/jmor.10661>).
- Stevens, J.D., West, G.J. & Mcloughlin, K.J. 2000. Movements, recapture patterns, and factors affecting the return rate of carcharhinid and other sharks tagged off northern Australia. *Marine and Freshwater Research* 51:127–141 (<http://dx.doi.org/10.1071/MF98158>).
- State of Queensland 2010. Moreton Bay Marine Park user guide. The State of Queensland, Department of State Development, 44 pp.
- State of Queensland 2011. Annual status report 2010. East Coast Inshore Fin Fish Fishery. Department of Employment, Economic Development and Innovation, 29 pp.
- State of Queensland 2012. Recreational fishing rules for Queensland, a quick guide 2011–2012. 26 pp
- State of Queensland 2013. Stock status of Queensland's fisheries resources. Department of Agriculture, Fisheries and Forestry, 121 pp.
- Taylor, S. 2008. Population structure and resource partitioning among Carcharhiniform sharks in Moreton Bay, southeast Queensland, Australia. University of Queensland. PhD thesis. (unpub.)
- Taylor, S.M. & Bennett, M.B. 2008. Cephalopod dietary specialization and ontogenetic partitioning of the Australian weasel shark *Hemigaleus australiensis* White, Last & Compagno. *Journal of Fish Biology* 72:917–936 (<http://dx.doi.org/10.1111/j.1095-8649.2007.01771.x>).
- Taylor, S.M. & Bennett, M.B. 2013. Size, sex and seasonal patterns in the assemblage of Carcharhiniformes in a sub-tropical bay. *Journal of Fish Biology* 82:228–241 (<http://dx.doi.org/10.1111/jfb.12003>).
- Taylor, S.M., Webley, J. & McInnes, K. 2013. 2010 Statewide Recreational Fishing Survey. Department of Agriculture, Fisheries and Forestry, 82 pp.
- Walker, T.I. 1998. Can shark resources be harvested sustainably? A question revisited with a review, of shark fisheries. *Marine and Freshwater Research* 49:553–572 (<http://dx.doi.org/10.1071/MF98017>).
- Werry, J.M., Lee, S.Y., Lemckert, C.J. & Otway, N.M. 2012. Natural or artificial? Habitat use by the bull shark, *Carcharhinus leucas*. *PLoS One* 7(11): e49796. <http://doi.10.1371/journal.pone.0049796>
- Werry, J.M., Lee, S.Y., Otway, N.M., Hu, Y. & Sumpton, Wu 2011. A multi-faceted approach for quantifying the estuarine-nearshore transition in the life cycle of the bull shark, *Carcharhinus leucas*. *Marine and Freshwater Research* 62:1421–1431.



# *Pallidelix simonhudsoni* sp. nov.: a new land snail from the central highlands of inland southern Queensland, Australia (Gastropoda: Eupulmonata: Camaenidae)

JOHN STANISIC

Honorary Research Fellow, Natural Environments Program, Queensland Museum, PO Box 3300, South Brisbane, Qld 4101, Australia. Email: john.stanisic@qm.qld.gov.au

<http://dx.doi.org/10.17082/j.2204-1478.59.2015.2015-01>

LSID urn:lsid:zoobank.org:pub:590F372C-1C7E-41AD-97CD-FDEE3445E8A1

Citation: Stanisic, J. 2015: *Pallidelix simonhudsoni* sp. nov.: a new land snail from the central highlands of inland southern Queensland, Australia (Gastropoda: Eupulmonata: Camaenidae). *Memoirs of the Queensland Museum-Nature* 59: 55-60. Brisbane. ISSN 2204-1478 (Online), ISSN 0079-8835 (Print). Accepted: 25 March 2015. First published online: 9 April 2015.

## ABSTRACT

*Pallidelix simonhudsoni* sp. nov. is described from vine thicket habitats on Carnarvon Station in the highlands of south central Queensland. The species is part of a much larger radiation of species of the camaenid genus *Pallidelix* Iredale, 1933 centred around the sandstone belt of inland central Queensland. *P. simonhudsoni* sp. nov. is distinguished by aspects of both shell sculpture and reproductive anatomy. The new species is hitherto only known from immediate environs of the type locality Carnarvon Station. The conservation status of the species is discussed within relation to: (1) its occurrence on a nature conservancy dedicated to biodiversity protection; (2) the endangered status of the species' primary habitat; and, (3) current land management practices on Carnarvon Station. □ *Pallidelix simonhudsoni* sp. nov., Eupulmonata, Camaenidae, systematics, new species, Queensland, Australia.

The Camaenidae is a family of land snails that is particularly diverse in the rainforests of eastern Queensland (Stanisic *et al.* 2010). Long recognised as a late Miocene invader from land masses to Australia's north (Bishop 1981; Solem 1992, 1997), the family has managed to radiate extensively in many areas of Australia. In eastern Australia camaenids are prominent snails in both the wetter humid coastal rainforests and the drier subcoastal and inland rainforests. Semi-evergreen vine thicket is a unique and widespread structural form of dry rainforest (Webb & Tracey 1981; Fensham 1996). Relatively few camaenids have made the transition to much drier eucalypt forests and woodland in eastern Australia. A mega-clade of semi-arid to arid-adapted, medium-sized

to large camaenids inhabiting inland parts of Queensland, coastal and inland New South Wales and the arid areas of South Australia and the Red Centre was identified by Hugall & Stanisic (2011, Clade 3). The Queensland endemic *Pallidelix* Iredale, 1933 (type *P. greenhilli*) is one of these Clade 3 genera with species centred in semi-arid inland southern and central Queensland in the Brigalow Lands bioregion.

*Pallidelix* currently includes three species: one from the semi-evergreen vine thickets of the central ranges (Expedition, Bigge and Carnarvon Ranges) [*P. greenhilli* (Cox 1866)], a second from south of the Great Dividing Range in the brigalow scrubs of the Dalby-Miles area of southern Queensland [*P. chinchilla* Stanisic,

2010] and a third from eucalypt woodland communities in southeastern Queensland [*P. beuueti* (Brazier 1872)] (see Stanisic *et al.* 2010). These species were collectively included in the genus on the basis of similarity of shell sculpture (coarse pustules and oblique to zigzag periostracal ridges) subject to future revision.

A new addition to this broad species inventory (*P. simonhudsoni* sp. nov.) was discovered on a recent Bush Blitz expedition to Carnarvon Station (a nature conservancy) situated on the western fringes of the central Queensland sandstone belt (see explanatory note in 'Acknowledgements'). Vegetation communities on Carnarvon Station although varied are dominated by native grasslands, brigalow, eucalypt woodland and a series of scattered semi-evergreen vine thickets in the sheltered gullies and on the surrounding hillsides. *P. simonhudsoni* sp. nov. lives primarily in semi-evergreen vine thickets. Less frequently it was also found to occur in adjacent woodland communities probably as result of 'leakage' from the thickets during periods of rain.

Although a taxonomic revision of *Pallidelix* is seen as overdue, this task will necessitate additional fieldwork to obtain specimens for molecular studies. In the meantime, the formal description of *P. simonhudsoni* sp. nov. is deemed necessary from a conservation perspective and the likely flow-on effects this action could achieve for terrestrial invertebrate communities on Carnarvon Station.

## MATERIALS AND METHODS

Material used in this study is held in the collections of the Queensland Museum (QMMO). Studies of shell characters were carried out on specimens in the museum's dry collection (RC) and anatomical studies were based on ethanol preserved samples (SC). Measurements of shell characters (height, diameter) were made using callipers with a precision of 0.01 mm. Whorl counts were made to the nearest 1/8 whorl. Three representatives of the species from the type locality (Carnarvon Station) were dissected and studied using a WILD M5 stereo microscope with drawing

apparatus in order to confirm stability of reproductive structures.

## SYSTEMATICS

### Infraorder EUPULMONATA

### Superfamily HELICOIDEA

### Family CAMAENIDAE

### Genus *Pallidelix* Iredale, 1933

**Type species.** *Helix greenhilli* Cox, 1866-by original designation.

**Diagnosis.** Shell large, yellowish brown, helicoid with an elevated spire and rounded whorls; teleoconch sculpture of closely spaced pustules that occasionally coalesce into micro-ridgelets and an overlying pattern of oblique to zigzag periostracal ridges; aperture roundly lunate, lip white, expanded and reflected; umbilicus narrowly open, reduced to a chink. Penis with a sheath, internally with smooth, thick longitudinal pilasters and a smooth papillate verge with a terminal pore; epiphallus thick, muscular; epiphallic flagellum present.

### *Pallidelix simonhudsoni* sp. nov. (Figs 1-4)

**Etymology.** Named for Simon Hudson, ecologist, colleague and environmental consultant.

**Material examined.** (All Carnarvon Station, south central Queensland).

**Holotype.** QMMO80282, Fig Tree Spring, (24° 47.813'S, 147° 41.593'E), semi-evergreen vine thicket on basalt scree, under rocks, 10.x.2014, coll. J. Stanisic. Height of shell 28.02 mm, diameter 31.89 mm, H/D = 0.88.

**Paratypes.** QMMO80231, same data as holotype; QMMO80124, 25C/9RC, rocky knoll NW homestead (24° 46.007'S, 147° 43.533'E), Ironbark woodland/rocky scree, under rocks/in litter, 9.x.2014, J. Stanisic; QMMO80227, 5RC, rocky knoll NW homestead (24° 46.007'S, 147° 43.533'E), Ironbark woodland/rocky scree, under rocks/in litter, 10.x.2014, J. Stanisic; QMMO80247, 25C/6RC, hillock N homestead, (24° 48.627'S, 147° 45.135'E), vine thicket/basalt scree, under rocks/in litter, 11.x.2014, J. Stanisic; QMMO80250, 15RC, homestead flats, (24° 48.423'S, 147° 45.149'E), grassy woodland, on ground,



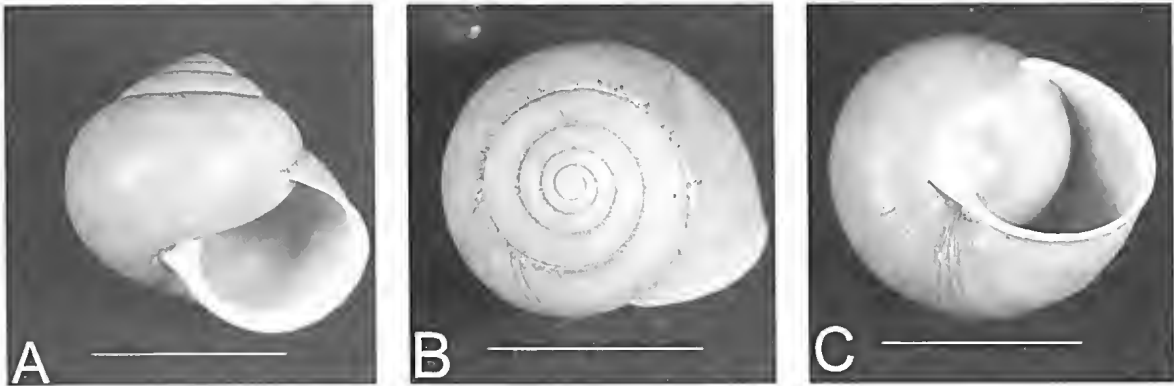


FIG. 1. *Pallidelix simonhudsoni* sp. nov. Shell views, holotype QMMO80261, Carnarvon Station. A, apertural; B, dorsal; C, ventral. Scale bars = 20 mm.

TABLE 1. Shell measurements for *Pallidelix simonhudsoni* sp.nov. [Range and mean].

	Number	Height (mm)	Diameter (mm)	H/D ratio	Whorls
<i>P. simonhudsoni</i> sp. nov. QMMO80231	5	23.50-25.88 Mean 24.69	26.53-29.63 Mean 28.41	0.82-0.90 Mean 0.88	5 5/8-6 1/2 Mean 5 5/8
<i>P. simonhudsoni</i> sp. nov. QMMO80227	4	24.79-27.53 Mean 25.89	24.34-31.17 Mean 29.78	0.84-0.88 Mean 0.87	5 5/8-5 3/4 Mean 5 5/8
<i>P. simonhudsoni</i> sp. nov. QMMO80124	4	23.38-26.14 Mean 24.23	25.57-29.59 Mean 28.24	0.83-0.92 Mean 0.86	5 3/8-5 1/2 Mean 5 1/2
<i>P. simonhudsoni</i> sp. nov. QMMO80247	4	23.33-26.13 Mean 24.43	27.17-29.57 Mean 28.27	0.84-0.88 Mean 0.86	5 1/2-5 3/4 Mean 5 5/8
<i>P. simonhudsoni</i> sp. nov. QMMO80250	15	23.47-28.30 Mean 22.88	24.87-31.15 Mean 27.75	0.81-0.93 Mean 0.88	5 3/8-5 3/4 Mean 5 5/8
<i>P. simonhudsoni</i> sp. nov. QMMO80261	4	22.79-24.32 Mean 23.63	26.55-28.82 Mean 27.94	0.82-0.87 Mean 0.85	5 1/4-5 3/4 Mean 5 1/2

12.x.2014, J. Stanisc; QMMO80261, 4RC, vine thicket N homestead, (24° 47.935'S, 147° 45.284'E), vine thicket/basalt scree, under rocks/in litter, 13.x.2014, J. Stanisc, K. & C. Wilson.

**Other material.** QMMO80219, 80220, 80258, 80271, 80274, 80275, 80280.

**Diagnosis.** Shell large, dark to yellowish brown, occasionally with a thin reddish brown subsutural band, helicoid with an elevated spire and rounded whorls; teleoconch sculpture of relatively fine, closely spaced pustules that occasionally coalesce into micro-ridgelets and scattered oblique to zigzag periostracal ridges. Penis long, thin with sheath; internally with smooth, thick longitudinal pilasters in the upper

part of the penial chamber becoming thinner and corrugated toward the atrium; epiphallus long with very thick, muscular ascending arm partially folded within sheath and a thinner descending arm; penial verge smooth, papillate with a terminal pore; epiphallic flagellum present.

**Description.** Shell large, dark to yellowish brown, helicoid with an elevated spire, whorls 5¼-5⅝ (mean 5⅝) evenly rounded, the last descending in front; apex and spire strongly elevated. Height of shell 22.79-28.30 mm (mean 24.29 mm), diameter of shell 24.87-31.17 mm (mean 28.40 mm), H/D = 0.85-0.88 (mean 0.87). Protoconch of 1¾ whorls sculptured with

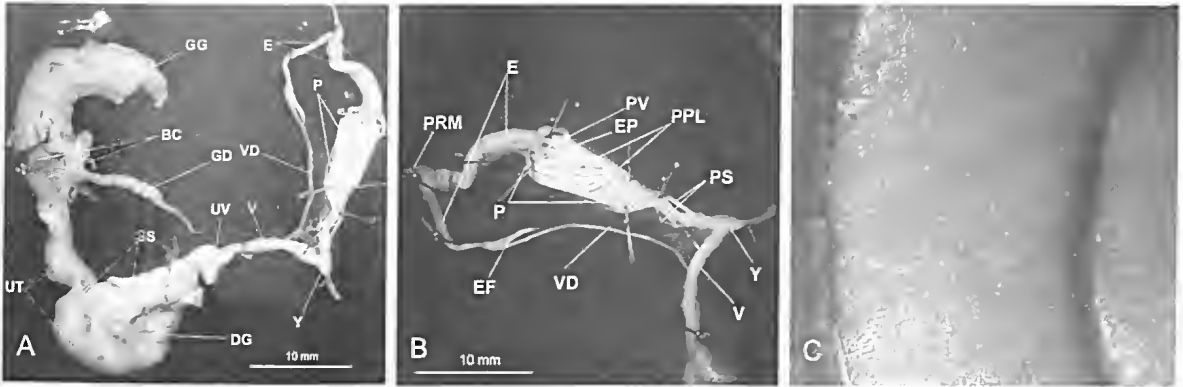


FIG. 2. *Pallidelix simonhudsoui* sp. nov. QMMO80124, paratype. A, Genital system; B, Penial complex; C, Close-up of shell whorls showing periostracal sculpture. Abbreviations used: BC, bursa copulatrix; DG, prostate; E, epiphallus; EF, epiphallus flagellum; EP, epiphallus pore; GD, hermaphroditic duct; GG, albumen gland; P, penis; PPL, penial pilasters; PRM, penial retractor muscle; PS, penial sheath; PV, penial verge; SS, bursa stalk; UT, uterus; UV, free oviduct; V, vagina; VD, vas deferens; Y, atrium. Scale bars as marked.

weak, low radial ridges that are often worn in adult specimens, teleoconch with a pattern of fine crowded pustules that occasionally coalesce into micro-ridgelets, and scattered oblique to zigzag periostracal ridges that become more prominent on the penultimate and body whorls. Aperture roundly lunate, lip expanded and strongly reflected, white. Umbilicus narrowly open, reduced to a chink. Animal orange grey with dark grey eyestalks. (Figs. 1A-C, 2C, 3).

**Genitalia.** Penis (P) long, tapered with slightly expanded apical bulb; thin sheath (PS) present; internally with a papillate verge (PV), walls of penial chamber with fleshy longitudinal pilasters (PPL) apically becoming corrugated basally and thinner descending into the atrium. Epiphallus (E) with relatively long, thick muscular ascending arm enveloped and partially folded within penial sheath, descending arm thin, relatively short; epiphallus entering penis through a simple pore (EP) situated terminally on verge. Penial retractor muscle (PRM) inserted at the junction of the two arms of the epiphallus. Vas deferens (VD) thin, attached to penial sheath with connective tissue; a short, thin epiphallus flagellum (EF) present, situated at epiphallus-vas deferens junction, tightly bound to vas deferens. Vagina (V) short, less than half length of penis, internally with several longitudinal pilasters. Atrium (Y) simple. Free oviduct (UV) shorter than vagina; bursa copulatrix (BC)

simple with a slender stalk (SS), situated at the base of the albumen gland (GG); prostate (DG), uterus (UT) and hermaphroditic duct (GD) without unusual features (Fig 2A, B).

**Habitat and ecology.** Semi-evergreen vine thicket and adjacent eucalypt woodland on Carnarvon Station. Additional collecting may extend the range south into other parts of the Chesterton Range. To the north-west the vine thickets of the Ka Ka Mundi Section, Carnarvon NP is home to a different and yet to be described species of *Pallidelix* (Stanisic, unpublished); it is unlikely to occur to the south and west due to the absence of suitable habitat. The species lives under rocks and woody debris.

**Comparative remarks.** *Pallidelix simonhudsoui* sp. nov. is similar to the type of the genus, *P. greenhilli* (Cox 1866) which is only definitively known from three shells: a syntype (registration number AMSC.5767, see Fig. 4) and one other specimen (AMSC.101192) which may also be considered a syntype, from the original Cox collections in the Australian Museum; and a further syntype in the National Museum of Wales (NMWZ1955.158.880). In the absence of definitive live material referable to the type, *P. simonhudsoui* sp. nov. can be distinguished from *P. greenhilli* by a combination of shell features here considered to indicate specific level separation. The shell of *P. simonhudsoui*



FIG. 3. *Pallidelix simonhudsoni* sp. nov. Live snail from Carnarvon Station.

sp. nov. has a more elevated spire than that of *P. greenhilli* (Fig. 4). But more significantly, *P. simonhudsoni* sp. nov. has a shell sculpture of very fine pustules with scattered oblique to zigzag periostracal ridges. In contrast, the shell of *P. greenhilli* has coarser pustules and very dominant oblique to zigzag periostracal ridges. In addition, the area around the umbilicus of *P. greenhilli* is slightly more excavate than that of *P. simonhudsoni* sp. nov.

The type locality of *P. greenhilli* was given by Cox (1866) as the 'Upper Dawson River' which is a large area extending from Taroom to the Carnarvon Ranges, Queensland. This range includes several apparent *Pallidelix* morphospecies. A key task of any revision will be to associate the specimens in the Australian and Welsh Museums with material from within this geographic range to enable accurate anatomical comparisons to be made. However, preliminary dissections show that *P. simonhudsoni* sp. nov. differs in aspects of the penial anatomy (comparatively narrower, elongate penis with a longer basal section) from all *Pallidelix* material hitherto examined from the 'Upper Dawson River' including specimens from both the Carnarvon Ranges and Taroom (Stanisic, unpublished).

## DISCUSSION

*Pallidelix* is currently broadly defined and includes three species from southeastern and

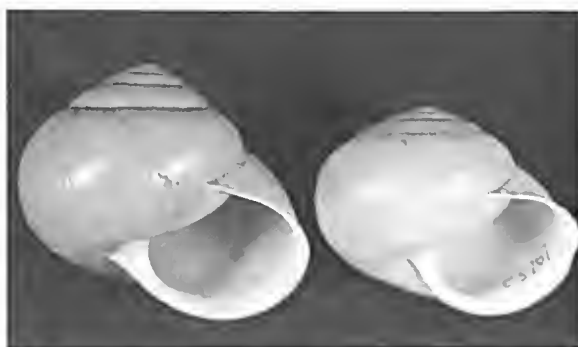


FIG. 4. *Pallidelix simonhudsoni* sp. nov. holotype QMMO80261 (left) and *P. greenhilli* (Cox (1866) syntype AMSC.5767 (right) showing relative spire elevations.

south central Queensland. Unpublished results of the author indicate that the genus as currently defined (Stanisic *et al.* 2010) is polyphyletic. The two southern species (*P. chinchilla* and *P. beunelli*) included by Stanisic *et al.* (2010) will be shown to belong elsewhere when a formal revision of the genus is completed. *Pallidelix* s.s. is essentially centred on the ranges of the sandstone belt in south central Queensland. Extensive material in the Queensland Museum shows that *Pallidelix* has a wide range in the central Queensland area that extends from Taroom and the Expedition Range in the east, through the Carnarvon Ranges to the Ka Ka Mundi Section of the Carnarvon NP in the west and north to the Drummond Range, west of Emerald. Preliminary dissection of this central Queensland material, all previously provisionally identified as *P. greenhilli*, has revealed the presence of several undescribed species within this broad geographic range. *P. simonhudsoni* sp. nov. is an integral part of this radiation chiefly living in the vine thickets of Carnarvon Station.

## CONCLUSIONS

The semi-evergreen vine thickets of Carnarvon Station are currently unmapped and largely unrecognised as particularly significant hubs of invertebrate biodiversity. For the station's land snails (20 native species recorded thus far), which have been found to largely inhabit only the vine thickets (17 species), these dry rainforests

are pivotal to their long-term survival and to the survival of a suite of other lesser known invertebrates (slaters, spiders, millipedes etc). In the short term the description of *P. simonludsoni* sp. nov. hopefully will highlight the importance of the vine thicket communities as important refugia for invertebrates. In the longer term it is hoped that this recognition will lead to a mapping of all the vine thicket patches on the property so that the station's management practices (particularly the use of fire) can be more sympathetically applied to their conservation. Semi-evergreen vine thicket as a community is a scattered archipelago occurring in small, isolated patches in semi-arid inland and monsoonal eastern and northern Australia. In Queensland the community has suffered greatly from largely unnecessary land clearing in the past and will require specific conservation measures if it is to be secured for the long-term (Fensham 1996).

Semi-evergreen vine thickets are now listed as an endangered ecological community under the Commonwealth's Environment Protection and Biodiversity Conservation Act 1999. Careful management of the Carnarvon Station vine thickets has the potential to permanently secure a small subset of this community and with them a unique suite of invertebrates.

On a no less significant scale, this study adds another species to the ever-increasing list of Australia's unique but largely unknown invertebrate fauna.

#### ACKNOWLEDGEMENTS

Thanks are due to the Bush Blitz team of Jo Harding, Brian Hawkins, Mim Jambrecina, Beth Tully, Earthwatch (Bruce Paton) and BHP-Billiton for funding, organising and supporting the Carnarvon Station land snail survey; and to the managers of Carnarvon Station (Chris and Alison Wilson), to Murray Haseler (Bush Heritage) and the Bush Heritage organisation for allowing access to the reserve. Thanks also to Darryl Potter, Queensland Museum for comments on the original manuscript.

[Note. Bush Blitz is a bio-discovery program co-funded by the Australian Commonwealth Government and BHP-Billiton and also involving Earthwatch Australia which seeks to document Australia's biodiversity. Carnarvon Station is a 56,000 ha. nature conservancy (a nature reserve outside the national reserve system) owned and managed by Bush Heritage which is a non-profit organisation acquiring land specifically for biodiversity conservation].

#### CITED LITERATURE

- Bishop, M. J. 1981. The biogeography and evolution of Australian land snails. Pp. 924-954. In Keast, A. (ed.), *Ecological biogeography of Australia*. (Dr W. Junk: The Hague). [http://dx.doi.org/10.1007/978-94-009-8629-9\\_32](http://dx.doi.org/10.1007/978-94-009-8629-9_32)
- Cox, J.C. 1866. Description d'espèces nouvelles provenant d'Australie et des îles Solomon et Norfolk. *Journal de Conchyliologie* 14: 45-48.
- Fensham, R. 1996. Land clearance and conservation of inland dry rainforest in north Queensland, Australia. *Biological Conservation* 75: 289-298. [http://dx.doi.org/10.1016/0006-3207\(95\)00057-7](http://dx.doi.org/10.1016/0006-3207(95)00057-7)
- Hugall, A.F. & Stanisic, J. 2011. Beyond the prolegomenon: a molecular phylogeny of the Australian camaenid land snail radiation. *Zoological Journal of the Linnean Society* 161: 531-572. <http://dx.doi.org/10.1111/j.1096-3642.2010.00644.x>
- Solem, A. 1992. Camaenid land snails from southern and eastern South Australia, excluding Kangaroo Island. Part 2. *Records of the South Australian Museum Monograph Series* No. 2: 339-425.
- Solem, A. 1997. Camaenid land snails from Western and central Australia (Mollusca: Pulmonata: Camaenidae). VII. Taxa from Dampierland through the Nullabor. *Records of the Western Australian Museum, Supplement* 50: 1461-1906.
- Stanisic, J., Shea, M., Potter, D. & Griffiths, O. 2010. *Australian land snails. Volume 1. A field guide to eastern Australian species*. (Bioculture Press: Mauritius). 596pp.
- Webb, L.J. & Tracey, J.G. 1981. Australian rainforests: patterns and change. Pp. 605-694. In, Keast, A. (ed.), *Ecological biogeography of Australia*. (Dr W. Junk: The Hague). [http://dx.doi.org/10.1007/978-94-009-8629-9\\_22](http://dx.doi.org/10.1007/978-94-009-8629-9_22)

# An Early Cretaceous (late Albian) halecomorph (? Ionoscopiformes) fish from the Toolebuc Formation, Eromanga Basin, Queensland

Alan BARTHOLOMAI

Director Emeritus, Queensland Museum, PO Box 3300, South Brisbane, Qld, 4101, Australia.

Citation: Bartholomai, A. 2015: An Early Cretaceous (late Albian) halecomorph (? Ionoscopiformes) fish from the Toolebuc Formation of the Eromanga Basin, Queensland. *Memoirs of the Queensland Museum - Nature* 59: 61–74. Brisbane. ISSN2204-1478 (Online) ISSN 0079-8835 (Print). Accepted: 14 Dec 2014. First published online: 8 May 2015.

<http://dx.doi.org/10.17082/j.2204-1478.59.2015.2014-05>

LSID urn:lsid:zoobank.org:pub:33AE497B-F8F9-4975-9CBA-7B8E515A7D9F

## ABSTRACT

The partial neurocranium of a relatively small, halecomorph fish is described as *Canaryichthys rozefeldsi* gen. et sp. nov. and represents the first possible ionoscopiform from the Cretaceous of Australia. The specimen was collected from the marine Toolebuc Formation of the Eromanga Basin, near Boulia, in the central west of Queensland, deposited during the Early Cretaceous (late Albian) when an epeiric sea covered much of the centre of the State. It is undistorted and preserved in 3-dimensions but lacks all but the cranial vault. *Canaryichthys* has many features in common with the enigmatic English Jurassic 'catirid' neurocranium redescribed and figured by Patterson (1975) as '*Aspidorhynchus*' sp., (originally described by Rayner, 1948) and also appears to have affinity with the Early Cretaceous (Aptian), *Oshunia*, from South America. □ *Halecomorphi*, *Ionoscopiformes*, *Canaryichthys rozefeldsi*, '*Aspidorhynchus*', *Oshunia*, *Macrepistius*, *Early Cretaceous (late Albian)*, *Toolebuc Formation*, *Eromanga Basin*.

The partial neurocranium of the relatively small halecomorph fish described here as a new genus and species, was collected from near Boulia in central western Queensland, exposed from a coquinite of the Toolebuc Formation. This sediment was deposited as shallow-water, marginal, marine deposits of Early Cretaceous (Late Albian) age, in the western part of the Eromanga Basin, within the Great Artesian Superbasin (Jell, Draper & McKellar 2013). This area and these deposits have been known to contain numerous remains of marine reptiles, especially ichthyosaurs but the fossil fauna also includes plesiosaurs, pliosaurs and turtles, as well as rare pterosaurs and birds, with the latter considered to add support for the suggestion of an in-shore depositional environment. Fossilised remains of fish, especially sharks

and teleosts are also commonly encountered. Bartholomai (2004) has recorded the presence of the aspidorhynchid, *Richmondichthys sweeti* (Etheridge Jnr. & Smith Woodward 1891). The pachyrhizodid, *Pachyrhizodus marathonensis* (Etheridge Jnr. 1905) has also been shown to be present (Bartholomai 1969, 2012). The Toolebuc pachycormid, *Australopachycormus hurleyi* Kear, 2007, was described from the Boulia area, while Kear & Hamilton-Bruce (2011) also record the presence of the ichthyodectiform, *Cooyoo australis* Lees & Bartholomai, 1986 from that area.

Cook (2012) regards the age of the Toolebuc Formation as being Early Cretaceous (Late Albian) but earlier work by Henderson (2004) has suggested the age be regarded as early Late Albian, based on ammonite and nannofossil

biostratigraphy. Smaller individuals and representatives of small species of fishes are infrequently encountered in the Toolebuc Formation and, when found in near shore deposits, are usually in a highly disassociated or fragmented state. It is considered unlikely that collections of better preserved and identifiable material relating to representatives of small taxa and immature individuals of larger species will be expanded in the near future.

The fossil record of the Halecomorphi is highly diverse (Brito & Alvarado-Ortega, 2013). However, most of the recorded Cretaceous occurrences have been from Northern and Central American deposits. Revisions and discoveries of the group over recent decades have concentrated on non-Gondwanan taxa and the presence of a broader halecomorph record in the Australian Cretaceous should lead to improved global understanding of the phylogeny of the group.

The holotype neurocranium that forms the basis for the description of the new taxon, *Canaryichthys rozefeldsi*, is preserved in an undistorted, 3-dimensional state, relatively common in many of the large individuals within fossil actinopterygian fishes from the Toolebuc Formation in the Boulia area and elsewhere in the marine Eromanga Basin sediments. Unfortunately, the holotype specimen lacks those characters considered by others to be phylogenetically diagnostic for determining halecomorph phylogenetic relationships. However, formal description of *Canaryichthys*, based on general comparisons with neurocrania of described halecomorphs, is felt reasonable, expanding the identified fish fauna of the Eromanga Basin and increasing knowledge of their Gondwanan radiation.

**Abbreviations.** acv = anterior cerebral vein fenestra; Apto = autopterotic; Asph = Autosphenotic; Boc = Basisoccipital; Bsp = Basisphenoid; df = dilator fossa; Dpto = Dermopterotic; dlpto = descending lamina of dermopterotic; Epo = Epiotic; Exo = Exoccipital; fhm = hyomandibular facet; fica = foramen of internal carotid artery; fm = foramen magnum; foca = foramen for occipital artery; fpt = facet for ligament to post-temporal; Fr = Frontal;

frla = foramen of recurrent branch of facial nerve; fvoc = posterior cerebral vein fenestra; Ic = Intercalar; jc = jugular canal; Le = Lateral Ethmoid; Leas = Lateral Ethmoid attachment surface; Ors = Orbitosphenoid; osc = otic sensory canal; Pa = Parietal; Pro = Prootic; prlm = process for origin of branchial levator muscles; Pspa = Parasphenoid attachment area; Opo = Opisthotic; potb = prootic bridge; Pas = Parasphenoid; ptf = post-temporal fossa; Pro = Prootic; Pto = Pterotic; Pts = Pterosphenoid; So = supraorbital; sosc = supraorbital sensory canal; Sot = Supraotic; stf = subtemporal fossa; Soc = Supraoccipital; vfon = vestibular fontanelle; I = olfactory tract fenestra; II = optic fenestra; III = oculomotor nerve foramen; IV = trochlea nerve foramen; V = trigeminal nerve foramen; VI = abducens nerve foramen; VII = facial nerve foramen, IX = glossopharyngeal nerve foramen; X = vagus nerve foramen.

Neopterygii Regan, 1923

Holostei *sensu* Grande, 2010

Subdivision Halecomorphi, Cope, 1872

Order ?Ionoscopiformes Grande & Bemis, 1998

Family *incertae sedis*

*Canaryichthys* gen. nov.

**Generic Diagnosis.** As for the specific diagnosis until such time as additional species are recognised.

**Etymology.** Named for 'Canary' Station, near Boulia, Central West Queensland (CWQ), from which the type species was recovered.

**Type Species.** *Canaryichthys rozefeldsi* sp. nov.

*Canaryichthys rozefeldsi* sp. nov.  
(Figs 1-3)

**Holotype.** QMF17025, partial neurocranium comprising the only the only known specimen at this time, from 'Canary' Station, SE of Boulia, CWQ, minimally prepared by mechanical techniques.

**Etymology.** Named for Dr Andrew Rozefelds (now Head of Geosciences, Queensland Museum), who collected and prepared the holotype specimen during his previous appointment in the geological section of the Queensland Museum.

**Formation and Age.** From the Toolebuc Formation of Early Cretaceous (Late Albian) age.

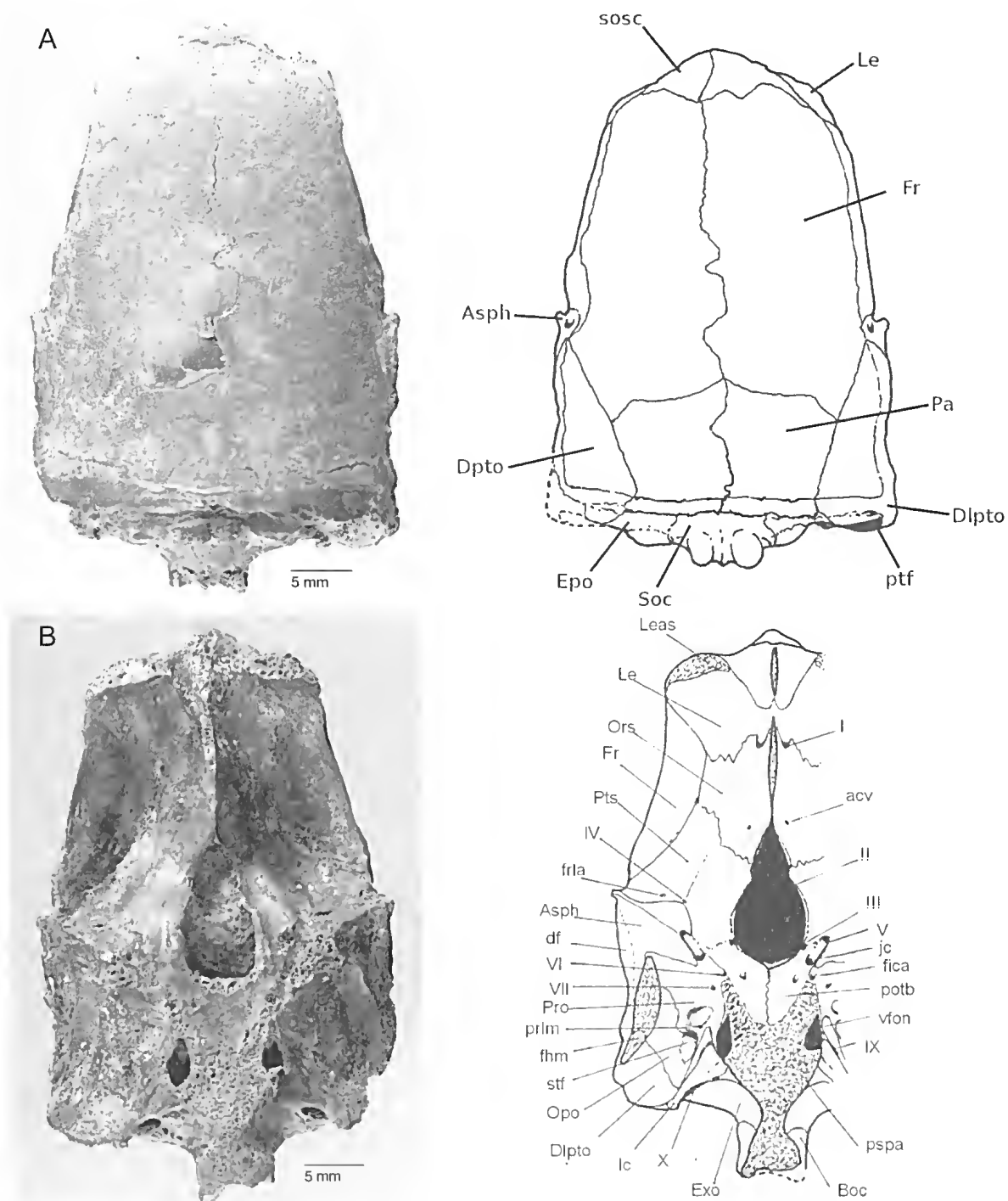


FIG. 1. *Canaryichthys rozefeldsi* gen. et sp. nov., QMF17025, Holotype. A, photograph and interpretative drawing of partial neurocranium in dorsal view. B, photograph and interpretative drawing of partial neurocranium in ventral view.



**Specific Diagnosis.** A small species with a shallow, broadly arched neurocranium, with sloping posterior surface. Skull roof ganoine covered with very fine 'orange skin' ornamentation internally with fine tubules often leading to minute surface pores. Frontals anteriorly stepped down and with interfrontal suture deeply interdigitating, especially posterior to orbits. Parietals with B:L ratio of 0.85, separated by deep, interdigitating suture. Cranial margins stepped down laterally and posteriorly. Circumorbital ring incomplete. Dermosphenotics only loosely attached to circumorbital margin, lacking inner orbital flange. Dermopterotics much longer than parietals. Post-temporal fossa angled anteromedially. Dilator fossa extends well onto autosphenotic. Short dorsal supraoccipital present, with prominent median bosses separating shallow, complex epiotics. Small pterotic present in post-temporal fossa. Exoccipitals very large, dished, meeting on broadly swollen, medial ridge above foramen magnum. Intercalar large, forming strong, grooved, elevated, ventrolateral bone fan. Nerve IX foramen in fold of intercalar fan. Vestibular fontanelle remnant present. No vertebral centrum fused with occipital condyle but basioccipital small, with very deeply, conically excavated notochordal pit. Vestibular fontanelle present. Subtemporal fossa small. Hyomandibular facet deeply concave, elongated, angled anteroventrally. Autosphenotic spine delicate. Pterosphenoid without pterosphenoid pedicle. Orbitosphenoid lacking ossified interorbital septum, firmly sutured to lateral ethmoid to form anterodorsal orbital margin. Parasphenoid reaching back of neurocranium and with process connected to base of autosphenotic.

**Description.** Neurocranium of this relatively small fish broad and shallow (see Figs. 1 and 2). Although lacking anterior, estimated length of skull is considered less than twice its maximum width (3 cm across both occipital and autosphenotic regions). Width across anterior of frontals 1.95 cm, while maximum depth of neurocranium at occiput is 1.89 cm. Cranial roof transversely relatively strongly convex (Fig. 2B) and slightly convex longitudinally. Anterior of neurocranium downturned at approximately 40°. Roofing bones ganoine covered and

extremely finely ornamented uniformly, with irregular short, low ridges separated by minute pits with ridges sometimes uniting into small rings around minute pockets (Fig. 1A). Stepped marginal areas not ornamented. Relatively numerous and elongated, slender tubules visible within ganoine, sometimes leading to surface pores, generally curving away from position of supraorbital sensory canal, especially medially and posteromedially from near centre of ossification of frontal.

Frontals comprise bulk of dorsal roof. Each meets its counterpart along a median suture deeply interdigitated behind orbits. Anterior of each frontal broad and stepped ventrally to accommodate overlap by the back of the anterior bones of skull roof, presumably including nasals. Lateral margin of frontal along and above orbital roof also stepped from autosphenotic to accommodate dermosphenotic (not preserved) but supraorbitals do not appear to have been present. Overall lateral margin of frontal part of the neurocranial roof slightly convergent anteriorly above orbit, while orbital margin very slightly concave laterally. Supraorbital sensory canal completely covered with no surface ridge. A small foramen present midway between median suture and lateral margin on anterior step believed to accommodate supraorbital sensory canal into frontal. Anteriorly, frontal partially overlies anterior of lateral ethmoid.

Parietal moderately large, longer than broad (B: L ratio of right parietal ca. 0.85), ornamented similar to frontals but with less obvious tubules visible in ganoine. Each does not reach as far anteriorly as front of dermosphenotic. Median suture deeply and irregularly interdigitated. Posterodorsally, parietal widely separated on stepped margin by supraoccipital. Parietal meets epiotic along posterior neurocranial step with a very short contact with dermosphenotic posterolaterally above inner margin of post-temporal fossa.

Dermosphenotic not preserved, not fused to frontal or dermosphenotic along their very short junctions. From the stepped surface present on the frontal, the bone was probably small,



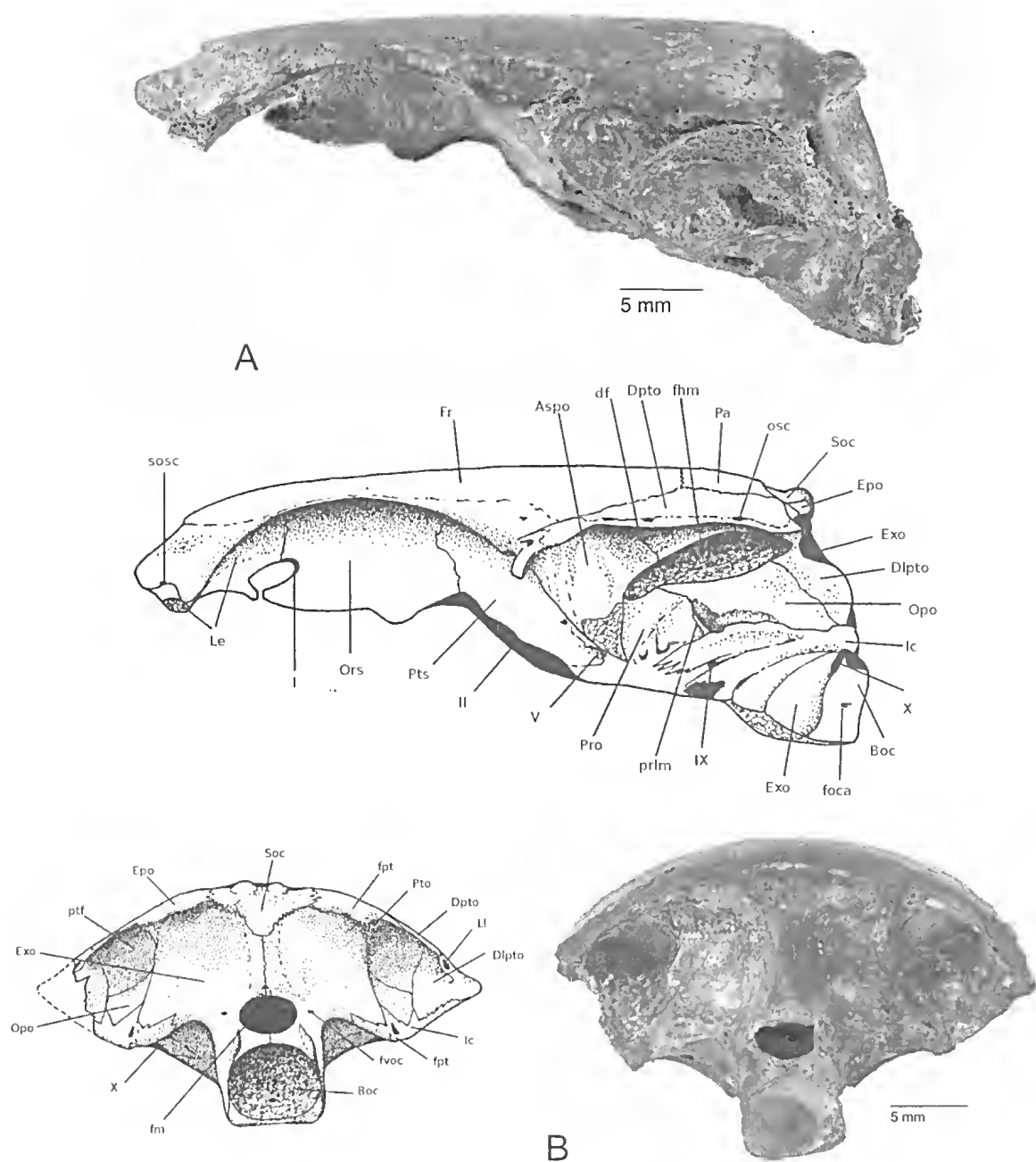


FIG. 2. *Canaryichthys rozefeldsi* gen. et sp. nov., QMF17025, Holotype. A, photograph of partial neurocranium in left lateral view above interpretative drawing. B, photograph of partial neurocranium in posterior view, beside interpretative drawing (slightly rotated anteroventrally to emphasise posterodorsal bones).

longer than broad and subovate in shape. A dorsal groove and indentation in rim of orbital wall present just in front of the autosphenotic spine, probably associated with sensory canal foramen directed ventrolaterally on the dorsal surface of the autosphenotic. No evidence of a ventral flange wrapping slightly around anterior of autosphenotic.

Dermopterotic with moderately large dorsal surface expression, ornamented similar to frontal. Lateral and posterodorsal margins bevelled and, except for minor contribution from autosphenotic, lateral edge provides roof for relatively deep dilatator fossa and bears otic sensory canal, with rare pores to surface, often within small processes above fossa roof. Canal opens posterolaterally above relatively large, external part of descending lamina of dermopterotic. Larger foramen opening posteriorly near dorsolateral margin of post-temporal fossa believed for entry of lateral line. Bone transversely and shallowly grooved just anterior to posterodorsal margin, with groove carrying numerous, minute pores. Descending lamina of dermopterotic provides posterolateral margin and wall of post-temporal fossa and appears to contribute to posterior of hyomandibular facet. Junction with opisthotic indistinct. Minor process of dermopterotic at dorsomedial rim of post-temporal fossa, lateral to epiotic adding support for supratemporal. Inside fossa, it extends anteriorly forming posterodorsal part of the inner wall, possibly uniting anteriorly with prootic. It appears to meet upper part of lateral margin of exoccipital along poorly defined junction near posterior of inner wall of post-temporal fossa.

Posterior neurocranial surface angled posteroventrally at angle of approximately 20° to vertical, with articulatory condyle for vertebral column projecting posteriorly even further (Fig. 2A). Sutural relationships of posterior neurocranial surface generally difficult to determine.

Supraoccipital relatively small, complex, extending broadly onto stepped, posterodorsal surface of neurocranium. Two prominent bosses present close to mid-line along posterodorsal neurocranial rim. Sutures with exoccipitals difficult to see at midline. Posterior surface

scooped dorsolaterally and continuing below epiotic (Fig. 2B).

Epiotic sturdy sutured medially to supraoccipital to provide epiotic process. Dorsally, epiotic meets parietal along base of posterior stepped margin and laterally has minimal contact with dermopterotic above the medial margin of the post-temporal fossa. Dorsomedially it carries a low swelling near junction with supraoccipital, apparently as support for supratemporal. Posterolateral surface ventrally scooped and broadly rounded onto medial wall of post-temporal fossa, meeting exoccipital ventrally. Posteromedially and within the dorsal margin and back of post-temporal fossa, it underlies dermopterotic. Epiotic process reduced.

Pterotic small, difficult to see, with anterior extent unknown, seen within post-temporal fossa as part of its inner wall, posteriorly meeting epiotic and dermopterotic dorsally.

Exoccipital forms largest element of posterior neurocranial surface. Junction with its counterpart present along base of foramen magnum; exoccipital provides lateral and dorsolateral margins of foramen magnum and extends dorsally to meet its counterpart along midline of broadly swollen, anterodorsally angled dorsoventral ridge from foramen magnum. Medial suture obscure. Element sharply flexed anteroventrally at level of top of foramen magnum and surface penetrated laterally by small foramen for posterior cerebral vein. Posterodorsal surface fanned and dished dorsolaterally, firmly fused with intercalar and epiotic. Below foramen magnum, it meets basioccipital just anterior to articulation for vertebral column; suture to basioccipital along the lateral neurocranial surface to near the posteroventral corner of intercalar, providing roof of foramen for nerve X.

Intercalar large, extending and expanding anteroventrally on lateral surface of neurocranium as longitudinally grooved, fan-shaped ridge of membranous bone from near lower corner of post-temporal fossa to cover most of anterolateral junctions between prootic and other elements and appears to meet flange from posterior process of parasphenoid. Intercalar provides posteroventral corner of subtemporal

fossa and supports narrow ridge dividing subtemporal fossa. Posteriorly, it surrounds lower margins of foramen for vagus nerve. Foramen for glossopharyngeal nerve contained in longitudinal flexure in anteroventral fan of intercalar, below subtemporal fossa. Sharply defined, anterodorsal ridge divides subtemporal fossa anteriorly, apparently above the prootic-opisthotic junction, probably providing an origin for branchial levator muscles.

Posterior of basioccipital preserved but anterior lacking. Articulating condyle includes very deep, conical notochordal pit, lined with dense, smooth, apparently lamellar bone. A small foramen, presumably for occipital artery, present laterally towards posteroventral rim of condyle. Anteriorly, large opening present above the element, representing remnants of vestibular fontanelle. Basioccipital contributes small dorsal process at ventrolateral margin of foramen magnum as vertebral condyle.

Opisthotic meets descending lamina of the dermopterotic to contribute significantly to the posterior of dorsolateral neurocranial surface. It meets prootic anteriorly and intercalar ventrally. Junction with prootic difficult to define but appears to be generally inclined anterodorsally before looping around front of deeply concave and anteroventrally angled, prominent hyomandibular facet. Subtemporal fossa is restricted but relatively deep above fan of intercalar

Prootic forms bulk of anteroventral lateral face of neurocranium. Dorsally, it meets dermopterotic at anterior edge of hyomandibular facet. Anteriorly, a small foramen present near side of roof of posterior myodome, interpreted as for internal carotid artery. Slightly above this is an indistinct foramen for nerve VII. Anterolaterally, a well-defined groove extends from foramen for nerve V back to foramen, possibly for entry of jugular canal. Medially directed plate of prootic meets its counterpart to form prootic bridge (Fig. 1B) above posterior myodome and is penetrated by a foramen, possibly for abducens nerve. Lateral to this is small foramen interpreted as for passage of facial nerve.

Autosphenotic relatively large, with a ventromedially angled sharp ridge to a delicate, well defined, anteroventrally projecting autosphenotic spine. Lateral face larger posterior to sharp ridge than the anterior. Foramen for recurrent branch of facial nerve present near margin of anterolateral face; several small foramina for ascending branches of superficial ophthalmic nerves also occur on anterior face. It meets prootic at anterior of hyomandibular facet, skirts anterodorsal margin of facet before turning anterodorsally then extended into short posteriorly narrowing process below dermopterotic margin of dilator fossa. Dorsal surface very small and is unornamented; surface penetrated above and posterior to autosphenotic spine by large foramen for anterior of sensory canal leading to shallow groove and marginal gap, below excavated shelf interpreted for dermosphenotic.

Pterosphenoid large, surrounding side of large opening for optic nerve. It smoothly and slightly bulges and, with anterior face of autosphenotic, forms the posterodorsal margin of orbit. Posteroventrally, it contributes to well-defined groove leading from foramen interpreted as being for trigeminal nerve, while foramen for oculomotor nerve exists at anteromedial edge of opening of optic nerve opening and outside scar for basisphenoid junction. No evidence exists for presence of pterosphenoid pedicle. Close to junction with autosphenotic, pterosphenoid penetrated by foramina for trochlea nerve and possibly that for recurrent branch of facial nerve. Anteriorly, bone firmly sutured to orbitosphenoid.

Orbitosphenoid relatively large, anteriorly surrounds central foramen for olfactory nerves. Ventromedially, bone lacks an ossified interorbital septum but is roughened, suggesting cartilagenous connection towards upper surface of parasphenoid. It also forms anteriorly 'V'-shaped anterodorsal roof of optic foramen. Small foramen for anterior cerebral vein present towards middle of bone.

Lateral ethmoid relatively short and firmly united with base of frontal, extending anteriorly from near middle of orbit to below stepped margin of the frontal. Broad plate of bone angled

anterolaterally beside anterolateral base of orbitosphenoid, thickening towards its roughened end. Anteriorly, its dorsal surface extends anterior to frontal and is slightly angled ventrally. Element linked to counterpart along a narrow, medial ridge that extends from its anterior extremity, posteriorly to short spine above foramen for olfactory nerves, approaching but not contacting an anteromedial spine of orbitosphenoid also above foramen for olfactory nerves. Body of bone curves anteroventrally, broadening from its junction with anterior margin of orbitosphenoid, with its end suggesting a cartilage junction to anteroventral neurocranial elements, most probably a pre-ethmoid. It has smoothly curved posteroventral surface forming anterodorsal margin of orbit.

## DISCUSSION

Description of *Canaryichthys rozefeldsi* gen. et sp. nov., adds to the diversity of neopterygian halecomorph fishes in the marine, Early Cretaceous (Albian), Toolebuc Formation sediments of the Eromanga Basin. Known only from the western rim of the Basin, from near Boulia, CW Qld, the species co-existed in that area with *Richmondichthys sweeti* (Etheridge Jnr. & Woodward 1891), revised by Bartholomai (2004) and *Australopachycormus hurleyi*, described by Kear (2007), representatives of the halecomorph orders Aspidorhynchiformes and Pachycormiformes respectively. Remains of other, as yet undescribed marine halecomorphs are known from largely incomplete or fragmentary fossils from the Toolebuc and contemporaneous Allaru Formations in the collections of the Queensland Museum. Although the partial neurocranium of *Canaryichthys* is preserved in a three-dimensional, undistorted condition, it unfortunately presents none of the characters considered by other researchers to be unquestionably diagnostic for its reference to any of the recognised halecomorph orders. The general characters presented in the neurocranium show that the species cannot be assigned to either of the previously described Eromanga taxa. Older marine Cretaceous deposits of mainly Aptian/ Early Albian age in the Eromanga Basin are noted to have a broad

reptilian fauna but only rarely have fish remains been recorded (Cook *et al.* 2014). Similarly, even the earlier Jurassic Gondwana fish record, as reported by Lopez-Arbarello *et al.* (2008), is highly incomplete both stratigraphically and geographically. They observe that this limits the ability to suggest phylogenetic relationships taking account of earlier fishes of the Southern Hemisphere.

The current study thus draws on comparison of the neurocranium of *Canaryichthys* with those described halecostome genera having general skull morphology similar to the new species, such comparisons suggesting the species is probably referable to the Order Ionoscopiformes (see Fig. 3). Relevant neurocranial characters were also compared in published data matrix analyses in Grande & Bemis (1998) for *Ionoscopus cyprinioides* from the Late Jurassic, Solenhofen Limestone of Germany, for *Oshunia brevis* from the Early Cretaceous, Santana Formation from Brazil, for the European *Ophiopsis procera* and for *Macrepistius arenatus*, from the Early Cretaceous (Albian) of Texas.

Grande and Bemis (1998) provided a cladistic analysis of the Halecomorphi based on 69 morphological characters mainly focused on the Amiidae and their study included both Caturoidea and Ionoscopiformes, among others, as outgroups. They indicated that groups closer to the Amiidae received more complete taxonomic coverage than more distantly related groups, like the caturoids and ionoscopiforms. The Amiiformes, including the caturoids, are defined by three characters, only two of which relate to *Canaryichthys*. These are the presence of an opisthotic and the presence of a pterotic. Grande & Bemis (1998) however, contradicted this by noting that the pterotic is absent in caturids, sinamiids and amiids. Of the characters defining the Caturoidea, none are represented in the partial neurocranium of *Canaryichthys*. Three characters were determined to define the halecomorph Section B (unnamed by Grande & Bemis 1998) that included the Amiiformes and the Ionoscopiformes. Of these, only the condition of the dermosphenotic has relevance to comparison with *Canaryichthys*.

This character is stated to be usually firmly sutured into the skull roof in adult halecomorphs, but must have been only loosely attached in *Canaryichthys* because it is missing and represented by a possible scar on both sides of the skull. Of the two characters identified as diagnostic for the Ionoscopiformes, the first refers to an inner-orbital dermosphenotic flange, not present in *Canaryichthys*. The other relates to parietal shape, where the parietal width to length ratio of 0.85 falls below the upper limit of 0.90, determined by Grande & Bemis (1998) for the order. However, they note that this character is homoplasious and polymorphic in the ophiostids, *Ophiopsis* and *Macrepistius* and is therefore of no value in interpreting phylogenetic relationships in these groups. Subsequent cladistic analyses by Alvarado-Ortega & Espinosa-Arrubarrena (2008) on the early Cretaceous, ionoscopiforms *Quetzalichthys* and *Teoichthys*, from the Early Cretaceous (Albian) Tlayua Formation of Mexico, regard the parietal character as plesiomorphic. Analysis of *Cipactlichthys*, also from Mexico, by Brito & Alvarado-Ortega (2013) who referred it to the Ionoscopiformes, does not include any additional characters, than those previously identified in Grande & Bemis (1998), that are relevant to understanding the phylogenetic relationships of *Canaryichthys*. Similarly, the analysis in Lopez-Arbarella *et al.* (2014) for the Triassic (?Ladinian) ionoscopiform, *Archaeosemionotus* of Europe does not provide additional characters relevant to the placement of *Canaryichthys*. Modifications to the phylogenetic relationships in this group, however, were proposed, as new taxa were described and with the reassessment of existing forms such as *Furo*.

The dermopterotic in *Caturus furcatus*, (illustrated in Grande & Bemis, 1998) is generally very expanded posteriorly and significantly longer than the parietal; supraorbitals are present in *C. furcatus* but are mostly absent in ionoscopiforms depicted; the presence of an opisthotic in ionoscopiforms contrasts with the caturids where it is absent. A small pterotic is present in *Canaryichthys* but is absent in caturids; unlike most halecomorphs,

the dermosphenotic is interpreted to be only loosely attached to the skull roof and no inner orbital flange appears present; and a supraoccipital is present. Regarding the occiput and occipital condyle, Grande & Bemis (1998) observed that those halecomorphs lacking ossified centra, such as the caturids, had occiputs that are difficult to interpret, with basioccipital/exoccipital sutures sometimes missing. The occiput in *Canaryichthys* involves the basioccipital, with the exoccipital only contributing to the base of the condyles. Based on these insights qualified reference of *Canaryichthys* to the Ionoscopiformes, as defined by Grande & Bemis (1998), rather than to the Caturidae seems preferable. The phylogenetic relationship of *Canaryichthys* within the order is not clear.

Our understanding of halecomorph phylogeny largely builds on Grande & Bemis (1998) who noted that 'many of the non-amiid halecomorph groups needed comprehensive phylogenetic study, using modern preparation techniques and new material including Ionoscopiformes'. With the description of new fish, the record of halecostomes has improved significantly, in part, due to the new discoveries from Mexican and Brazilian early Cretaceous deposits. Cladistic analysis of the Ionoscopiformes by Alvarado-Ortega & Espinosa-Arrubarrena (2008) recognised two monophyletic families, the Ionoscopidae and the Ophiopsidae, adding the Early Cretaceous genera *Quetzalichthys* from Mexico and *Oshunia* from Brazil to the ionoscopids (the latter previously having been placed in a separate family, the Oshuniidae by Grande and Bemis, 1998). *Taoichthys* from the Early Cretaceous of Mexico was added to the Ophiopsidae by Alvarado-Ortega & Espinosa-Arrubarrena (2008), as well as *Macrepistius*, supported by an additional species of *Teoichthys* by Machado *et al.* (2013). Brito & Alvarado-Ortega (2013) added their Early Cretaceous Mexican taxon, *Cipactlichthys*, as a monophyletic sister group of the ionoscopiformes + Amiiformes. The relationships within the ionoscopiforms were further addressed by Lopez-Arbarella *et al.* (2014), who concluded that *Furo*, *Archaeosemionotus* and *Robustichthys*

(see Xu *et al.* 2014) form a clade, and they included *Macrepistius* within the Ophiosidae. Based on the Grande & Bemis (1998) analysis, summarised previously above, the familial relationships of *Canaryichthys* can only be regarded as *incertae sedis*. Incompleteness of the holotype of *Canaryichthys* precludes it contributing significantly to resolution of the arguments relating to relationships within basal neopterygians (see Gardiner *et al.* 1996) but it does add to a better understanding of the morphology of the bones often masked by dermal elements.

Comparison of the neurocrania of *Canaryichthys* and *Ionoscopus*, here illustrated in Figs. 3A and 3B, shows considerable broad similarities, supporting a possible relationship within the Ionoscopiformes. However, the cranial vault in *Ionoscopus* is incompletely ossified and the opisthotic is very small and only weakly in contact with surrounding bones (Massey, 1999). Like *Canaryichthys*, its pterotic is small, wedged between the dermopterotic and epiotic within the post-temporal fossa. It does, however, have a supraotic bone, lacking in *Canaryichthys*. The posterior neurocranial surface in both is similarly sloped and the cranial vault is shallow. The parasphenoid process extends over more of the autosphenotic in *Ionoscopus*.

Reasonable superficial similarity also exists between the preserved neurocranium of *Canaryichthys* and the partial crania described and illustrated by Rayner (1948) as '*Aspidorhynchus*' sp. from Middle Jurassic (Bathonian) sediments of Great Britain (Figs. 3B and 3C). It was subsequently regarded as a caturid by Patterson (1973), who suggested it was intermediate between the Jurassic *Heterolepidotus* and the Cretaceous *Macrepistius*. Patterson (1975) undertook a further revision and restoration of this neurocranial material referring to it again as an undescribed caturid, '*Aspidorhynchus*' sp. This material was later given attention by Gardiner *et al.* (1996), who suggested that the presence of a pterotic and opisthotic and the non-sutured condition of the dermosphenotic conflict with it being firmly referred to the Caturidae and it was regarded

as 'enigmatic'. '*Aspidorhynchus*' sp. was omitted from their phylogenetic analysis of the fossil halecomorphs because it was too incompletely known. The slightly inclined posterior intracranial surface in *Canaryichthys* differs from the near-vertical posterior in '*Aspidorhynchus*' sp. It also differs in lacking a supraotic, present posterodorsally in '*Aspidorhynchus*' sp. The cranial vault width to depth ratio of 1.80 in *Canaryichthys* is considerably larger than the 1.33 in '*Aspidorhynchus*' sp., the supraoccipital is present and the epiotic is much less developed. The Queensland taxon also possesses a prominent, deep, inclined hyomandibular fossa and has a much smaller prootic, a larger and inclined opisthotic and a larger autosphenotic. The foramen for nerve IX in *Canaryichthys* lies in a fold of the intercalar while that in '*Aspidorhynchus*' sp. enters directly onto the prootic. Maisey (1999) concluded that '*Aspidorhynchus*' sp. 'may belong to an ionoscopid or some closely related halecomorph'. Although *Canaryichthys* shares some similarities with '*Aspidorhynchus*' sp., they do not appear to be closely related.

Gardiner *et al.* (1996) noted that the braincase in '*Aspidorhynchus*' sp. is 'remarkably similar (both in general appearance and in many details) to the braincase of *Oshunia*,' originally regarded as an Ionoscopiform by Wenz & Kellner (1986) and revised and illustrated by Maisey (1991). *Oshunia* is from the Lower Cretaceous (Aptian) Santana Formation of the Araripe Basin of Brazil. It was photographically illustrated in Grande & Bemis (1998) and had additional morphological detail added by Maisey (1999). The drawing here presented in Fig. 3D is based on the photograph and drawings of a near-complete, acid-prepared specimen of *Oshunia* figured in Maisey (1999).

The lateral aspect of the neurocranium of *Canaryichthys* (Fig. 3B) shows it has somewhat more strongly inclined posterior neurocranial and orbital surfaces than *Oshunia* (Fig. 3D). A supraotic bone present in *Oshunia* is lacking in *Canaryichthys*. The parietals are relatively longer in *Canaryichthys* and their sutural contact with the frontals is much less interdigitated. Further, *Oshunia* does not have a pterotic bone, present in the Queensland taxon. The prootics

in both are relatively of similar size but, while the opisthotic is much smaller in *Oshunia*, it is firmly attached to the surrounding bones (Fig. 3D). The supraoccipital separates the epiotics in *Canaryichthys* and there are two rounded, posterodorsal bosses near the midline. The supraoccipital is not present in *Oshunia* where the epiotics (= epioccipitals in Maisey, 1999) have an extensive suture. The exoccipital in *Canaryichthys* does not extend anterior to the foramen for the vagus nerve and the autosphenotic is only slightly relatively larger. Loss of the base of the neurocranium in *Canaryichthys* has exposed a ventrolateral void that most probably represents the remaining area of the vestibular fontanelle. The process from the intercalar, like that in *Oshunia*, provides the origin for the branchial levator muscles and is very well defined near the middle of the small but relatively deep subtemporal fossa in *Canaryichthys*. In dorsal view, Maisey (1991) indicates that the frontals in *Oshunia* are constricted above the orbits, then widen again over the ethmoid region. Those in *Canaryichthys* (Fig. 1A) narrow slightly. The lateral aspect of the neurocranium in *Oshunia*, shows that apart from the presence of a strongly developed, posterior dermopterotic spine, *Oshunia* has almost as many general morphological similarities with *Canaryichthys* as does '*Aspidorhynchus*' sp. (Fig. 3C). Gardiner *et al.* (1996) provide a detailed comparison of the basal neopterygians, including *Oshunia* and *Macrepistius arenatus*, revised by Schaeffer (1960) and supported by further description of the neurocranium of the latter taxon in Schaeffer (1971). *Macrepistius* is regarded as an ophiopid by Alvarado-Ortega & Espinosa-Arrubarrena (2008) along with *Teoichthys* (differing from *Canaryichthys* by possession of a series of supraorbital bones). The anterior foramen for the supraorbital sensory canal in *Canaryichthys* is similarly positioned with regard to the possible nasal to that in *Caturus porteri*, described and figured by Rayner (1948), a character that is not, however, considered to provide insights into relationships. However, although close relationship of *Canaryichthys* with *Oshunia* is unlikely, its reference to the ionoscopids is possible, based on the overall,

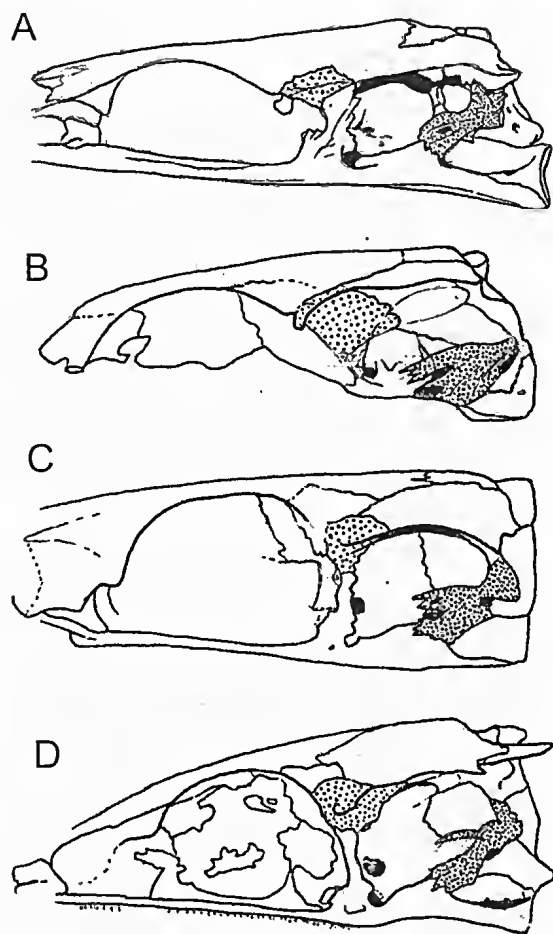


FIG. 3. Lateral view of neurocrania (not to scale) in the following- A, *Ionoscopus cyprinoides* (from photograph and drawing in Maisey, 1999); B, *Canaryichthys rozefeldsi* gen. et sp. nov.; C, '*Aspidorhynchus*' sp. (from Rayner, 1948); and D, *Oshunia brevis* (from photograph and drawing in Maisey, 1999). Dense stipple for intercalar and sparse stipple for autosphenotic.

broad similarities exhibited in its neurocranial remains.

Having regard to the comparisons with the genera discussed by Gardiner *et al.* (1996), the following notes are also considered to be relevant. Although the ascending process of the parasphenoid in *Canaryichthys* is not preserved, the scar left on the lateral surface of its braincase shows it most probably met



the lateral face of the autosphenotic towards its base, relatively lower than in *Oshunia* and '*Aspidorhynchus*' sp. Gardiner *et al.* (1996) regard the shortened parietals as primitive, although that in *Canaryichthys* with a W: L ratio of 0.85 is relatively close to the limit proposed for ionoscopiforms. The dermopterotic in the Queensland taxon is much longer than the parietal, unlike that in *Macrepistius* and more like that in other ionoscopids, as seen in *Oshunia*. The pterotic is also recorded as primitively present in extinct, non-amiid halecomorphs but is developed differently from one group to another. It is relatively small and present within the post-temporal fossa in *Canaryichthys* and in both *Oshunia* and *Ionoscopus*, as well as in '*Aspidorhynchus*' sp.

The intercalar in *Canaryichthys* (Fig. 2A) extends as a fan over the lower part of the saccular chamber that appears to have met the posterior process of the parasphenoid, as in *Macrepistius*, *Oshunia*, *Ionoscopus* and a number of other halecomorph fishes, a feature considered a possible synapomorphy by Gardiner *et al.* (1996). The orbitosphenoid is well developed in *Ionoscopus*, *Oshunia* and *Macrepistius*, similar to that in *Canaryichthys*. There is no evidence for the presence of an ossified interorbital septum in *Canaryichthys*, a well-developed structure in *Oshunia* and *Macrepistius* but the ventral base of the orbitosphenoid shows there was probably some cartilaginous interorbital septum development. The wide separation and spreading nature of the lateral ethmoids suggests that direct contact with the parasphenoid was unlikely in *Canaryichthys*. The bone probably contacted a pre-ethmoid, as in *Oshunia*, illustrated by Maisey (1991). *Canaryichthys* retains an opisthotic, as do non-amiid halecomorphs. The dermosphenotic was only loosely attached to the skull roof within a distinct, scarred recessed area within the autosphenotic and frontal. A shallow notch exists in the orbital margin in front of the autosphenotic spine but does not appear to have been associated with a flange that would have wrapped around the front of the spine. Until more complete material becomes available, further conjecture regarding the

phylogenetic significance of the element or its loss would be premature.

Ornamentation of the dorsal skull roof is similar to that in *Macrepistius*, as illustrated by Schaeffer (1971) but is much reduced in *Canaryichthys* (Fig. 1A). Bartram (1975) indicates the presence of ganoine tubules as ornamentation on dermal bones of the skull roof in the Upper Jurassic *Ophiopsis* from Europe (a genus also recorded from the Cretaceous of Brazil by Bartram, 1975 and Maisey, 1991). Tubules are visible within the ganoine in *Canaryichthys*. The dorsal aspect of the neurocranial roof in *Ophiopsis* has similar form to that in *Macrepistius* but is even more waisted above the orbits. The anterior shelf of the neurocranial roof in *Canaryichthys* descends at about the same angle from the rest of the roof as in *Macrepistius* but that in the former taxon is much shorter. Gardiner *et al.* (1996) recognised a monophyletic group that included *Oshunia* and *Ionoscopus*, as well as *Macrepistius*.

There appears to be slightly greater general morphological affinity present with the ionoscopid part of the group than with the ophiopsids. However, as noted above, diagnostic familial morphological characters are not preserved in the Eromanga specimen. Lopez-Arbarello, Rauhut & Moser (2008) indicated that ionoscopids were not represented in Gondwana faunas and were restricted to the Kimmeridgian-Tithonian of Europe, although the recent work by Alvarado-Ortega & Espinosa-Arrubarrena (2008) in describing *Quetzalichthys* from the Middle to Upper Albian limestones of Puebla, Mexico referred it to the Ionoscopidae and included *Oshunia* in that group, extended both stratigraphic and geographic limits for the family. *Quetzalichthys*, similar to *Oshunia*, had projecting processes from the posterior of the neurocranium. These were, however, more brush-like. As mentioned above, no such structure is present in *Canaryichthys*.

Brito & Yabumoto (2011) concluded that the southern and central American fishes had a close relationship with the Tethys fauna rather than supporting earlier ideas associating the fauna with the opening of the South Atlantic



Ocean. Regardless of the lack of firm ordinal and familial relationships between *Canaryichthys* and described ionoscopiforms, the taxon suggests a possible presence of greater ionoscopiformes radiation within the Gondwana fish fauna. Further discoveries from the Australian Lower Cretaceous sediments may shed additional information on Ionscopiformes relationships. The presence of *Canaryichthys* indicates the necessity for a broader overview of ionoscopiformes evolution generally.

### ACKNOWLEDGEMENTS

The author wishes acknowledge the mechanical preparation work undertaken on the specimen by Dr Andrew Rozefelds. His critical advice in his current capacity as Head of the Queensland Museum Geosciences Section, is greatly appreciated. Photography of the holotype was undertaken by Mr Geoff Thompson of the Queensland Museum.

### LITERATURE CITED

- Alvarado-Ortega, J. & Espinosa-Arrubarrena, L. 2008. A new genus of ionoscopiform fish from the Lower Cretaceous (Albian) lithographic limestones of the Tlayua Quarry, Puebla, Mexico. *Journal of Paleontology* 82: 163–75 (<http://dx.doi.org/10.1666/04-152.1>).
- Bartholomai, A. 1969. The Lower Cretaceous elopoid fish *Pachyrhizodus marathoniensis* (Etheridge Jnr.) Pp. 249–263. In Campbell, K.S.W., (ed.) *Stratigraphy and Palaeontology, Essays in Honour of Dorothy Hill* (ANU University Press: Canberra).
2004. The large aspidorhynchid fish, *Rielmundichthys sweeti* (Etheridge Jnr. and Smith Woodward, 1891) from Albian marine deposits of Queensland, Australia. *Memoirs of the Queensland Museum* 49: 521–36.
2012. The pachyrhizodontid teleosts from the marine Lower Cretaceous (latest mid to Late Albian) sediments of the Eromanga Basin, Queensland, Australia. *Memoirs of the Queensland Museum* 56: 119–48.
- Bartram, A.W.H. 1975. The holostean fish genus *Ophiopsis* Agassiz. *Zoological Journal of the Linnean Society* 56: 183–205 (<http://dx.doi.org/10.1111/j.1096-3642.1975.tb00263.x>).
- Brito, P.M. & Alvarado-Ortega, J. 2013. *Cipaetlichthys* scutatus from the Lower Cretaceous Tlayua Formation of Mexico. *PLoS ONE* 8(9): 0073551.
- Brito, P.M. & Yabumoto, Y. 2011. An updated review of the fish faunas from the Crato and Santana Formations in Brazil, a close relationship to the Tethys fauna. *Bulletin of the Kitakyushu Museum of Natural History, Series A*, 9: 107–36 (<http://dx.doi.org/10.1371/journal.pone.0073551>).
- Cook, A.G. 2012. Cretaceous faunas and events, northern Eromanga Basin, Queensland. *Episodes* 35: 153–9.
- Cook, A.G., Mc Kellar, J.L. & Draper, J.J. 2013. Eromanga Basin. Pp. 523–533. In, Jell, P.A. (ed.) *Geology of Queensland*. (Geological Survey of Queensland: State of Queensland).
- Gardiner, B.G., Maisey, J.G. & Littlewood, D.T.J. 1996. Interrelationships of basal neopterygians. Pp. 117–146. In, Stiassny, M., Parenti, L.R. & Johnson, G.D. (eds) *Interrelationships of Fishes* (Academic Press: San Diego) (<http://dx.doi.org/10.1016/B978-012670950-6/50007-2>).
- Grande, L. 2010. An empirical synthetic pattern study of gars (Lepisosteiformes) and closely related species, based mainly on skeletal anatomy. The resurrection of Holostei. *Copeia*, Special Publication 6: 1–871.
- Grande, L. & Bemis, W.E. 1998. A comprehensive phylogenetic study of amiid fishes (Amiidae) based on comparative skeletal anatomy. An empirical search for interconnected patterns of natural history. *Society of Vertebrate Paleontology, Memoir* 4. Supplement to *Journal of Vertebrate Paleontology*, 18(1): ix + 690pp.
- Jell, P.A., Draper, J.J. & McKellar, J. 2013. Great Artesian Superbasin. Pp. 517. In, Jell, P.A. (ed.) *Geology of Queensland* (Geological Survey of Queensland: State of Queensland).
- Kear, B.P. 2007. First record of a pachycormid fish (Actinopterygii: Pachycormiformes) from the Lower Cretaceous of Australia. *Journal of Vertebrate Paleontology* 27: 1033–1038 ([http://dx.doi.org/10.1671/0272-4634\(2007\)27\[1033:FROAPF\]2.0.CO;2](http://dx.doi.org/10.1671/0272-4634(2007)27[1033:FROAPF]2.0.CO;2)).
- Kear, B.P., & Hamilton-Bruce, R.J. 2011. Dinosaurs in Australia. *Mesozoic Life from the Southern Continent*. (CSIRO Publishing: Victoria). IX + 190 pp.
- Lopez-Arbarello, A., Rauhut, O.W.M. & Moser, K. 2008. Jurassic fishes of Gondwana. *Revista de la Asociacion Geologica Argentina* 63: 586–612.
- Lopez-Arbarello, A., Stockar, R. & Burgin, T. 2014. Phylogenetic relationships of the Triassic *Archeoscionotus* Deecke (Halecomorphi: Ionoscopiformes) from the 'Perledo Fauna'. *PLoS ONE* 9(10): 108665 (<http://dx.doi.org/10.1371/journal.pone.0108665>).
- Machado, G.P., Alvarado-Ortega, J.A., Machado, L.P. & Brito, P.M. 2013. *Teoichthys brevipinga* sp. nov. a new ophiopsid fish (Halecomorph, Ionoscopiformes) from the Lower Cretaceous Tlayua Formation, central Mexico. *Journal of Vertebrate Paleontology* 33(2): 482–487 (<http://dx.doi.org/10.1080/02724634.2013.729962>).

- Maisey, J.G. 1991. *Oshunia* Wenz & Kellner, 1986. Pp. 157–68. In, Maisey, J.G. (ed.) *Santana Fossils: an Illustrated Atlas. Contributions to IUGS-IGCP Project No. 242, the Cretaceous of South America* (TFH Publications Inc.: New Jersey).
- Maisey, J.G. 1999. The supraotic bone in neopterygian fishes (Osteichthyes, Actinopterygii). *American Museum Novitates* **3267**: 1–52.
- Patterson, C. 1973. Interrelationships of holosteans. In, Greenwood, P.H., Miles, R.S. & Patterson, C. (eds). 'Interrelationships of Fishes', Supplement No. 1, *Zoological Journal of the Linnean Society* **53**: 233–306.
- Patterson, C. 1975. The braincase of pholidophorid and leptolepid fishes, with a review of the actinopterygian braincase. *Philosophical Transactions of the Royal Society of London, B. Biological Sciences* **269**: 275–579 (<http://dx.doi.org/10.1098/rstb.1975.0001>).
- Rayner, D.H. 1948. The structure of certain Jurassic holostean fishes with special reference to their neurocrania. *Philosophical Transactions of the Royal Society of London, B. Biological Sciences* **233**: 287–345 (<http://dx.doi.org/10.1098/rstb.1948.0006>).
- Schaeffer, B. 1960. The Cretaceous holostean fish *Macrepistius*. *American Museum Novitates* **2011**: 1–18.
- Schaeffer, B. 1971. The braincase of the holostean fish *Macrepistius*, with comments on neurocranial ossification in the Actinopterygii. *American Museum Novitates* **2459**: 1–34.
- Xu, G-H, Zhao, L-J. & Coates, M. 2014. The oldest ionoscopiform from China sheds new light on the early evolution of halecomorph fishes. *Biological Letters* **10**(5): 20140204 (<http://dx.doi.org/10.1098/rsbl.2014.0204>).

# A taxonomic assessment of the Australian Dusky Antechinus Complex: a new species, the Tasman Peninsula Dusky Antechinus (*Antechinus vandycki* sp. nov.) and an elevation to species of the Mainland Dusky Antechinus (*Antechinus swainsonii mimetes* (Thomas))

Baker, A.M.

Queensland University of Technology, 2 George Street, Brisbane, Qld, 4001, Australia. Corresponding Author Email: am.baker@qut.edu.au

Queensland Museum, PO Box 3300, South Brisbane Qld 4101

Mutton, T.Y.

Mason, E.D.

Gray, E.L.

Queensland University of Technology, 2 George Street, Brisbane, Qld 4001 Australia.

Citation. Baker, A.M., Mutton, T.Y., Mason, E.D. & Gray, E.L. 2015. A taxonomic assessment of the Australian Dusky Antechinus Complex: a new species, the Tasman Peninsula Dusky Antechinus (*Antechinus vandycki* sp. nov.) and an elevation to species of the Mainland Dusky Antechinus (*Antechinus swainsonii mimetes* (Thomas)). *Memoirs of the Queensland Museum – Nature* 59: 75-126. Brisbane. ISSN 2204-1478 (Online), ISSN 0079-8835 (Print). Accepted: 25 November 2014. First published online: 26 May 2015.

<http://dx.doi.org/10.17082/j.2204-1478.59.2015.2014-10>

LSID - [lsid:zoobank.org/pub:OFC36E36-D655-4C82-A356-519105200E83](http://zoobank.org/pub:OFC36E36-D655-4C82-A356-519105200E83)

## ABSTRACT

In 2014, the northern outlying population of carnivorous marsupial Dusky Antechinus (*Antechinus swainsonii*) was nominated a new species, *A. arktos*. Here, we describe a further new species in the dasyurid *A. swainsonii* complex, which now contains five taxa. We recognise two distinct species from Tasmania, formerly represented by *A. swainsonii swainsonii* (Waterhouse); one species (and 2 subspecies) from mainland south-eastern Australia, formerly known as *A. swainsonii mimetes* (Thomas) and *A. swainsonii insulanus* Davison; and one species from the Tweed Caldera in mid-eastern Australia, formerly known as *A. s. mimetes* but recently described as *A. arktos* Baker, Mutton, Hines and Van Dyck. Primacy of discovery dictates the Tasmanian Dusky Antechinus *A. swainsonii* (Waterhouse) is nominate; the Mainland Dusky Antechinus taxa, one raised from subspecies within *A. swainsonii mimetes* (Thomas) is elevated to species (now *A. mimetes mimetes*) and the other, *A. swainsonii insulanus* Davison is transferred as a subspecies of *A. mimetes* (now *A. mimetes insulanus*); a species from Tasmania, the Tasman Peninsula Dusky Antechinus, is named *A. vandycki* sp. nov. These taxa are strongly differentiated: geographically (in allopatry), morphologically (in coat colour and craniodental features) and genetically (in mtDNA, 7.5-12.5% between species pairs). □ *Marsupialia*, *Dasyuridae*, *dasyurid*, *carnivorous marsupial*, *Antechinus swainsonii*, *mimetes*, *insulanus*, *vandycki*, *taxonomy*, *Tasmania*, *Tasman Peninsula*.

The first antechinus was discovered by Geoffroy more than 200 years ago (1803), but the genus was not formally erected for almost another 40 years (Macleay 1841), shortly following the description of two other species by Waterhouse (in 1838 and 1840). Later, there followed two further new species, named by Thomas (in 1904 and 1923). No other species was named under *Antechinus* until Van Dyck (1980). In the decades that followed Van Dyck's description, the advent of molecular techniques permitted resolution of numerous cryptic taxa across many organismal groups, including mammals. A range of genetic studies in the 1980s/1990s tested relationships among various families and genera of Australian mammals, including dasyurids (e.g. Armstrong *et al.* 1998; Baverstock *et al.* 1982; Krajewski *et al.* 1997) and this work prompted description of other antechinus species (Dickman *et al.* 1998, Van Dyck & Crowther 2000). Van Dyck (2002) then conducted a comprehensive morphological review of antechinus, recognising ten extant species: Swamp Antechinus, *A. minimus* (Geoffroy); Yellow-footed Antechinus, *A. flavipes* (Waterhouse); Brown Antechinus, *A. stuartii* Macleay; Dusky Antechinus, *A. swainsonii* (Waterhouse); Fawn Antechinus, *A. bellus* (Thomas); Rusty Antechinus, *A. adustus* (Thomas); Atherton Antechinus, *A. godmani* (Thomas); Cinnamon Antechinus, *A. leo* Van Dyck; Agile Antechinus, *A. agilis* Dickman, Parnaby, Crowther & King and Subtropical Antechinus, *A. subtropicus* Van Dyck & Crowther.

In the past three years, prompted by Van Dyck's suspicions that further cryptic taxa lay unresolved within antechinus, our research group undertook a systematic and taxonomic revision of the extant members of the genus; several new species were described as a result (see Baker, Mutton & Hines 2013; Baker, Mutton, Hines & Van Dyck 2014; Baker, Mutton & Van Dyck 2012; Baker & Van Dyck 2012, 2013a, b). The discovery sequence ran as follows. First, Baker, Mutton & Van Dyck (2012) diagnosed an eleventh species, the Buff-footed Antechinus *A. mysticus*, previously referred to the ubiquitous Yellow-footed Antechinus, *A. flavipes*. Then, in the process of investigating the distributional

range of *A. mysticus* between south-east and mid-east Queensland, Baker, Mutton & Hines (2013) found a twelfth antechinus species, the Silver-headed Antechinus, *A. argentus*. At about the time of discovering *A. argentus*, we began to shift our focus within the genus to the Dusky Antechinus, *Antechinus swainsonii*. The thirteenth species of Antechinus, *A. arktos*, was duly raised after comparison of northern outlying Dusky Antechinus populations with other mainland *A. s. mimetes* (Baker, Mutton, Hines & Van Dyck 2014). But further investigation showed that *A. swainsonii* was even more complex and better resolution of this group is the aim of the present work.

*Antechinus swainsonii* was originally described by Waterhouse (1840) from a Tasmanian specimen held in the private collection of William Swainson and later acquired by the British Museum. About three years after the description, Waterhouse, deferring to the judgment of Gould, synonymised *A. swainsonii* with *A. minimus* (Geoffroy 1803); however, it was another three years before Waterhouse was able to examine the *A. minimus* holotype and re-establish *swainsonii*. Subsequently, Thomas (1924) described the subspecies *A. swainsonii mimetes* from the Guy Fawkes district, NSW. In a checklist of Australian mammals, Iredale and Troughton (1934) attributed the distribution 'Northern New South Wales' to *A. s. mimetes*, and 'Tasmania, Victoria' to *A. s. swainsonii*. In response, Wakefield & Warneke (1963) noted the absence of a geographical break in the mainland distribution of *A. swainsonii*, a lack of morphological distinction between the populations from northern New South Wales and Victoria, and minimal morphological variation between the Victorian and Tasmanian populations. They therefore proposed the trinomial *A. s. swainsonii* be applied only to representatives of the species from Tasmania. They maintained that Thomas' trinomial *A. s. mimetes* should apply to the entire mainland population. However, some 46 years before Iredale and Troughton had published their checklist, Thomas (1888) had also made reference to the Victorian occurrence of the species. And later, Thomas (1924) again noted the Victorian distribution of the nominate form

in his description of *A. s. mimetes*. Evidently, the establishment of *A. s. mimetes* was intended to contrast with the Victorian population, not contain it. Wakefield and Warneke (1963) were duly obliged to demonstrate sufficient division between Tasmanian and Victorian populations to justify retention of the trinomial *A. s. mimetes*; they could not do so, but in any case chose not to sink the subspecies.

More recent works have addressed the distinctiveness of mainland and Tasmanian subspecies of *A. swainsonii* (Smith 1983; Davison 1986, 1991). Smith (1983) examined electrophoretic variation in *A. swainsonii* on either side of Bass Strait and concluded that given a mean genetic distance of  $0.085 \pm 0.015$  the trans-Bassian populations of *A. swainsonii* warranted (at least) subspecific status. The sampling of *A. swainsonii* in Smith's study was limited to a couple of Tasmanian populations (Arthur River and Mt Wellington) and no sampling of the mainland population was included near Guy Fawkes (north-east New South Wales, the type locality for *A. swainsonii mimetes*), being limited instead to two sites in southern Victoria (Gembrook and East Gippsland) and one in the ACT/NSW (Brindabella Ranges). Nevertheless, Smith's early genetic work clearly pointed towards the Tasmanian *A. swainsonii* being distinctive from mainland Victoria *A. swainsonii*. Later, Davison (1991) named *A. s. insulanus* based on morphology alone, in recognition of the generally larger animals from the Grampians Range, western Victoria, when compared with other mainland *A. s. mimetes*.

With the aforementioned studies in mind, and after the northern mainland *A. swainsonii* (now *A. arktos*) was recently recognised as specifically distinct from mainland *A. s. mimetes*, the stage was set for a thorough taxonomic revision of *A. swainsonii* across its geographic range. Here, we report the results of this work. We provide detailed holotype descriptions of *A. vandycki* sp. nov., *Antechinus swainsonii* (Waterhouse 1840) and *Antechinus swainsonii mimetes* (Thomas 1924), none of which have been described in detail previously. For detailed holotype descriptions of the remaining two members of the Dusky Antechinus complex, *A.*

*swainsonii insulanus* Davison 1991 and *A. arktos* Baker, Mutton, Hines and Van Dyck 2014, we direct the reader to Davison (1991) and Baker *et al.* (2014), respectively.

## MATERIALS AND METHODS

Fig. 1 describes and depicts the 30 skull and dental, and 5 external measurements taken. Measurements were made using Mitutoyo CD-8CSX digital calipers. Age variation was minimised by using only animals which possessed fully erupted permanent P<sup>3</sup> teeth and thus deemed to be adult. Tooth nomenclature follows Archer (1974) and basicranial nomenclature follows Archer (1976). Colour nomenclature used in the holotype pelage description follows Ridgway (1912).

Measured variables are as follows (and see Fig. 1): **wt** = body weight (grams); **hb** = head-body length (mm) from tip of nose to mid-vent; **tv** = tail-vent length (mm) from mid-vent to tip of tail proper (excluding hair at tip); **hf** = hind foot length (mm) from behind heel to tip of longest extended toe (excluding claw); **e** = ear length (mm) from extended ear tip to notch at rear base of tragus; **APV** = maximum anterior palatal vacuity length; **BL** = basicranial skull length, excluding incisors; **Dent** = dentary length, excluding incisors; **IBW** = minimum width between auditory bullae; **IOW** = minimum width of interorbital constriction; **IPV** = minimum interpalatal vacuity distance; **M<sup>2</sup>W** = maximum width of upper molar 2 measured diagonally from anterior lingual to posterior labial points; **NW** = width of nasals at the nasal / premaxilla / maxilla junction; **OBW** = basicranial width from outside right and left auditory bullae; **PPV** = maximum posterior palatal vacuity length; **R-LC<sup>1</sup>** = skull width level with the posterior of upper canines; **R-LM<sup>1</sup>** = skull width level with the junction of the first and second upper molars; **R-LM<sup>1</sup>T** = maximum width between the ectolophs of the left and right first upper molars; **R-LM<sup>2</sup>** = skull width level with the junction of the second and third upper molars; **R-LM<sup>3</sup>** = skull width level with the junction of the third and fourth upper molars; **ZW** = maximum zygomatic width; **HT**

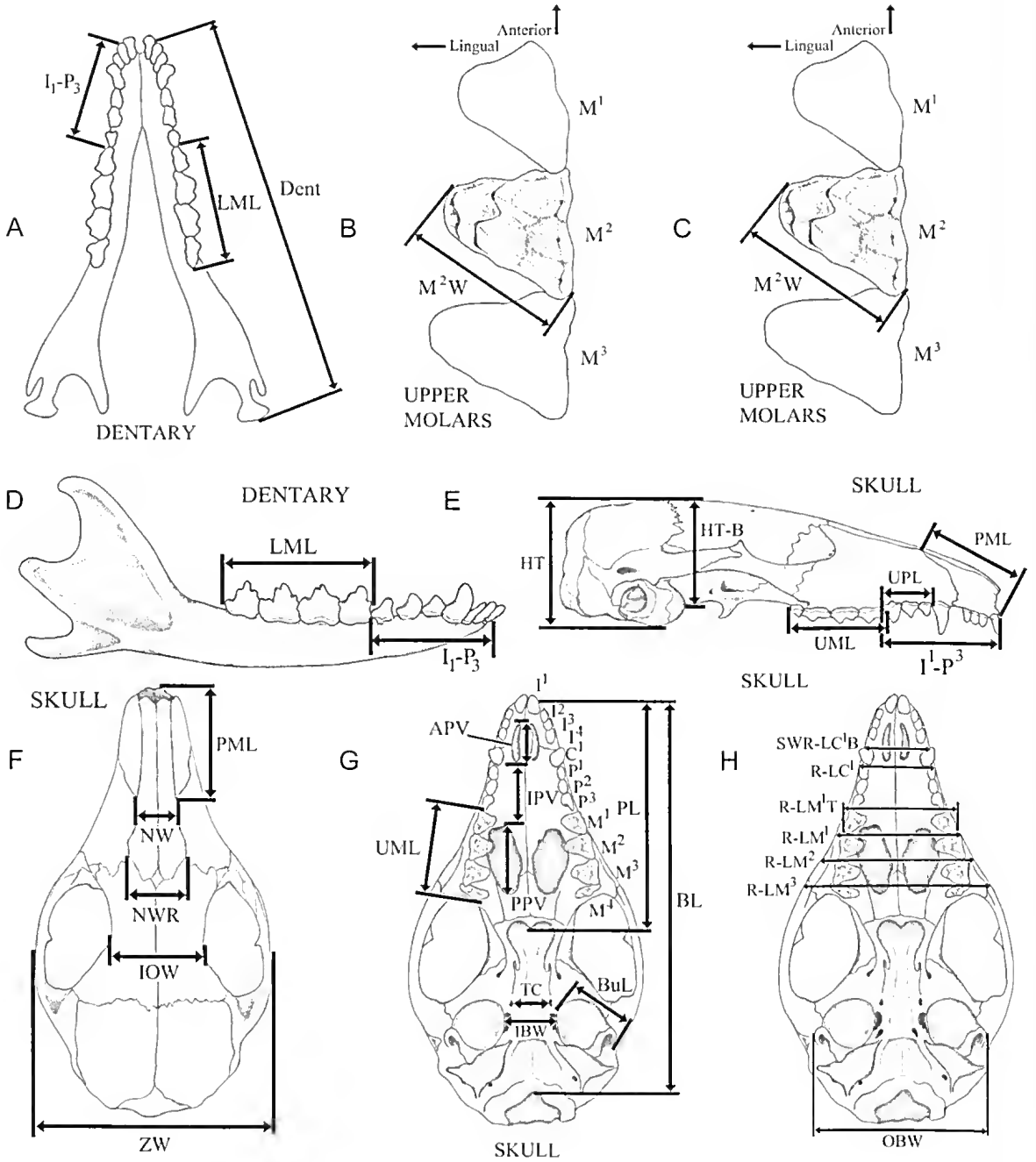


FIG. 1. Genus *Antechinus*; a guide to measurement of variables: skull and dentary (A-H).

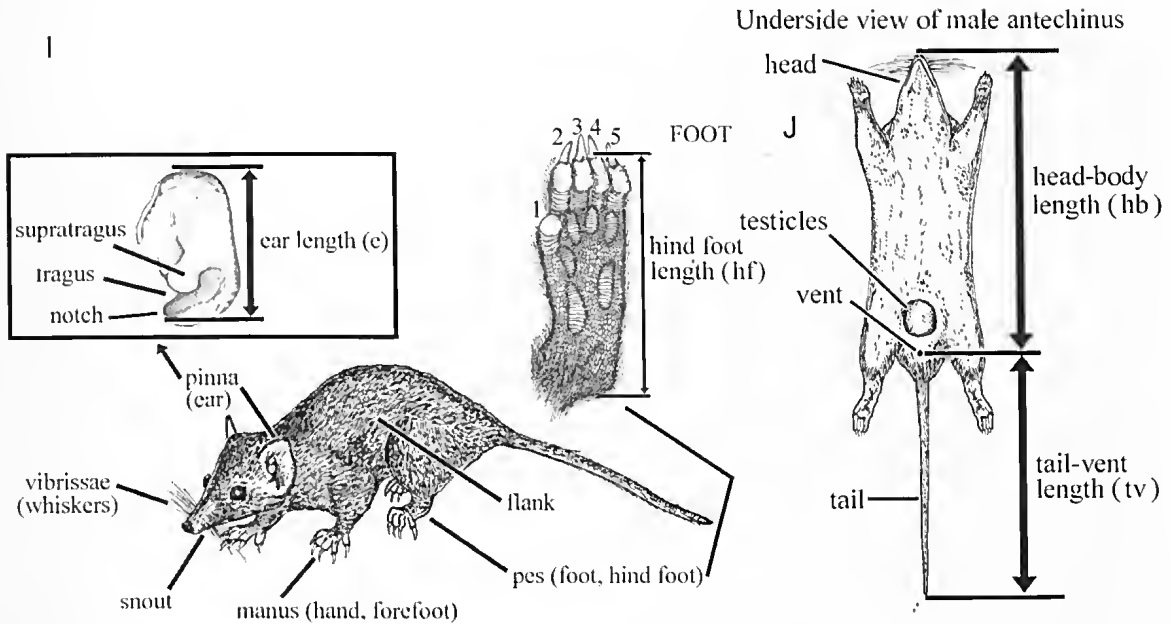


FIG. 1 continued. External body measures (I-J).

= skull height; **PL** = length of palate; **SWR-LC<sup>1</sup>B** = skull width level with the anterior of upper canines; **TC** = minimum distance separating transverse canals; **NWR** = width of nasals at the nasal / maxilla / frontal junction; **PML** = length of premaxilla; **UML** = maximum length of upper molar row,  $M_1$ - $M_4$ ; **HT-B** = skull height measured immediately anterior of auditory bullae; **BuL** = auditory bulla length; **I<sup>1</sup>-P<sup>3</sup>** = crown length from anterior edge of upper incisor 1 to posterior edge of upper premolar 3; **LML** = maximum length of lower molar row,  $M_1$ - $M_4$ ; **I<sub>1</sub>-P<sub>3</sub>** = crown length from anterior of lower incisor 1 to posterior of lower premolar 3; **M<sub>2</sub>W** = maximum width of lower molar 2 measured diagonally from anterior lingual to posterior labial points; **UPL** = crown length of upper premolar row,  $P^1$ - $P^3$ .

Species clades returned from constructed DNA-based phylogenies (see below) were used as testable hypotheses in subsequent morphological analyses; thus, multivariate analyses enabled us to predict membership of individuals in hypothesised species groups

based on a combination of skull morphology variables, whereas univariate ANOVAS (and subsequent post-hoc tests) for each variable enabled us to test for significant variation within each variable and determine which variables differed for comparisons of our putative new species with each species pair. The combination of univariate and multivariate analyses was essential to permit both fine-scale pairwise comparisons demonstrating species by species differences to facilitate best-practice species management and also broadscale comparisons among all species within the Dusky Antechinus complex, to best illustrate differences across all Antechinus measured variables.

Statistical analyses of morphometrics were undertaken using the program STATISTICA Version 7 (Statsoft Inc. 2004). Samples were initially tested for normality with the Kolmogorov-Smirnov and Lilliefors tests and homogeneity of sample variances using Levene's test. Analysis of Variance (ANOVA) was used to analyse variation in means among all putative antechinus species (from AMB's compiled

museum and live specimen measurement data), tested under separate hypotheses for each measured external and cranial/dentition variable. In each ANOVA, post-hoc unequal N HSD tests (a modification of Tukey's HSD) were used to test pairwise differences (at  $P < 0.05$ ) in external variables and cranial/dentition measures between *A. swainsonii* and each proposed congener, to compensate for potential Type 1 errors and since sample sizes differed between species. Multivariate analyses were conducted to optimise dimensionality of each variable set and maximise relationships between variable sets. Discriminant Function Analysis (DFA) was used to determine assignment reliability within proposed species groupings and subsequent Canonical Variate Analysis (CVA) generated independent functions that best discriminated between the putative species.

Univariate statistics (means, standard deviations, range minima and maxima) were compiled for each of the external and internal (cranial/dental) measures for the four species (and 5 taxa) within the Dusky Antechinus species complex: the Black-tailed Dusky Antechinus, *A. arktos*; the Mainland Dusky Antechinus *A. mimetes* (supporting two subspecies - *A. m. mimetes* and *A. m. insulamus*); the Tasmanian Dusky Antechinus *A. swainsonii*; and the Tasman Peninsula Dusky Antechinus, *A. vandycki* sp. nov. A range of scatterplots were constructed to show the main discriminating variable pairs among these species. All members of the Dusky Antechinus complex are strikingly different in both size and morphology to all congeners, so no other species were included for these comparisons. External body measures, while included in univariate analyses, were excluded from exploratory multivariate analyses because of missing data (numerous museum specimens included only skull material for the registered specimen) - this served to maximise the number of individuals of each species used in any given multivariate analysis. Antechinus are known to be sexually dimorphic in size (Marlow 1961; Soderquist 1995; Williams & Williams 1982), so sexes were analysed separately for all measured variables. No *A. vandycki* sp. nov. female could

be captured by us, so morphological analyses were conducted on males of that species only.

**Analyses of Genetic Data.** Comprehensive examination of genetic structuring in the genus *Antechinus* is the subject of an ongoing parallel research project and as such will not be presented in detail here. However, for the purpose of postulating DNA-based species groups that are subsequently tested with a comprehensive morphological data set, we present the preliminary DNA-based phylogenies for all recognised extant antechinus species, as well as DNA uncorrected percentage divergence ranges between each existing species paired with *A. swainsonii* (see results). A portion (607bp) of the mitochondrial Cytochrome B gene (CytB) and a portion (699bp) of the nuclear Interphotoreceptor Binding Protein gene (IRBP) were targeted using primers as described in Mutton (2011). Sequences were aligned by eye using Bioedit Version 7.1.11 (Hall 1999). Bayesian phylogenies (using mtDNA alone and also a concatenated dataset partitioned as mtDNA and nDNA) were reconstructed using MrBayes Version 3.2.1 (Ronquist & Huelsenbeck 2003), under the General Time Reversible Model of sequence evolution as determined by MrModelTest 2.3 (Nylander 2004), incorporating invariant sites and a gamma shape distribution of 2; in MrBayes, tree search was run for 10 million generations with a 25% burnin, as recommended by program guidelines. Resulting phylogenies were output in the program Treeview (Page 1996). A p-distance matrix was output based on aligned sequences in MEGA 6 (Tamura et al. 2013) and % divergences calculated by multiplying each value by 100; % divergence ranges incorporating minima and maxima were generated for each putative species pair.

Abbreviations for museums housing material examined in this paper are: BMNH, Natural History Museum, London (formerly British Museum of Natural History); C, Museum Victoria, Melbourne; J and JM, Queensland Museum, Brisbane; and QVM, Queen Victoria Museum and Art Gallery, Launceston.



## SYSTEMATICS

### *Antechinus vandycki* sp. nov.

(Figs 17–18)

**Etymology.** Named in honour of Dr Steve Van Dyck, former Senior Curator of Mammals and Birds at the Queensland Museum, for his pioneering taxonomic work on the genus *Antechinus*.

**Material examined.** *Holotype.* Queensland Museum, Brisbane. JM20111, Male. Study skin and skull; remainder of body tissues in spirit (refer Figs 17–18). Captured on 7 May, 2014, by Eugene Mason, Emma Gray and Hannah Maloney in an Elliott trap (type A, Elliott Scientific), baited with peanut butter, rolled oats, peanut oil and bacon.

*Paratypes.* All paratypes were genetically typed and were either the same haplotype as the holotype or were characterised as a second haplotype that was only 2 bases different (0.4% divergent) to the holotype specimen. Males: JM 20113, JM 20116 Fortescue Road, Fortescue Bay, Tasman Peninsula, Tasmania 43°08'40"S, 147°57'18"E; JM 20114 Balt's Road, Tasman Peninsula, Tasmania 43°04'48"S, 147°56'57"E; JM 20115, JM 20117 Lichen Road, Tasman Peninsula, Tasmania 43°03'07"S, 147°54'56"E.

**Referred specimen.** Male, BMNH 41.1246 Tasman's Peninsula, Tasmania.

**Type Locality.** Lichen Road, Tasman Peninsula, Tasmania, 43°03'07"S, 147°54'56"E, (refer Fig.19).

**Habitat.** Habitat of the type locality is wet sclerophyll temperate rainforest with many fallen logs and a dense understorey. Floristically, the area is typical of Tasmanian temperate rainforest, but there are only limited stands existent on Tasman Peninsula. The holotype locality featured Native Laurel, *Anopterus glandulosa*, with *Eucalyptus delegatensis* and *Eucalyptus obliqua* and an understorey of predominant *Blechnum nudum*.

**Diagnosis.** *Antechinus vandycki* sp. nov. differs from all other members of the *Antechinus swainsonii* complex in having longer anterior palatal vacuities, smaller inter-palatal vacuity distance and larger posterior palatal vacuities. *Antechinus vandycki* sp. nov. is most similar to *A. swainsonii*; both these species have predominantly greyish fur (although *A. vandycki* sp. nov. is darker), rather than the predominantly brownish *A. minnipes* and *A. arklos*. *Antechinus vandycki* sp. nov., like other Dusky Antechinus Complex

species, is easily distinguished from other antechinus, being notably larger and longer/more narrow-snouted than most other species, except *A. minimus*, to which it differs markedly in coat colour and body shape (*A. vandycki* sp. nov. is greyish brown, longer tailed and less squat, whereas *A. minimus* is greyish merging to yellowish/brown with a markedly short tail and heavy hind-quarters).

**Description.** Holotype skin and skull are shown in Figs 17–18.

**External Measurements.** body weight – 89.1 g; hindfoot length – 24.6 mm; head-body length – 132.6 mm; tail-vent length – 118.0 mm; ear length – 16.7 mm.

**Pelage.** Colours for the *A. vandycki* sp. nov. holotype are as follows: fur of the mid-back, up to 17 mm long with basal 14 mm Deep Gull Gray, median 1 mm Dresden Brown and apical 1 mm Fuscous black. The back appears overall to be Prout's Brown on the flanks but is darker, Slate Black, on the upper back such that the animal appears to have a broad blackish-coloured back (enhanced by the dense fuscous guard hairs), merging gradually to Prout's Brown and even tinges of Dresden Brown on the flanks. Guard hairs (medially-thickened) are Fuscous black; they are prominent giving an overall moderately shaggy appearance, and up to 20 mm long on the rump, reducing to 6 mm where they terminate at the crown of the head. The crown of the head and upper snout are Slate Black with Prout's Brown highlights merging to greyish-Dresden Brown highlights on the cheeks and under the eye. The holotype lacks a head-stripe and eye patches although there are mottled Dresden Brown highlights both above and particularly below the eye. The soft ventral fur, up to 10 mm long on the belly is Deep Neutral Gray on the basal 6 mm and Pale Olive-Buff-Whitish on the apical 4 mm. It is interspersed by medially-thickened spines up to 16 mm long. Forefeet and hindfeet are darkish; Dark Olive on the upper and lower surface; the underside of both fore and hindfeet are covered in Dark Olive pigmented granules, which give it its overall darkish appearance. The claws on the forefoot are exceptionally

long, up to 5.6 mm, and slightly longer than the claws on the hindfoot (up to 4.0 mm). The tail is dark, Chaetura Black on the upper surface and similar in colour to the darkish guard hairs on the rump; the tail is bicoloured, Chaetura Black on the dorsal surface with a lighter olive brown on the underside. The tail hairs are dense, fine and evenly moderate (6 mm). The overall impression of the animal is deep dark grey on the back, lighter dirty grey on the underside with brownish highlights on the body that are more notable on the flanks and also subtly towards the rump, with darkish brown-grey feet and a subtly bicoloured tail (dark grey on top and lighter brownish grey underneath).

*Vibrissae.* Approximately 20 mystacial vibrissae occur on each side and these are up to 27 mm long. They are Fuscous Black in colour some merging to lighter browns and even to colourless at the tips. Supra-orbital vibrissae (Fuscous Black) number 1 on the right and 1 on the left; genals (Fuscous Black and colourless) number 4 right and 4 left; ulna-carpals (fuscous-colourless) number 2 left and 2 right; and submentals (basally fuscous with colourless tips) number 2.

*Tail.* The tail is shorter than the head and body. It is thick at the base (6.5 mm) and tapers gradually towards the tip.

*Hindfoot.* Interdigital pads are separate. The elongate hallal and post-hallal pads are separate on the right foot but connected on the left foot. The metatarsal pad is long and oval shaped; all the foot pads are heavily striate. Claws are very long (longest on hindfoot measures 4.0 mm; longest on forefoot measures 5.6 mm).

*Ear.* For a large antechinus (89.1 g), the ears are smallish (16.7 mm); the supratragus is uncurled.

*Dentition.* Upper Incisors. All upper incisors are blade-like, procumbent. I<sup>1</sup> is broad, triangular, curved slightly anteriorly and uncurved posteriorly, two times taller-crowned than all other incisors and separated by a small (0.1 mm) diastema from I<sup>2</sup>. The flaring crown of I<sup>1</sup>, spreading posteriorly as well as anteriorly, does not quite meet the procumbent, flared I<sup>2</sup>. Left and right I<sup>1</sup> broadly contact to form a

cutting 'V'. In crown size I<sup>3</sup>=I<sup>2</sup>>I<sup>4</sup>. I<sup>2</sup> and I<sup>3</sup> lack buccal cingula, but posterior buccal cingula are present on both I<sup>4</sup> and to a lesser extent I<sup>1</sup>. There is no lack of differentiation between root and crown. All crowns are long antero-posteriorly, lower and rounded in I<sup>2</sup> and I<sup>3</sup>, but higher and peaked in I<sup>1</sup> and I<sup>4</sup>. I<sup>4</sup> and to a lesser extent I<sup>1</sup> carry a small posterior cusp.

Upper canines: C<sup>1</sup> is very slender and caniniform with a distinct anterior cusp but no posterior cusp. There is a very weak buccal cingulum and no lingual cingulum.

Upper premolars: All premolars are exceptionally narrow, slender and widely-spaced. Diastemata occur between C<sup>1</sup> and P<sup>1</sup> (0.6 mm), P<sup>1</sup> and P<sup>2</sup> (0.4 mm), P<sup>2</sup> and P<sup>3</sup> (0.3 mm), although P<sup>3</sup> contacts M<sup>1</sup>. All premolars carry buccal and lingual cingula. In crown size: (right) P<sup>3</sup>>P<sup>2</sup>>P<sup>1</sup>, (left) P<sup>3</sup>>P<sup>2</sup>>P<sup>1</sup>. Minute anterior cingular cusps occur on P<sup>1-3</sup>. Large posterior cusps occur on P<sup>1</sup>, P<sup>2</sup> and P<sup>3</sup>. No upper premolars possess posterolingual lobes, although there is a slight swelling in this area of P<sup>2</sup>.

Upper molars: In M<sup>1</sup>, the posterior tip of P<sup>3</sup> is positioned in the parastylar corner but lingual to and well below the minute stylar cusp A. The anterior cingulum below stylar cusp B is short, broad and incomplete. Stylar cusp B is moderately large, clearly peaked and about half the height of the paracone; there is no protoconule evident. Stylar cusps C and E are small, rounded peaks. M<sup>1</sup> lacks a posterior cingulum. The metacone is immediately lingual to, and larger than, stylar cusp D, the latter forming a large, rounded peak. The line from the metastylar corner of M<sup>1</sup> to the tip of the protocone is greatly indented and the post-protocrista is heavily swollen.

In M<sup>2</sup>, the broad anterior cingulum which contacts the metastylar corner of M<sup>1</sup> tapers quickly as it progresses down and along the base of the pre-paracrista and finally degenerates before meeting the trigon basin. The protocone forms a rounded peak; no protoconule is evident. M<sup>2</sup> has low and indistinct stylar cusps A, B, C and E. Stylar cusp D forms a clear, rounded peak but is smaller than the metacone; there is no posterior cingulum.

In  $M^3$ , the anterior cingulum is broader and slightly longer than in  $M^2$ . It becomes indistinct after covering 2/3 distance between stylar cusp B and the lingual base of the paracone. There is no protoconule evident. Stylar cusps A, C and E are low and rounded. Stylar Cusp B is a low, rounded peak and stylar cusp D is a distinct peak but barely as high as the paracone and only 1/3 as high as the metacone.

In  $M^4$ , the ectoloph between stylar cusps B and D is greatly indented. The narrow anterior cingulum terminates gradually away from the anterior corner of  $M^4$  and a posterior cingulum is absent. The protocone is greatly reduced and very narrow. In occlusal view, the angle made between the post-protocrista and the post-paracrasta is close to  $90^\circ$ .

Lower incisors: All lower incisors project horizontally from the tip of the dentary. In crown height:  $I_1 > I_2 > I_3$ .  $I_3$  is incisiform in lateral view with an inconspicuous posterior cusp at the base of the crest which descends posteriorly from the apex of the primary cusp. The lower canine rests against this posterior cusp. In occlusal view of  $I_3$ , a very small notch separates the posterior cusp from the prominent posterolingual lobe, and the crown enamel of the primary and posterior cusps fold lingually such that the crest of the two cusps bisects the tooth longitudinally.

Lower canines:  $C_1$  is premolariform and long. There is mild anterior but minimal posterior curvature from root to crown tip and the tooth is short-crowned. It has weak buccal and lingual cingulation and a clear posterior cusp. The posterior edge of the tooth peak descends at a point that falls in the front half of the total tooth length; thus this tooth appears in buccal view to be strongly peaked at the front but low-slung and long before terminating in a clearly peaked posterior cusp.

Lower premolars: All premolars are extremely elongate and narrow. There are clear, narrow (0.1-0.2 mm) diastemata separating all premolars, and  $C_1$ - $P_1$  as well as  $P_3$ - $M_1$ . In crown height:  $P_2 > P_3 > P_1$ . All premolars possess posterior cusps, which in  $P_1$  and  $P_2$  are very long. No premolars possess anterior cusps, except  $LP_1$ , where the

cusp is minute. The bulk of premolar mass is concentrated anteriorly to the line drawn transversely through the middle of the two premolar roots. Postero-lingual lobes are not features of the lower premolars but a narrow cingula surrounds each tooth.

Lower molars: All molars are very narrow. In  $M_1$ , the talonid is wider than the trigonid and no anterior cingulum is present. A narrow, weak posterior cingulum extends from the hypoconulid around to the posterior base of the protoconid, with a very narrow posterior buccal shelf. The narrow paraconid appears in occlusal view as a small, steeply sided spur with an appreciable shelf. The paraconid makes little contribution to the bulk of the ectoloph enamel. The metacristid and hypocristid are oblique to the long axis of the dentary. The cristid obliqua is short, shallow and extends from the hypoconid to the posterior wall of the trigonid, intersecting the trigonid at a point slightly buccal to that point directly below the tip of the protoconid. The protoconid is large, about twice the height of the metaconid, which itself is twice the height of the low paraconid. The hypocristid terminates at the buccal base of the hypoconulid. The entoconid is a broad, low, rounded hump. From the base of the metaconid posteriorly, the talonid endoloph follows the line of the dentary until the base of the hypoconulid, allowing for a lingual bulge formed by the entoconid.

In  $M_2$ , the trigonid is about as wide as the talonid. The anterior cingulum is poorly yet distinctly developed, originating lingually in a weak parastylid notch into which the hypoconulid of  $M_1$  is tucked. There is no buccal cingulum. A narrow, weak posterior cingulum extends from the hypoconulid to the posterior base of the hypoconid. The paraconid is well developed, but is the smallest trigonid cusp, with the metaconid slightly larger and protoconid clearly largest, and more than twice the height of the paraconid. The entoconid is a clearly, well-rounded peak, perhaps twice the height of the entoconid in  $M_1$ . A short cristid obliqua extends from the hypoconulid intersecting the posterior wall of the trigonid at a point directly below the tip of the protoconid, which is well

buccal to the metacristid fissure. From the base of the metaconid posteriorly, the endoloph follows the line of the dentary axis, allowing for the distinctive lingual swelling of the entoconid.

In  $M_3$ , the trigonid is wider than the talonid. A very weak parastylid wraps around the hypoconulid of  $M_2$ , and the  $M_3$  anterior cingulum is weak but clear. There is no buccal cingulum but the weak posterior cingulum is as in  $M_2$ , although even more poorly developed. The reduced cristid obliqua intersects the trigonid at a point slightly lingual to the tip of the protoconid, which is a great distance buccal to the metacristid fissure. A high, round-peaked entoconid is present, which is perhaps twice the height of the entoconid in  $M_2$ . The endoloph of the  $M_3$  talonid takes a slightly more buccal orientation than that seen in  $M_2$ . The rest of  $M_3$  morphology is as in  $M_2$ .

In  $M_4$ , the trigonid is much wider than the talonid. The anterior cingulum is as in  $M_3$  but the posterior cingulum is absent. A narrow buccal cingulum occurs between the trigonid and the talonid. Of the three main trigonid cusps, the metaconid is about 1.5 times taller than the paraconid but both are markedly smaller than the protoconid, the latter being about twice the height of the paraconid. The cristid obliqua forms a low, weak crest which contacts the trigonid wall slightly lingual to the metacristid fissure. Of the talonid cusps, the small, rounded hump of the entoconid is the largest cusp. The hypoconid is very weakly formed, while the hypoconulid is a rounded nubbin and all but absent.

**Skull.** The holotype skull is intact, in excellent condition, with only nominal tooth wear. The skull is characterised by a very long, narrow, low, rostrum which is tubular in cross section. The nasals are very narrow anteriorly and flare noticeably, posteriorly. Anteriorly the nasals are set well back from the inclined anterior edge of the premaxillaries. Slight flattening of the skull only occurs at the junction of the nasals and frontals, and the cranium is high and domed. The exceptionally large (7.16 mm) premaxillary vacuities extend from the level

of the posterior of the  $I^2$  root back to slightly posterior of the posterior of the  $P^2$  root. The maxillary vacuities are also exceptionally large (6.54 mm), extending from slightly anterior to the level of the protocone root of  $M^1$  back to the posterior of the protocone root of  $M^4$ .

**Comments.** We recommend the following common name be used in association with *A. vandycki* sp. nov.: Tasman Peninsula Dusky Antechinus.

### *Antechinus swainsonii* (Waterhouse, 1840)

*Phascogale swainsonii* Waterhouse, 1840

*Antechinus rolandensis* Higgins and Petterd, 1982

?*Antechinus niger* Higgins and Petterd, 1983

?*Antechinus moorei* Higgins and Petterd, 1984

?*Antechinus moorei* var. *assimilis* Higgins and Petterd, 1984

**Material examined.** *Holotype.* BMNH 60.1.5.18 (skin) and 60.1.5.26 (skull) (male) from the private collection of William Swainson, given to Waterhouse.

**Other material.** These specimens were formalin-fixed and old, so genetic analysis was not possible. Only adults were used for morphometrics and specimens were selected to be representative of the species' geographic range. Males: JM 20107 Mt Field NP off Lake Dobson Road, Tasmania 42° 41'S 146° 39'E; BMNH 87.5.18.10 Table Cape, Tasmania; BMNH 4.6.26.11 Magnet, Tasmania; QVM 1959:1:0012 Fingal, Tasmania; QVM 1963:1:0089 Mount Kate, Tasmania; QVM 1963:1:0189 Waratah, Corinna Rd, Tasmania; QVM 1965:1:0109 Renison Bell, Tasmania; QVM 1981:1:0152, QVM 1982:1:0136, QVM 1985:1:0005, QVM 1985:1:0006 Mount Barrow, Tasmania; QVM 1984:1:0116 Mount Arthur, Tasmania. Females: JM 4381 Button grass plains, eagle creek track, south-west Tasmania; QVM 1982:1:0133 Mount Barrow, Tasmania; QVM 1984:1:0143 Mount Arthur, Tasmania; QVM 1985:1:0016 Mount Barrow, Tasmania; QVM 1963:1:0043 between Erriba and Cradle Mountain, Tasmania; QVM 1963:1:0087 Mount Kate, Tasmania; QVM 1963:1:0187 Waratah, Corinna Road, Tasmania; QVM 1964:1:0042 Renison Bell, Tasmania; QVM 1964:1:0094 Mount Kate, Tasmania.

**Type Locality.** Van Diemen's Land, Tasmania.

**Rediagnosis.** *Antechinus swainsonii* sens. strict. differs from all other members of the Dusky Antechinus complex in having the slenderest-looking snout. *Antechinus swainsonii* is most similar to *A. vandycki* sp. nov. but has shorter anterior palatal vacuities, larger inter-palatal

vacuity distance and smaller posterior palatal vacuities; both species are greyish-brown in appearance, moderate-dark grey on the back, pale grey on the sides and light grey-white on the underside with brownish highlights on the body that are more notable on the flanks and also with brownish warming towards the rump. The tail in both species is bicoloured. However, *A. swainsonii* is distinctly paler in overall appearance than *A. vandycki* sp. nov. Both *A. swainsonii* and *A. vandycki* sp. nov. have predominantly greyish fur, rather than the predominantly brownish *A. mimetes* and *A. arktos*. *Antechinus swainsonii*, like other Dusky Antechinus complex species, is easily distinguished from other antechinus, being notably larger, shaggier and longer/ more narrow-snouted than most other species, except *A. minimus*, to which it differs markedly in coat colour and body shape (*A. swainsonii* is greyish brown, longer tailed and less squat, whereas *A. minimus* is greyish merging to yellowish/ brown with a markedly short tail and heavy hind-quarters). For individual species-pair comparisons of *A. swainsonii* to all congeners, refer to the species by species section in Results.

**Description.** Holotype, skin and skull are shown in Figs 13-14.

**Pelage.** Colours for the holotype are as follows: fur of the mid-back, up to 12.5 mm long with basal 10.5 mm Slate Colour, median 1 mm Prouts Brown and apical 1.0 mm Fuscous black. The back appears overall to be Chestnut Brown. Guard hairs (medially-thickened) are Fuscous black fading to Sepia. They are up to 20 mm long on the rump and reduce to 6 mm where they terminate at the crown of the head. Fur on, and below the shoulders, thighs, flanks and chin, lacks black tips and these areas appear as Deep Olive Gray. The tips of the guard hairs warm to a more rufous shade toward the rump.

The holotype lacks a head-stripe and there is no eye-ring present. The soft ventral fur, up to 10 mm long on the belly is Dark Mouse Gray on the basal 8.5 mm and Pale Smoke Grey on the apical 1.5 mm. It is interspersed by medially-thickened spines 11 mm long. The belly is thus an overall Deep Olive Gray. Forefeet are thinly

covered with Bister coloured hairs and hindfeet are more thickly covered with darker Sepia-coloured hairs. The tail is weakly bicoloured with hairs averaging 3 mm along its length and increasing to 4 mm at its tip. Dorsally, the tail-hairs are a uniform Clove Brown. Ventrally they are Olive Brown.

**Vibrissae.** Approximately 24 mystacial vibrissae occur on each side and are up to 16 mm long (many, however, are broken). All are Fuscous Black. Supra-orbital vibrissae (Fuscous Black) number 6 right and those on the left have been cut off; genals (Fuscous Black and colourless) number 6 right but those on the left cannot be seen; ulna-carpals (colourless) number 5 left and 1 right; and submentals (all cut) number 4.

**Tail.** The tail is shorter than the head and body. It is thin and tapers towards the tip.

**Hindfoot.** Interdigital pads are separate. The apical granule is enlarged, elongate and striate. The enlarged hallual and post-hallual pads are fused. Metatarsal pads are not visible in the holotype. Claws are very long.

**Ear.** On the holotype the pinnae are not present.

**Dentition.** Upper Incisors. All upper incisors are procumbent and badly worn.  $I^1$  is broad, triangular and uncurved, two times taller-crowned than all other incisors and is not separated by a diastema from  $I^2$ . The flaring crown of  $I^1$ , spreading posteriorly as well as anteriorly, meets the procumbent, flared  $I^2$  so that the natural diastema between  $I^1$  and  $I^2$  is filled. Left and right  $I^1$  contact to form a cutting 'V'. In crown size:  $I^3=I^2>I^4$  (but they are all badly worn). All upper incisors, but for  $I^4$ , lack buccal cingula and in  $I^4$  the cingula is positioned to the posterior of the tooth. There is no lack of differentiation between root and crown. All crowns are long antero-posteriorly and low.  $I^4$  carries no anterior or posterior cusp. The roots of  $I^4$  are wide.

Upper canines:  $C^1$  is very slender and caniniform with an indistinct boundary between the root and crown. There is a very weak buccal cingulum and no lingual cingulum. No anterior cusp is present but there is a minute posterior cusp.

Upper premolars: All premolars are exceptionally narrow and slender. Diastemata occur between  $C^1$  and  $P^1$ ,  $P^1$  and  $P^2$  (diastemata equally sized at 0.5 mm),  $P^2$  contacts  $P^3$  and  $P^3$  contacts  $M^1$ . All premolars carry very weak buccal and weak lingual cingula. In crown size: (right)  $P^2 > P^3 > P^1$ ; (left)  $P^3 = P^2 > P^1$ . Minute anterior cingular cusps occur on  $P^{1-3}$ . Large posterior cusps occur on  $P^2$  and  $P^3$ . No upper premolars possess posterolingual lobes.

Upper molars (note that  $LM^{2-4}$  are missing): The posterior tip of  $P^3$  is positioned in the parastylar corner of  $M^1$  but lingual to and well below the minute stylar cusp A. The anterior cingulum below stylar cusp B is short, broad and incomplete. Stylar cusp B is moderately large but the paracone is worn down to a nubbin and there is no protoconule present. Stylar cusps C and E are not present.  $M^1$  lacks a posterior cingulum. The metacone is immediately lingual to, and larger than, stylar cusp D. The line from the metastylar corner of  $M^1$  to the tip of the protocone is greatly indented and the post-protocrista is heavily swollen.

In  $RM^2$ , the broad (worn) anterior cingulum which contacts the metastylar corner of  $M^1$  tapers quickly as it progresses down and along the base of the pre-paracrista; it finally degenerates before meeting the trigon basin. The protocone is badly worn and no protoconule is present.  $M^2$  lacks stylar cusps A, C and E. Stylar cusp D is greatly reduced and smaller than the metacone and there is no posterior cingulum.  $LM^2$  is missing.

In  $RM^3$ , the worn anterior cingulum is broader and slightly longer than in  $RM^2$ . It becomes indistinct after covering 2/3 distance between stylar cusp B and the lingual base of the paracone. There is no protoconule. Stylar cusp D is reduced to a small, rounded peak, which is about half the height of the metacone. Stylar cusp C is absent and E is a worn rudament.  $LM^3$  is missing.

In  $RM^4$ , the ectoloph between stylar cusps B and D is greatly indented. The narrow anterior cingulum terminates quickly away from the anterior corner of  $M^4$  and a posterior cingulum is absent. The protocone is greatly reduced and

very narrow. In occlusal view, the angle made between the post-protocrista and the post-paracrista is close to  $90^\circ$ .  $LM^4$  is missing.

Lower incisors: All lower incisors are heavily worn and project horizontally from the tip of the dentary. In crown height:  $I_1 > I_3 > I_2$ .  $I_3$  is incisiform in lateral view with an inconspicuous posterior cusp at the base of the crest which descends posteriorly from the apex of the primary cusp. The lower canine rests against this posterior cusp. In occlusal view, a very small notch separates the posterior cusp from the prominent posterolingual lobe, and the crown enamel of the primary and posterior cusps fold lingually such that the crest of the two cusps bisects the tooth longitudinally.

Lower canines: The  $RC_1$  is broken off at the root.  $LC_1$  is premolariform and is characterised by excessive thegotic wear of the lower posterior surface. There is minimal curvature from root to crown tip and the tooth is short-crowned. It has weak buccal and lingual cingulation and a weak posterior cusp.

Lower premolars: All premolars are extremely elongate and narrow. There are no diastemata separating premolars, and contact is made between adjacent teeth from  $C_1$  to  $P_3$ ; however, there is a minute diastema between  $P_3$  and  $M_1$ . Although there is contact between lower premolars, there is no crushing. In crown height:  $P_2 > P_3 > P_1$ . All premolars possess weak posterior cusps, which in  $P_1$  and  $P_2$  are very long. No premolars possess anterior cusps. The bulk of premolar mass is concentrated anteriorly to the line drawn transversely through the middle of the two premolar roots. Postero-lingual lobes are not features of the lower premolars but a narrow cingula surrounds each tooth.

Lower molars: All molars are very narrow and heavily worn. In  $M_1$  the talonid is wider than the trigonid and no anterior cingulum is present. A narrow, weak posterior cingulum extends from the hypoconulid to the posterior base of the protoconid, with a very narrow posterior buccal shelf. The very narrow paraconid appears in occlusal view as a small, steeply sided spur with an appreciable shelf. The paraconid

makes little contribution to the bulk of the ectoloph enamel. The badly worn metacristid and hypocristid are oblique to the long axis of the dentary. The cristid obliqua is short and shallow and extends from the hypoconid to the posterior wall of the trigonid intersecting the trigonid at a point probably slightly lingual to that point directly below the tip of the protoconid. However, the posterior half of the protoconid is worn away so it is difficult to be precise. The hypocristid terminates at the buccal base of the hypoconulid. The entoconid is a rounded rudiment. From the base of the metaconid posteriorly, the talonid endoloph follows the line of the dentary until the base of the hypoconulid.

In  $M_2$ , the trigonid is slightly wider than the talonid. The anterior cingulum is very poorly developed originating lingually in a weak parastylid notch into which the hypoconulid of  $M_1$  is tucked. There is no buccal cingulum. A narrow, weak posterior cingulum extends from the hypoconulid to the posterior base of the hypoconid. The paraconid is well developed, but is the smallest trigonid cusp, with the metaconid larger and protoconid largest. However, the protoconid is poorly developed (likely due to wear) relative to the other lower molars  $M_3$  and  $M_4$ , and low crowned, while the metaconid is partly worn. The entoconid is poorly developed. A short cristid obliqua extends from the hypoconulid intersecting the posterior wall of the trigonid at a point directly below the tip of the protoconid, which is well buccal to the metacristid fissure. From the base of the metaconid posteriorly, the endoloph follows the line of the dentary axis.

In  $M_3$ , the trigonid is wider than the talonid. A very weak parastylid wraps around the hypoconulid of  $M_2$ , and the  $M_3$  anterior cingulum is very weak. There is no buccal cingulum but the weak posterior cingulum is as in  $M_2$  but more poorly developed. The reduced cristid obliqua intersects the trigonid at a point directly below the tip of the protoconid, which is a great distance buccal to the metacristid fissure. A low, rounded entoconid is present. The endoloph of the  $M_3$  talonid takes a slightly

more buccal orientation than that seen in  $M_2$ . The rest of  $M_3$  morphology is as in  $M_2$ .

In  $M_4$ , the trigonid is much wider than the talonid. The anterior cingulum is as in  $M_2$  but the posterior cingulum is absent. A small buccal cingulum occurs between the trigonid and the talonid. Of the three main trigonid cusps the metaconid is slightly taller than the paraconid but both are markedly smaller than the protoconid. The cristid obliqua forms a low, weak crest which contacts the trigonid wall slightly lingual to the metacristid fissure. Of the talonid cusps, the small entoconid is the largest cusp. The hypoconid is very weakly formed but the hypoconulid is absent.

**Skull.** The holotype skull is characterised by a long, narrow, low, rostrum which is tubular in cross section. The nasals are very narrow anteriorly and flare noticeably posteriorly. Anteriorly, the nasals are set well back from the inclined anterior edge of the premaxillaries. Slight flattening of the skull only occurs at the junction of the nasals and frontals, and the cranium is high and domed. The large premaxillary vacuities extend from the level of the  $I^2$  root back to the level of the middle of the  $P^2$  root. The maxillary vacuities extend from the level of the protocone root of  $M^1$  but all the palate is broken and smashed beyond this.

**Comments.** We recommend the following common name to be used in association with *A. swainsonii*: Tasmanian Dusky Antechinus.

There are several synonyms for *A. swainsonii*. First is *Antechinus rolandensis* Higgins and Petterd, 1882, based on a male, no registration number from Mount Roland (about 60 km west of Launceston), Tasmania. This species was initially assigned to synonymy with *A. minimus* (Thomas, 1888; Iredale and Troughton, 1934; Tate, 1947; Wakefield and Warneke, 1963; Mahoney and Ride, 1988 (who corrected the publication date from 1883 to 1882, probably on the authority of Thomas (1888) who nevertheless gives no indication that he examined the specimen)). However, Van Dyck (1997, 2002) noted measurements provided by the authors placed it as a very large animal and thus was most likely *A. swainsonii*. We concur with



Van Dyck's assessment. There are three other synonyms of *A. swainsonii* from elsewhere in Tasmania. First, *Antechinus niger* Higgins and Petterd (1883: 172), based on a female (no registration number) from (presumably) Upper Piper (now Lilydale, 28 km north-east of Launceston), Tasmania. Second, *Antechinus moorei* Higgins and Petterd (1884: 182), based on a male (no registration number) from Long Plains (north of Launceston), Tasmania. Third, *Antechinus moorei* var. *assiuilis* Higgins and Petterd (1884: 185), based on a specimen (sex unstated, 'in the museum of the Royal Society, Hobart') from 'Tasmania, West Coast. Thomas (1888), Iredale and Troughton (1934), Tate (1947) and Wakefield and Warneke (1963) all assign these three novelties to the synonymy of *A. swainsonii*.

And yet, all four type specimens noted above have never featured in the literature (as they are presumed lost), the descriptions are too inadequate to enable an accurate determination, and there is no indication that Thomas (1888) ever saw them. In their comprehensive review of the time, Wakefield and Warneke (1963) could not find any of the specimens and presumed them lost. Subsequently, Van Dyck (1997, 2002), who also could not locate the specimens, thereby classed these species and subspecies *incertae sedis*; we concur with Van Dyck's assessment and would add this note regarding their probable identity: three locations are near Launceston in the north of Tasmania, and the other in western Tasmania. Thus, based on distribution alone, the synonyms, if they indeed still exist, are highly likely to be *A. swainsonii*, since *A. swainsonii* are known from locations nearby and encompassing the regions where the mystery types are found and also *A. vandycki* sp. nov. is apparently limited to Tasman Peninsula, far to the south-east. While on the subject of type localities and identities, it is worth noting that the *A. swainsonii* holotype specimen unfortunately has a vague locality descriptor of 'Van Diemen's Land'. A thorough search by AMB of the BMNH archives in July 2013 found a log book of William Swainson covering his visit to Australia in the mid-1800s but there was no mention of him acquiring *A.*

*swainsonii*; thus, the generic type locality must stand. Measurements of this type specimen (BMNH 60.1.5.18 skin; BMNH 60.1.5.26 skull) indicate it is clearly *A. swainsonii* and not *A. vandycki* sp. nov. (based on APV and IPV, and several other craniodental measures). Furthermore, another specimen from the general collection held at the BMNH (41.1246) from 'Tasman's Peninsula, Tasmania' clearly clades out as *A. vandycki* sp. nov. rather than *A. swainsonii* (see species by species accounts and tables and figs therein).

*Antechinus mimetes mimetes*  
(Thomas 1924) **new status**

*Phascogale swainsonii mimetes* Thomas, 1924

**Rediagnosis of nominate form.** *Antechinus mimetes mimetes* differs from all other members of the Dusky *Antechinus* complex in having shorter anterior palatal vacuities than *A. vandycki* sp. nov. and *A. swainsonii*, but longer anterior palatal vacuities than *A. arktos*. *Antechinus mimetes mimetes* differs from both *A. vandycki* sp. nov. and *A. swainsonii* in being predominantly brownish on head and shoulders, rather than greyish. *Antechinus mimetes mimetes* is most similar to *A. mimetes insulanae*, but differ in that the latter has a generally broader skull, particularly at the base of the snout. *Antechinus mimetes mimetes* differs from *A. arktos* in being more evenly brownish from head to rump with a brownish tail and hind feet, whereas *A. arktos* has more colourful orange-tonings on the rump and both a black tail and hind feet. *Antechinus mimetes mimetes*, like other Dusky *Antechinus* complex species, is easily distinguished from other antechinus, being notably larger and longer/more narrow-snouted than most other species, except *A. minimus*, to which it differs markedly in coat colour and body shape (*A. mimetes mimetes* is brownish, longer tailed and less squat, whereas *A. minimus* is greyish merging to yellowish/brown with a markedly short tail and heavy hind-quarters).

**Material examined.** *Holotype.* BMNH 24.10.1.1 (skin and skull), female, collected by Captain G.H. Wilkins on 14 April, 1924.



*Other material.* These specimens were formalin-fixed and old, so genetic analysis was not possible. Only adults were used for morphometrics and specimens were selected to be representative of the species' geographic range. **Males:** J 3809 Ebor, Guy Fawkes District, north-east NSW, 30° 24'S 152°21'E; JM 20012 Weeping Rock Walking Track, New England NP, NSW 30° 29'S 152° 24'E; BMNH 24.10.1.2 Guy Fawkes District, NSW 30° 30'S 152°30'E; BMNH 86.5.15.7 Gippsland; C 875 Beech Forest, Victoria 38°38'S 143°34'E; C 9671 Kentbruck, Victoria 38° 10'S 141° 17'E; C 9725 Little Moleside Creek, Victoria 38° 07'S 141° 19'E; C 13574 14.4 km west of Noojee, Victoria 37°54'S 145°50'E, C 13725 Allambee, Victoria 38° 16'S 146° 02'E; C 13738 Cumberland picnic ground, Victoria 37° 33'S 148° 51'E; C 13759 Loch Valley, Victoria 37°49'S 146°01'E; C 15933 Pomonal, Victoria 37° 12'S 142° 37'E; C 7047 Neerim Junction, Victoria 37° 56'S 145° 58'E; C 28737 Orbost Region, Victoria 37°26'S 148° 37'E. **Females:** JM 20011 Cliff's Trail New England NP, NSW 30°31'S 152° 23'E; JM 20112 The Chalet, off Point Lookout Rd, New England NP, NSW 30° 30'S 152°24'E; C 426, C 427 Hordam Vale, Victoria 38°46'S 143°30'E; C 2584 Eyre Plantation, Beech Forest, Victoria 38° 38'S 143° 34'E; C 7432 Wyelangta, Arkin's Catchment, Victoria 38°40'S 143°26'E; C 7715 Gellibrand River, Victoria 38°31'S 143°33'E; C 9687 Belgrave area, Victoria 37°55'S 145°21'E; C 13570, C 13794 Loch Valley, Victoria 37°49'S 146°01'E; C 13740 Noorinbee North, Victoria 37°26'S 149°12'E; C 24892 Sherbrooke Forest, Victoria 37°01'S 147°07'E.

**Type Locality.** Guy Fawkes District, via Ebor, north-east New South Wales, 30°30'S 152°30'E.

**Description.** *Antechinus swainsonii* *mimetus* Holotype skin and skull are shown in Figs 15-16.

**Pelage.** Colours for the holotype are as follows: fur of the mid-back, up to 12.5 mm long with basal 10.5 mm Slate-Gray, median 1 mm Prouts Brown and apical 1 mm Fuscous black. The back appears overall to be Mummy Brown tending towards a Sepia colour on the rump. Guard hairs (medially-thickened) are Fuscous black fading to Sepia. They are up to 20 mm long on the rump and reduce to 6 mm where they terminate at the crown of the head. Fur on, and below the shoulders, thighs, flanks and chin, lacks black tips and these areas appear as Deep Olive Gray. The tips of the guard hairs warm to a more rufous shade toward the rump. The holotype lacks a head-stripe and there is

no eye-ring present, although the fur around the eye (particularly under it) and to a lesser extent between the eyes appears as Dresden Brown, as opposed to the generally Mummy Brown between the ears. The soft ventral fur, up to 10 mm long on the belly is Dark Mouse Gray on the basal 8.5 mm and Pale Smoke Gray on the apical 1.5 mm. It is interspersed by medially-thickened spines 11 mm long. The belly thus appears an overall Deep Olive Gray. Forefeet are thinly covered with Bister coloured hairs and hindfeet are more thickly covered with darker Sepia-coloured hairs. The tail is weakly bicoloured with hairs averaging 3 mm along its length and increasing to 4 mm at its tip. Dorsally, the tail-hairs are a uniform Clove Brown; ventrally, they are Buffy Brown.

**Vibrissae.** Approximately 24 mystacial vibrissae occur on each side and are up to 16 mm long (many, however, are broken). All are Fuscous Black. Supra-orbital vibrissae (Fuscous Black) number 6 right and those on the left have been cut off; genals (Fuscous Black and colourless) number 6 right but those on the left cannot be seen; ulna-carpals (colourless) number 5 left and 1 right; and submentals (all cut) number 4.

**Tail.** The tail is shorter than the head and body. It is thin and tapers towards the tip.

**Hindfoot.** Interdigital pads are separate. The elongate hallucal and post-hallucal pads are fused on the left hindfoot and separate on the right hindfoot. The metatarsal pad is long and oval shaped; all the foot pads are heavily striate. Claws are very long (longest on hindfoot measures 3.1 mm; longest on front foot measures 4.3 mm).

**Ear.** The ears appear to be smallish and the supratragus is uncurled.

**Dentition.** Upper Incisors. All upper incisors are procumbent. I<sup>1</sup> is broad, triangular with a curved anterior plane, two times taller-crowned than all other incisors and is not separated by a diastema from I<sup>2</sup>. The flaring crown of I<sup>1</sup>, spreading posteriorly as well as anteriorly, meets the slightly procumbent, flared I<sup>2</sup> so that the natural diastema between I<sup>1</sup> and I<sup>2</sup> is filled. Left and right I<sup>1</sup> contact to form a cutting

'V', although  $RI^1$  is worn at the tip. In crown size:  $I^3 > I^2 > I^4$ . All upper incisors, but for  $I^4$ , lack buccal cingula and in  $I^4$  the cingulum is positioned to the posterior of the tooth. There is no lack of differentiation between root and crown. All crowns are long antero-posteriorly and low.  $I^4$  carries no anterior or posterior cusp. The roots of  $I^4$  are wide.

Upper canines:  $C^1$  is very slender and caniniform with an indistinct boundary between the root and crown. There is a very weak buccal cingulum and no lingual cingulum. No anterior cusp is present but there is a minute posterior cusp.

Upper premolars: All premolars are exceptionally narrow and slender. Diastemata occur between  $C^1$  and  $P^1$ ,  $P^1$  and  $P^2$  (diastemata equally sized at 0.3 mm),  $P^2$  contacts  $P^3$  and  $P^3$  contacts  $M^1$ . All premolars carry very weak buccal and lingual cingula. In crown size, (right):  $P^3 > P^2 > P^1$ ; (left):  $P^3 > P^2 > P^1$ . Minute anterior cingular cusps occur on  $P^{1-3}$ . Large posterior cusps occur on  $P^{1-3}$ . No upper premolars possess posterolingual lobes.

Upper molars: The posterior tip of  $P^3$  is positioned in the parastylar corner of  $M^1$  but lingual to and slightly below the minute stylar cusp A. The anterior cingulum below stylar cusp B is short, broad and incomplete. Stylar cusp B is moderately large but smaller than the paracone and there is a small, rounded protoconule present; the paracone is smaller than stylar cusp D, which in turn is smaller than the metacone. Stylar cusp C is a worn rudiment and stylar cusp E is not present.  $M^1$  possesses a weak posterior cingulum formed at the base of the post-protocrista and tapering posteriorly to a point level with the base of the post-metacrista; thus the protocone appears notably broad. The metacone is immediately lingual to, and larger than, stylar cusp D. The line from the metastylar corner of  $M^1$  to the tip of the protocone is greatly indented and the post-protocrista is very heavily swollen.

In  $M^2$ , the very broad anterior cingulum which contacts the metastylar corner of  $M^1$  tapers quickly as it progresses down and along the base of the pre-paracrista and finally degenerates before meeting the trigon basin. Stylar cusp B is smaller than stylar cusp D, which is slightly smaller than the paracone, which in turn is much smaller

than the metacone; the protocone is well defined and about the same height as in  $M^1$ ; there is a small, rounded protoconule present.  $M^2$  lacks stylar cusp A, but stylar cusp E is a rounded rudiment and stylar cusp C is present, small and rounded.  $M^2$  possesses a weak posterior cingulum formed at the base of the post-protocrista and tapering posteriorly to a point level with the base of the post-metacrista; thus the protocone appears notably broad.

In  $M^3$ , the anterior cingulum is subequal in breadth and slightly longer than in  $M^2$ . It becomes indistinct after covering 3/4 of the distance between stylar cusp B and the lingual base of the paracone. There is a small, rounded protoconule. There is no stylar cusp A; stylar cusp B and D form subequal, small but distinct peaks, which are smaller than the paracone, which in turn is smaller than the metacone; stylar cusp C is very small and stylar cusp E is absent.  $M^3$  possesses a very weak posterior cingulum formed at the base of the post-protocrista and tapering posteriorly to a point level with the base of the post-metacrista; thus the protocone appears notably broad.

In  $M^4$ , the ectoloph between stylar cusps B and D is fairly straight. The narrow anterior cingulum tapers, forming a very narrow shelf that continues all the way to the base of the pre-protocrista; a posterior cingulum is absent. The protocone is greatly reduced and very narrow. In occlusal view, the angle made between the post-protocrista and the post-paracrista is about 50°.

Lower incisors: All lower incisors project horizontally from the tip of the dentary. In crown height:  $I_1 > I_2 > I_3$ .  $I_3$  is incisiform in lateral view with a distinct posterior cusp at the base of the crest which descends posteriorly from the apex of the primary cusp. The lower canine rests against this posterior cusp. In occlusal view,  $I_3$  has a very small notch separating the posterior cusp from the prominent posterolingual lobe, and the crown enamel of the primary and posterior cusps fold lingually such that the crest of the two cusps bisects the tooth longitudinally.  $I_3$  has a weak posterior buccal cingulum.

Lower canines:  $C_1$  is premolariform. There is moderate curvature from root to crown tip and the tooth is short-crowned, only slightly larger than  $P_2$ .  $C_1$  has weak buccal and lingual cingulation and a weak posterior cusp.

Lower premolars: All premolars are extremely elongate and narrow and there are clear diastemata separating all premolars from adjacent teeth. In crown height:  $P_2 > P_3 > P_1$ , such that  $P_2$  is about 1.5 times the height of  $P_3$  and about twice the height of  $P_1$ . All premolars possess distinct posterior cusps, which in  $P_2$  is very long. No premolars possess anterior cusps. The bulk of premolar mass is concentrated anteriorly to the line drawn transversely through the middle of the two premolar roots. Postero-lingual lobes are not features of the lower premolars but a narrow cingulum surrounds each tooth.

Lower molars: All molars are very narrow. In  $M_1$ , the talonid is wider than the trigonid and no anterior cingulum is present. A narrow, weak posterior cingulum extends from the hypoconulid to the posterior base of the protoconid, with a very narrow posterior buccal shelf. The very narrow paraconid appears in occlusal view as a small, steeply sided spur with an appreciable shelf. The paraconid makes little contribution to the bulk of the ectoloph enamel. The metacristid and hypocristid are oblique to the long axis of the dentary. The cristid obliqua is moderate, about  $45^\circ$  and extends from the hypoconid to the posterior wall of the trigonid intersecting the trigonid at a point buccal to that point directly below the tip of the protoconid. The hypocristid terminates at the buccal base of the hypoconulid. The entoconid is low and rounded. From the base of the small peaked metaconid posteriorly, the talonid endoloph roughly follows the line of the dentary until the base of the hypoconulid although there is a slight lingual bulge.

In  $M_2$ , the trigonid is very slightly wider than the talonid. The anterior cingulum is narrow, originating lingually in a weak parastylid notch into which the hypoconulid of  $M_1$  is tucked. A small buccal cingulum occurs between the trigonid and the talonid; a narrow, weak posterior cingulum extends from the hypoconulid to the

posterior base of the hypoconid. The paraconid is well developed, but is the smallest trigonid cusp, with the metaconid larger and protoconid largest. However, the protoconid is well developed and subequal with protoconids on  $M_3$  and  $M_4$ . The entoconid is a small but well-developed peak. A fairly steep ( $60^\circ$ ) cristid obliqua extends from the hypoconulid intersecting the posterior wall of the trigonid at a point directly below the tip of the protoconid, which is well buccal to the metacristid fissure. From the base of the metaconid posteriorly, the endoloph roughly follows the line of the dentary axis with a slight lingual bulge due to the entoconid swelling.

In  $M_3$ , the trigonid is wider than the talonid. A very weak parastylid wraps around the hypoconulid of  $M_2$ , and the  $M_3$  anterior cingulum is moderate. A small buccal cingulum occurs between the trigonid and the talonid; the weak posterior cingulum is as in  $M_2$ . The fairly steep ( $60^\circ$ ) cristid obliqua intersects the trigonid at a point directly below the tip of the protoconid, which is well buccal to the metacristid fissure. The entoconid is a moderate, well-developed peak. From the base of the well-developed metaconid posteriorly, the endoloph of the  $M_3$  talonid takes a slightly more buccal orientation than that seen in  $M_2$ .

In  $M_4$ , the trigonid is much wider than the talonid. The anterior cingulum is moderate but the posterior cingulum is absent. A small buccal cingulum occurs between the trigonid and the talonid. Of the three main trigonid cusps the metaconid is slightly taller than the paraconid but both are markedly smaller than the protoconid. The cristid obliqua forms a shallower ( $30^\circ$ ), smaller crest which contacts the trigonid wall slightly buccal to the metacristid fissure. Of the talonid cusps, the small hypoconid is the largest cusp. The hypoconulid is more weakly formed and the entoconid is absent.

*Skull.* The left and right alisphenoid tympanic bullae are widely separated and only moderately enlarged. The foramen pseudovale is large as is the eustachian canal opening. The internal jugular canal foramina are moderately large and

the canals poorly raised and inconspicuous. The posterior lacerate foramina are relatively small while the entocarotid foramina are large and exposed. Maxillary vacuities extend from the level of the M<sup>1</sup> paracone root back as far as the level of the M<sup>3</sup> metacone root. The premaxillary vacuities extend as far back as the P<sup>2</sup> anterior root.

**Comments.** We recommend the following common name to be used in association with *A. minimes*: Mainland Dusky Antechinus.

***Antechinus minimes insulanus* Davison, 1991  
new combination**

*Antechinus swainsonii insulanus* Davison, 1991

**Description.** Davison (1991) provides a detailed description of the holotype.

**Rediagnosis of Subspecies.** *Antechinus minimes insulanus* is distinguished from all other taxa in the *A. swainsonii* complex as recognised here, as detailed in the rediagnosis of the nominate form and also in the *A. vaudycki* sp. nov. diagnosis.

## SPECIES COMPARISONS

In total, more than 300 (male and female) specimens were examined for variation across the full suite of craniodental morphological characters in the 15 antechinus species. These combined data are from AMB's cumulative data set taken from both museum voucher and live specimens. The specimens encompassed the latitudinal geographic range of each species to represent maximal geographic variation and where possible at least 10 males and females of each species were examined for craniodental variation. However, for some species, such as *A. arktos* and *A. vaudycki* sp. nov. in the Dusky Antechinus complex, fewer than 10 specimens of each sex were available, despite accessing all registered museum specimens across Australia and conducting numerous field surveys across several years, representing many thousands of trap-nights.

All tests for normality and variance homogeneity of samples used in morphometric analyses were non-significant at  $p=0.05$ .

## Phylogenetic Structure

Figures 2-3 suggest that there are 15 putative species within antechinus. The phylogenies show the four species comprising the Dusky Antechinus complex and *A. minimus* clade is well-supported and deeply divergent compared with all congeners. Each of the four species of Dusky Antechinus and *A. minimus* are strongly supported and monophyletic with respect to each other; however, sister relationships between these taxa are unclear with the exception of the well-supported sister Dusky Antechinus from Tasmania, *A. swainsonii* and *A. vaudycki* sp. nov. (Figs 2-3). Within the Dusky Antechinus complex, the four species all form deep and well-supported clades with respect to each other, and within Augence between the two subspecies, *A. m. minimes* and *A. m. insulanus*; since there was only a single haplotype obtained for *A. minimes insulanus* (despite the fact that several individuals from two locations were sequenced), it is unclear if these taxa would form well-supported, reciprocally monophyletic clades. Fig. 2 is a phylogeny generated from mitochondrial (Cytochrome B - CytB) data and Fig. 3 combines the data from one mitochondrial gene (Cytochrome B - CytB) and one nuclear gene (Interphotoreceptor Binding Protein - IRBP); both phylogenies concord in their structuring of proposed species clades which then form the basis for testing individual assignment based on craniodental variation in multivariate analyses. Although the majority of the phylogenetic signal is generated from the mtDNA data, the nuclear gene corroborates the interspecific mitochondrial clade structure.

## Bivariate Scatterplots

A range of scatterplots are shown for dental variables differentiating *A. swainsonii* from the other three species (four taxa) of Dusky Antechinus. Figs 4-7 show differences among these taxa for a range of the most discriminating dental characters: APV, IPV and NWR, for males and females. The best skull characters for discriminating members of the Dusky Antechinus complex are the front / rear palatal vacuity lengths (APV, PPV) and the size of the gap separating them (IPV) - larger vacuities and

## Australian Dusky Antechinus Complex

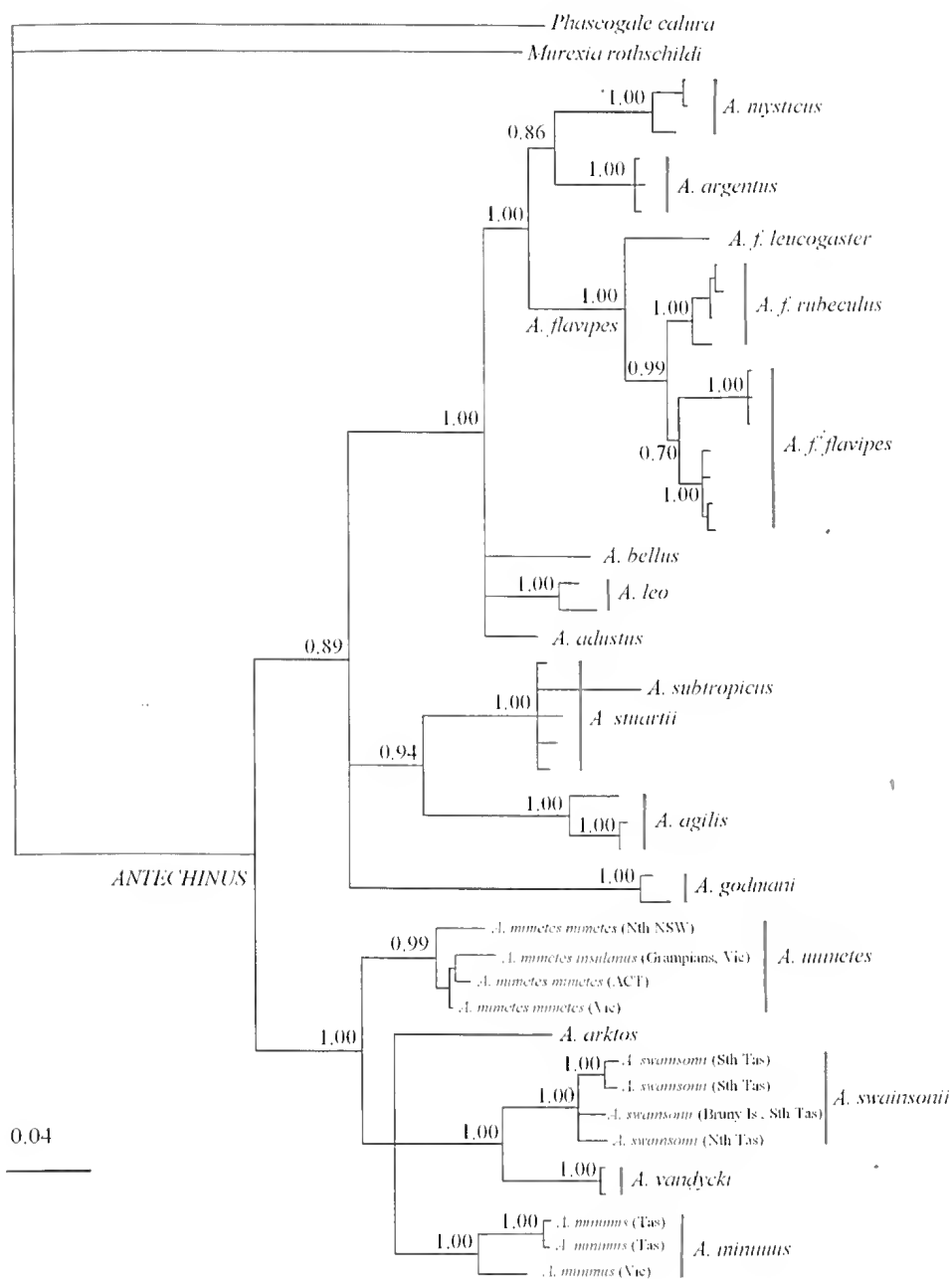


FIG. 2. Bayesian phylogeny of the genus *Antechinus* based on mitochondrial (Cytb) gene sequences. Posterior probabilities are shown at each node (those less than 0.70 are omitted).

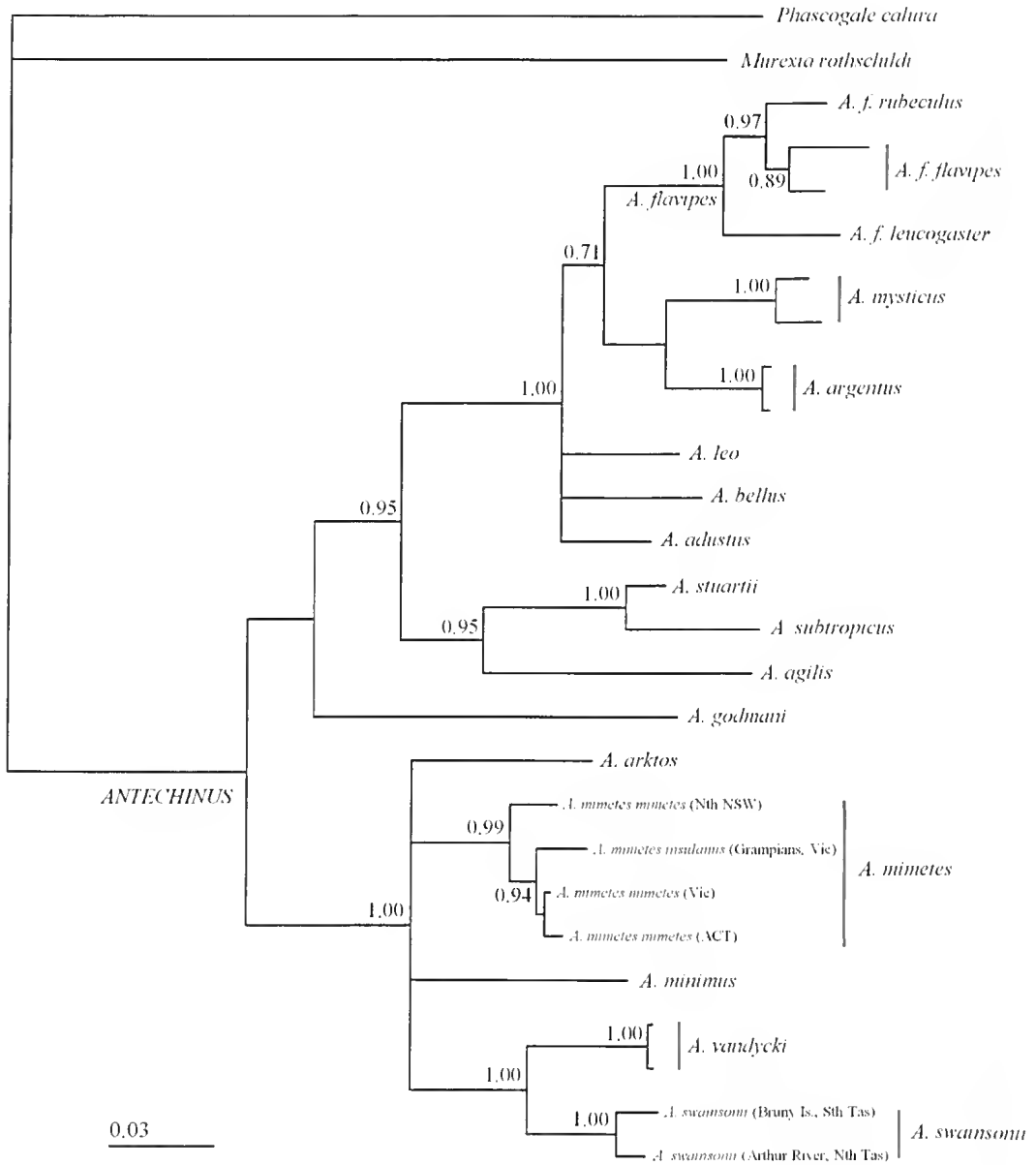


FIG. 3. Bayesian phylogeny of the genus *Antechinus* based on concatenated mitochondrial (Cytb) and nuclear (IRBP) gene sequences. Posterior probabilities are shown at each node (those less than 0.70 are omitted).

smaller separating gaps tend to be a feature of higher latitude species, with smaller holes and larger gaps as one moves into lower latitudes. *Antechinus vandycki* sp. nov. has larger anterior palatal vacuities than any congener.

## DFA and CVA

Discriminant Function Analysis (DFA) of members of the Dusky *Antechinus* complex indicated that 100% of females and males were clustered into the 5 proposed taxon groups

## Australian Dusky Antechinus Complex

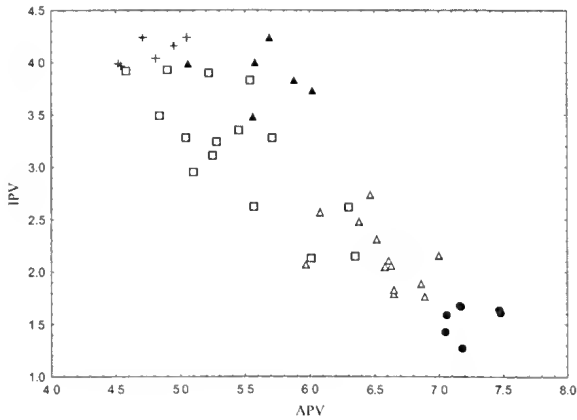


FIG. 4. Scatterplot of anterior palatal vacuity length (APV) versus inter palatal vacuity distance (IPV) measures for male *A. swainsonii* (open triangles), *A. vandycki* sp. nov. (closed circles), *A. mimetes mimetes* (open squares), *A. mimetes insulanus* (closed triangles) and *A. arktos* (crosses).

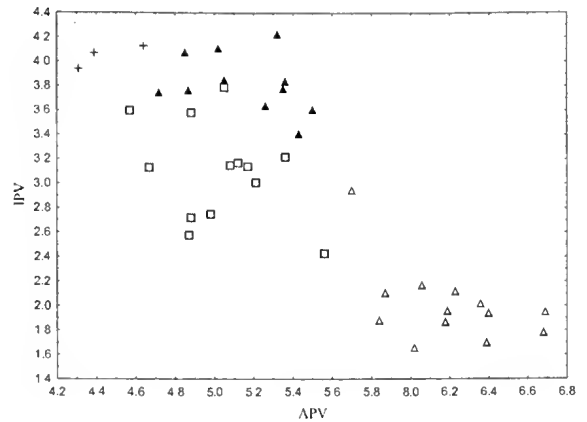


FIG. 5. Scatterplot of anterior palatal vacuity length (APV) versus inter palatal vacuity distance (IPV) measures for female *A. swainsonii* (open triangles), *A. vandycki* sp. nov. (closed circles), *A. mimetes mimetes* (open squares), *A. mimetes insulanus* (closed triangles) and *A. arktos* (crosses).

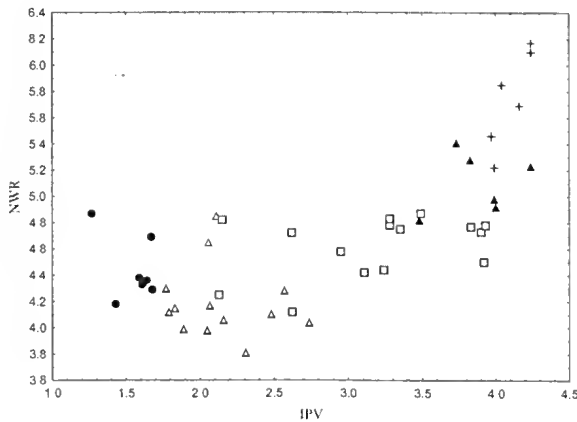


FIG. 6. Scatterplot of inter palatal vacuity distance (IPV) versus width of nasals at the nasal / maxilla / frontal junction (NWR) measures for male *A. swainsonii* (open triangles), *A. vandycki* sp. nov. (closed circles), *A. mimetes mimetes* (open squares), *A. mimetes insulanus* (closed triangles) and *A. arktos* (crosses).

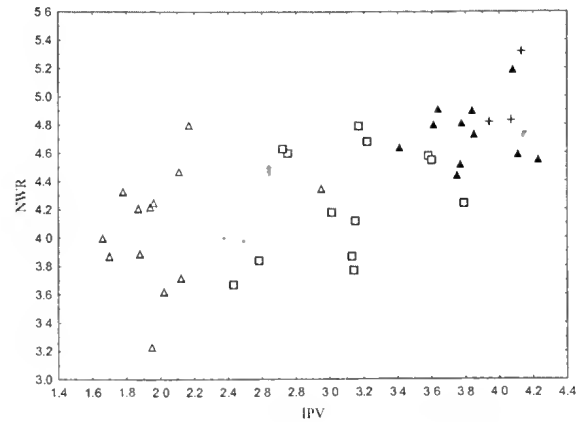


FIG. 7. Scatterplot of inter palatal vacuity distance (IPV) versus width of nasals at the nasal / maxilla / frontal junction (NWR) measures for female *A. swainsonii* (open triangles), *A. mimetes mimetes* (open squares), *A. mimetes insulanus* (closed triangles) and *A. arktos* (crosses).

(*A. swainsonii*, *A. vandycki* sp. nov., *Antechinus mimetes mimetes*, *A. mimetes insulanus* and *A. arktos*) correctly (posterior probabilities all equal to 1.00, not shown), based on the Mahalanobis distance of each individual from

the centroid of the *a priori* species group. For CVA, 100% of the variation in dental characters was explained in the first three canonical roots for males and females. Variation was very well resolved for both sexes, as eigenvalues for

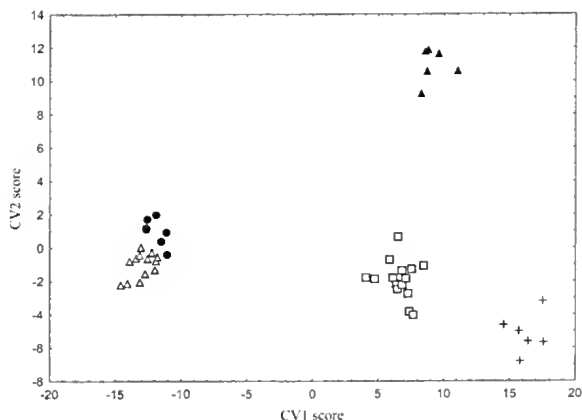


FIG. 8. Scatterplot of canonical variates scores (roots 1 and 2) for male *A. swainsonii* (open triangles), *A. vandycki* sp. nov. (closed circles), *A. mimetes mimetes* (open squares), *A. mimetes insulanus* (closed triangles) and *A. arktos* (crosses).

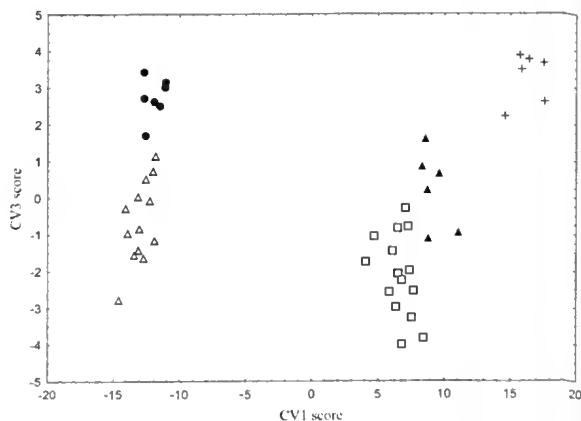


FIG. 9. Scatterplot of canonical variates scores (roots 1 and 3) for male *A. swainsonii* (open triangles), *A. vandycki* sp. nov. (closed circles), *A. mimetes mimetes* (open squares), *A. mimetes insulanus* (closed triangles) and *A. arktos* (crosses).

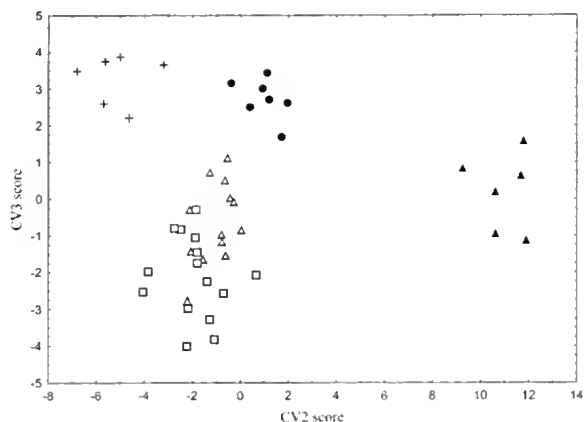


FIG. 10. Scatterplot of canonical variates scores (roots 2 and 3) for male *A. swainsonii* (open triangles), *A. vandycki* sp. nov. (closed circles), *A. mimetes mimetes* (open squares), *A. mimetes insulanus* (closed triangles) and *A. arktos* (crosses).

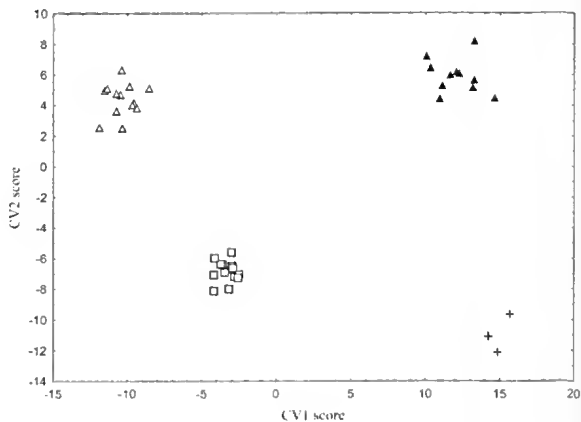


FIG. 11. Scatterplot of canonical variates scores (roots 1 and 2) for female *A. swainsonii* (open triangles), *A. vandycki* sp. nov. (closed circles), *A. mimetes mimetes* (open squares), *A. mimetes insulanus* (closed triangles) and *A. arktos* (crosses).

the first three canonical roots were well above 1 (males: root 1 = 141.2; root 2 = 22.8; root 3 = 4.5; females: root 1 = 105.7; root 2 = 44.4; root 3 = 4.0) and about four-fifths of the variation was explained in the first root (82%) for males, whereas about two-thirds (69%) was explained in the first root for females. Further, cumulatively the first two roots explained 96% of variation in males and 97% in females. Figs

8-12 show scatterplots of canonical roots 1-3, for males and females; all four taxa are tightly clustered within their taxon and well separated between taxa, for both sexes. Canonical analysis suggests that *A. vandycki* sp. nov. most closely resembles *A. swainsonii* and to a lesser extent *A. mimetes mimetes* and *A. m. insulanus* / *A. arktos*, which reflects their relative geographical proximities. This is a reflection of the longer,



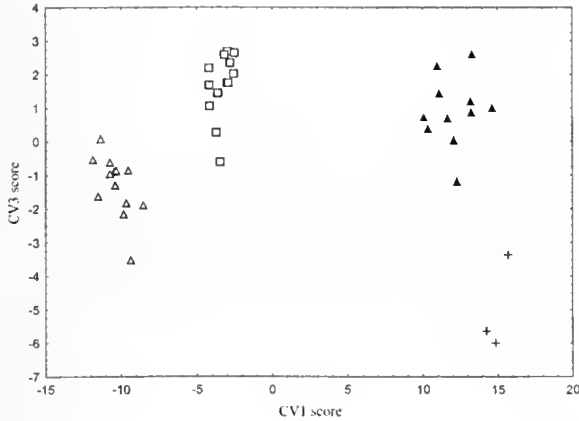


FIG. 12. Scatterplot of canonical variates scores (roots 1 and 3) for female *A. swainsonii* (open triangles), *A. mimetes mimetes* (open squares), *A. mimetes insulanus* (closed triangles) and *A. arktos* (crosses).

more narrow-snouted skulls with larger palatal vacuities characteristic of *A. swainsonii* and *A. vandycki* sp. nov. compared to the stouter skulls of *A. mimetes mimetes* and even more robust *A. mimetes insulanus* and *A. arktos*.

To facilitate direct comparison, univariate statistics (means, standard deviations, range minima and maxima) are shown for each of the external and craniodental measurements for all four species (and 5 taxa) within the Dusky Antechinus species complex: *A. swainsonii*, *A. vandycki* sp. nov., *A. mimetes mimetes*, *A. mimetes insulanus* and *A. arktos*. (refer Tables 1-5). All ANOVAs of measured variables among all antechinus species were significant (Table 6). In pairwise comparisons below, attention is given to diagnosing absolute differences (with no overlap in ranges) where they exist, compared to those that are significantly ( $P < 0.05$ ) different. *Antechinus swainsonii*, with primacy of discovery (Waterhouse 1840) within the complex, was chosen as the reference species, to which all other congeners are compared in pairwise fashion below.

## Taxon Comparisons

*Antechinus swainsonii* (Waterhouse)  
versus *Antechinus vandycki* sp. nov.  
Baker, Mutton, Mason and Gray

**Pelage.** Both species are greyish-brown in appearance; moderate-dark grey on the back, pale grey on the sides and light grey-white on the underside with brownish highlights on the body that are more notable on the flanks and also with brownish warming towards the rump. The tail in both species is bicoloured. However, *A. swainsonii* is distinctly paler than *A. vandycki* sp. nov.; *A. swainsonii* is slightly lighter grey dorsally, lighter grey on the cheeks, shoulders and throat; the underside of *A. swainsonii* is paler grey-white and the feet are lighter, appearing lighter brownish than those in *A. vandycki* sp. nov. The tail is more subtly bicoloured in *A. swainsonii*, with a lighter grey dorsally on the tail. *Antechinus swainsonii* is slightly more lightish grey in the front half of the body merging towards more distinct and slightly warmer brown on the rump, when compared with *A. vandycki* sp. nov.

**External Measurements.** *Antechinus swainsonii* and *A. vandycki* sp. nov. males are similar in external size (see Tables 1, 2 and 6).

**Craniodental Characters.** *Antechinus swainsonii* is smaller than *A. vandycki* sp. nov. in absolute measurement (i.e., with no overlap in ranges) for APV in males. *Antechinus swainsonii* is larger than *A. vandycki* sp. nov. in absolute measurement for IPV in males. *Antechinus swainsonii* is significantly smaller than *A. vandycki* sp. nov. for PPV in males (Tables 1, 2 and 6).

**Comments.** *Antechinus swainsonii* occur throughout most of Tasmania, except the far south-east on Tasman Peninsula. *Antechinus vandycki* sp. nov. have been found to date only in small patches of undisturbed forest on the east of Tasman Peninsula, Tasmania. Genetics: uncorrected pairwise difference at the mitochondrial gene CytB between *A. swainsonii* and *A. vandycki* sp. nov. is 7.3 - 8.6%.

*Antechinus swainsonii* versus *Antechinus mimetes mimetes* (Thomas) new status

**Pelage.** *Antechinus swainsonii* is greyish-brown in appearance, greyer at the front with a brownish warming on the rump whereas *A. mimetes mimetes* is more evenly brownish from head to rump. *Antechinus swainsonii* is light greyish on the belly, whereas *A. mimetes mimetes* tends to be light brownish on the belly.

**External Measurements.** *Antechinus swainsonii* and *A. mimetes mimetes* are similar in external size for males and females (see Tables 1, 3 and 6).

**Craniodental Characters.** *Antechinus swainsonii* is larger than *A. mimetes mimetes* in absolute measurement for APV in females. *Antechinus swainsonii* is significantly smaller than *A. mimetes mimetes* for IPV in males and females and for TC in males and significantly larger in APV for males (Tables 1, 3 and 6).

**Comments.** *Antechinus swainsonii* occur throughout most of Tasmania, except the far south-east on Tasman Peninsula. *Antechinus mimetes mimetes* is found on mainland Australia in Victoria and New South Wales. Genetics: uncorrected pairwise difference at the mitochondrial gene CytB between *A. swainsonii* and *A. mimetes mimetes* is 9.4 – 11.4%.

*Antechinus swainsonii* versus *Antechinus mimetes insulanus* Davison new status

**Pelage.** *Antechinus swainsonii* is greyish-brown in appearance, greyer at the front with a brownish warming on the rump whereas *A. mimetes insulanus* is more evenly brownish from head to rump. *Antechinus swainsonii* is light greyish on the belly, whereas *A. mimetes insulanus* tends to be light brownish on the belly.

**External measurements.** *Antechinus swainsonii* and *A. mimetes insulanus* are similar in external size for males and females (see Tables 1, 4 and 6).

**Craniodental Characters.** *Antechinus swainsonii* is smaller than *A. mimetes insulanus* in absolute measurement for IPV, M<sup>2</sup>W, R-LM<sup>3</sup>, TC, UML and LML in males and IPV, M<sup>2</sup>W, ZW and M<sub>2</sub>W in females. *Antechinus swainsonii* is larger than

*A. mimetes insulanus* in absolute measurement for APV in females. *Antechinus swainsonii* is significantly smaller than *A. mimetes insulanus* for Dent, IBW, NW, OBW, R-LM<sup>1</sup>T, NWR and PML in males and females and in BL, ZW, HT-B and M<sub>2</sub>W in males only and R-LM<sup>3</sup>, HT, TC, UML and LML in females only. *Antechinus swainsonii* is significantly larger than *A. mimetes insulanus* for APV in males (Tables 1, 3 and 6).

**Comments.** *Antechinus swainsonii* occur throughout most of Tasmania, except the far south-east on Tasman Peninsula. *Antechinus mimetes insulanus* is found on mainland Australia in the Grampians NP, Victoria. Genetics: uncorrected pairwise difference at the mitochondrial gene CytB between *A. swainsonii* and *A. mimetes insulanus* is 11.0 – 11.6%.

*Antechinus swainsonii* versus *Antechinus arktos*

Baker, Mutton, Hines and Van Dyck

**Pelage.** *Antechinus swainsonii* is greyish-brown in appearance, greyer at the front with a brownish warming on the rump whereas *A. arktos* is more brownish from head to rump with a very warm orangish rump and some orange fur around the eye. *Antechinus swainsonii* is light greyish on the belly, whereas *A. arktos* tends to be light brownish on the belly. *Antechinus swainsonii* has brownish hindfeet and a greyish-brown tail, whereas *A. arktos* has black hindfeet and tail.

**External Measurements.** *Antechinus swainsonii* has significantly smaller tail-vent length than *A. arktos* in males. *Antechinus swainsonii* and *A. arktos* are otherwise similar in external size for males and females (see Tables 1, 5 and 6).

**Craniodental Characters.** *Antechinus swainsonii* is smaller than *A. arktos* in absolute measurement for IBW, IPV, M<sup>2</sup>W, NW, R-LM<sup>1</sup>, TC, NWR and UML in males and IPV and UML in females. *Antechinus swainsonii* is larger than *A. arktos* in absolute measurement for APV in males and females. *Antechinus swainsonii* is significantly smaller than *A. arktos* for OBW and R-LM<sup>3</sup> in males only (Tables 1, 5 and 6).

**Comments.** *Antechinus swainsonii* occur throughout most of Tasmania, except the far south-east on Tasman Peninsula. *Antechinus arktos* is



FIG. 13. *Antechinus swainsonii* holotype specimen photographs of study skin BMNH 60.1.5.18 (male) (A-B): A, top view; B, bottom view. Photographs by Andrew Baker.

found on the border of Qld and NSW in the Tweed Volcano Caldera. Genetics: uncorrected pairwise difference at the mitochondrial gene CytB between *A. swainsonii* and *A. arktos* is 10.8–11.8%.

*Antechinus swainsonii* versus  
*Antechinus minimus* (Geoffroy)

**Pelage.** *Antechinus swainsonii* is greyish-brown in appearance, greyer at the front with a brownish warming on the rump whereas *A. minimus* has coarser fur and a leaden grey head that merges to brownish yellow fur on the rump and flanks.

**External Measurements.** *Antechinus swainsonii* has significantly larger tail-vent length and hindfoot length than *A. minimus* in males and females. (see Tables 1 and 6).

**Craniodental Characters.** *Antechinus swainsonii* is smaller than *A. minimus* in absolute measurement for IPV in males. *Antechinus swainsonii* is larger

than *A. minimus* in absolute measurement for APV, IOW, PL, I<sup>1</sup>-P<sup>3</sup>, I<sub>1</sub>-P<sub>3</sub> and UPL in males and APV, I<sup>1</sup>-P<sup>3</sup>, I<sub>1</sub>-P<sub>3</sub> and UPL in females. *Antechinus swainsonii* is significantly smaller than *A. minimus* for R-LC<sup>1</sup> and R-LM<sup>1</sup> in males and IPV, R-LC<sup>1</sup>, R-LM<sup>1</sup>, R-LM<sup>2</sup> and SWR-LC<sup>1</sup>B in females. *Antechinus swainsonii* is significantly larger than *A. minimus* for Dent, UML and LML in males and BL, Dent, IOW, PL, UML and LML in females (Tables 1 and 6).

**Comments.** *Antechinus swainsonii* occur throughout most of Tasmania, except the far south-east on Tasman Peninsula. *Antechinus minimus* is found in both Tasmania, Victoria and SA. In Tasmania, the two species may co-occur although *A. minimus* tends to be found in lower and more open habitats than *A. swainsonii*. Genetics: uncorrected pairwise difference at the mitochondrial gene CytB between *A. swainsonii* and *A. minimus* is 10.0–12.0%.

*Antechinus swainsonii* versus  
*Antechinus adustus* (Thomas)

**Pelage.** *Antechinus swainsonii* is greyish-brown in appearance, greyer at the front with a brownish warming on the rump whereas *A. adustus* has more uniformly dark brown fur with rusty tips on the head and back.

**External Measurements.** *Antechinus swainsonii* is larger than *A. adustus* in absolute measurement for body weight in males and females and in head-body length in females only. *Antechinus swainsonii* has significantly larger head-body length and hindfoot length than *A. adustus* in males only (see Tables 1 and 6).

**Craniodental Characters.** *Antechinus swainsonii* is smaller than *A. adustus* in absolute measurement for IPV in males and females. *Antechinus swainsonii* is larger than *A. adustus* in absolute measurement for APV, BL, Dent, IOW, HT,

PL, HT-B, I<sup>1</sup>-P<sup>3</sup>, I<sub>1</sub>-P<sub>3</sub> and UPL in males and females and PML in females only. *Antechinus swainsonii* is significantly smaller than *A. adustus* for R-LC<sup>1</sup> and SWR-LC<sup>1</sup>B in males and females. *Antechinus swainsonii* is significantly larger than *A. adustus* for PML, UML and LML in males and OBW, UML, BuL and LML in females (Tables 1 and 6).

**Comments.** *Antechinus swainsonii* occur throughout most of Tasmania, except the far south-east on Tasman Peninsula. *Antechinus adustus* is found in the wet tropics of north-east Qld. Genetics: uncorrected pairwise difference at the mitochondrial gene CytB between *A. swainsonii* and *A. adustus* is 14.7 – 16.3%.

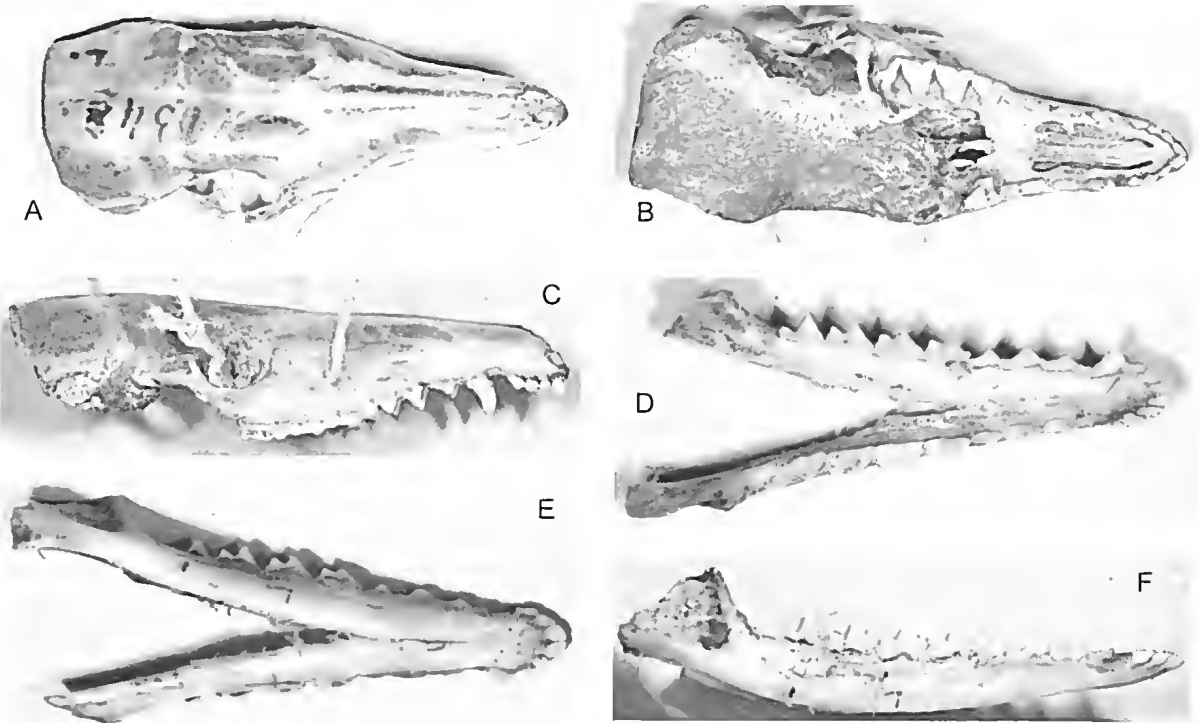


FIG. 14. *Antechinus swainsonii* holotype specimen photographs of skull and dentary BMNH 60.1.5.26 (male) (A-F): A, skull, top view; B, skull, bottom view; C, skull, side view; D, dentary, top view; E, dentary, bottom view; F, dentary, side view. Photographs by Andrew Baker.



FIG. 15. *Antechinus mimetes mimetes* holotype specimen photographs of study skin BMNH 24.10.1.1 (female) (A-B): A, top view; B, bottom view. Photographs by Andrew Baker.

*Antechinus swainsonii* versus  
*Antechinus agilis* Dickman,  
Parnaby, Crowther and King

**Pelage.** *Antechinus swainsonii* is greyish-brown in appearance, greyer at the front with a brownish warming on the rump whereas *A. agilis* is a uniform medium grey to greyish brown from head to rump. *Antechinus agilis* also has a light-coloured ring of fur around the eyes.

**External Measurements.** *Antechinus swainsonii* is larger than *A. agilis* in absolute measurement for body weight and hindfoot length in males and in body weight and head-body length in females. *Antechinus swainsonii* has significantly larger head-body length in males and hindfoot length in females (see Tables 1 and 6).

**Craniodental Characters.** *Antechinus swainsonii* is smaller than *A. agilis* in absolute measurement for IPV in males and females. *Antechinus swainsonii* is larger than *A. agilis* in absolute

measurement for APV, BL, Dent, IOW, PL, HT-B, I<sup>1</sup>-P<sup>3</sup>, LML, I<sub>1</sub>-P<sub>3</sub> and UPL in males and APV, BL, Dent, IBW, IOW, HT, PL, HT-B, I<sup>1</sup>-P<sup>3</sup>, I<sub>1</sub>-P<sub>3</sub> and UPL in females. *Antechinus swainsonii* is significantly smaller than *A. agilis* for R-LC<sup>1</sup>, R-LM<sup>2</sup> and SWR-LC<sup>1</sup>B in females. *Antechinus swainsonii* is significantly larger than *A. agilis* for IBW, OBW, PPV, HT, PML, UML and M<sub>2</sub>W in males and OBW, PPV, NWR, PML, UML and LML in females (Tables 1 and 6).

**Comments.** *Antechinus swainsonii* occur throughout most of Tasmania, except the far south-east on Tasman Peninsula, whereas *A. agilis* is known only from south-eastern Australia, south of around Sydney's (NSW) latitude. Genetics: uncorrected pairwise difference at the mitochondrial gene CytB between *A. swainsonii* and *A. agilis* is 14.7 – 16.9%.

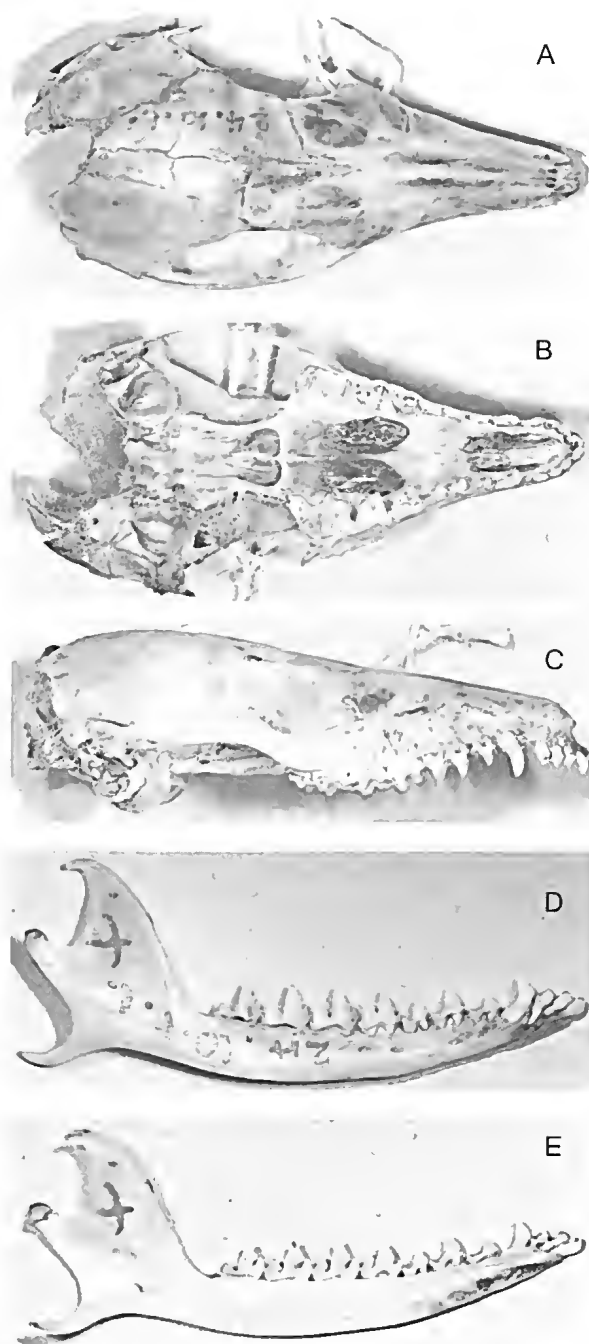


FIG. 16. *Antechinus mimetes mimetes* holotype specimen photographs of skull and dentary BMNH 24.10.1.1 (female) (A-E): A, skull, top view; B, skull, bottom view; C, skull, side view; D, dentary, outside view; E, dentary, inside view. Photographs by Andrew Baker.

# *Antechinus swainsonii* versus *Antechinus argentus* Baker, Mutton and Hines

**Pelage.** *Antechinus swainsonii* is greyish-brown in appearance, greyer at the front with a brownish warming on the rump whereas *A. argentus* has a silvery head and neck that merge subtly to deep olive-buff coloured fur on the rump and flanks.

**External Measurements.** *Antechinus swainsonii* is larger than *A. argentus* in absolute measurement for head-body length and hindfoot length in males and in body weight, head-body length and hindfoot length in females (see Tables 1 and 6).

**Craniodontal Characters.** *Antechinus swainsonii* is smaller than *A. argentus* in absolute measurement for IPV, R-LM<sup>1</sup> and R-LM<sup>2</sup> in males and in IPV for females. *Antechinus swainsonii* is larger than *A. argentus* in absolute measurement for APV, BL, Dent, IOW, HT, PL, HT-B, I<sup>1</sup>-P<sup>3</sup>, I<sub>1</sub>-P<sub>3</sub> and UPL in males and females and in PPV for females only. *Antechinus swainsonii* is significantly smaller than *A. argentus* for R-LC<sup>1</sup>, R-LM<sup>3</sup> and SWR-LC<sup>1</sup>B in males only. *Antechinus swainsonii* is significantly larger than *A. argentus* for LML in males only (Tables 1 and 6).

**Comments.** *Antechinus swainsonii* occur throughout most of Tasmania, except the far south-east on Tasman Peninsula, whereas *A. argentus* is known only from Kroombit Tops NP in south-east Qld. Genetics: uncorrected pairwise difference at the mitochondrial gene CytB between *A. swainsonii* and *A. argentus* is 16.0 – 17.1%.

# *Antechinus swainsonii* versus *Antechinus bellus* (Thomas)

**Pelage.** *Antechinus swainsonii* is greyish-brown in appearance, greyer at the front with a brownish warming on the rump whereas *A. bellus* is pale to medium grey above, sometimes with a fawn tinge, with pale grey belly, hands and feet.



FIG. 17. *Antechinus vandycki* sp. nov. holotype specimen photographs of study skin QM JM 20111 (male) (A-B): A, top view; B, bottom view. Photographs by Andrew Baker.

**External Measurements.** *Antechinus swainsonii* is smaller than *A. bellus* in absolute measurement for ear length in females. *Antechinus swainsonii* is significantly smaller than *A. bellus* in tail-vent length in males and females and in ear length for males. *Antechinus swainsonii* is significantly larger than *A. bellus* in body weight for females (see Tables 1 and 6).

**Craniodental Characters.** *Antechinus swainsonii* is smaller than *A. bellus* in absolute measurement for IPV, M<sup>2</sup>W, NW, R-LC<sup>1</sup>, R-LM<sup>1</sup>, R-LM<sup>2</sup>, R-LM<sup>3</sup>, SWR-LC<sup>1</sup>B and BuL for males and females and in M<sub>2</sub>W in females. *Antechinus swainsonii* is larger than *A. bellus* in absolute measurement for IPV, IOW, I<sub>1</sub>-P<sub>3</sub> and UPL in males and for APV, IBW, IOW, PPV, I<sub>1</sub>-P<sub>3</sub>, I<sub>1</sub>-P<sub>3</sub> and UPL in females. *Antechinus*

*swainsonii* is significantly smaller than *A. bellus* for OBW, R-LM<sup>1</sup>T, ZW and M<sub>2</sub>W in males and for OBW, R-LM<sup>1</sup>T, ZW, UML and LML in females. *Antechinus swainsonii* is significantly larger than *A. bellus* for IBW, PPV and I<sup>1</sup>-P<sup>3</sup> in males and for Dent, PL and HT-B in females (Tables 1 and 6).

**Comments.** *Antechinus swainsonii* occur throughout most of Tasmania, except the far south-east on Tasman Peninsula, whereas *A. bellus* is known only from northern Northern Territory. Genetics: uncorrected pairwise difference at the mitochondrial gene CytB between *A. swainsonii* and *A. bellus* is 15.9 – 18.3%.

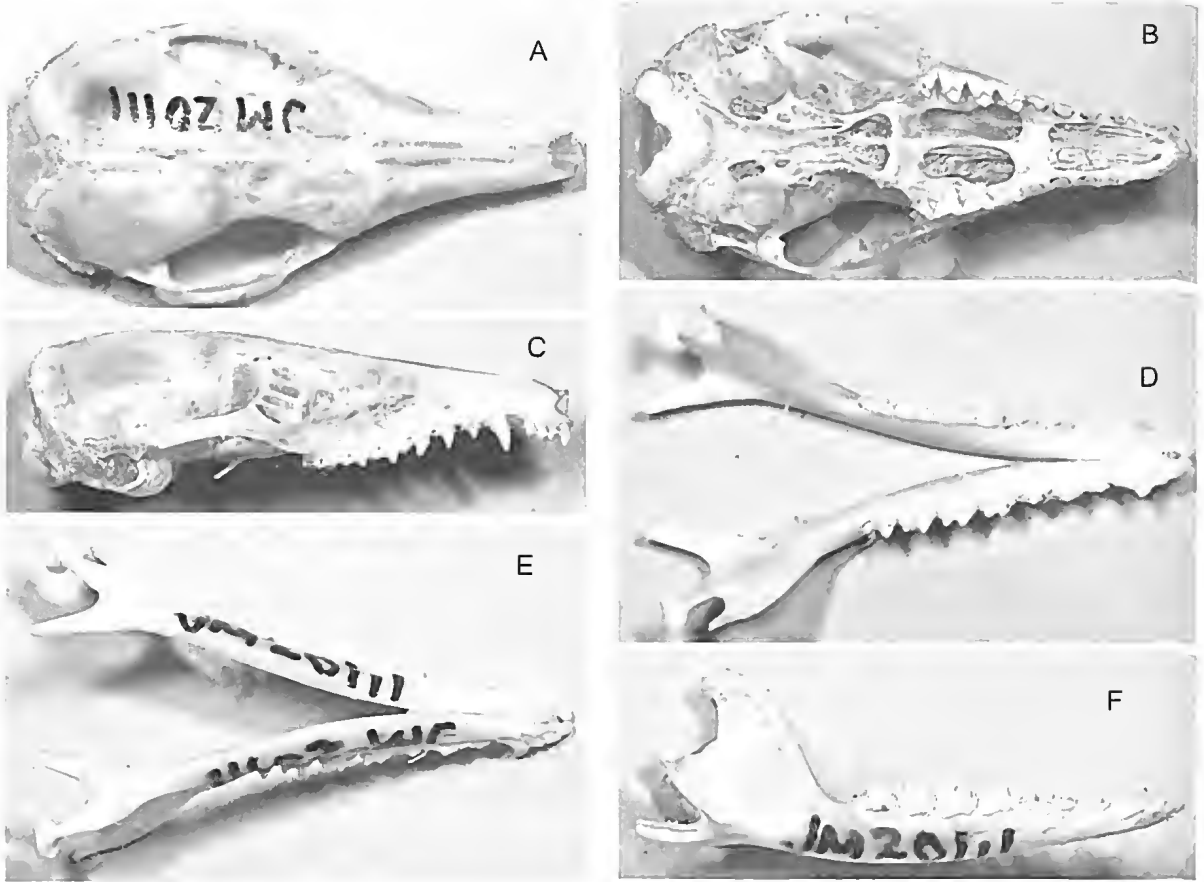


FIG. 18. *Antechinus vandycki* sp. nov. holotype specimen photographs of skull and dentary QM JM 20111 (male) (A-F): A, skull, top view; B, skull, bottom view; C, skull, side view; D, dentary, top view; E, dentary, bottom view; F, dentary, side view. Photographs by Andrew Baker.

*Antechinus swainsonii* versus  
*Antechinus flavipes flavipes* (Waterhouse)

**Pelage.** *Antechinus swainsonii* is greyish-brown in appearance, greyer at the front with a brownish warming on the rump whereas *A. f. flavipes* has marked orange-tonings on the hands, feet and tail base and a pale eye ring.

**External Measurements.** *Antechinus swainsonii* is significantly larger than *A. flavipes flavipes* in head-body length and hindfoot length for males and females (see Tables 1 and 6).

**Craniodental Characters.** *Antechinus swainsonii* is smaller than *A. flavipes flavipes* in absolute measurement for IPV, M<sup>2</sup>W and R-LM<sup>2</sup> in males and for IPV, M<sup>2</sup>W, R-LC<sup>1</sup>, R-LM<sup>2</sup>, R-LM<sup>3</sup> and SWR-LC<sup>1</sup>B in females. *Antechinus swainsonii* is larger than *A. flavipes flavipes* in absolute measurement for APV, IOW, I<sup>1</sup>-P<sup>3</sup>, I<sub>1</sub>-P<sub>3</sub> and UPL in males and females. *Antechinus swainsonii* is significantly smaller than *A. flavipes flavipes* for NW, R-LC<sup>1</sup>, R-LM<sup>1</sup>, R-LM<sup>1</sup>T, R-LM<sup>3</sup>, SWR-LC<sup>1</sup>B, BuL and M<sub>2</sub>W in males and for NW, R-LM<sup>1</sup>, R-LM<sup>1</sup>T, BuL and M<sub>2</sub>W in females. *Antechinus swainsonii* is significantly larger than *A. flavipes flavipes* for BL, Dent, IBW, PPV,



HT, PL and HT-B for males and females and for PML in females only (see Tables 1 and 6).

**Comments.** *Antechinus swainsonii* occur throughout most of Tasmania, except the far south-east on Tasman Peninsula, whereas *A. f. flavipes* occurs in a wide range of drier habitat in mainland south-east Australia. Genetics: uncorrected pairwise difference at the mitochondrial gene CytB between *A. swainsonii* and *A. flavipes flavipes* is 15.7 – 17.5%.

*Antechinus swainsonii* versus  
*Antechinus flavipes leucogaster* Gray

**Pelage.** *Antechinus swainsonii* is greyish-brown in appearance, greyer at the front with a brownish warming on the rump whereas *A. f. leucogaster* has marked yellowish-brown fur on the hands, feet and tail base and a pale eyering.

**External Measurements.** *Antechinus swainsonii* is significantly larger than *A. flavipes leucogaster* in body weight, head-body length and hind-foot length for males and females and for tail-vent length in females (see Tables 1 and 6).

**Craniodontal Characters.** *Antechinus swainsonii* is smaller than *A. flavipes leucogaster* in absolute measurement for IPV, R-LM<sup>1</sup> and R-LM<sup>2</sup> in males and for IPV, R-LC<sup>1</sup>, R-LM<sup>1</sup>, R-LM<sup>2</sup> and R-LM<sup>3</sup> in females. *Antechinus swainsonii* is larger than *A. flavipes leucogaster* in absolute measurement for APV, IOW, PL, I<sup>1</sup>-P<sup>3</sup>, I<sub>1</sub>-P<sub>3</sub> and UPL in males and for APV, Dent, IOW, PL, HT-B, I<sup>1</sup>-P<sup>3</sup>, I<sub>1</sub>-P<sub>3</sub> and UPL in females. *Antechinus swainsonii* is significantly smaller than *A. flavipes leucogaster* for NW, R-LC<sup>1</sup>, R-LM<sup>1</sup>T, R-LM<sup>3</sup>, SWR-LC<sup>1</sup>B and BuL in males and for M<sup>2</sup>W, NW, R-LM<sup>1</sup>T, SWR-LC<sup>1</sup>B, BuL and M<sub>2</sub>W in females. *Antechinus swainsonii* is significantly larger than *A. flavipes leucogaster* for BL, Dent, IBW, PPV, HT, UML, HT-B and LML in males and for BL, IBW, PPV, HT, PML, UML and LML in females (see Tables 1 and 6).

**Comments.** *Antechinus swainsonii* occur throughout most of Tasmania, except the far south-east on Tasman Peninsula, whereas *A. flavipes leucogaster* occurs in south-west Western Australia. Genetics: uncorrected pairwise difference at the

mitochondrial gene CytB between *A. swainsonii* and *A. flavipes leucogaster* is 15.3 – 17.1%.

*Antechinus swainsonii* versus  
*Antechinus flavipes rubeculus* Van Dyck

**Pelage.** *Antechinus swainsonii* is greyish-brown in appearance, greyer at the front with a brownish warming on the rump whereas *A. flavipes rubeculus* has orange-toned fur on the upper hind feet and tail base and a pale eyering.

**External Measurements.** *Antechinus swainsonii* is similar in size to *A. flavipes rubeculus* (see Tables 1 and 6).

**Craniodontal Characters.** *Antechinus swainsonii* is smaller than *A. flavipes rubeculus* in absolute measurement for IPV, M<sup>2</sup>W, R-LC<sup>1</sup>, R-LM<sup>1</sup>, R-LM<sup>1</sup>T, R-LM<sup>2</sup> and SWR-LC<sup>1</sup>B in males and for IPV, M<sup>2</sup>W, R-LC<sup>1</sup>, R-LM<sup>1</sup>, R-LM<sup>1</sup>T, R-LM<sup>2</sup>, R-LM<sup>3</sup>, ZW, SWR-LC<sup>1</sup>B, BuL and M<sub>2</sub>W in females. *Antechinus swainsonii* is larger than *A. flavipes rubeculus* in absolute measurement for APV, IOW, I<sup>1</sup>-P<sup>3</sup>, I<sub>1</sub>-P<sub>3</sub> and UPL in males and females and for PPV in females. *Antechinus swainsonii* is significantly smaller than *A. flavipes rubeculus* for NW, OBW, R-LM<sup>3</sup>, ZW, NWR, UML, BuL and M<sub>2</sub>W in males and for NW, OBW, UML and LML in females. *Antechinus swainsonii* is significantly larger than *A. flavipes rubeculus* for PL and HT-B in females only (see Tables 1 and 6).

**Comments.** *Antechinus swainsonii* occur throughout most of Tasmania, except the far south-east on Tasman Peninsula, whereas *A. flavipes rubeculus* is only found in the wet tropics of north-east Qld. Genetics: uncorrected pairwise difference at the mitochondrial gene CytB between *A. swainsonii* and *A. flavipes rubeculus* is 16.1 – 17.9%.

*Antechinus swainsonii* versus  
*Antechinus godmani* (Thomas)

**Pelage.** *Antechinus swainsonii* is greyish-brown in appearance, greyer at the front with a brownish warming on the rump whereas *A. godmani* is more uniformly brown on the head and back with a naked-looking tail.

**External Measurements.** *Antechinus swainsonii* is significantly smaller than *A. godmani* in body weight and tail-vent length in males and females and in ear length for females (see Tables 1 and 6).

**Craniodental Characters.** *Antechinus swainsonii* is smaller than *A. godmani* in absolute measurement for IBW, IPV, M<sup>2</sup>W, R-LC<sup>1</sup>, R-LM<sup>1</sup>, R-LM<sup>1</sup>T, SWR-LC<sup>1</sup>B, TC, UML, LML and M<sub>2</sub>W in males and for IPV, M<sup>2</sup>W, OBW, R-LC<sup>1</sup>, R-LM<sup>1</sup>, R-LM<sup>1</sup>T, R-LM<sup>2</sup>, R-LM<sup>3</sup>, ZW, SWR-LC<sup>1</sup>B, TC, UML, LML and M<sub>2</sub>W in females. *Antechinus swainsonii* is larger than *A. godmani* in absolute measurement for APV in males and females. *Antechinus swainsonii* is significantly smaller than *A. godmani* for BL, Dent, OBW, R-LM<sup>2</sup>, R-LM<sup>3</sup>, ZW and PL in males and for BL and IBW in females. *Antechinus swainsonii* is significantly larger than *A. godmani* for I<sub>1</sub>-P<sub>3</sub> in males and females (see Tables 1 and 6).

**Comments.** *Antechinus swainsonii* occur throughout most of Tasmania, except the far south-east on Tasman Peninsula, whereas *A. godmani* is known from only the wet tropics in north-east Qld. Genetics: uncorrected pairwise difference at the mitochondrial gene CytB between *A. swainsonii* and *A. godmani* is 16.3 – 19.1%.

*Antechinus swainsonii* versus  
*Antechinus leo* Van Dyck

**Pelage.** *Antechinus swainsonii* is greyish-brown in appearance, greyer at the front with a brownish warming on the rump whereas *A. leo* is uniformly cinnamon on the head and back with slightly darkened hair forming a mid-dorsal head stripe.

**External Measurements.** *Antechinus swainsonii* is significantly smaller than *A. leo* in tail-vent length, hindfoot length and ear length in males and females (see Tables 1 and 6).

**Craniodental Characters.** *Antechinus swainsonii* is smaller than *A. leo* in absolute measurement for IPV, M<sup>2</sup>W, NW, R-LC<sup>1</sup>, R-LM<sup>1</sup>, R-LM<sup>1</sup>T, R-LM<sup>2</sup>, R-LM<sup>3</sup>, SWR-LC<sup>1</sup>B and M<sub>2</sub>W in males and for IPV, M<sup>2</sup>W, NW, OBW, R-LC<sup>1</sup>, R-LM<sup>1</sup>, R-LM<sup>1</sup>T, R-LM<sup>2</sup>, R-LM<sup>3</sup>, ZW, SWR-LC<sup>1</sup>B, TC and M<sub>2</sub>W in females. *Antechinus swainsonii* is larger than

*A. leo* in absolute measurement for APV, IOW, I<sub>1</sub>-P<sub>3</sub> and UPL in males and females. *Antechinus swainsonii* is significantly smaller than *A. leo* for IBW, OBW, ZW, TC, NWR, PML, UML, BuL and LML in males and for IBW, NWR, UML, BuL and LML in females. *Antechinus swainsonii* is significantly larger than *A. leo* for I<sub>1</sub>-P<sub>3</sub> in males and females and HT-B in females (see Tables 1 and 6).

**Comments.** *Antechinus swainsonii* occur throughout most of Tasmania, except the far south-east on Tasman Peninsula, whereas *A. leo* is known only from north of Princess Charlotte Bay, on Cape York Peninsula in far northern Qld. Genetics: uncorrected pairwise difference at the mitochondrial gene CytB between *A. swainsonii* and *A. leo* is 15.7 – 17.9%.

*Antechinus swainsonii* versus  
*Antechinus mysticus* Baker,  
Mutton and Van Dyck

**Pelage.** *Antechinus swainsonii* is greyish-brown in appearance, greyer at the front with a brownish warming on the rump whereas *A. mysticus* has a greyish-brown head and neck, merging gradually to yellowish-buff on the rump and flanks, with a buff-brown tail base and slightly darkened tip.

**External Measurements.** *Antechinus swainsonii* is larger than *A. mysticus* in absolute measurement for hindfoot length in males. *Antechinus swainsonii* is significantly larger than *A. mysticus* in head-body length for males and for body weight, head-body length and hindfoot length in females (see Tables 1 and 6).

**Craniodental Characters.** *Antechinus swainsonii* is smaller than *A. mysticus* in absolute measurement for IPV and R-LC<sup>1</sup> in males and females and for SWR-LC<sup>1</sup>B in males. *Antechinus swainsonii* is larger than *A. mysticus* in absolute measurement for APV, IOW, PL, HT-B, I<sup>1</sup>-P<sup>3</sup>, I<sub>1</sub>-P<sub>3</sub> and UPL in males and females and for Dent and HT in females only. *Antechinus swainsonii* is significantly smaller than *A. mysticus* for M<sup>2</sup>W, R-LM<sup>1</sup>, R-LM<sup>2</sup> and R-LM<sup>3</sup> in males and for M<sup>2</sup>W, R-LM<sup>2</sup>, R-LM<sup>3</sup> and SWR-LC<sup>1</sup>B in females. *Antechinus swainsonii* is significantly larger than *A. mysticus* for BL,

Dent, IBW, HT, UML and LML in males and for BL, IBW, PML, UML and LML in females (see Tables 1 and 6).

**Comments.** *Antechinus swainsonii* occur throughout most of Tasmania, except the far south-east on Tasman Peninsula, whereas *A. mysticus* occurs in scattered coastal populations between the Qld / NSW border in far south-east Qld and Eungella NP near Mackay in mid-east Qld. Genetics: uncorrected pairwise difference at the mitochondrial gene CytB between *A. swainsonii* and *A. mysticus* is 15.5 – 17.5%.

*Antechinus swainsonii* versus  
*Antechinus stuartii* Macleay

**Pelage.** *Antechinus swainsonii* is greyish-brown in appearance, greyer at the front with a brownish warming on the rump whereas *A. stuartii* is more uniformly brownish-grey from head to rump.

**External Measurements.** *Antechinus swainsonii* is larger than *A. stuartii* in absolute measurement for hindfoot length in males and for body weight and head-body length in females. *Antechinus swainsonii* is significantly larger than *A. stuartii* in body weight and head-body length in males and for hind-foot length in females (see Tables 1 and 6).

**Craniodental Characters.** *Antechinus swainsonii* is smaller than *A. stuartii* in absolute measurement for IPV in males only. *Antechinus swainsonii* is larger than *A. stuartii* in absolute measurement for APV, IOW, PL, I<sup>1</sup>-P<sup>3</sup>, I<sub>1</sub>-P<sub>3</sub> and UPL in males and for APV, BL, Dent, IBW, IOW, HT, PL, HT-B, I<sup>1</sup>-P<sup>3</sup>, I<sub>1</sub>-P<sub>3</sub> and UPL in females. *Antechinus swainsonii* is significantly smaller than *A. stuartii* for R-LC<sup>1</sup> and SWR-LC<sup>1</sup>B in males and females and for IPV in females. *Antechinus swainsonii* is significantly larger than *A. stuartii* for BL, Dent, IBW, HT, PML, UML, HT-B and LML in males and for OBW, NWR, PML, UML and LML in females (see Tables 1 and 6).

**Comments.** *Antechinus swainsonii* occur throughout most of Tasmania, except the far south-east on Tasman Peninsula, *A. stuartii* occurs only on mainland Australia, in eastern NSW north of about Sydney to far south-east Queensland

(Girraween NP, Lamington NP, Main Range NP, Springbrook NP and Tamborine NP). Genetics: uncorrected pairwise difference at the mitochondrial gene CytB between *A. swainsonii* and *A. stuartii* is 13.4 – 15.9%.

*Antechinus swainsonii* versus  
*Antechinus subtropicus*  
Van Dyck and Crowther

**Pelage.** *Antechinus swainsonii* is greyish-brown in appearance, greyer at the front with a brownish warming on the rump whereas *A. subtropicus* is more uniformly brownish from head to rump.

**External Measurements.** *Antechinus swainsonii* is significantly larger than *A. subtropicus* in hindfoot length in males and for head-body length in females (see Tables 1 and 6).

**Craniodental Characters.** *Antechinus swainsonii* is larger than *A. subtropicus* in absolute measurement for APV, IOW, I<sup>1</sup>-P<sup>3</sup>, I<sub>1</sub>-P<sub>3</sub> and UPL in males and females and for HT-B in females only. *Antechinus swainsonii* is significantly smaller than *A. subtropicus* for M<sup>2</sup>W, PPV, R-LC<sup>1</sup>, SWR-LC<sup>1</sup>B and TC in males and for M<sup>2</sup>W, PPV, R-LC<sup>1</sup>, SWR-LC<sup>1</sup>B and M<sub>2</sub>W for females. *Antechinus swainsonii* is significantly larger than *A. subtropicus* for BL, Dent, HT and PL for males and females and for HT-B and LML for males only (see Tables 1 and 6).

**Comments.** *Antechinus swainsonii* occur throughout most of Tasmania, except the far south-east on Tasman Peninsula, whereas *A. subtropicus* appears to have a more subtropical distribution, occurring from Gympie south-east Qld south to Border Ranges NP in north-east NSW. Genetics: uncorrected pairwise difference at the mitochondrial gene CytB between *A. swainsonii* and *A. subtropicus* is 14.5 – 16.8%.

## DISCUSSION

### Systematics

The phylogenies reconstructed here (Figs 2-3) provide evidence of 15 putative species

TABLE 1. Univariate statistics: means, standard deviations and range minima and maxima of measured variables for *Antechinus swainsonii*.

MALES						FEMALES					
	Valid N	Mean	Min	Max	St. Dev.		Valid N	Mean	Min	Max	St. Dev.
wt	11	63.16	42.30	93.00	14.53	wt	15	41.59	31.00	57.00	7.36
hb	12	133.61	111.30	161.00	13.06	hb	16	116.70	103.19	127.00	8.69
tv	12	97.90	89.00	110.00	6.53	tv	16	87.75	77.00	101.42	6.13
hf	12	21.84	20.00	24.00	1.27	hf	15	19.30	18.00	21.00	0.81
e	12	16.86	15.01	21.00	1.47	e	14	15.28	14.50	16.00	0.54
APV	13	6.56	5.97	7.00	0.29	APV	13	6.20	5.70	6.69	0.30
BL	13	30.29	28.54	32.39	1.27	BL	13	28.70	26.80	30.36	1.17
Dent	13	24.62	23.05	26.61	1.19	Dent	13	23.28	21.74	24.72	0.94
IBW	13	4.50	4.15	4.81	0.19	IBW	13	4.33	4.14	4.65	0.15
IOW	13	7.95	7.61	8.77	0.30	IOW	13	7.84	7.38	8.43	0.34
IPV	13	2.14	1.77	2.74	0.31	IPV	13	2.01	1.66	2.95	0.32
M <sup>2</sup> W	13	2.29	2.19	2.38	0.06	M <sup>2</sup> W	13	2.22	2.08	2.34	0.08
NW	13	2.45	2.03	2.85	0.20	NW	13	2.45	2.20	2.73	0.16
OBW	13	12.24	11.31	13.30	0.54	OBW	13	11.80	11.21	12.18	0.29
PPV	13	5.33	4.39	5.99	0.44	PPV	13	5.00	4.52	5.56	0.30
R-LC <sup>1</sup>	13	4.64	3.99	5.20	0.33	R-LC <sup>1</sup>	13	4.27	3.93	4.56	0.20
R-LM <sup>1</sup>	13	8.52	7.70	9.07	0.47	R-LM <sup>1</sup>	13	8.32	7.78	8.67	0.31
R-LM <sup>1</sup> T	13	7.64	7.08	8.10	0.36	R-LM <sup>1</sup> T	13	7.35	6.99	7.72	0.25
R-LM <sup>2</sup>	13	10.42	9.58	11.27	0.51	R-LM <sup>2</sup>	13	10.01	9.48	10.51	0.30
R-LM <sup>3</sup>	13	12.73	11.89	13.64	0.53	R-LM <sup>3</sup>	13	12.17	11.21	12.59	0.40
ZW	13	16.68	15.43	18.49	0.97	ZW	13	15.63	14.16	16.42	0.58
HT	13	10.50	9.79	10.99	0.40	HT	13	10.10	9.61	10.77	0.37
PL	13	17.85	16.97	19.19	0.68	PL	13	17.08	15.91	17.87	0.62
SWR-LC <sup>1</sup> B	13	4.18	3.74	4.75	0.29	SWR-LC <sup>1</sup> B	13	3.81	3.54	4.16	0.21
TC	13	2.52	2.21	2.91	0.19	TC	13	2.62	2.22	2.87	0.21
NWR	13	4.19	3.81	4.85	0.28	NWR	13	4.07	3.23	4.80	0.41
PML	13	9.11	7.67	10.27	0.74	PML	13	8.62	7.99	10.23	0.75
UML	13	6.87	6.33	7.18	0.23	UML	13	6.65	6.23	7.01	0.29
HT-B	13	8.29	7.71	8.81	0.32	HT-B	13	8.08	7.68	8.52	0.26
BuL	13	4.19	3.62	4.50	0.26	BuL	13	4.02	3.76	4.28	0.16
I <sup>1</sup> -P <sup>3</sup>	13	10.00	9.43	10.45	0.28	I <sup>1</sup> -P <sup>3</sup>	13	9.54	8.88	10.12	0.37
LML	13	7.56	7.10	7.88	0.24	LML	13	7.33	6.96	7.71	0.29
I <sub>1</sub> -P <sub>3</sub>	13	7.96	7.51	8.43	0.27	I <sub>1</sub> -P <sub>3</sub>	13	7.57	7.09	8.03	0.36
M <sub>2</sub> W	13	2.19	2.00	2.33	0.10	M <sub>2</sub> W	13	2.09	1.94	2.22	0.08
UPL	13	4.44	4.16	5.08	0.25	UPL	13	4.20	3.86	4.45	0.19

TABLE 2. Univariate statistics: means, standard deviations and range minima and maxima of measured variables for *Antechinus vandycki* sp. nov.

MALES					
	Valid N	Mean	Min	Max	St. Dev.
wt	6	73.08	46.30	92.80	16.87
hb	6	120.21	104.91	132.60	9.82
tv	6	109.06	92.34	118.02	9.39
hf	6	22.47	20.34	24.62	1.67
e	6	16.37	14.94	17.55	1.00
APV	7	7.22	7.05	7.48	0.18
BL	7	31.71	29.90	33.20	1.04
Dent	7	25.92	24.48	27.76	1.02
IBW	7	4.48	4.21	4.75	0.21
IOW	7	7.95	7.67	8.11	0.15
IPV	7	1.56	1.27	1.68	0.15
M <sup>2</sup> W	7	2.33	2.24	2.38	0.05
NW	7	2.32	2.21	2.51	0.10
OBW	7	12.64	12.04	13.07	0.35
PPV	7	6.11	5.78	6.54	0.29
R-LC <sup>1</sup>	7	4.86	4.66	5.02	0.12
R-LM <sup>1</sup>	7	8.68	8.23	9.08	0.34
R-LM <sup>1</sup> T	7	7.87	7.61	8.15	0.16
R-LM <sup>2</sup>	7	10.55	9.70	10.97	0.47
R-LM <sup>3</sup>	7	12.91	12.39	13.44	0.37
ZW	7	17.25	15.99	18.39	0.71
HT	7	10.72	10.36	11.32	0.30
PL	7	18.73	17.89	19.38	0.56
SWR-LC <sup>1</sup> B	7	4.36	4.24	4.59	0.14
TC	7	2.66	2.44	2.88	0.18
NWR	7	4.44	4.18	4.87	0.24
PML	7	9.52	8.94	10.21	0.39
UML	7	6.94	6.78	7.08	0.11
HT-B	7	8.46	7.82	8.84	0.34
BuL	7	4.41	4.15	4.57	0.16
I <sub>1</sub> -P <sub>3</sub>	7	10.49	10.14	11.00	0.30
LML	7	7.58	7.37	7.68	0.11
I <sub>1</sub> -P <sub>3</sub>	7	8.41	8.18	8.63	0.17
M <sub>2</sub> W	7	2.21	2.17	2.27	0.04
UPL	7	4.66	4.45	4.79	0.11

in the genus *Antechinus*. Species delimitations based on *Antechinus* DNA work are necessarily arbitrary; depending on the strength of monophyletic clade support and relative depth/divergence of clades; all proposed antechinus species clades were distinctly clustered, deeply divergent (5-15% pairwise divergence at mtDNA), bearing strongly supported nodes (0.99-1.00 posterior probabilities).

Our DNA data corroborate the findings of Armstrong *et al.* (1998), who found similarly deep levels of divergence (using combined mtDNA and nDNA) among various antechinus species, including: *A. swainsonii*, *A. minivius*, *A. leo*, *A. bellus*, *A. godmani*, *A. flavipes*, *A. agilis* and *A. stuartii*. The present study provides a comparative analysis that encompasses a range of recently resolved antechinus taxa that could not be included in the work of Armstrong *et al.*: *A. adustus*, *A. subtropicus*, *A. mysticus*, *A. argentus*, *A. arktos*, *A. swainsonii* (Tas), *A. vandycki* sp. nov. (Tas), *A. minivius insularius* (Grampians, Vic).

Our DNA evidence of species distinction is consistently corroborated by a suite of other data sources, including: morphology (pelage colour, body size and craniodentary), biogeography (allopatric separation and/or relatively deep divergence across limited geographic distance) and/or ecology/behaviour (differences in breeding timing for a genus where breeding is known to be highly synchronised annually within any given species).

Assessing all data, we conclude the total evidence strongly supports the existence of 15 species of antechinus, including four species of Dusky Antechinus.

Our (direct sequencing) genetic work presented here corroborates the preliminary work of Smith (1983), who examined electrophoretic variation in *A. swainsonii* on either side of Bass Strait. He concluded that given a mean genetic distance of 0.085 ± 0.015 the trans-Bassian populations of *A. swainsonii* warranted at minimum subspecific status ('...or further elevation' p. 759). Smith (1983) analysed a total of 18 *A. swainsonii* individuals across a total of 4 populations on mainland Australia (1 in Canberra, 3 in Victoria) and compared them

TABLE 3. Univariate statistics: means, standard deviations and range minima and maxima of measured variables for *Antechinus mimetes mimetes*.

MALES						FEMALES					
	Valid N	Mean	Min	Max	St. Dev.		Valid N	Mean	Min	Max	St. Dev.
wt	6	60.55	42.00	112.00	26.01	wt	8	38.24	30.50	47.80	5.10
hb	20	122.18	89.20	150.00	16.50	hb	27	106.14	85.00	125.00	11.59
tv	20	101.11	82.43	113.75	8.83	tv	27	89.53	76.00	98.00	5.77
hf	20	21.41	18.69	24.00	1.41	hf	26	19.61	17.00	22.00	1.15
e	19	16.56	14.29	20.00	1.63	e	26	15.82	14.08	19.40	1.18
APV	15	5.41	4.58	6.35	0.52	APV	12	5.02	4.57	5.56	0.28
BL	15	30.39	28.53	31.72	0.93	BL	11	28.63	27.33	30.49	0.98
Dent	15	24.67	23.21	25.88	0.79	Dent	12	23.18	22.05	24.30	0.74
IBW	15	4.73	4.35	5.12	0.24	IBW	12	4.46	4.05	4.87	0.25
IOW	15	8.12	7.68	8.51	0.23	IOW	12	7.85	7.21	8.34	0.33
IPV	15	3.19	2.13	3.93	0.60	IPV	12	3.09	2.43	3.79	0.42
M <sup>2</sup> W	15	2.36	2.20	2.53	0.09	M <sup>2</sup> W	12	2.25	2.10	2.37	0.07
NW	15	2.70	2.41	2.92	0.15	NW	12	2.54	2.14	3.02	0.24
OBW	15	12.34	11.60	13.33	0.50	OBW	12	11.85	11.11	12.53	0.40
PPV	15	5.41	4.37	6.03	0.48	PPV	12	5.29	4.67	5.71	0.26
R-LC <sup>1</sup>	15	4.63	4.34	4.92	0.19	R-LC <sup>1</sup>	12	4.34	3.79	4.71	0.26
R-LM <sup>1</sup>	15	8.78	8.03	9.39	0.38	R-LM <sup>1</sup>	12	8.45	7.68	8.93	0.38
R-LM <sup>1</sup> T	15	7.68	7.27	8.15	0.29	R-LM <sup>1</sup> T	12	7.34	6.80	7.63	0.28
R-LM <sup>2</sup>	15	10.65	9.63	11.81	0.62	R-LM <sup>2</sup>	12	10.24	9.09	11.06	0.68
R-LM <sup>3</sup>	15	13.28	12.23	14.39	0.56	R-LM <sup>3</sup>	12	12.78	11.15	13.64	0.71
ZW	15	17.00	15.52	18.07	0.77	ZW	12	15.74	14.47	16.94	0.76
HT	15	10.76	10.28	11.15	0.28	HT	12	10.34	9.81	10.92	0.32
PL	15	17.51	16.66	18.27	0.51	PL	12	16.77	15.83	17.69	0.53
SWR-LC <sup>1</sup> B	15	4.18	3.78	4.63	0.22	SWR-LC <sup>1</sup> B	12	3.88	3.47	4.29	0.28
TC	15	2.90	2.50	3.41	0.29	TC	12	2.83	2.54	3.36	0.26
NWR	15	4.62	4.12	4.87	0.23	NWR	12	4.23	3.67	4.68	0.37
PML	15	9.39	8.21	10.70	0.69	PML	12	8.60	7.84	9.47	0.54
UML	15	6.93	6.29	7.52	0.34	UML	12	6.72	6.25	7.17	0.26
HT-B	15	8.57	8.21	9.04	0.24	HT-B	12	8.16	7.57	8.55	0.31
BuL	15	4.26	3.93	4.60	0.21	BuL	12	4.06	3.82	4.33	0.18
I <sup>1</sup> -P <sup>3</sup>	15	9.67	8.98	10.20	0.33	I <sup>1</sup> -P <sup>3</sup>	12	9.16	8.82	9.90	0.29
LML	15	7.60	7.00	8.19	0.37	LML	12	7.37	6.87	7.73	0.26
I <sub>1</sub> -P <sub>3</sub>	15	7.78	7.31	8.08	0.26	I <sub>1</sub> -P <sub>3</sub>	12	7.30	6.93	7.75	0.23
M <sub>2</sub> W	15	2.18	1.98	2.41	0.12	M <sub>2</sub> W	12	2.13	2.00	2.25	0.08
UPL	15	4.38	4.03	4.70	0.23	UPL	12	4.09	3.61	4.52	0.26

# Australian Dusky Antechinus Complex

TABLE 4. Univariate statistics: means, standard deviations and range minima and maxima of measured variables for *Antechinus mimetes insulanus*.

MALES						FEMALES					
	Valid N	Mean	Min	Max	St. Dev.		Valid N	Mean	Min	Max	St. Dev.
wt	4	70.63	46.00	87.00	17.55	wt	4	49.75	40.00	60.00	8.26
hb	6	138.87	117.10	165.00	17.48	hb	6	123.20	111.40	144.80	11.35
tv	6	111.86	105.00	121.90	7.62	tv	5	99.49	96.39	106.27	3.88
hf	6	22.04	20.00	24.26	1.49	hf	6	20.50	19.60	21.27	0.60
e	5	17.47	15.45	20.50	1.92	e	6	17.02	14.00	19.40	2.00
APV	6	5.63	5.06	6.02	0.33	APV	11	5.16	4.72	5.50	0.27
BL	6	32.57	30.19	33.85	1.37	BL	11	29.93	28.39	30.74	0.71
Dent	6	26.53	24.68	27.61	1.07	Dent	11	24.37	22.96	25.03	0.56
IBW	6	5.14	4.99	5.34	0.14	IBW	11	4.77	4.55	4.99	0.15
IOW	6	7.94	7.78	8.27	0.17	IOW	11	7.86	7.59	8.08	0.14
IPV	6	3.88	3.48	4.24	0.26	IPV	11	3.82	3.41	4.23	0.24
M <sup>2</sup> W	6	2.58	2.53	2.65	0.05	M <sup>2</sup> W	11	2.50	2.44	2.54	0.03
NW	6	2.93	2.77	3.19	0.16	NW	11	2.90	2.61	3.12	0.14
OBW	6	13.41	12.98	13.85	0.35	OBW	11	12.56	11.99	13.33	0.37
PPV	6	5.31	4.60	5.57	0.36	PPV	11	4.92	4.34	5.43	0.36
R-LC <sup>1</sup>	6	4.99	4.71	5.26	0.22	R-LC <sup>1</sup>	11	4.61	4.32	4.92	0.19
R-LM <sup>1</sup>	6	9.07	8.86	9.31	0.16	R-LM <sup>1</sup>	11	8.53	8.08	8.78	0.23
R-LM <sup>1</sup> T	6	8.29	8.01	8.76	0.27	R-LM <sup>1</sup> T	11	7.92	7.60	8.24	0.19
R-LM <sup>2</sup>	6	10.61	10.12	11.43	0.53	R-LM <sup>2</sup>	11	9.91	9.28	10.50	0.39
R-LM <sup>3</sup>	6	14.09	13.85	14.45	0.23	R-LM <sup>3</sup>	11	13.12	12.43	13.86	0.47
ZW	6	18.80	17.83	20.01	0.83	ZW	11	17.09	16.48	17.90	0.47
HT	6	11.20	10.65	11.89	0.46	HT	11	10.66	10.27	10.89	0.21
PL	6	18.84	17.88	19.36	0.53	PL	11	17.78	16.84	18.16	0.43
SWR-LC <sup>1</sup> B	6	4.47	4.22	4.74	0.21	SWR-LC <sup>1</sup> B	11	4.10	3.85	4.34	0.16
TC	6	3.11	2.96	3.28	0.14	TC	11	3.07	2.71	3.39	0.22
NWR	6	5.11	4.82	5.41	0.23	NWR	11	4.73	4.44	5.19	0.22
PML	6	10.64	9.90	11.30	0.47	PML	11	9.63	8.84	10.20	0.43
UML	6	7.46	7.35	7.62	0.11	UML	11	7.20	6.96	7.37	0.14
HT-B	6	8.97	8.49	9.48	0.36	HT-B	11	8.30	8.00	8.58	0.18
BuL	6	4.43	4.19	4.73	0.19	BuL	11	4.24	3.99	4.68	0.22
I <sup>1</sup> -P <sup>3</sup>	6	10.20	9.42	10.61	0.43	I <sup>1</sup> -P <sup>3</sup>	11	9.54	9.19	9.90	0.25
LML	6	8.13	8.00	8.43	0.17	LML	11	7.91	7.67	8.08	0.13
I <sub>1</sub> -P <sub>3</sub>	6	8.33	7.89	8.65	0.31	I <sub>1</sub> -P <sub>3</sub>	11	7.59	7.18	7.82	0.21
M <sub>2</sub> W	6	2.36	2.33	2.43	0.04	M <sub>2</sub> W	11	2.30	2.24	2.34	0.03
UPL	6	4.55	4.13	4.91	0.29	UPL	11	4.18	3.91	4.57	0.20

to a total of 4 *A. swainsonii* individuals from a total of two populations on Tasmania (Arthur River in the north and Mount Wellington in the south). Although based on small sample sizes, Smith found a striking pattern of markedly greater differentiation between *A. swainsonii* across Bass Strait compared to that among either mainland or Tasmanian populations of *A. swainsonii*.

Our genetic data from the present study indicate that four deeply divergent (pairwise mtDNA 7.5-12.5%) and distinctive species comprise the Dusky Antechinus complex; each species is deeply structured, monophyletic, very strongly supported and taken together all four, together with *A. minimus*, clade with strong support (1.00 posterior probability) to the exclusion of all other known species of antechinus (Figs 2-3). Although the two Tasmanian Dusky Antechinus, *A. swainsonii* and *A. vandycki* sp. nov. are clearly resolved as genetic sisters, the relationships between these taxa, *A. mimetes*, *A. arktos* and *A. minimus* are less clear.

Morphologically, the 4 species (5 taxa) of Dusky Antechinus are clearly allied with, but to the exclusion of, *A. minimus*; the latter is strikingly different in fur colour, body shape (squatter, shorter-tailed) and skull features, compared to all Dusky Antechinus, the various species of which differ distinctly but more subtly to each other as a discrete group. The fact that all members of the Dusky Antechinus complex do not form a discrete genetic clade to the exclusion of *A. minimus* speaks to the deep and comparable level of divergence between all Dusky Antechinus (7.5-12.5% between species pairs) and those between each Dusky Antechinus species and the Swamp Antechinus (7.6-12.0%). Moreover, it suggests that collectively, Dusky and Swamp Antechinuses shared a common ancestor sometime in the past.

Thus, based on comparative genetic and morphological (external colour and craniodental) differences, we have nominated two new species of antechinus as part of the *A. swainsonii* complex. The total recognised species in the complex shifts from two (*A. arktos*, *A. swainsonii*) as listed by Baker et al., (2014) to four (refer Fig.20), presented here,

thus: first, the Black-tailed Dusky Antechinus, *A. arktos* Baker, Mutton, Hines & Van Dyck; second, the Mainland Dusky Antechinus *A. mimetes* (Thomas) two subsp. raised, the nominate *A. m. mimetes* (Thomas) subsp. raised and secondarily *A. m. insulanus* Davison subsp. transferred; third, the Tasmanian Dusky Antechinus *A. swainsonii* (Waterhouse); fourth, the Tasman Peninsula Dusky Antechinus *A. vandycki* sp. nov.

Of species pairs within the Dusky Antechinus group, *A. swainsonii* and *A. vandycki* sp. nov. are closest genetically (and morphologically), ranging from 7.3-8.6% divergence at mtDNA. Comparatively, this is larger than the mtDNA divergence at some species pairs already named in the genus, such as *A. stuartii* / *A. subtropicus* (5%) and *A. leo* / *A. adustus* (5.4 - 6.9%). It is telling that from samples in our collection of *A. swainsonii* across Tasmania, ranging from Arthur River in the north to Bruny Island in the south, some 300 km straight-line distance, the genetic difference ranges from just 0 - 3.3%. And comparatively, for samples of *A. swainsonii* near Hobart to those of *A. vandycki* sp. nov. on Tasman Peninsula, a mere 40 km straight-line distance, the pairwise genetic difference is a striking 8% (refer Fig. 21). All 6 male *A. vandycki* sp. nov. captured in our surveys (3 sites across about 10 km maximum linear distance) were sequenced at mtDNA and represented in total 2 different genetic haplotypes, just 2 bases divergent to each other (about 0.4%).

Another interesting genetic pattern recovered here is that between the two subspecies of *A. mimetes*. *Antechinus m. mimetes* (Vic, NSW) and *A. m. insulanus* (Grampians NP, Vic) range from 2.0 - 4.3% divergent at mtDNA, with samples of the two subspecies in some cases less than 100 km apart geographically. In contrast, *A. m. mimetes* across its considerable geographic range from Cape Otway in southern Victoria to Ebor in north-east NSW, some 1,000 km straight-line distance, is just 0 - 4.1% (refer Fig.21). Notably, the two subspecies strongly clade together as part of the *A. mimetes* species clade to the exclusion of all other species, but the range of genetic divergence and (in particular) striking



# Australian Dusky Antechinus Complex

TABLE 5. Univariate statistics: means, standard deviations and range minima and maxima of measured variables for *Antechinus arktos*.

MALES						FEMALES					
	Valid N	Mean	Min	Max	St. Dev.		Valid N	Mean	Min	Max	St. Dev.
wt	2	89.85	59.70	120.00	42.64	wt	1	46.30	46.30	46.30	na
hb	5	131.53	108.58	145.00	14.91	hb	3	108.89	106.22	111.20	2.51
tv	6	118.01	100.42	131.00	14.22	tv	3	99.12	94.20	106.88	6.80
hf	6	23.27	21.88	24.00	0.80	hf	3	21.43	20.00	22.20	1.24
e	6	17.15	15.47	19.00	1.39	e	3	16.70	16.10	17.72	0.89
APV	6	4.76	4.52	5.05	0.22	APV	3	4.45	4.31	4.64	0.17
BL	6	32.44	30.45	33.75	1.55	BL	3	29.54	29.12	30.14	0.53
Dent	6	26.31	24.63	27.41	1.16	Dent	3	24.30	24.14	24.51	0.19
IBW	6	5.08	4.93	5.23	0.13	IBW	3	4.68	4.53	4.83	0.15
IOW	6	8.05	7.87	8.51	0.24	IOW	3	7.94	7.78	8.13	0.18
IPV	6	4.11	3.97	4.24	0.12	IPV	3	4.05	3.94	4.13	0.10
M <sup>2</sup> W	6	2.41	2.35	2.52	0.06	M <sup>2</sup> W	3	2.40	2.35	2.43	0.04
NW	6	3.15	2.99	3.43	0.16	NW	3	2.90	2.76	3.02	0.13
OBW	6	13.21	12.63	13.72	0.41	OBW	3	12.38	12.32	12.46	0.07
PPV	6	5.85	5.02	6.52	0.57	PPV	3	5.56	5.45	5.76	0.17
R-LC <sup>1</sup>	6	5.10	4.93	5.31	0.16	R-LC <sup>1</sup>	3	4.68	4.62	4.72	0.05
R-LM <sup>1</sup>	6	9.57	9.12	9.90	0.29	R-LM <sup>1</sup>	3	8.74	8.66	8.79	0.07
R-LM <sup>1</sup> T	6	8.15	7.97	8.29	0.14	R-LM <sup>1</sup> T	3	7.77	7.71	7.82	0.06
R-LM <sup>2</sup>	6	11.42	10.95	11.65	0.27	R-LM <sup>2</sup>	3	10.60	10.51	10.68	0.09
R-LM <sup>3</sup>	6	14.09	13.55	14.70	0.42	R-LM <sup>3</sup>	3	13.29	13.01	13.47	0.25
ZW	6	18.27	16.65	19.22	1.20	ZW	3	16.61	16.27	17.10	0.43
HT	6	10.95	10.55	11.38	0.27	HT	3	10.60	10.56	10.64	0.04
PL	6	18.38	17.45	19.04	0.61	PL	3	17.45	17.26	17.71	0.23
SWR-LC <sup>1</sup> B	6	4.60	4.33	5.03	0.25	SWR-LC <sup>1</sup> B	3	4.09	4.03	4.13	0.05
TC	6	3.22	2.97	3.38	0.15	TC	3	3.14	3.03	3.33	0.17
NWR	6	5.75	5.22	6.17	0.37	NWR	3	4.99	4.82	5.32	0.29
PML	6	10.23	9.68	10.78	0.44	PML	3	9.57	9.37	9.85	0.25
UML	6	7.35	7.21	7.55	0.11	UML	3	7.33	7.19	7.46	0.14
HT-B	6	8.76	8.53	9.08	0.20	HT-B	3	8.35	8.10	8.48	0.22
BuL	6	4.57	4.25	4.79	0.21	BuL	3	4.48	4.37	4.55	0.09
I <sup>1</sup> -P <sup>3</sup>	6	10.03	9.58	10.29	0.26	I <sup>1</sup> -P <sup>3</sup>	3	9.48	9.32	9.66	0.17
LML	6	7.83	7.72	8.07	0.12	LML	3	7.74	7.57	7.92	0.18
I <sub>1</sub> -P <sub>3</sub>	6	7.99	7.16	8.36	0.44	I <sub>1</sub> -P <sub>3</sub>	3	7.35	6.98	7.68	0.35
M <sub>2</sub> W	6	2.27	2.13	2.35	0.08	M <sub>2</sub> W	3	2.28	2.20	2.35	0.08
UPL	6	4.50	4.29	4.71	0.17	UPL	3	4.15	3.99	4.24	0.14

TABLE 6. ANOVA F-statistics (top two lines) for variation at each of the measured variables among all antechinus species and subspecies. Subsequent rows show significance values for ANOVA Post-Hoc tests of *Antechinus semnisonii* paired with each of its 14 congeners, for each measured variable. Shaded cells are significant at  $p=0.05$ , unshaded cells are not significant.

Comparison	sex	wt	hb	tv	hf	e	AI/V	BL	Dent	IBW	IOW	IPV	MPW	NW	OBW	PPV	R-LCI	R-LMI	R-LMIT
ANOVA F - all species	M	29.79	31.94	37.56	54.70	20.38	250.20	49.18	55.08	41.20	85.62	93.02	52.06	32.10	26.51	24.30	56.37	48.79	31.50
ANOVA F - all species	F	30.72	25.77	25.00	30.13	19.22	222.60	51.41	70.84	40.82	97.85	76.72	47.44	19.70	28.79	19.15	43.34	44.27	26.97
<i>A. vanhecki</i>	M	1.00	0.80	0.64	1.00	1.00	0.00	0.59	0.41	1.00	1.00	0.04	1.00	1.00	0.98	0.04	0.98	1.00	0.99
<i>A. mimetes mimetes</i>	M	1.00	0.54	1.00	1.00	1.00	0.00	1.00	1.00	0.64	0.95	0.00	0.87	0.15	1.00	1.00	1.00	0.38	1.00
<i>A. mimetes mimetes</i>	F	1.00	0.26	0.99	1.00	1.00	0.00	1.00	1.00	0.98	1.00	0.00	1.00	1.00	1.00	0.85	1.00	1.00	1.00
<i>A. mimetes insulanus</i>	M	1.00	1.00	0.22	1.00	1.00	0.00	0.04	0.03	0.00	1.00	0.00	0.00	0.00	0.00	1.00	0.61	0.66	0.03
<i>A. mimetes insulanus</i>	F	0.87	1.00	0.17	0.88	0.33	0.00	0.08	0.01	0.00	1.00	0.00	0.00	0.00	0.00	0.85	0.05	1.00	0.00
<i>A. arktos</i>	M	0.86	1.00	0.00	0.78	1.00	0.00	0.07	0.12	0.01	1.00	0.00	0.56	0.00	0.03	0.77	0.14	0.00	0.25
<i>A. arktos</i>	F	1.00	1.00	0.68	0.56	0.98	0.00	1.00	0.90	0.82	1.00	0.00	0.39	0.19	0.84	0.93	0.75	1.00	0.90
<i>A. minimus</i>	M	0.72	0.14	0.00	0.00	0.15	0.00	0.13	0.02	1.00	0.00	0.00	1.00	0.87	1.00	0.99	0.04	0.02	0.75
<i>A. minimus</i>	F	0.42	0.39	0.00	0.02	0.54	0.00	0.00	0.00	1.00	0.00	0.00	1.00	0.06	1.00	1.00	0.00	0.02	1.00
<i>A. adustus</i>	M	0.00	0.00	1.00	0.00	0.61	0.00	0.00	0.00	1.00	0.00	0.00	0.17	0.74	0.48	0.94	0.00	0.76	1.00
<i>A. adustus</i>	F	0.00	0.00	1.00	1.00	1.00	0.00	0.00	0.00	0.99	0.00	0.00	0.09	0.76	0.00	0.82	0.00	1.00	0.99
<i>A. agilis</i>	M	0.00	0.00	1.00	0.00	0.32	0.00	0.00	0.00	0.00	0.00	0.00	0.31	0.34	0.00	0.00	0.88	1.00	0.21
<i>A. agilis</i>	F	0.00	0.00	1.00	0.00	1.00	0.00	0.00	0.00	0.00	0.00	0.00	1.00	1.00	0.00	0.01	0.02	0.90	1.00
<i>A. argentus</i>	M	0.07	0.00	1.00	0.00	1.00	0.00	0.00	0.00	0.14	0.00	0.00	1.00	0.75	1.00	0.12	0.02	0.02	0.99
<i>A. argentus</i>	F	0.00	0.00	1.00	0.04	1.00	0.00	0.00	0.00	0.06	0.00	0.00	1.00	0.96	0.87	0.01	0.70	0.91	1.00
<i>A. bellus</i>	M	1.00	1.00	0.00	1.00	1.00	0.00	1.00	1.00	0.00	0.00	0.00	0.00	0.00	0.00	0.00	0.00	0.00	0.00
<i>A. bellus</i>	F	0.00	0.63	0.00	0.89	0.00	0.00	0.41	0.03	0.00	0.00	0.00	0.00	0.00	0.09	0.00	0.00	0.00	0.00
<i>A. flavipes flavipes</i>	M	0.51	0.00	0.97	0.00	1.00	0.00	0.00	0.00	0.00	0.00	0.00	0.00	0.00	1.00	0.00	0.00	0.00	0.00
<i>A. flavipes flavipes</i>	F	0.06	0.00	0.53	0.00	1.00	0.00	0.00	0.00	0.00	0.00	0.00	0.10	0.00	0.67	0.00	0.00	0.00	0.00
<i>A. flavipes leucogaster</i>	M	0.01	0.00	0.30	0.00	1.00	0.00	0.00	0.00	0.00	0.00	0.00	0.00	0.00	1.00	0.00	0.00	0.00	0.02
<i>A. flavipes leucogaster</i>	F	0.00	0.00	0.00	0.00	0.99	0.00	0.00	0.00	0.00	0.00	0.00	0.00	0.00	0.00	0.25	0.00	0.00	0.00
<i>A. flavipes rubecula</i>	M	1.00	0.78	1.00	1.00	1.00	0.00	1.00	0.81	1.00	0.00	0.00	0.00	0.00	0.00	0.00	0.00	0.00	0.00
<i>A. flavipes rubecula</i>	F	1.00	1.00	1.00	1.00	1.00	0.00	1.00	0.90	1.00	0.00	0.00	0.00	0.00	0.00	0.04	0.00	0.00	0.00
<i>A. godmani</i>	M	0.00	1.00	0.00	0.39	0.17	0.00	0.00	0.00	0.00	1.00	0.00	0.00	0.90	0.00	1.00	0.00	0.00	0.00
<i>A. godmani</i>	F	0.00	1.00	0.00	0.59	0.00	0.00	0.02	0.09	0.00	0.99	0.00	0.00	1.00	0.00	1.00	0.00	0.00	0.00
<i>A. leo</i>	M	0.16	1.00	0.00	0.00	0.01	0.00	0.14	0.66	0.00	0.00	0.00	0.00	0.00	0.00	1.00	0.00	0.00	0.00
<i>A. leo</i>	F	1.00	1.00	0.01	0.00	0.00	0.00	1.00	1.00	0.00	0.00	0.00	0.00	0.00	0.00	1.00	0.00	0.00	0.00
<i>A. mysticus</i>	M	0.08	0.00	1.00	0.00	1.00	0.00	0.00	0.00	0.00	0.00	0.00	0.01	0.38	1.00	0.92	0.00	0.00	0.05
<i>A. mysticus</i>	F	0.00	0.00	1.00	0.00	0.92	0.00	0.00	0.00	0.00	0.00	0.00	0.02	0.69	0.84	0.99	0.00	0.08	0.20
<i>A. stuartii</i>	M	0.00	0.00	0.99	0.00	1.00	0.00	0.00	0.00	0.00	0.00	0.00	0.96	0.25	0.26	1.00	0.02	1.00	1.00
<i>A. stuartii</i>	F	0.00	0.00	0.21	0.00	1.00	0.00	0.00	0.00	0.00	0.00	0.00	0.86	1.00	0.00	0.82	0.00	1.00	1.00
<i>A. subafricanus</i>	M	0.93	0.06	1.00	0.00	1.00	0.00	0.00	0.00	0.44	0.00	1.00	0.00	0.12	1.00	0.00	0.00	0.09	0.72
<i>A. subafricanus</i>	F	0.05	0.00	1.00	0.12	1.00	0.00	0.00	0.00	0.52	0.00	1.00	0.00	0.16	0.98	0.00	0.00	1.00	0.59

TABLE 6. continued ...

Comparison	sex	R-LM <sup>2</sup>	R-LM <sup>3</sup>	ZIV	HT	PL	SWR- LCIB	TC	NWR	PML	UML	HT-B	BuL	II-P <sup>3</sup>	LML	I <sub>1</sub> -P <sub>3</sub>	N <sub>1</sub> -V	UPL
ANOVA F - all species	M	49.52	30.88	18.67	37.40	71.93	44.90	27.15	14.90	20.66	57.00	39.00	24.89	87.10	56.54	130.45	34.96	101.34
ANOVA F - all species	F	48.30	29.58	20.39	52.18	79.90	37.71	31.92	14.70	28.47	58.75	58.78	24.47	46.78	62.14	126.25	47.89	95.59
<i>A. tancredii</i>	M	1.00	1.00	1.00	1.00	0.28	0.99	1.00	1.00	1.00	1.00	1.00	0.92	0.34	1.00	0.22	1.00	0.74
<i>A. mimetes mimetes</i>	M	1.00	0.70	1.00	0.91	0.99	1.00	0.00	0.46	1.00	1.00	0.73	1.00	0.50	1.00	0.96	1.00	1.00
<i>A. mimetes mimetes</i>	F	1.00	0.15	1.00	0.72	0.99	1.00	0.48	1.00	1.00	1.00	1.00	1.00	0.76	1.00	0.50	0.94	1.00
<i>A. mimetes insularis</i>	M	1.00	0.02	0.00	0.07	0.22	0.73	0.00	0.02	0.00	0.00	0.02	0.89	1.00	0.00	0.73	0.04	1.00
<i>A. mimetes insularis</i>	F	1.00	0.00	0.00	0.00	0.07	0.13	0.00	0.01	0.00	0.00	0.76	0.21	1.00	0.00	1.00	0.00	1.00
<i>A. arktos</i>	M	0.13	0.02	0.10	0.75	0.98	0.12	0.00	0.00	0.11	0.01	0.46	0.16	1.00	0.82	1.00	0.99	1.00
<i>A. arktos</i>	F	0.99	0.47	0.89	0.79	1.00	0.98	0.09	0.26	0.38	0.00	1.00	0.14	1.00	0.43	1.00	0.06	1.00
<i>A. minutus</i>	M	0.07	0.21	1.00	1.00	0.00	0.13	0.57	1.00	1.00	0.01	1.00	1.00	0.00	0.00	0.00	0.66	0.00
<i>A. minutus</i>	F	0.02	0.21	1.00	0.99	0.00	0.00	1.00	0.17	0.48	0.00	1.00	1.00	0.00	0.00	0.00	1.00	0.00
<i>A. adustus</i>	M	0.53	1.00	1.00	0.00	0.00	0.01	0.79	0.26	0.00	0.00	0.00	0.11	0.00	0.00	0.00	1.00	0.00
<i>A. adustus</i>	F	0.99	1.00	0.99	0.00	0.00	0.00	0.98	0.07	0.00	0.00	0.00	0.00	0.00	0.00	0.00	0.14	0.00
<i>A. agilis</i>	M	0.90	1.00	0.50	0.00	0.00	0.96	1.00	0.35	0.00	0.00	0.00	0.93	0.00	0.00	0.00	0.00	0.00
<i>A. agilis</i>	F	0.00	0.13	1.00	0.00	0.00	0.02	1.00	0.04	0.00	0.00	0.00	1.00	0.00	0.00	0.00	1.00	0.00
<i>A. argentus</i>	M	0.00	0.04	1.00	0.00	0.00	0.02	1.00	1.00	0.98	0.21	0.00	1.00	0.00	0.03	0.00	1.00	0.00
<i>A. argentus</i>	F	0.72	0.68	1.00	0.00	0.00	0.73	1.00	0.86	0.07	0.15	0.00	1.00	0.00	0.07	0.00	1.00	0.00
<i>A. bellus</i>	M	0.00	0.00	0.00	1.00	0.59	0.00	1.00	1.00	1.00	0.87	0.11	0.00	0.00	0.99	0.00	0.00	0.00
<i>A. bellus</i>	F	0.00	0.00	0.00	1.00	0.00	0.00	0.71	0.99	0.56	0.03	0.00	0.00	0.00	0.01	0.00	0.00	0.00
<i>A. flacipes flacipes</i>	M	0.00	0.00	0.06	0.01	0.00	0.00	1.00	1.00	0.39	1.00	0.00	0.00	0.00	1.00	0.00	0.00	0.00
<i>A. flacipes flacipes</i>	F	0.00	0.00	0.54	0.00	0.00	0.00	0.14	0.67	0.00	0.97	0.00	0.00	0.00	1.00	0.00	0.00	0.00
<i>A. flacipes leucogaster</i>	M	0.00	0.00	0.20	0.02	0.00	0.00	0.99	1.00	0.14	0.00	0.00	0.00	0.00	0.00	0.00	1.00	0.00
<i>A. flacipes leucogaster</i>	F	0.00	0.00	0.73	0.00	0.00	0.00	1.00	0.84	0.00	0.00	0.00	0.04	0.00	0.00	0.00	0.00	0.00
<i>A. flacipes rubeculus</i>	M	0.00	0.00	0.00	0.93	0.26	0.00	1.00	0.04	0.89	0.02	0.32	0.00	0.00	0.35	0.00	0.00	0.00
<i>A. flacipes rubeculus</i>	F	0.00	0.00	0.00	0.99	0.02	0.00	1.00	0.99	1.00	0.00	0.00	0.00	0.00	0.00	0.00	0.00	0.00
<i>A. godmani</i>	M	0.00	0.00	0.00	0.86	0.00	0.00	0.00	0.08	1.00	0.00	1.00	0.91	1.00	0.00	0.00	0.00	1.00
<i>A. godmani</i>	F	0.00	0.00	0.00	1.00	0.06	0.00	0.00	0.94	0.98	0.00	0.91	0.88	1.00	0.00	0.00	0.00	1.00
<i>A. leo</i>	M	0.00	0.00	0.00	1.00	1.00	0.00	0.00	0.00	0.00	0.00	0.99	0.00	0.00	0.00	0.00	0.00	0.00
<i>A. leo</i>	F	0.00	0.00	0.00	1.00	1.00	0.00	0.00	0.01	0.30	0.00	0.00	0.00	0.00	0.00	0.00	0.00	0.00
<i>A. mysticus</i>	M	0.00	0.00	0.94	0.00	0.00	0.00	1.00	1.00	0.66	0.00	0.00	0.28	0.00	0.00	0.00	1.00	0.00
<i>A. mysticus</i>	F	0.00 <sup>d</sup>	0.00	1.00	0.00	0.00	0.00	1.00	1.00	0.00	0.00	0.00	0.65	0.00	0.00	0.00	1.00	0.00
<i>A. stuartii</i>	M	1.00	1.00	0.95	0.00	0.00	0.02	0.75	1.00	0.00	0.00	0.00	1.00	0.00	0.00	0.00	1.00	0.00
<i>A. stuartii</i>	F	1.00	1.00	0.32	0.00	0.00	0.00	1.00	0.02	0.00	0.00	0.00	1.00	0.00	0.00	0.00	0.97	0.00
<i>A. subtropicus</i>	M	0.51	0.95	1.00	0.00	0.00	0.00	0.00	1.00	0.61	0.43	0.00	1.00	0.00	0.00	0.00	1.00	0.00
<i>A. subtropicus</i>	F	0.99	0.99	1.00	0.00	0.00	0.00	1.00	1.00	0.45	0.39	0.00	1.00	0.00	0.08	0.00	0.00	0.00

morphological differences between the two subspecies (*A. m. insulanus* have larger, broader skulls) is also clearcut. It is also interesting that both *A. m. insulanus* and *A. agilis* from the Grampians are both genetically and morphologically different to respective *A. m. mimetes* and *A. agilis* from surrounding areas in Victoria immediately outside the Grampians – this suggests a common history of geographical isolation for antechinus within Grampians NP. Comparatively, Crowther (2002) also noted the larger size of *A. agilis* from the Grampians, while Davison (1991) noted the relatively larger size of Grampians *A. swainsonii* from conspecifics, on the strength of which he raised the then *A. swainsonii insulanus* (now *A. mimetes insulanus*).

For clarity, common names of the four species are proposed here as variants of ‘Dusky Antechinus’. This necessitates a proposed common name change for *A. arktos* from our previous (Baker et al. 2014) ‘Black-tailed Antechinus’ to ‘Black-tailed Dusky Antechinus’. At the time of naming *A. arktos*, we were unaware of further variation within *A. swainsonii*; but given the suite of species now reported, retaining the original epithet nested within the common name of *A. arktos* seems most appropriate.

The *Antechinus swainsonii* from Tasmania named by Waterhouse in 1840 from a specimen in the private collection of William Swainson by primacy retains the original specific designator. Subsequently, Captain Wilkins collected an animal from Guy Fawkes district, near Ebor in north-east NSW, named by legendary BMNH taxonomist Oldfield Thomas in 1924 as the subspecies *A. swainsonii mimetes* (although then under genus *Phascogale*). Based on our reported striking genetic (on average 10% divergent at Cytb mtDNA) and morphological differences of *A. swainsonii mimetes* with both Tasmanian species, coupled with their separation in allopatry, we have raised Thomas’ subspecies *mimetes* to full species status, thus *A. mimetes*. Davison (in 1991) had nominated another subspecies of mainland *swainsonii* to account for larger animals from Grampians NP (Vic), his *A. s. insulanus*. We find that *insulanus* is a variant lying within the newly raised species *mimetes* based on both shallow but distinctive

genetic variation and clear craniodental variation. Thus, we have designated by primacy Thomas’ Guy Fawkes animals *Antechinus mimetes mimetes* and secondarily Davison’s Grampians animals are transferred to *Antechinus mimetes insulanus*. Other than *A. m. insulanus* from the Grampians, all other *swainsonii* complex individuals sampled from the Australian mainland between southern Victoria and Guy Fawkes (in north-east NSW) are apparently *A. m. mimetes* based on both morphology (see species by species differences in Results) and genetics (Figs 2-3 and AMB and TYM unpublished data).

To our knowledge, prior to the present study, there was only one collected voucher specimen of *A. vandycki*: sp. nov. This was obtained by John Gould (no date), held in the British Museum of Natural History, and registered there as a male *A. swainsonii*. Although no genetic data could be obtained for this specimen, morphologically it was clearly very similar to the six male *A. vandycki* sp. nov. that were included here and different to the suite of *A. swainsonii* from elsewhere in Tasmania.

All four species (and 5 taxa) within the *swainsonii* complex are distinctive morphologically. As one moves from south (higher latitudes) to north (lower latitudes) the fur colour generally changes from predominantly greyish (*vandycki* sp. nov. and *swainsonii*), to more predominantly brownish (*mimetes*) to predominantly brownish with more russet rump (*arktos*). Tail and hindfoot colour also predominantly darkens from southern (greyish/brown) to northern latitudes (through brown, dark brown, to black). The skull becomes generally stouter / broader from *swainsonii* through *mimetes mimetes* to *arktos/mimetes insulanus*. However, *vandycki* sp. nov. skulls are somewhat more robust than *swainsonii*; the latter are the most delicate of the group. Generally speaking, the length of the front holes in the skull palate (APV) and the distance between the front and back palate holes (IPV) are good diagnostics to separate the four species craniodentally; the front palate holes are very large indeed in *vandycki* sp. nov. and neatly separate this new animal from every other antechinus species. The front palate holes become smaller as one moves through each

Dusky Antechinus species, going northwards (*swainsonii*, *mimetes*, *arktos*); the functionality of these craniodental differences (if, indeed, any exists) remain a mystery.

### Biogeography

Resolving *Antechinus* phylogeography using genetic and fossil dating was not the aim of the present study; TYM's PhD, nearing completion, and incorporating a great many more mtDNA and nuclear sequences, will focus on this important task. However, it is worth discussing a few salient features of our phylogenetic tree as they may relate to biogeographic processes affecting the Dusky Antechinus complex. The genetic differences among (and relative to congeners, within) all members of the Dusky Antechinus complex are strikingly deep, suggesting this species group may be prone to geographic isolation. Certainly, their general preference for well-forested, high, cold and wet habitat types (Baker *et al.* 2014) may predispose the group to such isolating forces over time, especially as Australia has become drier and less-forested over time. The deep structuring between each of the two Tasmanian species (*A. swainsonii* and *A. vandycki* sp. nov.) and proximate mainland *A. mimetes* is particularly striking. Such deep divergences strongly suggest that speciation between these forms occurred well before separation of Tasmania from mainland Australia (regardless of which date for Tasmanian/mainland separation one ascribes to). Under one plausible scenario, even hundreds of thousands of years before continental separation, conditions may have favoured geographic isolation of some ancestral forms of this dasyurid complex and over time genetic isolation has conceivably resulted in their speciation; subsequently, Tasmania became separated from continental Australia, presumably carrying these already distinct taxa with it. Similar scenarios have been proposed to explain striking genetic divergences between Tasmanian and Victorian forms of the Tiger Quoll (*Dasyurus maculatus*; Firestone *et al.* 1999) and also the recently discovered deep divergences between mainland and Tasmanian

forms of our iconic monotreme, the Platypus (*Ornithorhynchus anatinus*; Gongora *et al.*, 2012).

The comparative biogeography of the three Tasmanian species of antechinus, *A. swainsonii*, *A. vandycki* sp. nov. and *A. minimus*, is also intriguing. It is plausible that *A. vandycki* sp. nov. has been isolated in the past by unsuitable habitat across the East Bay Neck between Dunalley and Blackman Bay (on Forestier Peninsula) and also further to the south at Eaglehawk Neck (Tasman Peninsula). In the latter location, the 200 metre long isthmus is so narrow that ferocious wild dogs and a handful of military guards were able to prevent escaped convicts from Port Arthur gaining safe passage north onto Tasmania proper some 150 years ago. *Antechinus vandycki* sp. nov. has been perhaps just as effectively confined to Tasman Peninsula over deeper time by geomorphology alone.

Interestingly, our research group have also caught *A. minimus* with *A. vandycki* sp. nov. on Fortescue Bay (at low altitude, 50 m), the southernmost capture site on Tasman Peninsula; *A. minimus* from there is genetically similar to *A. minimus* from other locations on Tasmania (data not shown). So, if these narrow necks of land have played a part in isolating *A. swainsonii* from *A. vandycki* sp. nov. then they have apparently not isolated the *A. minimus* population from conspecifics as effectively or for as long. This may at least partly be explained by their respective habitat preferences, because while members of the Dusky Antechinus complex typically prefer closed, wet, higher altitude forest (Baker *et al.* 2014; Dickman 2008), Swamp Antechinuses are more commonly found in lower altitude, more open habitat, as their name suggests (Gibson *et al.* 2004; Sale *et al.* 2006; Wilson & Bachmann 2008; Wilson *et al.*, 2001). Interestingly, *A. swainsonii* from South Bruny Island, which today is separated from mainland Tasmania, are only slightly different genetically (1-2%) from other *A. swainsonii* on southern Tasmania (Southwest NP and Mount Wellington). So whatever factors explain the evolutionary history of these antechinus species on Tasmania, it is not as simple as invoking isolation due to obvious geographic

## Ecology

Generally speaking, catchability of all four species in the Dusky Antechinus complex is low. Typically, even during late Autumn/ winter during pre-mating activity (optimum catchability) rarely is the catching rate higher than one every 200 trap/nights, although there are exceptions, such as some populations of *A. minutus minutus* (see e.g. Dickman 1986a, b; 1988a, b). For antechinus that probably spend much or most of the time foraging on the ground (Dickman, 1986a, b; 1988 a, b; 2008) (cf. their mostly semi-arboreal congeners, Baker *et al.*, 2014), this is in one sense a surprisingly low capture rate given that antechinus are typically captured in Elliott traps deployed on the ground. Because of this, it has been supposed that low catchability of Dusky Antechinus is best explained by their trap-shyness. This is certainly plausible. However, in the course of the present work we have done a lot of trapping of the various species within the Dusky Antechinus complex and in numerous cases have recaptured the same individuals across successive trap/nights, so there seems at least to be little reticence from the animals to re-enter traps after capture, if they are initially overly suspicious. Dusky Antechinus complex species are large antechinus (some males may even approach 200g) and if they are largely limited to the ground they may require relatively large home ranges to access food resources. Thus, in any given trapping grid, one may be less likely to catch such species that support a lower density of individuals. So low densities where Dusky Antechinus occur, especially as one moves north through NSW and into Qld where habitat requirements (high, cold, wet) are less often satisfied, may at least in part explain their characteristically low capture rates in many trapping surveys in those places. One of us (ELG) will be testing this idea with *A. arktos*, where they co-occur (apparently in low abundance) with a plethora of *A. stuartii* (regularly one *A. stuartii* captured in every 4-5 traps deployed) in Springbrook NP, using a combination of radio-tracking and baited remote RFID (Radio Frequency IDentification) camera stations (where already



FIG. 19. (A-C) Habitat photographs of the *A. vandycki* sp. nov. holotype locality – Lichen Road, Tasman Peninsula, Tasmania. Photographs by Eugene Mason (QUT).

barriers. At present, unfortunately we know little about *A. swainsonii*, especially in south-east Tasmania, and less still of *A. vandycki*. sp. nov. Our research group aims to spend the next few years further investigating the comparative biology of the species.





FIG. 20. Live photos of the four species in the Dusky Antechinus Species complex. Clockwise from top left: *Antechinus vandycki* sp. nov. (male, HOLOTYPE, QM JM 20111), *A. swainsonii* (male, general collection, QM JM 20107), *A. arktos* (male, PARATYPE, QM JM 2010), *A. mimetes* (female, general collection, QM JM 20112). Photographs by Gary Cranitch (QM).

pit-tagged individuals are recorded on each visit to the station). This data may indicate comparative home range size and over time hopefully relative abundance of each species using combined Elliott-trapping and remote cameras (the latter can be left in the field for a month at a time constantly recording data).

With respect to habitat requirements, *A. swainsonii* occurs in a range of forested habitats in Tasmania. Dominant species include: *Nothofagus cunninghamii*, *Atherosperma moschatum*, *Eucryphia lucida*, *Phyllocladus rhomboidalis* and *Anodopetalum biglandulosum*. In fire-affected areas, where the species is found, landscapes may be dominated by: *Eucalyptus* spp., understorey plants including *Olearia argyrophylla*, *Pittosporum bicolor*, *Drimys lanceolata*, *Persoonia gunnii*, *Anopterus glandulosa* and *Dicksonia antarctica*. Ecotonal regrowth habitats occupied by *A. swainsonii* are typically characterised by: *Ghania trifida*,

*Sprengelia incarnata*, *Epacris gunnii*, *Monotoca* sp., *Boronia rhomboidea*, *Leptospermum* sp., *Gleichenia alpina*, *Casuarina dystyla*, *Eucalyptus gunnii*, *Poa caespitosa*, *Calorophus lateriflorus*, *Restio australis* and *Lepidosperma filiforme*. Throughout the range of this species, rainfall may be in excess of 250 cm p.a. and temperatures may vary from as low as -12°C in subalpine habitat to 35°C in coastal areas; here, *A. swainsonii* is regularly found to occupy areas of dense cover and thick litter and is not trapped in treeless expanses of button grass (*Mesomelaena sphaerocephala*), where it is often replaced by *A. minimus* (Dickman 2008; Green 1972; Menkhorst 1995; Sanecki *et al.* 2006; Williams & Williams 1982).

The *Antechinus vandycki* sp. nov. type locality at Lichen Road on Tasman Peninsula features wet sclerophyll temperate rainforest with many fallen logs and a dense understorey. Floristically, the area is typical of Tasmanian temperate

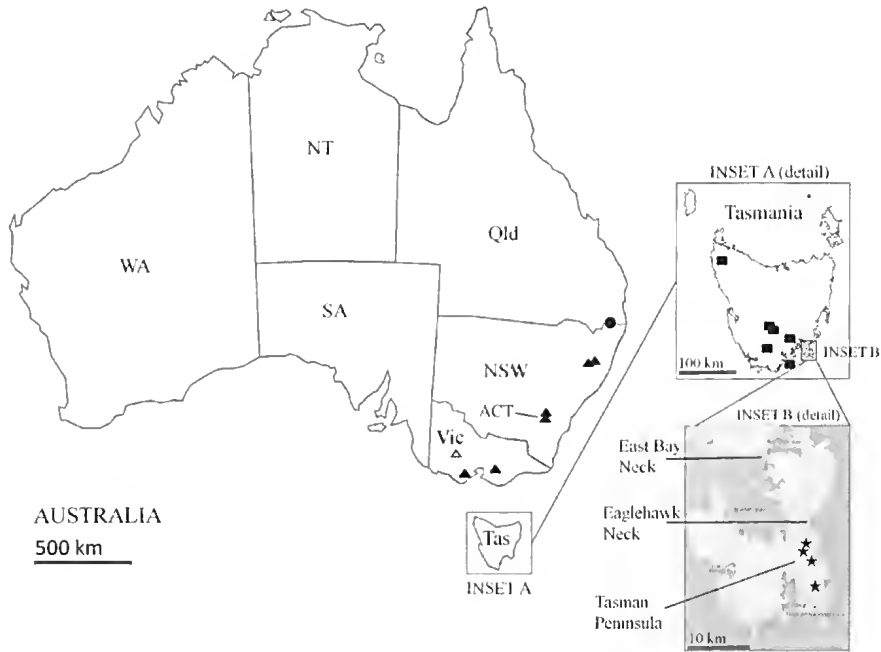


FIG. 21. Relative geographic distributions of Dusky Antechinus species, showing locations where combined genetic and morphological data was obtained from various individuals (*Antechinus arktos* [Qld] closed circle; *A. mimetes mimetes* closed triangles [NSW, ACT, Vic]; *A. mimetes insulanus* [Vic] open triangle; *A. swainsonii* [Tas, INSET A] closed squares; *A. vandycki* sp. nov. [Tasman Peninsula, Tas, INSET B] closed stars).

rainforest, but there are only limited stands existent on Tasman Peninsula, which in many places has already been cleared, is under plantation or has been fire-affected. The holotype locality featured Native Laurel, *Anopterus glandulosa*, with *Eucalyptus delegatensis* and *Eucalyptus obliqua* and an understorey of *Blechnum nudum*. In a study of mammalian predator and prey interactions and their responses to a range of predator odour cues, Lazenby & Dickman (2013) reported vegetation structure at one site on Tasman Peninsula which contained *A. vandycki* sp. nov. (that we have genetically confirmed). This site is roughly 1.5 km straight-line distance to the south of the *A. vandycki* sp. nov. holotype locality, and described generically by Lazenby and Dickman as cool temperate wet forest containing emergent eucalypts over rainforest/scrub communities, typically featuring *Nothofagus*, *Atherosperma*, *Encryphia* and *Athrotaxis*.

*Antechinus mimetes* in Victorian populations is largely restricted to dense vegetation in damp environments (>800 mm rainfall per annum) at altitudes from sea level to over 1,800 m, where vegetation types include alpine heath, woodland, high and low altitude rainforest, *Banksia* woodland and wet heath. In New South Wales, the subspecies is found on and east of the Great Dividing Range in wet sclerophyll and rainforest gullies, heathlands, coastal sand dunes and swamps, as well as sub-alpine woodland with dense shrubby understorey (Dickman 2008; Lunney *et al.* 2001; Menkhorst 1995; Williams & Williams 1982).

*Antechinus arktos* favours the highest altitude (>800 m), wettest, coldest patches of rainforest in the Tweed Volcano Caldera. The type locality at Best of All Lookout (Springbrook NP) featured complex notophyll vine forest in areas featuring moderately steep, bouldery headwater gully with Stream Lily, *Helmholtzia glaberrima*, and Antarctic Beech, *Nothofagus moorei* prominent



(Baker *et al.* 2014). This antechinus species was historically found in mountain mallee heath, approximately 162 ha in size, on rhyolitic soils, in the Dave's Creek area of Lamington National Park (28°13'S, 153°13'E, 840 m altitude). The area was surrounded by rainforest and wet sclerophyll forest. A prominent trachyte dyke known as Surprise Rock outcrops from nearby the capture site. Plant species present at this site included: *Leptospermum lanigerum* (now *L. trinervium*), *L. flavescens* (now *L. polygalifolium*), *Banksia collina* (now *B. neoaustralis*), *Leucopogon melaleucoides*, *Callistemon montanum* (now *Melaleuca montana*), *Lepidosperma caesecens* (now *L. clipeicola*) and the mallee *Eucalyptus codonocarpa* (Baker *et al.* 2014; Van Dyck & Ogilvie 1977).

Breeding ecology is little known for most members of the Dusky Antechinus complex. Mating timing in the group seems to range from May – September for *A. mimetes mimetes* (with coastal and low altitude populations breeding earliest; Williams & Williams 1982), May-June for *A. mimetes insulanus* (Davison 1991), September – October for *A. swainsonii* (Green 1972; AMB, pers. obs.), most likely mid-late September for *A. arktos* (ELG pers. obs.); there is no reliable information for breeding timing in *A. vandycki* sp. nov. although it is worth noting that a 92g adult male was caught by us at Lichen Road on Tasman Peninsula in early May 2014, suggesting an animal more than six months old which points towards an early November birth, at latest, the year before. Moreover, in the course of her PhD work, Lazenby (pers. comm.) caught three males between 8 and 12 March, 2011 that ranged from 60–65 g, which is also suggestive of adult animal size. Based on this (admittedly scant) data, and coupled with the notion that higher latitude populations of *A. swainsonii* tend to breed later (Dickman 1982; Williams & Williams 1982; McAllan 2003; McAllan *et al.*, 2006), one might guess that timing of breeding in *A. vandycki* sp. nov. is similar to that in *A. swainsonii* and *A. arktos* (Sep–Oct), or if not, slightly earlier (Aug). But this is sheer speculation until we study this *A. vandycki* sp. nov. population between July and October, where its breeding timing secrets

will be revealed in short order – this work is currently being planned.

Interestingly, in their investigation of mating timing across the genus *Antechinus*, McAllan *et al.* (2006) found rate of change of photoperiod to be the most important cue in most species. *Antechinus swainsonii* and *A. minimus* were an exception, being more variable, perhaps indicating a more plastic use of photoperiod to synchronise reproduction. The authors hypothesised that this may be in part attributable to interspecific interactions (*A. swainsonii* in Victoria are dominant to *A. agilis* and thus may be under less pressure to select for a particular rate of change of photoperiod) and in part associated with a more generalist diet (*A. swainsonii* and *A. minimus* eat a wider variety of prey than other antechinus, some of which may be less seasonably variable, thus there is less pressure to predict for insect flushes) (McAllan *et al.* 2006). They also noted the genetic and morphological distinctness of *A. swainsonii* and *A. minimus* compared to congeners, as recognised at the time (see also Armstrong *et al.*, 1998; Baverstock *et al.*, 1982; Krajewski *et al.*, 1997; Van Dyck, 2002). The present study, which reaffirms such distinctness and further suggests species level differences between Tasmanian and Victorian *A. swainsonii*, may also help to explain the variability in photoperiod response reported by McAllan *et al.* (2006), where they found mating at comparatively longer absolute photoperiod and ovulation at larger rate of change of photoperiod in Tasmanian versus mainland (Victorian and New South Wales) *A. swainsonii*. It is plausible that some aspects of speciation in the Dusky Antechinus complex may be associated with these variable responses to photoperiod.

Nipple count in females of the Dusky Antechinus complex ranges from 6–10 (Dickman 2008), with the typical condition being 8. Plausibly, there is a pattern in *A. mimetes* where lowland populations tend to have lower nipple numbers than upland populations (Williams & Williams, 1982). One population of *A. mimetes mimetes* studied in Kosciuszko NP consistently had females with 10 nipples (Happold 1989, 2011). *Antechinus swainsonii*

females tend to have 8 nipples, at least based on several females from different locations examined by AMB that are held in the QVM (Launceston). No female *A. vandycki* sp. nov. have yet been observed in breeding condition, so nipple count and other aspects of female breeding biology in this species are as yet unknown. Our research group are currently investigating comparative breeding ecology and diet of *A. vandycki* sp. nov. and *A. swainsonii*, as part of a proposed PhD project. Preliminary results from ELG's current PhD project on *A. arktos* in Qld suggest that nipple number in this species may be 6.

### Distribution & Conservation

*Antechinus mimetes mimetes* appears widely, if patchily, distributed across numerous sites between southern Victoria and north-east New South Wales (Dickman, 1982, 2008). *Antechinus swainsonii*, similarly, appears widely distributed across Tasmania, particularly in the central northern and western/south-western wilderness areas (AMB, pers. obs. of QVM specimens and data register, M.Dreissen, pers. comm.).

However, *A. vandycki*, sp. nov., *A. arktos* and *A. mimetes insulanus* all appear to be geographically limited (Baker et al., 2014; Davison, 1991; AMB, TYM, EDM, ELG pers. obs.).

*Antechinus mimetes insulanus*, found only within the confines of Grampians NP in Victoria (Davison 1991), has been regularly caught at several sites across the Park in annual mammal surveys conducted by our colleagues at Deakin over the last few years.

The northern limited *A. arktos* has plausibly retracted to the highest, wettest, coldest reaches of the Tweed Caldera in the face of global warming and may be restricted to just a couple of surviving populations (Springbrook NP, Border Ranges NP), supporting low numbers (Baker et al. 2014). This species is the subject of a current PhD project by one of us (ELG) investigating ecology, genetics and distribution. Monthly field surveys in 2014 (between April–October) have returned just 10 individuals (7 males, 3 females) in about 5,000 trap/nights at

the Qld type locality (Best of All Lookouts/Bilborough Ct, Springbrook NP) and 0 individuals in 1,500 trap/nights during a June, 2014 survey from the only known location of the species in NSW (Brindle Creek, Border Ranges NP). *Antechinus arktos* is currently being considered for Endangered species listing under both Qld and NSW state legislation with an application pending for federal EPBC listing.

Despite considerable trapping effort *A. vandycki* sp. nov. is thus far only known, in very low apparent density (6 male [and zero female] captures in 5,000 trap/nights across several field trips in recent years by us), on eastern Tasman Peninsula in a forest block encompassing just 40 km<sup>2</sup>. One of three study sites investigated by Lazenby and Dickman (2013) in their camera/capture/release study was on Tasman Peninsula, just 1.5 km south of the *A. vandycki* sp. nov. holotype locality. Between 2009 and 2011, they recorded several captures of *A. vandycki* sp. nov. (one of which has been genetically confirmed by us), including one 45 g female captured on the 16<sup>th</sup> of May, 2011 (all captures were released). We are currently investigating the ecology, genetics and distribution of *A. vandycki* sp. nov., which will permit us to formally assess status and conservation priorities with state and federal listings both pending. If *A. vandycki* sp. nov. is truly limited to Tasman Peninsula (south of EagleHawk Neck), it will certainly warrant listing in a threatened category because of geographical restriction, small apparent population size and because much of its known (and limited) natural habitat there falls within State Forest and is thus infested with timber plantations (within which the species has been targeted several times and never caught). Throughout the forest block (both intentional and unintentional) fires will also be a conservation concern, if *A. vandycki* sp. nov. behaves like *A. mimetes* in following a secondary succession pattern, typically not moving back into fire-affected / heavily disturbed areas until ten or more years post-disturbance (Dickman, 2008; Lunney et al. 2001). Indeed, the fragmented, harvested and fire-affected nature of the Tasman Peninsula forests over the last twenty years may account

in part for the very low trapping success for *A. vandycki* sp. nov. (just one male in every 830 trap/nights in our surveys). Another threat to *A. vandycki* sp. nov. (and other native Australian mammalian wildlife) exists in the form of feral cats (*Felis catus*). The Tasmanian Devil (*Sarcophilus harrisii*) population is small on Tasman Peninsula (30-40 disease-free animals, Mike Driessen pers. comm.) and such reduction/removal of a top native predator may result in increased feral cat numbers (Lazenby & Dickman, 2013); cats are common in the east of the Peninsula (often interfering with the Devil trapping program, Mike Driessen, pers. comm.) and will most likely opportunistically prey on *A. vandycki* sp. nov.

Nevertheless, the results of this study have generally positive implications for Tasmanian mammal conservation and tourism, with a new endemic and likely threatened species being identified (*A. vandycki* sp. nov.) and an existing species (*A. swainsonii*) now recognised as apparently endemic to the island. In a small Australian state boasting just six endemic (of 83) mammal species, an increase of two endemic species may prove important, raising its mammalian endemism rating from 7% to 10%.

## ACKNOWLEDGEMENTS

AMB especially wishes to thank his long-time friend and mentor Dr Steve Van Dyck (formerly of QM) for generously sharing his expertise on all things antechinus and making helpful comments on a draft of this work. AMB is also grateful to Harry Hines (QPWS) and Ian Gynther (EHP) for loan of Elliott traps to catch antechinus. This research would not have been possible without the unstinting help of Mike Driessen (DPIPWE), who provided invaluable advice, logistical support and ear clips of *A. swainsonii*. We warmly thank Hannah Maloney (QUT) for her sterling help on successive field trips in search of the elusive *A. vandycki* sp. nov. on Tasman Peninsula and typotypic *A. mimetes* from the chilly heights of Ebor. Billie Lazenby (DPIPWE) kindly provided ear clips of Tasmanian *A. swainsonii* and *A. vandycki* sp. nov. and her PhD trapping data for *A. vandycki* sp.

nov. was invaluable. ABRS (Aus. Govt) funded the trip led by TYM to the Tasmania wilderness areas. QUT supported AMB's sabbatical, where he spent a month happily ensconced in the British Museum of Natural History's extensive type collection. AMB thanks David Maynard and Craig Reid (QVM, Launceston) for making him welcome and providing unreserved access to their antechinus collection. AMB thanks Heather Janetzki (QM) for expertly crafting the type and study skins of *A. vandycki* sp. nov., *A. swainsonii*, *A. mimetes* and *A. arktos* and for her help in acquiring loans generously provided by staff at MVic and the AM. We thank two anonymous reviewers who made very useful comments on the manuscript.

## LITERATURE CITED

- Archer, M. 1974. The development of cheek teeth in *Antechinus flavipes* (Marsupialia, Dasyuridae). *Journal of the Royal Society of Western Australia* 57: 54-63.
1976. The dasyurid dentition and its relationships to that of didelphids, thylacinids, borhaenids (Marsupialia) and peramelids (Peramelina: Marsupialia). *Australian Journal of Zoology Supplementary Series* 39: 1-34.
- Armstrong, L.A., Krajewski, C. & Westerman, M. 1998. Phylogeny of the dasyurid marsupial genus *Antechinus* based on cytochrome-b, 12S-rRNA, and protamine-P1 genes. *Journal of Mammalogy* 79: 1379-1389 (<http://dx.doi.org/10.2307/1383028>).
- Baker, A.M., Mutton, T.Y. & Hines, H.B. 2013. A new dasyurid marsupial from Krombit Tops, south-east Queensland, Australia: the Silver-headed Antechinus, *Antechinus argentus* sp. nov. (Marsupialia: Dasyuridae). *Zootaxa* 3746(2): 201-239 (<http://dx.doi.org/10.11646/zootaxa.3746.2.1>).
- Baker, A.M., Mutton, T.Y., Hines, H.B. & Van Dyck, S. 2014. The Black-tailed Antechinus, *Antechinus arktos* sp. nov.: a new species of carnivorous marsupial from montane regions of the Tweed Volcano caldera, eastern Australia. *Zootaxa* 3765(2): 101-133 (<http://dx.doi.org/10.11646/zootaxa.3765.2.1>).
- Baker, A.M., Mutton, T.Y. & Van Dyck, S. 2012. A new dasyurid marsupial from eastern Queensland, Australia: the Bull-footed Antechinus, *Antechinus mysticus* sp. nov. (Marsupialia: Dasyuridae). *Zootaxa* 3515: 1-37.
- Baker, A.M., & Van Dyck, S. 2012. Taxonomy and redescription of the Fawn Antechinus, *Antechinus*

- bellus* (Thomas) (Marsupialia: Dasyuridae). *Zootaxa* 3613: 201-228.
- 2013a. Taxonomy and redescription of the Yellow-footed Antechinus, *Antechinus flavipes* (Waterhouse) (Marsupialia: Dasyuridae). *Zootaxa* 3649: 1-62 (<http://dx.doi.org/10.11646/zootaxa.3649.1>).
- 2013b. Taxonomy and redescription of the Atherton Antechinus, *Antechinus godmani* (Thomas) (Marsupialia: Dasyuridae). *Zootaxa* 3670: 401-439 (<http://dx.doi.org/10.11646/zootaxa.3670.4.1>).
- Baverstock, P.R., Archer, M., Adams, M., & Richardson, B.J. 1982. Genetic relationships among 32 species of Australian dasyurid marsupials. Pp. 641-650. In Archer M., (ed) *Carnivorans marsupials*. (Royal Zoological Society of New South Wales: Sydney).
- Crowther, M.S. 2002. Morphological variation within *Antechinus agilis* and *Antechinus stuartii* (Marsupialia: Dasyuridae). *Australian Journal of Zoology* 50: 339-356 (<http://dx.doi.org/10.1071/ZO01030>).
- Davison, A. 1986. Dentition of Victorian *Antechinus* species. *Australian Mammalogy* 9: 73-85.
1991. A new subspecies of dusky antechinus, *Antechinus swainsonii* (Marsupialia: Dasyuridae) from western Victoria. *Australian Mammalogy* 14: 103-113.
- Dickman, C.R. 1982. Some ecological aspects of seasonal breeding in *Antechinus* (Dasyuridae, Marsupialia). Pp. 139-150. In Archer, M. (ed) *Carnivorans Marsupials*. (Royal Zoological Society of New South Wales: Sydney).
- 1986a. An experimental manipulation of the intensity of interspecific competition: effects on a small marsupial. *Oecologia* 70(4): 536-543.
- 1986b. An experimental study of competition between two species of dasyurid marsupials. *Ecological Monographs* 56: 221-241.
- 1988a. Body size, prey size, and community structure in insectivorous mammals. *Ecology* 69(3): 569-580.
- 1988b. Sex ratio variation in response to interspecific competition. *The American Naturalist* 132(2): 289-297.
2008. Dusky Antechinus *Antechinus swainsonii*. Pp. 99-100. In, Van Dyck, S. & Strahan, R. (eds) *Mammals of Australia* (3<sup>rd</sup> edition). (New Holland: Australia).
- Dickman, C.R., Parnaby, H.E., Crowther, M.S. & King, D.H. 1998. *Antechinus agilis* (Marsupialia: Dasyuridae), a new species from the A. stuartii complex in south-eastern Australia. *Australian Journal of Zoology* 46(1): 1 - 26.
- Firestone, K.B., Elphinstone, M.S., Sherwin, W.B. & Houlden, B.A. 1999. Phylogeographical population structure of tiger quolls *Dasyurus maculatus* (Dasyuridae: Marsupialia), and endangered carnivorous marsupial. *Molecular Ecology* 8: 1613-1625.
- Geoffroy [Saint-Hilaire], E. 1803. Note sur les especes du genre dasyure. *Bulletin des Sciences par la Societe Philomathique de Paris* 3(81): 258-259.
- Gibson, L.A., Wilson, B.A., Cahill, D.M. & Hill, J. 2004. Modelling suitable habitat of the swamp antechinus (*Antechinus minimus maritimus*) in the coastal heathlands of southern Victoria, Australia. *Biological Conservation* 117: 143-150.
- Gongora, J., Swan, A.B., Chong, A.Y., Ho, S.Y.W., Damayanti, C.S., Kolomyjec, S., Grant, T., Miller, E., Blair, D., Furlan, E. & Gust, N. 2012. Genetic structure and phylogeography of platypuses revealed by mitochondrial DNA. *Journal of Zoology* 286(2012): 110-119.
- Green, R.H. 1972. The murids and small dasyurids in Tasmania. Parts 5 and 6. Records of the Queen Victoria Museum No. 46.
- Hall, T.A. 1999. BioEdit: a user-friendly biological sequence alignment editor and analysis program for Windows 95/98/NT. *Nucleic Acids Symposium Series* 41:95-98.
- Happold, D.C.D. 1989. Small mammals of the Australian Alps. Pp.221-239 In Good, R. (ed) *The scientific significance of the Australian Alps*. (Australian Alps National Parks Liason Committee and Australian Academy of Science).
2011. Reproduction and ontogeny of *Mastacomys fuscus* (Rodentia: Muridae) in the Australian Alps and comparisons with other small mammals living in alpine communities. *Mammalian Biology* 76(2011): 540-548.
- Higgins, E.T. & Petterd, W.F. 1882. Descriptions of hitherto undescribed *Antechini* and *Muridae* inhabiting Tasmania. *Papers and Proceedings of the Royal Society of Tasmania* 171-176.
1883. New species of Antechini and Mus. *Papers and Proceedings of the Royal Society of Tasmania* 184-186.
1884. Descriptions of new Tasmanian animals. *Papers and Proceedings of the Royal Society of Tasmania* 181-185.
- Iredale, T. & Troughton, E. 1934. A check-list of the mammals recorded from Australia. *Memoirs of the Australian Museum* 6: 1-122.
- Krajewski, C., Young, J., Buckley, L., Woolley, P.A. & Westerman, M. 1997. Reconstructing the Evolutionary Radiation of Dasyurine Marsupials with Cytochrome b, 12S rRNA, and Protamine P1 Gene Trees. *Journal of Mammalian Evolution* 4(3): 217-236 (<http://dx.doi.org/10.1023/A:1027349725642>).
- Lazenby B.T. & Dickman, C.R. 2013. Patterns of Detection and Capture Are Associated with Cohabiting Predators and Prey. *PLoS ONE* 8(4): e59846.

- Lunney, D., Matthews, A. & Grigg, J. 2001. The diet of *Antechinus agilis* and *A. swainsonii* in unlogged and regenerating sites in Mumbulla State Forest, south-eastern New South Wales. *Wildlife Research* 28: 459-464 (<http://dx.doi.org/10.1071/WR00015>).
- Macleay, W.S. 1841. Notice of a new genus of Mammalia discovered by J. Stuart, Esq., in New South Wales. *Annals and Magazine of Natural History* 8: 241-243.
- Mahoney, J.A. & Ride, W.D.L. 1988. Dasyuridae. Pp. 14-33. In Walton, D.W. (ed), 'Zoological Catalogue of Australia'. Vol. 5. (Australian Government Publishing Service: Canberra).
- Marlow, B. 1961. Reproductive behaviour of the marsupial mouse, *Antechinus flavipes* (Waterhouse) (Marsupialia) and the development of the pouch young. *Australian Journal of Zoology* 9: 203-220 (<http://dx.doi.org/10.1071/ZO9610203>).
- McAllan, B. 2003. Timing of reproduction in carnivorous marsupials. Pp. 147-168. In Jones, M., Dickman, C. & Archer, M. (eds). *Predators with Pouches: the Biology of Carnivorous Marsupials*. (CSIRO Publishing: Victoria).
- McAllan, B., Dickman, C.R. & Crowther, M.S. 2006. Photoperiod as a reproductive cue in the marsupial genus *Antechinus*: ecological and evolutionary consequences. *Biological Journal of the Linnean Society* 87: 365-379 (<http://dx.doi.org/10.1111/j.1095-8312.2006.00571.x>).
- Menkhorst, P. (ed.) 1995. *Mammals of Victoria*. (Oxford University Press Australia: Melbourne).
- Mutton, T.Y. 2011. *Systematics and Evolution of the Dasyurid Marsupial Genus Antechinus*. Honours Thesis, QUT: Brisbane, (Unpub.) 65 pp.
- Nylander, J.A.A. 2004. MrModeltest v2. Program distributed by the author. Evolutionary Biology Centre, (Uppsala University).
- Page, R.D.M. 1996. TREEVIEW: An application to display phylogenetic trees on personal computers. *Computer Applications in the Biosciences* 12: 357-358.
- Ridgway, R. 1912. *Colour Standards and Nomenclature*. (Published by the Author: United States National Museum).
- Ronquist, F. & Huelsenbeck, J.P. 2003. MRBAYES 3: Bayesian phylogenetic inference under mixed models. *Bioinformatics* 19: 1572-1574 (<http://dx.doi.org/10.1093/bioinformatics/btg180>).
- Sale, M.G., Ward, S.J. & Arnould, J.P.Y. 2006. Aspects of the ecology of swamp antechinus (*Antechinus minimus maritimus*) on a Bass Strait island. *Wildlife Research* 33:215-221 (<http://dx.doi.org/10.1071/WR05051>).
- Sanecki, G.M., Green, K., Wood, H., Lindenmayer, D. & Sanecki, K.L. 2006. The influence of snow cover on home range and activity of the bush-rat (*Rattus fuscipes*) and the dusky antechinus (*Antechinus swainsonii*). *Wildlife Research* 33: 489-496 (<http://dx.doi.org/10.1071/WR05012>).
- Smith, A.M.A. 1983. The subspecific biochemical taxonomy of *Antechinus minimus*, *A. swainsonii* and *Smintliopsis leucopus* (Marsupialia: Dasyuridae). *Australian Journal of Zoology* 32: 753-762 (<http://dx.doi.org/10.1071/ZO9830753>).
- StatSoft, Inc. 2004. STATISTICA (data analysis software system), version 7.
- Tamura, K., Stecher, G., Peterson, D., Filipski, A. & Kumar, S. 2013. MEGA6: Molecular Evolutionary Genetics Analysis Version 6.0. *Molecular Biology and Evolution* 30:2725-2729 (<http://dx.doi.org/10.1093/molbev/mst197>).
- Tate, G.H.H. 1947. Results of the Archbold Expeditions. No. 56. On the anatomy and classification of the Dasyuridae (Marsupialia). *Bulletin of the American Museum of Natural History* 88: 101-155.
- Thomas, M.O. 1888. *Catalogue of Marsupialia and Monotremata in the Collection of the British Museum*. (British Museum Natural History: London).
- Thomas, O. 1904. On a collection of mammals made by Mr. J.T. Tunney in Arnhem Land, Northern Territory of South Australia. *Novitates Zoologicae* 11: 222-229.
- Thomas, M.O. 1924. A new Pouched Mouse (*Plascogale*) from northern New South Wales. *Annals and Magazine of Natural History* 9(14): 528 (<http://dx.doi.org/10.1080/00222932408633152>).
- Van Dyck, S. 1980. The Cinnamon Antechinus, *Antechinus leo* (Marsupialia: Dasyuridae), a new species from the vine-forests of Cape York Peninsula. *Australian Mammalogy* 3: 5-17.
- Van Dyck, S. 1997. Revisionary studies in *Murexia* and *Antechinus* (Marsupialia: Dasyuridae). Unpublished PhD Thesis, University of New South Wales, Australia.
- Van Dyck, S. 2002. Morphology-based revision of *Murexia* and *Antechinus* (Marsupialia: Dasyuridae). *Memoirs of the Queensland Museum* 48: 239-330.
- Van Dyck, S.M. & Crowther, M.S. 2000. Reassessment of northern representatives of the *Antechinus stuartii* complex (Marsupialia: Dasyuridae): *A. subtropicus* sp. nov. and *A. adustus* new status. *Memoirs of the Queensland Museum* 45(2): 611-635.
- Van Dyck, S., & Ogilvie, P. 1977. *Antechinus swainsonii* (Waterhouse, 1840), the dusky marsupial mouse, an addition to the mammal fauna of Queensland. *Memoirs of the Queensland Museum* 18: 69-73.
- Wakefield, N.A. & Warneke, R.M. 1963. Some revision in *Antechinus* (Marsupialia) 1. *Victorian Naturalist* 80: 192-219.
- Waterhouse, G.R. 1840. Description of a new marsupial mammal belonging to the genus *Plascogale*. *Magazine of Natural History* 2(4): 299.

- Williams, R. & Williams, A. 1982. The life cycle of *Antechinus swainsonii* (Dasyuridae, Marsupialia). Pp. 91-95. In Archer, M. (ed), *Carnivorous Marsupials*. (Royal Zoological Society of New South Wales: Sydney, Australia).
- Wilson, B. A., Aberton, J. & Reichl, T. 2001. Effects of fragmented habitat and fire on the distribution and ecology of the Swamp Antechinus (*Antechinus minimus maritimus*) in the Eastern Otways, Victoria. *Wildlife Research* 28: 527-36 (<http://dx.doi.org/10.1071/WR00016>).
- Wilson, B.A. & Bachmann, M.R. 2008. Swamp Antechinus *Antechinus minimus*. Pp. 93-94. In Van Dyck, S. and Strahan, R. (eds) *Mammals of Australia (3rd edition)*. (New Holland: Australia).
- Woolley, P.A. 1966. Reproduction in *Antechinus* spp. and other dasyurid marsupials. *Symposia of the Zoological Society of London* 15: 281-294.

# Taxonomy and redescription of the Swamp Antechinus, *Antechinus minimus* (È. Geoffroy) (Marsupialia: Dasyuridae)

BAKER, A.M.

Queensland University of Technology, 2 George Street, Brisbane, Queensland, 4001, Australia.  
Email: am.baker@qut.edu.au

Queensland Museum, PO Box 3300, South Brisbane Qld 4101

VAN DYCK, S.

Queensland Museum, PO Box 3300, South Brisbane Qld 4101

Citation: Baker, A.M. & Van Dyck, S. 2015. Taxonomy and redescription of the Swamp Antechinus, *Antechinus minimus* (È. Geoffroy) (Marsupialia: Dasyuridae). *Memoirs of the Queensland Museum – Nature* 59: 127–170. Brisbane. ISSN 2204-1478 (Online), ISSN 0079-8835 (Print). Accepted: 25 November 2014. First published online: 31 July 2015

<http://dx.doi.org/10.17082/j.2204-1478.59.2015.2014-11>

LSID - urn:lsid:zoobank.org:pub:C74C6D50-090A-41EE-8EAB-90E9793A3436

## ABSTRACT

We provide a taxonomic redescription of the dasyurid marsupial Swamp Antechinus, *Antechinus minimus* (Geoffroy, 1803). In the past, *A. minimus* has been classified as two subspecies: the nominate *A. minimus minimus* (Geoffroy, 1803), which is found throughout much of Tasmania (including southern Bass Strait islands) and *A. minimus maritimus* (Finlayson, 1958), which is found on mainland Australia (as well as some near-coastal islands) and is patchily distributed in mostly coastal areas between South Gippsland (Victoria) and Robe (South Australia). Based on an assessment of morphology and DNA, we conclude that *A. minimus* is both distinctly different from all extant congeners and that the two existing subspecies of Swamp Antechinus are appropriately taxonomically characterised. In our genetic phylogenies, the Swamp Antechinus was monophyletic with respect to all 14 known extant congeners; moreover, *A. minimus* was well-positioned in a large clade, together with all four species in the Dusky Antechinus complex, to the exclusion of all other antechinus. Within *A. minimus*, between subspecies there were subtle morphological differences (*A. m. maritimus* skulls tend to be broader, with larger molar teeth, than *A. m. minimus*, but these differences were not significant); there was distinct, but only moderately deep genetic differences (3.9–4.5% at mtDNA) between *A. minimus* subspecies. Comparatively, across Bass Strait, the two subspecies of *A. minimus* are morphologically and genetically markedly less divergent than recently recognised species pairs within the Dusky Antechinus complex, found in Victoria (*A. mimetes*) and Tasmania (*A. swainsonii*) (9.4–11.6% divergent at mtDNA). □ *Marsupialia*, *Dasyuridae*, *dasyurid*, *carnivorous marsupial*, *Australia*.

In 1803, Étienne Geoffroy Saint-Hilaire, a French naturalist colleague of Lamarck, described a new carnivorous marsupial that had been collected by Peron from Tasmania. Geoffroy dubbed his new species *minimus*, placing it within the genus

*Dasyurus* that already contained three species, two of which were quolls; thus, the epithet *minimus*, meaning small, was appropriate for the time. Compared to the other 14 extant species of antechinus known today, *A. minimus* is in fact



medium-large in size, but it was to be another 35 years after Geoffroy coined *minimus* before a second antechinus was even discovered, by Waterhouse (*A. flavipes* [then *Phascogale*] in 1838), followed quickly by a third, *A. swainsonii* (Waterhouse 1840). The genus *Antechinus* was duly erected by Macleay in 1841, after the discovery of a fourth species, *A. stuartii*. More than 60 years later, there followed two further new species, named by renowned English taxonomist Oldfield Thomas (*bellus* in 1904 and *godmani* in 1923). No other species was named under *Antechinus* until Van Dyck's *leo* in 1980. In the decades that followed, the advent of molecular techniques allowed resolution of numerous cryptic taxa across many groups of organisms, including mammals. Pioneering genetic studies examined relationships among dasyurid genera (e.g., Armstrong *et al.* 1998; Baverstock *et al.* 1982; Krajewski *et al.* 1997) prompting description of other antechinus species (*agilis* by Dickman *et al.*, 1998, *subtropicus* and *adustus* [the latter raised from subspecies of *stuartii*] by Van Dyck & Crowther, 2000). So by the time of Van Dyck's (2002) morphological review, there were ten extant species of antechinus: Swamp Antechinus, *A. minimus* (Geoffroy); Yellow-footed Antechinus, *A. flavipes* (Waterhouse); Brown Antechinus, *A. stuartii* Macleay; Dusky Antechinus, *A. swainsonii* (Waterhouse); Fawn Antechinus, *A. bellus* (Thomas); Rusty Antechinus, *A. adustus* (Thomas); Atherton Antechinus, *A. godmani* (Thomas); Cinnamon Antechinus, *A. leo* Van Dyck; Agile Antechinus, *A. agilis* Dickman, Parnaby, Crowther and King and Subtropical Antechinus, *A. subtropicus* Van Dyck and Crowther. But in the years that followed Van Dyck's review, it became clear from aberrant specimens held in museum collections that other antechinus species lay waiting to be described.

To investigate this cryptic variation, three years ago our research group began a systematic and taxonomic revision of the extant members of the genus, which resulted in description of five new species of antechinus (see Baker, Mutton & Hines 2013; Baker, Mutton, Hines & Van Dyck 2014; Baker, Mutton, Mason & Gray 2015; Baker, Mutton & Van Dyck 2012) and redescription of

several others (Baker & Van Dyck 2012, 2013a,b). The new species description sequence ran as follows. First, Baker, Mutton & Van Dyck (2012) diagnosed an eleventh species, the Buff-footed Antechinus *A. mysticus*, found sheltering under the taxonomic umbrella of the ubiquitous Yellow-footed Antechinus, *A. flavipes*. Then, in the process of investigating the distributional range of *A. mysticus* between south-east and mid-east Queensland, Baker, Mutton & Hines (2013) stumbled across a twelfth antechinus species, the Silver-headed Antechinus, *A. argentus*, which is apparently restricted in distribution to just a few square kilometres, on the escarpment of Kroombit Tops NP in south-east Queensland. At about the time of discovering *A. argentus*, we shifted focus within the genus to the Dusky Antechinus, *Antechinus swainsonii*. The thirteenth species of Antechinus, the likely endangered *A. arktos*, was raised after comparison of northern outlying Dusky Antechinus populations with other mainland *A. s. mimetes* (Baker, Mutton, Hines & Van Dyck 2014). But after genetically screening some newly acquired tissue samples of Tasmanian *A. swainsonii*, it became clear there were further cryptic species within the Dusky Antechinus group. Our research group subsequently undertook a more comprehensive morphological and genetic review of Dusky Antechinus, duly naming a new (likely threatened) species apparently restricted to Tasman Peninsula, *A. vandycki*, and transferring the two mainland subspecies of *A. swainsonii* (*mimetes* and *insulanus*) to subspecies within the raised *A. mimetes* (Baker, Mutton, Mason & Gray 2015). This research indicated deep divergence between species on either side of Bass Strait, with *A. mimetes* (Vic, NSW) being about 10% divergent to both Tasmanian species: *A. swainsonii* and *A. vandycki*. Since the Swamp Antechinus, *A. minimus*, has a similar distribution to southern Dusky Antechinus, on either side of Bass Strait, with subspecies *maritimus* on the coastal mainland (SA, Vic and neighbouring islands) and subspecies *minimus* on Tasmania (and southern Bass Strait islands), we were prompted to investigate if there were also cryptic taxa hiding under *A. minimus*.



*A. minimus* (Geoffroy 1803) has an interesting taxonomic history. Although the original date of publication of this species was given as '1803...December (fide Sherbon)' by Iredale and Troughton (1934), they cited the page reference as p. 159 in the *Bulletin des Sciences par La Société Philomathique de Paris* No. 81. Tate (1947) did the same. This was later corrected to p. 259 (by Mahoney & Ride 1988), but relatively recently it was proposed that the species' publication date be amended to 1904 in favour of a subsequent, expanded description in the *Annales du Muséum d'Histoire Naturelle* (Julien-Laferrrière 1994). This amendment is most likely invalid.

Furthermore, the veracity of the *A. minimus* type locality received attention from Wakefield and Warneke (1963) who noted that Waterhouse's (1846) reference to Maria Island (near Hobart) as the type locality conflicted with Geoffroy's (1803) original statement that the holotype had come from an island found in Bass Strait. According to Wakefield and Warneke (1963), the confusion arose from an account by Péron (1807) of a single 'Dasyure' collected on Maria Island. The identity of this animal, Wakefield and Warneke argued, had confused Péron at the time as much as the description of events had later confused Waterhouse. The 'dasyure' was finally correctly identified and ended up being described as the holotype of the Eastern Pygmy-possum *Cercartetus nanus* (Desmarest, 1818). Thus, the only likely type locality attributable to *A. minimus* was eventually identified as (ironically) Waterhouse Island, a tiny (287 hectare) island located just 3 km off the north-eastern coast of Tasmania.

Unfortunately, further confusion followed, three years after the description of *A. swainsonii* (Waterhouse 1840), Waterhouse (1841: 142), deferring to the judgement of Gould, merged *swainsonii* under *minimus* 'I have altered the name I had applied to it, of *swainsonii* into *minima*, Mr. Gould, who has recently examined the original of Geoffroy's *Dasyurus minimus*, having informed me that that animal was specifically identical with the *swainsonii*. Geoffroy's specimen must be young, being only four French inches in length'. It was another

three years before Waterhouse was able to examine the *D. minimus* holotype himself and thereafter re-establish *swainsonii*, writing 'Mr. Gould imagined this species was identical with the *Dasyurus minimus* of Geoffroy; I have recently compared the two animals together, and find this is not the case. The skull of *P. swainsonii* is proportionately narrower...' (Waterhouse 1846: 412). Waterhouse must have been reasonably confident of his skills of external comparative assessment, since the skull of the *A. minimus* holotype was not removed from the mount until 1937 (Tate 1947)!

*A. minimus* was not knowingly collected from mainland Australia until 1962. However, Finlayson (1958) had encountered it earlier in South Australia and, mistaking it for a distinct form of *A. swainsonii*, named it *Plascogale (Antechinus) swainsonii maritima* from Port MacDonnell (collected in June, 1938). But Wakefield and Warneke (1963) noted Finlayson's error and referred *maritimus* to *A. minimus*.

Early genetic work addressed the distinctiveness of mainland and Tasmanian subspecies of *A. minimus* and *A. swainsonii*. Smith (1983) examined electrophoretic variation in *A. minimus* and *A. swainsonii* on either side of Bass Strait and concluded that respective mean genetic distances of 0.035  $\pm$  0.009 and 0.085  $\pm$  0.015 suggested that subspecies status was warranted in *A. minimus* and at least subspecies status was warranted for *A. swainsonii*. The sampling of *A. minimus* in Smith's study included a couple of Tasmanian populations: Flinders Island in the north and Bruny Island in the south, compared to four populations on the mainland (Vic): Gembrook, Dartmoor, Cape Liptrap and Cape Otway. Given that Smith's suspicions of deeper variation between *A. swainsonii* subspecies was recently born out by species level differences being attributed to these Dusky Antechinus populations after detailed morphological and comparative genetic assessment (see Baker, Mutton, Mason & Gray 2015), we were intrigued to investigate in more detail the comparative situation in *A. minimus*. Here, we report the results of this work.

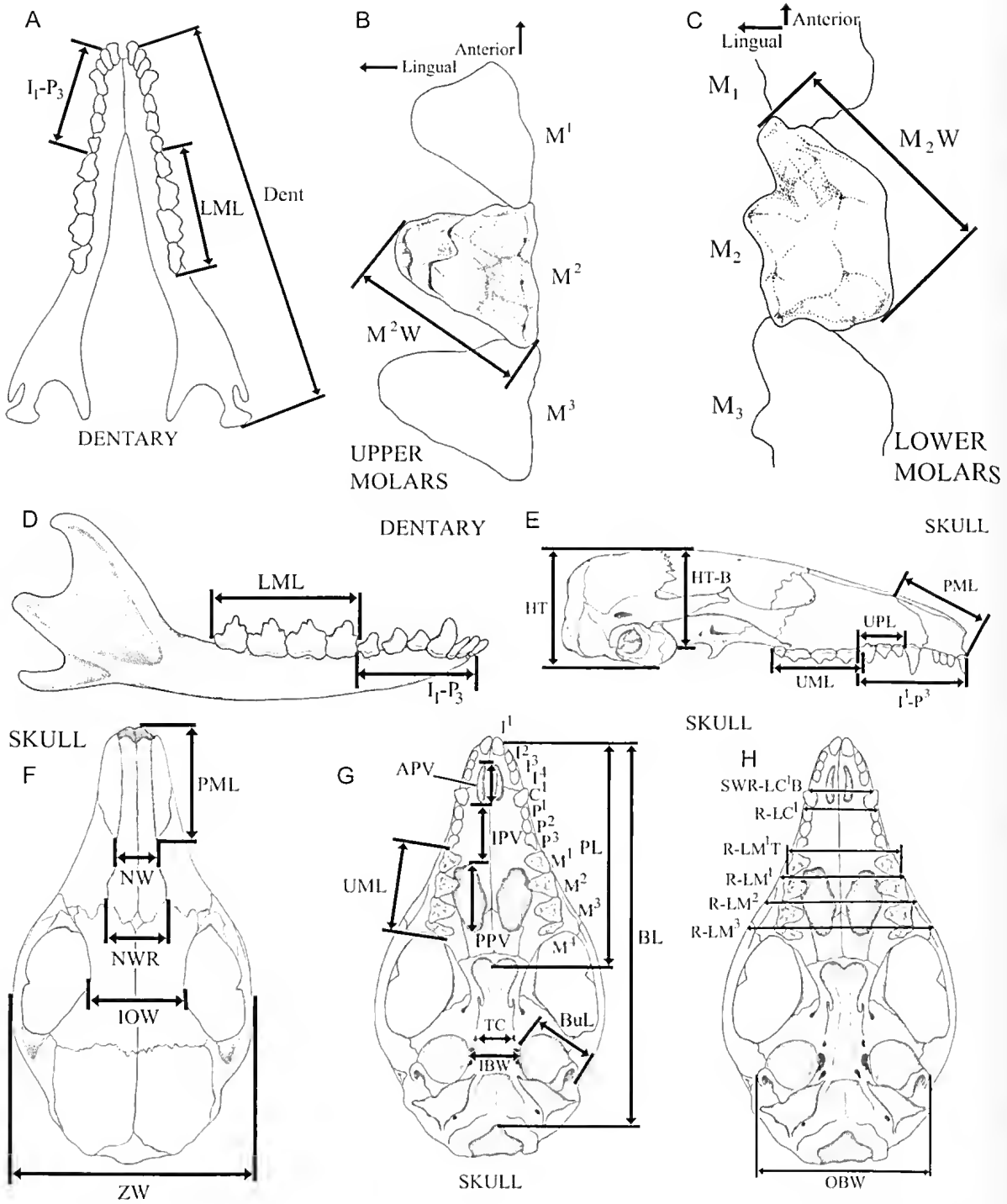


FIG. 1. A guide to measurement of variables: skull and dentary (A-H), and external body measures opposite page (I, J).

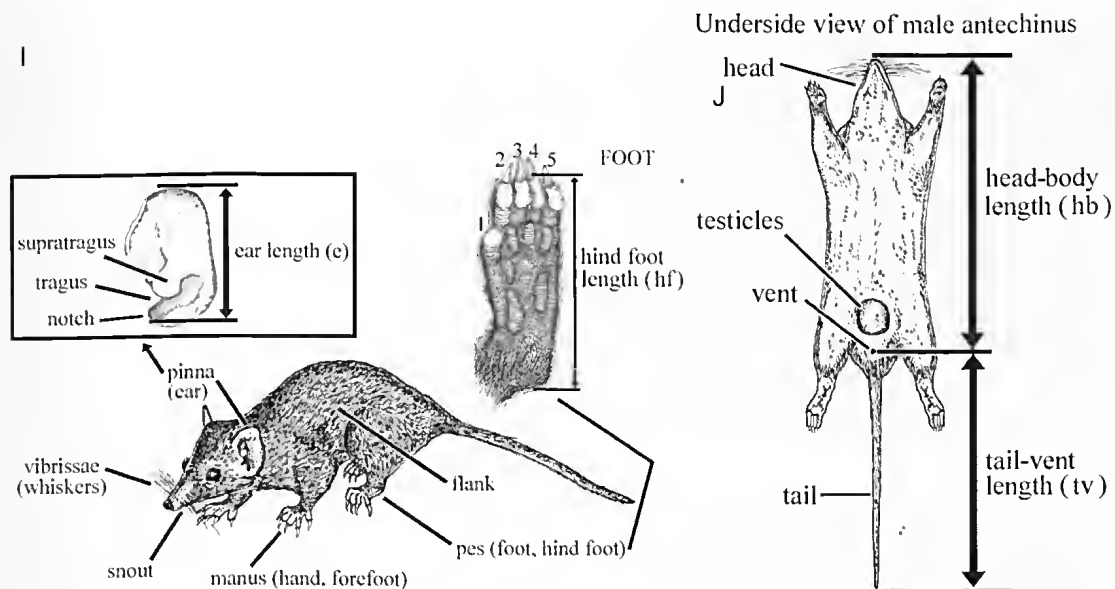


FIG. 1. Continued ...

## METHODS

### Analyses of morphological data

Figure 1 describes and depicts the 30 skull and dental, and 5 external measurements taken. Measurements were made using Mitutoyo CD-8CSX digital calipers (taken to the nearest 0.0 X mm). Age variation was minimised by using only animals which possessed fully erupted permanent P<sup>3</sup> teeth and thus deemed to be adult. Tooth nomenclature follows Archer (1974) and basicranial nomenclature follows Archer (1976). Colour nomenclature used in the holotype pelage description follows Ridgway (1912).

Measured variables are as follows (and see Fig 1): wt = body weight (grams); hb = head-body length (mm) from tip of nose to mid-vent; tv = tail-vent length (mm) from mid-vent to tip of tail proper (excluding hair at tip); hf = hind foot length (mm) from behind heel to tip of longest extended toe (excluding claw); e = ear length (mm) from extended ear tip to notch at rear base of tragus; APV = maximum anterior palatal vacuity length; BL = basicranial skull length, excluding incisors; Dent = dentary length, excluding incisors; IBW = minimum

width between auditory bullae; IOW = minimum width of interorbital constriction; IPV = minimum interpalatal vacuity distance; M<sup>2</sup>W = maximum width of upper molar 2 measured diagonally from anterior lingual to posterior labial points; NW = width of nasals at the nasal / premaxilla / maxilla junction; OBW = basicranial width from outside right and left auditory bullae; PPV = maximum posterior palatal vacuity length; R-LC<sup>1</sup> = skull width level with the posterior of upper canines; R-LM<sup>1</sup> = skull width level with the junction of the first and second upper molars; R-LM<sup>1</sup>T = maximum width between the ectolophs of the left and right first upper molars; R-LM<sup>2</sup> = skull width level with the junction of the second and third upper molars; R-LM<sup>3</sup> = skull width level with the junction of the third and fourth upper molars; ZW = maximum zygomatic width; HT = skull height; PL = length of palate; SWR-LC<sup>1</sup>B = skull width level with the anterior of upper canines; TC = minimum distance separating transverse canals; NWR = width of nasals at the nasal / maxilla / frontal junction; PML = length of premaxilla; UML = maximum length of upper molar row, M<sup>1</sup>-M<sup>4</sup>; HT-B = skull height measured immediately anterior of auditory bullae; BuL = auditory bulla length; I<sup>1</sup>-P<sup>3</sup> = crown length from anterior edge



FIG. 2. *Antechinus minimus minimus* holotype mount of MNHN C.G. 1987-233; No. 381; Type No. 628

of upper incisor 1 to posterior edge of upper premolar 3; LML = maximum length of lower molar row,  $M_1$ - $M_4$ ;  $I_1$ - $P_3$  = crown length from anterior of lower incisor 1 to posterior of lower premolar 3;  $M_2W$  = maximum width of lower molar 2 measured diagonally from anterior lingual to posterior labial points; UPL = crown length of upper premolar row,  $P^1$ - $P^3$ .

Species clades returned from constructed DNA-based phylogenies (see below) matched to voucher specimens were used as testable hypotheses in subsequent morphological analyses; thus, multivariate analyses enabled us to predict membership of individuals in hypothesised species groups based on a combination of skull morphology variables, whereas univariate ANOVAS (and subsequent post-hoc tests) for each variable enabled us to test for significant variation within each variable and determine which variables differed for comparisons of our putative *A. minimus minimus* with each other putative species pair. The combination of univariate and multivariate analyses was essential to permit both fine-scale pairwise comparisons demonstrating species by species differences to facilitate best-practice species management for the future and also broadscale comparisons among all species within both *A. minimus* and the closely related Dusky Antechinus complex, to best illustrate broader differences across all measured variables.

Statistical analyses of morphometrics were undertaken using the program STATISTICA

Version 7 (Statsoft Inc. 2004). Samples were initially tested for normality with the Kolmogorov-Smirnov and Lilliefors tests and homogeneity of sample variances using Levene's test. Analysis of Variance (ANOVA) was used to analyse variation in means among all putative antechinus species, tested under separate hypotheses for each measured external and cranial/dentition variable. In each ANOVA, Post-hoc Unequal N HSD tests (a modification of Tukey's HSD) were used to test pairwise differences (at  $P < 0.05$ ) in external variables and craniodental measures between *A. minimus minimus* and each proposed congener, to compensate for potential Type 1 errors and since sample sizes differed between species. Multivariate analyses were conducted to optimise dimensionality of each variable set and maximise relationships between variable sets. Discriminant Function Analysis (DFA) was used to determine assignment reliability within proposed species groupings and subsequent Canonical Variate Analysis (CVA) generated independent functions that best discriminated between the putative species.

Baker, Mutton, Mason and Gray (2015) recognised the close genetic relationship between *A. minimus* and all members of the Dusky Antechinus complex, indicating that these taxa formed a combined well-supported clade to the exclusion of all congeners. Thus, univariate statistics (means, standard deviations, range minima and maxima) were compiled for each of the external and internal (cranial/dental) measures for Swamp Antechinus, *A. minimus minimus* and *A. minimus maritimus* as well as the four species (5 taxa) within the dusky antechinus species complex: Tasmanian Dusky Antechinus, *A. swainsonii*; Tasman Peninsula Dusky Antechinus, *A. vandycki*; Mainland Dusky Antechinus, *A. mimetes mimetes*, *A. mimetes insulans*; and Black-tailed Dusky Antechinus, *A. arktos*. A range of scatterplots were constructed to show the main discriminating variable pairs among these species. *Antechinus minimus* and all members of the Dusky Antechinus complex are strikingly different in both size and morphology to all congeners, so no other species were included

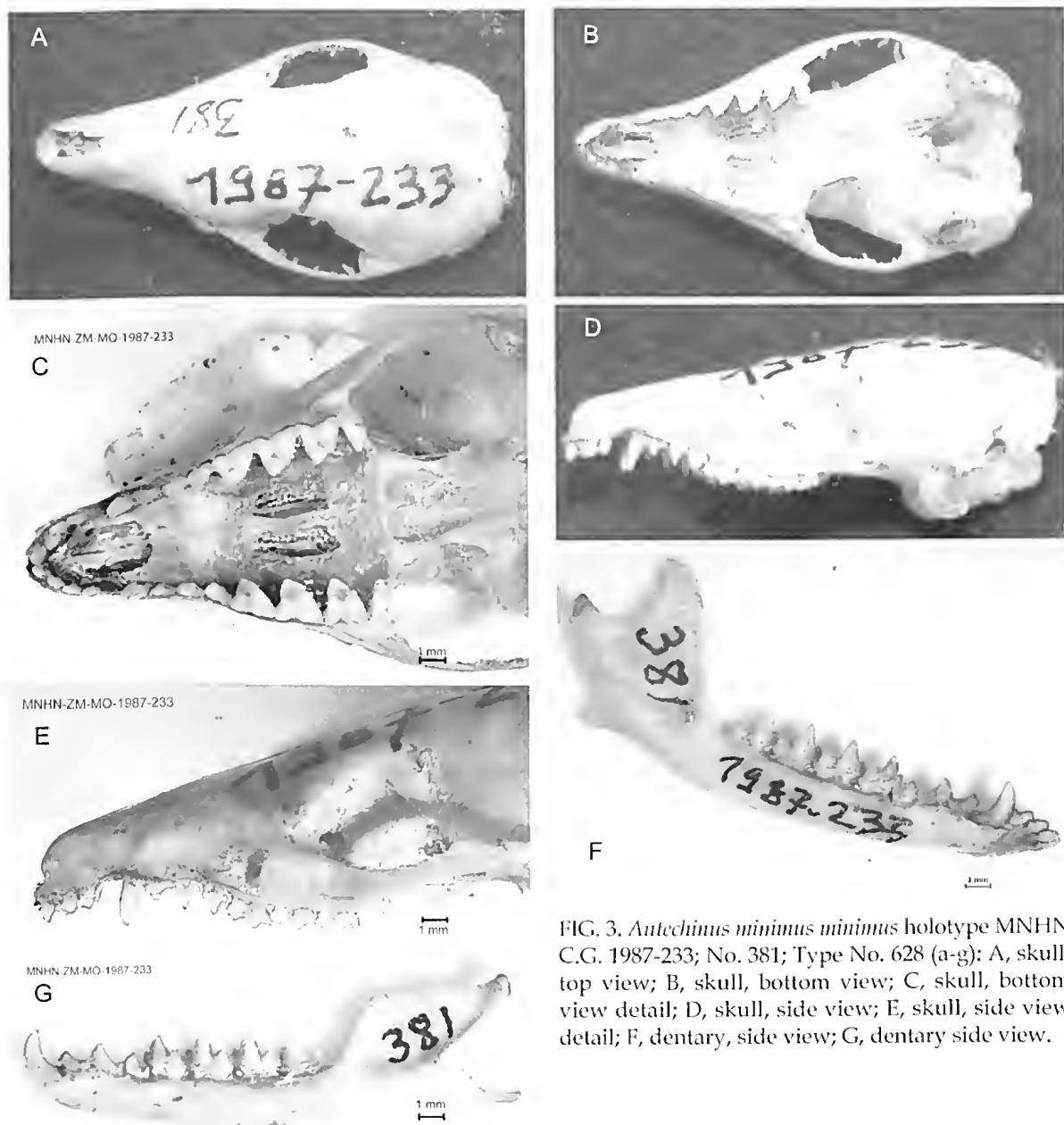


FIG. 3. *Antechinus minimus minimus* holotype MNHN C.G. 1987-233; No. 381; Type No. 628 (a-g): A, skull, top view; B, skull, bottom view; C, skull, bottom view detail; D, skull, side view; E, skull, side view detail; F, dentary, side view; G, dentary side view.

for these comparisons. DFA and CVA were conducted for *A. minimus minimus* and *A. minimus maritimus*, as well as the four species (5 taxa) within the Dusky Antechinus species complex. External body measures, while included in univariate analyses, were excluded from multivariate analyses because of missing data (numerous museum specimens included

only skull material for the registered specimen) - this served to maximise the number of individuals of each species used in any given multivariate analysis. Antechinuses are known to be sexually dimorphic in size (Marlow 1961; Soderquist 1995; Williams & Williams 1982), so sexes were analysed separately for all measured variables.

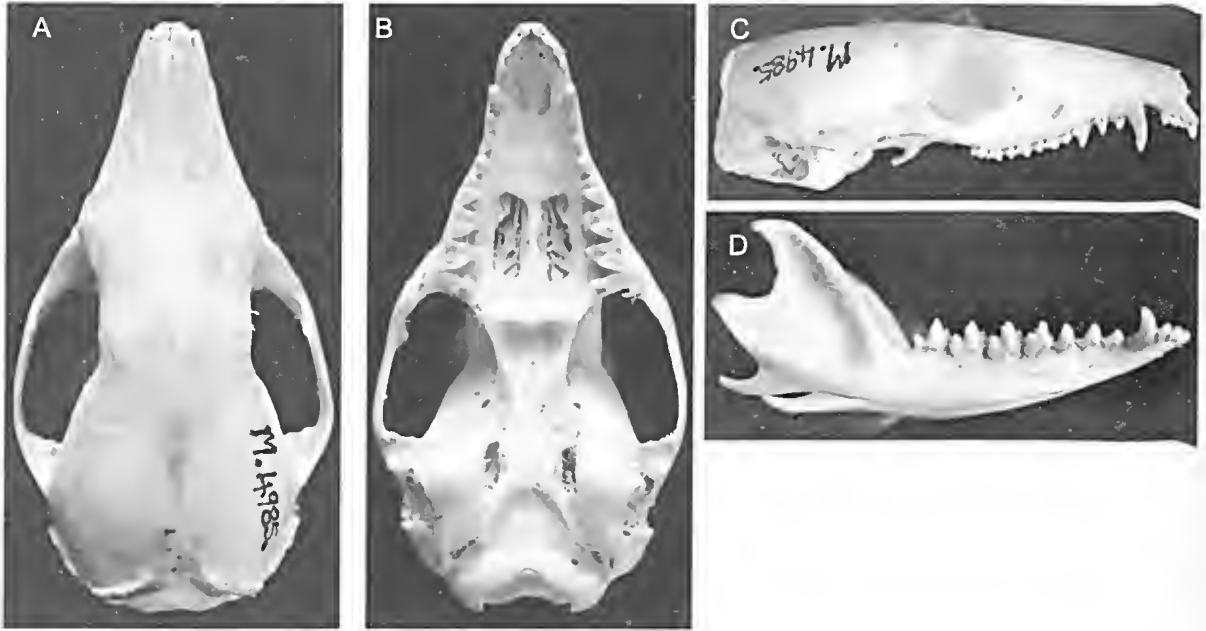


FIG. 4. *Antechinus minimus maritimus* holotype SAM M4985 (a-d): A, skull, top view; B, skull, bottom view; C, skull, side view; D, dentary, side view.

#### Analyses of Genetic Data.

Comprehensive examination of genetic structuring in the genus *Antechinus* is the subject of an ongoing parallel research project and as such will not be presented in detail here. However, for the purpose of postulating DNA-based species groups that were matched with vouchers and subsequently tested with a comprehensive morphological data set, we present the preliminary DNA-based phylogenies for all recognised extant antechinus species, as well as DNA uncorrected percentage divergence ranges between each existing species paired with *A. minimus minimus* (see results). A portion (607 bp) of the mitochondrial Cytochrome B gene (CytB) and a portion (699bp) of the nuclear Interphotoreceptor Binding Protein gene (IRBP) were targeted using primers as described in Mutton (2011). Sequences were aligned by eye using Bioedit Version 7.1.11 (Hall 1999). Bayesian phylogenies (using mtDNA alone and also a concatenated dataset partitioned as mtDNA and nDNA) were reconstructed using MrBayes Version 3.2.1 (Ronquist & Huelsenbeck 2003) under the General Time

Reversible Model of sequence evolution as determined by MrModelTest 2.3 (Nylander, 2004), incorporating invariant sites and a gamma shape distribution of 2; in MrBayes, tree search was run for 10 million generations with a 25% burnin, as recommended by program guidelines. Resulting phylogenies were output in the program Treeview (Page, 1996). A p-distance matrix was output based on aligned sequences in MEGA 6 (Tamura *et al.* 2013) and % divergences calculated by multiplying each value by 100; % divergence ranges incorporating minima and maxima were generated for each putative species pair.

Abbreviations used for Institutions housing specimens examined in this study are as follows: QM – Queensland Museum, Brisbane, Queensland, Australia; QVM – Queen Victoria Museum, Launceston, Tasmania, Australia; MTAS – Tasmanian Museum and Art Gallery, Hobart, Tasmania, Australia; MVIC – Museum Victoria, Melbourne, Victoria, Australia; BMNH – British Museum Natural History, London, England; MNHN – Muséum National D'Histoire

A



B

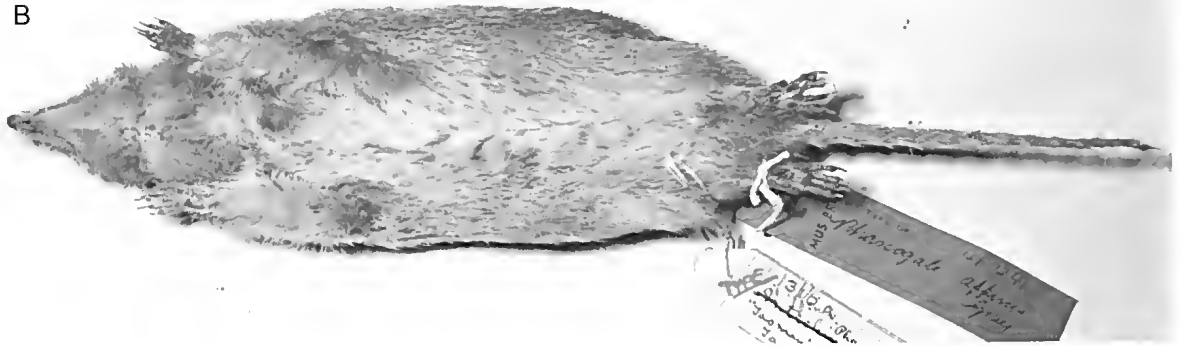


FIG. 5. *Phascogale affinis* syntype study skin BMNH 41.1241 (a-b): A, above; B, below.

Naturelle, Paris, France; SAM - South Australian Museum, Adelaide, Australia.

## RESULTS

We provide below detailed holotype descriptions of *Antechinus minimus minimus* and *A. m. maritimus*, neither of which has been adequately described in the past.

## Systematics

*Antechinus minimus* (É. Geoffroy, 1803)

*Dasyurus minimus* Geoffroy, 1803

*Phascogale affinis* Gray, 1841

**Material examined.** Holotype. MNHN (Muséum National D'Histoire Naturelle, Paris), Catalogue Général No. C.G. 1987-233; Nouveau Catalogue de

la Galerie Zoologie No. 381; Type No. 628 (refer Figs 2-3). Collected by F. Peron.

Adult male, faded ('...the little animal described by Geoffroy has been exposed to the action of light in a museum for upwards of forty years, we cannot but suppose its colouring has changed' Waterhouse, 1846) mount and skull, No. 192A, with basicranium smashed, lower dentary separated at LC<sub>1</sub> and LA ramus missing ('the hinder part of the palate is mutilated', Waterhouse, 1841), and both in poor condition (notwithstanding recent reassurances from the French... 'Montage en bon état sauf yeux absents. Crâne en bon état' [Julien-Laferrrière, 1994: 7]).

**Type Locality.** Waterhouse Island, Bass Strait, Tasmania, c. 40°40'S 148°10'E. Altitude not supplied.

**Rediagnosis.** There are no significant morphological differences between *A. minimus minimus* and *A. minimus maritimus*. However, *A. minimus minimus* differs from *A. minimus maritimus* in having a typically narrower skull at a point level with the molar teeth and often

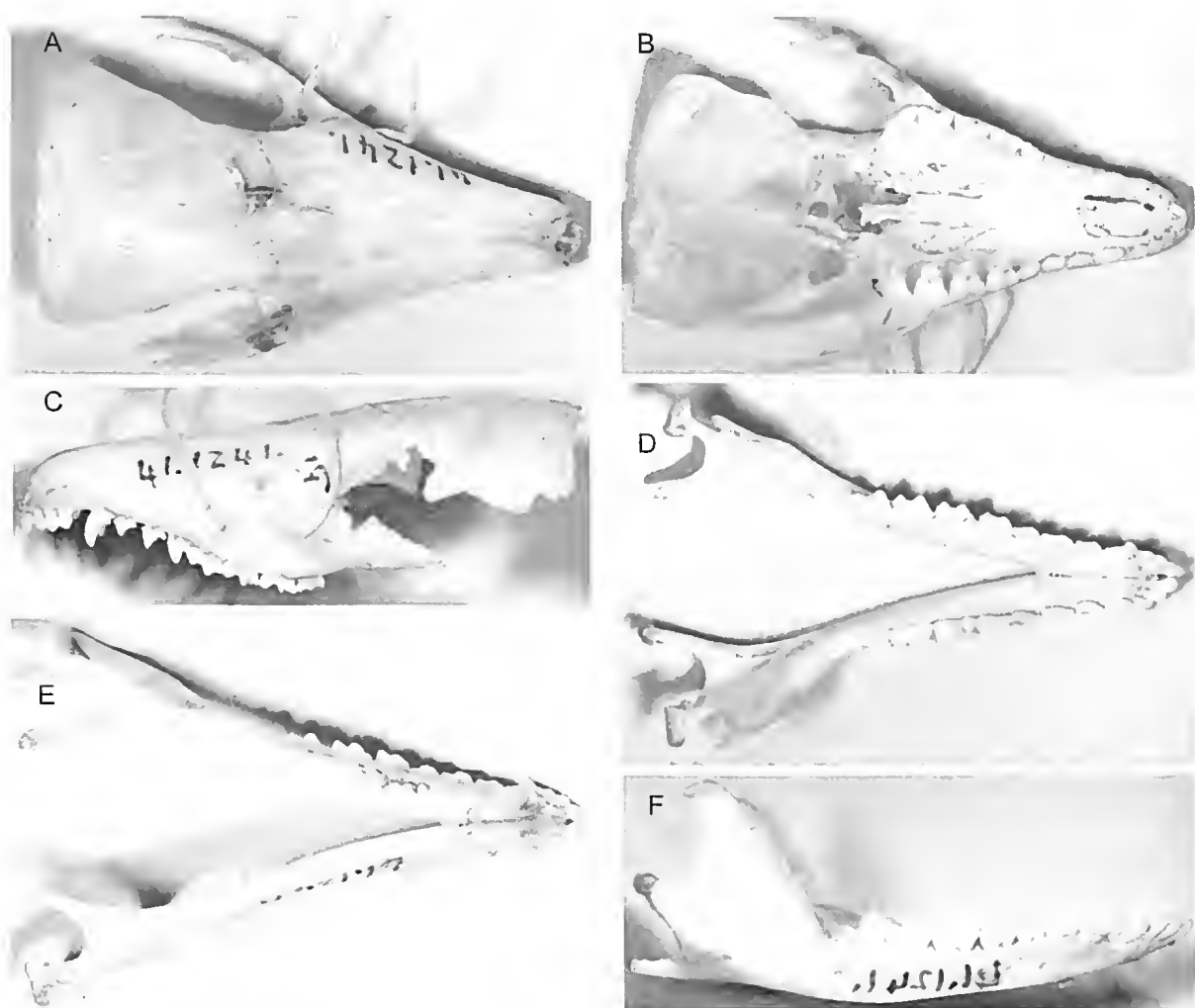


FIG. 6. *Phascogale affinis* syntype BMNH 41.1241 (a-f): A, skull, top view; B, skull, bottom view; C, skull, side view; D, dentary, top view; E, dentary, bottom view; F, dentary, side view.

smaller upper and lower second molar teeth. *Antechinus minimus minimus* also tends to have a longer tail and larger feet than *A. minimus maritimus*. *Antechinus minimus minimus* differs from all members of the Dusky Antechinus complex in having a leaden grey head merging to yellowish (rather than brownish) rump. Also, *A. minimus minimus* tends to have a heavier rump and shorter tail relative to body length compared to all members of the Dusky Antechinus complex. *Antechinus minimus minimus* is easily distinguished from all other antechinus species, being notably

larger, heavier bodied, relatively shorter tailed (compared to head-body length) and smaller-eared; also, the snout is relatively longer/narrower with relatively long anterior palatal vacuities compared to most other antechinus species outside the Dusky Antechinus complex.

**Description.** Holotype. *Pelage*. The skin of the mounted holotype is so faded that a formal pelage description will not be presented here. Nevertheless, the mount shows a definite warming of dorsal fur from head to rump and flanks. The skin of the better preserved *A. affinis* is described in detail under SYNONYMS.



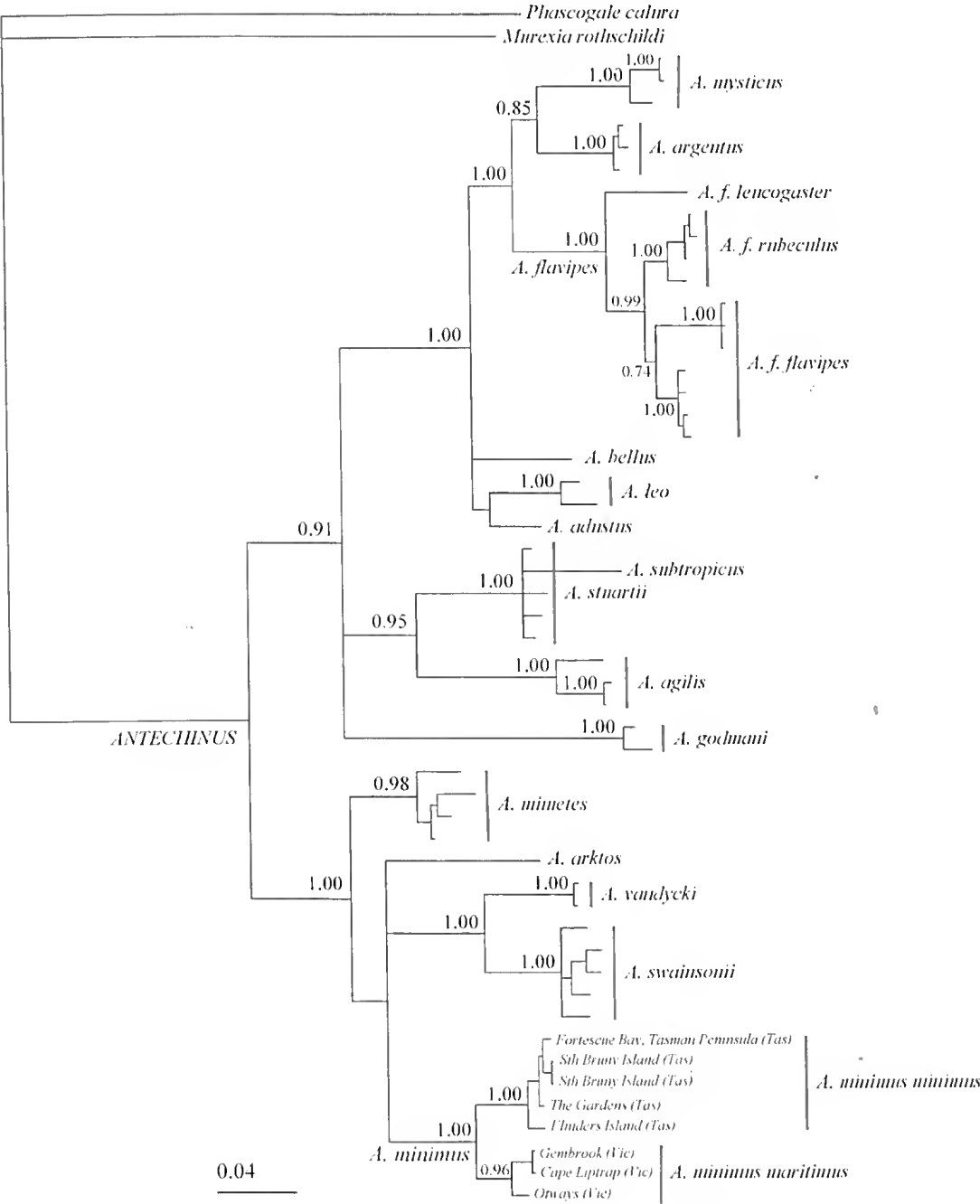


FIG. 7. Bayesian phylogeny of the genus *Antechinus* based on mitochondrial (Cytb) gene sequences. Posterior probabilities are shown at each node (those less than 0.70 are omitted).

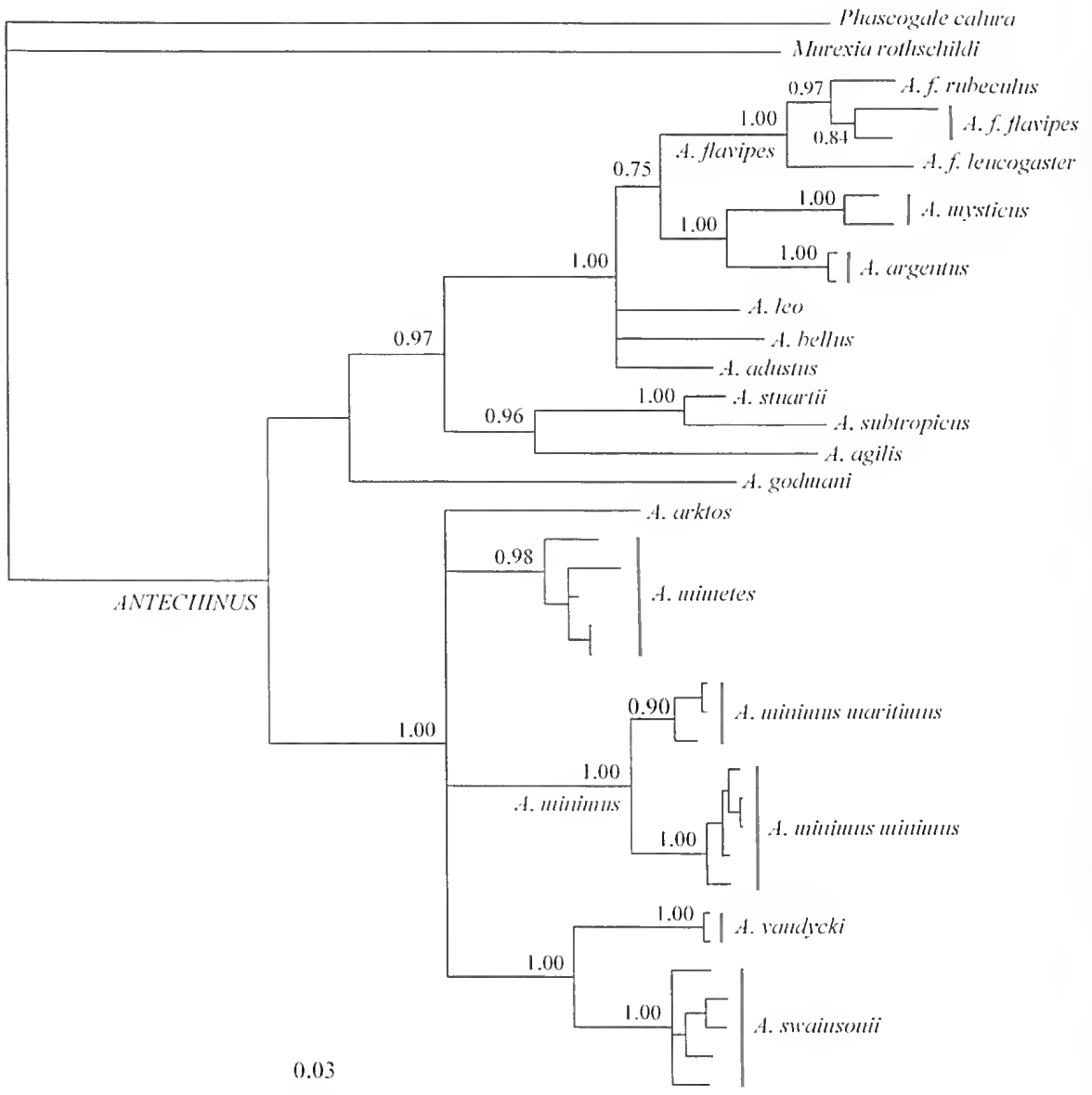


FIG. 8. Bayesian phylogeny of the genus *Antechinus* based on concatenated mitochondrial (Cytb) and nuclear (IRBP) gene sequences. Posterior probabilities are shown at each node (those less than 0.70 are omitted).

**Dentition.** Upper incisors.  $I^1$  is broad, non-procumbent and relatively curved. It is taller-crowned than all other upper incisors. It is not separated from  $I^2$  by a diastema. Left and right  $I^1$  contact each other. For  $I^2$ – $I^4$ , crown height:  $I^4 > I^3 > I^2$ . In crown length,  $I^2$ – $I^4$  are subequal.

All upper incisors have weak buccal cingula.  $I^4$  carries no anterior or posterior cusp. The roots of  $I^4$  are wide.

Upper canines:  $C^1$  is slender and almost straight, with an indistinct boundary between

root and crown. There is no buccal cingulum and no lingual cingulum. Neither an anterior cusp nor posterior cusp is present.

Upper premolars: There are no diastemata between  $C^1$  and  $P^1$ ,  $P^1$  and  $P^2$  or  $P^2$  and  $P^3$ , although there is not quite contact between  $C^1$ - $P^1$ ,  $P^1$ - $P^2$  or  $P^2$ - $P^3$ . All upper premolars carry weak buccal and weak lingual cingula, which are more pronounced at the rear of the tooth. In crown size:  $P^3 > P^2 > P^1$ . Posterior cusps are present in  $P^3$  (very large),  $P^2$  (notably smaller than  $P^3$ ) and  $P^1$  (slightly smaller than  $P^2$ ). Small anterior cusps are present in  $P^1$  and  $P^2$ , but not in  $P^3$ .

Upper molars: The posterior tip of  $P^3$  lies immediately below the prominent stylar cusp A. The anterior cingulum below stylar cusp B appears as a broad flange and is just complete. Stylar cusp B and the paracone are relatively unworn and a minute, worn protoconule is present on the trigon basin. The paracone is approximately half the height of the metacone. Stylar cusp C is just visible on L and  $RM^1$ , but E is a worn rudiment. There is no posterior cingulum on  $M^1$ .

In  $M^2$ , the anterior cingulum appears as a very broad wing which contacts the metastylar corner of  $M^1$  and tapers away quickly, as it progresses down and along the base of the paracone. It finally degenerates mesially to the base of the paracone apex. There is no protoconule.  $M^2$  lacks stylar cusps A and C; E is a worn rudiment. Stylar cusp D is subequal in height to its condition in  $M^1$  but is slightly more sharply peaked. The paracone is about 2.5 times the height of the metacone. There is no posterior cingulum.

In  $M^3$ , the protocone is greatly reduced, the anterior cingulum is narrower and shorter than that in  $M^2$  and it becomes indistinct after covering 1/2 of the distance between stylar cusp B and the base of the paracone; the anterior cingulum degenerates mesially well buccal to the base of the paracone apex. There is no evidence of an anterior cingulum at the base of the paracone, nor is there a protoconule. Stylar cusp D is reduced to a small sharp peak, barely taller than B. Stylar cusp C is low and worn, whereas E is a worn nubbin.

In  $M^4$ , the protocone is very small and narrow, and the metastylar corner is greatly developed. The anterior cingulum is about as broad as that in  $M^3$ , and tapers gradually away from the anterior corner of  $M^4$ , becoming indistinct at a point just labial to the paracone apex. The paracone is large and sharply peaked. The posterior cingulum is absent. In occlusal view, the angle made between the post-protocrista and the post-paracrista is close to  $90^\circ$ .

Lower incisors: In crown height:  $I_1 > I_2 > I_3$ . The incisors project almost horizontally from the tip of the dentary.  $I_1$  and  $I_2$  are oval in anterolateral view and scoop-like in occlusal view.  $I_3$  is premolariform in lateral view with a very large posterior cusp at the base of the crest which descends posteriorly from the apex of the primary cusp; the anterior edge of  $C_1$  rests inside this posterior cusp. In occlusal view, a small notch separates the posterior cusp from the prominent, heavy posterolingual lobe, and crown enamel of the primary and posterior cusps folds lingually such that the crest of the two cusps bisects the tooth longitudinally.

Lower canines:  $C_1$  is caniniform and characterised by strong curvature from root to crown. It possesses strong buccal and lingual cingula and there is no posterior cusp.

Lower premolars: Premolars are roughly equally spaced but  $C_1$  clearly does not contact  $P_1$  and  $P_3$  does not quite contact  $M_1$ . They are well cingulated buccally and lingually and this is particularly prominent towards the rear of the tooth. In crown height:  $P_2 > P_3 > P_1$ . All premolars are narrow and elongate. All possess very strong posterior cusps and  $P_2$  possesses a small anterior cusp. The bulk of each premolar mass is concentrated anterior to the line drawn transversely through the middle of the two premolar roots. Postero-lingual lobes are not a feature of the lower premolars.

Lower molars: All the molars are narrow. The  $M_1$  talonid is wider than the trigonid and the anterior cingulum is present but very poorly developed; it terminates at the posterior base of the protoconid. There is a weak, broken buccal cingulum. The narrow paraconid appears in occlusal view as a small steeply-sided spur,

the lingual edge of which makes a considerable swelling on the endoloph of  $M_1$ . The paracristid is almost  $45^\circ$  to the horizontal from paraconid to paracristid fissure and vertical from the paracristid fissure to the anterior base of the pre-protocristid. The metacristid and hypocristid are both roughly oblique to the long axis of the dentary. The cristid obliqua is long and extends from the hypoconid to the posterior wall of the trigonid, intersecting the trigonid at a point directly below the apex of the protoconid. The hypocristid terminates at the tip of the metastylid. From the metaconid posteriorly, the talonid endoloph follows the line of the dentary until the base of the hypoconulid. The entoconid is low and broadly rounded.

In  $M_2$ , the trigonid is slightly narrower than the talonid. The anterior cingulum is poorly developed, terminating lingually in a weak parastylid notch into which the hypoconulid of  $M^1$  is tucked, and terminating buccally at a point below the protoconid apex. There is a small, incomplete buccal cingulum at the base of the protoconid-hypoconid junction. The strong posterior cingulum extends from the hypoconulid to the posterior base of the hypoconid. The paraconid is well developed but is the smallest trigonid cusp, smaller than the metaconid which is in turn smaller than the protoconid. The entoconid is low and broad, but about twice the height of that in  $M_1$ . The cristid obliqua extends from the hypoconulid to the posterior wall of the trigonid, intersecting the trigonid at a point slightly buccal to the apex of the protoconid but well buccal to the metacristid fissure. The hypocristid extends from slightly anterior and buccal to the hypoconulid to the tip of the hypoconid. From the base of the metaconid posteriorly, the endoloph follows the line of the dentary axis.

In  $M_3$ , the trigonid is as wide as the talonid. A small parastylid wraps around the hypoconulid of  $M_2$  and there is a weak anterior cingulum on  $M_3$ , slightly narrower than that of  $M_2$ . Buccal and posterior cingula are as in  $M_2$  but more poorly developed. The reduced cristid obliqua intersects the trigonid at a point just lingual to the longitudinal vertical midline drawn through the apex of the protoconid, but

slightly buccal to the metacristid fissure. The entoconid on  $M_3$  is long and tall and crushes against the hypoconulid anterior base. The endoloph on the talonid of  $M_3$  takes a more buccal orientation than that seen in  $M_2$ . The rest of  $M_3$  morphology is as in  $M_2$ .

In  $M_4$ , the trigonid is much wider than the talonid. The anterior cingulum is as in  $M_3$ . The posterior cingulum is absent. Of the three main trigonid cusps, the metaconid is marginally taller than the paraconid but both are dwarfed by the almost twice as tall protoconid. The hypoconid of  $M_4$  is absent from the talonid, as is the entoconid. The cristid obliqua forms a low, weak crest which degenerates before contacting the trigonid wall. A significant feature of  $M_4$  morphology is the reduction of talonid crown enamel below the cristid obliqua which results in the talonid appearing (in occlusal view) as a narrow oblique spur jutting off the trigonid wall.

*Skull.* *Antechinus minimus uinius* is characterised by a long, narrow, low rostrum which is tubular in cross section. The rostrum rises gradually along the nasals, then more steeply through the frontals to a high, domed cranium. The nasals are narrow anteriorly and flare very wide posteriorly. In lateral view, there is minimal depression of the rostrum at the junction of the frontals and nasals, and the posterior dorsal surface of the skull is only gently curved across the cranium. The right and left alisphenoid bullae are moderately enlarged and widely separated. The basicranium is smashed behind the alisphenoid bullae. The right foramen pseudovalve appears to have been reasonably small and kidney-shaped. The large premaxillary vacuities extend from the level of the  $I^2$  root back to the level of the anterior root of  $P^1$ . The large maxillary vacuities extend from the level of the anterior of the protocone root of  $M^1$  back as far as the level of the posterior of the protocone root of  $M^3$ .

**Material Examined.** Bridport  $41^\circ 00' S$   $147^\circ 23' E$  (QVM 1987.1.29, QVM 1987.1.82, QVM 1986.1.3, QVM 1986.1.47, QVM 1988.1.84); Brooks Creek (QVM 1981.1.113, QVM 1981.1.102, QVM 1981.1.53, QVM 1981.1.47, QVM 1981.1.68, QVM 1981.1.45, QVM 1981.1.44, QVM 1981.1.101, QVM 1981.1.106, QVM

Swamp Antechinus, *Antechinus minimus* (È. Geoffroy)

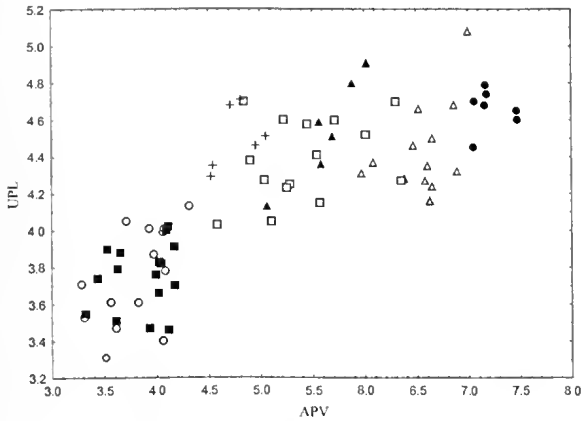


FIG. 9. Scatterplot of anterior palatal vacuity length (APV) versus upper premolar row length (UPL) measures for male *A. minimus minimus* (○), *A. minimus maritimus* (■), *A. swainsonii* (△), *A. vandycki* (●), *A. minetes minetes* (□), *A. minetes insularis* (▲) and *A. arktos* (+).

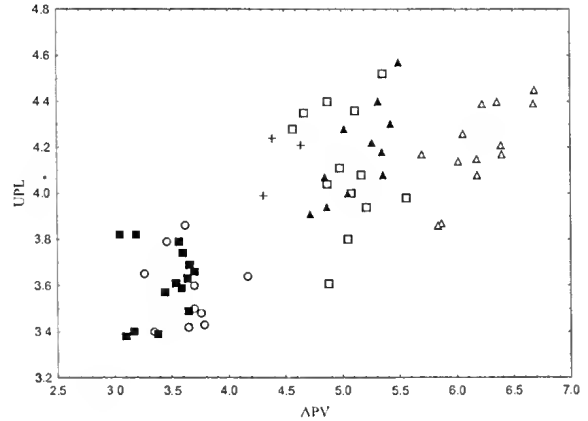


FIG. 10. Scatterplot of anterior palatal vacuity length (APV) versus crown length of upper premolar row (UPL) measures for female *A. minimus minimus* (○), *A. minimus maritimus* (■), *A. swainsonii* (△), *A. vandycki* (●), *A. minetes minetes* (□), *A. minetes insularis* (▲) and *A. arktos* (+).

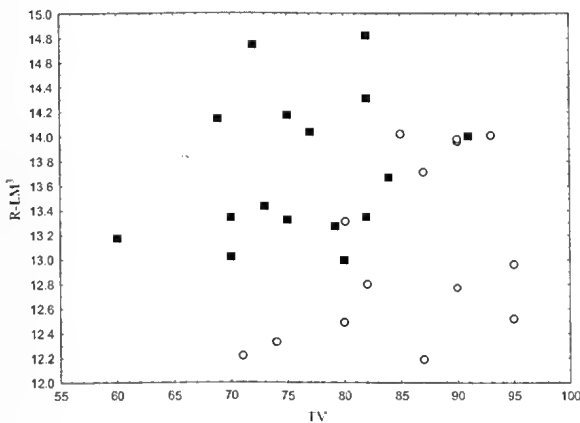


FIG. 11. Scatterplot of tail-vent length (tv) versus skull width level with the junction of the third and fourth upper molars (R-LM³) measures for male *A. minimus minimus* (○), *A. minimus maritimus* (■), *A. swainsonii* (△), *A. vandycki* (●), *A. minetes minetes* (□), *A. minetes insularis* (▲) and *A. arktos* (+).

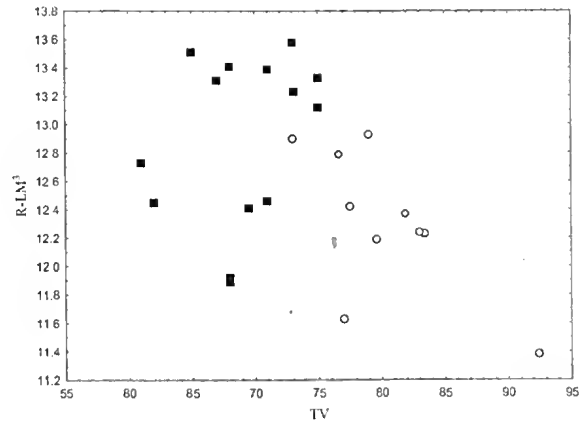


FIG. 12. Scatterplot of tail-vent length (tv) versus skull width level with the junction of the third and fourth upper molars (R-LM³) measures for female *A. minimus minimus* (○), *A. minimus maritimus* (■), *A. swainsonii* (△), *A. vandycki* (●), *A. minetes minetes* (□), *A. minetes insularis* (▲) and *A. arktos* (+).

1981.1.48, QVM 1981.1.105, QVM 1981.1.85); Bruny Island, Tasmania 43°21' S 147°19'E (MTAS A1500); Cockle Creek, Tasmania 43°36' S 146°51'E (QM JM20118); Eriba - Cradle Mt. Rd 41°39' S 145°57'E (QVM 1963.1.70); Flinders Is, Tasmania 40°01'S 148°02'E (MVIC C21965); Fortescue Bay, Tasmania 43°09' S 147°57'E (QM JM20118); Hummock Island, Bass Strait 40°26'S 144°54'E (BMNH 58.12.27.120);

Lake Pedder, Tasmania 42°57'S 146°12'E (MTAS A801, MTAS A802); Maatsuyker Island 43°39' S 146°17'E (MTAS A610, MTAS A611, MTAS A612, MTAS A616, MTAS A617, MTAS A618, MTAS A872; MVIC C216, MVIC C217, MVIC C6337, MVIC C6338, MVIC C6339); Martha Lavinia Beach, King Is 39°39' S 144°04'E (QVM 1986.1.52); Mount Direction, Tasmania 41°15' S 147°01'E (QVM 1988.1.45); Queenstown, Tasmania 42°05' S

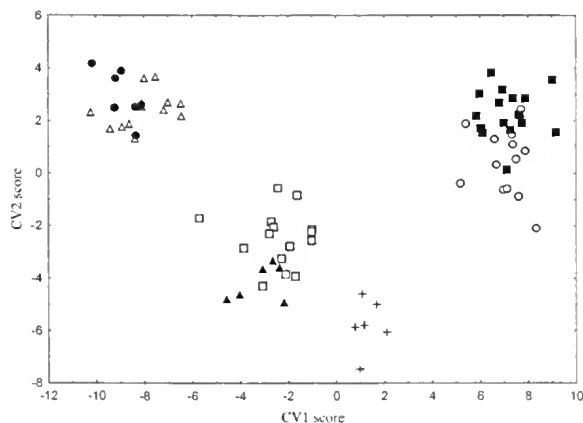


FIG. 13. Scatterplot of canonical variates scores (roots 1 and 2) for male *A. minimus minimus* (○), *A. minimus maritimus* (■), *A. swainsonii* (△), *A. vandycki* (●), *A. mimetes mimetes* (□), *A. mimetes insulanus* (▲) and *A. arktos* (+).

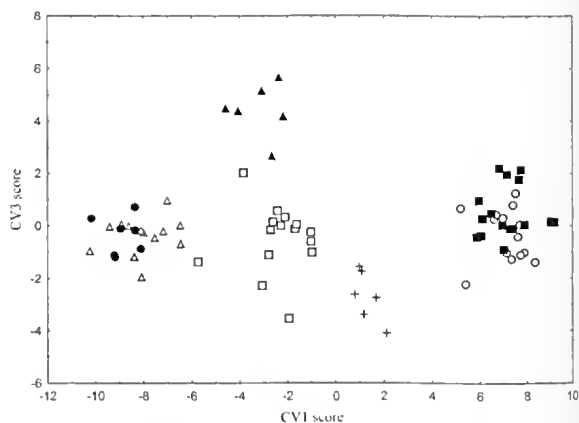


FIG. 14. Scatterplot of canonical variates scores (roots 1 and 3) for male *A. minimus minimus* (○), *A. minimus maritimus* (■), *A. swainsonii* (△), *A. vandycki* (●), *A. mimetes mimetes* (□), *A. mimetes insulanus* (▲) and *A. arktos* (+).

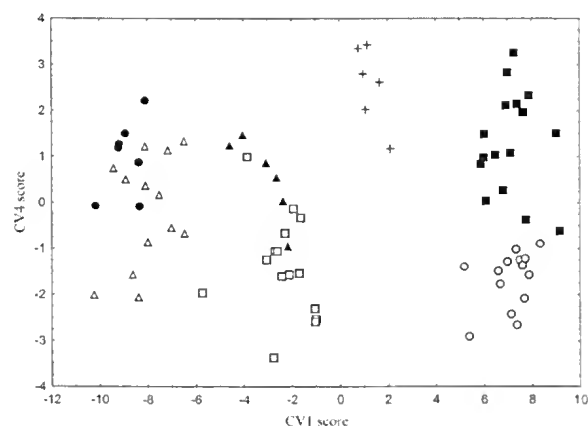


FIG. 15. Scatterplot of canonical variates scores (roots 1 and 4) for male *A. minimus minimus* (○), *A. minimus maritimus* (■), *A. swainsonii* (△), *A. vandycki* (●), *A. mimetes mimetes* (□), *A. mimetes insulanus* (▲) and *A. arktos* (+).

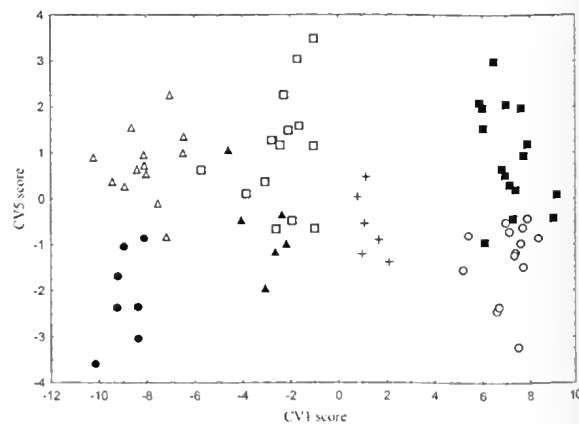


FIG. 16. Scatterplot of canonical variates scores (roots 1 and 5) for male *A. minimus minimus* (○), *A. minimus maritimus* (■), *A. swainsonii* (△), *A. vandycki* (●), *A. mimetes mimetes* (□), *A. mimetes insulanus* (▲) and *A. arktos* (+).

145°33'E (QVM 2014.1.15, QVM 1998.1.1); South Mount Cameron, Tasmania 41°02' S 147°57'E (QVM 1944.1.57); Tasmania (BMNH 52.1.15.7); Turners Marsh 41°16' S 147°08'E (QVM 2007.1.2); Waratah 41°27' S 145°32'E (QVM 1963.1.213, QVM 1963.1.214, QVM 1963.1.134, QVM 1963.1.212, QVM 1963.1.161, QVM 1963.1.162, QVM 1963.1.125, QVM 1963.2.123, QVM 1963.1.163).

#### *Antechinus minimus maritimus* (Finlayson, 1958)

*Phascogale swainsonii maritima*, Finlayson 1958

**Material examined.** Holotype. South Australian Museum, SAM M4985. Adult male in spirit with the skull extracted; both spirit and skull components are in good condition (refer Fig 4). Collected by G.H.Tilley.

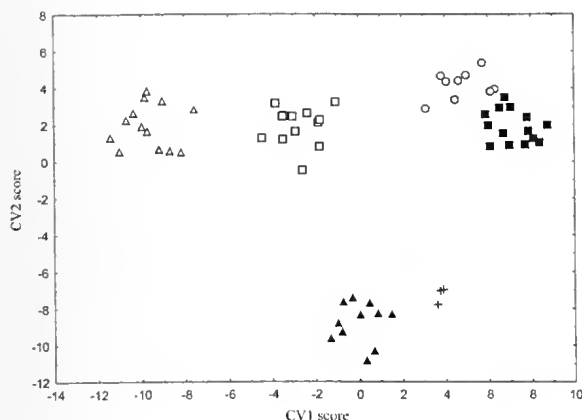


FIG. 17. Scatterplot of canonical variates scores (roots 1 and 2) for female *A. minimus minimus* (○), *A. minimus maritimus* (■), *A. swainsonii* (△), *A. vandycki* (●), *A. mimetes mimetes* (□), *A. mimetes insulanus* (▲) and *A. arktos* (+).

**Type locality.** Port MacDonnell, south-eastern South Australia, 38°03'S 140°42'E at sea level.

**Rediagnosis.** There are no statistically significant morphological differences between *A. minimus maritimus* and *A. minimus minimus*. However, *A. minimus maritimus* differs from *A. minimus minimus* in having a typically broader skull at a point level with the molar teeth and often larger upper and lower second molar teeth. *Antechinus minimus maritimus* also tends to have a shorter tail and smaller feet than *A. minimus minimus*. *Antechinus minimus maritimus* differs from all members of the Dusky Antechinus complex in having a leaden grey head merging to yellowish (rather than brownish) rump. Also, *A. minimus maritimus* tends to have a heavier rump and markedly shorter tail (especially) relative to body length compared to all members of the Dusky Antechinus complex. *Antechinus minimus maritimus* is easily distinguished from all other antechinus species, being typically larger, heavier bodied, relatively shorter tailed (compared to head-body length) and smaller-eared; also, the snout is relatively longer / narrower with relatively long anterior palatal vacuities compared to most other antechinus species outside the Dusky Antechinus complex.

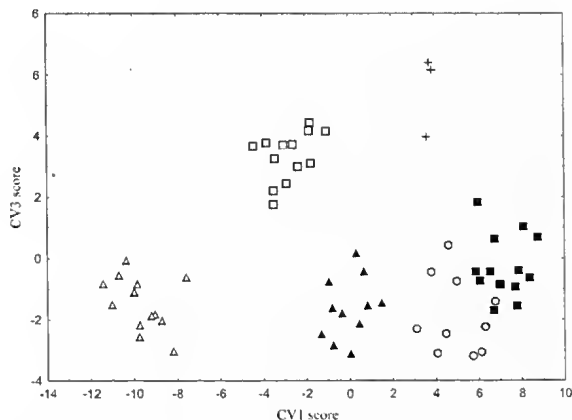


FIG. 18. Scatterplot of canonical variates scores (roots 1 and 3) for female *A. minimus minimus* (○), *A. minimus maritimus* (■), *A. swainsonii* (△), *A. vandycki* (●), *A. mimetes mimetes* (□), *A. mimetes insulanus* (▲) and *A. arktos* (+).

**Description of Holotype.** Pelage. We have not examined the alcoholic body of this holotype, but a detailed description is provided by Finlayson (1958) who described it thus, 'the head, nape and shoulders a cold, grizzled grey increasingly suffused posteriorly with rufous which may become very rich over the rump... Ventrums a uniform greyish white, but variably and sometimes strongly washed with yellow or buff and deep plumbeous for the basal two thirds.' (p. 149)

**Dentition.** I<sup>1</sup> contacts I<sup>2</sup>. In crown height: I<sup>2</sup>>I<sup>3</sup>>I<sup>4</sup>. I<sup>4</sup> carries no anterior or posterior cusp. C<sup>1</sup> has no posterior cusp. In the upper premolars, slight diastemata occur between C<sup>1</sup>-P<sup>1</sup>, P<sup>1</sup>-P<sup>2</sup> and P<sup>2</sup>-P<sup>3</sup>. The gap separating P<sup>1</sup> and P<sup>2</sup> is greater than that separating P<sup>2</sup> and P<sup>3</sup> and greater than that separating C<sup>1</sup> and P<sup>1</sup>. In M<sup>4</sup>, the angle made between post-protocrista and post-paracrista is close to 135°. Lower premolars with P<sub>1</sub> just contacting P<sub>2</sub> and P<sub>3</sub> is in contact with M<sub>1</sub>. The rest of the craniodental features are as for the holotype of *A. minimus minimus* described above.

**Skull.** The left and right alisphenoid tympanic bullae are very widely separated. The foramen pseudovale is large, as is the eustachian canal opening. The internal jugular canal foramina are moderately large and the canals are only poorly raised and non-prominent. The posterior lacerate foramina are small, while the

entocarotid foramina are large. The maxillary vacuities extend from the level of the M<sup>1</sup> protocone root back as far as the level of the M<sup>3</sup> metacone root. The larger left premaxillary vacuity extends from the level of the I<sup>2</sup> root back to the level of the posterior edge of C<sup>1</sup>; the smaller right premaxillary vacuity terminates at the level of the middle of the C<sub>1</sub> root.

**Material examined.** Anglesea 38°25'S 144°11'E (MVIC C26888, C27051, C27042, C27044, C27045, C27039, C27050, C27062, C27064, C27065, C27048, C26986, C29803); Birnam Otways, Victoria 38°27'S 143°35'E (MVIC C26485); Bridgewater Lakes 38°19'S 141°24'E (MVIC C13820, MVIC C13863, MVIC C15878); Buck's Lake, South Australia 37°55'S 140°24'E (SAM M11464); Cape Liptrap, Victoria 38°54'S 145°56'E (MVIC C31198); Carpenter Rocks, South Australia 37°54'S 140°23'E (SAM M11978, SAM M12996); Casterton 37°36'S 141°24'E (MVIC C27030, C27043, C27031, C27041); Dartmoor 37°55'S 141°16'E (MVIC C24345, MVIC C24347, MVIC C26889, MVIC C27047, MVIC C27049); Greater Glennie Island 39°05'S 146°15'E (MVIC C13830, C13829, C13822); Hut Gully, Victoria (MVIC C13818, C13819, C22156); Kennett River Foreshore, Otways, Victoria 38°40'S 143°51'E (MVIC C11619); Kilcun, 2 km west (MV C13447); Kongorong 37°54'S 140°33'E (SAM M10052); Millicent, South Australia 37°35'S 140°21'E (SAM M22405); Moonlight Head 38°46'S 143°14'E (MVIC C13826); Mount Roundback, Victoria 38°52'S 146°26'E (MVIC C17100); Otways, Victoria 38°27'S 143°58'E (MVIC C11619); Parker River Inlet 38°50'S 143°33'E (SAM M4985); near Point Danger, Portland, Victoria 38°21'S 144°20'E (MVIC C23475); Port Campbell NP, Victoria 38°37'S 143°00'E (MVIC C22199); Port MacDonnell 38°03'S 140°42'E (SAM M4985); Snake Island, Victoria 38°45'S 146°34'E (MVIC C26018); Southend, South Australia 37°34'S 140°08'E (SAM M10930); Tucker Orchard, Victoria 38°34'S 143°29'E (MVIC C26831); Upper Yarra, Victoria 37°42'S 145°50'E (MVIC C6351); Venus Bay, Victoria 38°40'S 145°47'E (MVIC C36842); Yanakie 38°49'S 146°13'E (MVIC C25817).

## SYNONYMS

The status of *Phascogale affinis* Gray, 1841

**Syntypes.** BMNH 41.1241, puppet skin and skull (skin in good condition, skull broken and basicranium missing) (refer Figs 5-6). Collected by J. Gould.

**Type Locality.** Tasman Peninsula, Tasmania. Altitude not supplied.

**Description.** Holotype BMNH 41.1241 differs from *Antechinus minimus minimus* in the following respects:

**Pelage.** The fur of the mid-back is 13 mm long with the basal 10 mm Slate Colour, median 2 mm Buckthorn Brown and the apical 1 mm black. The back appears overall to be a speckled Olive Brown. Medially-thickened guard hairs are interspersed thickly through the fur and are 15 mm long on the rump and reduce to 6 mm where they terminate at the crown of the head. Fur on and below the shoulders, thighs flanks and chin lacks the black tips or coarse guard hairs and these areas and the belly appear as Old Gold. There is no head stripe and no eye-ring. The soft ventral fur (10 mm long on the belly) is Mouse Gray on the basal 2/3 and Naples Yellow on the apical 1/3 and is interspersed by Naples Yellow medially-thickened spines 13 mm long. The belly is thus an overall Old Gold. Forefeet and thinly covered with Olive Brown hairs. Hindfeet are more thickly covered with lighter Buffy Brown coloured hairs. The tail is weakly bicoloured with hairs averaging 3 mm along its length and increasing 4 mm at its tip. Dorsally the hairs are a uniform Olive Brown with Fuscous Black tips. Ventrally, the black tips are lost and the overall colour is Buffy Brown.

**Vibrissae.** Approximately 16 mystacial vibrissae occur on each side of the face; they are, however, twisted and broken off, and are a maximum length of 11 mm. Supra-orbital vibrissae could not be located; genals (Fuscous Black and Colourless) number 3 (left) and 4 (right); ulna-carpals (colourless) number 3 on the right (left vibrissae could not be found). No submentals could be found.

**Tail.** The tail is slightly shorter than the nose-vent length. It is thin and tapers toward the tip.

**Hindfoot.** The claws are long. The apical granule of the hindfoot is elongated, enlarged and striate. The enlarged hallucal pad is just separate from the post-hallucal pad. Metatarsal granules are not visible in the holotype.



**Ears.** The ears are small and the supratragus appears to be simple and flat.

**Dentition.**  $I^1$  is separated from  $I^2$  by a slight diastema. In crown height:  $I^2 > I^3 > I^4$ .  $I^4$  carries no anterior or posterior cusp.  $C^1$  has a large posterior cusp. In the upper premolars, diastemata occur between  $C^1$ - $P^1$ ,  $P^1$ - $P^2$ ,  $P^2$ - $P^3$ . The gap separating  $P^1$  and  $P^2$  is greater than that separating  $P^2$  and  $P^3$  is greater than that separating  $C^1$  and  $P^1$ . In the upper molars, stylar cusp B is very large in  $M^1$  which also lacks a posterior cingulum. In  $M^2$ , stylar cusp B is again very large. Stylar cusp C is present and D is reduced in comparison to  $M^1$  but is still very large. In  $M^3$ , the anterior cingulum is as large as it is in  $M^2$  and it becomes indistinct after covering 1/2 the distance between stylar cups B and the base of the paracone. In  $M^4$ , the angle made between post-protocrista and post-paracrista is close to  $90^\circ$ . Lower premolars are equally spaced with  $P_3$  in contact with  $M_1$ . In  $M_3$ , the entoconid is seen to crush against the hypoconulid and in  $M_4$  a small entoconid is present. A tall hypoconid is also present and the cristid obliqua intersects the trigonid wall well lingual to the metacrista fissure. There is no hypoconulid.

**Skull.** The entire basicranium is smashed and missing posterior from the maxillary vacuities. The premaxillary vacuities extend from the level of the  $I^2$  root back to the level of the middle of  $P^1$ . The larger maxillary vacuities extend from the level of the protocone root of  $M^1$ , but are open-ended posteriorly with the missing basicranium.

**Note.** When Gray (1841) described *Phascogale affinis* (the description is a catalogue listing), he and Gould (from whom he obtained the specimen) and, perhaps more reluctantly, Waterhouse (at least by 1841), considered *A. minimus* and *A. swainsonii* synonymous (see Gray, 1841: 401). Of his *P. affinis*, Gray (1841) maintained 'This may be the same *P. minima* of Geoffroy, but the tail is longer for its size' (p. 407). Gray lists two specimens collected (nominations of holotypes was not practised at that stage), a male and a female; however, BMNH 1841.1241 is the only specimen of the pair now represented

in the research collection of the British Museum (Natural History) ('one of two syntypes, location of other specimen unknown', Jenkins & Knutson, 1983). The sex of the remaining specimen is not identified on attached labels, nor is it immediately apparent from the skin. Our interest in the sex of the holotype centres on a possibility that the missing syntype may have been an example of *A. swainsonii* or *A. vandycki* and not *A. minimus*. Measurements provided by Gray for the female (HB: 4.5" [114 mm]; T: 2.75" [70 mm]) sit comfortably within the range of measurements from females available today (taking into account that for head-body/tail lengths, the 'root' of the tail was where head-body and tail measurements ended, not the 'vent'); for total length in female *A. minimus*  $\bar{x}$  = 178.83, R = 165 - 203, N = 12 (data from Green, 1972),  $\bar{x}$  = 175.4, R = 165 - 182, N = 5 (our research), for total length in males  $\bar{x}$  = 195.5, R = 174 - 230, N = 10 (data from Green, 1972),  $\bar{x}$  = 190.2, R = 174 - 204 (N = 5, our research). However, data provided for the male type specimen (HB: 6.5" [165 mm]; T: 4.5" [114 mm]) describes an extraordinarily large animal (total length 279 mm), well outside the maximum values available from our research (226 mm, MV C13826 from Moonlight Head Victoria), or from Green (1972), whose maximum value (230 mm) exceeded that provided by Wakefield and Warneke (1963). Indeed, so large is the animal described by Gray (1841), that it falls just outside those values available for the maximum total length of males of the much larger *A. swainsonii* (253 mm, N = 8, Green [1972]). The short tail length, for which *P. affinis* was named (4.5" [114 mm]) is 43 mm longer than the longest 'Tasmanian' record available to us for a male specimen of *A. minimus* (MTAS A1404, adult male, TV = 71 mm, Cockle Creek) and 14 mm longer than the longest record available to Wakefield and Warneke (1963) (TV = 100 mm, registration and provenance details unavailable). The length, however, is compatible with the upper limit of values available for males of *A. swainsonii*. Having obtained the specimens from Gould, it is not unreasonable to suggest the published values could have represented field measurements, particularly as neither of Gray's published

measurements (total length for male = 11" [279 mm]; female = 7.25" [184 mm]) correspond with the total length of the study skin BMNH 41.1241 = 237 mm).

Sexual dimorphism for body size (reflected through cranial and dental morphology) is at its most insignificant in this species (compared with e.g., *A. godmani*). The sex of BMNH 1841.1241, therefore, could not be established on these grounds. If the puppet skin of BMNH 1841.1241, which shows no evidence of a scrotum, is in fact the female referred to by Gray (1841), then the preparation of the skin has resulted in the addition of 33 mm to the overall length. If, on the other hand, BMNH 1841.1241 is the male, with scrotum removed, preparation must account for shrinkage of approximately 53 mm.

Gray noted that the male was darker. This could further implicate an example of *A. swainsonii* as Green (1972) found no sexual dimorphism for pelage colour in *A. minimus*; however, ranges in depth of pelage colour from 1 to 3 (where 5 represents almost black pelage, 1 represents light fawn-brown) have been recorded (Van Dyck, S. pers. obs.) from individuals collected at a particular locality (e.g., Brooks Ck) in Tasmania.

Given that *A. affinis* was described for the relatively short length of its tail, and taking into account the other factors mentioned above, we suggest that one of Gray's syntypes was an example of *A. minimus* and the other, an example of *A. swainsonii*; the surviving syntype, BMNH 1841.1241, is most likely the (slightly stretched) *A. minimus* female.

*Antechinus concinnus* Higgins and Petterd  
(1883) *incertae sedis*

The sex and locality of this specimen in Tasmania is unknown; no registration number; formerly in the collection of the Royal Society of Tasmania; holotype lost. This novelty has, in the past, been assigned to the synonymy of *A. minimus* (Thomas, 1888; Iredale & Troughton, 1934; Tate, 1947; Wakefield & Warneke, 1963; Mahoney & Ride, 1988, who corrected the publication date from 1884 to 1883) probably

on the authority of Thomas (1888) who may not have even examined the specimen. The animal is small (total length = 203.6 mm) and could pass for a young *A. swainsonii* or an adult *A. minimus*. Green (1972) used the change in dorsum pelage colour from dark brownish grey to rich tan over the rump, flanks and round the base of the tail to distinguish adult *A. minimus* from *A. swainsonii*. If the holotype was an adult *A. minimus*, however, Higgins and Petterd make no mention of a warming change in dorsal pelage colour, although they describe the fur as 'brownish-grey on the upper surface'. Considering all the above, we consider this form to be *incertae sedis*.

## SPECIES BY SPECIES COMPARISONS

All tests for normality and variance homogeneity of samples used in morphometric analyses were non-significant at  $p=0.05$ .

### Phylogenetic Structure

Figures 7-8 suggest that there are 15 putative species within antechinus. The phylogenies show the four species comprising the Dusky Antechinus complex and *A. minimus* clade is well-supported and deeply divergent compared with all congeners. Each of the four species of Dusky Antechinus and *A. minimus* are strongly supported and monophyletic with respect to each other; however, species-level sister relationships between these taxa are unclear with the exception of the well-supported sister Dusky Antechinus from Tasmania, *A. swainsonii* and *A. vandycki* (Figs 7-8). Within *A. minimus*, *A. minimus minimus* (Tasmania) and *A. minimus maritimus* (mainland) are strongly-supported (0.9-1.0 posterior probabilities) and reciprocally monophyletic; there is moderate genetic divergence within each subspecies.

Figure. 7 is a phylogeny generated from mitochondrial (Cytochrome B - CytB) data and Fig. 8 combines the data from one mitochondrial gene (Cytochrome B - CytB) and one nuclear gene (Interphotoreceptor Binding Protein - IRBP); both phylogenies accord in their structuring of putative species clades which, once matched with morphological vouchers, then form the

Swamp Antechinus, *Antechinus minimus* (È. Geoffroy)

TABLE 1. Univariate statistics: means, standard deviations and range minima and maxima of measured variables for *Antechinus minimus minimus*.

MALES						FEMALES					
	Valid N	Mean	Min	Max	St. Dev.		Valid N	Mean	Min	Max	St. Dev.
wt	13	74.38	37.00	118.00	30.05	wt	7	38.43	24.00	58.00	11.93
hb	13	130.68	114.00	155.00	14.66	hb	13	112.64	103.00	132.00	8.56
tv	13	85.31	71.00	95.00	7.61	tv	13	78.19	68.00	92.40	6.33
hf	14	19.98	18.00	22.50	1.33	hf	12	18.41	17.00	20.56	1.28
e	14	14.94	13.00	19.00	1.61	e	13	14.05	12.78	15.00	0.59
APV	14	3.81	3.28	4.31	0.31	APV	10	3.65	3.26	4.17	0.26
BL	14	28.71	26.32	31.46	1.56	BL	10	26.27	24.93	27.60	0.94
Dent	14	23.16	21.54	25.04	1.12	Dent	10	21.07	19.92	22.34	0.76
IBW	14	4.63	4.13	5.08	0.29	IBW	10	4.37	4.02	4.82	0.25
IOW	14	7.78	7.36	8.27	0.27	IOW	10	7.45	7.11	7.76	0.21
IPV	14	4.05	3.37	4.59	0.39	IPV	10	3.42	3.08	3.90	0.27
M <sup>2</sup> W	14	2.27	2.13	2.40	0.07	M <sup>2</sup> W	10	2.16	2.08	2.20	0.04
NW	14	2.75	2.39	3.18	0.23	NW	10	2.70	2.33	2.93	0.16
OBW	14	12.32	11.42	12.91	0.44	OBW	10	11.52	11.14	12.22	0.31
PPV	14	5.04	4.00	6.05	0.54	PPV	10	4.77	4.45	5.14	0.28
R-LC <sup>1</sup>	14	5.18	4.80	5.60	0.26	R-LC <sup>1</sup>	10	4.67	4.30	5.14	0.26
R-LM <sup>1</sup>	14	9.10	8.51	9.66	0.42	R-LM <sup>1</sup>	10	8.65	8.12	9.07	0.30
R-LM <sup>1</sup> T	14	7.82	7.45	8.52	0.37	R-LM <sup>1</sup> T	10	7.37	7.01	7.68	0.22
R-LM <sup>2</sup>	14	10.85	10.02	11.90	0.69	R-LM <sup>2</sup>	10	10.33	9.49	10.83	0.46
R-LM <sup>3</sup>	14	13.09	12.19	14.02	0.72	R-LM <sup>3</sup>	10	12.31	11.38	12.93	0.51
ZW	14	16.95	15.66	18.74	1.01	ZW	10	15.32	14.44	15.94	0.57
HT	14	10.66	9.87	11.34	0.49	HT	10	10.13	9.83	10.55	0.21
PL	14	16.52	15.63	17.77	0.66	PL	10	15.20	14.61	16.00	0.49
SWR-LC <sup>1</sup> B	14	4.54	4.20	4.85	0.22	SWR-LC <sup>1</sup> B	10	4.07	3.80	4.48	0.20
TC	14	2.92	2.67	3.21	0.18	TC	10	2.69	2.52	2.89	0.12
NWR	14	4.66	4.13	5.32	0.35	NWR	10	4.32	3.89	4.80	0.35
PML	14	8.79	7.72	9.53	0.55	PML	10	7.92	7.66	8.52	0.26
UML	14	6.48	6.11	6.89	0.26	UML	10	6.21	5.95	6.51	0.20
HT-B	14	8.52	8.01	9.11	0.38	HT-B	10	8.06	7.59	8.59	0.31
BuL	14	4.17	3.86	4.37	0.14	BuL	10	3.84	3.49	4.03	0.16
I <sup>1</sup> -P <sup>3</sup>	14	9.03	8.34	9.72	0.43	I <sup>1</sup> -P <sup>3</sup>	10	8.30	7.99	8.65	0.23
LML	14	6.96	6.60	7.41	0.24	LML	10	6.73	6.48	7.08	0.21
I <sub>1</sub> -P <sub>3</sub>	14	7.26	6.83	7.65	0.29	I <sub>1</sub> -P <sub>3</sub>	10	6.56	6.17	7.10	0.27
M <sub>2</sub> W	14	2.06	1.98	2.16	0.06	M <sub>2</sub> W	10	2.02	1.90	2.10	0.06
UPL	14	3.75	3.31	4.13	0.27	UPL	10	3.58	3.40	3.86	0.16

basis for testing individual assignment based on craniodental variation in subsequent multivariate analyses. Although the majority of the phylogenetic signal is generated from the mtDNA data, the nuclear gene corroborates the interspecific mitochondrial clade structure.

Bivariate Scatterplots

A range of scatterplots are shown for dental variables differentiating *A. minimus* from the four species (five taxa) of Dusky Antechinus. Figs 9-10 show differences among these taxa for

TABLE 2. Univariate statistics: means, standard deviations and range minima and maxima of measured variables for *Antechinus minimus maritimus*.

MALES						FEMALES					
	Valid N	Mean	Min	Max	St. Dev.		Valid N	Mean	Min	Max	St. Dev.
wt	6	62.27	42.00	91.00	18.33	wt	5	44.20	35.00	60.00	9.68
hb	11	123.49	99.98	148.00	15.18	hb	8	108.94	91.00	123.00	10.53
tv	11	77.09	60.00	97.93	9.87	tv	8	70.20	62.00	75.00	4.35
hf	11	18.57	17.20	20.00	0.79	hf	7	17.33	16.00	18.20	0.78
e	10	15.03	13.10	17.00	1.15	e	6	14.80	14.01	16.00	0.80
APV	16	3.87	3.32	4.17	0.28	APV	14	3.45	3.05	3.70	0.23
BL	16	28.77	27.14	32.25	1.42	BL	14	26.82	24.52	28.11	0.94
Dent	16	23.19	21.80	26.00	1.09	Dent	14	21.47	19.97	22.34	0.63
IBW	16	4.49	3.99	5.09	0.30	IBW	14	4.31	3.84	4.62	0.23
IOW	16	7.47	7.07	7.98	0.25	IOW	14	7.34	6.88	7.71	0.25
IPV	16	3.91	3.52	4.64	0.32	IPV	14	3.77	3.28	4.52	0.38
M <sup>2</sup> W	16	2.29	2.16	2.50	0.08	M <sup>2</sup> W	14	2.27	2.16	2.45	0.09
NW	16	2.73	2.32	3.25	0.24	NW	14	2.61	2.36	2.85	0.16
OBW	16	12.31	11.82	13.76	0.52	OBW	14	11.70	11.22	12.04	0.29
PPV	16	5.13	4.04	6.02	0.50	PPV	14	4.92	4.46	5.25	0.21
R-LC <sup>1</sup>	16	5.27	4.86	5.81	0.31	R-LC <sup>1</sup>	14	4.77	4.43	5.00	0.19
R-LM <sup>1</sup>	16	9.42	8.94	10.11	0.35	R-LM <sup>1</sup>	14	8.80	8.45	9.09	0.22
R-LM <sup>1</sup> T	16	8.05	7.59	8.49	0.26	R-LM <sup>1</sup> T	14	7.65	6.97	8.08	0.29
R-LM <sup>2</sup>	16	11.45	10.65	12.59	0.59	R-LM <sup>2</sup>	14	10.82	9.94	11.44	0.47
R-LM <sup>3</sup>	16	13.74	12.99	14.82	0.59	R-LM <sup>3</sup>	14	12.91	11.89	13.58	0.59
ZW	16	17.00	15.73	19.23	1.08	ZW	14	15.72	14.40	16.73	0.61
HT	16	10.61	9.71	11.70	0.53	HT	14	10.20	9.60	10.78	0.30
PL	16	16.43	15.48	18.26	0.76	PL	14	15.47	14.51	16.20	0.55
SWR-LC <sup>1</sup> B	16	4.69	4.16	5.13	0.27	SWR-LC <sup>1</sup> B	14	4.23	3.84	4.49	0.20
TC	16	2.75	2.48	3.10	0.15	TC	14	2.63	2.45	2.83	0.13
NWR	16	4.58	3.59	5.34	0.48	NWR	14	4.34	3.88	4.84	0.32
PML	16	9.20	8.63	10.01	0.38	PML	14	8.36	7.85	8.85	0.32
UML	16	6.50	6.34	6.72	0.12	UML	14	6.38	6.18	6.67	0.16
HT-B	16	8.42	7.69	9.23	0.43	HT-B	14	8.10	7.63	8.47	0.23
BuL	16	4.17	3.73	4.66	0.21	BuL	14	4.04	3.79	4.29	0.17
I <sup>1</sup> -P <sup>3</sup>	16	9.02	8.29	9.87	0.38	I <sup>1</sup> -P <sup>3</sup>	14	8.50	7.82	8.89	0.28
LML	16	7.08	6.67	7.35	0.19	LML	14	7.02	6.74	7.33	0.21
I <sub>1</sub> -P <sub>3</sub>	16	7.17	6.60	7.90	0.30	I <sub>1</sub> -P <sub>3</sub>	14	6.76	6.15	7.16	0.29
M <sub>2</sub> W	16	2.10	2.00	2.19	0.07	M <sub>2</sub> W	14	2.08	2.00	2.19	0.06
UPL	16	3.75	3.46	4.02	0.18	UPL	14	3.61	3.38	3.82	0.15

the most discriminating dental characters: APV and UPL, for males and females, respectively. There is no overlap in APV between *A. minimus* and the four species in the Dusky Antechinus complex, with *A. minimus* having smaller anterior

palatal vacuities; within the Dusky Antechinus complex, larger vacuities tend to be a feature of higher latitude species, with smaller holes and larger gaps as one moves into lower latitudes. *Antechinus vandycki* from Tasman Peninsula, for

Swamp Antechinus, *Antechinus minimus* (È. Geoffroy)

TABLE 3. Univariate statistics: means, standard deviations and range minima and maxima of measured variables for *Antechinus swainsonii*.

MALES						FEMALES					
	Valid N	Mean	Min	Max	St. Dev.		Valid N	Mean	Min	Max	St. Dev.
wt	11	63.16	42.30	93.00	14.53	wt	15	41.59	31.00	57.00	7.36
hb	12	133.61	111.30	161.00	13.06	hb	16	116.70	103.19	127.00	8.69
tv	12	97.90	89.00	110.00	6.53	tv	16	87.75	77.00	101.42	6.13
hf	12	21.84	20.00	24.00	1.27	hf	15	19.30	18.00	21.00	0.81
e	12	16.86	15.01	21.00	1.47	e	14	15.28	14.50	16.00	0.54
APV	13	6.56	5.97	7.00	0.29	APV	13	6.20	5.70	6.69	0.30
BL	13	30.29	28.54	32.39	1.27	BL	13	28.70	26.80	30.36	1.17
Dent	13	24.62	23.05	26.61	1.19	Dent	13	23.28	21.74	24.72	0.94
IBW	13	4.50	4.15	4.81	0.19	IBW	13	4.33	4.14	4.65	0.15
IOW	13	7.95	7.61	8.77	0.30	IOW	13	7.84	7.38	8.43	0.34
IPV	13	2.14	1.77	2.74	0.31	IPV	13	2.01	1.66	2.95	0.32
M <sup>2</sup> W	13	2.29	2.19	2.38	0.06	M <sup>2</sup> W	13	2.22	2.08	2.34	0.08
NW	13	2.45	2.03	2.85	0.20	NW	13	2.45	2.20	2.73	0.16
OBW	13	12.24	11.31	13.30	0.54	OBW	13	11.80	11.21	12.18	0.29
PPV	13	5.33	4.39	5.99	0.44	PPV	13	5.00	4.52	5.56	0.30
R-LC <sup>1</sup>	13	4.64	3.99	5.20	0.33	R-LC <sup>1</sup>	13	4.27	3.93	4.56	0.20
R-LM <sup>1</sup>	13	8.52	7.70	9.07	0.47	R-LM <sup>1</sup>	13	8.32	7.78	8.67	0.31
R-LM <sup>1</sup> T	13	7.64	7.08	8.10	0.36	R-LM <sup>1</sup> T	13	7.35	6.99	7.72	0.25
R-LM <sup>2</sup>	13	10.42	9.58	11.27	0.51	R-LM <sup>2</sup>	13	10.01	9.48	10.51	0.30
R-LM <sup>3</sup>	13	12.73	11.89	13.64	0.53	R-LM <sup>3</sup>	13	12.17	11.21	12.59	0.40
ZW	13	16.68	15.43	18.49	0.97	ZW	13	15.63	14.16	16.42	0.58
HT	13	10.50	9.79	10.99	0.40	HT	13	10.10	9.61	10.77	0.37
PL	13	17.85	16.97	19.19	0.68	PL	13	17.08 <sup>†</sup>	15.91	17.87	0.62
SWR-LC <sup>1</sup> B	13	4.18	3.74	4.75	0.29	SWR-LC <sup>1</sup> B	13	3.81	3.54	4.16	0.21
TC	13	2.52	2.21	2.91	0.19	TC	13	2.62	2.22	2.87	0.21
NWR	13	4.19	3.81	4.85	0.28	NWR	13	4.07	3.23	4.80	0.41
PML	13	9.11	7.67	10.27	0.74	PML	13	8.62	7.99	10.23	0.75
UML	13	6.87	6.33	7.18	0.23	UML	13	6.65	6.23	7.01	0.29
HT-B	13	8.29	7.71	8.81	0.32	HT-B	13	8.08	7.68	8.52	0.26
BuL	13	4.19	3.62	4.50	0.26	BuL	13	4.02	3.76	4.28	0.16
I <sup>1</sup> -P <sup>3</sup>	13	10.00	9.43	10.45	0.28	I <sup>1</sup> -P <sup>3</sup>	13	9.54	8.88	10.12	0.37
LML	13	7.56	7.10	7.88	0.24	LML	13	7.33	6.96	7.71	0.29
I <sub>1</sub> -P <sub>3</sub>	13	7.96	7.51	8.43	0.27	I <sub>1</sub> -P <sub>3</sub>	13	7.57	7.09	8.03	0.36
M <sub>2</sub> W	13	2.19	2.00	2.33	0.10	M <sub>2</sub> W	13	2.09	1.94	2.22	0.08
UPL	13	4.44	4.16	5.08	0.25	UPL	13	4.20	3.86	4.45	0.19

example, has larger anterior palatal vacuities than any congener. Within *A. minimus*, the most discriminating morphological features are tv and R-LM<sup>3</sup>, with *A. minimus maritimus* tending to be shorter-tailed and broader-skulled than *A. minimus minimus*, although there is overlap in both characters for both sexes (Figs 11-12).

DFA and CVA

Discriminant Function Analysis (DFA) of *A. minimus* with members of the Dusky Antechinus complex indicated that 100% of females and males were clustered into both *A. minimus* taxa (*A. minimus minimus*, *A. minimus*

*maritimus*) and the five Dusky *Antechinus* taxon groups (*A. swainsonii*, *A. vandycki*, *A. mimetes mimetes*, *A. mimetes insulanus* and *A. arktos*) correctly (posterior probabilities all equal to 1.00, not shown), based on the Mahalanobis distance of each individual from the centroid of

TABLE 4. Univariate statistics: means, standard deviations and range minima and maxima of measured variables for *Antechinus vandycki*.

MALES					
	Valid N	Mean	Min	Max	St. Dev.
wt	6	73.08	46.30	92.80	16.87
hb	6	120.21	104.91	132.60	9.82
tv	6	109.06	92.34	118.02	9.39
hf	6	22.47	20.34	24.62	1.67
e	6	16.37	14.94	17.55	1.00
APV	7	7.22	7.05	7.48	0.18
BL	7	31.71	29.90	33.20	1.04
Dent	7	25.92	24.48	27.76	1.02
IBW	7	4.48	4.21	4.75	0.21
IOW	7	7.95	7.67	8.11	0.15
IPV	7	1.56	1.27	1.68	0.15
M <sup>2</sup> W	7	2.33	2.24	2.38	0.05
NW	7	2.32	2.21	2.51	0.10
OBW	7	12.64	12.04	13.07	0.35
PPV	7	6.11	5.78	6.54	0.29
R-LC <sup>1</sup>	7	4.86	4.66	5.02	0.12
R-LM <sup>1</sup>	7	8.68	8.23	9.08	0.34
R-LM <sup>1</sup> T	7	7.87	7.61	8.15	0.16
R-LM <sup>2</sup>	7	10.55	9.70	10.97	0.47
R-LM <sup>3</sup>	7	12.91	12.39	13.44	0.37
ZW	7	17.25	15.99	18.39	0.71
HT	7	10.72	10.36	11.32	0.30
PL	7	18.73	17.89	19.38	0.56
SWR-LC <sup>1</sup> B	7	4.36	4.24	4.59	0.14
TC	7	2.66	2.44	2.88	0.18
NWR	7	4.44	4.18	4.87	0.24
PML	7	9.52	8.94	10.21	0.39
UML	7	6.94	6.78	7.08	0.11
HT-B	7	8.46	7.82	8.84	0.34
BuL	7	4.41	4.15	4.57	0.16
I <sup>1</sup> -P <sup>3</sup>	7	10.49	10.14	11.00	0.30
LML	7	7.58	7.37	7.68	0.11
I <sub>1</sub> -P <sub>3</sub>	7	8.41	8.18	8.63	0.17
M <sub>2</sub> W	7	2.21	2.17	2.27	0.04
UPL	7	4.66	4.45	4.79	0.11

the *a priori* species group. For CVA, 100% of the variation in dental characters was explained in the first six canonical roots for males and the first five roots for females. Variation was well resolved for both sexes, as eigenvalues for the first three canonical roots were well above 1 (males: root 1 = 43.9; root 2 = 8.9; root 3 = 2.5; females: root 1 = 40.1; root 2 = 22.8; root 3 = 5.7) and about three-quarters of the variation was explained in the first root (74%) for males, whereas just over half (56%) was explained in the first root for females. Further, cumulatively the first two roots explained 90% of variation in males and 88% in females. Figs 13-16 show scatterplots of canonical roots for males and Figs 17-18 for females; all species are tightly clustered within their taxon and well separated between species, for both sexes, but particularly females. However, there is some overlap between subspecies of *A. minimus*, particularly in males; canonical variates 4 and 5 (Figs 15-16) are important for discriminating the subspecies of *A. minimus* in males, whereas canonical variates 1 and 2 defined adjacent but distinct clusters of *A. minimus minimus* and *A. minimus maritimus*. The close and sometimes overlapping positions of the *A. minimus* subspecies in the multivariate analysis reflects the subtle morphological and only moderate genetic differences between them.

To facilitate direct comparison, univariate statistics (means, standard deviations, range minima and maxima) are shown for each of the external and internal (cranial/dental) measures for both subspecies of *A. minimus* and all four species (5 taxa) within the Dusky *Antechinus* species complex: *A. swainsonii*, *A. vandycki*, *A. mimetes mimetes*, *A. mimetes insulanus* and *A. arktos* (refer Tables 1-7). All ANOVAs of measured variables among all antechinus species were significant (Table 8). In pairwise comparisons below, attention is given to diagnosing absolute differences (with no overlap in ranges) where they exist, compared to those that are significantly ( $P < 0.05$ ) different. *Antechinus minimus minimus*, with primacy of discovery within *A. minimus*, was chosen as the reference species, to which all other congeners are compared in pairwise fashion below.

Swamp Antechinus, *Antechinus minimus* (É. Geoffroy)

TABLE 5. Univariate statistics: means, standard deviations and range minima and maxima of measured variables for *Antechinus mimetes mimetes*.

MALES						FEMALES					
	Valid N	Mean	Min	Max	St. Dev.		Valid N	Mean	Min	Max	St. Dev.
wt	6	60.55	42.00	112.00	26.01	wt	8	38.24	30.50	47.80	5.10
hb	20	122.18	89.20	150.00	16.50	hb	27	106.14	85.00	125.00	11.59
tv	20	101.11	82.43	113.75	8.83	tv	27	89.53	76.00	98.00	5.77
hf	20	21.41	18.69	24.00	1.41	hf	26	19.61	17.00	22.00	1.15
e	19	16.56	14.29	20.00	1.63	e	26	15.82	14.08	19.40	1.18
APV	15	5.41	4.58	6.35	0.52	APV	12	5.02	4.57	5.56	0.28
BL	15	30.39	28.53	31.72	0.93	BL	11	28.63	27.33	30.49	0.98
Dent	15	24.67	23.21	25.88	0.79	Dent	12	23.18	22.05	24.30	0.74
IBW	15	4.73	4.35	5.12	0.24	IBW	12	4.46	4.05	4.87	0.25
IOW	15	8.12	7.68	8.51	0.23	IOW	12	7.85	7.21	8.34	0.33
IPV	15	3.19	2.13	3.93	0.60	IPV	12	3.09	2.43	3.79	0.42
M <sup>2</sup> W	15	2.36	2.20	2.53	0.09	M <sup>2</sup> W	12	2.25	2.10	2.37	0.07
NW	15	2.70	2.41	2.92	0.15	NW	12	2.54	2.14	3.02	0.24
OBW	15	12.34	11.60	13.33	0.50	OBW	12	11.85	11.11	12.53	0.40
PPV	15	5.41	4.37	6.03	0.48	PPV	12	5.29	4.67	5.71	0.26
R-LC <sup>1</sup>	15	4.63	4.34	4.92	0.19	R-LC <sup>1</sup>	12	4.34	3.79	4.71	0.26
R-LM <sup>1</sup>	15	8.78	8.03	9.39	0.38	R-LM <sup>1</sup>	12	8.45	7.68	8.93	0.38
R-LM <sup>1</sup> T	15	7.68	7.27	8.15	0.29	R-LM <sup>1</sup> T	12	7.34	6.80	7.63	0.28
R-LM <sup>2</sup>	15	10.65	9.63	11.81	0.62	R-LM <sup>2</sup>	12	10.24	9.09	11.06	0.68
R-LM <sup>3</sup>	15	13.28	12.23	14.39	0.56	R-LM <sup>3</sup>	12	12.78	11.15	13.64	0.71
ZW	15	17.00	15.52	18.07	0.77	ZW	12	15.74	14.47	16.94	0.76
HT	15	10.76	10.28	11.15	0.28	HT	12	10.34	9.81	10.92	0.32
PL	15	17.51	16.66	18.27	0.51	PL	12	16.77	15.83	17.69	0.53
SWR-LC <sup>1</sup> B	15	4.18	3.78	4.63	0.22	SWR-LC <sup>1</sup> B	12	3.88	3.47	4.29	0.28
TC	15	2.90	2.50	3.41	0.29	TC	12	2.83	2.54	3.36	0.26
NWR	15	4.62	4.12	4.87	0.23	NWR	12	4.23	3.67	4.68	0.37
PML	15	9.39	8.21	10.70	0.69	PML	12	8.60	7.84	9.47	0.54
UML	15	6.93	6.29	7.52	0.34	UML	12	6.72	6.25	7.17	0.26
HT-B	15	8.57	8.21	9.04	0.24	HT-B	12	8.16	7.57	8.55	0.31
BuL	15	4.26	3.93	4.60	0.21	BuL	12	4.06	3.82	4.33	0.18
I <sup>1</sup> -P <sup>3</sup>	15	9.67	8.98	10.20	0.33	I <sup>1</sup> -P <sup>3</sup>	12	9.16	8.82	9.90	0.29
LML	15	7.60	7.00	8.19	0.37	LML	12	7.37	6.87	7.73	0.26
I <sub>1</sub> -P <sub>3</sub>	15	7.78	7.31	8.08	0.26	I <sub>1</sub> -P <sub>3</sub>	12	7.30	6.93	7.75	0.23
M <sub>2</sub> W	15	2.18	1.98	2.41	0.12	M <sub>2</sub> W	12	2.13	2.00	2.25	0.08
UPL	15	4.38	4.03	4.70	0.23	UPL	12	4.09	3.61	4.52	0.26

*Antechinus minimus minimus* (Geoffroy)  
versus  
*Antechinus minimus maritimus* (Finlayson)

**Pelage.** *Antechinus minimus minimus* and *A. minimus maritimus* are similar in appearance, with coarse fur and a leaden grey head that

merges to brownish yellow fur on the rump and flanks.

**External Measurements.** *Antechinus minimus minimus* is similar in size compared to *A. minimus maritimus*, although *A. minimus minimus* tends to



TABLE 6. Univariate statistics: means, standard deviations and range minima and maxima of measured variables for *Antechinus mimetes insulanus*.

MALES						FEMALES					
	Valid N	Mean	Min	Max	St. Dev.		Valid N	Mean	Min	Max	St. Dev.
wt	4	70.63	46.00	87.00	17.55	wt	4	49.75	40.00	60.00	8.26
hb	6	138.87	117.10	165.00	17.48	hb	6	123.20	111.40	144.80	11.35
tv	6	111.86	105.00	121.90	7.62	tv	5	99.49	96.39	106.27	3.88
hf	6	22.04	20.00	24.26	1.49	hf	6	20.50	19.60	21.27	0.60
e	5	17.47	15.45	20.50	1.92	e	6	17.02	14.00	19.40	2.00
APV	6	5.63	5.06	6.02	0.33	APV	11	5.16	4.72	5.50	0.27
BL	6	32.57	30.19	33.85	1.37	BL	11	29.93	28.39	30.74	0.71
Dent	6	26.53	24.68	27.61	1.07	Dent	11	24.37	22.96	25.03	0.56
IBW	6	5.14	4.99	5.34	0.14	IBW	11	4.77	4.55	4.99	0.15
IOW	6	7.94	7.78	8.27	0.17	IOW	11	7.86	7.59	8.08	0.14
IPV	6	3.88	3.48	4.24	0.26	IPV	11	3.82	3.41	4.23	0.24
M <sup>2</sup> W	6	2.58	2.53	2.65	0.05	M <sup>2</sup> W	11	2.50	2.44	2.54	0.03
NW	6	2.93	2.77	3.19	0.16	NW	11	2.90	2.61	3.12	0.14
OBW	6	13.41	12.98	13.85	0.35	OBW	11	12.56	11.99	13.33	0.37
PPV	6	5.31	4.60	5.57	0.36	PPV	11	4.92	4.34	5.43	0.36
R-LC <sup>1</sup>	6	4.99	4.71	5.26	0.22	R-LC <sup>1</sup>	11	4.61	4.32	4.92	0.19
R-LM <sup>1</sup>	6	9.07	8.86	9.31	0.16	R-LM <sup>1</sup>	11	8.53	8.08	8.78	0.23
R-LM <sup>1</sup> T	6	8.29	8.01	8.76	0.27	R-LM <sup>1</sup> T	11	7.92	7.60	8.24	0.19
R-LM <sup>2</sup>	6	10.61	10.12	11.43	0.53	R-LM <sup>2</sup>	11	9.91	9.28	10.50	0.39
R-LM <sup>3</sup>	6	14.09	13.85	14.45	0.23	R-LM <sup>3</sup>	11	13.12	12.43	13.86	0.47
ZW	6	18.80	17.83	20.01	0.83	ZW	11	17.09	16.48	17.90	0.47
HT	6	11.20	10.65	11.89	0.46	HT	11	10.66	10.27	10.89	0.21
PL	6	18.84	17.88	19.36	0.53	PL	11	17.78	16.84	18.16	0.43
SWR-LC <sup>1</sup> B	6	4.47	4.22	4.74	0.21	SWR-LC <sup>1</sup> B	11	4.10	3.85	4.34	0.16
TC	6	3.11	2.96	3.28	0.14	TC	11	3.07	2.71	3.39	0.22
NWR	6	5.11	4.82	5.41	0.23	NWR	11	4.73	4.44	5.19	0.22
PML	6	10.64	9.90	11.30	0.47	PML	11	9.63	8.84	10.20	0.43
UML	6	7.46	7.35	7.62	0.11	UML	11	7.20	6.96	7.37	0.14
HT-B	6	8.97	8.49	9.48	0.36	HT-B	11	8.30	8.00	8.58	0.18
BuL	6	4.43	4.19	4.73	0.19	BuL	11	4.24	3.99	4.68	0.22
I <sup>1</sup> -P <sup>3</sup>	6	10.20	9.42	10.61	0.43	I <sup>1</sup> -P <sup>3</sup>	11	9.54	9.19	9.90	0.25
LML	6	8.13	8.00	8.43	0.17	LML	11	7.91	7.67	8.08	0.13
I <sub>1</sub> -P <sub>3</sub>	6	8.33	7.89	8.65	0.31	I <sub>1</sub> -P <sub>3</sub>	11	7.59	7.18	7.82	0.21
M <sub>2</sub> W	6	2.36	2.33	2.43	0.04	M <sub>2</sub> W	11	2.30	2.24	2.34	0.03
UPL	6	4.55	4.13	4.91	0.29	UPL	11	4.18	3.91	4.57	0.20

have larger hind feet and a longer tail (Tables 1, 2 and 8).

**Craniodental Characters.** *Antechinus minimus minimus* is not significantly different to *A. minimus maritimus* for any craniodental characters, but *A. minimus minimus* tend to have a narrower skull

(smaller R-LM<sup>1</sup>T, R-LM<sup>2</sup>, R-LM<sup>3</sup>) in both sexes and narrower M<sup>2</sup>W in females (Tables 1, 2 and 8).

**Comments.** *Antechinus minimus minimus* occurs throughout most of Tasmania (including southern Bass Strait Islands) whereas *A. minimus maritimus* is found on mainland Australia (as



Swamp Antechinus, *Antechinus minimus* (È. Geoffroy)

TABLE 7. Univariate statistics: means, standard deviations and range minima and maxima of measured variables for *Antechinus arktos*.

MALES						FEMALES					
	Valid N	Mean	Min	Max	St. Dev.		Valid N	Mean	Min	Max	St. Dev.
wt	2	89.85	59.70	120.00	42.64	wt	1	46.30	46.30	46.30	na
hb	5	131.53	108.58	145.00	14.91	hb	3	108.89	106.22	111.20	2.51
tv	6	118.01	100.42	131.00	14.22	tv	3	99.12	94.20	106.88	6.80
hf	6	23.27	21.88	24.00	0.80	hf	3	21.43	20.00	22.20	1.24
e	6	17.15	15.47	19.00	1.39	e	3	16.70	16.10	17.72	0.89
APV	6	4.76	4.52	5.05	0.22	APV	3	4.45	4.31	4.64	0.17
BL	6	32.44	30.45	33.75	1.55	BL	3	29.54	29.12	30.14	0.53
Dent	6	26.31	24.63	27.41	1.16	Dent	3	24.30	24.14	24.51	0.19
IBW	6	5.08	4.93	5.23	0.13	IBW	3	4.68	4.53	4.83	0.15
IOW	6	8.05	7.87	8.51	0.24	IOW	3	7.94	7.78	8.13	0.18
IPV	6	4.11	3.97	4.24	0.12	IPV	3	4.05	3.94	4.13	0.10
M <sup>2</sup> W	6	2.41	2.35	2.52	0.06	M <sup>2</sup> W	3	2.40	2.35	2.43	0.04
NW	6	3.15	2.99	3.43	0.16	NW	3	2.90	2.76	3.02	0.13
OBW	6	13.21	12.63	13.72	0.41	OBW	3	12.38	12.32	12.46	0.07
PPV	6	5.85	5.02	6.52	0.57	PPV	3	5.56	5.45	5.76	0.17
R-LC <sup>1</sup>	6	5.10	4.93	5.31	0.16	R-LC <sup>1</sup>	3	4.68	4.62	4.72	0.05
R-LM <sup>1</sup>	6	9.57	9.12	9.90	0.29	R-LM <sup>1</sup>	3	8.74	8.66	8.79	0.07
R-LM <sup>1</sup> T	6	8.15	7.97	8.29	0.14	R-LM <sup>1</sup> T	3	7.77	7.71	7.82	0.06
R-LM <sup>2</sup>	6	11.42	10.95	11.65	0.27	R-LM <sup>2</sup>	3	10.60	10.51	10.68	0.09
R-LM <sup>3</sup>	6	14.09	13.55	14.70	0.42	R-LM <sup>3</sup>	3	13.29	13.01	13.47	0.25
ZW	6	18.27	16.65	19.22	1.20	ZW	3	16.61	16.27	17.10	0.43
HT	6	10.95	10.55	11.38	0.27	HT	3	10.60	10.56	10.64	0.04
PL	6	18.38	17.45	19.04	0.61	PL	3	17.45	17.26	17.71	0.23
SWR-LC <sup>1</sup> B	6	4.60	4.33	5.03	0.25	SWR-LC <sup>1</sup> B	3	4.09	4.03	4.13	0.05
TC	6	3.22	2.97	3.38	0.15	TC	3	3.14	3.03	3.33	0.17
NWR	6	5.75	5.22	6.17	0.37	NWR	3	4.99	4.82	5.32	0.29
PML	6	10.23	9.68	10.78	0.44	PML	3	9.57	9.37	9.85	0.25
UML	6	7.35	7.21	7.55	0.11	UML	3	7.33	7.19	7.46	0.14
HT-B	6	8.76	8.53	9.08	0.20	HT-B	3	8.35	8.10	8.48	0.22
BuL	6	4.57	4.25	4.79	0.21	BuL	3	4.48	4.37	4.55	0.09
I <sup>1</sup> -P <sup>3</sup>	6	10.03	9.58	10.29	0.26	I <sup>1</sup> -P <sup>3</sup>	3	9.48	9.32	9.66	0.17
LML	6	7.83	7.72	8.07	0.12	LML	3	7.74	7.57	7.92	0.18
I <sub>1</sub> -P <sub>3</sub>	6	7.99	7.16	8.36	0.44	I <sub>1</sub> -P <sub>3</sub>	3	7.35	6.98	7.68	0.35
M <sub>2</sub> W	6	2.27	2.13	2.35	0.08	M <sub>2</sub> W	3	2.28	2.20	2.35	0.08
UPL	6	4.50	4.29	4.71	0.17	UPL	3	4.15	3.99	4.24	0.14

well as some near-coastal islands) and is patchily distributed in mostly coastal areas between South Gippsland (Victoria) and Robe (South Australia). Genetics: uncorrected pairwise difference at the mitochondrial gene CytB between *A. minimus minimus* and *A. minimus maritimus* is 3.9 - 4.5%.

*Antechinus minimus minimus* versus *Antechinus swainsonii* (Waterhouse)  
Pelage. *Antechinus minimus minimus* has coarse fur and a leaden grey head that merges to brownish yellow fur on the rump and flanks whereas *A. swainsonii* is greyish-brown in

TABLE 8. ANOVA F-statistics (top two lines) for variation at each of the measured variables among all antechinus species and subspecies. Subsequent rows show significance values for ANOVA post-hoc tests of *Antechinus minimus minimus* paired with each of its 14 congeneric species, for each measured variable. Shaded cells are significant at  $p=0.05$ , unshaded cells are not significant.

Comparison	sex	wt	hb	tv	hf	e	APV	BL	Dent	IBW	IOW	IPV	MBW	NW	OBW	PPV	R-IC <sub>1</sub>	R-IM <sub>1</sub>	R-LIM <sub>1</sub>
ANOVA F - all species	male	22.90	29.66	37.28	50.49	21.31	235.90	41.94	48.85	37.85	86.90	90.51	58.12	29.49	24.38	21.61	50.91	46.38	29.76
ANOVA F - all species	female	26.69	24.47	25.22	29.42	19.61	219.10	48.39	65.25	39.25	97.55	74.40	51.69	19.39	28.13	18.55	43.46	41.46	25.68
<i>minimus maritimus</i>	male	1.00	0.99	0.68	0.29	1.00	0.96	1.00	1.00	0.99	0.11	1.00	1.00	1.00	1.00	1.00	1.00	0.87	0.90
<i>minimus maritimus</i>	female	0.99	1.00	0.42	0.91	1.00	0.96	1.00	1.00	1.00	1.00	0.85	0.14	1.00	1.00	1.00	1.00	1.00	0.71
<i>scottsonii</i>	male	0.96	1.00	0.02	0.01	0.05	0.00	0.06	0.01	1.00	0.98	0.00	1.00	0.04	1.00	0.97	0.00	0.03	0.99
<i>scottsonii</i>	female	1.00	1.00	0.00	0.84	0.23	0.00	0.00	0.01	1.00	0.03	0.00	0.95	0.16	1.00	0.99	0.01	0.89	1.00
<i>vancouveri</i>	male	1.00	0.98	0.00	0.02	0.94	0.00	0.00	0.00	1.00	1.00	0.00	1.00	0.02	1.00	0.00	0.68	0.93	1.00
<i>minimoides minimoides</i>	male	1.00	0.95	0.00	0.33	0.20	0.00	0.02	0.00	1.00	0.04	0.00	0.46	1.00	1.00	0.69	0.00	0.84	1.00
<i>minimoides minimoides</i>	female	0.98	0.97	0.00	0.18	0.00	0.00	0.00	0.01	1.00	0.00	0.93	0.24	0.90	0.99	0.12	0.16	1.00	1.00
<i>minimoides insularis</i>	male	1.00	1.00	0.00	0.16	0.23	0.00	0.00	0.00	0.06	1.00	1.00	0.00	0.99	0.00	1.00	1.00	1.00	0.47
<i>minimoides insularis</i>	female	0.48	0.80	0.00	0.06	0.00	0.00	0.00	0.01	0.00	0.02	0.65	0.00	0.61	0.00	1.00	1.00	1.00	0.00
<i>aklos</i>	male	1.00	1.00	0.00	0.00	0.30	0.00	0.00	0.00	0.18	0.94	1.00	0.30	0.10	0.09	0.10	1.00	0.90	0.94
<i>aklos</i>	female	1.00	1.00	0.00	0.04	0.19	0.00	0.00	0.01	0.95	0.52	0.88	0.03	1.00	0.41	0.41	1.00	1.00	0.95
<i>adustus</i>	male	0.00	0.00	0.00	0.99	1.00	0.00	0.01	0.00	0.99	0.00	1.00	0.04	1.00	0.26	1.00	1.00	1.00	1.00
<i>adustus</i>	female	0.00	0.00	0.00	1.00	0.87	0.00	0.80	0.21	1.00	0.00	0.27	0.00	1.00	0.18	1.00	0.71	1.00	1.00
<i>agilis</i>	male	0.00	0.00	0.02	0.00	1.00	0.00	0.01	0.00	0.00	0.00	1.00	0.55	1.00	0.00	0.00	0.04	0.20	0.00
<i>agilis</i>	female	0.00	0.00	0.39	0.02	1.00	0.00	0.03	0.00	0.00	0.00	0.81	0.51	0.28	0.17	0.41	1.00	1.00	1.00
<i>argutus</i>	male	0.00	0.00	0.40	0.81	0.57	0.00	0.45	0.07	0.02	0.00	1.00	1.00	1.00	1.00	0.88	1.00	0.99	1.00
<i>argutus</i>	female	0.02	0.00	1.00	0.64	0.90	0.01	0.39	0.21	0.02	0.00	1.00	0.68	1.00	1.00	0.21	1.00	1.00	1.00
<i>bellus</i>	male	0.12	1.00	0.00	0.00	0.00	0.00	0.07	0.28	0.00	0.00	0.00	0.00	0.00	0.00	0.00	0.00	0.00	0.00
<i>bellus</i>	female	0.46	1.00	0.00	0.01	0.00	0.00	0.03	0.01	0.00	0.00	0.00	0.00	0.00	0.00	0.00	0.00	0.00	0.00
<i>flavipes flavipes</i>	male	0.00	0.00	0.81	0.89	0.21	0.00	1.00	0.87	0.00	0.00	0.00	0.00	0.00	0.25	0.22	0.00	0.01	0.00
<i>flavipes flavipes</i>	female	0.98	0.00	0.95	0.54	0.00	0.00	1.00	1.00	0.00	0.00	0.00	0.00	1.00	0.66	0.13	0.00	0.84	0.00
<i>flavipes leucogaster</i>	male	0.00	0.00	1.00	0.87	0.06	0.00	0.93	0.59	0.00	0.00	0.00	0.00	0.26	0.91	0.15	0.16	0.01	0.22
<i>flavipes leucogaster</i>	female	0.04	0.00	1.00	0.41	0.00	0.00	1.00	1.00	0.00	0.00	0.00	0.00	1.00	1.00	0.37	0.51	0.01	0.08
<i>flavipes rubiculus</i>	male	1.00	0.99	0.00	0.19	0.16	0.00	0.51	0.10	0.78	0.00	0.00	0.00	0.00	0.00	1.00	0.00	0.00	0.00
<i>flavipes rubiculus</i>	female	1.00	1.00	0.00	0.53	0.92	0.00	0.00	0.00	1.00	0.00	0.00	0.00	0.00	0.00	0.75	0.00	0.00	0.00
<i>gordmani</i>	male	0.21	0.90	0.00	0.00	0.00	0.00	0.00	0.00	0.00	1.00	0.00	0.00	0.98	0.00	0.32	0.00	0.04	0.00
<i>gordmani</i>	female	0.00	0.82	0.00	0.00	0.00	0.00	0.00	0.00	0.00	0.67	0.00	0.00	0.88	0.00	0.70	0.00	0.11	0.00
<i>leo</i>	male	1.00	0.99	0.00	0.00	0.00	0.00	0.00	0.00	0.00	0.00	0.00	0.00	0.00	0.00	1.00	0.00	0.00	0.00
<i>leo</i>	female	1.00	1.00	0.00	0.00	0.00	0.00	0.00	0.00	0.02	0.00	0.00	0.00	0.00	0.00	1.00	0.00	0.00	0.00
<i>myotis</i>	male	0.00	0.00	0.00	0.01	0.26	0.00	1.00	0.31	0.00	0.00	1.00	0.00	1.00	1.00	1.00	0.04	1.00	0.90
<i>myotis</i>	female	0.00	0.00	0.06	0.26	0.00	0.00	1.00	0.60	0.00	0.00	0.76	0.00	1.00	1.00	1.00	0.00	1.00	0.61
<i>stuartii</i>	male	0.00	0.00	0.64	0.01	0.59	0.00	0.00	0.00	0.00	0.00	0.00	0.69	1.00	0.08	0.69	0.95	0.53	1.00
<i>stuartii</i>	female	0.00	0.00	1.00	0.31	0.46	0.00	0.03	0.00	0.00	0.00	0.86	0.04	0.50	0.30	0.10	1.00	0.23	1.00
<i>subtropicus</i>	male	0.13	0.37	0.10	1.00	0.00	0.97	1.00	0.98	0.03	0.00	0.00	0.00	0.00	1.00	0.00	1.00	1.00	1.00
<i>subtropicus</i>	female	0.58	0.00	0.50	1.00	0.17	1.00	1.00	1.00	0.20	0.00	0.00	0.00	1.00	1.00	0.00	0.91	1.00	0.77

TABLE 8. cont ...

Comparison	sex	R-LM <sup>2</sup>	R-LM <sup>3</sup>	ZW	HT	PL	SVR- LC-B	TC	NWR	PNL	UNIL	HT-B	BuL	I-P <sup>3</sup>	LMIL	I-P <sup>3</sup>	M <sub>2</sub> W	UPL
ANOVA F - all species	male	45.96	29.84	16.46	35.27	63.05	42.04	27.23	14.61	20.45	55.11	40.40	23.95	78.64	56.11	127.60	40.06	90.44
ANOVA F - all species	female	47.29	29.48	20.11	52.35	74.68	38.58	31.24	14.46	28.72	56.33	59.21	24.64	46.45	59.31	121.10	49.32	90.68
<i>minimus minimus</i>	male	0.30	0.37	1.00	1.00	1.00	0.98	0.82	1.00	0.94	1.00	1.00	1.00	1.00	1.00	1.00	1.00	1.00
<i>minimus minimus</i>	female	0.66	0.54	1.00	1.00	1.00	0.98	1.00	1.00	0.69	0.79	1.00	0.56	1.00	0.11	0.95	0.88	1.00
<i>scotinotii</i>	male	0.92	1.00	1.00	1.00	1.00	0.00	0.00	0.30	1.00	0.00	0.94	1.00	0.00	0.00	0.00	0.01	0.00
<i>scotinotii</i>	female	0.99	1.00	1.00	1.00	1.00	0.00	0.36	0.99	0.03	0.00	1.00	0.79	0.00	0.00	0.00	0.84	0.00
<i>rundolphi</i>	male	1.00	1.00	1.00	1.00	1.00	1.00	0.69	1.00	0.68	0.00	1.00	0.85	0.00	0.00	0.00	0.06	0.00
<i>minimetus minimetus</i>	male	1.00	1.00	1.00	1.00	1.00	0.00	1.00	1.00	0.39	0.00	1.00	1.00	0.00	0.00	0.00	0.01	0.00
<i>minimetus minimetus</i>	female	1.00	0.78	0.95	0.96	0.00	0.96	0.99	1.00	0.04	0.00	1.00	0.48	0.00	0.00	0.00	0.03	0.00
<i>minimetus insulanus</i>	female	0.90	0.08	0.00	0.00	0.00	1.00	0.00	0.58	0.00	0.00	0.75	0.00	0.00	0.00	0.00	0.00	0.00
<i>arkles</i>	male	0.96	0.35	0.46	1.00	0.00	1.00	0.62	0.00	0.00	0.00	0.99	0.10	0.00	0.00	0.00	0.00	0.00
<i>arkles</i>	female	1.00	0.73	0.52	0.87	0.00	1.00	0.27	0.78	0.00	0.00	0.99	0.00	0.04	0.00	0.00	0.00	0.00
<i>adustus</i>	male	1.00	1.00	0.87	0.00	0.00	1.00	0.67	1.00	0.00	1.00	0.00	0.17	0.00	1.00	0.00	0.00	0.00
<i>adustus</i>	female	1.00	1.00	1.00	0.00	0.10	0.34	1.00	0.92	0.00	1.00	0.00	0.80	0.03	1.00	0.00	0.00	0.00
<i>agilis</i>	male	1.00	1.00	0.09	0.00	0.00	0.62	0.00	0.00	0.00	0.00	0.00	0.97	0.00	0.00	0.00	0.94	0.00
<i>agilis</i>	female	0.12	0.43	1.00	0.00	0.00	1.00	0.90	0.00	1.00	0.90	0.00	0.40	0.00	0.95	0.00	1.00	0.00
<i>argenteus</i>	male	0.14	0.46	1.00	0.00	0.02	1.00	0.39	0.27	1.00	1.00	0.00	1.00	0.00	1.00	0.00	0.92	0.00
<i>argenteus</i>	female	1.00	0.91	1.00	0.00	0.15	1.00	1.00	0.20	1.00	1.00	0.00	0.76	0.14	1.00	0.00	0.98	0.00
<i>bellus</i>	male	0.00	0.00	0.00	0.96	0.15	0.00	0.00	0.28	1.00	0.00	0.00	0.00	0.99	0.00	0.00	0.00	0.14
<i>bellus</i>	female	0.00	0.00	0.00	0.99	0.26	0.00	0.17	0.20	1.00	0.00	0.00	0.00	1.00	0.00	0.00	0.00	0.04
<i>flavipes flavipes</i>	male	0.00	0.00	0.44	0.00	0.76	0.00	0.00	0.44	1.00	0.00	0.00	0.00	0.00	0.00	0.00	0.00	0.00
<i>flavipes flavipes</i>	female	0.00	0.00	0.11	0.00	0.96	0.00	0.04	0.04	0.96	0.00	0.00	0.00	0.00	0.00	0.00	0.00	0.00
<i>flavipes leucogaster</i>	male	0.00	0.00	0.78	0.00	0.00	0.09	0.04	0.00	0.94	1.00	0.00	0.00	0.00	1.00	0.00	0.00	0.00
<i>flavipes leucogaster</i>	female	0.00	0.00	0.13	0.00	0.38	0.00	0.98	0.05	0.95	1.00	0.00	0.00	0.03	1.00	0.00	0.00	0.00
<i>flavipes rubicollis</i>	male	0.00	0.00	0.00	0.41	0.76	0.00	0.25	1.00	0.13	0.00	0.00	0.00	0.75	0.00	0.00	0.00	0.02
<i>flavipes rubicollis</i>	female	0.00	0.00	0.00	0.98	0.00	0.00	1.00	1.00	0.18	0.00	0.00	0.00	1.00	0.00	0.00	0.00	0.08
<i>godmani</i>	male	0.00	0.00	0.00	1.00	0.00	0.00	0.00	1.00	0.62	0.00	1.00	0.81	0.00	0.00	0.46	0.00	0.00
<i>godmani</i>	female	0.00	0.00	0.00	1.00	0.00	0.00	0.00	1.00	0.00	0.00	0.99	0.01	0.00	0.00	0.00	0.00	0.00
<i>leo</i>	male	0.00	0.00	0.00	1.00	0.00	0.00	0.00	0.03	0.00	0.00	0.16	0.00	1.00	0.00	0.00	0.00	0.99
<i>leo</i>	female	0.00	0.00	0.00	1.00	0.00	0.00	0.00	0.38	0.00	0.00	0.01	0.00	0.98	0.00	0.11	0.00	1.00
<i>mysticus</i>	male	0.85	0.04	1.00	0.00	0.24	0.00	0.00	0.81	1.00	1.00	0.00	0.15	0.00	1.00	0.00	0.29	0.00
<i>mysticus</i>	female	0.55	0.20	0.88	0.00	0.18	0.00	1.00	0.89	1.00	1.00	0.00	0.00	0.00	1.00	0.00	0.11	0.00
<i>stuartii</i>	male	0.98	1.00	0.48	0.00	0.00	1.00	0.35	0.00	0.06	1.00	0.00	1.00	0.00	1.00	0.00	0.04	0.00
<i>stuartii</i>	female	0.98	1.00	1.00	0.00	0.00	1.00	0.93	0.00	0.59	1.00	0.00	1.00	0.00	1.00	0.00	0.04	0.00
<i>subtropicus</i>	male	1.00	1.00	1.00	0.00	0.88	0.93	1.00	0.05	1.00	0.95	0.00	1.00	0.00	0.92	0.00	0.00	0.08
<i>subtropicus</i>	female	1.00	1.00	1.00	0.00	1.00	0.04	1.00	0.49	1.00	0.38	0.00	0.78	0.93	0.05	0.00	0.00	0.00

appearance, greyer at the front with a brownish warming on the rump.

**External Measurements.** *Antechinus minimus minimus* is significantly smaller than *A. swainsonii* in tv and hf length in males and for tv length in females (Tables 1, 3 and 8).

**Craniodental Characters.** *Antechinus minimus minimus* is larger than *A. swainsonii* in absolute measurement (i.e., with no overlap) for IPV in males and females. *Antechinus minimus minimus* is significantly larger than *A. swainsonii* in NW, R-LC<sup>1</sup>, R-LM<sup>1</sup>, SWR-LC<sup>1</sup>B and TC in males and for R-LC<sup>1</sup> in females. *Antechinus minimus minimus* is smaller than *A. swainsonii* in absolute measurement for APV in both sexes and for UPL in males. *Antechinus minimus minimus* is significantly smaller than *A. swainsonii* in Dent, PL, UML, I<sup>1</sup>-P<sup>3</sup>, LML, I<sub>1</sub>-P<sub>3</sub> and M<sub>2</sub>W in males and for BL, Dent, IOW, PL, PML, UML, I<sup>1</sup>-P<sup>3</sup>, LML, I<sub>1</sub>-P<sub>3</sub> and UPL in females (Tables 1, 3 and 8).

**Comments.** *Antechinus minimus minimus* occurs throughout most of Tasmania (including southern Bass Strait Islands) and may co-occur with *A. swainsonii*, which occurs throughout much of Tasmania, except the far south-east on Tasman Peninsula. Genetics: uncorrected pairwise difference at the mitochondrial gene CytB between *A. minimus minimus* and *A. swainsonii* is 10.0 – 12.0%.

*Antechinus minimus minimus* versus  
*Antechinus vandycki* Baker,  
Mutton, Mason and Gray

**Pelage.** *Antechinus minimus minimus* has coarse fur and a leaden grey head that merges to brownish yellow fur on the rump and flanks whereas *A. vandycki* is dark greyish-brown in appearance, greyer at the front with a brownish warming on the rump.

**External Measurements.** *Antechinus minimus minimus* is significantly smaller than *A. vandycki* in tv and hf length in males (Tables 1, 4 and 8).

**Craniodental Characters.** *Antechinus minimus minimus* is larger than *A. vandycki* in absolute measurement for IPV in males. *Antechinus minimus minimus* is significantly larger than *A.*

*vandycki* in NW for males. *Antechinus minimus minimus* is smaller than *A. vandycki* in absolute measurement for APV, PL, I<sup>1</sup>-P<sup>3</sup>, LML, I<sub>1</sub>-P<sub>3</sub> and UPL in males. *Antechinus minimus minimus* is significantly smaller than *A. vandycki* in BL, Dent, PPV and UML in males (Tables 1, 4 and 8).

**Comments.** *Antechinus minimus minimus* occurs throughout most of Tasmania (including southern Bass Strait Islands) whereas *A. vandycki* occurs only in the far south-east on Tasman Peninsula. The two species may co-occur on Tasman Peninsula. Genetics: uncorrected pairwise difference at the mitochondrial gene CytB between *A. minimus minimus* and *A. vandycki* is 9.4-10.2%.

*Antechinus minimus minimus* versus  
*Antechinus mimetes mimetes* (Thomas)

**Pelage.** *Antechinus minimus minimus* has coarse fur and a leaden grey head that merges to brownish yellow fur on the rump and flanks whereas *A. mimetes mimetes* is more evenly brownish from head to rump.

**External Measurements.** *Antechinus minimus minimus* is significantly smaller than *A. mimetes mimetes* in tv for males and for tv and e in females (Tables 1, 5 and 8).

**Craniodental Characters.** *Antechinus minimus minimus* is significantly larger than *A. mimetes mimetes* in IPV, R-LC<sup>1</sup> and SWR-LC<sup>1</sup>B for males. *Antechinus minimus minimus* is smaller than *A. mimetes mimetes* in absolute measurement for APV in males and females and for I<sup>1</sup>-P<sup>3</sup> in females. *Antechinus minimus minimus* is significantly smaller than *A. mimetes mimetes* in BL, Dent, IOW, PL, UML, I<sup>1</sup>-P<sup>3</sup>, LML, I<sub>1</sub>-P<sub>3</sub>, M<sub>2</sub>W and UPL for males and for BL, Dent, IOW, PL, PML, UML, LML, I<sub>1</sub>-P<sub>3</sub>, M<sub>2</sub>W and UPL for females (Tables 1, 5 and 8).

**Comments.** *Antechinus minimus minimus* occurs throughout most of Tasmania (including southern Bass Strait Islands) whereas *A. mimetes mimetes* is found on mainland Australia in Victoria and New South Wales. Genetics: uncorrected pairwise difference at the mitochondrial gene CytB between *A. minimus minimus* and *A. mimetes mimetes* is 8.6-10.6%.

*Antechinus minimus minimus* versus  
*Antechinus mimetes insulanus* Davison

**Pelage.** *Antechinus minimus minimus* has coarse fur and a leaden grey head that merges to brownish yellow fur on the rump and flanks whereas *A. mimetes insulanus* is more evenly brownish from head to rump.

**External Measurements.** *Antechinus minimus minimus* is smaller than *A. mimetes insulanus* in absolute measurement (i.e., with no overlap) for tv in males and females. *Antechinus minimus minimus* is significantly smaller than *A. mimetes insulanus* in e for females (Tables 1, 6 and 8).

**Craniodental Characters.** *Antechinus minimus minimus* is smaller than *A. mimetes insulanus* in absolute measurement for APV, M<sub>2</sub>W, OBW, PL, PML, UML, LML, I<sub>1</sub>-P<sub>3</sub> and M<sub>2</sub>W in males and for APV, BL, Dent, M<sub>2</sub>W, ZW, PL, PML, UML, I<sup>1</sup>-P<sup>3</sup>, LML, I<sub>1</sub>-P<sub>3</sub>, M<sub>2</sub>W and UPL in females. *Antechinus minimus minimus* is significantly smaller than *A. mimetes insulanus* in BL, Dent, ZW, I<sub>1</sub>-P<sub>3</sub> and UPL for males and for IBW, IOW, OBW, R-LM<sup>1</sup>T, HT, TC and BuL for females (Tables 1, 6 and 8).

**Comments.** *Antechinus minimus minimus* occurs throughout most of Tasmania (including southern Bass Strait Islands) whereas *A. mimetes insulanus* is found on mainland Australia in the Grampians NP, Victoria. Genetics: uncorrected pairwise difference at the mitochondrial gene CytB between *A. minimus minimus* and *A. mimetes insulanus* is 9.2-9.6%.

*Antechinus minimus minimus* versus  
*Antechinus arktos* Baker, Mutton,  
Hines & Van Dyck

**Pelage.** *Antechinus minimus minimus* has coarse fur and a leaden grey head that merges to brownish yellow fur on the rump and flanks whereas *A. arktos* is more brownish from head to rump with a very warm orangish rump and some orange fur around the eye.

**External Measurements.** *Antechinus minimus minimus* is smaller than *A. arktos* in absolute measurement for tv in males and females. *Antechinus minimus minimus* is significantly

smaller than *A. arktos* in hf for males and females (Tables 1, 7 and 8).

**Craniodental Characters.** *Antechinus minimus minimus* is smaller than *A. arktos* in absolute measurement for APV, PML, UML, LML and UPL for males and for APV, BL, Dent, M<sub>2</sub>W, PL, PML, UML, BuL, I<sup>1</sup>-P<sup>3</sup>, LML, M<sub>2</sub>W and UPL in females. *Antechinus minimus minimus* is significantly smaller than *A. arktos* in BL, Dent, PL, NWR, I<sup>1</sup>-P<sup>3</sup>, I<sub>1</sub>-P<sub>3</sub> and M<sub>2</sub>W in males and for I<sub>1</sub>-P<sub>3</sub> in females (Tables 1, 7 and 8).

**Comments.** *Antechinus minimus minimus* occurs throughout most of Tasmania (including southern Bass Strait Islands) whereas *A. arktos* is found on the border of Qld and NSW in the Tweed Volcano Caldera. Genetics: uncorrected pairwise difference at the mitochondrial gene CytB between *A. minimus minimus* and *A. arktos* is 9.2-10.4%.

*Antechinus minimus minimus* versus  
*Antechinus adustus* (Thomas)

**Pelage.** *Antechinus minimus minimus* has coarse fur and a leaden grey head that merges to brownish yellow fur on the rump and flanks whereas *A. adustus* has more uniformly dark brown fur with rusty tips on the head and back.

**External Measurements.** *Antechinus minimus minimus* is larger than *A. adustus* in absolute measurement for hb in females. *Antechinus minimus minimus* is significantly larger than *A. adustus* in wt and hb in males and for wt in females (Tables 1 and 8).

**Craniodental Characters.** *Antechinus minimus minimus* is larger than *A. adustus* in absolute measurement for APV, IOW, HT, HT-B, I<sub>1</sub>-P<sub>3</sub> in both sexes and for I<sup>1</sup>-P<sup>3</sup> in females only. *Antechinus minimus minimus* is significantly larger than *A. adustus* in BL, Dent, PL, PML, I<sup>1</sup>-P<sup>3</sup> and UPL for males and for PML and UPL in females. *Antechinus minimus minimus* is smaller than *A. adustus* in absolute measurement for M<sub>2</sub>W in females. *Antechinus minimus minimus* is significantly smaller than *A. adustus* in M<sub>2</sub>W and M<sub>2</sub>W in males and for M<sub>2</sub>W in females (Tables 1 and 8).

**Comments.** *Antechinus minimus minimus* occurs throughout most of Tasmania (including southern Bass Strait Islands) whereas *A. adustus* is found in the wet tropics of north-east Qld. Genetics: uncorrected pairwise difference at the mitochondrial gene CytB between *A. minimus minimus* and *A. adustus* is 14.3-15.7%.

*Antechinus minimus minimus* versus  
*Antechinus agilis* Dickman,  
Parnaby, Crowther and King

**Pelage.** *Antechinus minimus minimus* has coarse fur and a leaden grey head that merges to brownish yellow fur on the rump and flanks whereas *A. agilis* is a uniform medium grey to greyish brown from head to rump.

**External Measurements.** *Antechinus minimus minimus* is larger than *A. agilis* in absolute measurement for hb in females. *Antechinus minimus minimus* is significantly larger than *A. agilis* in wt, hb and hf in males and for wt and hf in females. *Antechinus minimus minimus* is significantly smaller than *A. agilis* in tv for males (Tables 1 and 8).

**Craniodontal Characters.** *Antechinus minimus minimus* is larger than *A. agilis* in absolute measurement for APV, PL, HT-B, I<sub>1</sub>-P<sub>3</sub> in males and for APV, IBW, IOW, HT, NWR, HT-B, I<sub>1</sub>-P<sub>3</sub>, I<sub>1</sub>-P<sub>3</sub> and UPL in females. *Antechinus minimus minimus* is significantly larger than *A. agilis* in BL, Dent, IBW, IOW, OBW, PPV, R-LC<sup>1</sup>, R-LM<sup>1</sup>T, HT, TC, NWR, PML, UML, I<sub>1</sub>-P<sub>3</sub>, I<sub>1</sub>-P<sub>3</sub>, LML and UPL in males and for BL, Dent and PL in females (Tables 1 and 8).

**Comments.** *Antechinus minimus minimus* occurs throughout most of Tasmania (including southern Bass Strait Islands) whereas *A. agilis* is known only from south-eastern Australia, south of around Sydney's (NSW) latitude. Genetics: uncorrected pairwise difference at the mitochondrial gene CytB between *A. minimus minimus* and *A. agilis* is 14.3-15.5%.

*Antechinus minimus minimus* versus  
*Antechinus argentus* Baker,  
Mutton and Hines

**Pelage.** *Antechinus minimus minimus* has coarse fur and a leaden grey head that merges to brownish yellow fur on the rump and flanks whereas *A. argentus* has a silvery head and neck that merge subtly to deep olive-buff coloured fur on the rump and flanks.

**External Measurements.** *Antechinus minimus minimus* is larger than *A. argentus* in absolute measurement for hb in males and for wt and hb in females. *Antechinus minimus minimus* is significantly larger than *A. argentus* in wt for males (Tables 1 and 8).

**Craniodontal Characters.** *Antechinus minimus minimus* is larger than *A. argentus* in absolute measurement for APV, IOW, HT, PL, HT-B, I<sub>1</sub>-P<sub>3</sub>, I<sub>1</sub>-P<sub>3</sub> for males and for APV, IOW, HT, HT-B, I<sub>1</sub>-P<sub>3</sub> and UPL in females. *Antechinus minimus minimus* is significantly larger than *A. argentus* in IBW for both sexes and for UPL in males only (Tables 1 and 8).

**Comments.** *Antechinus minimus minimus* occurs throughout most of Tasmania (including southern Bass Strait Islands) whereas *A. argentus* is known only from Kroombit Tops NP in south-east Qld. Genetics: uncorrected pairwise difference at the mitochondrial gene CytB between *A. minimus minimus* and *A. argentus* is 14.1-14.7%.

*Antechinus minimus minimus* versus  
*Antechinus bellus* (Thomas)

**Pelage.** *Antechinus minimus minimus* has coarse fur and a leaden grey head that merges to brownish yellow fur on the rump and flanks whereas *A. bellus* is pale to medium grey above, sometimes with a fawn tinge, with pale grey belly, hands and feet.

**External Measurements.** *Antechinus minimus minimus* is smaller than *A. bellus* in absolute measurement for tv and e in males and for e in females. *Antechinus minimus minimus* is significantly smaller than *A. bellus* in hf for males and for tv and hf in females (Tables 1 and 8).

**Craniodental Characters.** *Antechinus minimus minimus* is larger than *A. bellus* in absolute measurement for APV and IOW in males and for IBW, IOW and PPV in females. *Antechinus minimus minimus* is significantly larger than *A. bellus* in IBW, PPV, TC, HT-B and I<sub>1</sub>-P<sub>3</sub> in males and for APV, HT-B, I<sub>1</sub>-P<sub>3</sub> and UPL in females. *Antechinus minimus minimus* is smaller than *A. bellus* in absolute measurement for IPV, M<sup>2</sup>W, R-LC<sup>1</sup>, R-LM<sup>1</sup>, R-LM<sup>2</sup>, R-LM<sup>3</sup>, SWR-LC<sup>1</sup>B, BuL and M<sub>2</sub>W in males and for IPV, M<sup>2</sup>W, R-LC<sup>1</sup>, R-LM<sup>1</sup>, R-LM<sup>2</sup>, R-LM<sup>3</sup>, SWR-LC<sup>1</sup>B, UML, BuL, LML and M<sub>2</sub>W in females. *Antechinus minimus minimus* is significantly smaller than *A. bellus* in NW, OBW, R-LM<sup>1</sup>T, ZW, UML and LML in males and for BL, NW, OBW, R-LM<sup>1</sup>T and ZW in females (Tables 1 and 8).

**Comments.** *Antechinus minimus minimus* occurs throughout most of Tasmania (including southern Bass Strait Islands) whereas *A. bellus* is known only from northern Northern Territory. Genetics: uncorrected pairwise difference at the mitochondrial gene CytB between *A. minimus minimus* and *A. bellus* is 13.8-14.5%.

*Antechinus minimus minimus* versus  
*Antechinus flavipes flavipes* (Waterhouse)

**Pelage.** *Antechinus minimus minimus* has coarse fur and a leaden grey head that merges to brownish yellow fur on the rump and flanks whereas *A. flavipes flavipes* has a similarly coloured head and rump but with marked orange-tonings on the hands, feet and tail base as well as a pale eye ring.

**External Measurements.** *Antechinus minimus minimus* is significantly larger than *A. flavipes flavipes* for wt and hb in males and hb in females. *Antechinus minimus minimus* is significantly smaller than *A. flavipes flavipes* in e for females (Tables 1 and 8).

**Craniodental Characters.** *Antechinus minimus minimus* is larger than *A. flavipes flavipes* in absolute measurement for IOW and I<sub>1</sub>-P<sub>3</sub> for males and for APV, IOW, I<sub>1</sub>-P<sub>3</sub> and UPL for females. *Antechinus minimus minimus* is significantly larger than *A. flavipes flavipes* in APV, IBW, HT, TC, HT-B, I<sup>1</sup>-P<sup>3</sup> and UPL for males and for IBW, HT, TC, NWR, HT-B and

I<sup>1</sup>-P<sup>3</sup> in females. *Antechinus minimus minimus* is smaller than *A. flavipes flavipes* in absolute measurement for M<sup>2</sup>W and M<sub>2</sub>W in both sexes. *Antechinus minimus minimus* is significantly smaller than *A. flavipes flavipes* in IPV, NW, R-LC<sup>1</sup>, R-LM<sup>1</sup>, R-LM<sup>1</sup>T, R-LM<sup>2</sup>, R-LM<sup>3</sup>, SWR-LC<sup>1</sup>B, UML, BuL and LML in males and for IPV, R-LC<sup>1</sup>, R-LM<sup>1</sup>T, R-LM<sup>2</sup>, R-LM<sup>3</sup>, SWR-LC<sup>1</sup>B, UML, BuL and LML in females (Tables 1 and 8).

**Comments.** *Antechinus minimus minimus* occurs throughout most of Tasmania (including southern Bass Strait Islands) whereas *A. flavipes flavipes* occurs in a wide range of drier habitat in mainland south-east Australia. Genetics: uncorrected pairwise difference at the mitochondrial gene CytB between *A. minimus minimus* and *A. flavipes flavipes* is 15.1-16.5%.

*Antechinus minimus minimus* versus  
*Antechinus flavipes leucogaster* Gray

**Pelage.** *Antechinus minimus minimus* has coarse fur and a leaden grey head that merges to brownish yellow fur on the rump and flanks whereas *A. flavipes leucogaster* has a similarly coloured head and rump but with yellowish-brown fur on the hands, feet and tail base and a pale eyering.

**External Measurements.** *Antechinus minimus minimus* is significantly larger than *A. flavipes leucogaster* for wt and hb in both sexes. *Antechinus minimus minimus* is significantly smaller than *A. flavipes leucogaster* in e for females (Tables 1 and 8).

**Craniodental Characters.** *Antechinus minimus minimus* is larger than *A. flavipes leucogaster* in absolute measurement for APV, IOW and I<sub>1</sub>-P<sub>3</sub> for males and for APV and IOW for females. *Antechinus minimus minimus* is significantly larger than *A. flavipes leucogaster* in IBW, HT, PL, TC, NWR, HT-B, I<sup>1</sup>-P<sup>3</sup> and UPL for males and for IBW, HT, HT-B, I<sup>1</sup>-P<sup>3</sup>, I<sub>1</sub>-P<sub>3</sub> and UPL in females. *Antechinus minimus minimus* is smaller than *A. flavipes leucogaster* in absolute measurement for IPV, M<sup>2</sup>W, R-LM<sup>2</sup> and M<sub>2</sub>W in females only. *Antechinus minimus minimus* is significantly smaller than *A. flavipes leucogaster* in IPV, M<sup>2</sup>W, R-LM<sup>1</sup>, R-LM<sup>2</sup>, R-LM<sup>3</sup>, BuL and



M<sub>2</sub>W for males and for R-LM<sup>1</sup>, R-LM<sup>3</sup>, SWR-LC<sup>1</sup>B and BuL in females (Tables 1 and 8).

**Comments.** *Antechinus minimus minimus* occurs throughout most of Tasmania (including southern Bass Strait Islands) whereas *A. flavipes leucogaster* occurs in south-west Western Australia. Genetics: uncorrected pairwise difference at the mitochondrial gene CytB between *A. minimus minimus* and *A. flavipes leucogaster* is 12.6-14.5%.

#### *Antechinus minimus minimus* versus *Antechinus flavipes rubeculus* Van Dyck

**Pelage.** *Antechinus minimus minimus* has coarse fur and a leaden grey head that merges to brownish yellow fur on the rump and flanks whereas *A. flavipes rubeculus* has orange-reddish toned fur on the upper hind feet and tail base and a pale eyering.

**External Measurements.** *Antechinus minimus minimus* is significantly smaller than *A. flavipes rubeculus* in tv in both sexes (Tables 1 and 8).

**Craniodental Characters.** *Antechinus minimus minimus* is larger than *A. flavipes rubeculus* in absolute measurement for I<sub>1</sub>-P<sub>3</sub> in males and for APV in females. *Antechinus minimus minimus* is significantly larger than *A. flavipes rubeculus* in APV, IOW, HT-B and UPL for males and for IOW, HT-B and I<sub>1</sub>-P<sub>3</sub> in females. *Antechinus minimus minimus* is smaller than *A. flavipes rubeculus* in absolute measurement for IPV, M<sub>2</sub>W, R-LC<sup>1</sup>, R-LM<sup>1</sup>, R-LM<sup>2</sup>, SWR-LC<sup>1</sup>B, BuL and M<sub>2</sub>W in males and for IPV, M<sub>2</sub>W, R-LC<sup>1</sup>, R-LM<sup>1</sup>T, R-LM<sup>2</sup>, R-LM<sup>3</sup>, ZW, SWR-LC<sup>1</sup>B, UML, BuL, UML and M<sub>2</sub>W in females. *Antechinus minimus minimus* is significantly smaller than *A. flavipes rubeculus* in NW, OBW, R-LM<sup>1</sup>T, R-LM<sup>3</sup>, ZW, UML and LML in males and for BL, Dent, NW, OBW, R-LM<sup>1</sup> and PL in females (Tables 1 and 8).

**Comments.** *Antechinus minimus minimus* occurs throughout most of Tasmania (including southern Bass Strait Islands) whereas *A. flavipes rubeculus* is only found in the wet tropics of north-east Qld. Genetics: uncorrected pairwise difference at the mitochondrial gene CytB between *A. minimus minimus* and *A. flavipes rubeculus* is 15.1-16.3%.

#### *Antechinus minimus minimus* versus *Antechinus godmani* (Thomas)

**Pelage.** *Antechinus minimus minimus* has coarse fur and a leaden grey head that merges to brownish yellow fur on the rump and flanks whereas *A. godmani* is more uniformly brown on the head and back with a naked-looking tail.

**External Measurements.** *Antechinus minimus minimus* is smaller than *A. godmani* in absolute measurement in tv for males. *Antechinus minimus minimus* is significantly smaller than *A. godmani* in hf and e in males and for wt, tv, hf and e in females (Tables 1 and 8).

**Craniodental Characters.** *Antechinus minimus minimus* is larger than *A. godmani* in absolute measurement for APV in females. *Antechinus minimus minimus* is significantly larger than *A. godmani* in APV for males. *Antechinus minimus minimus* is smaller than *A. godmani* in absolute measurement for IPV, M<sub>2</sub>W, PL, TC, UML, LML and M<sub>2</sub>W in males and for BL, Dent, IPV, M<sub>2</sub>W, OBW, R-LM<sup>1</sup>T, R-LM<sup>2</sup>, R-LM<sup>3</sup>, ZW, PL, TC, UML, I<sup>1</sup>-P<sub>3</sub>, I<sub>1</sub>-P<sub>3</sub>, LML, M<sub>2</sub>W and UPL in females. *Antechinus minimus minimus* is significantly smaller than *A. godmani* in BL, Dent, IBW, OBW, R-LC<sup>1</sup>, R-LM<sup>1</sup>, R-LM<sup>1</sup>T, R-LM<sup>2</sup>, R-LM<sup>3</sup>, ZW, SWR-LC<sup>1</sup>B, I<sup>1</sup>-P<sub>3</sub> and UPL in males and for IBW, R-LC<sup>1</sup>, SWR-LC<sup>1</sup>B, PML, BuL and I<sub>1</sub>-P<sub>3</sub> in females (Tables 1 and 8).

**Comments.** *Antechinus minimus minimus* occurs throughout most of Tasmania (including southern Bass Strait Islands) whereas *A. godmani* is only found in the wet tropics of north-east Qld. Genetics: uncorrected pairwise difference at the mitochondrial gene CytB between *A. minimus minimus* and *A. godmani* is 15.0-16.7%.

#### *Antechinus minimus minimus* versus *Antechinus leo* Van Dyck

**Pelage.** *Antechinus minimus minimus* has coarse fur and a leaden grey head that merges to brownish yellow fur on the rump and flanks whereas *A. leo* is uniformly cinnamon on the head and back with slightly darkened hair forming a mid-dorsal head stripe.



**External Measurements.** *Antechinus minimus minimus* is smaller than *A. leo* in absolute measurement in tv for males and e in females. *Antechinus minimus minimus* is significantly smaller than *A. leo* in hf and e in males and for tv and hf in females (Tables 1 and 8).

**Craniodental Characters.** *Antechinus minimus minimus* is larger than *A. leo* in absolute measurement for IOW in males and for APV in females. *Antechinus minimus minimus* is significantly larger than *A. leo* in APV and I<sub>1</sub>-P<sub>3</sub> for males and for IOW in females. *Antechinus minimus minimus* is smaller than *A. leo* in absolute measurement for M<sup>2</sup>W, NW, OBW, R-LC<sup>1</sup>, R-LM<sup>1</sup>T, R-LM<sup>2</sup>, R-LM<sup>3</sup>, SWR-LC<sup>1</sup>B, UML, BuL, LML and M<sub>2</sub>W in males and for BL, Dent, IPV, M<sup>2</sup>W, OBW, R-LC<sup>1</sup>, R-LM<sup>1</sup>, R-LM<sup>1</sup>T, R-LM<sup>2</sup>, R-LM<sup>3</sup>, ZW, SWR-LC<sup>1</sup>B, TC, PML, UML, BuL, LML and M<sub>2</sub>W in females. *Antechinus minimus minimus* is significantly smaller than *A. leo* in BL, Dent, IBW, IPV, R-LM<sup>1</sup>, ZW, PL, TC, NWR and PML in males and for IBW, NW and PL in females (Tables 1 and 8).

**Comments.** *Antechinus minimus minimus* occurs throughout most of Tasmania (including southern Bass Strait Islands) whereas *A. leo* is known only from north of Princess Charlotte Bay, on Cape York Peninsula in far northern Qld. Genetics: uncorrected pairwise difference at the mitochondrial gene CytB between *A. minimus minimus* and *A. leo* is 13.4-15.1%.

#### *Antechinus minimus minimus* versus *Antechinus mysticus* Baker, Mutton and Van Dyck

**Pelage.** *Antechinus minimus minimus* has coarse fur and a leaden grey head that merges to brownish yellow fur on the rump and flanks whereas *A. mysticus* has a greyish-brown head and neck, merging gradually to yellowish-buff on the rump and flanks, with a buff-brown tail base and slightly darkened tip.

**External Measurements.** *Antechinus minimus minimus* is significantly larger than *A. mysticus* in wt, hb and hf for males and wt and hb in females. *Antechinus minimus minimus* is

significantly smaller than *A. mysticus* in tv for males and for e in females (Tables 1 and 8).

**Craniodental Characters.** *Antechinus minimus minimus* is larger than *A. mysticus* in absolute measurement for IOW, HT, HT-B and I<sub>1</sub>-P<sub>3</sub> in males and for APV, IOW, HT, HT-B and I<sub>1</sub>-P<sub>3</sub> in females. *Antechinus minimus minimus* is significantly larger than *A. mysticus* in APV, IBW, TC, I<sup>1</sup>-P<sup>3</sup> and UPL in males and for IBW, I<sup>1</sup>-P<sup>3</sup> and UPL in females. *Antechinus minimus minimus* is significantly smaller than *A. mysticus* in M<sup>2</sup>W, R-LC<sup>1</sup>, R-LM<sup>3</sup> and SWR-LC<sup>1</sup>B in males and for M<sup>2</sup>W, R-LC<sup>1</sup>, SWR-LC<sup>1</sup>B and BuL in females (Tables 1 and 8).

**Comments.** *Antechinus minimus minimus* occurs throughout most of Tasmania (including southern Bass Strait Islands) whereas *A. mysticus* occurs in scattered coastal populations between the Qld / NSW border in far south-east Qld and Eungella NP near Mackay in mid-east Qld. Genetics: uncorrected pairwise difference at the mitochondrial gene CytB between *A. minimus minimus* and *A. mysticus* is 14.5-15.2%.

#### *Antechinus minimus minimus* versus *Antechinus stuartii* Macleay

**Pelage.** *Antechinus minimus minimus* has coarse fur and a leaden grey head that merges to brownish yellow fur on the rump and flanks whereas *A. stuartii* is more uniformly brownish-grey from head to rump.

**External Measurements.** *Antechinus minimus minimus* is larger than *A. stuartii* in absolute measurement hb in both sexes. *Antechinus minimus minimus* is significantly larger than *A. stuartii* in wt for both sexes and hf for males only (Tables 1 and 8).

**Craniodental Characters.** *Antechinus minimus minimus* is larger than *A. stuartii* in absolute measurement for APV, IOW and HT-B for males and for APV, IOW, HT, HT-B, I<sup>1</sup>-P<sup>3</sup>, I<sub>1</sub>-P<sub>3</sub> and UPL in females. *Antechinus minimus minimus* is significantly larger than *A. stuartii* in BL, Dent, IBW, HT, PL, NWR, I<sup>1</sup>-P<sup>3</sup>, I<sub>1</sub>-P<sub>3</sub> and UPL for males and for BL, Dent, IBW, PL and NWR in females. *Antechinus minimus minimus*

is significantly smaller than *A. stuartii* in M<sup>2</sup>W for females only and for M<sub>2</sub>W in both sexes (Tables 1 and 8).

**Comments.** *Antechinus minimus minimus* occurs throughout most of Tasmania (including southern Bass Strait Islands) whereas *A. stuartii* occurs only on mainland Australia, in eastern NSW north of about Sydney to far south-east Queensland (Girraween NP, Lamington NP, Main Range NP, Springbrook NP and Tamborine NP). Genetics: uncorrected pairwise difference at the mitochondrial gene CytB between *A. minimus minimus* and *A. stuartii* is 12.1-14.9%.

*Antechinus minimus minimus* versus  
*Antechinus subtropicus*  
Van Dyck and Crowther

**Pelage.** *Antechinus minimus minimus* has coarse fur and a leaden grey head that merges to brownish yellow fur on the rump and flanks whereas *A. subtropicus* is more uniformly brownish from head to rump.

**External Measurements.** *Antechinus minimus minimus* is significantly larger than *A. subtropicus* in hb for females. *Antechinus minimus minimus* is significantly smaller than *A. subtropicus* in e for males only (Tables 1 and 8).

**Craniodental Characters.** *Antechinus minimus minimus* is larger than *A. subtropicus* in absolute measurement for IOW, IPV and I<sub>1</sub>-P<sub>3</sub> for males and for IOW, IPV, HT and HT-B in females. *Antechinus minimus minimus* is significantly larger than *A. subtropicus* in IBW, HT, HT-B and I<sup>1</sup>-P<sup>3</sup> for males and for I<sub>1</sub>-P<sub>3</sub> and UPL in females. *Antechinus minimus minimus* is smaller than *A. subtropicus* in absolute measurement for M<sup>2</sup>W and M<sub>2</sub>W in females only. *Antechinus minimus minimus* is significantly smaller than *A. subtropicus* in M<sup>2</sup>W, PPV and M<sub>2</sub>W for males and for PPV and SWR-LC<sup>1</sup>B in females (Tables 1 and 8).

**Comments.** *Antechinus minimus minimus* occurs throughout most of Tasmania (including southern Bass Strait Islands) whereas *A. subtropicus* occurs only on mainland Australia, from far south-east Queensland north to just

north of Gympie in south-east Queensland. Genetics: uncorrected pairwise difference at the mitochondrial gene CytB between *A. minimus minimus* and *A. subtropicus* is 14.3-15.2%.

## DISCUSSION

### Systematics and Biogeography

The phylogenies reconstructed here (Figs 7-8) provide evidence of 15 putative species in the genus *Antechinus*. Species delimitations based on DNA work are necessarily arbitrary, depending on the strength of monophyletic clade support and relative depth/divergence of clades; all proposed antechinus species clades were distinctly clustered, deeply divergent (5-15% pairwise divergence at mtDNA), bearing strongly supported nodes (0.99-1.00 posterior probabilities).

Our DNA data corroborate the findings of Armstrong *et al.* (1998), who found similarly deep levels of divergence (using combined mtDNA and nDNA) among various antechinus species, including: *A. swainsonii*, *A. minimus*, *A. leo*, *A. bellus*, *A. godmani*, *A. flavipes*, *A. agilis* and *A. stuartii*. The present study provides a comparative genetic analysis that encompasses a range of recently resolved antechinus taxa that could not be included in the earlier work: *A. adustus*, *A. subtropicus*, *A. mysticus*, *A. argentus*, *A. arktos*, *A. swainsonii* (Tas), *A. vandycki* (Tas), *A. mimeles insulanus* (Grampians, Vic) and both *A. minimus minimus* (Tas and southern Bass Strait Islands) and *A. m. maritimus* (Victoria) from a range of geographic locations.

Our DNA evidence of species distinction within the genus *Antechinus* is consistently corroborated by a suite of other data sources, including: morphology (pelage colour, body size and craniodentary), biogeography (allopatric separation and/or relatively deep divergence across limited geographic distance) and/or ecology/behaviour (differences in breeding timing for a genus where breeding is known to be highly synchronised annually within any given species and asymmetrical between sympatric congeners.).

Assessing all comparative data, we conclude the total evidence strongly supports the existence of 15 species of antechinus, including a single species of Swamp Antechinus, *A. minimus*, that is appropriately characterised into two subspecies, *A. m. minimus* (Tas and southern Bass Strait Islands) and *A. m. maritimus* (Vic, SA, and nearby offshore islands).

The (direct sequencing) genetic work presented here broadly corroborates the (allozyme) genetic work of Smith (1983), who examined electrophoretic variation in *A. minimus* across Bass Strait. He concluded that given a mean genetic distance of  $0.035 \pm 0.009$ , the trans-Bassian populations of *A. minimus* warranted their subspecific status. Our genetic phylogenies suggest that *A. minimus* is distinctly different (monophyletic) with respect to all congeners; there were distinct but moderate genetic (3.9–4.5% at mtDNA) differences between subspecies and notable genetic divergence within each subspecies (*A. m. minimus* 0–1.2%; *A. m. maritimus* 0–1.8%). In our genetic phylogenies, *A. minimus* was positioned in a large clade, together with all four species in the Dusky Antechinus complex, to the exclusion of all other antechinus, indicating that these taxa have shared a common ancestor some time in the past (see also Baker, Mutton, Mason & Gray, 2015). The present subspecies status for *A. m. minimus* and *A. m. maritimus* would seem appropriate because comparatively, across Bass Strait, the subspecies of *A. minimus* (3.9–4.5%) are morphologically only subtly divergent for craniodental characters, where there are no significant differences (see below), and only about half as genetically divergent as recognised species pairs within the Dusky Antechinus complex that are found in Victoria (*A. mimetes*) and Tasmania (*A. swainsonii*) (9.4–11.6%), where there were numerous significant (and absolute) morphological differences (refer Baker, Mutton, Mason & Gray 2015). This relative pattern was also recovered by Smith (1983), who found that electrophoretic variation in *A. minimus* and *A. swainsonii* across Bass Strait differed markedly, with mean genetic distances of  $0.035 \pm 0.009$  and  $0.085 \pm 0.015$ , respectively, prompting his suggestion at the time that subspecies status was

warranted in *A. minimus* and at least subspecies status was warranted for *A. swainsonii*.

The sampling of *A. minimus* in Smith's (1983) study included a couple of Tasmanian populations: Flinders Island (N=14) in the north and Bruny Island (N=13) in the south, compared to four populations on the mainland (Vic): Gembrook (N=1), Dartmoor (N=2), Cape Liptrap (N=7) and Cape Otway (N=10). Interestingly, Smith (1983) reported a mean genetic distance between the Flinders Island and Victorian *A. minimus* populations of  $0.007 \pm 0.010$ , whereas the mean distance between the Victorian and Bruny Island *A. minimus* populations was  $0.037 \pm 0.015$ ; the genetic distance between Flinders Island and Bruny Island was 0.029. Thus, Smith concluded that the Flinders Island population was significantly closer genetically to the Victorian populations than to the Bruny Island population and he cautiously referred the Flinders Island *A. minimus* to the mainland *A. minimus maritimus*. Smith's view contrasted with Johnston and Sharman's (1977, 1979) referral of the Flinders Island populations of *Potorous tridactylus* and *Macropus rufogriseus* to their respective Tasmanian subspecies, and the prevailing view that the fauna of the Bass Strait islands are primarily Tasmanian (Hope 1973). In this regard, the results of the present study also contrast with that of Smith, because we sampled several Flinders Island *A. minimus* and also two individuals from Sth Bruny Island and found that they both claded strongly together with all other Tasmanian samples in our (mtDNA and nDNA) phylogenies to the exclusion of mainland *A. m. maritimus*. Interestingly, in our study the Flinders Island samples were slightly (1.2%) divergent to all other Tasmanian samples, except the sample from the Gardens in north-east Tasmania (closest to Flinders Island), to which they were 0.8% divergent. And yet all Tasmanian samples showed similar divergence to Victorian (mainland) samples: Flinders Island to Victorian samples (4.3–4.5% divergent) and all other Tasmanian samples to all Victorian samples (3.9–4.5%). The slightly greater mtDNA genetic difference of Flinders Island samples compared with all other Tasmanian samples (taken from both north and south Tasmania)

observed here may explain why Smith recovered some distinct allozyme differences between Flinders Island and Bruny Island samples, but cannot explain why he found a relatively closer connection between Flinders Island and Victorian samples, since our Flinders Island and Victorian Swamp Antechinus were relatively deeply divergent (4.3-4.5%). Interestingly, the single morphological (skull) specimen from Flinders Island available for inclusion in our analysis, MVIC C21965, is a very large male, that exceeds both *A. minimus minimus* and *A. minimus maritimus* in most length and width measures. This animal may be an example of the 'island effect' where small mammals may evolve rapidly towards larger size under reduced predation and competition (see Foster, 1964; Lomolino, 1985, 2005; Millien & Damuth 2004; Sondaar 1991; Van Valen 1973), which can accelerate morphological evolution in mammals, when compared to mainland conspecifics, by up to 3-fold (Millien 2006). Similarly, we found relatively larger skulls in *A. minimus minimus* from Maatsuyker Island (5.5 km off the south coast of Tasmania) compared to *A. minimus minimus* from mainland Tasmania.

Taken together, our results suggest that Flinders Island and Maatsuyker Island *A. minimus* should be regarded as *A. minimus minimus*, along with the rest of the Tasmanian *A. minimus minimus*. While no genetic samples could be obtained from Waterhouse Island, the supposed type locality of *A. minimus minimus*, it seems likely they would clade genetically with other Tasmanian *A. minimus*, since the geographic range between our Flinders Island and the Gardens samples encapsulates Waterhouse Island, with Flinders Island lying about 70 km to its north-east and the Gardens just 50 km to its south-east. We were unable to include a comparative genetic sample of *A. minimus* from King Island, which lies to the north-west of Tasmania; however, one voucher specimen we examined was from Martha Lavinia Beach on King Island, 39°39'S 144°04'E (QVM 1986.1.52). The craniodental features of this specimen were consistent with Tasmanian *A. minimus minimus*, bearing large anterior palatal vacuities and narrower measures across

the snout and upper molar teeth, compared to mainland *A. minimus maritimus*. Thus, based on morphology of this specimen, King Island's geographic proximity (just 80 km off the Tasmanian north-west coast) and geological history (see below), it seems reasonable to assume these animals, like those on Flinders Island, are best considered *A. minimus minimus*. Recent work on the King Island Emu by Heupink *et al.* (2011) showed that models (Hope 1973; Lambeck & Chappell 2001) of sea level change indicate that Tasmania, including King and Flinders Islands, was isolated from the Australian mainland around 14,000 years ago. Up to several thousand years later, King Island (and presumably Flinders Island) was then separated from Tasmania. Heupink *et al.* suggested that initially a King Island/Tasmanian Emu population was isolated from the mainland taxon, after which the King Island and Tasmanian populations were separated. Our mtDNA results would suggest a similar evolutionary scenario for divergence initially between Tasmanian and mainland *A. minimus* (almost certainly predating physical continental separation) followed by Flinders Island (and likely King Island) *A. minimus* with Tasmanian *A. minimus*.

*Antechinus minimus maritimus* is also known from several neighboring islands off the south-east coast of Australia (Menkhorst & Seebeck 1999), including both Great Glennie Island and Kanowna Island, which are situated several kilometres off Wilson's Promontory (the southern tip of Victoria on mainland Australia); these islands have apparently been separated from mainland Australia for about 10,000 years (Wallis 1998) and the Swamp Antechinus found there have been purported as *A. m. maritimus* (Sale *et al.* 2006; Wainer 1976, 1978); we were unable to source genetic or morphological samples from either of these locations, but we assume them to be *A. m. maritimus* based on geographic proximity to the mainland and geological history; it would be interesting to see how genetically differentiated they are from Victorian populations of the subspecies.

*Antechinus minimus* is distinctly different in morphology compared with congeners. There

is sexual dimorphism for size, with males larger than females. Swamp Antechinus are leaden grey on the head and shoulders grading into rich yellowish brown on the rump and flanks; belly fur colour is greyish yellow or buff. The tail is short-haired, grizzled dark brown above, lighter below. The fur is coarse and grizzled; the foreclaws are long. The tail is short and the eyes and ears small. When compared with congeners, Swamp Antechinus are most similar, based on external body colouring (only), to *A. flavipes*. But *A. flavipes* have a marked pale eye ring, more orange-toned rump, fur on the feet and tail base, as well as a more marked darkened tail tip. The tail length is proportionately closer to head-body length in *A. flavipes*, compared with *A. minimus* and *A. minimus* is much more heavy-bodied than *A. flavipes*. In regard to their large body size, small ears and long claws on the forefeet, *A. minimus* are similar to members of the Dusky Antechinus complex.

Based on craniodontal features, *A. minimus* is distinctive from every species of antechinus but most similar to members of the Dusky Antechinus complex, with large skulls bearing moderate-long palatal vacuities and long, well-spaced premolar rows. Our morphological analyses corroborate the DNA data in finding subtle craniodontal differences between *A. m. minimus* and *A. m. maritimus*, where there were some size difference trends but none were significant. Specifically, *A. m. maritimus* tends to have a shorter tail and smaller feet than *A. m. minimus*. Also, *A. m. maritimus* tends to be larger than *A. m. minimus* for a range of craniodontal features associated with breadth of the skull across the snout (R-LM<sup>1</sup>T, R-LM<sup>2</sup>, R-LM<sup>3</sup>), width of molar teeth (M<sup>2</sup>W, M<sub>2</sub>W) and (to a lesser extent) length of molar row (UML, LML). These various size differences between *A. m. maritimus* and *A. m. minimus* are more pronounced in females than males, which is often the case in antechinus, because males vary more markedly in size range (both in overall body size and skulls) than females (see, for example, Baker, Mutton & Hines 2013; Baker, Mutton, Hines & Van Dyck, 2014; Baker, Mutton, Mason & Gray 2015; Baker, Mutton & Van Dyck 2012; Baker & Van Dyck 2012, 2013a,b).

*Antechinus m. maritimus* (Victoria) also tends to have smaller anterior palatal vacuities (APV) than *A. m. minimus* (Tasmania) (particularly in females). This morphological skull difference in APV is also notable in members of the Dusky Antechinus complex, which share similar biogeography and may co-occur with *A. minimus* on the mainland and Tasmania. Comparatively, in Tasmanian *A. swainsonii* and mainland *A. mimetes*, the former tend to have larger anterior palatal vacuities, together with narrower snouts and smaller molar teeth (Baker, Mutton, Mason & Gray 2015). The other Tasmanian Dusky Antechinus, *A. vandycki* from Tasman Peninsula, has even larger anterior palatal vacuities than *A. swainsonii* and is similarly less robust in skull breadth than the mainland *A. mimetes* (Baker, Mutton, Mason & Gray 2015). Such patterns of less robust skulls and longer anterior palatal vacuities in Tasmanian compared to mainland antechinus, while intriguing, are difficult to explain. Length of holes in the palate in fact varies among many species of dasyurid (Van Dyck, Gynther & Baker 2013). Archer (1981) speculated the size of palatal vacuities (and hypotympanic sinuses) in dunnarts (*Sminthopsis*) seemed, in general, to correlate with relative environmental aridity. This may relate to a rete-like exchange system at the interface between the narial and oral cavities via the soft tissue that spans the palatal cavities in the palatine, maxilla and premaxilla. Heat exchange was postulated to be involved, such that hot dry air breathed in by animals living in drier areas, would trigger increased evaporation within the oral cavity via the relatively larger palatal vacuities in the inland (more arid) species, which would in turn lower the temperature of the incoming air into the lungs, which itself in turn may result in less water being stripped out from the lungs on its way out. This interesting idea has never been formally tested, and it would probably be technologically difficult to do so (M. Archer, pers. comm.). In any case, such processes could not adequately explain the patterns observed here, since Tasmania tends to be both cooler and wetter than many mainland environments where *A. minimus maritimus* and *A. mimetes* occur, both of which exhibit the smaller incisive vacuities than their Tasmanian congeners (rather

than the larger maxillary/palatine vacuities observed in more arid-occurring *Smuntropsis*).

## Ecology

### *Antechinus minimus minimus*

**Distribution.** *Antechinus minimus minimus* is widely distributed in wet sedgeland and swampy drainage areas mainly throughout western Tasmania, where it has been found at altitudes ranging from sea level to 1000 m (Green 1972). It occurs in habitats containing dominant species such as: button grass *Mesomelaena sphaerocephala* in association with *Calorophus lateriflorus*, *Restio australis* and *Lepidosperma filiforme*. Rainforest ecotonal and regrowth habitats occupied by *A. m. minimus* are characterised by *Glania trifida*, *Sprengelia incarnata*, *Epacris gunnii*, *Monotoca* sp., *Boronia rhomboidea*, *Leptospermum* sp., *Gleichenia alpina*, *Casuarina thystyla*, *Eucalyptus gunnii* and *Poa caespitosa*. According to Green (1972), sphagnum moss bogs are also a preferred habitat. Green also notes that throughout its range, rainfall may average in excess of 250 cm p.a. and temperatures may vary from as low as -12°C in subalpine habitat to 35°C on the coast. *Antechinus m. minimus* may often be confined under snow drifts for weeks at a time.

**Reproduction.** Wakefield and Warneke (1963) and Green (1972) report a nipple number of six for *A. minimus minimus* (although one female held in the QVM confirmed by AMB had 8 young). Green (1972) reported a female with pouch young collected 6 December 1964 and suggested a breeding period from September to the end of December.

Little is known of diet or movement/range in *A. minimus minimus* populations. The status of this subspecies on Tasmania is regarded as secure because it occurs widely, and sometimes in apparent high density, across a range of habitats throughout much of Tasmania and the southern Bass Strait Islands.

### *Antechinus minimus maritimus*

**Distribution.** Because of its affinity for dense wet heath, tussock grass and sedgeland *A.*

*minimus maritimus* occurs in a patchy, near-coastal distribution from south-eastern Victoria (Sunday Island) west to Robe in the south-eastern district of South Australia (Menkhorst 1995; Finlayson 1958). In Victoria, it may be found in both treeless vegetation and forests with a wet heath understorey (Wainer & Gibson 1976; Menkhorst & Beardsell, 1982) provided a dense ground cover is present for one or two metres above the ground. In south-western heaths, it has been found in areas that receive over 650 mm rainfall per year, where dominant species of vegetation included *Leptospermum myrsinoides*, *Xanthorrhoea minor*, *Banksia marginata*, *Melaleuca squarrosa*, *Sprengelia incarnata*, *Eucalyptus baxteri*, *Leptocarpus tenax* and *Allocasuarina paludosa* (Menkhorst 1995; Menkhorst & Beardsell 1982). In south-eastern heaths (Great Glennie Island), upper stratum species included *Banksia marginata*, *Leptospermum laevigatum*, *Correa alba*, *Olearia philloggopappa* and *Myoporum laetifolium* with an understorey of *Poa poiformis* (Wainer 1976). *Antechinus minimus maritimus* is found in high density on the 60-ha Great Glennie Island, 6km west of Wilson's Promontory (the southern tip of Victoria) where it co-occurs with *Rattus fuscipes* (Wainer 1976, 1988) and also in high density on the 31-ha Kanowna Island, situated about 5km south-east of Great Glennie Island, where it is apparently the sole mammal species (Sale *et al.* 2006).

**Reproduction.** Ovulation and mating are synchronised but may occur a month later at Anglesea and Great Glennie Island than in the Wannon region (Wilson 1986). Earliest matings have been recorded in May and extend through to July. Young are born in July and August (Wilson 1986; Wilson & Bourne 1984; Wilson *et al.* 1990). All males succumb to a post-mating die-off, parturition occurs 28-32 days after mating and only a few females live through a second year. Females possess eight nipples (Wainer & Wilson 1995).

**Diet.** In one study, the diet of Swamp Antechinus on Kanowna Island was found to include a wide variety of prey. Remains of insect larvae, beetles, spiders, flies and ants were frequently



identified items in the scats of trapped animals; centipedes, scorpions, grasshoppers and lizards were also occasionally found to occur in Swamp Antechinus scats (Allison *et al.* 2006; Sale *et al.* 2006). Similarly, a wide variety of arthropods were found in the scats of individuals from a mainland population in the Otway Ranges, and on Great Glennie Island. This large variety of prey items would suggest *A. minimus* is a generalist species. The study on Kanowna Island found a high incidence of moth larvae in the *A. minimus* diet; moth larvae remains were found in about 95% of scats between August and October. Interestingly, even though this frequency of moth prey items fell in November and January, larvae were still the most important prey item in the diet, in terms of number, bulk and frequency (Sale *et al.* 2006; Wainer 1976, 1988).

**Movements.** In the eastern Otway Ranges of Victoria, the dispersal of nine litters of pouch young ( $n = 62$ ) was assessed following two breeding seasons. Young males were found to remain on the natal site until December–January, dispersing before the breeding season. New males entered the population between January and June. More than 50% of females were residents at the study site and remained there to breed; the remaining females were trapped a single time. After the male die-off, movements of pregnant females increased, appearing to expand their home ranges. *Antechinus minimus* exhibits philopatry of females and dispersal of males, as observed in other *Antechinus* species. However, most antechinus disperse abruptly after weaning, whereas the Otways population of Swamp Antechinus were found to disperse 2–3 months after weaning (Magnusdottir *et al.* 2008).

**Conservation.** The preferred habitat of *A. minimus maritimus* is limited, so the Swamp Antechinus is patchily distributed and considered sensitive to human disturbance, particularly land clearance and urban development. *Antechinus minimus* prefers late successional vegetation; it is noteworthy that some populations were eliminated by bushfire in the eastern Otway Ranges, Victoria, and have unfortunately taken 20 years to re-establish (Wilson & Bachmann

2008; Wilson *et al.* 2001). Current threats to the species are habitat and population fragmentation, drainage of swamp habitat and frequent fire. Peak density of *A. minimus maritimus* in the eastern Otways area is 1–30 animals ha<sup>-1</sup>. Comparatively, maximum densities at Walkerville in south Gippsland were estimated at 10 animals ha<sup>-1</sup>. This in turn is in contrast to the islands off Wilsons Promontory, such as Great Glennie Island and Kanowna Island, where astonishing densities of 80 and 98 animals ha<sup>-1</sup>, respectively, have been recorded. Such high densities on islands are well known among small mammals and have mainly been attributed to less interspecific competition and predation than is experienced by mainland populations (Gibson *et al.* 2004; Magnusdottir *et al.* 2008; Sale *et al.* 2006; Wilson & Bachmann 2008; Wilson *et al.* 2001).

## ACKNOWLEDGEMENTS

We are grateful to Harry Hines (QPWS) and Ian Gynther (EHP) for generous loan of Elliott traps to catch antechinus. We warmly thank Thomas Mutton, Gene Mason, Emma Gray and Hannah Maloney (QUT) for their sterling help on successive field trips in search of *A. minimus*. Mike Driessen (DPIPWE) provided invaluable advice, logistical support and ear clips of *A. minimus*. Billie Lazenby (DPIPWE) kindly furnished ear clips of Tasmanian *A. minimus*. ABRS (Australian Government) funded the trips to the Tasmania wilderness areas.

Grants from the Joyce W. Vickery Scientific Research Fund (Linnean Society of New South Wales), the Ethel Mary Read Research Grant (Royal Zoological Society of New South Wales) and financial support from the Queensland Museum Board of Trustees allowed SVD to examine overseas type and comparative material. SVD gratefully acknowledges the help and hospitality of Paulina Jenkins (Natural History Museum, London).

QUT supported AMB's sabbatical, where he spent a month happily ensconced in the British Museum of Natural History's (BMNH) extensive type collection where he was hosted

by Roberto Portela Miguez and also in the MNHN of Paris, where he was hosted by Cecile Callou. Cecile kindly photographed the type specimens of *A. minimus* held in the MNHN collection. AMB thanks David Maynard and Craig Reid (QVM, Launceston) for making him welcome and providing unreserved access to their antechinus collection. AMB thanks Heather Janetzki (QM) for her help in acquiring loans generously provided by staff at Tasmanian Museum and Art Gallery, MVIC and the SAM. AMB thanks Jesse Rowland and Tyrone Lavery for providing comparative congeneric specimens to include in the analyses. We thank two anonymous reviewers who made very helpful comments on the manuscript.

## LITERATURE CITED

- Allison, L.M., Gibson, L.A. & Aberton, J.G. 2006. Dietary strategy of the Swamp Antechinus (*Antechinus minimus maritimus*) (Marsupialia: Dasyuridae) in coastal and inland heath habitats. *Wildlife Research* 33: 67-76 <http://dx.doi.org/10.1071/WR05038>.
- Archer, M. 1974. The development of cheek teeth in *Antechinus flavipes* (Marsupialia, Dasyuridae). *Journal of the Royal Society of Western Australia* 57: 54-63.
1976. The dasyurid dentition and its relationships to that of didelphids, thylacinids, borhaenids (Marsupicarnivora) and peramelids (Peramelina: Marsupialia). *Australian Journal of Zoology Supplementary Series* 39:1-34 <http://dx.doi.org/10.1071/AJZS039>.
1981. Results of the Archbold Expeditions. No. 104. Systematic revision of the marsupial dasyurid genus *Sminthopsis* Thomas. *Bulletin of the American Museum of Natural History* 168: 61-224.
- Armstrong, L.A., Krajewski, C. & Westerman, M. 1998. Phylogeny of the dasyurid marsupial genus *Antechinus* based on cytochrome-b, 12S-rRNA, and protamine-P1 genes. *Journal of Mammalogy* 79: 1379-1389 <http://dx.doi.org/10.2307/1383028>.
- Baker, A.M., Mutton, T.Y. & Hines, H.B. 2013. A new dasyurid marsupial from Kroombit Tops, south-east Queensland, Australia: the Silver-headed Antechinus, *Antechinus argentus* sp. nov. (Marsupialia: Dasyuridae). *Zootaxa* 3746(2): 201-239 <http://dx.doi.org/10.11646/zootaxa.3746.2.1>.
- Baker, A.M., Mutton, T.Y., Hines, H.B. & Van Dyck, S. 2014. The Black-tailed Antechinus, *Antechinus arktos* sp. nov.: a new species of carnivorous marsupial from montane regions of the Tweed Volcano caldera, eastern Australia. *Zootaxa* 3765(2): 101-133 <http://dx.doi.org/10.11646/zootaxa.3765.2.1>.
- Baker, A.M., Mutton, T.Y., Mason, E.D. & Gray, E.L. 2015. A new species (*Antechinus vandyckii*) and an elevation to species (*Antechinus minetes*) within the Australian Dusky Antechinus complex. *Memoirs of the Queensland Museum - Nature*. 59: 75-126 <http://dx.doi.org/10.17082/j.2204-1478.59.2015.2014-10>.
- Baker, A.M., Mutton, T.Y. & Van Dyck, S. 2012. A new dasyurid marsupial from eastern Queensland, Australia: the Buff-footed Antechinus, *Antechinus mysticus* sp. nov. (Marsupialia: Dasyuridae). *Zootaxa* 3515: 1-37.
- Baker, A.M., & Van Dyck, S. 2012. Taxonomy and redescription of the Fawn Antechinus, *Antechinus bellus* (Thomas) (Marsupialia: Dasyuridae). *Zootaxa* 3613: 201-228.
- 2013a. Taxonomy and redescription of the Yellow-footed Antechinus, *Antechinus flavipes* (Waterhouse) (Marsupialia: Dasyuridae). *Zootaxa* 3649: 1-62. <http://dx.doi.org/10.11646/zootaxa.3649.1.1>.
- 2013b. Taxonomy and redescription of the Atherton Antechinus, *Antechinus godmani* (Thomas) (Marsupialia: Dasyuridae). *Zootaxa* 3670: 401-439 <http://dx.doi.org/10.11646/zootaxa.3670.4.1>.
- Baverstock, P.R., Archer, M., Adams, M. & Richardson, B.J. (1982). Genetic relationships among 32 species of Australian dasyurid marsupials. Pp. 641-650. In, Archer, M. (ed) *Carnivorous Marsupials* (Royal Zoological Society of New South Wales: Sydney).
- Desmarest, A.G. 1818. *Nouveau Dictionnaire d'Histoire Naturelle* (Nouv. Edn. Paris: Deterville Tom. 25 ed).
- Dickman, C.R., H.E. Parnaby, Crowther, M.S. & King, D.H. 1998. *Antechinus agilis* (Marsupialia: Dasyuridae), a new species from the *A. stuartii* complex in south-eastern Australia. *Australian Journal of Zoology* 46: 1-26. <http://dx.doi.org/10.1071/ZO97036>.
- Finlayson, H.H. 1958. A case of duplex convergence in Australian mammals, with a review of some aspects of the morphology of *Phascogale* (Antechinus) *swainsonii* Waterhouse and *Phascogale* (Antechinus) *flavipes* Waterhouse. *Proceedings of the Royal Society of South Australia* 81: 141-151.
- Foster, J.B. 1964. Evolution of mammals on islands. *Nature* 202: 234-235. <http://dx.doi.org/10.1038/202234a0>.
- Geoffroy [Saint Hilaire], É. 1803. Note sur les espee du genre dasyure. *Bulletin des Sciences par la Societe Philomathique de Paris* 3(81): 258-259.
- Gibson, L.A., Wilson, B.A., Cahill, D.M. & Hill, J. 2004. Modelling habitat suitability of the swamp antechinus (*Antechinus minimus maritimus*)



- in the coastal heathlands of southern Victoria. *Australian Biological Conservation* **117**: 143–50. [http://dx.doi.org/10.1016/S0006-3207\(03\)00288-X](http://dx.doi.org/10.1016/S0006-3207(03)00288-X).
- Gray, J.E. 1841. Contributions toward the geographical distribution of the Mammalia of Australia, with notes on some recently discovered species. Appendix C, pp. 397–414. In, Grey, G. (ed), *Journal of Two Expeditions of discovery in North-west and Western Australia, During the Years 1837, 38, and 39, Under the Authority of Her Majesty's Government*. Vol. 2 (T & W Boone: London).
- Green, R.H. 1972. The murids and small dasyurids in Tasmania. Parts 5 and 6. *Records of the Queen Victoria Museum* No. 46.
- Heupink T.H., Huynen L. & Lambert D.M. 2011. Ancient DNA Suggests Dwarf and 'Giant' Emu Are Conspecific. *PLoS ONE* **6**(4): e18728. <http://dx.doi.org/10.1371/journal.pone.0018728>.
- Hope, J. 1973. Mammals of the Bass Strait islands. *Proceedings of the Royal Society of Victoria* **85**: 163–196.
- Iredale, T. & Troughton, E. 1934. A check-list of the mammals recorded from Australia. *Memoirs of the Australian Museum* **6**: 1–122. <http://dx.doi.org/10.3853/j.0067-1967.6.1934.516>.
- Jenkins, P.D. & Knutson, L. 1983. *A catalogue of the type specimens of Monotremata and Marsupialia in the British Museum (Natural History)*. (Trustees of the British Museum (Natural History): Great Britain).
- Johnston, P.G. & Sharman, G.B. 1977. Studies on populations of Potorous Desmarest (Marsupialia). I. Electrophoretic, chromosomal and breeding studies. *Australian Journal of Zoology* **25**: 433–747. <http://dx.doi.org/10.1071/zo9770733>.
- Johnston, P.G. & Sharman, G.B. 1979. Studies on the red-necked wallaby *Macropus rufogriseus* (Desmarest). *Australian Journal of Zoology* **27**: 433–443. <http://dx.doi.org/10.1071/ZO9790433>.
- Julien-Laferrriere, D. 1994. Catalogue des types de marsupiaux (Marsupialia) du Museum National D'Histoire Naturelle, Paris. *Mammalia* **58**(1): 1–39. <http://dx.doi.org/10.1515/mamm.1994.58.1.1>.
- Krajewski, C., Blacket, M., Buckley, L., & Westerman, M. 1997. A multigene assessment of phylogenetic relationships within the dasyurid marsupial subfamily Sminthopsinae. *Molecular Phylogenetics and Evolution* **8**: 236–248. <http://dx.doi.org/10.1006/mpev.1997.0421>.
- Lambeck, K. & Chappell, J. 2001. Sea level change through the last glacial cycle. *Science* **292**: 679. <http://dx.doi.org/10.1126/science.1059549>.
- Lomolino, M.V. 1985. Body size of mammals on islands: The island rule reexamined. *American Naturalist* **125**: 310–316. <http://dx.doi.org/10.1086/284343>.
2005. Body size evolution in insular vertebrates: Generality of the island rule. *Journal of Biogeography* **32**: 1683–1699.
- Mahoney, J.A. & Ride, W.D.L. 1988. Dasyuridae. Pp. 14–33. In, Walton, D.W. (ed) *Zoological Catalogue of Australia*. Vol. 5. (Australian Government Publishing Service: Canberra).
- Magnusdottir, R., Wilson, B.A. & Hersteinsson, P. 2008. Dispersal and the influence of rainfall on a population of the carnivorous marsupial Swamp Antechinus (*Antechinus minimus maritimus*). *Wildlife Research* **35**: 446–454. <http://dx.doi.org/10.1071/WR06156>.
- Marlow, B. 1961. Reproductive behaviour of the marsupial mouse, *Antechinus flavipes* (Waterhouse) (Marsupialia) and the development of the pouch young. *Australian Journal of Zoology* **9**: 203–220. <http://dx.doi.org/10.1071/ZO9610203>.
- Menkhorst, P. (ed) 1995. *Mammals of Victoria*. (Oxford University Press Australia: Melbourne).
- Menkhorst, P.W. & Beardsell, C.M. 1982. Mammals of southwestern Victoria from the Little Desert to the coast. *Proceedings of the Royal Society of Victoria* **94**: 221–247.
- Menkhorst, P. & Seebeck, J. 1999. A list of native mammals of Wilsons Promontory National Park. *Victorian Naturalist* **116**: 26–27.
- Millien, V. 2006. Morphological evolution is accelerated among island mammals. *PLoS Biology* **4**(10): e321: 1863–1868.
- Millien, V. & Damuth, J. 2004. Climate change and size evolution in an island rodent species: New perspectives on the island rule. *Evolution* **58**: 1353–1360. <http://dx.doi.org/10.1111/j.0014-3820.2004.tb01713.x>.
- Mutton, T.Y. 2011. Systematics and Evolution of the Dasyurid Marsupial Genus *Antechinus*. Honours Thesis, (Queensland University of Technology: Brisbane) 65 pp.
- Peron, F. *Antechinus* 1807. *Voyage de decouvertes aux Terres Australes, sur les corvettes la Geographie, le Naturaliste, et la goelette le Casuarina, 1800–4'*. Vol. 1. Paris.
- Ridgway, R. 1912. *Colour Standards and Nomenclature*. (Published by the Author, United States National Museum) 43 pp.
- Ronquist, F. & Huelsenbeck, J.P. 2003. MRBAYES 3: Bayesian phylogenetic inference under mixed models. *Bioinformatics* **19**: 1572–1574. <http://dx.doi.org/10.1093/bioinformatics/btg180>.
- Sale, M.G., Ward, S.J. & Arnould, J.P.Y. 2006. Aspects of the ecology of swamp antechinus (*Antechinus minimus maritimus*) on a Bass Strait island. *Wildlife Research* **33**: 215–221. <http://dx.doi.org/10.1071/WR05051>.

- Smith, A.M.A. 1983. The subspecific biochemical taxonomy of *Antechinus minimus*, *A. swainsonii* and *Sminthopsis leucopus* (Marsupialia: Dasyuridae). *Australian Journal of Zoology* 32: 753-762. <http://dx.doi.org/10.1071/ZO9830753>.
- Sondaar, P.Y. 1991. Island mammals of the past. *Science Progress* 75: 249-264.
- Soderquist, T.R. 1995. Ontogeny of sexual dimorphism in size among polytocous mammals: tests of two carnivorous marsupials. *Journal of Mammalogy* 76: 376-390. <http://dx.doi.org/10.2307/1382349>.
- Statsoft, Inc. 2004. STATISTICA (data analysis software system), version 7.
- Tate, G.H.H. 1947. Results of the Archbold Expeditions. No. 56. On the anatomy and classification of the Dasyuridae (Marsupialia). *Bulletin of the American Museum of Natural History* 88: 101-155.
- Van Dyck, S. 2002. Morphology-based revision of Murexia and Antechinus (Marsupialia: Dasyuridae). *Memoirs of the Queensland Museum* 48: 239-330.
- Van Dyck, S.M. & Crowther, M.S. (2000). Reassessment of northern representatives of the *Antechinus stuartii* complex (Marsupialia: Dasyuridae): *A. subtropicus* sp. nov. and *A. adustus* new status. *Memoirs of the Queensland Museum* 45(2): 611-635.
- Van Dyck, S., Gynther, I. & Baker, A.M. 2013. *Field companion to the mammals of Australia*. (New Holland: Australia).
- Van Valen, L. 1973. Pattern and the balance of nature. *Evolutionary Theory* 1: 31-49.
- Wakefield, N.A. & Warneke, R.M. 1963. Some revision in Antechinus (Marsupialia) 1. *Victorian Naturalist* 80: 192-219.
- Wainer, J. W. 1976. Studies of an island population of *Antechinus minimus* (Marsupialia: Dasyuridae). *Australian Zoologist* 19: 1-7.
1988. Ecological studies of island and mainland populations of *Rattus fasciipes* and *Antechinus minimus* in coastal heathland in southern Victoria. Ph. D. Thesis (Unpub.) University of Melbourne.
- Wainer, J.W. & Gibson, R.J. 1976. Habitat of the Swamp Antechinus in Victoria. *Victorian Naturalist* 93: 253-255.
- Wainer, J.W. & Wilson, B.A. 1995. Swamp Antechinus *Antechinus minimus*. Pp. 93-94. In, Strahan, R. (ed), *The Mammals of Australia* (Reed Books: Chatswood).
- Wallis, G. 1998. The geology of Wilsons Promontory. *Victorian Naturalist* 115: 300-306.
- Williams, R. & Williams, A. 1982. The life cycle of *Antechinus swainsonii* (Dasyuridae, Marsupialia). Pp. 91-95. In, Archer, M. (ed) *Carnivorous Marsupials*. (Royal Zoological Society of New South Wales: Sydney).
- Wilson, B.A. 1986. Reproduction in the female dasyurid *Antechinus minimus maritimus* (Marsupialia, Dasyuridae). *Australian Journal of Zoology* 34: 189-97. <http://dx.doi.org/10.1071/ZO9860189>.
- Wilson, B. A., Aberton, J. & Reichl, T. 2001. Effects of fragmented habitat and fire on the distribution and ecology of the Swamp Antechinus (*Antechinus minimus maritimus*) in the Eastern Otways, Victoria. *Wildlife Research* 28: 527-36. <http://dx.doi.org/10.1071/WR00016>.
- Wilson, B.A. & Bachmann, M.R. 2008. Swamp Antechinus *Antechinus minimus*. In, Van Dyck, S. & Strahan, R. (eds) *Mammals of Australia* (3rd edition). (New Holland: Australia).
- Wilson, B.A. & Bourne, A.R. 1984. Reproduction in the male dasyurid *Antechinus minimus* (Marsupialia: Dasyuridae). *Australian Journal of Zoology* 32: 311-318. <http://dx.doi.org/10.1071/ZO9840311>.
- Wilson, B.A., Robertson, D., Moloney, D.J., Newell, G.R. & Laidlaw, W.S. 1990. Factors affecting small mammal distribution and abundance in the eastern Otway Ranges, Victoria. Pp.379-396. In, Saunders, D.A., Hopkins, A.J.M. & How, R.A. (eds), *Australian Ecosystems: 200 Years of Utilisation, Degradation and Reconstruction* (Surrey Beatty & Sons, and Ecological Society of Australia: Sydney).
- Waterhouse, G.R. 1840. Description of a new marsupial mammal belonging to the genus Phascogale. *Magazine of Natural History* 2(4): 299.
1841. Marsupialia or Pouched Animals. *Mammalia*. Vol. XI. Pp. 1-323. In, Jardine W. (ed), *The Naturalist's Library* Vol. XXIV. (W.H. Lizars: Edinburgh).
1846. *A Natural History of Mammalia*. Vol 1. Containing the Order Marsupialia, or pouched animals. (Bailliere: London).

# A new species of *Diplotrema* (Acanthodrilinae, Metagynophora, Crassiclitellata, Oligochaeta) from the Einasleigh Uplands Bioregion of Queensland

**B.G.M. JAMIESON**

Emeritus Professor, Department of Zoology and Entomology, School of Biological Sciences, University of Queensland, Brisbane 4072 Qld. Honorary Associate, Queensland Museum. Email: b.Jamieson@uq.edu.au

**K.R. McDONALD**

Honorary Research Fellow, Queensland Museum, Natural Environments Programme Southbank, 4101, Queensland, Australia

**Sam JAMES**

Adjunct Associate Professor, Department of Biology, 143 Biology Building, University of Iowa, Iowa City, Iowa 52242-1324, USA

Citation: Jamieson B.G.M., McDonald, K.R. & James, S. 2015 A new species of *Diplotrema* (Acanthodrilinae, Metagynophora, Crassiclitellata, Oligochaeta) from the Einasleigh Uplands Bioregion of Queensland. *Memoirs of the Queensland Museum – Nature* 59: 171-176. Brisbane. ISSN 2204-1478 (Online), ISSN 0079-8835 (Print). Accepted: 24 November 2014. First published online: 14 August 2015.

<http://dx.doi.org/10.17082/j.2204-1478.59.2015.2014-12>

LSID urn:lsid:zoobank.org:pub:13698CC3-FCB7-493C-A73A-1D8FD9ECF273

## ABSTRACT

Descriptions are provided of a new species of Acanthodrilinae, *Diplotrema anomala*, with anomalous segmentation. □ new species, *Diplotema*, Queensland.

This account of a new species of the earthworm genus *Diplotrema*, collected in the Australian Einasleigh Uplands Bioregion in March 2007, augments the CD of Dyne and Jamieson (2004), on all known *Acanthodrilinae* (Megascolecidae) of Australia. The specimens were collected as part of an ongoing study of molecular phylogeny of the Oligochaeta.

The Acanthodrilinae + Megascolecinae were shown to be jointly part of the sister group of Ocnerodrilidae in the molecular analysis of Jamieson *et al.* (2002). Therefore, as the familial status of the Ocnerodrilidae was accepted, the former two groups were correctly accorded subfamilial status. However, Csuzdi and Mischis (2010) accord familial rank, as the

Acanthodrilidae. In a molecular investigation of earthworm phylogeny James and Davidson (2012) advocated an Acanthodrilidae *sensu lato* that corresponded to the Acanthodrilinae *sensu* Jamieson (2000, 2001) and Jamieson and Ferraguti (2006). This concept of Acanthodrilidae suppressed the Octochaetidae and Exxidae in the Acanthodrilidae, and recognised within it the subfamily Benhamiinae. These changes, including rejection of the Octochaetidae, as in Dyne and Jamieson (2004), are accepted here but subfamilial rank for the Acanthodrilinae is retained as the molecular analysis confirmed the sister status of the family Ocnerodrilidae relative to the Megascolecidae *sensu lato*.

## Acanthodrilinae

### *Diploptrema* Spencer, 1900

**Type species.** *Diploptrema fragilis* Spencer, 1900: 31 (Gayndah, Queensland).

*Eodrilus* Michaelsen, 1907: 141. (Australian species only).

*Diploptrema*; (part. excluding *Notiodrilus* and *Microscolex*) Jamieson, 1971: 100–102.

*Microscolex* (*Diploptrema*); Jamieson and Dyne, 1976: 447–448.

*Diploptrema*; Dyne, 1987, 1997: 1; Dyne and Jamieson, 1998: 487–493.

Dyne and Jamieson, 2004: 20.

**Generic Diagnosis.** Setae 8 per segment. Prostates 2 pairs, tubular, rarely tubuloracemose to racemose, their pores on XVII and XIX; rarely a single pair, on XVII; male pores a single pair, on XVIII, occasionally in 17/18, or rarely, combined with the prostatic pores on XVII; exceptionally, with prostatic pores in XVII, and male pores at 17/18 or (*D. anomala*), where I and II are fused, appearing to be translocated forward by one segment. Spermathecal pores 2 pairs, at 7/8 and 8/9, ventrolateral, or a single pair at 8/9; rarely transposed to 8/9 and 9/10; exceptionally (*D. anomala*) appearing to lie in 6/7 and 7/8. Nephropores in a single series on each side, or, exceptionally, alternating regularly between *cd* and a point far dorsal of *d*. Gizzard usually well developed, muscular, in V (or, rarely, in VI). Calciferous glands present or absent. Holonephric, avesiculate. Holandric or rarely metandric. Testis-sacs absent. Penial setae invariably present; genital setae usually present. Nephridial bladders absent.

**Distribution.** *Australia*: coastal and adjacent inland Queensland; ranging from the vicinity of Narrabri in New South Wales to northern Queensland and across northern Australia to the Kimberley region of Western Australia; with a single species in south-western Australia. The precise northerly limit of the genus in Cape York Peninsula is unknown, the most northerly record being from the vicinity of Weipa. It is thus uncertain whether *Diploptrema* is replaced by the meronephric *Neodiploptrema* further northwards. However, the two genera are sympatric in the Cape Melville National Park and McIlwraith Range (Jamieson 1997; Dyne 1997). *Extralimital*: Two Mexican acanthodrilids with a single gizzard but otherwise referable to

*Diplocardia* were reasonably placed by James (1990) in *Diploptrema* on morphological grounds but their close relationship to Australian species is questionable. Fragoso and Rojas (1994) have erected *Kaxdrilus* for *Diploptrema*-like species of Mexico and Central America with calciferous glands in the region of VII–XII but it is perhaps questionable that the ‘pebbly internal texture’ in this region in the two species of James (1990) qualifies to be considered calciferous.

For keys to species, see Dyne and Jamieson (2004). The new species is distinguished from all other species of *Diploptrema* in fusion of the peristomium and first setigerous segment so that the prostate pores are in patent segments XVI and XVIII. However, in the following account and illustrations the fused peristomium and first setigerous segment is designated I & II and the segments of the prostate porophores are designated XVII and XIX, as usual for acanthodrilids.

### *Diploptrema anomala* nov. sp. (Figs 1–6)

**Material Examined.** Holotype. Einasleigh Uplands Bioregion of Queensland, 18°19′21″S 145°24′10″E, Girringun National Park, Princess Hills section, 3.1 km by road from main entrance gate towards Princess Hills Ranger Station. Melaleuca and Eucalypt woodland on gentle slope with moist, lateritic, sandy soil. Earthworms were in the upper 20 cm and above the water table. Altitude 625 metres, PFA fixation, K.R. McDonald, 5 Mar 2007. QM G231042.

Paratypes. Same locality, 5 specimens, 100% ethanol, QM G231043–231047.

Non-types. Same locality, 15 specimens, mostly clitellate.

**Description.** Length (Holotype) 114 mm; width (midclitellum) 4 mm. Segments approximately 246. Colour in life unpigmented, pinkish (Fig. 1A–C); in preservation, light brown with dark brown clitellum. Prostomium (Fig. 2) epilobous 1/3 (relative to fused peristomium and first setigerous segment), squarish, demarcated posteriorly and laterally by a straight groove. Dorsal pores minute apparently commencing in 11/12, sometimes not observable until the caudal end. Setae 8 per segment, closely paired, but the lateral pair (*c,d*) much narrower than the

ventral pair (*a,b*), the ventral pair being larger; setal ratios (mm) *aa:ab:bc:cd* = 1.3:0.21:1.3:0.11. Nephropores in *c* lines. Clitellum weakly developed, annular, XII–XVIII. Prostate pores two pairs, in segments 16 and 17 by external counting but these here designated XVII and XIX (Figs 1A–B, 3, 4), on small elliptical papillae, in *ab*; male pores not certainly visible. Accessory genital markings (holotype): a faint circular protuberance visible in the anterior two-thirds of VIII anterior to the spermathecal pore of 8/9 (Fig. 3). Female pores anteromedian of setae *a* of XIV. Spermathecal pores 2 pairs, indistinct, in 7/8 and 8/9, in *b* lines.

Last hearts in XII. Gizzard large, firm, globular, in VI. Oesophagus with dorsal vascularized swelling in XIII. Intestine commencing in XIX(?), Holonephric, with stomate, avesculate nephridia. Sperm funnels large, in XI only, giving rise to a clearly visible vas deferens, egress of which distally was not determinable. Very large racemose seminal vesicles in XII. Ovaries not seen. Prostates two pairs, in XVII and XIX; tubular, those in XVII on left extending across the gut to the other side and almost straight; those in XIX short and winding; both sets of prostates with slender muscular ducts each accompanied by a penisetal follicle. Penial setae (paratype QM G231047) filiform, bent in a gentle arc (Fig. 5A); the tip in the form of a shepherd's crook, i.e. strongly curved on itself and then reflexed in the opposite direction; the shaft with fairly regular transverse cicatriciing but the terminal bend with only a few pit-like markings (Fig. 5B, C); lengths of three penial setae 16.97–18.55 (mean 17.6) mm. Spermathecae two pairs, in VIII and IX, each with a subspherical ampulla and a diverticulum of size and shape similar to the ampulla, which is sessile on the duct which it obscures and which contains iridescent sperm balls. Spermathecae in IX each preceded by a curved follicle containing two spermathecal setae. Each seta (Fig. 6) moderately stout, gently curved and with a pointed tip; the distal region of the seta with periodic incisions in profile, each of which extends for approximately half of the circumference and confers a toothed appearance on the profile; lengths of the two

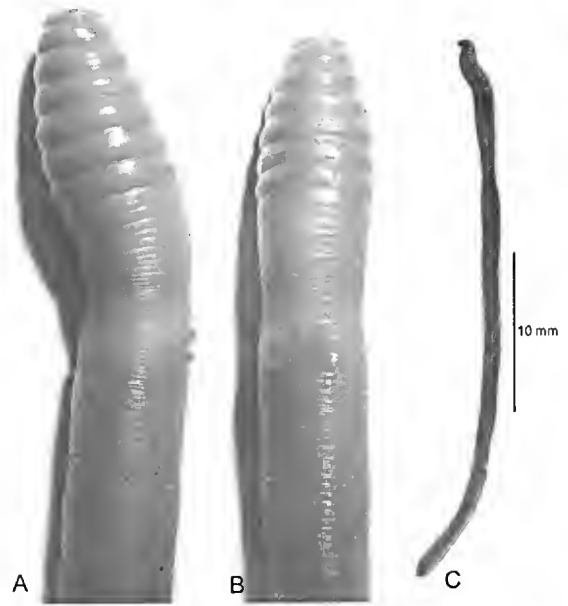


FIG. 1. *Diplotrema anomala* sp. nov. A, B, Anterior, genital region of a live specimen, showing the male genital field with two pairs of protuberant male porophores; A, Lateral view; B, Ventral view; C, Lateral view of an entire worm.



FIG. 2. *Diplotrema anomala* sp. nov. Anterior region of paratype QM G231047 to show form of prostomium.

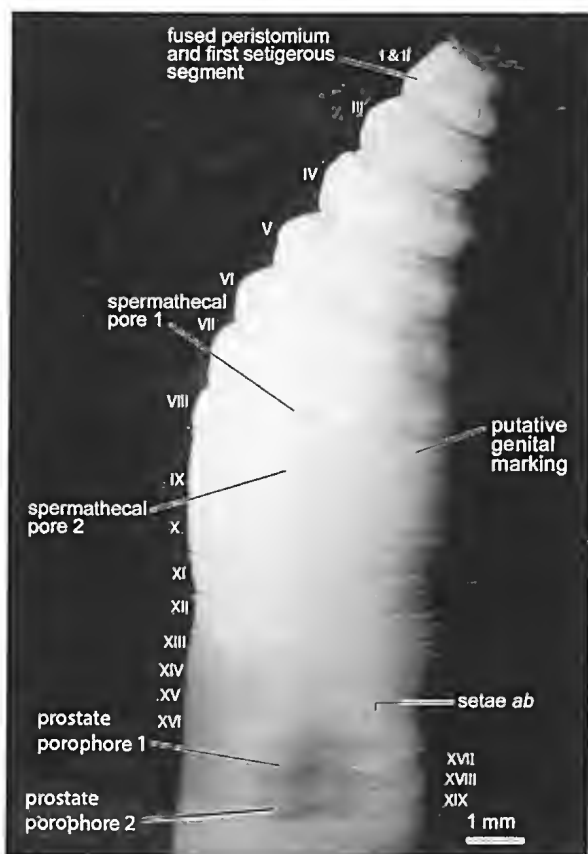


FIG. 3. *Diplotrema anomala* sp. nov. Ventral view of anterior, genital region of holotype, QM G231042.

left setae, measured in a straight line from base to tip, 0.873 and 0.933 cm.

**Etymology.** ‘*anomala*’ referring to the anomalous segmentation.

**Remarks.** In the above description the first observable ‘segment’, consisting of the peristomium fused with the first setigerous segment, is designated segment I & II. That it is the result of such fusion is shown by its possession of setae in its posterior half. No other species of *Diplotrema* is known to show this segmental fusion. If apparent segments are counted externally, the spermatheca, female, and prostate pores therefore appear to be translocated anteriorly by one segment, though not by homeosis.

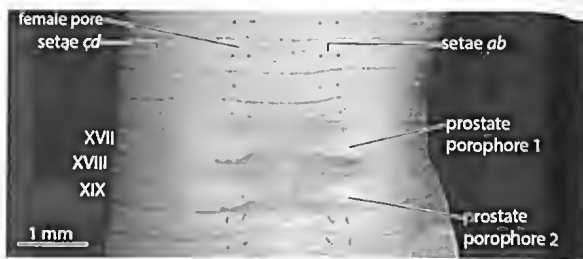


FIG. 4. *Diplotrema anomala* sp. nov. Detail of male genital field of holotype, QM G231042.

The spermathecal (genital) setae in the type genus of the Acanthodrilinae, *Acanthodrilus*, are almost straight and exhibit rows of deep scallops (notches); the posterior lip of each notch forming a crescent (Jamieson & Bennett 1979). This type of spermathecal seta is also seen in the Queensland genus *Kayarmacia* and in many species of *Diplotrema* (references in Dyne & Jamieson 2004), illustrated by scanning electron microscopy for *D. ridei*, *D. shandi* and *D. socialis*. The spermathecal setae of *D. anomala* differ from this form in lacking the deep gauging (notching) of the setae but have a fine denticulation. The notched setae may represent a symplesiomorphy for *Acanthodrilus* + *Diplotrema* + *Kayarmacia* (while being a synapomorphy of a common ancestor) and the alternative form of setae, seen in *D. anomala*, may provide grounds for taxonomic distinction of such species as possess it.

The large, subspherical diverticulum seen in *D. anomala* spermathecae also occurs in the type-species *D. fragilis*, in *D. armifera* and *D. cornigravei* but those species differ from *D. anomala* in having typical acanthodrilid scalloped genital setae and in lacking anterior segmental fusion.

In the Melaleuca areas where *D. anomala* is found, when the water table rises to the surface it is possible to locate them under logs with their posterior ends above the water. When touched the exposed end is withdrawn below the water surface and ground. Later, when the water table drops, the earthworms are found in the upper surface of the soil horizon above the water table (K.R. McDonald, pers. ob.).

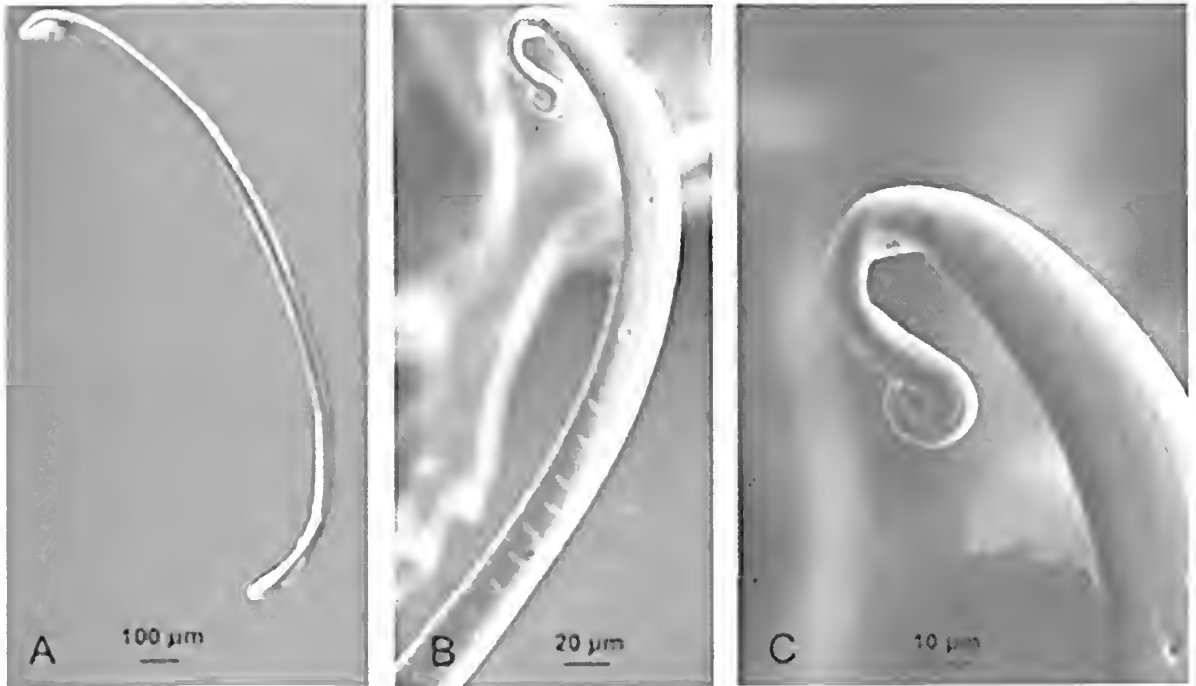


FIG. 5. *Diplotrema anomala* sp. nov. Scanning electron micrographs of penial setae of paratype QM G231043. A, whole seta; B and C, Detail of anterior region of seta.

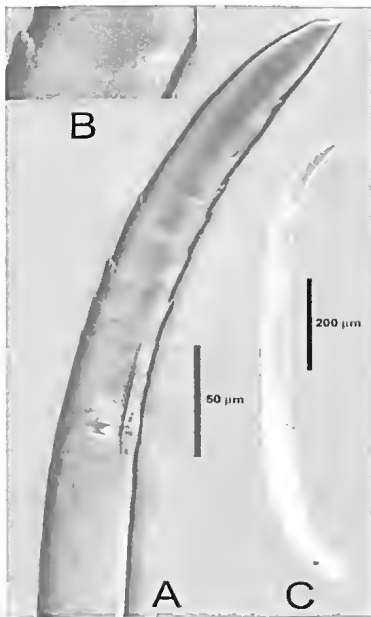


FIG. 6. *Diplotrema anomala* sp. nov. Left spermathecal seta of holotype QM G231042. A, Distal region; B, Detail of denticulation; C, Whole seta.

#### ACKNOWLEDGMENTS

We are grateful for the kind cooperation of the Environmental Protection Agency, Atherton, Queensland. This study resulted from a collaboration of Barrie Jamieson with Sam James and Seana Davidson (Research Assistant Professor, Department of Civil and Environmental Engineering, University of Washington), supported by US National Science Foundation grant DEB-0516439. Queensland Museum staff, Dr Mal Bryant is thanked for impeccable curation of specimens, Dr Owen Seeman for photographing the spermathecal setae and Dr Robert Raven kindly provided facilities.

#### LITERATURE CITED

Csuzdi, C. & Mischis, C.C. 2010. Earthworms from Argentinian Patagonia with descriptions of two remarkable new species (Oligochaeta, Acanthodrilidae, Lumbricidae and Megascolecidae). *Journal of Natural History* 44 (1-2): 31-40.

- Dyne, G.R. 1987. Two new *acanthodriline* earthworms (Oligochaeta: Megascolecidae) from the Northern Territory, Australia. *The Beagle, Records of the Northern Territory Museum of Arts and Sciences* 4(1): 1-6.
- Dyne, G.R. 1997. Two new genera of *Acanthodrilinae* (Megascolecidae, Oligochaeta) from Cape York Peninsula and the Torres Strait. *Memoirs of the Queensland Museum* 42 (1): 139-157.
- Dyne, G.R. & Jamieson, B.G.M. 1998. Two new semi-aquatic species of *Diploptrema* (Oligochaeta: Megascolecidae: Acanthodrilinae), with a redescription of the type species. *Memoirs of the Queensland Museum* 42(2): 487-493.
- Dyne, G.R. & Jamieson, B.G.M. 2004. Native Earthworms of Australia II (Megascolecidae, Acanthodrilinae). Australian Government Department of Environment and Heritage. CD Rom.
- Fragoso, C. & Rojas-Fernandez, P.1994 Earthworms from southeastern Mexico, new acanthodriline genera and species (Megascolecidae, Oligochaeta). *Megadrilogica* 6: 1-12.
- James, S.W. 1990. *Diploptrema murchiei*, new species and *Diploptrema papillata*, new species new earthworms (Oligochaeta: Megascolecidae) from Mexico. *Acta Zoologica Mexicana Nueva Serie* 0: 18-27.
- James, S.W. & Davidson, S.K. 2012. Molecular phylogeny of earthworms (Annelida : Crassicitellata) based on 28S, 18S and 16S gene sequences. *Invertebrate Systematics* 26: 213-229.
- Jamieson, B.G.M. 1971. A review of the megascolecoid earthworm genera (Oligochaeta) of Australia. Part II – The subfamilies *Oncerodrilinae* and *Acanthodrilinae*. *Proceedings of the Royal Society of Queensland* 82: 95-108.
- Jamieson, B.G.M. & Bennett J.D. 1979. New species of *Acanthodrilinae* and a new genus of *Perionychini* (Oligochaeta, Megascolecidae), from New Caledonia, their phylogeny and zoogeography. *Bulletin du Muséum National d'Histoire Naturelle*, 4e Série 1, section A, 353-403.
- Jamieson, B.G.M. 1997. Some new and previously known earthworm species from Cape York Peninsula (Annelida: Oligochaeta: Megascolecidae). *Memoirs of the Queensland Museum* 42(1): 233-270.
2000. The native earthworms of Australia (Megascolecidae Megascolecinae). (Science Publishers: Enfield) (CD-ROM).
2001. The native earthworms of Australia (Megascolecidae Megascolecinae). Supplement. B.G.M. Jamieson, Department of Zoology and Entomology, University of Queensland, Brisbane.) (CD-ROM).
- Jamieson, B.G.M. & Dyne, G.R. 1976. The acanthodriline earthworm genus *Microscolex* (*Diploptrema*) (Megascolecidae: Oligochaeta) in the Northern Territory of Australia. *Australian Journal of Zoology* 24: 445-476.
- Jamieson, B.G.M. & Ferraguti, M. 2006. Non-leech Clitellata. In, G. Rouse & F. Pleijel (Eds) *Reproductive biology and phylogeny of Annelida*. Pp. 235-392. (Science Publishers: Enfield, NH.)
- Jamieson, B.G.M., Tillier, S., Tillier, A., Justine J.-L., Ling E., James S., McDonald, K. & Hugall, A.F. 2002. Phylogeny of the Megascolecidae and Crassicitellata (Annelida, Oligochaeta): combined versus partitioned analysis using nuclear (28S) and mitochondrial (12S, 16S) rDNA. *Zoosystema* 24(4): 707-734.
- Michaelson, W. 1907. Oligochaeta, In, W. Michaelson & R. Hartmeyer (Eds) *Die Fauna Südwest-Australiens*, Gustav Fischer, Jena, pp. 117-232.
- Spencer, W.B. 1900. Further descriptions of Australian earthworms, Part I. *Proceedings of the Royal Society of Victoria* 13(n.s.) (1): 29-67.



# Additional chimaeroid specimens from the Early Cretaceous (Late Albian) Toolebuc formation, Queensland, Australia

Alan BARTHOLOMAI

Director Emeritus, Queensland Museum PO Box 3300, South Brisbane Qld 4101

Citation: Bartholomai, A. 2015: Additional chimaeroid specimens from the Early Cretaceous (Late Albian) Toolebuc Formation, Queensland, Australia. *Memoirs of the Queensland Museum - Nature* 59: 177–185. Brisbane. ISSN 2204-1478 (Online) ISSN 0079-8835 (Print). Accepted: 10 June 2015. First published online: 15 September 2015.

<http://dx.doi.org/10.17082/j.2204-1478.59.2015.2015-03>

LSID: urn:lsid:zoobank.org:pub:255CFAE2-CDFF-4942-A6AA-AC2C114D6D48

## ABSTRACT

Associated upper and lower tooth plates, comprising both vomerine dental plates, one incomplete left palatine dental plate and one partial left mandibular dental plate from a single individual of the chimaeroid *Ptyktoptychion wadeae* Bartholomai, 2008, have been collected from near Richmond, north-central Queensland, Australia. This material came from the usually poorly exposed, marine Early Cretaceous (Late Albian) Toolebuc Formation in the north of the Eromanga Basin. The new, associated tooth plates support the reference of palatine and mandibular dental plates identified by Bartholomai (2008) as all belonging to *P. wadeae*, possibly from a single individual; and also confirms the reference of an isolated vomerine tooth (QMF52605) from the west of the Basin to that species. The first chimaeroid fin spine from the Toolebuc Formation is tentatively referred to *?Ptyktoptychion* sp. □ *Chimaeroidei*, *Ptyktoptychion wadeae*, *?Ptyktoptychion* sp., Eromanga Basin, Toolebuc Formation, Early Cretaceous (Late Albian).

The first chimaeroid (Chondrichthyes: Chimaeriformes) recovered from the Lower Cretaceous (Late Albian) Toolebuc Formation of the Eromanga Basin in Queensland was described as *Ptyktoptychion tayyo* by Lees (1986). Further chimaeroid remains from the Toolebuc Formation were subsequently added to the collections of the Queensland Museum by field work by museum staff, resulting in a more complete knowledge of the dental plates of *P. tayyo* and description of a further species, *P. wadeae* by Bartholomai (2008). Both species were based on isolated plates that show evidence of partial loss through fracturing. Older chimaeroid material identified as *Edaphodon eyrensis* by Long (1985) has been described from the Eromanga Basin

in the Aptian Bulldog Shale, west of Bopeechee Siding in northern South Australia.

Additional, recently discovered, chimaeroid fossils have been donated to the Queensland Museum and are described herein. Both specimens were recovered from excavations in quarries operated by the Richmond Council for road making purposes and reflect increasing interest in the Toolebuc fossil fauna resulting from the development of the Kronosaurus Korner display centre in Richmond and its promotion of public involvement in finding and excavating elements of the fauna. The appointment of professional palaeontological and technical curatorial staff at Kronosaurus Korner has also provided interpretation and identification support, leading to increased public interest in the local Toolebuc fauna and recognition and

recovery of more complete skeletons of fossil fishes. This has led to deposition of many new species to the Kronosaurus Korner collection and to the Queensland Museum, including the isolated chimaeroid spine (QMF43006) referred questionably to *Ptyktoptychion* sp.

The Eromanga Basin was part of the Great Artesian Superbasin (Jell *et al.* 2013) that was covered by a relatively shallow layered epeiric sea. The thin (25–45 m thick), organic-rich Toolebuc Formation reflected dysoxic to anoxic benthic conditions (Cook *et al.* 2013) and together with its conformable and similarly aged Allaru Formation, was not well exposed and is now best seen at the surface along the northern and western rims of the Basin. The Toolebuc Formation is rich in fossil vertebrates, including many actinopterygians (Bartholomai 2015), most of which are from predatory, pelagic species. Relatively rare occurrence of chimaeroids in the Lower Cretaceous sediments probably reflected their presence in both the general shallow-water environments of the Eromanga Basin exposed in what was most probably near-shore or even littoral deposits, and the paucity of bottom dwelling invertebrates resulting from the adverse benthic conditions. The Eromanga chimaeroid community is very restricted taxonomically when compared with Eurasian Albian-Cenomanian chimaeroid associations where, for example, 10 genera were present in the Upper Albian of Belgorod Province, Russia (Popov & Machalski 2014, Fig. 8).

The specimen of *Ptyktoptychion wadeae*, QMF55449, discussed and illustrated herein in Figs. 1 and 2, was located in one of the Richmond Council quarries exposing the Toolebuc Formation. This specimen was excavated and donated by Queensland Museum Honorary Research Fellow, Mr Ian Sobbe and was prepared by the Museum's preparator, Mrs Jo Wilkinson. It comprises associated dental plates. Such undoubted associated remains are important in confirming the original reference of disassociated dental plates to this species by Bartholomai (2008).

The originally described material, including the holotype palatine dental plate, QMF52601, came from the Toolebuc Formation exposures along the anabranches of the Flinders River at 'Boree Park' Station, as were the referred mandibular dental plates QMF52602 and QMF52603. An additional partial palatine tooth plate was also referred to the species from the Late Albian, Allaru Formation at 'Currane' Station, near Dartmouth in central Queensland. The vomerine tooth plate referred to *P. wadeae*, QMF52605, however, was found in the Toolebuc Formation on 'Canary' Station, near Boulia and, at that time, was the only chimaeroid specimen referable to *P. wadeae* recovered from the western rim of the Basin. Before location of the associated tooth plates, QMF55449, the vomerine tooth plate illustrated by Bartholomai (2008, Fig. 6) could have been of *P. tayyo* or even the Aptian 'E.' *eyreensis* rather than of *P. wadeae*. *Ptyktoptychion tayyo* is currently known only from the Boulia area. The holotype tooth plate of *P. tayyo*, QMF12987, was originally described by Lees (1986) as a mandibular tooth plate but the specimen was reinterpreted by Averianov (1992), supported later by Stahl (1999) to be a palatine tooth plate which was confirmed by Bartholomai (2008) who showed that it differed from that attributed to *P. wadeae*.

Terminology mostly follows that summarised by Stahl (1999). The higher level taxonomy generally follows that outlined in Popov & Machalski (2014) and Stahl (1999).

#### ABBREVIATIONS

adt	.....	additional outer tritor
aot	.....	anterior outer tritor
bp	.....	basal perforation
bt	.....	beak tritor
fbp	.....	field of basal perforation
fpl	.....	fragment pleromin
lbm	.....	labial margin
lgm	.....	lingual margin
mm	.....	mesial margin
mt	.....	median tritor

mtp-l ..... mandibular tooth plate (left)  
 pot ..... posterior outer tritor  
 pt ..... plesiosaur tooth  
 ptp-l ..... palatine tooth plate (left)  
 sm ..... symphyseal margin  
 st ..... shark tooth  
 vtp-l ..... vomerine tooth plate (left)  
 vtp-r ..... vomerine tooth plate (right)

Class CHONDRICHTHYES Huxley, 1880

Subclass HOLOCEPHALI Bonaparte, 1832

Superorder HOLOCEPHALOMORPHA  
 Nelson, 2006

Order CHIMAERIFORMES Obruchev, 1953

Suborder CHIMAEROIDEI Patterson, 1965

Superfamily CHIMAEROIDEA  
 Bonaparte, 1832

Family CALLORHYNCHIDAE Garman, 1901

Subfamily CALLORHYNCHINAE  
 Garman, 1901

*Ptyktoptychion wadeae* Bartholomai, 2008  
 (Figs 1A–B; 2A–B)

*Ptyktoptychion wadeae*, Bartholomai, 2008: 53–6.

**Material.** See Bartholomai (2008) for detail of QMF52601, holotype palatine tooth plate, and referred specimens QMF52602 (left mandibular tooth plate) and QMF52603 (right mandibular tooth plate), all from Early Cretaceous (Late Albian) Toolebuc Formation of 'Boree Park', near Richmond, NCQ., and QMF52605 (vomerine tooth plate), from same formation, 'Canary' Station, near Boulia, CWQ. QMF52604, (palatine tooth plate) from the Early Cretaceous (Late Albian) Allaru Formation, 'Curran' Station near Dartmouth, CWQ.

QMF55449, associated upper and lower dental plates comprising both vomerine dental plates, one incomplete left palatine dental plate and one partial left mandibular dental plate, together with an isolated chondrichthyan tooth. This is referable to *Echinorhinus australis* and was illustrated by Kemp (1991, Pl. 4W) as *Pseudocorax australis*. An additional, unidentifiable base of a shark tooth is also present, along with an

isolated plesiosaur tooth. The specimen was collected from a Richmond Council quarry on 'Cambridge Downs' Station, northwest of Richmond, NCQ., from calcareous shale of the Early Cretaceous (Late Albian) Toolebuc Formation.

**Description.** The associated dental plates here referred to *Ptyktoptychion wadeae* are morphologically inseparable from those described by Bartholomai (2008). For that reason, a full revised description of the species has not been undertaken. Minor differences that add to the original description have been included with the following comments.

The left mandibular tooth plate (Figs 1, 2) is incomplete, lacking the extreme tip of the mandibular beak and the majority of the lingual and posterosymphyseal margins. Distribution of the tritors is very similar to that seen in QMF52603 but because the specimen has a more complete labial margin, it shows more of the edge of the sharply angular, dentate labial margin and the extent of the beak tritor is slightly extended mesially. The symphyseal surface is more distinctly grooved close to the oral surface. The new specimen is slightly smaller than QMF52603 and appears less robust. An apparently disassociated, adhering piece of pleromin is present in the broad groove on the oral surface that opens towards the lingual margin. No pleromin body is seen to be associated with this floating fragment at the lingual surface of the plate. This floating fragment is in a similar position to a similar structure seen in QMF52603 that was incorrectly identified by Bartholomai (2008) as a posterior inner tritor. In that specimen, some vascular pleromin was evident with the fragment. No posterior outer tritor has been preserved in QMF55449.

The vomerine tooth plate in QMF55449 is also morphologically very similar to QMF52605, described as *P. wadeae* by Bartholomai (2008) but is very slightly smaller. The cupped shape of oral surfaces is similar, as is the presence of labial tritors as low, parallel ridges from the deep centre of the cupped surface. The mesial beak differs slightly, with the tip of the beak bent laterally around the innermost tritors. The labial margin is less dentate on the right

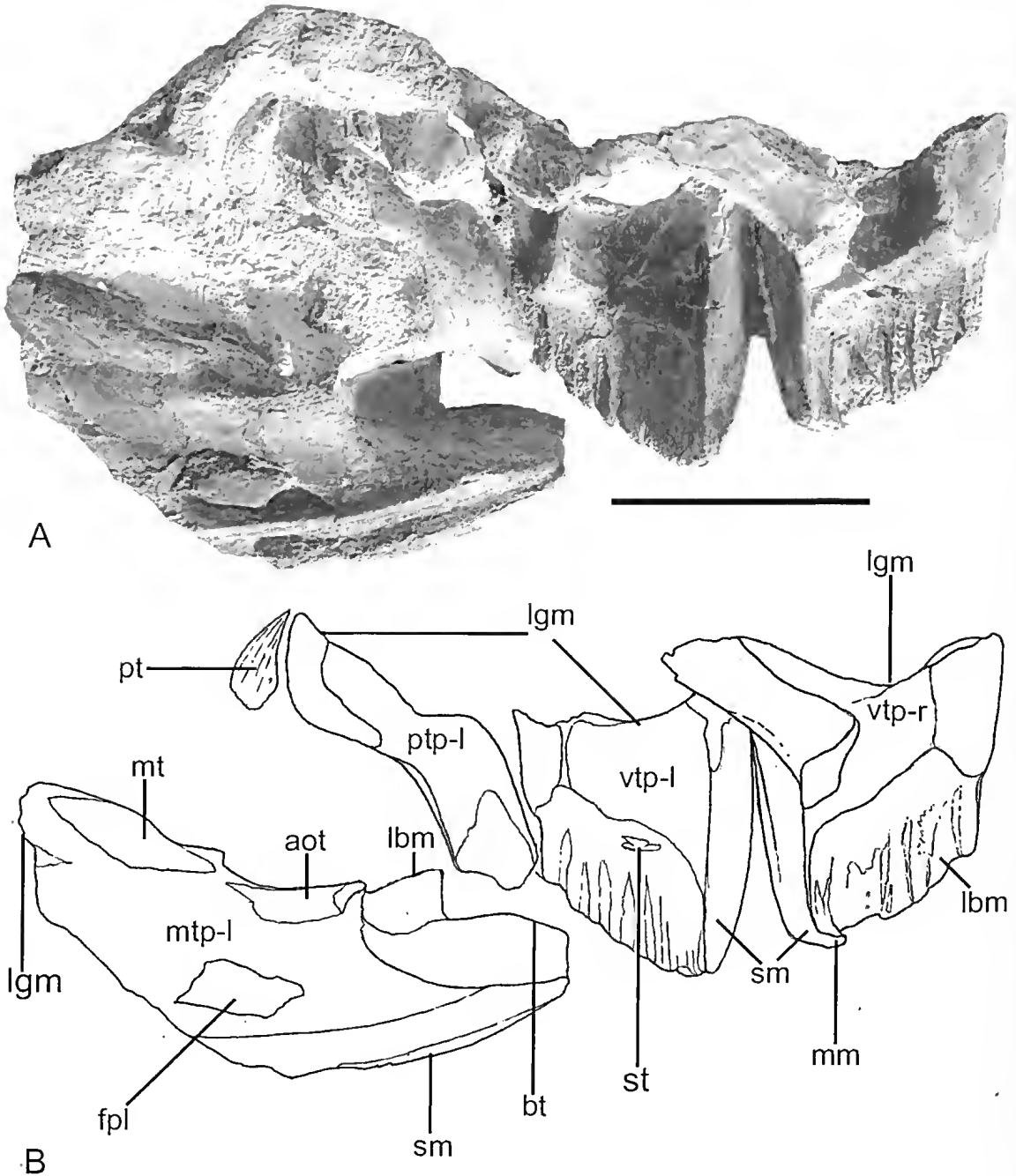


FIG. 1. *Ptyktoptychion wadeae*, QMF55449, associated tooth plates. A, photograph of the near complete dentition from a single individual showing both vomerine tooth plates, the partial left palatine tooth plate and the left mandibular tooth plate. Also present is an isolated chondrichthyan tooth of *Echinorhinus australis* in the middle of the left vomerine tooth plate and an isolated plesiosaur tooth; B, An interpretative line illustration of photograph 1A. Scale bar = 4 cm.

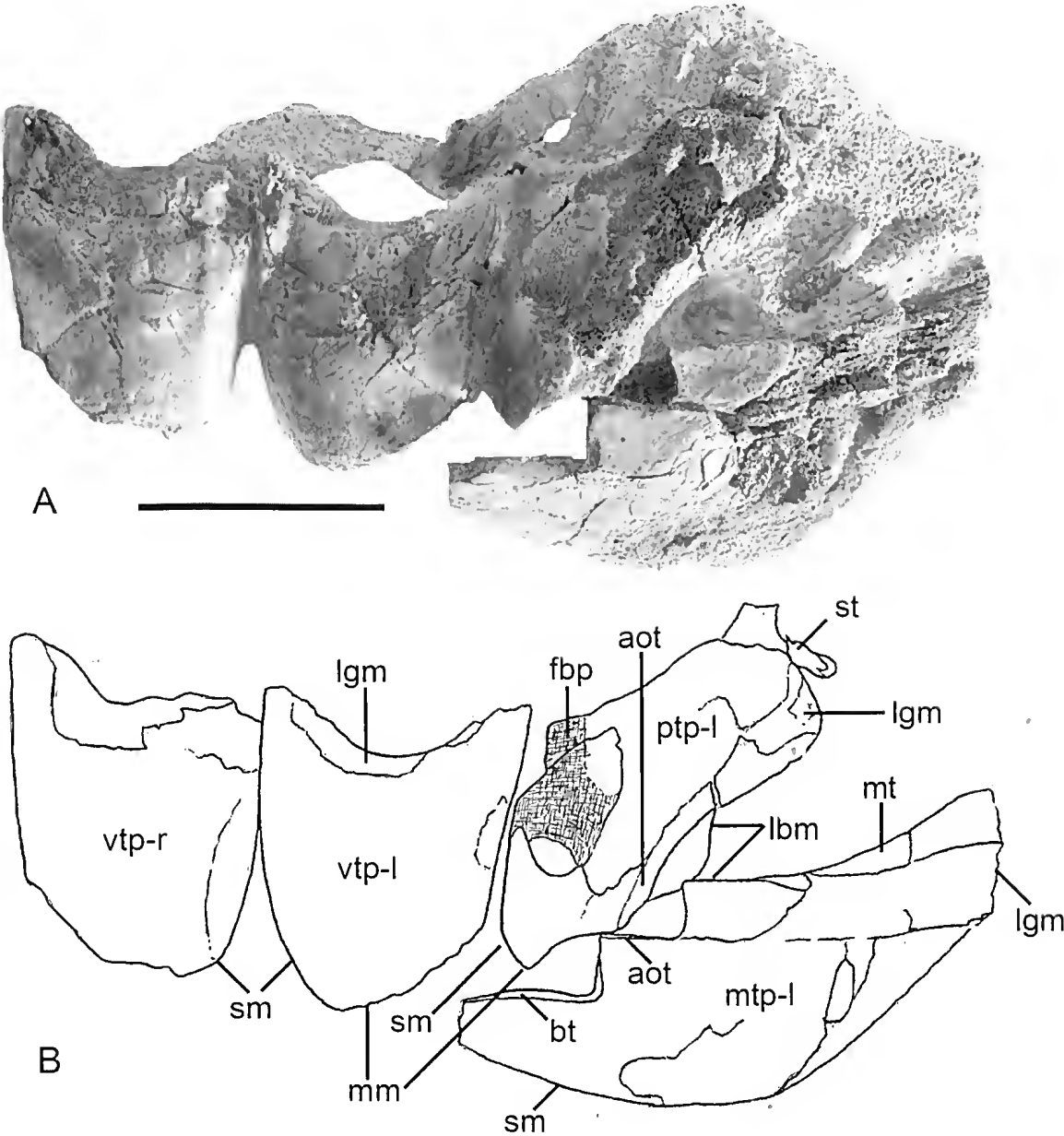


FIG. 2. *Ptyktoptychion wadeae*, QMF55449, reverse view of associated tooth plates. A, photograph of the near complete dentition showing both vomerine tooth plates, the partial left palatine tooth plate and the left mandibular tooth plate; B, an interpretive line illustration of photograph 2A. Scale bar = 4 cm.

vomerine plate than on the left as a result of fracturing and loss of the plate edge.

Although incomplete, the palatine tooth plate in QMF55449, shows more of the morphology of the anterior of the beak than that in QMF52601, the holotype of *P. wadeae*, where breakage and margin loss has reduced its mesial and anterolabial indentation. The occlusive surface of the beak is deeply excavated in QMF55449. The tip of its mesial margin is convexly rounded, leading posteriorly into a shallow but broad groove in the aboral surface and with the indentation of the anterior of the labial margin sharply shelved to the middle ridge above the basal pocket of the plate. Only a short remnant of the symphyseal descending lamina is preserved. Otherwise, the preserved remains of the palatine dental plate are similar to that of the holotype.

**Discussion.** The associated dental plates in QMF55449, discussed and illustrated herein in Figs 1 and 2, are partially masked by matrix left during preparation to maintain the original configuration of the elements as they were found. Allowing for this and for the incompleteness of the partially preserved palatine dental plate, the morphology of all of the elements is very similar to those upon which the callorhynchine chimaeroid, *Ptykyoptychion wadeae* Bartholomai, 2008, was based.

Popov (2011) considered that *Edaphodon eyrensis* Long should be transferred to *Ptykyoptychion*, but did not formally make a new combination. In a later paper, Popov & Machalski (2014), concluded that *Edaphodon* was not present in the Eromanga Basin, but they recorded *Ischyodus* cf. *thurnmanni*, in Fig. 8, from the Basin. It is therefore inferred that they favoured referral of *Edaphodon eyrensis* to *Ischyodus* over *Ptykyoptychion*, but did not discuss this in detail. Due to this uncertainty of the generic placement, '*Edaphodon*' *eyrensis* is thus placed in inverted commas. Thus, the chimaeroid fauna of the Eromanga Basin is currently considered to be restricted to species of two genera, endemic *Ptykyoptychion* and '*Edaphodon*' *eyrensis* which might have affinities with the cosmopolitan genus *Ischyodus*.

Sufficient morphological features are present, especially relating to the tritor development, to maintain separation of '*E.*' *eyrensis* and *P. wadeae*. It was noted by Bartholomai (2008) that the holotype of *P. wadeae* and the referred specimens, QMF52602 and QMF52603, were all collected from 'Boree Park' Station near Richmond. They could have come originally from the same individual but full details of their collection had been lost when located in the effects of Dr Mary Wade following her death. The 'Boree Park' specimens were therefore treated as separate specimens in the original paper. Not only does the current associated specimen (QMF55449) confirm referral of the vomerine dental plate (QMF52605) from near Boulia, CW Qld to *P. wadeae* but the remainder of its upper and lower dental plates validates the assumptions for association of all of the referred dental plates described for this species by Bartholomai (2008).

*Ptykyoptychion wadeae* was shown to differ from the type species, *P. tayyo* Lees, 1986, currently known only from the western exposures of the Toolebuc Formation in the Eromanga Basin, and the morphological differences between the species were discussed in Bartholomai (2008). The holotype tooth plate of *P. tayyo*, QMF12987, was originally described by Lees (1986) as a mandibular tooth plate but the specimen was reinterpreted by Averianov (1992), supported later by Stahl (1999) to be a palatine tooth plate which was confirmed by Bartholomai (2008) who also showed that it differed from that attributed to *P. wadeae*. Popov (2011) initially suggested that the two species of *Ptykyoptychion*, could be conspecific but later maintained them as separate taxa (Popov & Machalski 2014, Fig. 8).

**?*Ptykyoptychion* sp.**  
(Fig. 3A– B)

**Material.** QMF43006, an isolated, incomplete dorsal fin spine with detached distal tip and lacking an undetermined amount of the inserted portion of the spine, collected from the Richmond Council 8-mile pits on the Richmond-Croydon road, from calcareous shale of the Toolebuc Formation of Early Cretaceous (Albian) age. Collected and donated to the Queensland Museum by Mr. John Towning.

**Description.** Preserved portion of the dorsal fin spine measures 22.3 cms in length and is slightly curved posteriorly and laterally. Spine is laterally compressed, sub-triangular in cross section, with near flat posterior wall meeting lateral walls around rounded corners and with lateral walls meeting anteriorly to form a sharp keel distally, becoming sharply rounded proximally. Spine widest basally, tapering apically. Keel lacks denticles. Lateral walls with numerous, fine, longitudinal striations, finer towards keel.

Distally, each posterolateral margin with a single row of numerous, small, sharply lunate, posteroventrally curved, hooked denticles that diminish slightly in size away from dorsal tip of the spine. Bases of denticles are ovate and are generally organised in an en eschalon way with the axes directed anteromedially. The tip of each denticle is formed by a sharp, acutely curved and posteriorly directed, scooped margin around the back of the denticle tip. Each denticle is smooth, formed of a thin coating of enameloid. The lateral rows of denticles are separated by a shallow, longitudinal, medial groove that extends proximally beyond the area occupied by the denticles.

Lateral compression of the spine is evident proximally, making it difficult to see the structure of the spine in section. It appears that the keel consists of solid trabecular tissue, probably with fine vascular canals. Posterolaterally, the vascular canals are larger on each side of the median groove, while the lateral surfaces are of lamellar tissue, apparently free of vascular canals. A central, large pulp cavity has allowed partial inward crushing of part of the lateral walls but the shape of the cavity is masked by the compression.

**Discussion.** Dorsal fin spines are not diagnostic to species or even to genera within a family when not found associated with dental or skeletal elements (Takeuchi & Huddleston 2006, Popov pers. comm. 2015). Two genera, *Ptyktoptychion* and another taxon that is possibly referable to *Ichthyodus* (see above) are represented in the Toolebuc Formation, neither

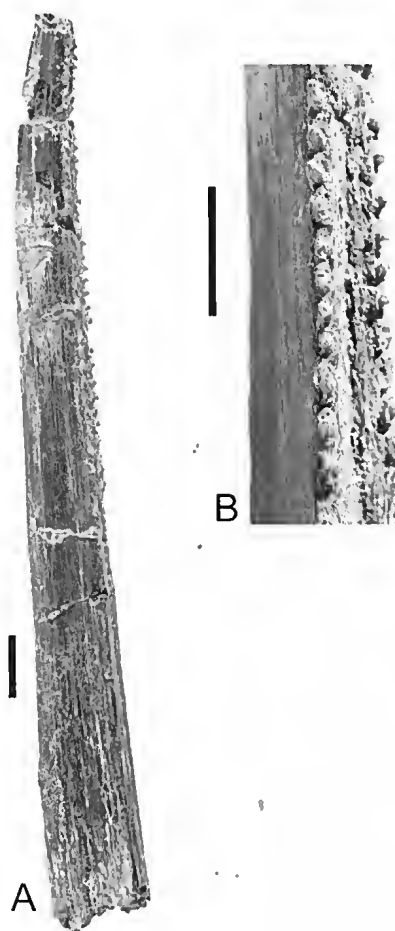


FIG. 3. ?*Ptyktoptychion* sp., QMF43006, isolated dorsal fin spine. A, photograph of spine in left lateral view; B, Further enlargement of left side of spine showing double row of denticles along posterior margins and median groove. Scale bar A = 1 cm, B = 1 cm.

of which was preserved with associated dorsal fin spines.

QMF43006 has generalised similarities to those referred to *Ischyodus*, and they were described by Ward & Grande (1991) as laterally compressed, smooth or longitudinally striated, with a double series of posterior denticles. Spines of *Edaphodon* also have similarities, e.g., in particular to the spine described and illustrated by Duffin & Reynders (1995) from the Maastrichtian of Belgium as *Edaphodon* sp.



and further material illustrated by Takeuchi & Huddleston (2006) and Stahl (1999). QMF43006 has insufficient morphological differences to enable it to be shown to have unquestioned referral to either *Ptyktoptychion* or *Ischyodus*. Its possible reference to *Ptyktoptychion* is based solely on the observation that species of that genus are the more widely distributed in the Toolebuc Formation. As has occurred with the tooth plates described above, this suggestion can only be clarified at the generic and/or specific levels when associated tooth plates and a dorsal fin spine are found.

Although the preserved part of the spine QMF43006 lacks a large percentage of its overall length and part of its distal tip, an additional, non-associated dorsal spine from the Toolebuc Formation in the Richmond Council Quarry, (Kronosaurus Korner collection, KK F553 from Site 2, 8 mile pits, 20° 38' 43.75" S, 143° 5' 40.23" E) is near complete and appears to differ only slightly from QMF43006. The *Kronosaurus* Korner specimen has a shorter series of posterior denticles immediately below the dorsal tip, which is separated by a short gap from the remainder of the denticles. In this it differs from QMF43006, although both spines have similar curvature and their proportions are similar as is the morphology of individual denticles. The *Kronosaurus* Korner specimen measures 46 cms in length and 2.9 cms across its proximal base and its basal opening to accommodate basal cartilage extends slightly more than 18% up the base of the spine. This virtually complete specimen is considered by Popov (pers. comm. 2015) to be one of the largest fossil chimaeroid spines known.

#### ACKNOWLEDGEMENTS

The author wishes to acknowledge the valuable suggestions, assistance and information provided by Dr Andrew Rozefelds, Head of Geosciences, Queensland Museum and Dr Timothy Holland, Curator, *Kronosaurus* Korner, Richmond. I am grateful to both reviewers, particularly for Dr Evgenii V. Popov's comments which significantly improved the paper.

#### LITERATURE CITED

- Averionov, A.O. 1992. New Jurassic chimaeroids of Russia. *Paleontological Journal*, **3**: 57-62.
- Bartholomai, A. 2008. Lower Cretaceous chimaeroids (Chondrichthyes: Holocephali) from the Great Artesian Basin, Australia. *Memoirs of the Queensland Museum*, **52**: 49-56.
- Bartholomai, A. 2015. An Early Cretaceous (late Albian) halecomorph (?lonoscapiformes) fish from the Toolebuc Formation of the Eromanga Basin, Queensland. *Memoirs of the Queensland Museum- Nature*. <http://dx.doi.org/10.17082/j.2204-1478.59.2015.2014-5>
- Chapman, F. & Pritchard, G.B. 1907. Fossil fish remains from the Tertiaries of Australia, *Proceedings of the Royal Society of Victoria*, **20**: 59-75.
- Cook, A.G., McKellar, J.L. & Draper, J.J. 2013. Eromanga Basin. In, *Jell, P.A. (ed.) Geology of Queensland*. (Geological Survey of Queensland: State of Queensland). 523-33.
- Duffin, J. & Reynnders, J.P.H. 1995. A fossil chimaeroid from the Gronsvelt Member, Late Maastrichtian, Late Cretaceous of northeastern Belgium, *Bulletin de la Société belge de Géologie, de Paléontologie et d'Hydrologie, Belgian Geological Survey Professional Paper*, **278**: 111-56.
- Garman, S. 1901. Genera and families of the chimaeroids. *Proceedings of the New England Zoological Club*, **2**: 75-7.
- Jell, P.A., Draper, J.J. & McKellar, J.L. 2013. Great Australian Superbasin. In, *Jell, P.A. (ed.) Geology of Queensland* (Geological Survey of Queensland: Brisbane). 517.
- Kemp, N.R. 1991. Chondrichthyans in the Cretaceous and Tertiary of Australia. In, *Vickers-Rich, P., Monaghan, J.M., Baird, R.F. & Rich, T.H. (eds), "Vertebrate Palaeontology of Australia"*. (Pioneer Design Studios Pty Ltd: Monash University Publications Committee). 497-568.
- Long, J.A. 1985. A new Cretaceous chimaerid (Pisces: Holocephali) from South Australia. *Transactions of the Royal Society of South Australia*, **109**: 49-53.
- Lees, T. 1986. A new chimaeroid *Ptyktoptychion tayyo* gen. et sp. nov. (Pisces: Holocephali) from the marine Cretaceous of Queensland. *Alcheringa*, **10**: 187-93. <http://dx.doi.org/10.1080/03115518608619154>.
- Migdalski, E.C. & Fichter, G.S. 1976. The fresh and saltwater fishes of the world. (Bay Books: Sydney and London), 316 pp.
- Patterson, C. 1965. The phylogeny of the chimaeroids. *Philosophical Transactions of the Royal Society of London, Series B, Biological Sciences*, No. 757, **249**: 101-219. <http://dx.doi.org/10.1098/rstb.1965.0010>



- Popov, E.V. 2011. New data on chimaeroid fishes (Holocephali; Chimaeroidei) from the Cretaceous and Neogene of Australia. Pp. 40-41. In, Lebedev, O. & Ivanov, A. (eds), *Abstract volume of the II International Obruchev Symposium "Palaeozoic Early Vertebrates"* (A. Ivanov: St Petersburg)
- Popov, E.V. & Machalski, M. 2014. Late Albian chimaeroid fishes Holocephali, Chimaeroidei) from Annopol, Poland. *Cretaceous Research*, 47: 1-18. <http://dx.doi.org/10.1016/j.cretres.2013.09.011>.
- Stahl, B.J. 1999. Chondrichthyes III - Holocephali, In, Schultze, H.-P. (ed.), *Handbook of Paleichthyology*, 4, (Dr. Friedrich Pfeil: München): 6-164.
- Takeuchi, G.T. & Huddleston, R.W. 2006. A Miocene chimaeroid fin spine from Kern County, California, *Bulletin of the Southern Californian Academy of Science*, 105: 85-90. [http://dx.doi.org/10.3160/0038-3872\(2006\)105\[85:AMCFSF\]2.0.CO;2](http://dx.doi.org/10.3160/0038-3872(2006)105[85:AMCFSF]2.0.CO;2).
- Ward, D.J. & Grande, L. 1991. Chimaeroid fish remains from Seymour Island, Antarctic Peninsula. *Antarctic Science* 3: 323-330. <http://dx.doi.org/10.1017/S095410209100038X>.

# A presumed Leichhardt geological specimen in the Queensland Museum

*Memoirs of the Queensland Museum - Nature* 59: 186. 2015:– The number of geological specimens collected by Ludwig Leichhardt during his extensive travels, in Australia, is not known. However, in July 1844 prior to departing from Sydney on his ill-fated expedition to cross the continent from east to west (Erdos 1967) he dispatched 288 mineral and rock specimens to the Museum d'Histoire Nationale in Paris and a collection of fossils to Richard Owen at the Royal College of Surgeons in London (Darragh 2013). Nonetheless, as Darragh acknowledged, other specimens may lie unrecognised in Australian geological collections, and especially those of the Australian Museum, which in Leichhardt's time was the only institution in the Colony of New South Wales functioning as a museum.

The presence, in the Queensland Museum, of an axial sandstone cast (QMF3275) of *Leptophloeum australe* (McCoy) Walton, labelled 'Leichhardt Clarke River,' (Clifford 1996 1b) and presumably collected during Leichhardt's Expedition from Moreton Bay to Port Essington, was overlooked by Darragh and is therefore noteworthy. Subsequent to 1996 the label has become detached from the specimen and neither it nor the negative of Fig. 1 has been located and so both may be assumed lost. However, there are no reasons to doubt the wording of the inscription for it is remembered clearly by both the present authors. Regrettably, it has not been possible to determine either the donor of the specimen or the date it was incorporated into the Museum collection. The earliest Register in which reference is made to the specimen is dated 1948 and the entry provides no information additional to that given on the label.

Neither the exact date nor location at which the cast was collected is known but in April 1844 the Expedition was in the vicinity of 145.5E, 19.4S close to the junction of the Clarke and Burdekin Rivers (Leichhardt 1847 p. 225), about 200 km west of Townsville. Thereabouts, shallow water Mississippian sediments of both the Venetia and Ruxton Formations outcrop. Casts of *Leptophloeum australe* have been reported from both Formations (Henderson & Withnall 2013) and are sometimes exposed on the weathered surfaces of Ruxton Formation sandstones. (Cook pers. obs). As such sediments do not occur elsewhere along the expedition's route it is reasonable to assume the specimen was collected at the above cited locality.

By September the Expedition was in difficulty and on 7th October 1844 Leichhardt parted, 'with a small collection of rocks made by Mr. Gilbert,' so as to ease the burden

of a packhorse (Leichhardt 1847, p. 428). Disaster struck again, a fortnight later, when three of the pack-horses, each carrying specimens, drowned after slipping into the Roper River (Leichhardt 1847, p. 445).

It is clear Leichhardt did not dispose of all his geological specimens when he discarded the Gilbert collection because the published account of the expedition includes a description of *Cyathophylloids leichhardtii*, a fossil coral, collected some months earlier, near the Burdekin River, far to the south. This specimen was described by Reverend W.B. Clarke (Leichhardt 1847, p.212), a geologist of Parramatta, and was almost certainly lost on 22nd September 1882, when fire destroyed the Garden Palace, Sydney, where 'the palaeontological specimens of the recently deceased W.B. Clarke' were stored (Gilbert 1986, p. 107). The name, *Cyathophylloids leichhardtii*, was not synonymised by Zhen & Jell (1996), in their work on Devonian corals and so its status will remain unclear unless the original specimen is located.

Unfortunately, the history of the cast, prior to its acquisition by the Queensland Museum, is not known. However, it is probable that before setting out from the Darling Downs, in February 1848 on what was to his final Expedition Leichhardt left, for safe keeping, the specimen together with a chest and other items, (David Parkhill pers. comm. 15 May 2015), with Thomas Alford, a hotel keeper, on the Darling Downs. The two men were acquainted, as Leichhardt had stayed at 'Alford's House of Accommodation' in June 1842 when en route to Brisbane (Darragh & Fensham 2013, p. 239).

Throughout it has been accepted that the cast of *Leptophloeum australe* and the specimen of *Cyathophylloids leichhardtii* were collected by Leichhardt (Fig. 1). However, the possibility that he rescued them from the 'small collection of rocks' made by the zoologist-ornithologist John Gilbert cannot be discounted, because his death did not occur until some weeks after the Expedition had left the Clarke River area (Leichhardt 1847) and so the name on the Queensland Museum label may refer to the Expedition rather than its leader.

The authors thank their Museum colleagues Megan Lloyd, who searched the Museum Registers for entries relevant to Leichhardt's specimen, and David Parkhill who is studying the history of the wooden chest, left with Alford, for safe keeping.

## Literature Cited

- Clifford, H.T. 1996. Geometrical study of a cast of *Leptophloeum australe* (McCoy) Walton from Queensland. *Memoirs of the Queensland Museum* 39: 227–230.
- Darragh, T.A. 2013. Leichhardt as a geologist. *Memoirs of the Queensland Museum-Culture* 7: 575–597.
- Darragh, T.A. & Fensham, R.J. 2013. The Leichhardt Diaries: Early travels in Australia during 1842–1844. *Memoirs of the Queensland Museum - Culture* 7: 1–540.
- Erdos, R. 1967. Leichhardt, Friedrich Wilhelm Ludwig. In Kemp, J. (Ed.) *Australian Dictionary of Biography* 2: 102–104.
- Gilbert, L.A. 1986. *The Royal Botanic Gardens, Sydney; a history, 1816–1985*. (Melbourne: Oxford University Press).
- Henderson, R.A. & Withnall, W. 2013. Mossman Orogen, Broken River Province. In Jell, P.A. (ed.) *Geology of Queensland*, Pp. 250–279.
- Leichhardt, L. 1847. *Journal of an overland expedition in Australia from Moreton Bay to Port Essington, a distance of upwards of 3000 miles, during the years 1844–1845*. (London: T. & W. Boone).
- Zhen, Y.Y. & Jell, J.S. 1996. Middle Devonian rugose corals from the Fanning River Group, north Queensland. *Palaeontographica A* 242: 15–89.
- H. Trevor Clifford & Alex G. Cook, Queensland Museum, PO Box 3300 South Brisbane Qld 4101 P 186 First published online 21 September 2015 <http://dx.doi.org/10.17082/j.2204-1478.59.2015.2015-05>

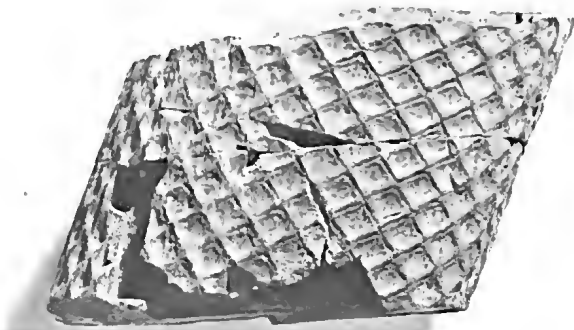


FIG. 1. Specimen of *Leptophloeum australe* labelled Leichhardt Clarke River (QMF3275).

# A critical re-evaluation of the hindlimb myology of moa (Aves: Dinornithiformes)

Peter J. BISHOP

Geosciences Program, Queensland Museum, 122 Gerler Rd, Hendra, QLD 4011, Australia. E-mail: peter.bishop@qm.qld.gov.au.

Centre for Musculoskeletal Research, Griffith University, Parklands Drive, Southport, QLD 4222, Australia.

Citation: Bishop, P.J. 2015. A critical re-evaluation of the hindlimb myology of moa (Aves: Dinornithiformes). *Memoirs of the Queensland Museum - Nature* 59: 187–234. Brisbane. ISSN 2204-1478 (Online), ISSN 0079-8835 (Print). Accepted: 23 July 2015. First published online: 6 November 2015.

DOI - <http://dx.doi.org/10.17082/j.2204-1478.59.2015.2015-02>

LSID - urn:lsid:zoobank.org:pub:2FC7B3DA-F6D3-4CB6-800F-64A860F5A34E

## ABSTRACT

The extinct moa of New Zealand were an enigmatic group of flightless birds, some attaining gigantic size. To better understand the biomechanical consequences of their large size and unique anatomy on stance and locomotion, a critical re-evaluation of the evidence for muscular attachment in the hindlimb of moa was undertaken. Three focal taxa, *Dinornis robustus*, *Emeus crassus* and *Pachyornis elephantopus*, were studied in detail, although other moa species were also addressed. More than one thousand individual bones from a diverse array of localities across the South Island of New Zealand were examined, and interpretations were made within the context of extant palaeognath birds. The interpretations and reconstructions produced largely concur with those of previous workers in many respects. The reconstructed myology of these moa species is also quite comparable to that in extant palaeognaths, although some important differences are hypothesised to exist. The most significant of these is that moa are posited to have had a very well-developed iliotochantericus caudalis in comparison to extant palaeognaths. Digital computer reconstruction of this muscle in an adult female *D. robustus* supports this hypothesis. The great development of the iliotochantericus caudalis in moa may be related to their large size, or reflect a different locomotor behaviour compared to extant palaeognath species. Finally, a number of myology-related features have been identified that may prove useful in the taxonomic identification of isolated or poorly preserved bones. □ Moa; hindlimb; myology; extinct; fossil; palaeognath; *Dinornis robustus*; *Emeus crassus*; *Pachyornis elephantopus*.

The extinct moa (Aves: Palaeognathae: Dinornithiformes) of New Zealand are an intriguing group of flightless birds that included some of the largest birds to have ever existed. It has been estimated that some moa species may have weighed 250 kg or more (Alexander 1983a; Anderson 1989; Worthy & Holdaway 2002; Murray & Vickers-Rich 2004; Brassey *et al.* 2013). In addition to their large body size, moa possessed a suite of anatomical features

that may have influenced their stance and gait in comparison to extant birds. Moa completely lacked any wings (unique among Aves), had an acarinate sternum and their pelvises were very broad caudal to the acetabulum (except in the smaller species, *Megalapteryx didinus* and *Anomalopteryx didiformis*). The whole-body centre of mass in moa may consequently have been more caudally located in comparison to extant birds, which in turn would influence

how the limbs were positioned when standing and during locomotion (Alexander 1983a). The femoral trochanter in moa is exceptionally developed among palaeognaths, raised well above the level of the femoral head. This makes the facies for articulation with the antitrochanter markedly concave, and in turn the antitrochanteric facies on the pelvis is markedly convex. In addition, non-*Dinornis* moa possess a well-defined, ball-shaped femoral head that is separate from the remainder of the femur by a distinct neck (Worthy & Holdaway 2002). Among large palaeognaths, such a feature is only seen elsewhere in *Casuarinus* and *Emuarius* (Boles 1992).

A further interesting aspect of moa anatomy concerns the proportions of their main hindlimb bones. Moa have the most extreme limb segment proportions of any flightless, terrestrial bird (extinct or extant), in possessing a long tibiotarsus and short tarsometatarsus (Gatesy & Middleton 1997). Moreover, in non-*Dinornis* species the tarsometatarsus is shorter than the femur, often significantly so (Worthy & Holdaway 2002). The limb bones of several moa species also appear to be exceptionally robust compared to other birds. This is not simply due to these birds' large absolute size, however, for several comparative studies have shown that moa hindlimb bones are in fact more robust than would be expected for their body size (Alexander 1983a,b; Doube *et al.* 2012; Brassey *et al.* 2013).

Questions concerning how the aforementioned anatomical features may have influenced moa stance and gait, and why such features may have evolved, can be addressed through comparative biomechanical analysis of the hindlimbs of moa and extant bird species. Fundamental to such analysis is having a thorough understanding of the musculoskeletal anatomy of the hindlimbs in these animals (Hutchinson *et al.* 2005; Maidment & Barrett 2011; Bates & Schachner 2012; Dilkes *et al.* 2012; Maidment *et al.* 2014). Two previous attempts have been made at reconstructing parts of the hindlimb myology in moa. Kooyman (1985, 1991) restricted his analysis of all moa species to the femur, tibiotarsus and tarsometatarsus. Without considering the pelvis, fibula and phalanges, his interpretations may have been significantly

influenced, and in any case cannot be related to these particular bones. Additionally, Kooyman drew his inferences largely from comparison with the hindlimb myology of only kiwi (*Apteryx* spp.), which could have further influenced his interpretations. More recently, Zinoviev (2013) produced a complete myological reconstruction for two species of moa, the dinornithid *Dinornis robustus* and the emeid *Emeus crassius*.

Whilst Zinoviev's (2013) work was thorough, he only had very limited fossil material (one specimen per species) upon which to base his reconstructions. This prevented him from assessing variability in surface morphology both within and across species, which can be considerable in moa (Worthy 1988; Kooyman 1991; Worthy & Holdaway 2002). Furthermore, it is clear from several of the photographs figured by Zinoviev that most of the bones studied by him were incomplete or were of sub-ideal preservation. The generality of his interpretations therefore remain uncertain.

To build and improve upon this research, a critical re-evaluation of the osteological evidence of muscle attachment in the hindlimb of moa was undertaken here. In addition to the two species addressed by Zinoviev (2013), a further species, *Pachyornis elephantopus*, was also investigated in detail, although the bones of most species of moa were examined throughout the course of this study. Besides producing a more soundly supported set of myological reconstructions, it was also sought to identify myology-related features which tend to be found only in certain species. These features may in the future help distinguish between species, and hence prove useful in identifying the taxonomic affinity of isolated, incomplete or poorly preserved bones. They may also help to better understand potential differences in locomotor behaviour between different moa species.

## MATERIALS AND METHODS

The taxonomy for moa outlined by Worthy & Scofield (2012) is followed here. This study was based upon the very extensive collection of moa bones in the Canterbury Museum, Christchurch, New Zealand, as well as the much smaller

collection in the Queensland Museum, Brisbane, Australia. A list of the exemplar specimens studied is given in Appendix 1 (available online <http://www.qm.qld.gov.au/About+Us/Publications/Memoirs+of+the+Queensland+Museum/MQM+Vol+59>); specimens with the prefix CM are from the Canterbury Museum collections and specimens with the prefix QMF are from the Queensland Museum collections. The specimens examined derive from many localities throughout the South Island of New Zealand, including the large swamp deposits of Pyramid Valley (Waikari), Glenmark, Cheviot, Kapua (Waimate) and Enfield (Oamaru). Hence, the observations and interpretations detailed herein are not biased by one or two select populations. Only bones from skeletally mature adults was examined (cf. Turvey & Holdaway 2005), as muscle scarring is usually only minimally developed in immature individuals. Furthermore, only specimens whose taxonomic identity was certain were studied. In many cases, such as the Pyramid Valley and Cheviot swamp specimens, this was known because the bones derived from articulated or associated specimens. In concert with the large number of bones studied, this scrutinization allows for the nature of intraspecific variation in a given anatomical feature to be properly assessed and interpreted.

**Myological Reconstructions.** Interpretation of osteological evidence for muscle attachment, and subsequent reconstruction of myology in the hindlimbs of moa, follows the approach of the 'extant phylogenetic bracket' (EPB; Witmer 1995; Carrano & Hutchinson 2002; Maidment & Barrett 2011). Here, soft tissues in the extinct taxon are reconstructed on the basis of inferred homology within a phylogenetic framework comprising extant species. A phylogenetic approach facilitates the identification of homologous osteological correlates of soft tissue attachment in the extant taxa that phylogenetically 'bracket' the extinct taxon. These homologous osteological correlates may then be identified as present or absent in the extinct taxon. By considering multiple extant outgroup taxa, such an approach also allows ancestral (symplesiomorphic) and derived (apomorphic)

character states to be identified for a particular soft tissue attachment. This helps avoid false comparisons with derived extant taxa, and in turn the most phylogenetically parsimonious inferences can be made in the extinct taxon. Additionally, by focusing on extant 'bracket' taxa, this avoids potentially misleading comparisons to more distantly related taxa, such as neognaths in the case of the present study. By framing musculoskeletal hypotheses for extinct taxa within a phylogenetic context, this therefore allows for the degree of uncertainty present in a given reconstruction to be more easily qualified.

The EPB approach minimally requires the bracketing of the extinct taxon of interest between the two most closely related extant taxa (Bryant & Russell 1993; Witmer 1995). In the case of moa, however, strict application of the EPB approach is problematic, since it is uncertain as to exactly what taxa constitute their EPB. Most recent studies of palaeognath phylogeny that have utilised molecular (genetic) data strongly suggest that tinamous are the sister taxon to moa (Phillips *et al.* 2010; Haddrath and Baker, 2012; Smith *et al.* 2013; Mitchell *et al.* 2014). However, it remains unresolved as to what constitutes the next most closely related taxon, despite a multitude of molecular and morphological phylogenetic studies. Thus, in recent years the EPB of moa has been hypothesised to be: *Apteryx* and all other 'ratites' (Livezey & Zusi 2007; Bourdon *et al.* 2009; Worthy & Scofield 2012); tinamous and 'ratites' (Baker & Pereira 2009); tinamous and *Apteryx* + casuariids (Phillips *et al.* 2010; Mitchell *et al.* 2014); *Rhea* and *Apteryx* + casuariids (Johnston 2011); tinamous and non-ostrich 'ratites' (Haddrath & Baker 2012); tinamous and *Rhea* + *Pterocnemia* (Smith *et al.* 2013). In light of this lack of consensus, the EPB approach is employed here in a somewhat loose fashion: assuming a tinamou-moa sister relationship, any extant palaeognath group could be the next most closely related taxon. Moreover, as moa have never been hypothesised to be the most basal of the 'modern' palaeognaths, their EPB has always comprised extant palaeognath species (i.e., no neognath groups). Hence, in this study the myological reconstructions were

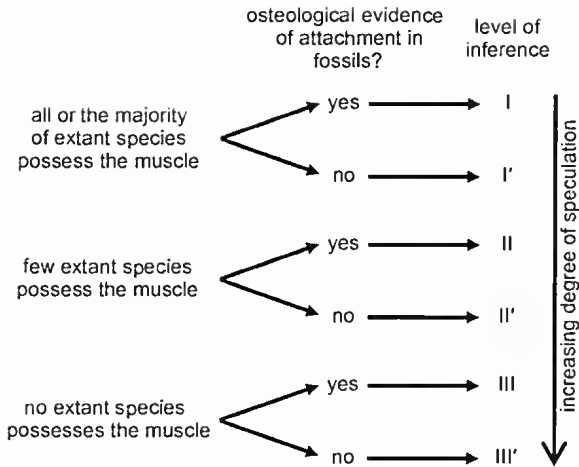


FIG. 1. Defining the level of speculation inherent in a soft tissue reconstruction, according to the scheme of Witmer (1995). This is based on the degree of support the reconstruction receives from extant taxa that phylogenetically bracket the extinct taxon of interest (indirect evidence), as well as osteological evidence in the fossils themselves (direct evidence). A level I inference is less speculative (better supported) than a level I' inference, which is less speculative than a level II inference, and so on.

framed within the context of the anatomy of extant palaeognaths only.

In lieu of undertaking first-hand dissections, a comparative basis of hindlimb myology in extant palaeognaths was drawn from the literature thus: *Dromaius* (Patak & Baldwin 1998; Lamas *et al.* 2014), *Casuarius* (Gadow 1880; Pycraft 1900), *Struthio* (Gangl *et al.* 2004; Smith *et al.* 2006; Zinoviev 2006; Schaller *et al.* 2009; Hutchinson *et al.* 2015); *Rhea* (Gadow 1880; Pycraft 1900; Picasso 2010); *Apteryx* (Owen 1879; McGowan 1979; Kooyman 1991); tinamous (Hudson *et al.* 1972). A comparative basis of hindlimb osteology in extant palaeognaths was developed through examination of neontological skeletal material in the collections of the Queensland Museum, Canterbury Museum and Museum Victoria, Melbourne, Australia.

By considering all extant palaeognaths as forming a loosely defined EPB of moa, without a strict phylogenetic framework in place, this

may lead to ambiguity in character polarity, and hence how a muscle is interpreted to have appeared in moa, if it in fact did exist. Given that different taxa can display different topologies or characteristics for a particular muscle or muscle group, this uncertainty could lead to the reconstructed musculature of a given moa species becoming somewhat 'generalised'.

This problem is countered to some extent by the great prevalence of direct osteological evidence for muscle attachment on the fossil limb bones of moa, as described below. In many cases this can eliminate the problem of uncertainty in the presence or absence of a muscle, or its nature of origin or insertion. This issue is further addressed by use of Witmer's (1995) 'levels of inference' (Fig. 1; see also Carrano & Hutchinson 2002). These gauge the level of speculation inherent in the reconstruction of a particular muscle, based on the amount of support it has from osteological data (direct evidence) and comparative data (indirect evidence). Thus, it helps define the confidence that can be placed in the reconstructions. More importantly, they provide a means by which to objectively compare alternative interpretations, hence allowing the most parsimonious one to be identified. This study follows Carrano & Hutchinson (2002) in minimally requiring a level II inference in order to reconstruct a muscle; a reconstruction of level II' or lower is deemed too speculative. It should be noted that reconstructions of the main ligaments of the hindlimb (collateral ligaments) are presented here with limited discussion or justification. The reason for this is that in almost every case the situation in extant palaeognaths is unambiguous and consistent, and moreover, there are clear scars on the fossil moa bones which are readily interpretable as such (i.e., level I inferences throughout).

Every bone of the hindlimb of *D. robustus* is illustrated here, to show the pattern of surface morphology and muscle scarring in the moa hindlimb skeleton. Features of the bones of the other species that were studied are illustrated only where they differ significantly from that exemplified by *D. robustus*. Each illustration is a composite, based upon many specimens so as to depict the 'typical' appearance of each

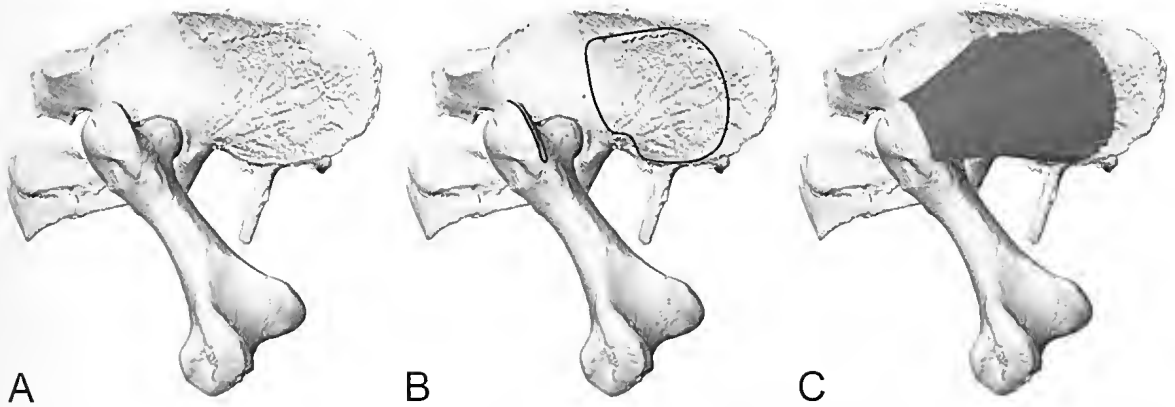


FIG. 2. Estimating the size of the ilioprochantericus caudalis in *D. robustus* using a digital computer model. A, the digital model of the pelvis and femur in articulation (only the right side is shown for clarity); B, the boundaries of the area of origin and insertion of the muscle on the bones are identified; C, computer-aided design software is used to render a solid geometric representation of the muscle. From this the volume, and in turn mass, of the muscle is estimated.

bone. In some illustrations several of the scars are enhanced, to show their appearance more clearly. All illustrations are of bones from the right side of the body.

**Digital Muscle Modelling.** Throughout the course of myological reconstruction, a point of biomechanical interest became apparent, in regards to the size of the ilioprochantericus caudalis in moa. The reconstructions produced here (detailed below) posit that this muscle originated from much of the preacetabular iliac blade. As the ilium of moa (especially *Dinornis*) is distinctive among large palaeognaths, in that the preacetabular ilium is dorsoventrally deep and is considerably longer than the postacetabular ilium (Worthy & Holdaway 2002), this suggests that the ilioprochantericus caudalis may have been enlarged in moa compared to extant palaeognaths.

This hypothesis was investigated by developing a digital computer model of the pelvis and femur in a large female individual of *D. robustus*, CM Av8422, and using it to estimate the volume of the ilioprochantericus caudalis (Fig. 2; cf. Persons & Currie 2011a, b; Hutchinson *et al.* 2011; Persons & Currie 2012). The geometry of the bones was obtained, as part of another study, through X-ray computed tomographic scanning (Siemens Somatom Definition Flash,

140 kV peak voltage, 307 mAs exposure for pelvis, 166 mAs exposure for femur, 1000 ms exposure time, slice thickness 0.4 mm, 0.96 mm pixel resolution for pelvis, 0.50 mm pixel resolution for femur) and digital segmentation and rendering of the resulting scans (Mimics 17.0, Materialize NV, Belgium). The models of the pelvis and femur were then virtually articulated in the computer-aided design software Rhinoceros 4.0 (McNeel, USA) (Fig. 2A). The articulation followed current consensus regarding the habitual position of the moa femur (Worthy & Holdaway 2002; Zinoviev 2013), namely that the bone was oriented subhorizontally with the trochanter in close apposition to the antitrochanter. Subsequently, the boundary of the area of origin on the pelvis was mapped out according to the reconstructions (Fig. 2B). The insertion on the femur was taken to be the cranial aspect of the appropriate portion of the trochanter (described below), in order to keep the model as simple and assumption-free as possible. Using the 'loft' option in Rhinoceros, these boundaries were used to produce a prismatic object that forms a first approximation of the bulk of the ilioprochantericus caudalis (Fig. 2C). The volume of this object was then calculated in Rhinoceros. It is important to note that as the muscle would likely have been rounded to some degree in life, rather than purely straight-sided, the geometric model developed here



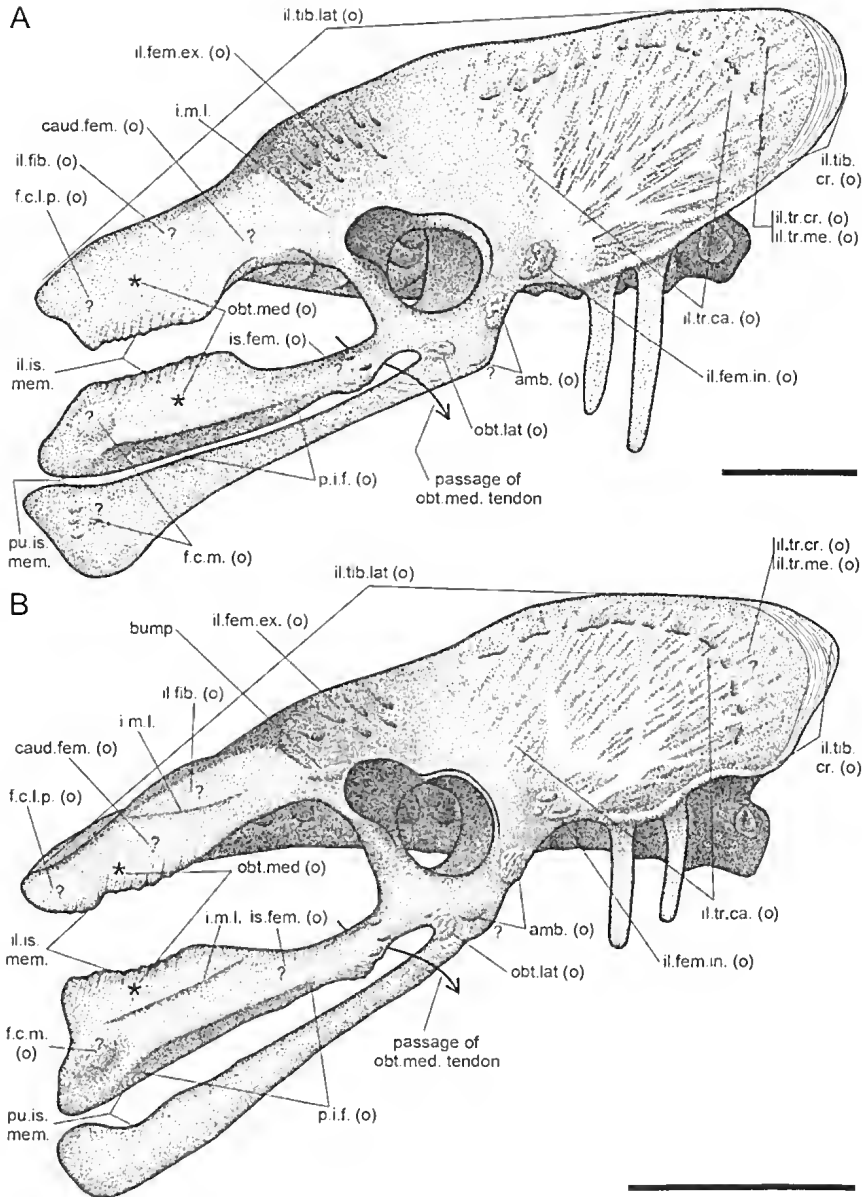


FIG. 3. Osteological evidence of muscle attachment on the pelvis of moa, with corresponding myological interpretations. A, *D. robustus*; B, *E. crassus*. The asterisk indicates that the origin of the obturatorius medialis is inferred to have been situated on the medial aspect of the bones or membrane to which it attached. In this figure and those that follow, question marks indicate uncertainty as to the exact location or extent of a given muscle attachment. Scale bars = 100 mm. Abbreviations: *amb.*, ambiens; *caud.fem.*, caudofemoralis; *f.c.l.p.*, flexor cruris lateralis pars pelvica; *f.c.m.*, flexor cruris medialis; *il.fem.ex.*, iliofemoralis externus; *il.fem.in.*, iliofemoralis internus; *il.fib.*, iliofibularis; *il.is.mem.*, ilioischadic membrane; *il.tib.cr.*, iliotibialis cranialis; *il.tib.lat.*, iliotibialis lateralis; *il.tr.ca.*, iliotrochantericus caudalis; *il.tr.cr.*, iliotrochantericus cranialis; *il.tr.me.*, iliotrochantericus medius; *i.m.l.*, intermuscular line; *is.fem.*, ischiofemoralis; *(o)*, muscle origin; *obt.lat.*, obturatorius lateralis; *obt.med.*, obturatorius medialis; *p.i.f.*, puboischiofemoralis; *pu.is.mem.*, pubischadic membrane.



is almost certainly an underestimate of the muscle's true bulk.

## RESULTS

For each muscle, a synopsis of the comparative anatomical context in extant palaeognaths is provided, and the osteological evidence observed in moa is detailed. The interpretations and myological reconstructions are also presented and discussed here, for the sake of fluency and clarity. In addition to the osteological illustrations provided (Figs 3–13), a restoration of the muscles as they may have appeared in life is presented (Fig. 14). This restoration is tentative and is not designed to illustrate the relative size of the muscles, nor the extent (or nature) of their attachments, but rather is intended to help place many of the muscles in the context of the whole limb. All references to the anatomy of extant palaeognaths are drawn from the abovementioned literature sources, unless noted otherwise. The more general terms of hip, knee and ankle are used instead of the more formal *junctura coxae*, *junctura genus* and *junctura tarsi*, respectively.

### Ilioischadic membrane (Fig. 3; il.is.mem.)

**General comments.** The ilioischadic membrane is present in all extant palaeognaths, spanning much of the space between the ilium and ischium.

**Observations.** The presence of the membrane in moa is indicated by well-defined, and often fimbriate, ridges on the ventrolateral surface of the postacetabular ilium and the dorsal surface of the ischium. These ridges are usually most pronounced caudally, although they are present for most of the length of their respective elements, a condition also observed in extant palaeognaths.

**Remarks.** Reconstruction of this soft tissue is a level I inference.

### Puboischadic membrane (Fig. 3; pu.is.mem.)

**General comments.** The puboischadic membrane is present in all extant palaeognaths, spanning between the ischium and pubis.

**Observations.** As with the ilioischadic membrane, its presence in all moa species is given by marked ridges on the ventral aspect of the ischium and dorsal aspect of the pubis for most of their length.

**Remarks.** Reconstruction of this soft tissue is a level I inference. In some species, such as *P. elephantopus* and *Dinornis* spp., very little of the puboischadic membrane would have actually existed in life, for the pubis and ischium are typically in close proximity along their entire length.

### Iliotibialis (Figs 3, 6, 7; il.tib.)

**General comments.** In extant palaeognaths, this muscle is divided into three parts, the iliotibialis cranialis (il.tib.cr), lateralis pars preacetabularis and lateralis pars postacetabularis (il.tib.lat.); the lateralis pars postacetabularis is itself further divided into two parts in *Struthio* (Gangl *et al.* 2004). They take origin from the dorsal iliac crest (cranial to the acetabulum) and the dorsolateral iliac crest (caudal to the acetabulum), and insert on the patellar tendon and surrounding connective tissue. This in turn inserts on one or both of the cnemial crests of the tibiotarsus, and perhaps also the proximomedial tibiotarsus (iliotibialis cranialis in *Dromaius* and *Struthio*).

**Observations.** Both the dorsal and dorsolateral iliac crests of *D. robustus*, *P. elephantopus* and *E. crassus* are pronounced, and are indeed slightly proud of the surrounding bone surface. The fine, striated scarring on these crests indicates the attachment of the iliotibiales in these species. In *D. robustus*, the dorsolateral iliac crest may also bear several ill-defined tubercles. In all three species, the scarring of the dorsal iliac crest extends around the cranial margin of the preacetabular iliac blade, where it widens to cover a significant area behind

the cranial margin of the bone, indicating that the iliotibialis cranialis also extended onto the cranial edge, as in *Apteryx* and *Rhea*. The striations here are more or less parallel with the margins of the bone. There is no evidence from the osteology as to the exact delimitations of the attachment of each part of the iliotibialis to the ilium, and it is possible that they originated via a shared aponeurosis. The presence of both cnemial crests on the moa tibiotarsus attests to the presence of strong, tendinous insertions of the iliotibiales and patellar tendon, and indeed the margins of the crests are often slightly recessed into the surrounding bone as a result of this attachment.

**Remarks.** Moa appear not to have had an osseous patella, unlike some extant palaeognath species; the presumed 'patella' noted by Owen (1883) in a specimen of *A. didiformis* is more likely to have been a misinterpreted tarsal sesamoid (Regnault *et al.* 2014). Regardless of this fact, reconstructing the iliotibiales cranialis et lateralis in *D. robustus*, *P. elephantopus* and *E. crassus* is a level I inference, although inferring the presence of separate partes preacetabularis and postacetabularis has only level I' support, since osteological evidence is lacking.

### Iliofemoralis externus (Figs 3–5; il.fem.ex.)

**General comments.** This muscle is present in all extant palaeognaths, originating from the ilium dorsal to the acetabulum and just ventral to the dorsal iliac crest. It inserts on the lateral aspect of the femoral trochanter along with the iliotrochantericus heads, obturatorius heads and the ischiofemoralis. Whilst different variations in the exact spatial pattern of insertion occur in extant palaeognaths, a common basic topology exists, which is evident throughout all neornithine birds (Hutchinson 2001). The cranialmost insertions on the trochanter are those of the iliotrochanterici, proceeding proximal to distal in the order of caudalis, medius, cranialis; sometimes the medius and cranialis heads are fused to a variable degree, as in *Struthio*, *Dromaius*, *Apteryx* and at least some tinamous (*Tinamus* and *Crypturellus*).

The obturatorius medialis et lateralis insert on the proximocaudal aspect of the trochanter, with the insertion of the medialis proximal to that of the lateralis; sometimes the two share a common insertion. The ischiofemoralis inserts distal to the insertion (or insertions) of the obturatorius, and the iliofemoralis externus inserts somewhere in the middle of the aforementioned insertions.

**Observations.** The pelves of *D. robustus*, *P. elephantopus* and *E. crassus* exhibit a broad area of marked surface rugosity (with individual rugae directed toward the acetabulum) in the area corresponding to the origin of this muscle in extant palaeognaths. This is interpreted as marking the origin of the iliofemoralis externus in moa. In several specimens of *D. robustus* and *P. elephantopus* examined, a faint striated ridge, directed toward the acetabulum, forms the posterior boundary of this area. This ridge is interpreted to be an intermuscular line bounding the posterior extent of the origin of the iliofemoralis externus in these species. The pattern of surface scarring on the femoral trochanter of moa is evidently no exception to the general neornithine pattern noted above, and a clear, rugose scar of insertion of the iliofemoralis externus is evident in the middle of the trochanter in *D. robustus*, *P. elephantopus* and *E. crassus*. Its fibrous texture, directed proximally to cranioproximally, is suggestive of the presence of abundant Sharpey's fibres (Carrano & Hutchinson 2002).

On the pelvis of *E. crassus*, as well as *Euryapteryx curtus*, there is a subcircular bump, ventral to the inferred origin of the iliofemoralis externus and dorsocaudal to the antitrochanter (bump, Fig. 3B). It ranges in size from quite small (< 5 mm diameter) to large (>20 mm in greatest dimension); in one specimen of *E. crassus* examined (CM Av8331), the bump is present on the left side of the pelvis but not the right. The surface texture of the bump varies from being rough (with tubercles, pits and striations) to completely smooth; typically the larger bumps are smoother. What soft tissue attachment this bump was for is uncertain, but its position on the pelvis suggests that it could be associated with the iliofemoralis externus,

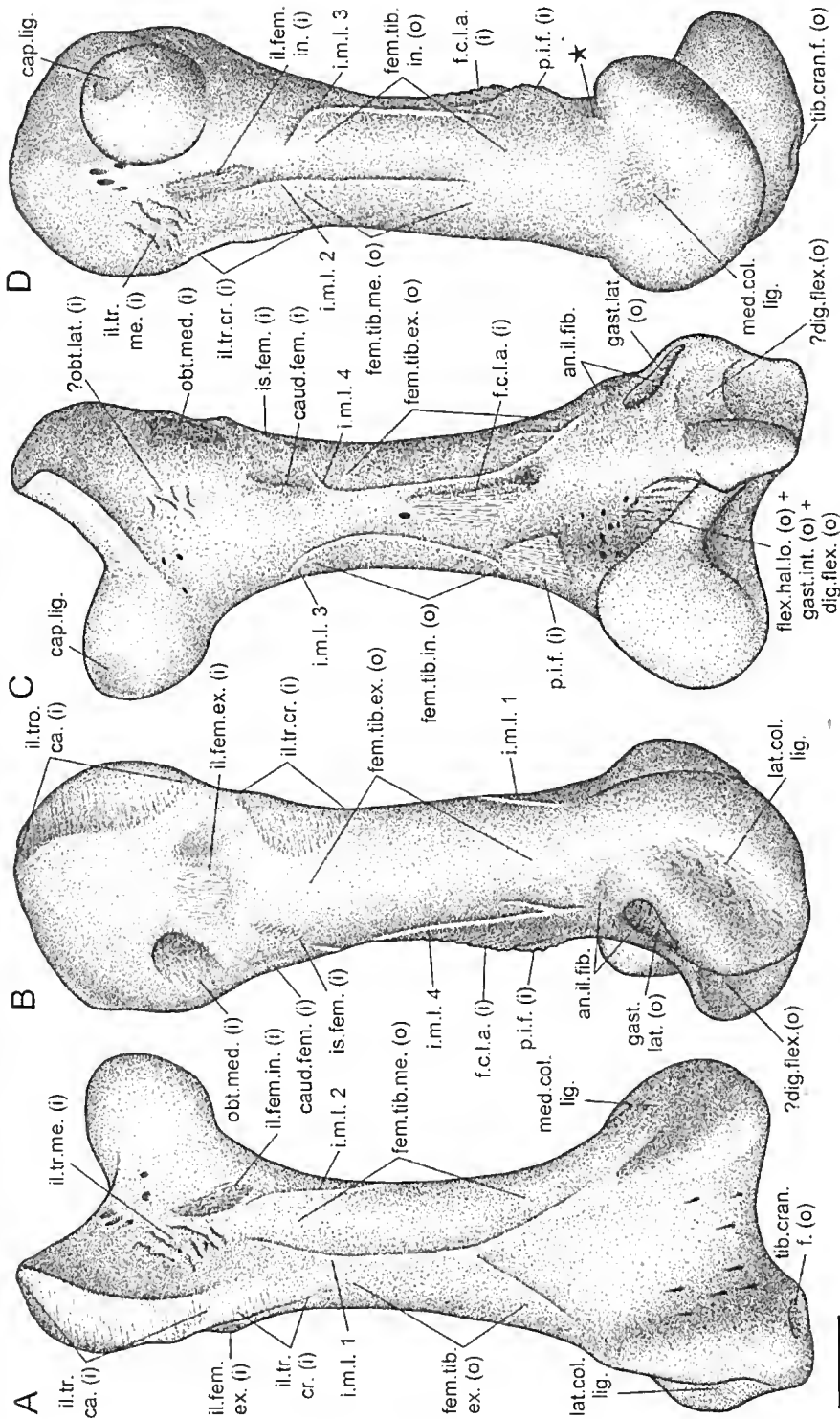


FIG. 4. Osteological evidence of muscle attachment on the femur of *D. robustus*, with corresponding myological interpretations. A, cranial view; B, lateral view; C, caudal view; D, medial view. The star indicates the small scar which may be for a fourth head of the gastrocnemius, or alternatively the flexor perforatus digiti III. Scale bar = 50 mm. Abbreviations: *an.il.fib.*, ansa iliofibularis; *cap.lig.*, capital ligament; *caud.*, caudofemoralis; *dig.flex.*, digital flexors; *f.c.l.a.*, flexor cruris lateralis pars accessoria; *fem.tib.ex.*, femorotibialis externus; *fem.tib.in.*, femorotibialis internus; *fem.tib.me.*, femorotibialis medius; *flex.hall.o.*, flexor hallucis longus; *gast.int.*, gastrocnemius intermedia; *gast.lat.*, gastrocnemius lateralis; *i.*, muscle insertion; *il.fem.ex.*, iliofemoralis externus; *il.fem.in.*, iliofemoralis internus; *il.tr.ca.*, iliotochantericus caudalis; *il.tr.cr.*, iliotochantericus cranialis; *il.tr.me.*, iliotochantericus medius; *i.m.l.* 1–4, intermuscular lines 1–4; *is.fem.*, ischiofemoralis; *lat.col.lig.*, lateral collateral ligament; *med.col.lig.*, medial collateral ligament; *o.*, muscle origin; *obt.lat.*, obturatorius lateralis; *obt.med.*, obturatorius medialis; *p.i.f.*, puboischiofemorialis; *tib.cran.f.*, tibialis cranialis caput femorale.

iliofibularis or caudofemoralis pars pelvica (see below), or perhaps even a ligament spanning the hip joint. What does appear certain, however, is that this feature is only present in *E. crassus* and *E. curtus*.

**Remarks.** Reconstruction of the iliofemoralis externus in moa is a level I inference.

### Iliofemoralis internus (Figs 3–5; il.fem.in.)

**General comments.** Among extant palaeognaths the iliofemoralis internus typically originates from the caudoventral rim of the preacetabular ilium, cranial to the preacetabular tubercle. In *Struthio*, however, it originates from between the origins of the iliotrochanterici cranialis et medialis (Gangl *et al.* 2004; Zinoviev 2006), while in *Rhea* it does so from the cranial aspect of the acetabulum (Picasso, 2010). The insertion of this muscle is on the medial to craniomedial surface of the femur, distal to the base of the femoral neck.

**Observations.** In *D. robustus*, *P. elephantopus* and *E. crassus* there exists a discrete elevation of variable rugosity on the caudolateral rim of the preacetabular ilium, immediately cranial to the pubic peduncle of the ilium; this corresponds to the origin of the iliofemoralis externus in most extant palaeognaths, and is interpreted as such. Its development varies within and between species, ranging from being constricted in size with highly pronounced scarring, through to being a broad, oval-shaped region of less pronounced rugosity. In some instances (particularly in *E. crassus*) it may form one or two heavily striated flanges of bone which project laterally to ventrolaterally. Regardless of its morphology, in all cases this scar is clearly distinct from that of the ambiens (see below), the two being of different character and being separated by smooth bone. The craniomedial surface of the proximal femur of moa always possesses a region of complex rugosity, although its appearance and extent varies. This feature is recognised as homologous to the insertion scar of the iliofemoralis internus in extant palaeognaths. In *E. crassus* this region is strongly recessed into the bone surface, forming a deeply excavated pit (Worthy & Holdaway 2002).

**Remarks.** In addition to the iliofemoralis internus, Zinoviev (2013) posited that the iliotrochantericus medius also originated from the caudolateral rim of the preacetabular ilium, on the basis of finding two rugosities on the surface of his specimens. As noted above, however, the appearance of the scar of the iliofemoralis internus is variable in moa, and the large sample of specimens studied here illustrates that this variation is expressed along a continuum, from a single discrete scar to two apparently distinct rugosities. Furthermore, among extant palaeognaths the iliotrochantericus medius is only closely associated with the iliofemoralis internus in *Struthio*, owing to a more dorsal location of the latter muscle's origin (Gangl *et al.* 2004; Zinoviev 2006), and even then the two muscles never actually fuse. Elsewhere among extant palaeognaths, the iliotrochantericus medius originates from a more cranial position on the preacetabular ilium. These observations suggest that the scarring in moa is for a single muscle, albeit one that may vary in internal architecture (e.g., the presence and number of internal fibrous planes). The most parsimonious interpretation is that the scar marks the origin of the iliofemoralis internus (a level I inference).

As regards the insertion of the iliofemoralis internus, Worthy & Holdaway (2002), Worthy & Scofield (2012) and Zinoviev (2013) considered the possibility that the pronounced scar on the femur was for the insertion of the iliofemoral ligament, rather than a muscle. This is not supported by osteological evidence (as noted above), and moreover, a mummified femur of *E. crassus*, described by Hutton & Coughtrey (1875b) and figured by Rawlence *et al.* (2012b), shows that muscle fibres and not a ligament inserted here. The most parsimonious interpretation therefore is that the scar indicates the insertion of the iliofemoralis internus in all moa (also a level I inference).

### Iliotrochanterici (Figs 3–5)

**General comments.** The iliotrochanterici cranialis (il.tr.cr.), medius (il.tr.me.) et caudalis (il.tr.ca.) occur in all extant palaeognaths, with the caudalis being the largest of the three. The

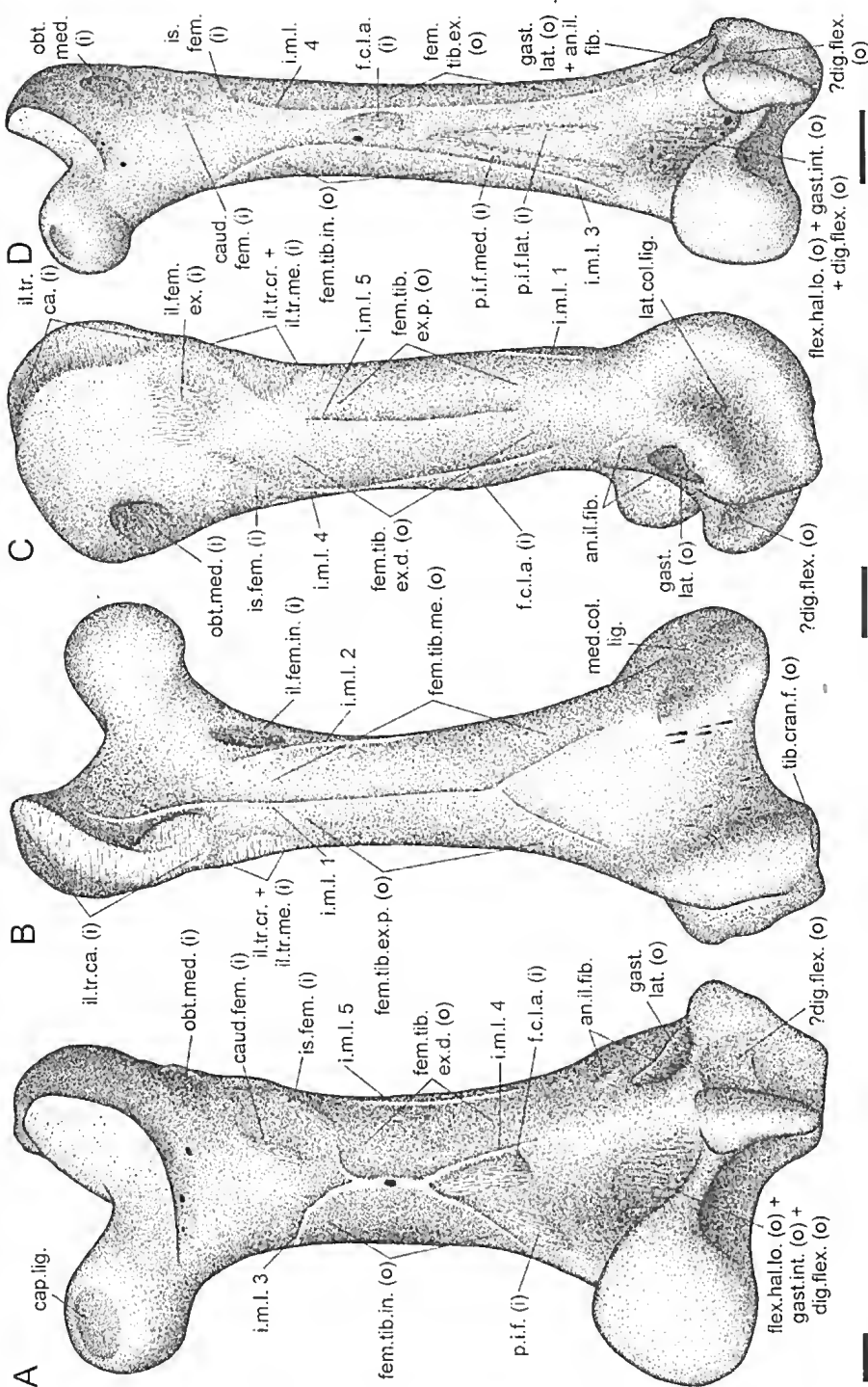


FIG. 5. Osteological evidence of muscle attachment on the femora of non-*Dinornis* moa, with corresponding myological interpretations. A, *P. elephantopus*, caudal view; B, *E. crassus*, cranial view; C, *M. didinus*, lateral view; D, *M. didinus*, caudal view. Scale bars = 20 mm. Abbreviations: *an.il.fib.*, ansa iliofibularis; *cap.lig.*, capital ligament; *caud.fem.*, caudofemoralis; *dig.flex.*, digital flexors; *f.c.l.a.*, flexor cruris lateralis pars accessorius; *fem.tib.ex.d.*, femorotibialis externus pars distalis; *fem.tib.ex.p.*, femorotibialis externus pars proximalis; *fem.tib.in.*, femorotibialis internus; *fem.tib.me.*, femorotibialis medius; *flex.hal.lo.*, flexor hallucis longus; *gast.int.*, gastrocnemius intermedia; *gast.lat.*, gastrocnemius lateralis; *i.*, muscle insertion; *il.fem.ex.*, iliofemoralis externus; *il.fem.in.*, iliofemoralis internus; *il.tr.ca.*, iliotochantericus caudalis; *il.tr.cr.*, iliotochantericus cranialis; *il.tr.me.*, iliotochantericus medius; *i.m.l.* 1–5, intermuscular lines 1–5; *is.fem.*, ischiofemoralis; *lat.col.lig.*, lateral collateral ligament; *med.col.lig.*, medial collateral ligament; *obt.med.*, obturatorius medialis; *p.i.f.*, puboischiofemoralis; *p.i.f.lat.*, puboischiofemoralis lateralis; *p.i.f.med.*, puboischiofemoralis medialis; *tib.cran.f.*, tibialis cranialis caput femorale.

muscles' origination typically occupies almost the entire preacetabular iliac blade, and their insertion on the femoral trochanter follows a fairly consistent pattern (see above).

**Observations.** In *D. robustus*, *P. elephantopus* and *E. crassus*, the three muscles' origin from the preacetabular ilium is indicated by an uneven surface texture with extensive and strong, often striated, ridges and elongate tubercles, directed toward the acetabulum. (These scars should not be confused with the numerous anastomosing, smooth-surfaced blood vessel channels that etch the iliac surface.) Toward the dorsal and cranial margins of the preacetabular ilium is a long line of tuberosities and short ridges, which runs from the dorsal part of the preacetabular ilium and around the cranial margin, and often loops back along the cranioventral margin. Each tubercle or ridge is striated, with the striations directed toward the acetabulum. The degree of development of these tuberosities and ridges is variable in all species studied: in some specimens they are well developed and unite to form a single, well-defined ridge, whereas in others they consist of several low tubercles that are broadly aligned. This line of scarring is interpreted as an intermuscular line separating the origins of at least two of the iliotrochanterici, with the origin of the iliotrochantericus caudalis likely being situated caudal to the line. The exact location of origins of the iliotrochanterici cranialis et medius is not able to be determined. The distinctive scarring of the iliotrochanterici does not extend onto the sacral ribs fused with the ilium in any species, suggesting that the muscles' origins did not either.

The existence of the iliotrochanterici in *D. robustus*, *P. elephantopus* and *E. crassus* is also evidenced by their well-marked scars of insertion on the femoral trochanter, which although variable in appearance, is consistent with that observed in extant palaeognaths (level I inference). The topography of the femoral trochanter in all moa is dominated cranially by a very long and deep furrow which parallels the cranial margin of the bone; this gives the cranial part of the trochanteric ridge a medial inflection in proximal view. At its caudal end, the furrow

is strongly scarred, with striations and ridges pointing cranially to cranioproximally; here the furrow can also become so deeply recessed that it forms a long pocket. In *E. crassus* the scarring in the distal part of this region extends onto the cranial aspect of the trochanter. The entire region of scarring corresponds to the insertion of the iliotrochantericus caudalis in extant palaeognaths, and is interpreted as such here for *D. robustus*, *P. elephantopus* and *E. crassus*. Distal to this scar is a broad region of coarse striations, which are again cranially to cranioproximally directed; the striations are most strongly developed around the margins of this area. This scarring, which extends onto the cranial aspect of the trochanter in *P. elephantopus*, is distinct from the aforementioned scarring located proximal to it, and often they are separated by smooth bone. In extant palaeognaths this region of scarring corresponds to the insertion of both the iliotrochantericus cranialis and medius. In lieu of any further discrete scarring in this region of the femur in *P. elephantopus* and *E. crassus*, it is hypothesised that both iliotrochanterici cranialis et medius inserted here in these species, sharing a common insertion.

In *D. robustus* the situation is different. Here, the craniomedial aspect of the femoral trochanter is scarred with well-developed tubercles and ridges (Fig. 4A). (This area of the bone is relatively smooth in *P. elephantopus* and *E. crassus*; any uneven texture is related to the presence of pneumatic diverticula.) They often bear fine striations (presumably Sharpey's fibres), which are directed transverse to their long axes, roughly toward the femoral head. That the striations are pointing in this direction, and not distally, argues against them being associated with the femorotibialis muscles (see below), where they would be expected to point distally. Indeed, in a number of specimens the medial extent of the scarring is bounded by an intermuscular line of the femorotibialis medius (see below). It is posited here that these scars are for the insertion of the iliotrochantericus medius. In two specimens (CM Av 8469, 13461), these scars are united into a single, massive tubercle some 20 mm across, pointing toward the femoral head.



Thus, the ilioprochantericus cranialis in *D. robustus* is posited to have inserted separately in the usual position on the lateral aspect of the trochanter. The medial aspect of the trochanter in *D. robustus* also shows a variable level of pneumatization, with pockets, furrows and large foramina dotting the surface (indicating the presence of diverticula), but these are easily distinguished from the hypothesised insertion of the ilioprochantericus medius because they produce no positive surface relief, and the bone surface itself is smooth, as opposed to the coarse and fibrous scarring of the muscle insertion.

**Remarks.** Although evidence for each separate ilioprochantericus head is not always present on the bones of a given moa species, inferring the presence of all three heads in moa is supported by the fact that they exist in all extant palaeognaths (a level I inference). Both the origin and insertion of the ilioprochantericus caudalis is evidenced by well-developed and unambiguous osteological indicators of its attachment to the pelvis and femur, respectively. Hence, the proposed reconstruction of this head is well supported (level I inference).

The origins of the ilioprochantericus cranialis et medius are proposed here to have likely originated more or less cranial to the origin of the ilioprochantericus caudalis. This arrangement differs markedly from that hypothesised by Zinoviev (2013), who reconstructed both heads as originating ventral to the origin for the ilioprochantericus caudalis. His specimens were both incomplete, however, lacking the cranial part of the preacetabular iliac blade. Consequently, he may not have been able to observe the long line of tuberosities and ridges that are consistently present, which are interpreted here as an intermuscular line. This may in turn have influenced his interpretations. Moreover, the ilioprochantericus cranialis at least is typically wholly or partially cranial to the main bulk of the ilioprochantericus caudalis in extant palaeognaths. Considering both osteological and comparative evidence together, the proposed arrangement receives level II support, whereas Zinoviev's reconstruction only has level II support.

The ilioprochantericus cranialis et medius on the femur of *P. elephantopus* and *E. crassus* are both posited to have shared a single common insertion, based on the osteological evidence. A common insertion of the ilioprochantericus cranialis et medius is a feature seen in several extant palaeognaths (*Dromaius*, *Struthio*, *Apteryx*, *Tinamus* and *Crypturellus*), such that the interpretation for *P. elephantopus* and *E. crassus* is a level II inference. The reconstructed position of the insertion for the ilioprochantericus medius in *D. robustus*, on the medial aspect of the femoral trochanter and separate to that of the ilioprochantericus cranialis, is distinct from that observed in all extant palaeognaths. Nonetheless, its proximodistal position on the femur is comparable to that observed in extant palaeognaths and inferred in other moa species. Furthermore, hypothesizing that the scars on the medial aspect of the trochanter are for a different muscle would be more speculative, as all other muscles in the general region of the bone can be accounted for with other surface scars (detailed above and below).

#### Femorotibialis (Figs 4–7; fem.tib.)

**General comments.** This comprises a minimum of four parts in extant palaeognaths, namely, externus pars proximalis (fem.tib.ex.p.), externus pars distalis (fem.tib.ex.d.), medius (fem.tib.me.) and internus (fem.tib.in.). (Note that Hudson *et al.* (1972) termed the femorotibialis externus pars proximalis of tinamous the 'lateral head of the femorotibialis medius', and also termed the femorotibialis medius the 'medial head of the femorotibialis medius'.) Except in *Apteryx*, the pars internus is further subdivided in the various species of palaeognaths, although the homology of these parts between species is uncertain, especially of the 'pars pectineus' of *Struthio* (Zinoviev 2006; Hutchinson *et al.* 2015). The origins of the various heads of the femorotibialis effectively enclose the whole shaft of the femur in extant palaeognaths, and they typically insert on the cranial cnemial crest of the tibiotarsus, either directly or via the patellar tendon and surrounding connective tissue. The femorotibialis externus pars distalis,

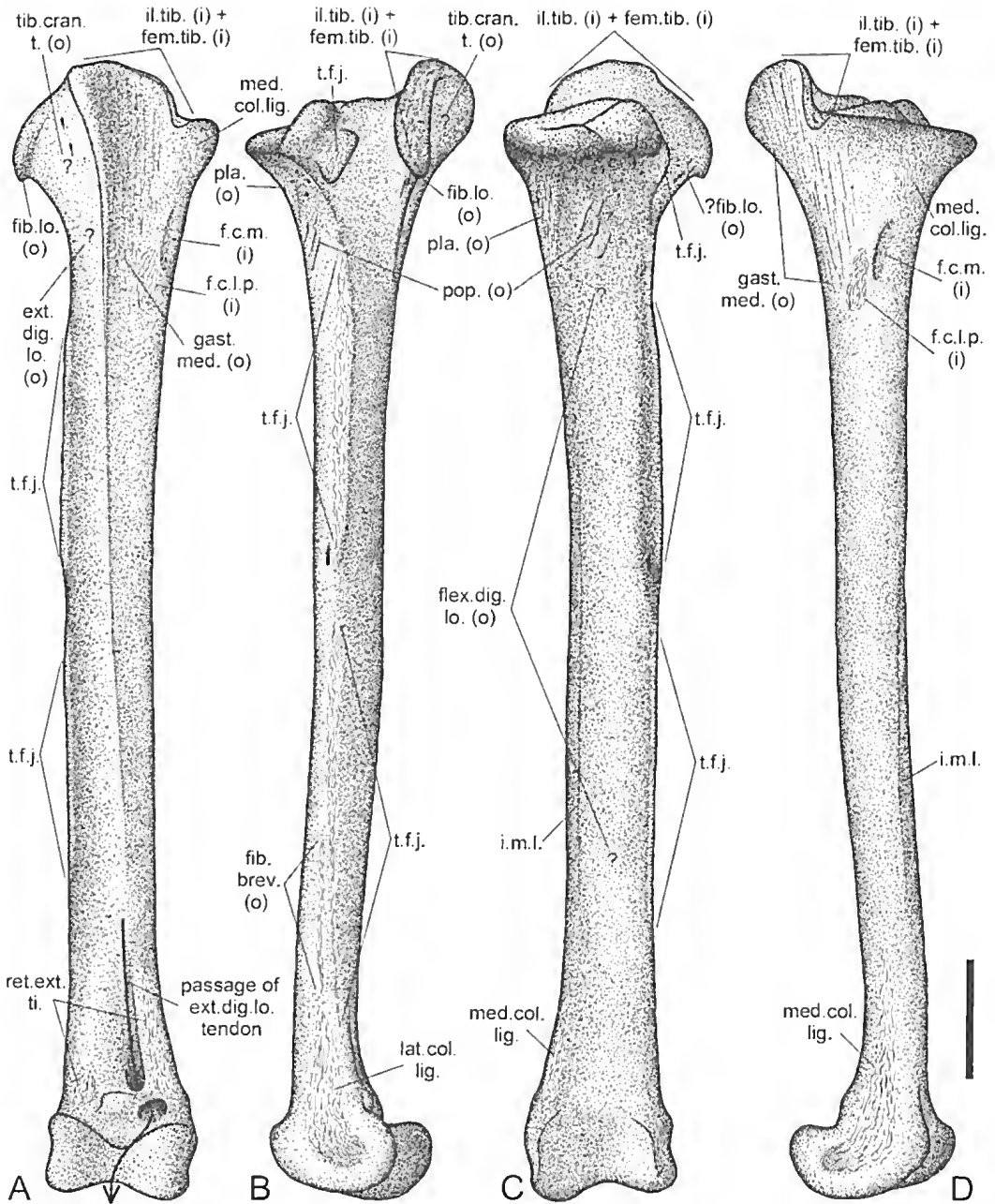


FIG. 6. Osteological evidence of muscle attachment on the tibiotarsus of *D. robustus*, with corresponding myological interpretations. A, cranial view; B, lateral view; C, caudal view; D, medial view. Scale bar = 100 mm. Abbreviations: *ext.dig.lo.*, extensor digitorum longus; *f.c.l.p.*, flexor cruris lateralis pars pelvica; *f.c.m.*, flexor cruris medialis; *fem.tib.*, femorotibialis; *fib.br.*, fibularis brevis; *fib.lo.*, fibularis longus; *flex.dig.lo.*, flexor digitorum longus; *gast.med.*, gastrocnemius medialis; (i), muscle insertion; *il.tib.*, iliotibialis; *i.m.l.*, intermuscular line; *lat.col.lig.*, lateral collateral ligament; *med.col.lig.*, medial collateral ligament; (o), muscle origin; *pla.*, plantaris; *pop.*, popliteus; *ret.ext.ti.*, retinaculum extensorium tibiotalaris; *t.f.j.*, ligament of the tibiofibular junction; *tib.cran.t.*, tibialis cranialis caput tibiale.



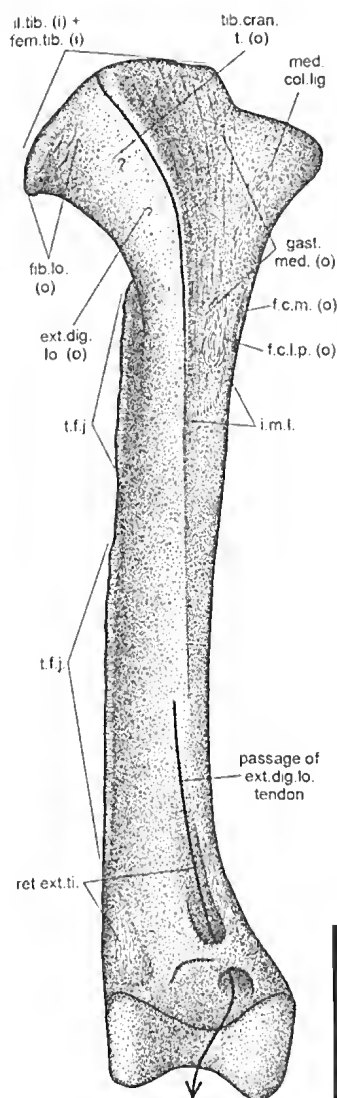


FIG. 7. Osteological evidence of muscle attachment on the cranial tibiotarsus of *P. elephantopus*. Note in particular the coarse intermuscular line bounding the distal extent of the origin of the gastrocnemius medialis. Scale bar = 100 mm. Abbreviations: *ext.dig.lo.*, extensor digitorum longus; *f.c.l.p.*, flexor cruris lateralis pars pelvica; *f.c.m.*, flexor cruris medialis; *fem.tib.*, femorotibialis; *fib.lo.*, fibularis longus; *gast.med.*, gastrocnemius medialis; *(i)*, muscle insertion; *il.tib.*, iliotibialis; *i.m.l.*, intermuscular line; *med.col.lig.*, medial collateral ligament; *(o)*, muscle origin; *ret.ext.ti.*, retinaculum extensorium tibiotarsi; *t.f.j.*, ligament of the tibiofibular junction; *tib.cran.t.*, tibialis cranialis caput tibiale.

however, inserts on the lateral aspect of the lateral cnemial crest.

**Observations.** The femur of *D. robustus*, *P. elephantopus* and *E. crassus* possesses several well-defined, longitudinal ridges along the shaft, which occupy the same general position as the femorotibialis intermuscular lines on the femora of extant large palaeognaths, and they are therefore interpreted as such. These ridges usually bear fine striations along their length, which are always directed distally. The longest ridge (intermuscular line 1) runs from the craniomedial aspect of the trochanter down the cranial aspect of the shaft; it bifurcates halfway to three-fifths of the way down, sending a branch each to the proximal extent of the lateral and medial condyles. This ridge is homologous with the linea intermuscularis cranialis of extant birds (cf. Baumel *et al.* 1993). In moa its proximal extent along the craniomedial trochanter is variable, sometimes reaching up to the level of the proximal aspect of the femoral head. A second, fainter ridge (intermuscular line 2) runs proximodistally along the craniomedial shaft, distal to the insertion scar of the iliofemoralis internus. Intermuscular line 2 sometimes extends proximal to the insertion of the iliofemoralis internus (in *E. crassus* it can run either lateral or medial to the iliofemoralis internus scar). In some specimens it is so proximally extensive that it joins up with intermuscular line 1 on the craniomedial aspect of the femoral trochanter. This feature is particularly prevalent in *E. crassus* and *Euryapteryx curtus*, where intermuscular line 1 also has a considerable proximal extent (cf. Fig. 5B).

Two ridges are present on the caudal surface of the femur, which run along the bone's caudo-medial aspect (intermuscular line 3) and caudolateral aspect (intermuscular line 4). In *D. robustus* these ridges are always well separated, whereas in *E. crassus*, they can be quite close to each other, although the fine striations on the apices of the ridges remain separate. In *P. elephantopus* the ridges are very close to one another, and in the great majority of cases they actually unite along the middle of the caudal shaft to form a single intermuscular line which runs adjacent to – or indeed straight across –

the central nutrient foramen (Fig. 5A). Thus, in *P. elephantopus*, the entire femoral shaft (at the level of the midpoint in the bone) is enveloped by the femorotibiales. It is proposed here that both intermuscular lines 3 and 4 (or the union thereof) are homologous with the single linea intermuscularis caudalis of extant birds (cf. BaumeI *et al.* 1993); moa seem to be exceptional here in that these lines are largely separate in most species. In *Apteryx* spp. the caudal aspect of the femur possess two faint longitudinal ridges on its caudal aspect, but one is not a femorotibialis intermuscular line, rather it marks the (extended) attachment of the caudofemoralis pars caudalis (McGowan 1979).

In all moa, the proximal end of intermuscular line 3 curves medially and heads towards the insertion scar of the iliofemoralis internus. Intermuscular line 4 typically runs all the way from the ventral edge of the insertion scar of the ischiofemoralis (see below), down past the pronounced caudal tuberosities and nearly to the ectocondylar fossa. In *D. robustus* a small accessory line of similar scarring (with striations directed distally) is occasionally present, branching off the distal part of intermuscular line 4. A fifth ridge (intermuscular line 5) is present in most specimens examined, although it is only rarely present on the femora of *D. robustus*. It is situated between intermuscular lines 1 and 4 on the bone's lateral aspect, typically in line with the scar of insertion of the iliofemoralis externus, and runs proximodistally. This ridge is homologous with the linea intermuscularis lateralis of extant birds (cf. Hutchinson 2001).

As in extant palaeognaths, the abovementioned intermuscular lines would have delimited, to a large extent, the areas of origin of the femorotibialis heads. The femorotibialis externus would have originated from much of the lateral surface of the shaft, between intermuscular lines 1 and 4. Furthermore, the presence of intermuscular line 5 in most specimens supports reconstructing the division of this muscle into partes proximalis and distalis; as in extant palaeognaths, the pars proximalis would presumably have originated cranial to the pars distalis. It is uncertain as to whether the division of the femorotibialis externus was a consistent feature in *D. robustus*.

The femorotibialis medius would have originated along the cranial aspect of the shaft between intermuscular lines 1 and 2; the great proximal extent of line 1 in *E. crassus* and *Euryapteryx curtus* indicates that the muscle took origin from the medial aspect of the trochanter, as in *Apteryx* (McGowan 1979; Kooyman 1991). The femorotibialis internus would have originated from much of the medial aspect of the shaft between intermuscular lines 2 and 3.

The proximal and lateral margins of both cnemial crests in moa show evidence of soft tissue attachment, with distinct areas of a roughened, fibrous texture, slightly recessed into the surrounding bone surface. Although the femorotibiales presumably inserted on these parts, as in extant palaeognaths, it is not possible to differentiate the insertions of the femorotibialis from those of the iliotibiales.

**Remarks.** Identification of the femorotibialis intermuscular lines on the moa femur, and the largely conservative nature of the femorotibialis in extant palaeognaths, means that reconstruction of the femorotibialis externus pars proximalis, externus pars distalis, medius and internus in moa are all strongly supported (level I inferences). However, a lack of osteological evidence precludes determining whether the femorotibialis internus was further subdivided or not.

The interpretations presented here differ slightly from those offered by Zinoviev (2013) in two respects. Firstly, Zinoviev reconstructed the proximal part of the femorotibialis medius as originating from the distocranial aspect of the trochanter, but this is not supported by the osteological evidence. Specifically, intermuscular lines 1 and 2 indicate that if the muscle's origin did indeed reach as far proximally as the trochanter, it would have been restricted to the medial aspect of the trochanter only. The second difference in interpretations relates to the subdivision of the femorotibialis medius. Zinoviev suggested that a second part of the femorotibialis medius existed, the 'pars distalis', which took origin from the distal femur between the two branches of intermuscular line 1. No evidence for this attachment was observed in any of the specimens examined in this study; the

surface of the bone here is either smooth, or any unevenness present appears to be fluting caused by blood vessel channels. Furthermore, only in *Struthio* does such a second part exist. Thus, without osteological evidence, it is less parsimonious to reconstruct a 'pars distalis' in moa (a level II' inference) than to refrain from doing so (a level I' inference).

### Ambiens (Fig. 3; amb.)

**General comments.** Except in *Struthio*, where it originates from the ventrolateral margin of the preacetabular ilium (Gangl *et al.* 2004; Zinoviev 2006; but see Hutchinson *et al.* 2015), the ambiens originates from the preacetabular tubercle (or 'pectineal process') in extant palaeognaths. The ambiens runs down to the knee, where it becomes a tendon that perforates the aponeurosis surrounding the knee medially. Two exceptions to this are tinamous, where the perforation occurs on the lateral side (Hudson *et al.* 1972), and *Apteryx*, where it the tendon actually perforates the patella (McGowan, 1979). Distal to the knee, the tendon inserts on the origin (or origins) of the flexor perforatus digiti II, the flexor perforatus digiti III, or both. In casuariids, the tendon terminates at the knee (Gadow, 1880; Patak & Baldwin 1998; Lamas *et al.* 2014).

**Observations.** Moa lack a preacetabular tubercle, but a low, broad area of pronounced rugosity is present in the same region of the pelvis, on the craniolateral aspect of the acetabular rim; this is taken to mark the origin of the ambiens (level I inference). In one specimen of *D. robustus* (CM Av9049) and two specimens of *P. elephantopus* (CM Av8383, 8387), this scar is slightly recessed into the surrounding bone surface. In *D. robustus*, *P. elephantopus* and *E. crassus*, there is also occasionally a poorly developed area of roughened bone, sometimes with a small tubercle or flange, located ventral to this broad area of rugosity on the craniolateral 'corner' of the proximal pubis. This may mark the origin of a second head of the ambiens, as evidenced by the fact that the tubercle or flange points ventrolaterally, towards the in-life position of the knee. The ambiens of moa would

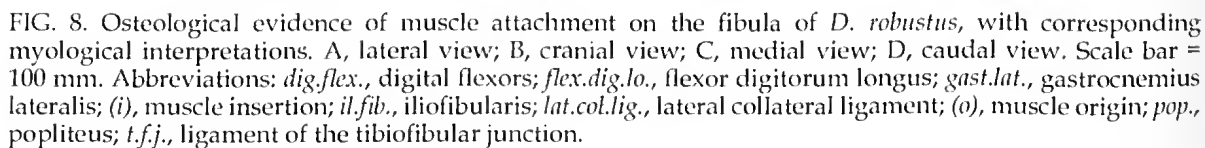
have presumably run at least as far as the knee, but whether it terminated or continued toward the distal limb, and in what manner, cannot be determined.

**Remarks.** Reconstructing the site of origination for this muscle in moa is well supported (a level I inference), as is the hypothesis that it ran toward the knee (a level I' inference). How it may have terminated, and where in the limb it may have done so, remains uncertain, as there is no osteological evidence in the moa fossils, and the situation in extant palaeognaths is variable; any reconstruction would have level II' support at best.

### Iliofibularis (Figs 3–5, 8; il.fib.)

**General comments.** In all extant palaeognaths, the iliofibularis takes origin from most of the length of the postacetabular ilium, immediately ventral to the origin of the iliotibialis lateralis pars postacetabularis on the dorsolateral iliac crest. It inserts via a thick tendon on a pronounced tubercle on the posterolateral shaft of the fibula. (*Struthio* possesses a small second insertion, the 'crus caudale' of Gangl *et al.* (2004), which separates from the main muscle mass distally and inserts on the caudal fascia of the gastrocnemii). Before it inserts on the fibula, the tendon of this muscle always runs through a ligamentous loop, the ansa iliofibularis (an.il.fib.). The nature of bony attachment of the ansa is poorly documented in extant palaeognaths. It may also be variable, as Owen (1879) described attachments to the lateral femur and tibia in *Apteryx*, yet McGowan (1979) and Kooyman (1991) found two attachments to the femur only. In *Rhea*, Gadow (1880) described one attachment of the ansa to the distal lateral femur, and another apparently to the lateral collateral ligament of the knee. In *Struthio* there are two attachments to the distal femur, which are very close together (J.R. Hutchinson, pers. comm. 7.2.13).

**Observations.** Although visible surface scarring is lacking in the vast majority of specimens examined, the iliofibularis is inferred to have occupied the same relative position on the ilium in *D. robustus*, *P. elephantopus* and *E.*



*crassus* as in extant palaeognaths. In a few *P. elephantopus* and *E. crassus* specimens examined, there existed a broad, roughened ridge with longitudinal striations, positioned a little ventral to the dorsolateral iliac crest. This ridge may be some form of intermuscular line demarcating the boundary between the origin of the iliofibularis and another muscle. The insertion of the iliofibularis in moa is unambiguous, for the fibula possesses a very distinct tubercle on its posterolateral aspect. It is large and broad, although its degree of development is variable; in some specimens of *P. elephantopus*, the scar of insertion is slightly recessed into the surrounding bone. The tubercle is always well separated, and distinct, from the large area of strong scarring proximally; this area would have been for the attachment of the lateral collateral ligament, as indicated by the coarse striations and fine tubercles directed proximally.

There are two candidate attachment sites for the ansa on the femur of moa, the ectocondylar fossa (as also suggested by Worthly & Scofield 2012), and a small scar cranioproximal to this (Figs 4B, C, 5A, C, D). Both are recognisable in *Apteryx* as the attachments for the ansa (McGowan 1979; Kooyman 1991).

**Remarks.** The reconstruction of this muscle in moa in the typical palaeognath condition is supported, both proximally (a level I inference) and distally (a level I inference). The nature of its associated ansa is somewhat uncertain, however. Two attachments for the ansa are reconstructed here, but Zinoviev (2013) suggested that a third attachment existed, to the proximolateral fibula. This is the condition present in most neognaths (Baumel *et al.* 1993). No discrete scar on the proximolateral fibula, separate from that of the lateral collateral ligament of the knee, was discernable in any of the material examined in this study, nor is any appropriate scar evident on the lateral tibiotarsus. Hence, it is deemed too speculative to reconstruct a third attachment for the ansa in moa, especially in light of the lack of knowledge of this feature in most extant palaeognaths.

### Flexor cruris lateralis (Figs 3–7)

**General comments.** In extant palaeognaths, the flexor cruris lateralis comprises two parts, the partes pelvica (f.c.l.p.) and accessoria (f.c.l.a.). The pars pelvica originates from the caudal end of the postacetabular ilium, caudal to the origin of the iliotibialis, although in various taxa it may also take origin from the first few unfused caudal vertebrae (*Casuaris*, *Rhea*, tinamous), the caudal end of the ischium (*Struthio* and *Rhea*, related to the fusion of the caudal ilium and ischium in these taxa), or ilioischadic membrane (*Struthio*). The pars pelvica gives off the pars accessoria distally, which inserts on the caudal aspect of the femoral shaft; see the description of the puboischiofemorals below for a treatment of this muscle's insertion in moa. The pars pelvica itself becomes tendinous distally and inserts on the proximomedial surface of the tibiotarsus, adjacent to that of the flexor cruris medialis (the two may share a common insertion, as in *Struthio* and sometimes *Rhea*).

**Observations.** Although no osteological evidence has been observed in *D. robustus*, *P. elephantopus* or *E. crassus*, this muscle likely originated from the caudal end of the postacetabular ilium or the region thereabouts. On the proximomedial tibiotarsus of *D. robustus*, *P. elephantopus* and *E. crassus*, there are three diffuse areas of roughened, sometimes rugose, bone. One of these is more proximal to the other two, and the three areas are not always completely separate from each other. The proximal area is suggested to be the scar of the lateral collateral ligament of the knee, and the distal two are the insertion scars of the flexores cruris medialis et lateralis pars pelvica. In *Dromaius*, the flexor cruris lateralis pars pelvica inserts cranial to the flexor cruris medialis (Lamas *et al.* 2014), and without any evidence to the contrary this was probably also the case in moa. In *E. crassus*, *Euryapteryx curtus* and *A. didiforuiis*, the flexor cruris lateralis pars pelvica may have been associated with the head of the gastrocnemius medialis (see below), as the scar of insertion of the former muscle is often more cranially situated, where it almost contacts the procnemial ridge and thereby would have been

very close to the latter's origin. Moreover, the scar of the flexor cruris lateralis pars pelvica is often sometimes closely associated with the striations of the gastrocnemius medialis origin (see below).

**Remarks.** Reconstructing this muscle in the manner typical among palaeognaths is well-supported, being a level I' inference proximally and level I inference distally. Zinoviev (2013) suggested that the more cranial of the two distal scars on the proximomedial tibiotarsus of moa was for the insertion of both the flexor cruris lateralis pars pelvica and the flexor cruris medialis (implying a common insertion), and that the more caudal scar was for the insertion of the medial collateral ligament of the knee; he did not mention the proximal scar. It is more likely that the more proximal scar was for the insertion of the collateral ligament, rather than either of the distal ones; this is because the distal scars are always a fair distance from the proximal end of the bone compared to other birds, including ostriches (Chadwick *et al.* 2014).

#### **Flexor cruris medialis** (Figs 3, 6, 7; f.c.l.m.)

**General comments.** In extant palaeognaths, this muscle usually takes origin from the lateral aspect of the caudal end of the pubis, or the caudal end of the pubis and ischium and the lateral aspect of the intervening puboischiadic membrane; in *Struthio* it may also originate from the ilioischiadic membrane (Gangl *et al.* 2004). *Rhea* is distinct different from all other extant palaeognaths in that the muscle takes origin from the cranioventral ischium, just caudal to the acetabulum (Picasso 2010). As noted above, the muscle invariably inserts on the proximomedial tibiotarsus, adjacent to (or with) that of the flexor cruris lateralis pars pelvica.

**Observations.** The muscle very likely existed in *D. robustus*, *P. elephantopus* and *E. crassus*. On the distal ischium or pubis of these species, there is usually some form of low, broad tubercle with a rougher surface texture than the surrounding bone, sometimes associated with a localised thickening of the bone. This is

likely associated with the origin of the flexor cruris medialis, although the muscle may have also originated from the puboischiadic or ilioischiadic membranes. As described above, a scar exists on the proximomedial tibiotarsus in all moa that is interpreted as that for the insertion of the flexor cruris medialis. The scar for the collateral ligament may be confluent with the scar of the flexor cruris medialis, although they can be easily distinguished: the scar of the muscle is recessed, often deeply, into the bone surface, whilst that of the ligament is not.

**Remarks.** Reconstructing both the origin and insertion of this muscle in moa is a level I inference.

#### **Obturatorius medialis** (Figs 3–5; obt.med.)

**General comments.** Always present in palaeognaths, this muscle has a variable origin, which can include the medial surface of the ischium (the most common manifestation), the medial surfaces of the puboischiadic membrane and pubis, and, less frequently, the medial surface of the ilioischiadic membrane and even the ventral postacetabular ilium. *Struthio* is unusual in that this muscle originates from the lateral aspect of the puboischiadic membrane (Gangl *et al.* 2004; Zinoviev 2006). In the casuariids and *Rhea* it comprises two separate parts (Gadow 1880; Patak & Baldwin 1998; Picasso 2010; Lamas *et al.* 2014). In marked contrast to this variation, the muscle's manner of insertion in extant species is highly consistent: it sends a tendon through the obturator foramen (formed between the closely aligned proximal pubis and ischium; Fig. 3), to insert on the proximocaudal aspect of the femoral trochanter.

**Observations.** All moa likely possessed an obturatorius medialis, although it is not certain as to where it originated; presumably, it would have originated from the medial surface of whatever element or membrane it attached to. As described above, a suitable insertion for this muscle is present on the proximal femur of *D. robustus*, *P. elephantopus* and *E. crassus*,

as indicated by a large, roughened depression rimmed with coarse-textured bone. In all three species the scar is often so well developed that it is recessed into the surrounding bone surface at its cranial end, forming a pocket. In *D. robustus*, there is sometimes a secondary pocket within the main pocket, which may mark the insertion of the obturatorius lateralis (see below).

**Remarks.** This muscle's reconstruction in moa is well supported both at its origin (level I' inference) and insertion (level I inference). Zinoviev (2013) posited that the obturatorius medialis in *D. robustus* was bipartite, comprising dorsal and ventral bellies. He cited osteological evidence in support of this – “[t]races of its origin in *D. robustus* suggest that it must have had two bellies” (p. 259; see also his fig. 1B) – yet he did not describe the evidence itself. A bipartite obturatorius medialis does exist in some extant palaeognaths, and this is typically associated with a faint longitudinal ridge along at least part of the ventromedial aspect of the ischium, probably marking the junction of the aponeuroses of the two bellies with the bone. However, no ridge or any other feature, was observed on the medial surface of the ischium in any moa specimen examined in this study. Reconstructing a bipartite obturatorius medialis in moa is therefore not well supported (level II' inference), and is avoided here.

#### Obturatorius lateralis (Figs 3, 4; obt.lat.)

**General comments.** This muscle is always present in extant palaeognaths, typically originating from the margin of the obturator foramen, just caudal to the acetabulum. The point of insertion of the obturatorius lateralis on the proximocaudal femur is closely associated with that of the obturatorius medialis in extant palaeognaths, although they are usually distinct.

**Observations.** The scarring surrounding the obturator foramen on the pelvis of *D. robustus*, *P. elephantopus* and *E. crassus* is exceptionally variable, in terms of the number, position and degree of development of tubercles and ridges. One feature which does appear to be consistent in each species is the presence of a prominent

and coarse tuberosity immediately cranial to the obturator foramen, which is interpreted as marking the origin (or part thereof) of the obturatorius lateralis. Other scars in the vicinity may also mark the origin of this muscle, but they may also be where the ischiofemoralis originated from (see below). There is often a small, rugose area on the proximocaudal surface of the femur of *D. robustus*, *P. elephantopus* and *E. crassus*, caudal to the insertion scar of the obturatorius medialis, which could be the insertion scar of the obturatorius lateralis, although this was not present in every specimen examined. In *D. robustus*, an accessory pocket inside the main scar of the obturatorius medialis may indicate that the two muscles were more closely associated in that species.

**Remarks.** Reconstructing the general areas of origin and insertion of this muscle is well supported (level I inferences), although the exact position of each are difficult to identify. Moreover, these positions may vary somewhat both within and between species.

#### Ischiofemoralis (Figs 3–5; is.fem.)

**General comments.** In extant palaeognaths this muscle originates from the dorsolateral aspect of the ischium and the adjacent ilioischadic membrane, although there are minor differences between species. For example, its area of origin includes most of the ischium in *Apteryx* and tinamous, but only the cranial third of the ischium in *Struthio*, and only the caudal part of the ischium in *Dromaius* (where it is often fused with the caudofemoralis pars pelvica; but see Lamas *et al.* 2014). As described above, the ischiofemoralis inserts on the caudolateral aspect of the femoral trochanter in extant palaeognaths, just distal to the insertion of the obturatorius.

**Observations.** Unambiguous osteological evidence of this muscle's origin is wanting in *D. robustus* and *P. elephantopus*. The muscle presumably took origin from part of the dorsolateral ischium, and in the proximal part of the bone there are usually a number of tubercles or ridges, but these may be associated with the origin of the obturatorius lateralis. In *E. crassus*, there



is sometimes a faint, but distinct, ridge on the lateral surface of the distal ischium, trending roughly parallel with the bone (Fig. 3B). This may be an intermuscular line demarcating part of the origin of the muscle in this species. The femora of all moa exhibit a strongly developed scar in the region corresponding to the insertion of the ischiofemoralis in extant palaeognaths, distal to the insertion scar of the obturatorius medialis. This scar typically consists of an elongate oval-shaped to linear region of raised bone with pronounced roughness. In *D. robustus*, the scar is sometimes developed into a roughened depression with a pronounced and rugose distal rim. In *E. crassus*, it may be partly confluent with the scar of insertion of the iliofemoralis externus, but they can always be distinguished by the different orientation of the fibres or striations in each scar (directed proximally to cranioproximally in the iliofemoralis externus scar, directed proximocaudally to caudally in the ischiofemoralis scar).

**Remarks.** Reconstructing the ischiofemoralis in moa is well supported both for its origin (level I' inference) and its insertion (a level I inference), although the exact size and position of its origin in *D. robustus* and *P. elephantopus* is uncertain.

### Caudofemoralis (Figs 3–5; caud.fem.)

**General comments.** This muscle consists of two parts in extant palaeognaths, the pars caudalis and the pars pelvica. The pars caudalis is absent in *Dromaius* and *Rhea*, but in other palaeognaths it originates from the lateral aspect of several unfused caudal vertebrae (which vertebrae are involved varies from species to species). The pars pelvica has a more varied origin, which can include the ventrolateral postacetabular ilium, ventral to the origin of the iliofibularis, ilioischadic membrane, dorsocaudal pubis and the synsacral caudal vertebrae. In *Dromaius*, the pars pelvica is often fused with the ischiofemoralis (but see Lamas *et al.* 2014), the combined muscle originating from the caudal ilium, ischium and ilioischadic membrane. The two parts of the caudofemoralis (when both are present) both insert on the proximal

caudolateral surface of the femoral shaft, near the insertion of the ischiofemoralis; their insertions are often fused into a single attachment. *Apteryx* is distinctive in that the insertion continues distally for a considerable distance along the caudal aspect of the femur (McGowan 1979).

**Observations.** The unfused caudal vertebrae of *D. robustus*, *P. elephantopus* and *E. crassus* possess a slightly fluted or uneven surface on their ventral and ventrolateral aspects, but this varies both within and between individuals of the same species, as well as between species. Other caudal muscles were likely also present in this region of the tail, and since there is no discrete scarring which may be recognised as the attachment of the caudofemoralis pars caudalis, it is uncertain as to whether these taxa possessed this muscle or not. Moa almost certainly possessed a pars pelvica, but the great variability in its origin in extant palaeognaths, and lack of visible surface scarring on the pelvis, precludes an identification of its exact area of origin.

On the proximal caudal surface of the femur of *D. robustus*, *P. elephantopus* and *E. crassus* is an area of relatively faint scarring, located caudal to (and distinct from) the large insertion scar of the ischiofemoralis on the caudolateral aspect of the femoral trochanter. This scarring corresponds to similarly positioned scarring for the caudofemoralis in extant palaeognaths, and is interpreted as such for moa. The scarring in *P. elephantopus* is usually more medially situated away from the scar of the ischiofemoralis, lying proximal to the bend in intermuscular line 3; the two scars are well separated by smooth bone. The scar's exact size, shape and positioning vary modestly in *E. crassus*, and in roughly half of the specimens examined the scar is confluent with that of the ischiofemoralis. In *Euryapteryx curtus*, the scar is almost always confluent with that of the ischiofemoralis; sometimes only a single large area of scarring is present in this part of the femur. In *D. robustus*, *P. elephantopus* and *E. curtus*, a small but rugose region of scarring is occasionally found proximal to scar of insertion of the caudofemoralis, caudal to the scar of the obturatorius insertion. This



may be for the caudofemoralis (perhaps the pars caudalis, if it existed) or instead may be for the obturatorius (perhaps the smaller lateralis head).

**Remarks.** It is currently too ambiguous to reconstruct the caudofemoralis pars caudalis in moa (it would be a level II' inference), but reconstructing the pars pelvica is more supported (level I' inference for origin, level I inference for insertion). No scarring on the proximal caudal femur of any kind was mentioned by Zinoviev (2013), and consequently the caudofemoralis pars pelvica (his 'iliofemoralis') was reconstructed as inserting elsewhere, on intermuscular line 4. This has been argued above to instead reflect the attachment of the femorotibialis externus, or part thereof. That intermuscular line 4 (as with the other intermuscular lines) typically bears fine striations that point distally further refutes Zinoviev's interpretation, for the striations would be expected to point proximally if the caudofemoralis inserted there. Moreover, the scar inferred here as marking the insertion of the caudofemoralis is clearly separated from intermuscular line 4 by smooth bone, indicating that the insertion of the caudofemoralis did not extend onto the ridge. Zinoviev did concur with the current study in considering that the caudofemoralis pars caudalis (his 'caudofemoralis') was possibly absent in moa.

### Puboischiofemoralis (Figs 3–5, p.i.f.)

**General comments.** In all extant palaeognaths, this muscle comprises two parts, lateralis (p.i.f.lat.) and medialis (p.i.f.med.), which are closely associated. They typically originate from the ventral ischium and adjacent puboischadic membrane, and in *Struthio* and tinamous the origin extends onto the dorsal pubis (Hudson *et al.* 1972; Gangl *et al.* 2004). The insertion of the puboischiofemorales on the caudal femur is somewhat variable in extant taxa, with the insertion being extensive in some, such as along almost the entire length of the femur in *Apteryx* (McGowan 1979) and *Rhea* (Picasso 2010), and relatively restricted in others. In all cases its insertion is medial to that of the flexor cruris lateralis pars accessoria. Furthermore, the two

parts of the puboischiofemoralis tend to have a more or less single, common insertion.

**Observations.** The caudal ischium of *D. robustus*, *P. elephantopus* and *E. crassus* typically bears a long ridge of coarse, longitudinally striated bone on its ventral half, which can extend as far cranially so as to become confluent with the scarring on the obturator flange. This ridge is often well developed, forming an overhang above the ventralmost part of the ischium, especially in larger individuals. In small individuals the ridge may be entirely absent. The ridge and associated scarring is interpreted to be the dorsal border of the origin of the puboischiofemoralis in all three species. The muscle in moa would presumably have comprised both lateralis and medialis parts, as in extant palaeognaths.

In *D. robustus*, there are always two prominent and large tuberosities on the caudal femoral shaft, that are well separated from each other by smooth bone; the smaller, medial one is more distally located than the larger, lateral one. This feature is diagnostic for *Dinornis* (Worthy 1988; Worthy & Holdaway 2002; Worthy & Scofield 2012). Both tuberosities are also present in *M. didinus* and emeid moa, although in emeids they are associated with each other to a variable degree: their appearance ranges from two distinct points of elevation, the fibrous textures of which are separate, through to a single discernable tuberosity. The presence of two tuberosities – which are separated by smooth bone in *D. robustus* and *M. didinus* – suggests that two muscles inserted on this part of the moa femur, rather than one. Given that the medial of the two caudal tuberosities is separated from intermuscular line 3 by smooth bone, and likewise the lateral caudal tuberosity is separated from intermuscular line 4 by smooth bone, it is suggested that the medial caudal tuberosity is for the insertion of the puboischiofemoralis, and the lateral caudal tuberosity is for the insertion of the flexor cruris lateralis pars accessoria. This interpretation implies that in emeid moa the puboischiofemorales and flexor cruris lateralis pars accessoria are closely associated distally, to a varying degree.

The condition in *M. didinus* is unusual (Fig. 5D). The scars of insertion of the flexor cruris lateralis pars accessoria and puboischiofemoralis on the femur are clearly distinct and well-separated from each other (as in *Dinornis* spp.), with the scar of the flexor cruris lateralis pars accessoria situated just proximal to the shaft's midpoint. More importantly, the scar of the puboischiofemoralis consists of two parts, both long and linear, which are nearly fully separated for their entire

length; the lateral part of the scar is typically less developed than the medial part. These are both clearly separate from intermuscular line 3 that runs adjacent to the medial scar. This arrangement indicates that in *M. didinus* the puboischiofemoralis comprised well-separated lateralis and medialis parts; in this respect, *M. didinus* is unusual among palaeognaths, where the two parts of the puboischiofemoralis are usually closely associated with each other.

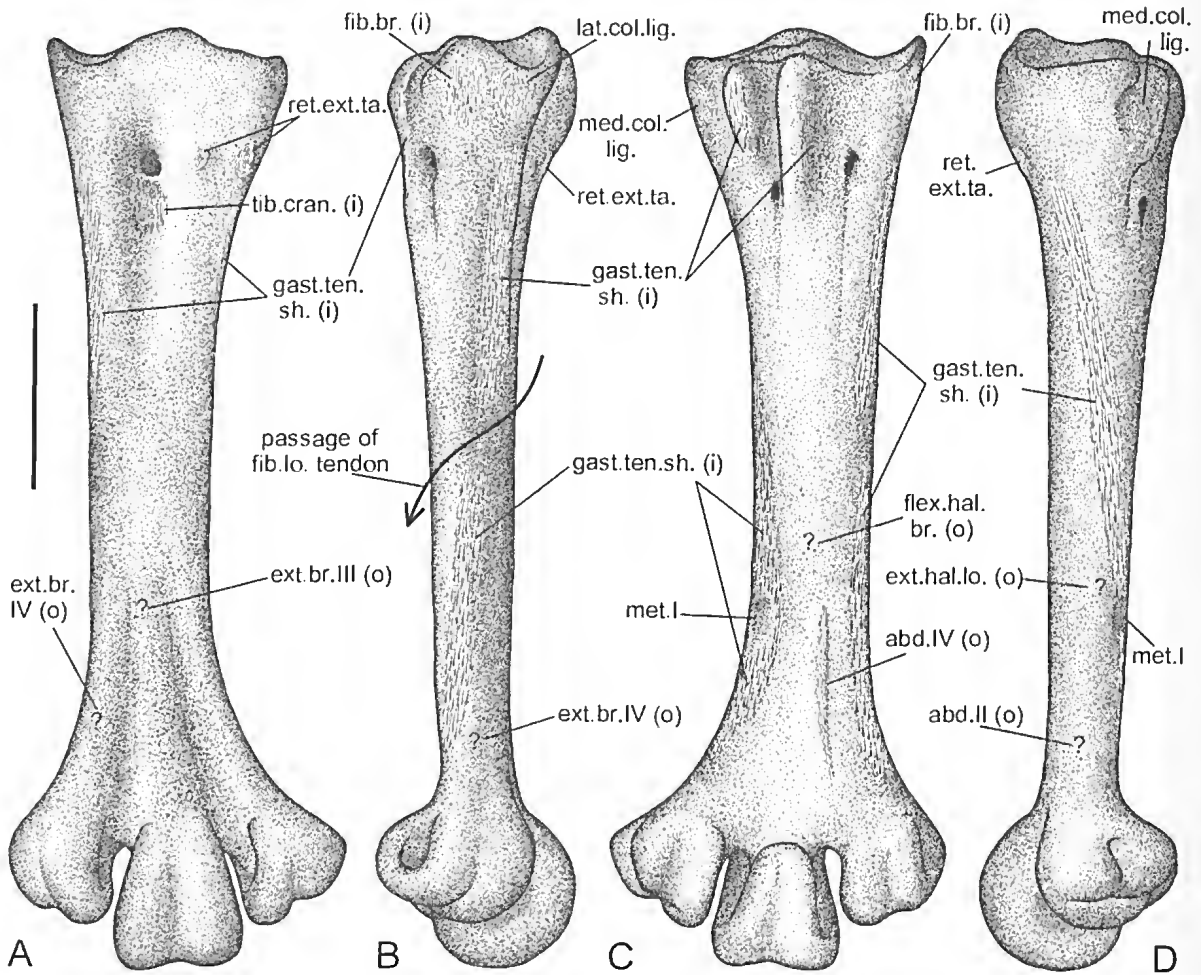


FIG. 9. Osteological evidence of muscle attachment on the tarsometatarsus of *D. robustus*, with corresponding myological interpretations. A, cranial view; B, lateral view; C, caudal view; D, medial view. Scale bar = 100 mm. Abbreviations: *abd.II*, abductor digiti II; *abd.IV*, abductor digiti IV; *ext.br.III*, extensor brevis digiti III; *ext.br.IV*, extensor brevis digiti IV; *ext.hal.lo.*, extensor hallucis longus; *fib.br.*, fibularis brevis; *fib.lo.*, fibularis longus; *flex.hal.br.*, flexor hallucis brevis; *gast.ten.sh.*, tendinous sheath of gastrocnemii; (i), muscle insertion; *lat.col.lig.*, lateral collateral ligament; *med.col.lig.*, medial collateral ligament; *met.I*, attachment scar of metatarsal I; (o), muscle origin; *ret.ext.ta.*, retinaculum extensorium tarsometatarsi; *tib.cran.*, tibialis cranialis.

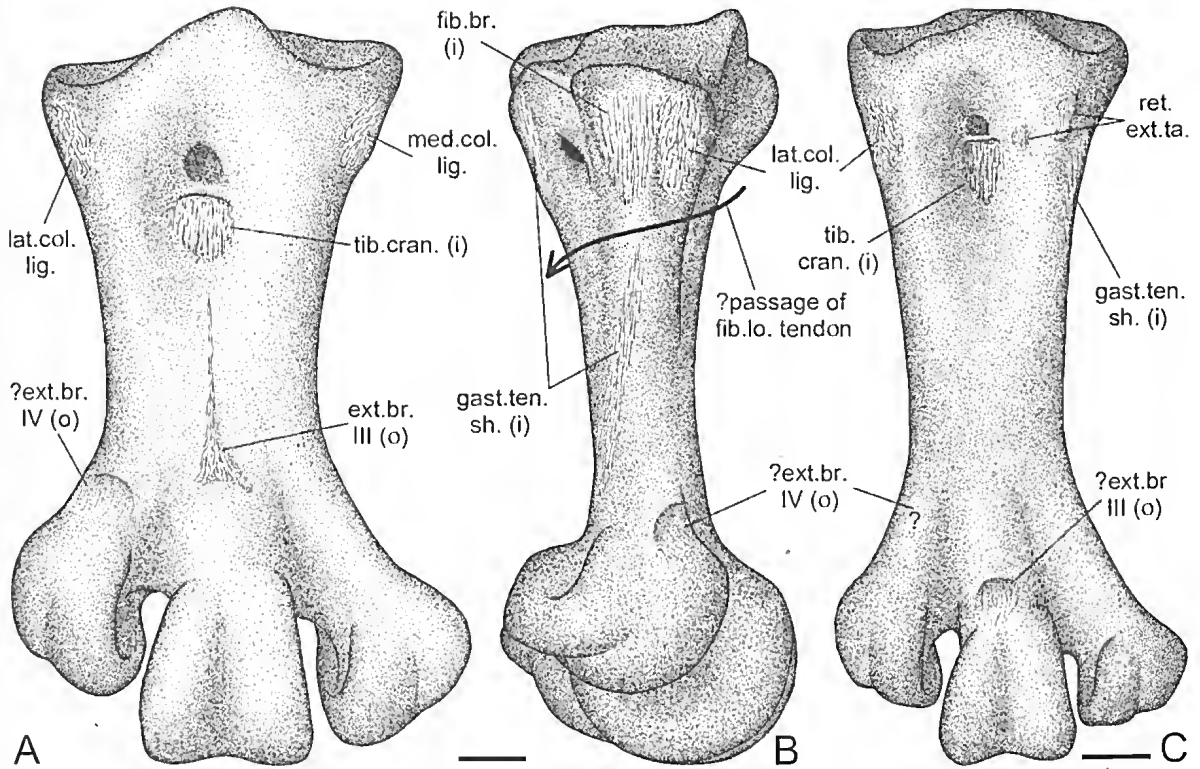


FIG. 10. Osteological evidence of muscle attachment on the tarsometatarsi of non-*Dinornis* moa, with corresponding myological interpretations. A, *P. elephantopus*, cranial view; B, *P. elephantopus*, lateral view; C, *E. crassus*, cranial view. Scale bars = 20 mm. Abbreviations: *ext.br.III*, extensor brevis digiti III; *ext.br.IV*, extensor brevis digiti IV; *fib.br.*, fibularis brevis; *fib.lo.*, fibularis longus; *gast.ten.sh.*, tendinous sheath of gastrocnemii; (i), muscle insertion; *lat.col.lig.*, lateral collateral ligament; *med.col.lig.*, medial collateral ligament; (o), muscle origin; *ret.ext.ta.*, retinaculum extensorium tarsometatarsi; *tib.cran.*, tibialis cranialis.

**Remarks.** Reconstruction of this muscle in *D. robustus*, *P. elephantopus* and *E. crassus* is well supported by osteology and comparative anatomy (level I inferences for both origin and insertion). That the medial caudal tuberosity of moa is for the insertion of the puboischiofemorales was also reached independently by Kooyman (1991) in his study. Zinoviev (2013) did not mention either the medial or lateral caudal tuberosities, and his reconstructions for both *D. robustus* and *E. crassus* show that the area where both tuberosities are situated was occupied only by the insertion of the flexor cruris lateralis pars accessoria. Additionally, the puboischiofemorales would have inserted on the ridge on the caudomedial aspect of the shaft (which has been identified as intermuscular

line 3 here). This reconstruction is rejected on the grounds that all longitudinal ridges on the femur of all moa can be homologized with the femorotibialis intermuscular lines of extant palaeognaths, and hence they reflect the origins of the femorotibialis, not the insertions of other muscles. Furthermore, the presence of two distinct tuberosities argues strongly against a single muscle insertion on this area of the femur.

### Gastrocnemius (Figs 4–10)

**General comments.** The gastrocnemius is ubiquitously the largest muscle of the crus in extant palaeognaths, comprising three heads, lateralis (*gast.lat.*), intermedia (*gast.int.*) and medialis (*gast.med.*); in *Dromaius* and *Rhea*,

the intermedia is further divided into partes medialis and caudalis (Patak & Baldwin 1998; Picasso 2010). The gastrocnemius lateralis takes origin from the lateral aspect of the lateral condyle of the femur, in common with (or immediately adjacent to) the distal attachment of the ansa iliofibularis. In some extant palaeognaths, the gastrocnemius lateralis also takes origin from the lateral aspect of the patellar tendon of the knee (*Dromains*, *Struthio*) or from the cranial or lateral aspects of the fibular head (*Dromains*, *Rhea*). The gastrocnemius intermedia originates from the distocaudal shaft of the femur, either from (via an aponeurosis) or just proximal to the popliteal fossa. The medial head of the gastrocnemius always originates from the medial aspect of the cranial cnemial crest of the tibiotarsus in extant palaeognaths, although this origin can also extend onto the patellar tendon and the proximal shaft of the tibiotarsus. In some tinamou genera, such as *Tinamus* and *Crypturellus*, the origin of this head is very extensive, including the entire cranial (and even craniolateral) aspect of the patellar tendon.

The three heads of the gastrocnemius give off tendons which unite proximal to the ankle; the common tendon goes around the caudal aspect of the ankle (being the most superficial one that does so in extant palaeognaths) and inserts on the caudal surface of the tarsometatarsus. It usually inserts on just the proximal part of the bone (including in some cases the hypotarsal ridge or ridges), although in tinamous this insertion extends for most of the bone's length. In all cases, the tendon forms a broad sheath (the tendo calcaneus, gast.ten.sh.) which covers the tendons of the digital flexors. In doing so, it inherently attaches to the tarsometatarsus only along its lateral and medial edges.

**Observations.** The ectocondylar fossa of the femur of moa is the appropriate site for the distal insertion of the ansa iliofibularis, and its exceptional size and degree of scarring in moa indicates that the gastrocnemius lateralis originated from here as well. In some specimens, the fibres or striations are so well developed that they come straight out of the bone surface, directed roughly caudally. A pronounced tuberosity is present on the

craniolateral corner of the head of the fibula of *D. robustus*, *P. elephantopus* and *E. crassus*, which can be plausibly interpreted as a second origin of the gastrocnemius lateralis. The tuberosity bears many fine striations and tubercles (<1 mm diameter), which are directed distally.

On the distocaudal femur of moa is a pronounced tuberosity (medial caudal tuberosity), but this is interpreted as the attachment of the puboischiofemoralis (see above), rather than one of the heads of the gastrocnemius. Evidence supporting this interpretation is seen in the fine striations on the tuberosity, which probably reflect Sharpey's fibres (Carrano & Hutchinson 2002), and which are directed proximally. This would be expected if the puboischiofemoralis inserted here, whereas if the gastrocnemius intermedia inserted here, the striations would be expected to point distally. Given the lack of other visible scars in this region of the femur, the gastrocnemius intermedia probably originated from the popliteal fossa (or some part thereof), the surface of which is very heavily scarred in all moa, with pockets, striations and tubercles.

Reconstructing the origin of the gastrocnemius medialis in *D. robustus*, *P. elephantopus* and *E. crassus* as on the medial surface of the cranial cnemial crest is supported by osteological evidence, as much of this part of the tibiotarsus is covered with fine, longitudinally oriented striations. These scars almost merge onto the distinct and more rugose (and unstriated) scar of insertion of the flexor cruris lateralis, suggesting a close association between the two muscles (see above). In *P. elephantopus* and *E. crassus*, there is often a curved line of scarring located about two-fifths of the way down the shaft of the tibiotarsus, where the scars consist of fine striations oriented longitudinally, transverse to the line (Fig. 7); this is interpreted as an intermuscular line delimiting the distal extent of the origin of the gastrocnemius medialis. Furthermore, in *E. crassus* the insertion of the flexor cruris lateralis encroaches upon the procnemial ridge, such that near its origin the gastrocnemius medialis would have been divided nearly into two.

There is usually a small scar of pronounced surface rugosity located proximomedial to

the proximal end of the medial condyle of the femur on its caudomedial aspect (Fig. 4D); it is absent in *M. didimus*, although this may be related to the relatively small size of the femora examined. Its appearance is somewhat variable with regards to size, degree of development and exact position. What soft tissue attached here is ambiguous. In *Dromaius* and *Rhea*, there exists a small, fourth head to the gastrocnemius which takes origin from this general area of the femur (Patak & Baldwin 1998; Picasso 2010). Additionally in *Dromaius*, the flexor perforatus digiti III also takes origin from the same general area, but more from the medial aspect of the medial condyle, not proximal to it (Patak & Baldwin 1998). Hence, the attachment responsible for the scar could plausibly be that of a fourth head of the gastrocnemius or the flexor perforatus digiti III; both hypotheses are equally speculative.

Concerning the insertion of the gastrocnemius, direct evidence of the nature and extent of the insertion in *D. robustus* is given by way of a remarkable partial mummified foot, described by Hutton & Coughtrey (1875a). The tendinous sheath of the muscle in this specimen had an insertion most similar to that seen in tinamous, where it extended for most of the length of the caudal aspect of the tarsometatarsus. This produces two tracts of striated texture on the bone, which start proximally on the lateral and medial aspects and progress caudolaterally and caudomedially going towards the distal end (level I inference). In *D. robustus* the lateral tract is interrupted by smooth bone about midway down the shaft, marking the point where the tendon of the fibularis longus would have likely passed (Fig. 9B; see also below). A similar pattern of scarring is also present on the tarsometatarsus of *P. elephantopus* and *E. crassus*, although there is no break in the lateral tract, suggesting that the passage of the fibularis longus tendon was very proximally situated, possibly passing between the gastrocnemius tendinous sheath and the lateral collateral ligament of the ankle (Fig. 10B). There is also evidence for insertion of the gastrocnemius on some part of the hypotarsal ridges in *D.*

*robustus*, *P. elephantopus* and *E. crassus*, in the form of similar striations.

**Remarks.** Reconstruction of the origin of each head of the gastrocnemius is supported by both osteology and comparative anatomy (level I inferences). Inferring the presence of a second head to the gastrocnemius lateralis, originating from the cranial aspect of the fibular head, is less supported (level II inference). Reconstructing the insertion of the common tendinous sheath on the tarsometatarsus is also supported (level I inference). Zinoviev (2013) did not mention the presence of any tuberosity or scarring on the cranial aspect of the fibular head in the material he studied, and consequently no fibular origin of the gastrocnemius lateralis was reconstructed. Likewise, no mention was made of the small rugosity located proximomedial to the proximal end of the medial condyle of the femur, although this feature is variable in its degree of development.

### Popliteus (Figs 6, 8; pop.)

**General comments.** The popliteus is present in all extant palaeognaths (except *Apteryx*: McGowan 1979) as a small muscle, running from the proximocaudal tibiotarsus, lateral to the origin of the plantaris, to the proximal fibula (either the head or just distal to it).

**Observations.** In all large extant palaeognaths the origin of this muscle is associated with obliquely oriented, subparallel ridges on the proximocaudal tibiotarsus, which are often strongly developed, and are directed towards the in-life position of the head of the fibula. A similar condition is observed on the proximocaudal tibiotarsus of moa, and these are therefore interpreted as marking the origin of this muscle. The insertion of this muscle on the proximal caudal or medial fibula is not readily identifiable from scarring on the bones. There are usually one or more small tubercles on the proximocaudal fibula where the shaft starts to expand into the head; in small specimens they can be reduced to a small area of relatively faint scarring, in the form of a 'mottled' texture. This may mark the insertion of the popliteus, as suggested by Zinoviev (2013). However, the fine

striations on the tubercles are directed distally (rather than medially), which suggests that the tubercles were more likely for the attachment of one or more digital flexors (see below).

**Remarks.** Reconstruction of this muscle is well supported (level I inference for origin, level I' inference for insertion).

### Plantaris (Fig. 6; pla.)

**General comments.** The plantaris occurs in all extant palaeognaths. Its origin is largely fleshy, and is somewhat variable in size and position. It originates from the caudal or caudomedial aspect of the proximal tibiotarsus, near the insertions of the flexores cruris lateralis et medialis and the medial collateral ligament of the knee. The muscle usually inserts, via a long tendon, on the proximal tibial cartilage surrounding the ankle joint, but in some species its tendon also merges with that of the gastrocnemii.

**Observations.** On the proximocaudal tibiotarsus of *D. robustus*, *P. elephantopus* and *E. crassus* is a faintly depressed area, roughly oval-shaped (sometimes elongate) and with fine longitudinal striations; in *P. elephantopus* these striations may also be accompanied by a 'mottled' texture. This depression is interpreted here as marking the origin of the plantaris in moa. It is distinct from the strong ridges of the popliteus located immediately lateral to it, the two regions sometimes separated by a raised 'wall' of bone. In *P. elephantopus* the medial edge of the depression is often bounded by a pronounced ridge with longitudinal striations; a similar ridge is less frequently present on the lateral edge of the depression. The plantaris of moa may have originated from the medial collateral ligament of the knee, as occurs in *Apteryx* (where it originates from both the ligament and the caudal tibiotarsus), but this is not supported by osteological evidence. Currently it is not possible to recognise the presumably soft-tissue insertion of the plantaris in moa, although examination of mummified specimens may yield otherwise.

**Remarks.** Whilst osteological evidence on the proximocaudal tibiotarsus supports the reconstruction of a plantaris in *D. robustus*, *P. elephantopus* and *E. crassus* (level I inference), the nature of its distal insertion remains uncertain (level I' inference). Kooyman (1991) suggested that the plantaris of moa originated from the proximocaudal tibiotarsus on an area with strong subparallel ridges oriented obliquely to the bone's long axis. His interpretation was based on *Apteryx*, however, in which the popliteus is absent; as noted above, in other extant palaeognaths, it is the popliteus which takes origin from these coarse, linear rugosities.

### Tibialis cranialis (Figs 4–7, 9, 10; tib.cran.)

**General comments.** In all extant palaeognaths this muscle has two heads, the caput femorale (tib.cran.f.), which originates from a small fovea on the distal end of the lateral condyle of the femur, and the caput tibiale (tib.cran.t.), which usually originates from much of the broad sulcus between the cranial and lateral cnemial crests of the tibiotarsus. In some extant palaeognaths the caput tibiale may also extend its origin onto the lateral aspect of the patellar tendon (*Apteryx*: McGowan 1979), or even the fibular head (*Rhea*: Picasso 2010). The manner of insertion of this muscle is highly conserved among extant palaeognaths: the two heads fuse and the tendon of insertion passes under a retinaculum on the distal tibiotarsus (retinaculum extensorium tibiotarsi) before inserting on the proximocranial tarsometatarsus. Its insertion leaves a characteristically distinct region of strong scarring.

**Observations.** Both of the osteological correlates for the origins of the tibialis cranialis are present in moa, and are comparable to that seen in extant palaeognaths, although in *E. crassus* the attachment of the caput femorale on the femur is sometimes a low, broad tubercle rather than a fovea. The insertion of this muscle in moa is in the same position of the tarsometatarsus as in extant palaeognaths, and is indicated by a subcircular region of very coarse texture; it is often well excavated to the point that the area



is recessed into the surrounding bone. The scars of attachment of the retinaculum extensorium tibiotarsi to the distal cranial tibiotarsus are also present and are clearly identifiable as such, corresponding to those present on the surface of the tibiotarsus of extant palaeognaths.

**Remarks.** The reconstruction of this muscle in moa is supported by both osteological and comparative data (level I inferences both proximally and distally).

### **Extensor digitorum longus** (Figs 6, 7, 9–12; ext.dig.lo.)

**General comments.** This muscle is present in all palaeognaths, typically originating from the distal lateral and cranial cnemial crests of the tibiotarsus, as well as the sulcus in between. Lying deep to the tibialis cranialis caput tibiale, its origin is just distal to that of the former muscle. The muscle gives off a tendon distally which passes under the retinaculum extensorium tibiotarsi and the pons supratendinous (which may or may not be ossified: Worthy & Scofield 2012), before crossing the ankle joint. It then passes under another retinaculum, the retinaculum extensorium tarsometatarsi, after which it trifurcates, sending a branch each to digits II, III and IV (except in *Struthio*, where digit II is absent: Gangl *et al.* 2004). The manner of insertion of each branch onto the phalanges of its respective toe is variable among extant palaeognaths; a commonality, however, is that they insert on the extensor processes of the unguals of each digit.

**Observations.** The distal extent of the origin of the extensor digitorum longus, down the cranial surface of the tibiotarsus, is variable among extant palaeognaths and cannot be determined precisely for *D. robustus*, *P. elephautopus* and *E. crassus*. However, it probably continued down along much of the shaft in these species, given the extent of the procnemial ridge, to which the muscle would have likely had an aponeurotic attachment (the procnemial ridge taking on the form of an intermuscular line distally). The presence of the retinaculum extensorium tarsometatarsi on the tarsometatarsus of *D. robustus* and *E. crassus* is indicated by two small

tuberosities located proximomedially to the scar of insertion of the tibialis cranialis. In large *D. robustus* individuals (e.g., CM Av8422, 8473, 8488), these tubercles are sometimes drawn out into proximodistally elongate patches of scarring. No such tuberosities or scars were observed on the cranial tarsometatarsus in any *P. elephautopus* material examined. The extensor processes of the unguals in all moa species are well developed, particularly the larger species, and they bear fine, proximodistally oriented striations, ridges or tubercles, which presumably indicate the insertion of the extensor digitorum longus.

**Remarks.** Reconstruction of the extensor digitorum longus in moa is well supported (level I inference proximally, level I at ankle and toes), the only uncertainty lying in the extent of the muscle's origin, and whether the muscle inserted on non-ungual phalanges.

### **Fibularis longus** (Figs 6, 7, 9, 10; fib.lo.)

**General comments.** This muscle, the most superficial of the cranial crus, typically originates in extant palaeognaths from one or both cnemial crests of the tibiotarsus and also the cranial aspect of the patellar tendon; in tinamous it also takes origin from a considerable area on the lateral surface of the fibula (Hudson *et al.* 1972). The muscle sends a tendon distally which typically bifurcates, inserting on the tibial cartilage of the ankle joint, and also on the tendon of the flexor perforator digiti III at the level of the proximal tarsometatarsus, on its caudal aspect.

**Observations.** The fibularis longus is probably responsible for coarse ridges and tubercles on the apex of the lateral cnemial crest in *D. robustus*, *P. elephautopus* and *E. crassus*, which are often swollen into a pronounced, craniodistally directed tuberosity. There is also occasionally a very faint fluted texture adjacent to the tuberosity on the lateral cnemial crest, on the caudolateral aspect of the ectocnemial ridge (Fig. 6C), which may have been for attachment of the fibularis longus. Where else the muscle may have originated from cannot be

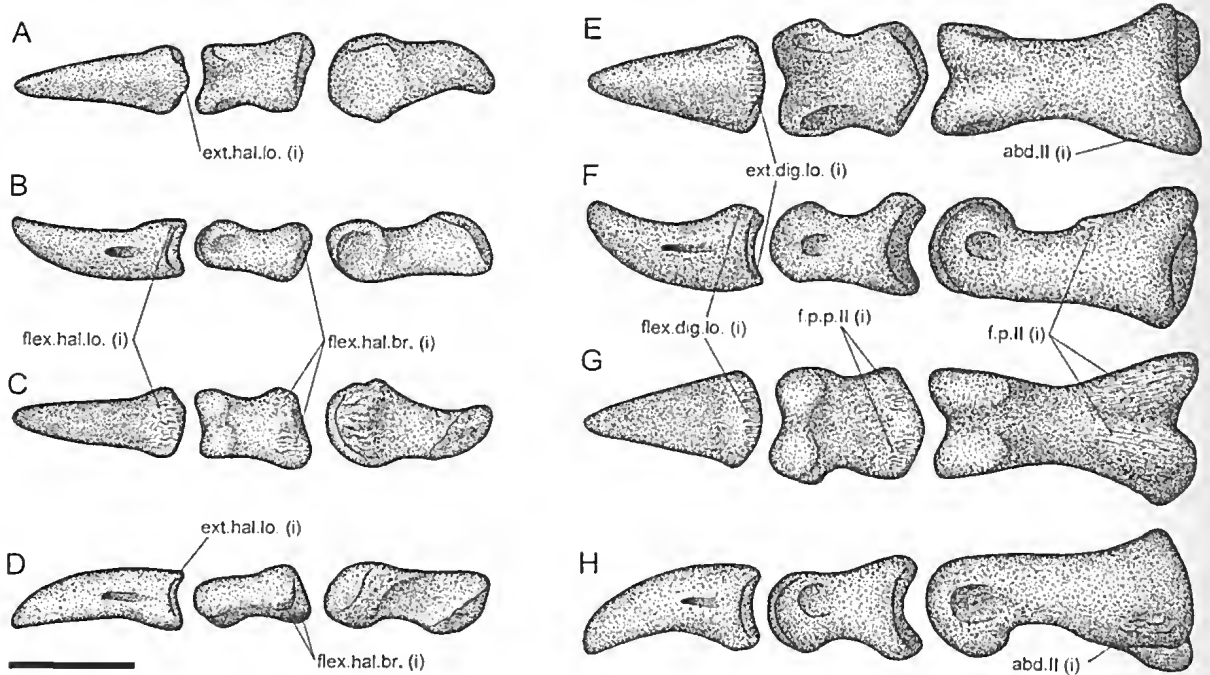


FIG. 11. Osteological evidence of muscle attachment on digits I and II of *D. robustus*, with corresponding myological interpretations. A–D, digit I; E–H, digit II; A and E are dorsal views, B and F are lateral views, C and G are plantar views, D and H are medial views. Scale bar = 50 mm. Abbreviations: *abd.II*, abductor digiti II; *ext.dig.lo.*, extensor digitorum longus; *ext.hal.lo.*, extensor hallucis longus; *flex.dig.lo.*, flexor digitorum longus; *flex.hal.br.*, flexor hallucis brevis; *flex.hal.lo.*, flexor hallucis longus; *f.p.II*, flexor perforans et perforatus digiti II; *f.p.p.II*, flexor perforans et perforatus digiti II; (i), muscle insertion.

determined with certainty, since other muscles attach to the cnemial crests too (iliotibialis, femorotibialis), and no attachment to the fibula is evident, either. Although there is no direct osteological evidence of the muscle's insertion in *D. robustus*, *P. elephantopus* and *E. crassus*, the typical pattern may be reconstructed for these species, since it is quite consistent among extant taxa. In *D. robustus*, the lateral scar of the gastrocnemius insertion on the tarsometatarsus is interrupted by a span of smooth bone about halfway along the bone's length. This corresponds to the point, noted by Hutton & Coughtrey (1875a), where the tendon of the fibularis longus passes from the cranial side to the caudal side of the tarsometatarsus, underneath the tendinous sheath of the gastrocnemius, to insert on the tendon of the flexor perforatus digiti III. As discussed above, in *P. elephantopus* and *E. crassus* the likely

passage of the tendon around to the caudal tarsometatarsus was very proximally situated, so much so that the tendon may have passed between the tendinous sheath and the lateral collateral ligament of the ankle.

**Remarks.** Reconstructing this muscle as having the typical palaeognath condition is well supported (level I inference proximally, level I' inference distally). The postulated origin of this muscle in moa, from the apex of the lateral cnemial crest, was also suggested by Kooyman (1991), although he also suggested that it may have also served as the origin for the flexores perforantes et perforatus digitorum II et III (see below for a treatment of these muscles).

Zinoviev (2013) suggested that the origin of the fibularis longus in *D. robustus* and *E. crassus* also included the cranial surface of the fibula and the proximolateral surface of the



tibiotarsus, immediately cranial to the fibular crest and distal to the lateral cnemial crest. The only osteological evidence Zinoviev (2013) cited in support of this interpretation was an “uneven surface on the cranial surface of the fibula” (p. 269). Aside from the tubercle on the fibular head (which is here proposed as the origin of a second head of the gastrocnemius lateralis), no evidence of muscular attachment was observed in the material studied here. Additionally, this topology is not present in any extant palaeognath; only in tinamous does the muscle gain origin from the fibula (Hudson *et al.* 1972), and here it is from the lateral, not cranial, surface of the bone. Zinoviev’s interpretation of an extended origin for the fibularis longus is hence not well supported (a level II’ inference).

#### Fibularis brevis (Figs 6, 9, 10; fib.br.)

**General comments.** This muscle only occurs in some extant palaeognaths, and in these species it varies in both degree of development and area of origination. In *Struthio* it is reduced to a tendinous vestige that originates from a small area on the lateral tibiotarsus just distal to the end of the fibular spine (Schaller *et al.* 2009), whereas in *Apteryx* it is very well developed, originating from much of the lateral surface of the fibular shaft (distal to the insertion of the iliofibularis) and the proximal caudolateral surface of the tibiotarsus (McGowan 1979). The insertion of the fibularis brevis in extant palaeognaths, where present, is typically on the proximal caudolateral surface of the tarsometatarsus, except in *Apteryx*, where the tendon of insertion fuses with that of the flexor digitorum longus (McGowan 1979).

**Observations.** On the distal lateral tibiotarsus of *D. robustus*, *P. elephautopus* and *E. crassus* is a well-defined linear area of fibrous scarring, proximal to the scar of attachment of the lateral collateral ligament of the ankle. In large *D. robustus* specimens this scarring can become elevated into a course ridge. This scarring does not reflect the attachment of the fibula, and is not a proximal extension of the origin of the collateral ligament, because the scarring

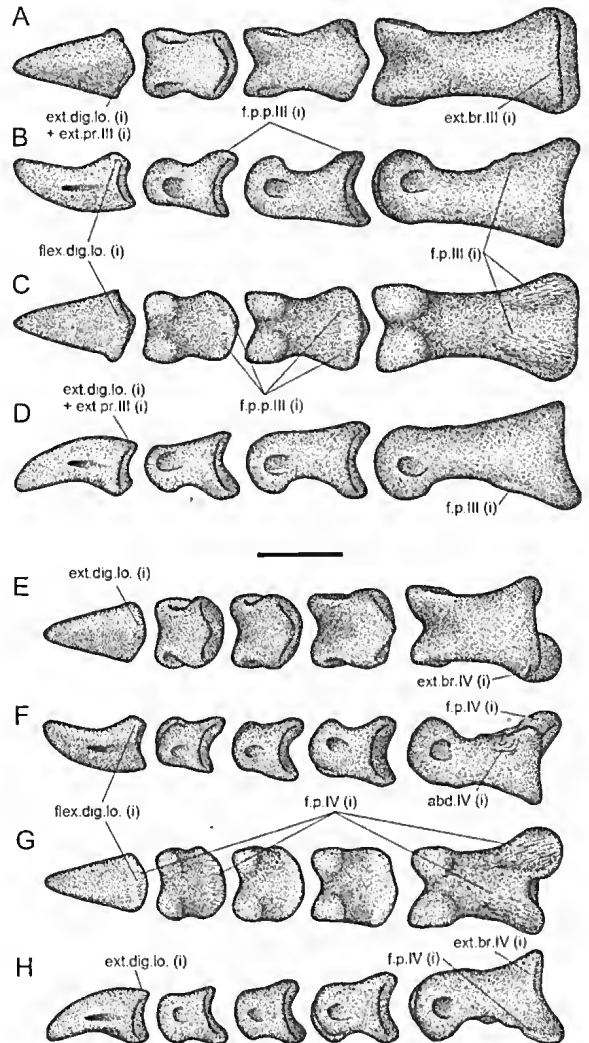


FIG. 12. Osteological evidence of muscle attachment on digits III and IV of *D. robustus*, with corresponding myological interpretations. A–D, digit III; E–H, digit IV; A and E are dorsal views, B and F are lateral views, C and G are plantar views, D and H are medial views. Scale bar = 50 mm. Abbreviations: *abd.IV*, abductor digiti IV; *ext.br.III*, extensor brevis digiti III; *ext.br.IV*, extensor brevis digiti IV; *ext.dig.lo.*, extensor digitorum longus; *ext.pr.III*, extensor proprius digiti III; *flex.dig.lo.*, flexor digitorum longus; *f.p.III*, flexor perforatus digiti III; *f.p.IV*, flexor perforatus digiti IV; *f.p.p.III*, flexor perforans et perforatus digiti III; (i), muscle insertion.

is separated from the fibular crest scarring and the collateral ligament scar by smooth bone. It is therefore inferred that this scar marks the origin of the fibularis brevis. In several specimens, such as CM Av8381 (*P. elephantopus*), the scarring of the fibular crest is unbroken and continues cranial to the scar for the fibularis brevis, indicating that the muscle originated caudal to the fibular spine. In *D. robustus*, *P. elephantopus* and *E. crassus* the proximolateral tarsometatarsus bears two distinct – although often not fully separated – areas of coarse scarring, which are interpreted as the insertions of the lateral collateral ligament (the cranial one) and the fibularis brevis (the caudal one). The cranial scar is a diffuse area of rough, somewhat mottled scarring, and the caudal one is occasionally recessed in *D. robustus* and *P. elephantopus* to form a rough fovea.

**Remarks.** Reconstructing the origin and insertion of the fibularis brevis is a level II inference, receiving support from osteology and comparative anatomy. Zinoviev (2013) suggested that this muscle was absent in moa, for he did not find evidence of a retinaculum on the distal lateral tibiotarsus that would have held the tendon of the muscle in place, or evidence of its insertion on the tarsometatarsus. The supposedly ‘required’ retinaculum may well have been present, but simply could have been part of the large lateral collateral ligament, leaving no trace of its own on the bones. Furthermore, plausible osteological correlates of both the origin and insertion of the fibularis brevis have been identified in the material examined here.

**Flexores perforantes et  
perforatus digitorum II et III, flexores  
perforatus digitorum II, III et IV  
(Figs 4, 5, 8, 11, 12)**

**General comments.** These digital flexor muscles are invariably present in all extant palaeognaths (except *Struthio*, where those associated with digit II are absent: Gangl *et al.* 2004). They exhibit extreme interspecific variability in their origins, which include the origin of the gastrocnemius lateralis on the distal femur (*Dromaius*), proximal fibula (*Dromaius*, *Rhea*, tinamous), medial aspect of the medial condyle of the femur (*Dromaius*), cranial

cnemial crest (*Struthio*, tinamous), popliteal fossa (*Struthio*, *Rhea*, *Apteryx*, tinamous; usually via an aponeurosis from which other digital flexors can also originate), ansa iliofibularis (*Casuarinus*, *Struthio*, *Rhea*), origin of the gastrocnemius intermedia (tinamous) and the patellar tendon or its surrounding aponeuroses (casuariids). Furthermore, in some taxa particular muscles have multiple heads of origin rather than just one, and some muscles may take origin from the heads of others (e.g., casuariids, *Struthio*).

All of these digital flexors in extant palaeognaths give off tendons which run distally to pass around the caudal aspect of the ankle, before typically running through the sulcus associated with the hypotarsal ridge (or ridges) on the proximal caudal tarsometatarsus. Some of the tendons pass through the tibial cartilage on their way and some pass superficial to it (deep to the tendo calcaneus), but there is no consistent pattern in the extant species as to what a given muscle does. There is, however, some consistency in the manner of insertion of these muscles’ tendons onto the phalanges:

- The flexor perforans et perforatus digiti II (f.p.p.II) inserts on the proximoplantar aspect of II-2; in tinamous this insertion extends proximally to include the distoplantar aspect of II-1 (Hudson *et al.* 1972).
- The flexor perforans et perforatus digiti III (f.p.p.III) inserts on III-2, typically on the proximoplantar aspect, but in *Struthio* and the tinamous it inserts on the distoplantar aspect, in which the insertion extends to the proximoplantar aspect of III-3 (Hudson *et al.* 1972; Gangl *et al.* 2004).
- The flexor perforatus digiti II (f.p.II), when present, invariably inserts on the proximoplantar aspect of II-1 in extant palaeognaths.
- The flexor perforatus digiti III (f.p.III) either inserts on the proximoplantar aspect of III-1 (casuariids, *Rhea* and *Apteryx*) or alternatively on the distoplantar aspect of III-1, in which it extends to the proximoplantar aspect of III-2 (*Struthio* and tinamous).

- The flexor perforatus digiti IV (f.p.IV) always inserts on IV-1 in extant palaeognaths, although it may also have further insertions on IV-2 (*Dromaius*, tinamous), IV-3 (tinamous), IV-4 (tinamous), and the first and second interphalangeal joints (*Struthio*).

**Observations.** The great variability in the nature of these muscles' origins in extant palaeognaths renders it extremely difficult to reconstruct the origins of any of them in moa with great clarity. Their ubiquitous presence among extant species, however, does imply that they were all present in moa. The popliteal fossa of the moa femur, as noted above, is heavily scarred and probably served as the origin (likely via an aponeurosis) for at least some of the digital flexors. There is usually a small scar located proximomedial to the proximal end of the medial condyle of the femur, which may be for the flexor perforatus digiti III, or alternatively for a fourth head to the gastrocnemius (see above). Additionally, on the femur, there also exists a distinct region immediately distal to the ectocondylar fossa between the proximal extents of the lateral and fibular condyles, which may have also served as the origin for one or more of these muscles, although it often does not show any surface scarring *per se*. Alternatively, it may have functioned as a receptacle for the fibular head during strong flexure of the knee. On the caudal aspect of the proximal fibula of *D. robustus*, *P. elephantopus* and *E. crassus*, below the expansion of the head, there are usually several small tubercles and ridges of varying shape and size. In specimens where the tuberosities are very well developed, distinct striations or fibres are evident; these are directed distally. In *P. elephantopus* (and occasionally in *E. crassus*) most of these scars sometimes unite to form a large C-shaped ridge of striated bone; this feature was observed in every *P. elephantopus* specimen examined from Cheviot Swamp, but it is less prevalent in other sampled populations. This may indicate the origin of one or more of the digital flexors, or the flexor digitorum longus, or both.

Two well-developed hypotarsal ridges are present on the proximal caudal tarsometatarsus

in all moa species, such that at least some of the tendons of the digital flexors probably ran through the sulcus formed between them, on their way to the digits. As regards the insertions of the individual muscles, the following interpretations are presented:

- In *D. robustus*, *P. elephantopus* and *E. crassus* there are two subtle tubercles on the proximoplantar aspect of II-2, which may be confluent with each other in some instances. These probably mark the insertion of the flexor perforans et perforatus digiti II.
- In *D. robustus* there are faint raised rugosities on both the proximoplantar and distoplantar aspects of III-2 (the distoplantar ones are less frequently present), indicating the insertion of the flexor perforans et perforatus digiti III. The proximoplantar aspect of III-3 also bears faint rugosities, suggesting that the muscle had a 'dual insertion' on both phalanges, as in *Struthio* and the tinamous. A similar condition exists in *P. elephantopus* and *E. crassus*, although no scarring on the distoplantar aspect of III-2 was observed.
- Phalanx II-1 of *D. robustus*, *P. elephantopus* and *E. crassus* possesses two very large and well-developed rugosities on its proximoplantar aspect, signifying the attachment of the flexor perforatus digiti II.
- The proximoplantar aspect of III-1 in *D. robustus*, *P. elephantopus* and *E. crassus* possesses two large, heavily scarred rugosities, which likely mark the insertion of the flexor perforatus digiti III. Similar scars are present on the proximoplantar aspects of III-2 and III-3; these could have been for both the flexor perforans et perforatus and the flexor perforatus, or just the flexor perforans et perforatus (see above).
- In *D. robustus* there are two strong scars on the proximoplantar aspect of IV-1, and a more diffuse region of fainter scarring on the proximoplantar aspect of IV-4, as well as the flexor tubercle of the ungual. These probably all mark the attachment of the

tendon of the flexor perforatus digiti IV. In one specimen (CM Av8422), there was also distinct scarring on the proximoplantar aspect of IV-2, suggesting a further insertion to this phalanx. In *P. elephantopus* and *E. crassus*, scarring of a similar character to that observed in *D. robustus* is present on the proximoplantar aspects of phalanges IV-1 to IV-4 (IV-4 being the ungual in *E. crassus*, which only has four phalanges in digit IV), although that on IV-3 is typically less substantial.

**Remarks.** Whilst the exact origins of each muscle in *D. robustus*, *P. elephantopus* and *E. crassus* are uncertain, reconstructing them is nevertheless well supported by comparative data (level I' inference). The presence of clear scars on the phalanges also supports this; distally, each muscle can be reconstructed with considerable confidence (level I inferences). The observations of mummified foot specimens of *D. robustus* and *P. elephantopus*, made by Hutton & Coughtrey (1875a) and Buller (1888), respectively, further support the inferences made here. One small difference, however, is that Hutton & Coughtrey (1875a) did not find an attachment of the flexor perforans et perforatus digiti III to III-2 in their specimen. This may reflect individual anatomical variation with respect to this muscle. In the phalanges of smaller *E. crassus* individuals (e.g., CM Av8344), some of the scars on the phalanges are less well developed, and in some instances are even absent.

### Flexor digitorum longus (Figs 6, 11, 12; flex.dig.lo.)

**General comments.** The deepest of the caudal muscles of the crus, the flexor digitorum longus is present in all extant palaeognaths. It originates from the caudal aspects of the tibiotarsus and fibula, except in *Apteryx*, where it comes from the popliteal fossa (McGowan 1979). Gadow (1880) described a second small head to the muscle in *Rhea*, as originating from the distocaudal femur. The extent of origin of the muscle from the tibiotarsus is variable, being restricted to the proximal end in *Rhea* (Picasso 2010), but extending across two-thirds of the

caudal surface of the bone in *Struthio* (Gangl *et al.* 2004). In all extant palaeognaths, the flexor digitorum longus gives off a tendon which passes around the caudal margin of the ankle, through the tibial cartilage, before trifurcating on the caudal aspect of the tarsometatarsus, sending a branch each to digits II, III and IV (except *Struthio*, where digit II is absent; Gangl *et al.* 2004). The tendons typically insert on the flexor tubercles of the unguals of each digit, although in tinamous they also give off slips to various other phalanges as well (Hudson *et al.* 1972).

**Observations.** On the caudomedial aspect of the tibiotarsus in *D. robustus* and *P. elephantopus*, and rarely in *E. crassus*, about two-thirds to three-quarters of the way towards the distal end, there is sometimes a faint, longitudinal ridge. This ridge may be extensive proximally, and is interpreted as an intermuscular line demarcating the medial extent of the origin of the flexor digitorum longus; it thus indicates that the muscle had an extensive origin. An origin from the caudal fibula in moa seems probable, and in *D. robustus*, *P. elephantopus* and *E. crassus*, there is often some form of linear scarring (striations, or more rarely, ridges and elongate, distally directed tubercles) running down the caudal or caudolateral surface of the shaft. This scarring starts at about the level of the iliofibularis insertion scar and progresses distally, and probably marks an additional attachment of the flexor digitorum longus. Although the fibularis brevis may also take origin from this region of the fibula in *Apteryx* (McGowan 1979) and most tinamous (Hudson *et al.* 1972), there is, as noted above, a distinct region of scarring distal to the fibular crest on the tibiotarsus which seems the more probable origin of that muscle in moa. The flexor digitorum longus may have also taken origin from the small tubercles and ridges on the caudal aspect of the proximal fibula, but these may have alternatively been for other digital flexor muscles (see above). The unguals of digits II, III and IV of all moa all have strongly scarred flexor tubercles (which tend to be better developed in larger individuals), attesting to the muscle's insertions.

**Remarks.** Reconstruction of this muscle is well supported (level I inferences both proximally and distally), although the extent of its origin is not entirely certain.

**Flexor hallucis longus**  
(Figs 4, 5, 11; flex.hal.lo.)

**General comments.** This muscle originates from the distocaudal femur in extant palaeognaths, typically from the popliteal fossa, although in *Dromaius* and *Rhea* it also takes origin, via a second head, from an area proximal to the lateral femoral condyle on the caudal surface of the femur (Pataki & Baldwin 1998; Picasso 2010). In extant palaeognaths lacking digit I, the tendon of insertion of this muscle fuses with that of the flexor digitorum longus prior to the latter muscle splitting to the toes, about halfway down the tarsometatarsus. In tinamous that have retained digit I, the tendon of the flexor hallucis longus inserts on the flexor tubercle of the ungual (Hudson *et al.* 1972). *Apteryx* is unusual in that the muscle (termed the 'ligament to hallux' by McGowan 1979) is vestigial and entirely tendinous, originating from the tendon of the flexor digitorum longus and inserting on the ungual.

**Observations.** No distinct area of scarring is present on the distocaudal femur of *D. robustus*, *P. elephautopus* and *E. crassus* that would be in the appropriate position for this muscle's origin. It seems likely that the flexor hallucis longus originated from the popliteal fossa, probably along with other muscles as noted above. The ungual of digit I in *D. robustus*, *P. elephautopus* and *E. crassus* has a modestly developed flexor tubercle with fine scarring, suggesting the insertion of this muscle here.

**Remarks.** As only tinamous and *Apteryx* have retained digit I among extant palaeognaths, comparisons between moa and extant outgroups are limited. Consequently, any inference concerning the muscles of digit I in moa can only receive limited support. Reconstructing the origin of the flexor hallucis longus in moa as done here is a level I inference, whilst the reconstructed insertion is a level II inference. The muscle may have been vestigial

and displayed an *Apteryx*-like condition, but this is a more speculative suggestion (level II inference).

**Flexor hallucis brevis**  
(Figs 9, 11; flex.hal.br.)

**General comments.** In extant palaeognaths, this muscle is only present in tinamous, where it originates from the middle of the caudal surface of the tarsometatarsus and inserts on the base of I-1 (Hudson *et al.* 1972).

**Observations.** There is no osteological evidence of this muscle's origin in *D. robustus*, *P. elephautopus* or *E. crassus*, distinct from the scarring of the gastrocnemius (but see below). However, the proximoplantar aspect of I-1 presents two faint flexor tubercles, which may be interpreted as the insertion of this muscle.

**Remarks.** Reconstruction of this muscle in *D. robustus*, *P. elephautopus* and *E. crassus* is tentative (level II inference).

**Extensor hallucis longus**  
(Figs 9, 11; ext.hal.lo.)

**General comments.** Among extant palaeognaths this muscle is only present in *Apteryx* and those species of tinamou with a hallux (Hudson *et al.* 1972; McGowan 1979). It typically originates from about the medial aspect of the tarsometatarsus, just proximal to the attachment of metatarsal I, and inserts on the dorsolateral aspect of I-1 (*Apteryx*) or the ungual (tinamous).

**Observations.** No distinct osteological evidence exists as to its origin on the tarsometatarsus in *D. robustus*, *P. elephautopus* or *E. crassus*, but the ungual of the hallux normally possesses an extensor process with fine (< 1 mm diameter) tubercles, supporting its reconstruction in these species. In small individuals the extensor process of the ungual can be poorly developed or even absent. In *D. robustus* there is occasionally a small, elongate, proximodistally trending tubercle on the caudomedial aspect of the proximal tarsometatarsus. This may be for the origin of the extensor hallucis longus in

this species, but this would be unusual being so proximally situated.

**Remarks.** Reconstructing this muscle in *D. robustus*, *P. elephautopus* or *E. crassus* is a level II inference.

### Extensor proprius digiti III (Fig. 12; ext.pr.III)

**General comments.** This muscle typically originates from some part of the soft tissues of the ankle joint in extant palaeognaths, either the joint capsule or the lateral meniscus, except in *Dromaius*, where it originates from the proximocranial tarsometatarsus, just distal to the insertion of the tibialis cranialis (Patak & Baldwin 1998). In all extant palaeognaths this muscle inserts on the extensor process of III-4 (ungual), along with a branch of the extensor digitorum longus.

**Observations.** No evidence of the *Dromaius*-type origin from the proximocranial tarsometatarsus was observed, so although its exact origin is uncertain, it is nevertheless reasonable to reconstruct this muscle in *D. robustus*, *P. elephautopus* and *E. crassus*. An extensor process is present on III-4 in moa, suggesting that the extensor proprius digiti III may have inserted here.

**Remarks.** No unequivocal osteological evidence exists to support the reconstruction of this muscle in moa, yet its wide distribution among extant palaeognaths suggests that it was present (level I' inference). As regards the insertion, whilst the extensor process of III-4 may have only received the tendon of the extensor digitorum longus, it is more parsimonious to reconstruct the extensor proprius digiti III as inserting here as well (level I inference), than to be inserting elsewhere (level II' inference).

### Extensor brevis digiti III (Figs 9, 10, 12; ext.br.III).

**General comments.** The extensor brevis digiti III is present in all extant palaeognaths, but its origin on the cranial aspect of the tarsometatarsus is fleshy and variable in location and extent. It typically inserts on the proximodorsal aspect of III-1.

**Observations.** No discernable scarring exists on the cranial surface of the tarsometatarsus of *D. robustus*. In contrast, on the cranial surface of the tarsometatarsus of *P. elephautopus*, about two-thirds of the way towards the distal end, is a gently elevated rugosity. This may extend proximally to form a long, proximodistally oriented ridge (as seen in the type specimen illustrated by Owen 1858, pl. 44). This scar was likely for the origin of the extensor brevis digiti III (a level I inference). In many specimens of *E. crassus*, there is a small depression (approximately 10 mm in diameter) on the cranial aspect of the distal tarsometatarsus, just proximal to the trochlea for digit III. It has a rough surface texture, and is usually rimmed by rough bone as well, although in specimens from Kapua the depression is mostly smooth. This depression may mark the origin of the extensor brevis digiti III in this species, or alternatively it may simply be present to facilitate hyperextension of the tarsometatarsophalangeal joint. The middle of the proximodorsal aspect of III-1 in *D. robustus*, *P. elephautopus* and *E. crassus* bears a small patch of fine, subparallel ridges that are oriented proximodistally, suggesting the insertion of the extensor brevis digiti III here.

**Remarks.** Reconstructing the origin and insertion of this muscle is well-supported in *P. elephautopus* (level I inference), slightly less so for *D. robustus* and *E. crassus* (level I' inference proximally, level I inference distally). The rugosity and ridge on the cranial surface of the tarsometatarsus of *P. elephautopus* may have alternatively (or additionally) been for the origin of the extensor proprius digiti III, similar to that seen in *Dromaius*, but this is more speculative (a level II inference) than what is reconstructed here.

### Extensor brevis digiti IV (Figs 9, 10, 12; ext.br.IV)

**General comments.** Present in all extant palaeognaths except *Dromaius* (Patak & Baldwin 1998), this muscle is very much like the extensor brevis digiti III in that it has a fleshy and variable origin on the cranial tarsometatarsus, lateral to the origin of the latter muscle. The extensor

brevis digiti IV typically inserts on the medial or dorsomedial aspect of the proximal end of IV-1.

**Observations.** Significant scarring can be present on the craniolateral aspect of the proximal third of the tarsometatarsus of *D. robustus*, *P. elephantopus* and *E. crassus*, but as it covers one diffuse area, it likely is for the insertions of the gastrocnemius and lateral collateral ligament of the ankle too. In contrast, in about two thirds of *P. elephantopus* specimens examined, and most *M. didimus* specimens, there is a small oval patch of slightly roughened bone, immediately proximal to the trochlea for digit IV. This patch is gently recessed somewhat, and often bears a roughened rim. This may mark the origin of the extensor brevis digiti IV in these two species, or (as with the depression proximal to the middle trochlea in *E. crassus*) it may be present to facilitate tarsometatarsophalangeal hyperextension. The proximal end of IV-1 in *D. robustus*, *P. elephantopus* and *E. crassus* often bears a small, elongate area of marked roughness, suggesting the insertion of the extensor brevis digiti IV in these species.

**Remarks.** Zinoviev (2013) suggested that the origin of the extensor brevis digiti IV in *D. robustus* occupied much of the lateral half of the cranial aspect of the tarsometatarsus, but no scars have been observed that supports this interpretation. Nevertheless, inferring the presence of this muscle in *D. robustus*, *P. elephantopus* and *E. crassus* is well supported (level I' inference or higher for origin, level I inference for insertion).

#### Abductor digiti II (Figs 9, 11; abd.II)

**General comments.** Present in all palaeognaths except *Struthio* (where digit II is absent; Gangl *et al.* 2004), this muscle originates from the distomedial aspect of the tarsometatarsus, although in tinamous the origin can encroach onto the craniomedial aspect (Hudson *et al.* 1972). It typically inserts on the proximomedial aspect of II-1.

**Observations.** The distomedial tarsometatarsus of *D. robustus*, *P. elephantopus* and *E. crassus* is

smooth, with no osteological evidence of muscle attachment. However, phalanx II-1 in all three species bears a broad area of rough scarring proximomedially, either as a shallow depression or a low tuberosity; this is presumably for the insertion of the abductor digiti II. The scarring in *E. crassus* is somewhat continuous with that found on the plantar surface.

**Remarks.** The muscle's reconstruction is supported both proximally (level I' inference) and distally (level I inference). Of the mummified foot of *D. robustus* discussed above, Hutton & Coughtrey (1875a p. 273) described a small tendon running to the first phalanx of digit II, "ending in the outer side of the base of this bone." They probably used the word 'outer' to mean 'medial' in this instance, for the outer aspect of digit II in life would be the medial aspect of the pes. If this is correct, then Hutton & Coughtrey (1875a) were referring to an abductor digiti II, and since no other tendon running to the base of II-1 was described by these authors (except the flexor perforatus digiti II, noted above), this would imply the absence of the adductor digiti II (see below). On the other hand, if Hutton & Coughtrey (1875a) used the word 'outer' to mean 'lateral', then the tendon they so described would be that of the adductor digiti II, which in turn would imply that the abductor digiti II was absent in their specimen. The first possibility is considered more likely here, since there is a distinct scar for reception of a tendon on the fossil specimens examined.

#### Abductor digiti IV (Figs 9, 12; abd.IV)

**General comments.** This muscle occurs in all extant palaeognaths. It originates from the caudolateral aspect of the tarsometatarsus, although its extent is rather variable between species. It characteristically inserts on the proximolateral aspect of IV-1.

**Observations.** In *D. robustus*, *P. elephantopus* and *E. crassus* there is a coarse, longitudinally elongate scar or ridge on the distocaudal shaft of the tarsometatarsus, positioned on the lateral half of the bone, which may mark the origin of the abductor digiti IV. The proximolateral



aspect of IV-1 in all three species bears a broad area of surface rugosity, suggesting the insertion of the muscle here (level I inference). This scarred area is usually confluent with the more prominent scars on the proximoplantar aspect of the bone, for insertion of the flexor perforatus digiti IV.

**Remarks.** Reconstructing the abductor digiti IV in the three species is a level I inference for both origin and insertion. In contrast to the reconstruction proposed here, Kooyman (1991) and Zinoviev (2013) suggested that the abductor digiti IV originated from the lateral aspect of the proximal end of the tarsometatarsus, adjacent to the insertion of the lateral collateral ligament of the ankle. This interpretation is not supported by the osteological evidence observed here. Fine striations in the scarring in this region of the bone all point proximally (reflecting the insertion of the collateral ligament and the fibularis brevis; see above); if the abductor digiti IV attached here then a portion of them would be expected to point distally. Kooyman (1991) also suggested that the longitudinal ridge on the distocaudal tarsometatarsus was associated with the lumbricalis (see below), rather than the abductor digiti IV. However, in all extant palaeognaths the lumbricalis originates from the dorsal (deep) surface of the tendon of the flexor digitorum longus; having no direct interaction with the tarsometatarsus itself, the lumbricalis would not be expected to leave any osteological correlates on that bone. The scarring may alternatively indicate the origin of the flexor hallucis brevis, or alternatively marks the origin of both muscles, acting as an intermuscular line. Whilst the situation is unclear, it seems more likely that the scarred area in question is for the abductor digiti IV only, since it is located on the lateral half of the caudal surface of the tarsometatarsus, and is always rougher on its lateral side.

### Adductor digiti II

**General comments.** This muscle is absent in *Struthio* (owing to the loss of digit II: Gangl *et al.* 2004), and is also absent in *Apteryx* (McGowan 1979). In other extant palaeognaths it originates

from the distocaudal tarsometatarsus. The insertion of this muscle in digit II is varied, ranging from II-1 in tinamous to II-3 in *Dromains*; typically, it inserts on the lateral aspect of the phalanx.

**Observations.** In *D. robustus*, *P. elephantopus* and *E. crassus* the distocaudal tarsometatarsus lacks any osteological evidence of muscle attachment, separate from that interpreted as the scar of the abductor digiti IV. Additionally, no scar of attachment is evident on the lateral aspect of any phalanx examined.

**Remarks.** It is too speculative to reconstruct this muscle in moa (level II' inferences proximally and distally). Additionally, Hutton & Coughtrey (1875a) appear not to have found this muscle in their mummified specimen of *D. robustus* (see above).

### Adductor digiti IV

**General comments.** This muscle has only been reported in *Dromains* where it originates from the distal cranio-lateral tarsometatarsus and inserts on the medial aspect of IV-1 (Patak & Baldwin 1998).

**Observations.** No osteological evidence of either origin or insertion was observed in any of the *D. robustus*, *P. elephantopus* or *E. crassus* material examined.

**Remarks.** Reconstructing the adductor digiti IV in moa is too speculative (level II' inference).

### Lumbricalis

**General comments.** The lumbricalis is present in all extant palaeognaths, taking origin from the dorsal (deep) surface of the tendon of the flexor digitorum longus just before it trifurcates (or bifurcates in the case of *Struthio*). Its insertion is somewhat varied, but it is typically the trochleae or surrounding soft tissues of metatarsi III and IV (and II in *Apteryx*: McGowan 1979); in *Casuarinus* and *Rhea*, it inserts on III-1 instead (Gadow 1880).



**Observations.** No direct, osteological evidence of this muscle was observed on the bones of *D. robustus*, *P. elephantopus* and *E. crassus*.

**Remarks.** Despite the lack of osteological evidence, the ubiquity of this muscle in extant palaeognaths implies that the lumbricalis was also present in moa (level I' inference).

#### Soft tissues surrounding the tarsal sesamoid (Fig. 13)

**General comments.** Moa are distinct among 'modern' palaeognaths in possessing a sizeable tarsal sesamoid, located in the lateral half of the ankle joint, between the tibiotarsus and the tarsometatarsus. The sesamoid is, very roughly, a triangular prism in shape with three faces.

**Observations.** The two faces that articulate with the tibiotarsus (cranioproximal face) and tarsometatarsus (craniodistal face) are smooth and devoid of any texture. The third, caudal face presents a fibrous, roughened texture suggestive of a broad attachment of collagenous soft tissue. Whilst no discrete regions of scarring are observable, a consistent pattern is present in that there are strong 'fibres' directed proximally at the proximal margin, and there are also strong 'fibres' directed medially at the bone's medial margin.

**Remarks.** Hutton and Coughtrey (1875a) observed in their mummified *D. robustus* pes that the sesamoid was connected to the proximal tarsometatarsus (and possibly also the tibiotarsus) by a number of ligaments. Hence, it seems possible that the sesamoid was an ossified complement to the tibial cartilage: no muscles *per se* appear to have inserted on it or originated from it, but their tendons may have crossed over it (caudally) as they ran to the pes. This can potentially be investigated further through examination of other mummified specimens.

**Size of the ilirotrochantericus caudalis.** The volume of the ilirotrochantericus caudalis in the geometric model of *D. robustus* was determined to be 2275.02 cm<sup>3</sup>. Assuming a bulk density for striated muscle of 1.06 g/cm<sup>3</sup> (Hutchinson *et al.* 2015), this equates to a mass of 2.412 kg.

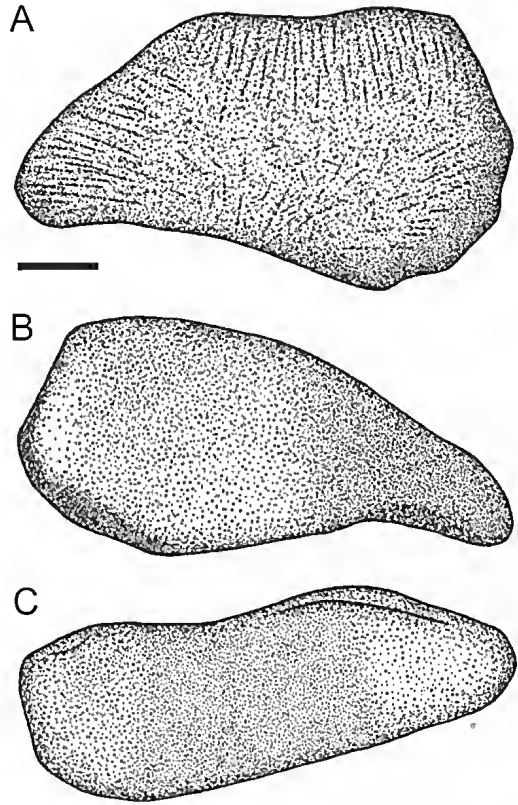


FIG. 13. Osteological evidence of soft tissue attachment on the tarsal sesamoid of *D. robustus*. A, outer (caudal) face; B, cranioproximal face; C, craniodistal face. In A and B, proximal is to top of page; in C, cranial is to top of page. Scale bar = 10 mm.

## DISCUSSION

### Comparison to the work of Zinoviev (2013)

The reconstructions of Zinoviev and those produced here are largely in agreement as regards the presence or absence of certain muscles, and the general location of their origins and insertions. Nonetheless, there are a number of important differences between the two sets of reconstructions, pertaining to the exact location of a given muscle's origin or insertion. These include the site of origin of the ilirotrochanterici medius et cranialis, the extent of origin and manner of subdivision of the femorotibialis medius, the manner of subdivision of the obturatorius medialis, the insertions of

the flexores cruris lateralis pars pelvica, lateralis pars accessoria et medialis, the insertions of the flexor cruris lateralis pars accessoria, caudofemoralis and puboischiofemoralis, insertion of the popliteus, the extent of origin of the fibularis longus and the site of origin of the abductor digiti IV. Additionally, Zinoviev did not reconstruct two muscles in the distal limb, the fibularis brevis and flexor hallucis brevis, which have been reconstructed here.

Many of the differences between the interpretations of Zinoviev (2013) and those made here likely stem from the limited material Zinoviev had at his disposal. It is clear from this study that, just as with whole-bone osteology (Worthy 1988; Kooyman 1991; Worthy & Holdaway 2002; Worthy & Scofield 2012), muscle scarring in the hindlimb of moa shows a high degree of intraspecific and interspecific variation. Hence, it is important to study abundant and well-preserved material when making myological inferences in this group of birds. The differences in interpretations probably also result from differences in the approach used. Zinoviev drew his inferences through comparison to the anatomy of all extant birds, whereas the phylogenetic scope of this study was restricted solely to palaeognaths. Additionally, the inferences made in this study were framed in the context of homology (Bryant & Seymour 1993; Witmer 1995), in order to identify the most phylogenetically parsimonious myological reconstructions.

This study also differs from that of Zinoviev (2013) in that it refrains from interpreting the exact boundaries of attachment for most muscles, whereas Zinoviev explicitly reconstructed the areas of muscle origins and insertions for all muscles. Some of the boundaries illustrated by Zinoviev were rather complex in geometry, yet osteological evidence was not described in support of his reconstructions. That the fleshy origin of many muscles in extant palaeognaths varies both between and within species (cf. Owen 1879; McGowan 1979; Kooyman 1991; Patak & Baldwin 1998; Gangl *et al.* 2004; Smith *et al.* 2006; Zinoviev 2006; Lamas *et al.* 2014; Hutchinson *et al.* 2015) cautions against making such explicitly detailed reconstructions without supporting osteological evidence. This point

is all the more pertinent given the high level of variation in the nature of muscle scarring in moa as described in this study.

In some parts of the moa skeleton, such as the preacetabular iliac blade and the femoral shaft, there exist well-defined intermuscular lines that delineate much of the area of attachment of one or more muscles. In the majority of cases, however, there is simply not enough (if any) osteological evidence to permit an accurate reconstruction of the shape of a muscle's attachment in its entirety (cf. McGowan 1979; Bryant & Seymour 1990). For instance, the postacetabular ilium and the distal ischium and pubis of *D. robustus* is interpreted here to have been the site of origin (or part thereof) of at least six muscles (Fig. 3). Yet for only one of these muscles can a boundary be consistently identified (puboischiofemoralis, delineated dorsally by a pronounced, striated ridge), and even then its entire area of origin remains uncertain. Hence, it remains ambiguous as to exactly where these muscles would have attached to the bones. Without explicitly detailing how much evidence a given reconstruction is based upon, this can limit the reliability of the reconstructions as a whole. Identifying the areas of uncertainty in a reconstruction is also important in that it can point out aspects for future research. One such line of enquiry is the examination of mummified moa remains (see Rawlence *et al.* 2012b).

### The utility of muscle scarring in taxonomic identification.

Despite variability in the nature of muscle scars, a number of patterns were found in the presence or nature of muscle scarring that may be used to distinguish between moa species.

The femora of *P. elephantopus* and South Island populations of *Euryapteryx curtus* are very similar in appearance, to the extent that isolated bones can be exceedingly difficult to assign to one or the other species, owing to population-dependent variation in bone robusticity. Features that have been used to aid identification previously (e.g., Worthy 1988; Worthy & Holdaway 2002), such as the relative location of the popliteal and ectocondylar fossae and the caudal extent of

# Hindlimb myology in moa

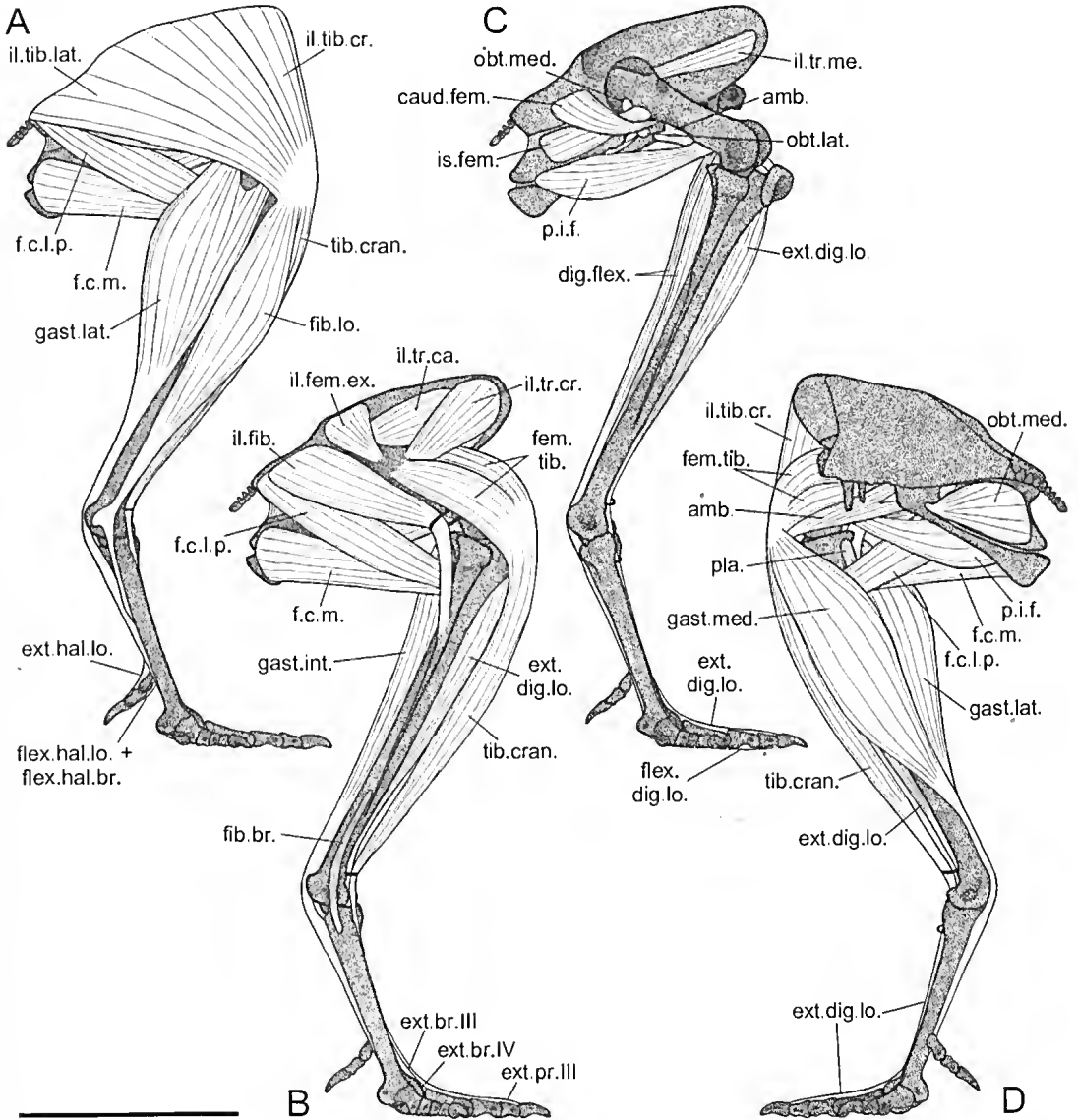


FIG. 14. Tentative restoration of how the hindlimb musculature of *D. robustus* may have appeared in life. A, lateral view showing superficial musculature; B, lateral view showing deeper muscles with outer muscles removed; C, lateral view showing deepest muscles; D, medial view showing superficial musculature. Scale bar = 500 mm. Abbreviations: *amb.*, ambiens; *caud.fem.*, caudofemoralis; *dig.flex.*, digital flexors; *ext.br.III*, extensor brevis digiti III; *ext.br.IV*, extensor brevis digiti IV; *ext.dig.lo.*, extensor digitorum longus; *ext.hal.lo.*, extensor hallucis longus; *ext.pr.III*, extensor proprius digiti III; *f.c.l.p.*, flexor cruris lateralis pars pelvica; *f.c.m.*, flexor cruris medialis; *fem.tib.*, femorotibialis; *fib.br.*, fibularis brevis; *fib.lo.*, fibularis longus; *flex.dig.lo.*, flexor digitorum longus; *flex.hal.br.*, flexor hallucis brevis; *flex.hal.lo.*, flexor hallucis longus; *gast.int.*, gastrocnemius intermedia; *gast.lat.*, gastrocnemius lateralis; *gast.med.*, gastrocnemius medialis; *il.fem.ex.*, iliofemoralis externus; *il.fib.*, iliofibularis; *il.tib.cr.*, ilirotibialis cranialis; *il.tib.lat.*, ilirotibialis lateralis; *il.tr.ca.*, ilirotrochantericus caudalis; *il.tr.cr.*, ilirotrochantericus cranialis; *il.tr.me.*, ilirotrochantericus medius; *is.fem.*, ischiofemoralis; *obt.lat.*, obturatorius lateralis; *obt.med.*, obturatorius medialis; *p.i.f.*, puboischiofemoralis; *pla.*, plantaris; *tib.cran.*, tibialis cranialis.

the trochanteric ridge, have been found to be variable in these species (T.H. Worthy, pers. comm., 7.1.14; pers. obs.). Additionally, it was considered that *P. elephantopus* femora could be distinguished from those of *E. curtus* on the basis of the cross-sectional shape of the shaft at the mid-point of the bone (Worthy 1988, 1989; Worthy & Holdaway 2002), with the craniocaudal depth typically being markedly greater than the mediolateral width in *P. elephantopus*. This criterion is usually successful, and the distinction is clearly apparent when the femora of both species are compared side-by-side. With isolated specimens, however, it is difficult to apply this criterion with certainty.

Two myology-related features may help resolve this problem. The first is that, in *P. elephantopus*, intermuscular lines 3 and 4 are always in very close proximity, and are almost always fused to form a single intermuscular line on the middle of the caudal surface of the bone (Fig. 5A). These intermuscular lines were observed to be distinctly separate in all *E. curtus* femora examined. Hence, whilst the presence of a single intermuscular line on the middle of the caudal femur is indicative of *P. elephantopus*, the presence of two intermuscular lines is ambiguous, because a very small fraction of *P. elephantopus* femora examined showed two separate, although closely spaced, lines. The second myology-related feature is the relative disposition of the scars of insertion of the ischiofemoralis and caudofemoralis pars pelvica. In *P. elephantopus* the two scars are always well-separated by smooth bone, whereas in *E. curtus* the two are usually confluent (normally at their distal ends), sometimes so much so that only a single large area of scarring is present.

Paralleling the situation with the femur, the tarsometatarsus of *P. elephantopus* and South Island populations of *E. curtus* can also be difficult to distinguish in isolation. This is again due to variation within and between populations, even in those features previously proposed as taxonomically useful, such as the morphology of the middle trochlea (Worthy 1988; Worthy & Holdaway 2002; T.H. Worthy pers. comm. 7.1.14). Two myology-related features were observed which may be of use. The two small

tuberosities for attachment of the retinaculum extensorium tarsometatarsi are absent in *P. elephantopus* (Fig. 10A), whereas they were present in approximately half of the *E. curtus* specimens examined. (In some individuals of *E. curtus*, the tuberosities were present on one tarsometatarsus but not on that from the other foot.) Thus, whilst the absence of the tuberosities is an ambiguous result, their presence indicates that the tarsometatarsus is of *E. curtus*. The other feature is a roughened depression proximal to the trochlea for digit IV on the cranial aspect of the bone, which is present in approximately two-thirds of the *P. elephantopus* specimens examined (Fig. 10A,B), but which is absent in *E. curtus*. The presence of this feature, which may or may not be associated with the extensor brevis digiti IV (see above), is therefore indicative of *P. elephantopus*, but its absence is an ambiguous result.

The femur of *M. didimus* is usually easily distinguished from that of other moa species by virtue of its slenderness and small size, although the femur of large individuals are difficult to distinguish from that of *A. didiformis*, especially if the distal end is poorly preserved (Worthy & Holdaway 2002). Uniquely among moa, however, is the nature of the two caudal tuberosities in *M. didimus* (Fig. 5D). The lateral caudal tuberosity (insertion for the flexor cruris lateralis pars accessoria) is positioned in the proximal half of the bone, whereas in all other species it is located in the distal half. Additionally, the medial caudal tuberosity in *M. didimus* (insertion for the puboischiofemoralis) is bipartite, whereas in all other species it is singular. The clear separation of the lateral and medial caudal tuberosities in *M. didimus* is also seen in *Dinornis* spp. Considering the current consensus of moa interrelationships (Bunce *et al.* 2009; Worthy & Scofield 2012), this indicates that an association between the puboischiofemoralis and the flexor cruris lateralis pars accessoria is apomorphic for emeids.

### Moa and the reconstruction of musculature in extinct vertebrates

Moa have been shown to display a considerable degree of variability in the manifestation

of muscle attachment. Despite this, the basic topology and location of muscle scarring in moa is relatively consistent across species, and is generally comparable with extant palaeognaths. Coupled with overall conservatism in palaeognath hindlimb myology, this has made the task of myological reconstruction in moa relatively straightforward for most muscles. Also aiding the process is that moa are a group of animals for which there are abundant fossil remains, and in which muscle scarring is well pronounced on the bones studied. This is due to several factors, the most important being the exceptional preservation of many of the specimens examined. These specimens are very recent, in some instances less than 1,000 years old, and have undergone little taphonomic degradation (e.g., Allentoft *et al.* 2012, 2014; Rawlence *et al.* 2012a). Furthermore, in some swamp localities, such as Pyramid Valley, Kapua and Cheviot, differential staining of the bones has highlighted muscle attachment scars. An additional factor is that the muscles of larger animals tend to leave larger, more distinct scars of attachment on the bones.

The prevalence of muscle scarring in moa, and the relatively straightforward process of myological reconstruction in this group, prompts reflection on the sentiments of McGowan (1979), who raised concerns over the ability of palaeontologists to accurately reconstruct the myology of extinct species. Using moa as an example, he was only able to recognise osteological correlates of a small proportion of hindlimb muscles in a skeleton of *E. crassus*, and thus claimed that it would be impossible to accurately reconstruct the hindlimb musculature in moa.

McGowan based his work only on the musculo-skeletal anatomy of *Apteryx mantelli*, however, and attempted to extrapolate his findings directly from this small bird to a much larger species. The osteological correlates of muscle attachment in *Apteryx* spp. are small and usually poorly developed, or are absent entirely (McGowan 1979; pers. obs.). Consequently, McGowan was able to recognise fewer osteological correlates common to both *Apteryx* and *E. crassus*. Being a much larger bird, however, there are a multitude

of other attachment scars on the bones of *E. crassus* that are not evident in *Apteryx*, which would have further hampered McGowan's comparison. Indeed, of the 48 muscles (or muscle parts) that have been reconstructed here in *D. robustus*, *P. elephantopus* and *E. crassus*, the proportion that are consistently recognisable by osteological correlates is 44%, 50% and 46 % (respectively) for muscle origins and 88%, 83% and 83% (respectively) for muscle insertions. Considering origins or insertions together, the proportion of muscles which can be consistently recognised by osteological correlates is 96%, 94% and 94% (respectively). That is, almost every muscle in the hindlimb of these three species can be recognised by an osteological correlate of attachment somewhere on the skeleton. This means that the origins and insertions of a considerable number of these muscles, particularly those of the proximal limb, may be confidently inferred for moa. Considering the great prevalence of scars of muscle attachment in moa, the preservation of the fossil bones, their recent extinction and the overall conservatism in extant palaeognath hindlimb myology, moa may be seen as an exception to the general difficulty facing palaeontologists who attempt to reconstruct musculature in extinct vertebrates (Bryant & Seymour 1990).

McGowan's inability to reconstruct the hindlimb myology of *E. crassus* more fully also highlights the importance of making comparisons to multiple extant relatives, as done here. In the years following McGowan's (1979) work, the advent of the EPB approach (Bryant & Russell 1993; Witmer 1995) has helped facilitate defensible inferences of musculature (and other soft tissues), even when direct osteological evidence is absent. For those few muscles that lacked any osteological evidence, they were still able to be hypothesised as present and so reconstructed here in *D. robustus*, *P. elephantopus* and *E. crassus* through this approach. Moreover, where osteological evidence of an origin or insertion is wanting, the EPB can guide the reconstruction of the approximate region from which the origin or insertion would have most likely been. As with all extinct vertebrates, however, little, if anything, may be inferred

about muscle size, gross geometry, internal architecture (parallel-fibred *versus* pennate) or histochemistry (Bryant & Seymour 1990).

### Biomechanical considerations

The myological reconstructions produced for the three moa species studied will help facilitate comparative biomechanical analysis of locomotor behaviour in moa. Throughout the course of the current study, two points of interest concerning the biomechanics of the moa hindlimb have arisen. These are briefly discussed here.

#### Relative size of the iliotochantericus caudalis.

The iliotochantericus caudalis is active during the stance (support) phase of walking and running in extant birds (Gatesy 1994, 1999), and is hypothesised to be the main muscle responsible for maintaining stability of the hip joint during stance. Specifically, its contraction effects medial (inward) long-axis rotation of the femur, which, because of the subhorizontal orientation of the femur in birds, helps to resist adduction of the limb as a whole under the weight of the body (Hutchinson & Gatesy 2000). The muscle is hence one of the most important antigravity muscles in the avian hindlimb. Digital computer modelling of the iliotochantericus caudalis in an adult female *D. robustus* has estimated that the muscle in this individual had a mass of 2.412 kg. As explained above, this estimate should be viewed as an absolute minimum.

The *D. robustus* individual utilised here (CM Av 8422) is very similar in size to that studied by Brassey *et al.* (2013), who estimated its mass as 196 kg (with a 95% confidence interval of 155–245 kg). Assuming these values here, the modelled iliotochantericus caudalis thus occupies a minimum of 0.984–1.56% of total body mass. This is a very large proportion. For comparison, in a 65.3 kg ostrich, Hutchinson *et al.* (2015) measured the mass of the iliotochantericus caudalis as 0.311 kg, or approximately 0.476% of body mass; and in a 42 kg emu, Lamas *et al.* (2014) measured the mass of the muscle as 0.336 kg, or approximately 0.8 % of body mass. Therefore, the iliotochantericus caudalis in *D. robustus* is disproportionately large compared

to both the emu and ostrich, by a factor of at least 1.2 for the emu and 2.1 for the ostrich. This supports the hypothesis that, in having an enlarged preacetabular iliac blade, at least some species of moa had a relatively enlarged iliotochantericus caudalis in comparison to other palaeognaths. Being a primary antigravity muscle, the large size of the iliotochantericus caudalis in moa undoubtedly reflects the larger size of moa compared to ostriches and emus. Its disproportionately greater size may be an allometric effect, since the force-generating capacity of muscle scales with negative allometry: all other factors being equal, force scales proportional to cross-sectional area, and thus length<sup>2</sup>, whereas mass scales proportional to volume, and thus length<sup>3</sup> (Vogel 2003). Indeed, Lamas *et al.* (2014) found that the mass of the iliotochantericus caudalis scaled with positive allometry across an ontogenetic sample of emus. The great size of the iliotochantericus caudalis in moa may alternatively, or additionally, reflect a difference in the locomotor behaviour of moa compared to ostriches and emus, and thus opens up further avenues for future biomechanical investigation.

**Function of the tarsal sesamoid.** As discussed above, no muscle appears to have originated or inserted on this bone in moa, but the tendons of one or more digital flexors may have passed over it as they ran around the caudal aspect of the ankle joint. If this interpretation is correct, then the tarsal sesamoid of moa may have possibly functioned in an analogous fashion to the proximal sesamoid bone of the horse metacarpus, which acts to increase the moment arm of the digital flexors as they cross the metacarpophalangeal joint (Thomason 1985). Interestingly, biomechanical modelling by Hutchinson (2004a, b) suggested that the ankle joint is the 'weakest link' in the hindlimb of a biped, in terms of the ability of extensor (antigravity) muscles to support the limb during stance and prevent it from collapsing. The presence of a tarsal sesamoid in moa may have therefore been advantageous in these large birds, by increasing the mechanical efficacy of distal limb muscles in preventing limb collapse during locomotion. An alternative, or perhaps



even complementary, function that the tarsal sesamoid may have conferred is providing a measure of stability to the ankle joint.

## CONCLUSIONS

Utilising a large sample of fossil specimens from many localities throughout the South Island of New Zealand, the hindlimb myology of three moa species, *D. robustus*, *P. elephantopus* and *E. crassus*, has been reconstructed in detail. The reconstructions presented here are well supported by both osteological correlates of muscle attachment on the fossil bones themselves, as well as through comparison with extant, phylogenetically close birds (palaeognaths). Nevertheless, the high level of variation in moa osteology and muscle scarring morphology suggests that it would be worthwhile testing these reconstructions on hitherto unsampled populations from other sites around the South Island. It would also be worthwhile studying the mummified remains of moa to better understand their hindlimb musculoskeletal anatomy, through the non-destructive approaches of magnetic resonance imaging and X-ray computed tomography.

Several features pertaining to the attachments of muscles have been identified that may be of use in the taxonomic identification of isolated, incomplete or poorly preserved moa limb bones.

Moa are rather unique among extinct vertebrates in that the reconstruction of much of their hindlimb musculature has proven to be a relatively straightforward process. It remains to be seen as to whether this holds true for other parts of the moa body, such as the neck and head.

The myological reconstructions produced here provide a solid anatomical basis upon which comparative biomechanical investigation of moa locomotor behaviour can be undertaken. This can help shed light on the posture and gait of moa, as well as the reason or reasons underlying the unique skeletal proportions of the moa hindlimb. Additional features have also been identified which would be worthy of biomechanical investigation, such

as the significance of a large preacetabular iliac blade, and the role of the tarsal sesamoid.

## ACKNOWLEDGEMENTS

The staff of the Geosciences Program of the Queensland Museum is thanked for help with access to the collection and in the production of the figures. Great appreciation is extended to Dr R.P. Scofield and Mr M. Shaw of the Canterbury Museum, for access to the moa fossils in their care, and for assistance with the CT scanning. Likewise, the access to comparative material of extant palaeognath birds, afforded by Dr R.P. Scofield, Ms H. Janetzki (Queensland Museum) and Dr K.K. Roberts (Museum Victoria), is much appreciated. The assistance of Mr D. Hely and the Christchurch Hospital Radiology Department, with CT scanning, and Ms M. Lloyd (Queensland Museum Library), with obtaining literature, is gratefully acknowledged. For helpful discussion of various aspects covered in this work, or for the provision of unpublished observations or information, the following people are sincerely thanked: Profs. J.R. Hutchinson and S.A. Hocknull, and Drs T.H. Worthy, R.P. Scofield and M.B.J. Picasso. The final manuscript benefited greatly from the constructive comments and suggestions of Drs T.H. Worthy and P. Johnston, as well as those of the editor, Dr A.C. Rozefelds. This study was financially supported by an Australian Postgraduate Award.

## LITERATURE CITED

- Alexander, R.McN. 1983a. Allometry of the leg bones of moas (*Dinornithes*) and other birds. *Journal of Zoology* **200**: 215–231.
- Alexander, R.McN. 1983b. On the massive legs of a moa (*Pachyornis elephantopus*, *Dinornithes*). *Journal of Zoology* **201**: 363–376.
- Allentoft, M.E., Collins, M., Harker, D., Haile, J., Oskam, C.L., Hale, M.L., Campos, P.F., Samaniego, J.A., Gilbert, M.T.P., Willerslev, E., Zhang, G., Scofield, R.P., Holdaway, R.N. & Bunce, M. 2012. The half-life of DNA in bone: measuring decay kinetics in 158 dated fossils. *Proceedings of the Royal Society of London Series B Biological Sciences* **279**: 4724–4733.
- Allentoft, M.E., Heller, R., Oskam, C.L., Lorenzen, E.D., Hale, M.L., Gilbert, M.P.T., Jacomb, C., Holdaway,

- R.N. & Bunce, M. 2014. Extinct New Zealand megafauna were not in decline before human colonization. *Proceedings of the National Academy of Sciences* **111**: 4922–4927.
- Anderson, A.J. 1989. *Prodigious Birds: Moas and Moa-Hunting in Prehistoric New Zealand*. (Cambridge University Press: Cambridge).
- Baker, A.J. & Pereira, S. 2009. Ratites and tinamous (Palaeognathae). Pp. 412–414. In Hedges, S.B. & Kumar, S. (eds) *The Timetree of Life*. (Oxford University Press: Oxford).
- Bates, K.T. & Schachner, E.R. 2012. Disparity and convergence in bipedal archosaur locomotion. *Journal of the Royal Society Interface* **9**: 1339–1353.
- Baumel, J.J., King, A.S., Breazile, J.E., Evans, H.E. & Vanden Berge, J.C. (eds) 1993. *Handbook of Avian Anatomy: Nomina Anatomica Avium, 2nd Edition*. (Nuttall Ornithological Club: Cambridge).
- Boles, W.E. 1992. Revision of *Dromaius gidju* Patterson and Rich 1987 from Riversleigh, northwestern Queensland, Australia, with a reassessment of its generic position. *Los Angeles County Museum Science Series* **36**: 195–208.
- Bourdon, E., de Ricqlès, A. & Cubo, J. 2009. A new transantarctic relationship: morphological evidence for a Rheidae-Dromaiidae-Casuariidae clade (Aves: Palaeognathae, Ratitae). *Zoological Journal of the Linnean Society* **156**: 641–663.
- Brassey, C.A., Holdaway, R.N., Packham, A.G., Anne, J., Manning P.L. & Sellers, W.I. 2013 More than one way of being a moa: Differences in leg bone robustness map divergent evolutionary trajectories in Dinornithidae and Emeidae (Dinornithiformes). *PLoS ONE* **8**: e82668.
- Bryant, H.N. & Russel, A.P. 1993. The occurrence of clavicles within the Dinosauria: implications for the homology of the avian furcula and the utility of negative evidence. *Journal of Vertebrate Paleontology* **13**: 171–184.
- Bryant, H.N. & Seymour, K.L. 1990. Observations and comments on the reliability of muscle reconstruction in fossil vertebrates. *Journal of Morphology* **206**: 109–117.
- Buller W.L. 1888. *A history of the birds of New Zealand, 2nd edition*. (Buller: London).
- Bunce, M., Worthy, T.H., Phillips, M.J., Holdaway, R.N., Willerslev, E., Halle, J., Shapiro, B., Scofield, R.P., Drummond, A., Kamp, P.J.J. & Cooper, A. 2009. The evolutionary history of the extinct ratite moa and New Zealand Neogene paleogeography. *Proceedings of the National Academy of Sciences* **106**: 20646–20651.
- Carrano, M.T. & Hutchinson, J.R. 2002. Pelvic and hindlimb musculature of *Tyrannosaurus rex* (Dinosauria: Theropoda). *Journal of Morphology* **253**: 207–228.
- Chadwick, K.P., Regnault, S. Allen, V. & Hutchinson, J.R. 2014. Three-dimensional anatomy of the ostrich (*Struthio camelus*) knee joint. *PeerJ* **2**: e706.
- Dilkes, D.W., Hutchinson, J.R., Holliday, C.M. & Witmer, L.M. 2012. Reconstructing the musculature of dinosaurs. Pp. 151–190. In, Brett-Surman, M.K., Holtz, T.R. Jr & Farlow, J.O. (eds) *The Complete Dinosaur, 2nd edition*. (Indiana University Press: Bloomington).
- Doube, M., Yen, S.C.W., Klosowski, M.M., Farke, A.A., Hutchinson, J.R. & Shefelbine, S.J. 2012. Whole-bone scaling of the avian pelvic limb. *Journal of Anatomy* **221**: 21–29.
- Gadow, H. 1880. *Zur Vergleichenden Anatomie der Muskulatur des Beckens und der Hinteren Gliedmasse der Ratiten*. (Gustav Fischer: Jena). [In German]
- Gangl, D., Weissengruber, G.E., Egerbacher, M. & Forstenpointner, G. 2004. Anatomical description of the muscles of the pelvic limb in ostrich (*Struthio camelus*). *Anatomia Histologia Embryologia* **33**: 100–114.
- Gatesy, S.M. 1994. Neuromuscular diversity in archosaur deep dorsal thigh muscles. *Brain, Behavior and Evolution* **43**: 1–14.
- Gatesy, S.M. 1999. Guineafowl hind limb function. II. Electromyographic analysis and motor pattern evolution. *Journal of Morphology* **240**: 127–142.
- Gatesy, S.M. & Middleton, K.M. 1997. Bipedalism, flight and the evolution of theropod locomotor diversity. *Journal of Vertebrate Paleontology* **17**: 308–329.
- Haddrath, O. & Baker, A.J. 2012. Multiple nuclear genes and retroposons support vicariance and dispersal of the palaeognaths, and an Early Cretaceous origin of modern birds. *Proceedings of the Royal Society of London Series B Biological Sciences* **279**: 4617–4625.
- Hudson, G.E., Schreiweis, D.O., Wang, S.Y.C. & Lancaster, D.A. 1972. A numerical study of the wing and leg muscles of tinamous (Tinamidae). *Northwest Science* **46**: 207–255.
- Hutchinson, J.R. 2001. The evolution of femoral osteology and soft tissues on the line to extant birds (Neornithes). *Zoological Journal of the Linnean Society* **131**: 169–197.
- 2004a. Biomechanical modeling and sensitivity analysis of bipedal running ability. I. Extant Taxa. *Journal of Morphology* **262**: 421–440.
- 2004b. Biomechanical modeling and sensitivity analysis of bipedal running ability. II. Extinct Taxa. *Journal of Morphology* **262**: 441–461.
- Hutchinson, J.R. & Gatesy, S.M. 2000. Adductors, abductors, and the evolution of archosaur locomotion. *Paleobiology* **26**: 734–751.
- Hutchinson, J.R., Anderson, F.C., Blemker, S.S. & Delp, S.L. 2005. Analysis of hindlimb muscle moment arms in *Tyrannosaurus rex* using a



- three-dimensional musculoskeletal computer model: implications for stance, gait, and speed. *Paleobiology* 31: 676–701.
- Hutchinson, J.R., Bates, K.T., Molnar, J., Allen, V. & Makovicky, P.J. 2011. A computational analysis of limb and body dimensions in *Tyrannosaurus rex* with implications for locomotion, ontogeny, and growth. *PLoS ONE* 6: e26037.
- Hutchinson, J.R., Rankin, J. W., Rubenson, J., Rosenbluth, K.H., Siston, R.A. & Delp, S.L. 2015. Musculoskeletal modeling of an ostrich (*Struthio camelus*) pelvic limb: influence of limb orientation on muscular capacity during locomotion. *PeerJ* 3: e1001.
- Hutton, F.W. & Coughtrey, M. 1875a. Description of some moa remains from the Kobby Ranges. With anatomical notes. *Transactions of the New Zealand Institute* 7: 266–273.
- 1875b. Notice of the Earnsclough Cave. With remarks on some of the more valuable moa remains found in it. *Transactions of the New Zealand Institute* 7: 138–144.
- Johnston, P. 2011. New morphological evidence supports congruent phylogenies and Gondwana vicariance for palaeognathous birds. *Zoological Journal of the Linnean Society* 163: 959–982.
- Kooyman, B.P. 1985. *Moa and Moa Hunting: An Archaeological Analysis of Big Game Hunting in New Zealand*. PhD thesis, University of Otago, Dunedin.
1991. Implications of Bone Morphology for Moa Taxonomy and Behaviour. *Journal of Morphology* 209: 53–81.
- Lamas, L., Main, R.P. & Hutchinson, J.R. 2014. Ontogenetic scaling patterns and functional anatomy of the pelvic limb musculature in emus (*Dromaius novaehollandiae*). *PeerJ* 2: e716.
- Livezey, B.C. & Zusi, R.L. 2007. Higher-order phylogeny of modern birds (Theropoda, Aves: Neornithes) based on comparative anatomy. II. Analysis and discussion. *Zoological Journal of the Linnean Society* 149: 1–95.
- Maidment, S.C.R. & Barrett, P.M. 2011. The locomotor musculature of basal ornithischian dinosaurs. *Journal of Vertebrate Paleontology* 31: 1265–1291.
- Maidment, S.C.R., Bates, K.T., Falkingham, P.L., Van Buren, C., Arbour, V. & Barrett, P.M. 2014. Locomotion in ornithischian dinosaurs: an assessment using three-dimensional computational modelling. *Biological Reviews* 89: 588–617.
- McGowan, C. 1979. The hind limb musculature of the Brown Kiwi, *Apteryx australis mantelli*. *Journal of Morphology* 160: 33–74.
- Mitchell, K.J., Llamas, B., Soubrier, J., Rawlence, N.J., Worthy, T.H., Wood, J., Lee, M.S.Y. & Cooper, A. 2014. Ancient DNA reveals elephant birds and kiwi are sister taxa and clarifies ratite bird evolution. *Science* 344: 898–900.
- Murray, P.F. & Vickers-Rich, P. 2004. *Magnificent Mihirungs: The Colossal Flightless Birds of the Australian Dreamtime*. (Indiana University Press: Bloomington).
- Owen, R. 1858. On *Dinornis* (Part VII): containing a description of the bones of the leg and foot of the *Dinornis elephantopus*, Owen. *Transactions of the Zoological Society of London* 4: 149–158.
1879. *Memoirs on the Extinct Wingless Birds of New Zealand*. (Van Voorst: London).
1883. On *Dinornis* (Part XXIII): containing a description of the skeleton of *Dinornis parvus*, Owen. *Transactions of the Zoological Society of London* 11: 233–256.
- Patak, A.E. & Baldwin, J. 1998. Pelvic limb musculature in the emu *Dromaius novaehollandiae* (Aves: Struthioniformes: Dromaiidae): adaptations to high-speed running. *Journal of Morphology* 238: 23–37.
- Persons, W.S. IV & Currie, P.J. 2011a. Dinosaur speed demon: the caudal musculature of *Carnotaurus sastrei* and implications for the evolution of South American abelisaurids. *PLoS ONE* 6: e25763.
- Persons, W.S. IV & Currie, P.J. 2011b. The tail of *Tyrannosaurus*: reassessing the size and locomotive importance of the *M. caudofemoralis* in non-avian theropods. *The Anatomical Record* 294: 119–131.
- Persons, W.S. IV & Currie, P.J. 2012. Dragon tails: convergent caudal morphology in winged archosaurs. *Acta Geologica Sinica (English Edition)* 86: 1402–1412.
- Phillips, M.J., Gibb, G.C., Crimp, E.A. & Penny, D. 2010. Tinamou and moa flock together: mitochondrial genome sequence analysis reveals independent losses of flight among ratites. *Systematic Biology* 59: 90–107.
- Picasso, M.B.J. 2010. The hindlimb muscles of *Rhea americana* (Aves, Palaeognathae, Rheidae). *Anatomia Histologia Embryologia* 39: 462–472.
- Pycraft, W.P. 1900. On the morphology and phylogeny of the Palaeognathae (Ratitae and Crypturi) and Neognathae (Carinatae). *Transactions of the Zoological Society of London* 15: 149–290.
- Rawlence, N.J., Metcalf, J.L., Wood, J.R., Worthy, T.H., Austin, J.J. & Cooper, A. 2012a. The effect of climate and environmental change on the megafaunal moa of New Zealand in the absence of humans. *Quaternary Science Reviews* 50: 141–153.
- Rawlence, N.J., Wood, J.R., Scofield, R.P., Fraser, C. & Tennyson, A.J.D. 2012b. Soft tissue specimens from pre-European extinct birds of New Zealand. *Journal of the Royal Society of New Zealand* 43: 154–181.

- Regnault, S., Pitsillides, A.A. & Hutchinson, J.R. 2014. Structure, ontogeny and evolution of the patellar tendon in emus (*Dromaius novaehollandiae*) and other palaeognath birds. *PeerJ* 2: e711.
- Schaller, N.U., Herkner, B., Villa, R. & Aerts, P. 2009. The intertarsal joint of the ostrich (*Struthio camelus*): anatomical examination and function of passive structures in locomotion. *Journal of Anatomy* 214: 830–847.
- Smith, J.V., Braun, E.L. & Kimball, R.T. 2013. Ratite nonmonophyly: Independent evidence from 40 novel loci. *Systematic Biology* 62: 35–49.
- Smith, N.C., Wilson, A.M., Jespers, K.J. & Payne, R.C. 2006. Muscle architecture and functional anatomy of the pelvic limb of the ostrich (*Struthio camelus*). *Journal of Anatomy* 209: 765–779.
- Thomason, J.J. 1985. Estimation of locomotor forces and stresses in the limb bones of Recent and extinct equids. *Paleobiology* 11: 209–220.
- Turvey, S.T. & Holdaway, R.N., 2005. Postnatal ontogeny, population structure, and extinction of the giant moa *Dinornis*. *Journal of Morphology* 265: 70–86.
- Vogel, S. 2003. *Comparative Biomechanics: Life's Physical World*. (Princeton University Press: Princeton).
- Witmer, L.M. 1995. The extant phylogenetic bracket and the importance of reconstructing soft tissues in fossils. Pp. 19–33. *In* Thomason, J.J. (ed.) *Functional Morphology in Vertebrate Paleontology*. (Cambridge University Press: Cambridge).
- Worthy, T.H. 1988. An illustrated key to the main leg bones of moas (Aves: Dinornithiformes). *National Museum of New Zealand Miscellaneous Publication Series* 17: 1–37.
- Worthy, T.H. 1989. Aspects of the biology of two moa species (Aves: Dinornithiformes). *New Zealand Journal of Archaeology* 11: 77–86.
- Worthy, T.H. & Holdaway, R.N. 2002. *The Lost World of the Moa*. (Indiana University Press: Bloomington).
- Worthy, T.H. & Scofield, R.P. 2012. Twenty-first century advances in knowledge of the biology of moa (Aves: Dinornithiformes): a new morphological analysis and moa diagnoses revised. *New Zealand Journal of Zoology* 39: 87–153.
- Zinoviev, A.V. 2006. Notes on the hind limb myology of the ostrich (*Struthio camelus*). 1551 *Ornithologia* 33: 53–62.
2011. Notes on the hindlimb myology and syndesmology of the Mesozoic toothed bird *Hesperornis regalis* (Aves: Hesperornithiformes). *Journal of Systematic Palaeontology* 9: 65–84.
2013. Notes on the pelvic and hindlimb myology and syndesmology of *Emeus crassus* and *Dinornis robustus* (Aves: Dinornithiformes). Pp. 253–278. *In*, Göhlich, U.B. & Kroh, A. (eds) *Proceedings of the Eighth International Meeting of the Society of Avian Paleontology and Evolution*, Vienna, 11–16 June, 2012. (Naturhistorisches Museum Wien: Vienna).

# A drift log from Cape York Peninsula, Australia identified as *Vatica* (Dipterocarpaceae), and the use of botanical, zoological, geological and ethnographic data in interpreting the direction of oceanic drift

A.C. ROZEFELDS

Queensland Museum, GPO Box 3300, South Brisbane Qld 4101, Australia. Corresponding author  
email: andrew.rozefelds@qm.qld.gov.au

J. WALKER

Department of Agriculture, Box 96, Cairns International Airport, Cairns Qld 4878, Australia

E. NORRIS

D. WICKS

PO Box 1070, Mossman Qld 4873, Australia

J. ILIC

19 Benambra Street, Oakley South Vic 3167, Australia

Citation: Rozefelds, A.C., Walker, J., Norris, E., Wicks, D. & Ilic, J. 2015. A drift log from Cape York Peninsula, Australia identified as *Vatica* (Dipterocarpaceae), and the use of botanical, zoological, geological and ethnographic data in interpreting the direction of oceanic drift. *Memoirs of the Queensland Museum – Nature* 59: 235-243. Brisbane ISSN 2204-1478 (Online) ISSN 0079-8835 (Print) Accepted: 19 August 2015. First published online: 24 November 2015

<http://dx.doi.org/10.17082/j.2204-1478.59.2015.2015-04>

LSID: urn:lsid:zoobank.org:pub:DA74E240-2269-4806-85C8-EDC0BE946D92

## ABSTRACT

Information on oceanic currents along with botanical, zoological, geological data and ethnographic records are used to interpret drift patterns in north eastern Australia. A log of *Vatica* sp. (Dipterocarpaceae), other botanical disseminules, and ethnographic objects, such as indigenous canoes and plastic bottles, found in north eastern Queensland are interpreted as coming from New Guinea. The southerly drift of these objects from New Guinea is facilitated, in part, by the Gulf of Papua Current and/or seasonal south westerly directed winds from October through to March. The identification of source areas for geological (pumice), zoological (*Nautilus*) and some anthropological items demonstrates predominantly westerly drift due to the South Equatorial Current and south eastern trade winds from April to October. Thus, seasonal factors determine, in part, the direction of drift in parts of north east Queensland. □ *Dipterocarpaceae*, *Vatica*, wood anatomy, Cape York Peninsula, New Guinea, drift trajectory, long-distance dispersal, Gulf of Papua Current (GPC), South Equatorial Current (SEC).

The action, prevailing direction and interplay of oceanic currents and wind lead to the translocation and accumulation of drift material from disparate source areas onto oceanic beaches. In many cases the origins of these drift objects

can only be speculated upon, but occasionally, as in this study, the sources of different classes of drift objects, i.e. zoological, botanical, geological and ethnographic, can be identified with some certainty and it is therefore possible

to infer the direction of drift of these objects in relation to the predominant oceanic currents and winds in the region.

A modern tree trunk was found by one of us (D. Wicks) washed up on the eastern coast of Cape York Peninsula, north eastern Queensland. Its wood anatomy is described, and it is shown to be referable to the Malesian genus, *Vatica* (Dipterocarpaceae). Based upon the prevailing oceanic currents in this part of north east Queensland, and knowledge as to where the Dipterocarpaceae currently occur, the likely drift trajectory of the *Vatica* log can be proposed. This trajectory is compared with that seen for different classes of drift objects in this region, and we examine the extent to which these patterns can be correlated with information on oceanic currents and wind direction (see Schiller *et al.* 2008, SPICE community). From this combined data we can identify generalised patterns for the oceanic drift of objects and the potential for oceanic dispersal of fauna and flora throughout this region.

## MATERIALS AND METHODS

This study is largely based upon a log which was found at the mouth of the Nesbit River (13° 33'S 143° 33'E), Cape York Peninsula, Australia that had a diameter of 40-50 cm, and over two metres in length. While much of the outer wood is weathered and partially decomposed (Fig. 1A-B), samples from the centre of the trunk were sufficiently well preserved to allow identification (Fig. 1C-E). Transverse, radial and tangential sections were prepared, stained with methyl violet and examined under a Nikon MKII (Fig. 1C-E). The standard procedures for wood identification were carried out by the last author, a wood anatomist, based on an examination of the wood anatomical characteristics (features) of the unknown specimen. Its features were compared with authentic specimens and slides of *Vatica* according to accepted IAWA (International Association of Wood Anatomists) procedures (Wheeler *et al.* 1989). The identification is only feasible to generic level, and was conferred through reference to the systematic descriptions in PROSEA (Sosef *et al.* 1993). The critical features for *Vatica* include the

presence of diffuse axial gum canals, vessel size and frequency, nature of the inter-vessel pitting and absence of silica inclusions as summarised below in 'Description of the wood anatomy'. A sample of the wood (AQ798211) has been donated to the Queensland Herbarium (BRI).

Published papers and ethnographic records from the Cultural Heritage section of the Queensland Museum, recording the occurrence of dugout canoes in eastern Australia were assessed. Papers dealing with the geochemical analysis of pumice samples and with botanical and zoological records of drift items from the region were also reviewed. The data from these different object classes was examined to see what patterns exist.

The different oceanic currents in the Coral Sea are described in terms of their prevailing wind direction, so the northerly-directed winds from October through to March result in a south-westerly drift; similarly the south easterly trade winds that drive the South Equatorial Current result in a predominantly westerly drift.

Records in the Atlas of Living Australia website (<http://www.ala.org.au>) were assessed to determine the distribution of *Vatica* in New Guinea and *Nautilus* in eastern Australia. Authorities to extant plant taxa are available at the International Plant Names Index website: <http://www.ipni.org>, and to animal names: <http://www.organismnames.com>.

## DESCRIPTION OF WOOD SAMPLE

### Dipterocarpaceae Blume (1825)

#### *Vatica* L.

**Description of wood anatomy.** Wood reddish-brown with streaks of pale-coloured decay and resinous deposits with a faint odour. Growth rings indistinct. Vessels small, numerous, mostly solitary and heavily tylosed, approximately 100-120µm in diameter. Rays appear to be of two types, 1, 4-7 cells wide, narrow and medium width with occasional sheath cells, - the latter almost as wide as the vessels. Vertical canals diffuse and difficult to detect, appear

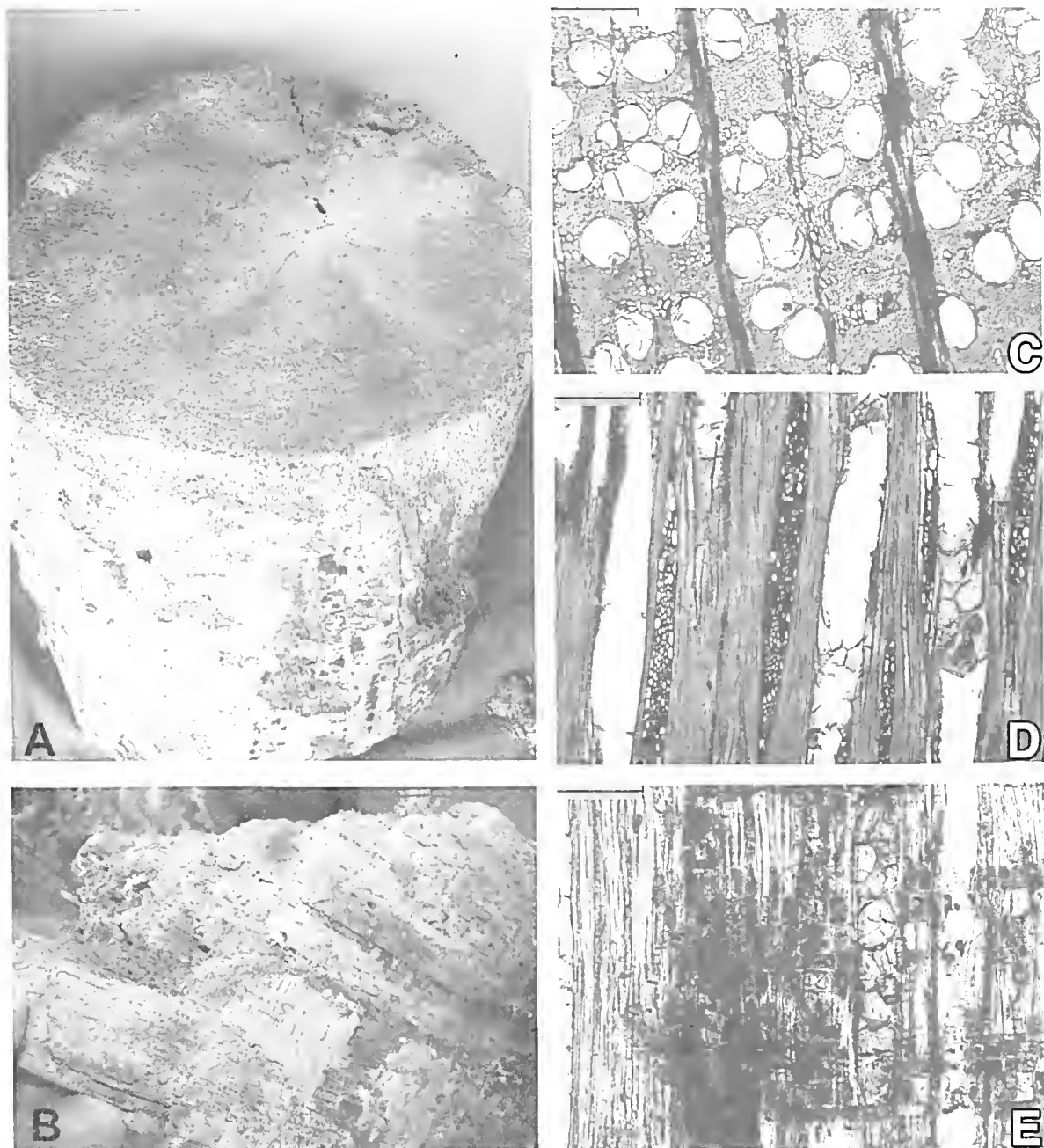


FIG. 1. A–E. *Vatica* wood. A, View of log showing the resin on the outside of the trunk; B, detail showing resin; C, Transverse Section; D, Longitudinal Section; E, Radial Section. Scale bar = 200µm.

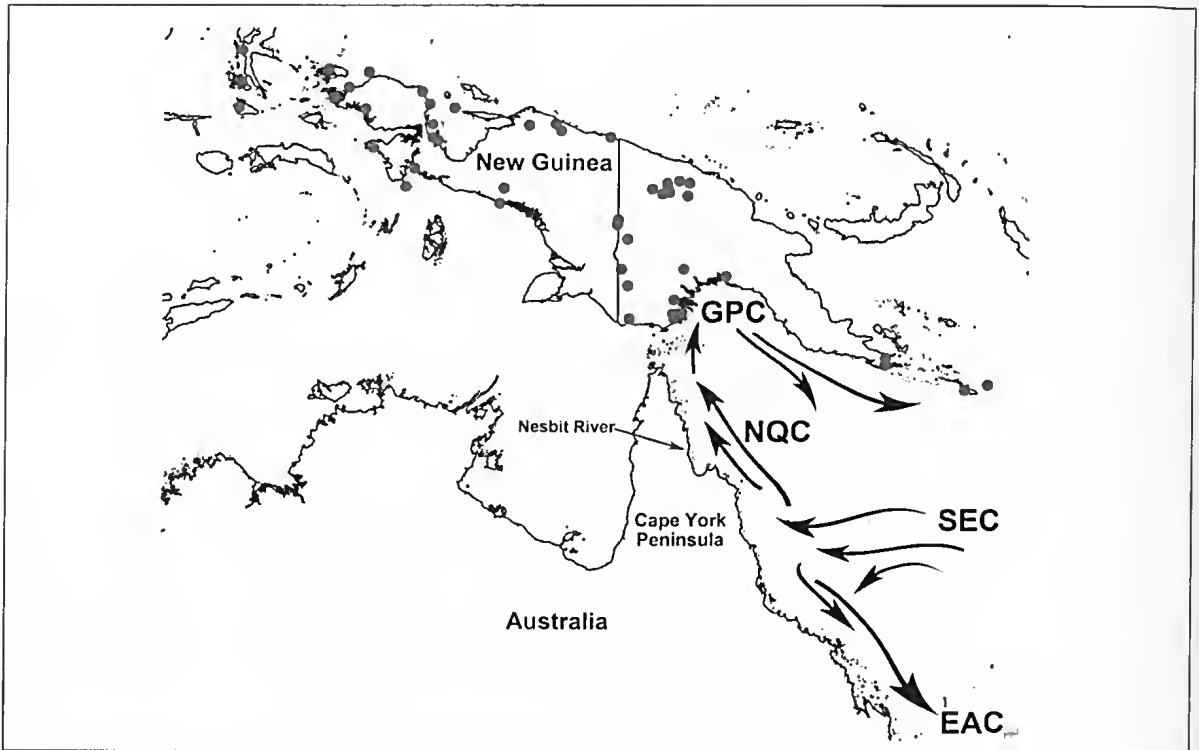


FIG. 2. Map showing distribution of *Vatica* spp. (in circles) records in New Guinea from the Atlas of Living Australia ([ala.org.au](http://ala.org.au)), 22 January 2013. The location, Nesbit River, where the log was found, is highlighted and the generalised oceanic currents in this region, i.e. SEC South Equatorial Current; EAC East Australian Current, NQC North Queensland Current, GPC Gulf of Papua Current, based upon Ridgway & Hill (2009) are shown.

smaller in diameter than the vessels. Rays weakly heterocellular with 1–3 rows of square to upright marginal cells. Parenchyma apotracheal – diffuse and paratracheal – vessels partially surrounded by parenchyma cells. Intercellular canals surrounded by parenchyma cells. Perforation plates simple. Pits to vessels rare, opposite to scalariform. Vessel-ray pits simple, large, rounded to elongated. Fibres thick walled, non-septate. Silica and crystals absent.

**Remarks.** The log found at the mouth of the Nesbit River is from a species of *Vatica* L. (Dipterocarpaceae). The family includes 17 genera and about 500 species and is most diverse in the South East Asian region; with a few additional taxa occurring in Africa and South America (Ashton 2003). Most genera in South East Asia are restricted to the western side of Wallace's line. Only *Anisoptera*, *Hopea*

and *Vatica*, with a combined total of 15 species, are found in New Guinea (Ashton 1982: fig. 3). The Dipterocarpaceae reach their eastern limit in New Guinea in the Louisiade Archipelago (Frodin 2001: 501). The family does not occur in Australia (Hoogland 1972) and neither is there any fossil record in this continent (Mary Dettmann pers. comm. 2013), so we can conclude that the log came from outside Australia.

There is only has a single species of *Vatica* in New Guinea, and *V. rassak* is widespread across the Island (Fig. 2). It does not occur in the Solomon Islands, Vanuatu or New Caledonia. As *Vatica* is found throughout New Guinea, it seems probable that this island was the source of the tree trunk implying a southerly drift trajectory, although drift from islands west of New Guinea is also a possibility.

## OCEANIC CURRENTS IN NORTH EASTERN AUSTRALIA

Based upon current oceanographic models we can predict the direction in which oceanic currents and winds move objects in this region (Schiller *et al.* 2008; SPICE community). While surface currents vary throughout the year (Anonymous 1973), the predominant current affecting north eastern Queensland is the South Equatorial Current (SEC), which is the prevailing westerly directed current in this area (Schiller *et al.* 2008; SPICE community) (Fig. 2). The SEC bifurcates on reaching the Australian coast, generating the East Australian Current (EAC) that flows south along the Queensland coast and the North Queensland Current (NQC) flows north towards New Guinea. The surface currents in north-eastern Australia and southern Papua New Guinea, from March through to October, have a predominantly north westerly direction, which is driven by the south easterly trade winds. We would therefore anticipate that the SEC and south east trade winds are important for determining the drift trajectory of objects onto eastern Australia at this time of year.

The Gulf of Papua Current (GPC) (SPICE Community) which runs along the southern coast of Papua New Guinea is associated with the Coral Sea Gyre which is a strong and dominating feature in oceanic circulation between north-eastern Australia and Papua New Guinea. From October through to February the surface currents have a predominantly south westerly direction and are driven by northerly to north westerly winds (Anonymous 1973), that are referred to colloquially as the “northerlies” in north Queensland. At this time of year, these surface currents and winds are responsible for moving drift objects away from New Guinea and towards the north east coast of Australia. Where the southern arm of Gulf of Papua Current intersects the prevailing South Equatorial Current (Ridgway & Hill 2009), the trajectory for drift objects is westerly, which may also result in them washing up on the northern coast of Australia (Schiller *et al.* 2008). Large tropical (cyclonic) storms, between September and April are also likely to affect the drift trajectory of objects in this region

(Gillespie *et al.* 2012; Bryan *et al.* 2012); and floods from the Fly River are also responsible for moving flood debris, including vegetation, into the Gulf of Papua (Jeffries 2015).

## EVIDENCE OF DRIFT TRAJECTORY IN NORTH EASTERN AUSTRALIA

To infer the trajectory of a drift object, the item must (a) have a restricted distribution, and be endemic to a particular geographical area and/or (b) have a source that can be identified with certainty, e.g. through analysis of geochemical data (for pumice), or molecular data (for animals and plants). Objects, or species, with widespread or cosmopolitan distributions will be therefore largely uninformative in determining drift patterns. The underlying assumption is that objects are likely to respond to oceanic currents in similar ways, and it should therefore be possible to identify generalised patterns of drift through the study of different classes of objects and whether these patterns are consistent with oceanic currents in north east Queensland, and whether they can explain the occurrence of a *Vatica* log on the east coast of Cape York Peninsula.

### Geological evidence

The source of pumice can be identified using geochemistry and it is therefore possible to infer the drift trajectory of samples that have washed up on beaches in Australia. The geochemical signatures of pumice from north eastern Queensland show diverse origins although most specimens on the east Australian Coast are from the Tongan – Kermadec Island arc, in the western Pacific, and therefore demonstrate a predominantly western drift trajectory on the South Equatorial current (Stanton 1992; Sutherland & Barron 1998; Bryan *et al.* 2012). However, while the majority of pumice samples indicate a West Pacific origin, consistent with drift on the SEC, two samples, found on beaches between Cardwell and Cape Upstart in North Queensland, have been identified as coming from Indonesia; suggesting that easterly drift from the Indian Ocean also occurs (Stanton 1992). Judd (in Symonds 1888) also noted that a pumice sample collected at Cape York Peninsula was



from the 1883 eruption of Krakatoa (Indonesia) and geochemical analysis confirmed this origin (Frick & Kent 1984).

### Botanical evidence

Smith (1994) recorded 47 species of drift disseminules in north west Coral Sea and provided an overview of their drift patterns. He identified the disseminules of a number of non-Australian species from beaches in northern Australia, including *Excoecaria indica*, *Lithocarpus* spp. and *Inocarpus fagifer*, and concluded that their occurrence were due to southward drift from New Guinea. *Lithocarpus*, like *Vatica*, has its most easterly distribution in New Guinea (Hoogland 1972; Frodin 2001), and its fruits have been recorded from beaches in the Torres Strait, north east Cape York Peninsula and eastern Australia as far south as Raine Island (George Batianoff, pers. comm. in Smith (1994)). *Excoecaria indica* and *Inocarpus fagifer* have more widespread distributions in the Malesian region, so the suggestion by Smith (1994) that disseminules of these species were from New Guinea may be incorrect, although it is still the closest, and therefore the most likely source area. Many of the other drift species recorded by Smith (1994) occur widely throughout the region, and are thus uninformative in inferring the origin of the drift material.

A log washed up at Seisia boat ramp, Cape York on 8th March 2012 was identified as *Octomeles* (Tetramelaceae) by the botanist, John Ford (James Walker pers. obs.). This genus contains a single species, *O. sumatrana*, which is a rainforest timber known as 'Erina'. It grows in Malaysia, Indonesia, Brunei, the Philippines, the Solomon Islands and Papua New Guinea but is not known from Australia. While the closest source area for this log is again New Guinea, it could conceivably have come from another part of south east Asia. Anecdotal evidence also exists of other logs washing up on northern Australian beaches (James Walker pers. obs.), but as their taxonomic affinities remain unknown, we cannot speculate on their origins.

### Zoological evidence

The shells of three species of *Nautilus*, *N. pompilius*, *N. stenomphalus* and *N. macromphalus* have been found on beaches in north eastern Queensland (Bonacum et al. 2011). While *Nautilus pompilius* and *N. stenomphalus* occur in the seas off north eastern Australia, shells of *N. macromphalus* are due to long distance drift from New Caledonia, where this species is endemic (Bonacum et al. 2011). Shells of *N. macromphalus* have been found along the eastern coast of Australia, from north eastern Queensland to near Sydney (Atlas of Living Australia (ala.org.au) data retrieved Dec 2014, Queensland Museum malacology records) and their distribution is consistent with a westerly drift trajectory due to the South Equatorial Current and drift on either the East Australian Current south along the Queensland coast or the North Queensland Current towards New Guinea.

### Ethnographic evidence

Ethnographic evidence can also be used to infer the direction of drift, if the source of objects can be identified with certainty. We focussed on canoes and other large wooden items as we assumed that they would respond to oceanic currents in a similar way to tree trunks. However, the origin of some canoes is not always certain (see below).

A canoe (QME2168) from Point Lookout, Stradbroke Island, South East Queensland and a Kanak door jam or *chambranle* (QME4018) from Lizard Island in north eastern Queensland, have been identified as either Vanuatuan or New Caledonian in origin (QM ethnographic records). Boyd (1999) provided an overview of the drift canoes, than known, that have washed up on the eastern Australian coast and he argued that one found in the Solitary Islands off the northern New South Wales coast was likely to be from Vanuatu. He concluded that the source of canoes, particularly those in South Eastern Queensland and northern New South Wales, was likely to be islands in the western Pacific, indicating westerly drift via the South Equatorial Current.



Many of the canoes found in northern Queensland are, however, assumed to have come from New Guinea to the north. Beaton (1978) noted that dugout canoes are common flotsam on Great Barrier Reef islands and he considered that their likely source, probably based upon geographical proximity, was the islands of the Torres Strait or New Guinea. Canoes have been recorded from the eastern side of Cape York Peninsula at Noah's Beach, Cape Tribulation; Hummock Beach, north of Starcke River, Cape Flattery; Cape Hillsborough; near Bowen; and further south but their provenance and origins are often uncertain (Boyd 1999, QM Ethnographic records).

Dugout canoes are thought to have been introduced from New Guinea through the Torres Strait Aboriginal groups to Cape York communities (Haddon 1913; Thomson 1934; Clarke 2012). Canoes identified as "New Guinean" have also been collected, or noted, from the western side of Cape York Peninsula at Weipa, Kowanyama and Crabbe Island, near the mouth of the Jardine River (Cameron & Cogger 1992; QM Ethnographic records; Patrick Couper pers. comm. 2013). These are more likely to have come from communities either in the Torres Strait Islands or the southern coast of New Guinea. Roth (1910) also claimed that pre 1910, Torres Strait islanders, would travel south down the Great Barrier Reef during the monsoon in summer (November-February) due to the prevailing south westerly winds and return with the south east trade winds during the dry season (April-September). So the occurrence of these water craft in parts of the Torres Strait and northern Cape York may be through drift or oceanic currents but could equally be the result of trade and the movement of people between communities. Identifying the provenance of some dugout canoes can be difficult. Michael Quinnell, Senior Curator of Anthropology, at the Queensland Museum pointed out, in a letter to Mr W Fisher (6 April 1990), Regional Director of the Department of Environment and Heritage that these drift canoes resemble coastal canoes from areas as far apart as Melakula in Vanuatu and the Fly River in Papua New Guinea.

While there are problems in using these ethnographic records, uncritically, the overall evidence suggests a southerly movement of at least some canoes in northern Australia. Evidence of this movement also comes from KKK bleach bottles, identified as originating from New Guinea, which washed up at Archer Point, near Cooktown, in north eastern Queensland (Hinchcliffe & Howley 2009).

## DISCUSSION

Evidence for the direction of movement of drift objects washed up on north Queensland beaches comes from: (a) direct observations of their movement by oceanic currents and (b) indirectly through determining, or knowing, the source of geological, zoological, ethnographic and botanical objects. The ability to determine the direction of drift requires that we know both their source and that we apply the principle of Occam's Razor that we use the simplest explanation for the movement of a drift object in preference to a more complex scenario. It is also evident, particularly from ethnographic and geological samples that assumptions about the origins of objects need to be examined critically.

This study demonstrates that where their source can be identified drift objects found on in Cape York Peninsula, have come from several diverse areas including islands in the western Pacific to the east, from New Guinea to the north, and from Indonesia to the west. However, the predominant current affecting north eastern Queensland is the South Equatorial Current which moves in a prevailing westerly direction (Ridgway & Hill 2009). Most of the drift records of pumice and its associated epifauna (Bryan *et al.* 2012), drift shells of *Nautilus macromphalus* and some ethnographic drift objects show western Pacific origins.

The occurrence of a log of *Vatica* sp. (Dipterocarpaceae) in north eastern Australia is interesting because the family is unknown from Australia, New Guinea being the most easterly distribution of this family and therefore the most likely source area. New Guinea also represents the most easterly distribution for other genera, such as *Lillocarpus*. We speculate that the *Vatica*

sp. log came from New Guinea, which is the closest source area for these trees. Anecdotal records indicate that large (unidentified) trees, are washed down the Fly River and have been recorded 30 km, out to sea, at Bramble Cay, south of the river's delta (Jeffries 2015). This supports Smith's (1994) suggestion that disseminules of *Lithocarpus* spp., and probably *Luocarpus fagifer* and *Excoecaria indica*, are from the Fly and other large rivers flowing into the Gulf of Papua. These disseminules are washed into the Gulf of Papua Current and surface currents and seasonal south westerly winds move them away from New Guinea, towards Australia. The prevailing Southern Equatorial Current may also have led to the log being washed onto the northern coast of Australia (Schiller et al. 2008). A similar southerly drift trajectory is also evident for ethnographic objects such as canoes and bleach bottles.

Drift logs occur commonly on the North Queensland coast are also important as a raft and habitat for other species. For instance, living colonies of non-Australian termites (Isoptera: Blattellidae) have been found in beach-washed logs on Cape York Peninsula (James Walker pers. obs. 2014). The likely origin of these termites is yet to be determined and they may have come from the Pacific Islands to the east, or New Guinea to the north but they have not yet become established in Australia (James Walker pers. obs. 2014).

We suggest that seasonal factors, determine, in part the patterns of drift and therefore the movement of objects onto this part of the Queensland Coast. Understanding drift patterns is important because the drift of animals or plant disseminules have the potential to result in dispersal events and hence the colonisation of new geographic localities. While the *Vatica* log does not demonstrate successful colonisation, it, along with *Lithocarpus* fruits does provide evidence of a southerly drift of objects between New Guinea and north east Queensland.

## ACKNOWLEDGEMENTS

We thank Michael Quinnett, Jeanette Covacevich and Patrick Couper, Queensland Museum (QM),

for their comments and advice regarding canoes washing up in North Eastern Queensland. Alex Cook (Honorary QM) provided advice on pumice records in Eastern Australia. We thank the QM ethnographic section for access to canoe records and Brit Asmussen commented in the ethnographic content in the text. John Healy (QM) provided advice on records of *Nautilus* in Australia. Comments from Laurie Jessup, an anonymous referee and Prof. H.T. Clifford have also improved the manuscript.

## LITERATURE CITED

- Anonymous 1973. *Australia Pilot Vol 3 Sixth Edition*, Hydrographic Department; Great Britain. 320pp.
- Ashton, P.S. 1982. Dipterocarpaceae. *Flora Malesiana*, Series 1 (9): 237–552.
- Ashton, P.S. 2003. Dipterocarpaceae. Pp. 182–197. In Kubitzki, K. & Bayer, C. (eds). *The families and genera of vascular plants Vol. V: Flowering plant Dicotyledons – Malvales, Capparales and non-betain Caryophyllales*, Springer: Berlin, Heidelberg, New York.
- Beaton, J.M. 1978. Archaeology and the Great Barrier Reef. *Philosophical Transactions of the Royal Society of London Series B* 284: 141–147.
- Bonacum, J., Landman, N.H., Mapes, R.H., White, M.M., White, A.J., & Irlam, J. 2011. Evolutionary radiation of present-day *Nautilus* and *Allonautilus*. *American Malacological Bulletin* 29: 77–93.
- Boyd, W.E. 1999. The probable origin of a wooden dug-out canoe discovered in the Solitary Islands Marine Park, eastern Australia. *Bulletin Australian institute for maritime archaeology* 23: 93–98.
- Bryan, S.E., Cook, A.G., Evans, J.P., Hebden, K., & Hurrey, L. 2012. Rapid, long-distance dispersal by pumice rafting. *PLoS ONE* 7(7): e40583. doi:10.1371/journal.pone.0040583.
- Clarke, P.A. 2012. *Australian plants as Aboriginal tools*. Rosenberg: Dural Delivery Centre, NSW.
- Cameron, E.E., & Cogger, H.G. 1992. *The herpetofauna of the Weipa Region, Cape York Peninsula*. 200pp. Technical Report Australian Museum No 7.
- Frick, C. & Kent, L.E. 1984. Drift pumice in the Indian and South Atlantic Oceans. *Transactions of the Geological Society of South Africa* 87: 19–33.
- Frodin, D.G. 2001. *Guide to Standard Floras of the World*. 2nd Edit. Cambridge University Press, Cambridge.
- Gillespie, R.G., Baldwin, B.G., Waters, J.M., Fraser, C.I., Nikula, R. & Roderick, G.K. 2012. Long-distance dispersal: a framework for hypothesis testing. *Trends in Ecology and Evolution* 27: 47–56.

- Haddon, A.C. 1913. The outrigger canoes of Torres Straits and North Queensland. Pp. 609–634. In Quiggen, E.C. (ed.) *Essays and studies presented to William Ridgeway*, Cambridge University Press, Cambridge.
- Hinchcliffe, J. & Howley, C. 2009. *Eastern Cape York Peninsula Beach Rubbish Assessment 2007 & 2008*. Cape York Marine Advisory Group (CYMAG) Environmental Inc., Cooktown.
- Hoogland, R.D. 1972. Plant distribution patterns across the Torres Strait, Pp. 131–152. In Walker, D. (ed.) *Bridge and Barrier: the natural and cultural history of Torres Strait*. (Australian National University: Canberra).
- Jeffries, R. 2015. Diving at reefs end. *Club Marine Magazine* 30(2): 104–110.
- Ridgway, K., & Hill, K. 2009. The East Australian Current. Pp. 1–16. In Poloczanska, E.S. Hobday, A.J., & Richardson, A.J. (eds) *A Marine Climate Change Impacts and Adaptation Report Card for Australia*, NCCARF Publication 05/09, ISBN 978-1-921609-03-9.
- Roth, W.E. 1910. *North Queensland ethnography*. Transport and Trade Bull. 14. (Government Printer: Brisbane).
- Schiller, A., Oke, P.R., Brassington, G., Entel, M., Fiedler, R., Griffin, D.A., & Mansbridge, J.V. 2008. Eddy resolving ocean circulation in the Asian Australian region inferred from an ocean reanalysis effort. *Progress in Oceanography* 16: 334–365.
- Smith, J.M.B. 1994. Patterns of disseminule dispersal by drift in the north-west Coral Sea. *New Zealand Journal of Botany* 32: 453–461.
- Sosef, M.S.M., Soerianegara, I., Lemmens, R.H.M.J. (eds.). 1993. PROSEA Plant Resources of South-East Asia 5-1. Timber trees: major commercial timbers. Pudoc Scientific Publishers Wageningen.
- SPICE community 2012. Naming a western boundary current from Australia to the Solomon Sea. *CLIVAR Exchanges* 58(17): 28.
- Stanton, J.B. 1992. *Proposed south western Pacific sources of drift pumice collected from the North Queensland coast between Cardwell and Cape Upstart*. James Cook University of North Queensland BSc (Hons) Thesis (unpublished).
- Sutherland, F.L. & Barron, B.J. 1998. Balmoral Beach Aboriginal shell midden, Port Jackson, Australia: pumice petrology and sources. *Records of the Australian Museum* 50: 241–262.
- Symonds, G.J. 1888. *The eruption of Krakatoa and subsequent phenomena*. Report of the Krakatoan Committee. Royal Society of London, Harrison and Sons: London.
- Thomson, D.F. 1934. *The dugong hunters of Cape York*. *Journal of the Royal Anthropological Institute*. 64: 27–235.
- Wheeler, E., Baas, P. & Gasson, P.E. (eds.). 1989. IAWA List of Microscopic Features for Hardwood Identification. *IAWA Bulletin* n. series 10(3), 219–332, Leiden.



# Predation of the Early Cretaceous (Late Albian) pachycormiform, *Australopachycormus hurleyi* Kear, in Queensland's Eromanga Basin

Alan BARTHOLOMAI

Director Emeritus, Queensland Museum, PO Box 3300, South Brisbane, Qld 4101, Australia.

Citation: Bartholomai, A. 2015. Predation of the Early Cretaceous (Late Albian) pachycormiform, *Australopachycormus hurleyi* Kear, in Queensland's Eromanga Basin. *Memoirs of the Queensland Museum – Nature* 59: 245–255. Brisbane. ISSN 2204-1478 (Online) ISSN 0079-8835 (Print): Accepted 18 Dec 2014. First published online: 30 November 2015.

<http://dx.doi.org/10.17082/j.2204-1478.59.2015.2014-04>

LSID - urn:lsid:zoobank.org:pub:D351FC80-BDBA-47C6-BEB4-1A9C0A2FB4D0

## ABSTRACT

Additional remains of the marine pachycormiform fish, *Australopachycormus hurleyi* Kear, 2007, have been located in collections of the Queensland Museum from the Early Cretaceous (Late Albian) Toolebuc Formation of the Eromanga Basin, near Boulia in central western Queensland. The specimens significantly extend knowledge of the neurocranium, especially relating to the morphology of the orbital area, maxilla and mandible. The additional specimens show evidence of predation, with one possibly also having been regurgitated in a partially digested state. □ *Australopachycormus hurleyi*; neopterygian; pachycormiform; Early Cretaceous (Late Albian); Eromanga Basin; Toolebuc Formation.

Investigation of collections of fossil actinopterygian fishes in the Queensland Museum, both in Brisbane and in its material loaned to the Stonehouse Museum in Boulia, central western Queensland, has revealed the presence of two additional neurocranial specimens of the pachycormiform, *Australopachycormus hurleyi*, Kear, 2007. These not only provide additional morphological detail to that outlined in Kear (2007) but also exhibit details of preservation that help interpret their taphonomy. Currently known material of *A. hurleyi*, including the holotype, QMF52641, has mostly come from the marine Toolebuc Formation of Early Cretaceous (Late Albian) age, from the poorly exposed western rim of the Eromanga Basin near Boulia, within the Great Artesian Superbasin, defined by *Jell et al.* (2013). Only an isolated rostrodermethmoid has been identified by *Wretman and Kear*

(2013) from near Richmond in the north of the Basin, also from the Toolebuc Formation.

The Toolebuc Formation is a thin, organic rich unit, generally 20–45 m thick, that includes coquinitic limestone and shales (including oil and kerigenous shales). *Cook et al.* (2013) indicate that the Formation was deposited in a layered epeiric sea, with dysoxic to anoxic benthic conditions. *Henderson* (2004) showed that the Formation contained shell beds in response to benthic oxygen fluctuations during a maximum deepening event. Many of the fossil vertebrates from near Boulia have been collected as isolated neurocrania or partial skeletons in calcareous concretions that have been concentrated and exposed on the soil surface by physical factors, with little or no evidence of lateral transport. This is the case with the current specimens. However, in recent

years, more complete skeletons particularly of large reptiles have been found.

Preparation of the specimens involved mechanical and acetic acid techniques.

#### Abbreviations

bc	brain case
cfct	compression fracture
cdk	coronoid tusk
co	coronoid
den	dentary
dt	dentary teeth
dpal	dermopalatine
ecp	ectopterygoid
fr	frontal
ga	gill arch element
gr	gill rakers
ha	hyoid arch element
hm	hyomandibular
le	lateral ethmoid
mx	maxilla
pmx	premaxilla
pa	parietal
par	parasphenoid
pro-op	prootic-opisthotic
qu	quadrate
rder	rostrodermethmoid
sc pl	sclerotic plate
sph-pts-obs	sphenotic-pterosphenoid orbitosphenoid
ve	vertebral arch

#### CLASS ACTINOPTERYGII

#### SUBCLASS NEOPTERYGII

#### ORDER PACHYCORMIFORMES

#### *Australopachycormus hurleyi* Kear, 2007 (Figs 1–4)

*Australopachycormus hurleyi* Kear, 2007: 1033–8.

**Material Examined.** QMF52641, holotype (see Kear 2007). QMF49220, an incomplete skull and a plaster cast of the specimen before preparation. The specimen is from 'Lorna Downs' Station (at 23° 22.127' S and 140° 11.858' E) near Boulia, CWQ. QMF10913, a partial

acetic acid prepared neurocranium and a coloured fibre glass cast of the specimen prior to acetic acid preparation. The specimen was collected 15 miles (ca. 24 km) north of 'Springvale' Station, NE of Boulia, CWQ.

**Age and Formation.** From the marine Toolebuc Formation of Early Cretaceous (Late Albian) age.

**Description.** The following descriptive notes augment the original description of *Australopachycormus hurleyi* by Kear (2007). Measurements for the specimens are presented in the Appendix.

The cranial roof is obtusely angular across the dermopterotic-parietal area, becoming broadly convex across the back of the orbits and narrowing to a more tightly dorsally convex cross section anteriorly; no fronto-parietal boss appears present; the anterodorsal neurocranial surface slopes posteriorly at a low angle to the horizontal, then bends slightly dorsally above the brain case. The posterior of the neurocranium has suffered bone loss in QMF10913 (Fig. 1A–D) making it difficult to identify most individual elements of the brain case. The brain case appears to have been almost fully ossified. Posteriorly, only dorsolateral surface bone remains. The lateral margin of the dermopterotic is damaged by conical, compaction fracturing and compression into the post-temporal fossa. The dermosphenotic forms much of the dorsal margin of the orbit and is attenuated anteriorly. The hyomandibular facet exhibits local, dorsal compressed fracturing into the base of the post-temporal fossa. Other isolated, circular, pressure fractures are also evident on the parasphenoid. The posterior portion of the anterior semi-circular canal is exposed in dorsal view. Laterally, the subtemporal fossa is insignificant.

The orbit is best preserved in QMF10913 (Fig. 1A) but neurocranial elements within the orbit are mostly fractured and somewhat displaced on the right side. Very eroded and often fractured elements are exposed on the right side of QMF49220. The eye was large (see Appendix) and was supported by two, heavy sclerotic plates joined dorsally and ventrally, with each expanded mesially and transversely; the

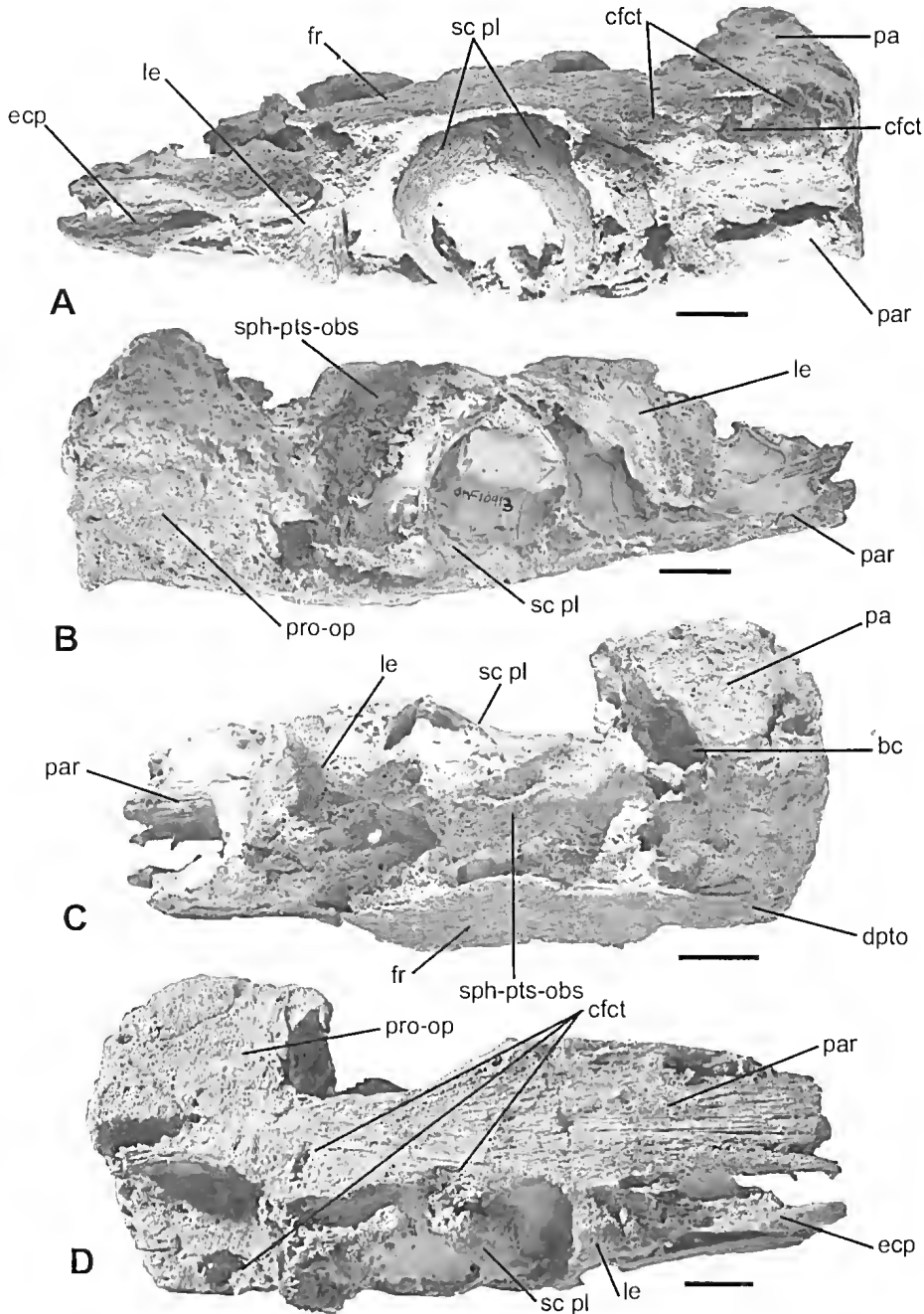


FIG. 1. *Australopachycormus hurleyi* Kear, 2007, specimen QMF10913; **A**, left lateral view of partial skull showing conical compression fractures along and below dermopterotic margin and large sclerotic plates; **B**, right lateral view showing displaced lateral ethmoid, united sphenotic-pterosphenoid- orbitosphenoid and lack of defined junctions in braincase; **C**, dorsal view showing enlarged parietals and displaced but little corrosion of lateral ethmoid and united sphenotic-pterosphenoid-orbitosphenoid and arched dorsal surface of parasphenoid; and **D**, ventral view showing broad parasphenoid with several conical compression fractures. Scale bar = 1 cm.

plates are gently convex externally and gently concave internally. The surface of each plate is ornamented over the outer moiety by very fine, reticulating ridges, especially ventrally.

The lateral ethmoid is large and complex in QMF10913 (Fig. 4A) but is corroded in QMF49220 (Fig. 4B). The anterior is poorly preserved in both specimens examined. The posterior surface is curved, smooth and expanded medially, forming the anterior border of the orbit; it expands dorsally and curves posteriorly to broadly support the back of the rostrodermethmoid and dorsal margin of the frontal; its dorsolateral surface is rugose in QMF10913, possibly to support the front of the supraorbital immediately above a large scooped opening that is believed to be the nasal opening. The lateral ethmoid is expanded medially to meet its counterpart from the other side and is excavated transversely into a large, posteromedially orientated, trough-like, olfactory capsule that is penetrated by variable small foramina; it medially appears to have met the anterior of the orbitosphenoid and presumably carried the passage for the olfactory nerves; the bone extended anterolaterally to be overlain by a posterodorsal plate of the ectopterygoid and dorsally by the rostrodermethmoid. Laterally, the anterodorsal surface supports a partial element believed to be part of the nasal, lying outside the ectopterygoid, while its anteroventral surface supports the upper margin of the maxilla.

The rostrodermethmoid is largely lacking in the specimens. That above the parasphenoid in QMF10913 exhibits two large, anteriorly directed cavities. These were not associated with paramedial teeth, replicating similar structures in the holotype in which paramedial teeth are also represented below them. A near complete rostrodermethmoid from near Richmond, North Central Queensland, identified as *A. lurleyi*, was illustrated by Wretman and Kear (2013).

The sphenotic, pterosphenoid and orbitosphenoid are strongly united and contribute the bulk of the dorsomedial wall of the orbit but junctions of the three elements are difficult to define. However, the sphenotic appears to be a small bone with a curved dorsolateral rim

above a smoothly concave outer surface that is overlain ventrally by the upper margin of the pterosphenoid. The pterosphenoid is small, penetrated anteriorly by a large optic fenestra. A foramen for the trochlear nerve penetrates the bone above the optic fenestra. Internally, the pterosphenoid contributes to the base of the braincase. The orbitosphenoid appears to be the largest of the bones. It internally contributes to the anterior of the cranial cavity and externally provides the smoothly concave upper wall of the orbit; it is separated from the sphenotic by a shallow, broad, oblique groove and appears as a raised, overhanging rim posteriorly with its broadened upper surface loosely underlying and supporting the frontal. The bone appears to contribute to the margin of the large opening for the olfactory tract. The basisphenoid is poorly preserved. The anterior of the prootic is fractured and difficult to interpret.

The parasphenoid is imperfectly preserved in QMF10913, extending anteriorly to beyond two tapering cavities that appear too far back to represent sockets of the paramedial teeth. These cavities are large and sub-ovate and are anteriorly directed with slight divergence. The parasphenoid is broad and ventrally flattened by significant bone loss (but arched in the holotype). Compression fracturing of the right lateral margin suggests tooth damage during predation. Posterior to the back of the orbit, the parasphenoid steps up slightly and curves slightly dorsally (again exhibiting an indication of predator tooth damage) while narrowing and twisting to lie along the sides and base of the basi-exoccipital; it is linked laterally to the prootic by poorly defined ascending processes. Anterodorsally, the parasphenoid surface above the twin cavities is markedly convex and is densely ridged longitudinally.

Remains of a broad, thin, sheet-like ectopterygoid are present in both referred specimens. This is angled anteroventrally inside the premaxilla and terminates in a swollen base that narrows posteriorly and ventrally parallels the parasphenoid margin. Fragmentary anterior remains of an elongated, thin, possible endopterygoid are present external to the parasphenoid in QMF49220. Fragmentary evidence for possible



right dermopalatines are present in QMF49220. The bones are reduced to a fine splint posteriorly and support a single series of very small, blade-like teeth, reducing in size posteriorly.

Remains of the jaws are preserved in QMF49220. Although eroded and with loss of surface enamel from the teeth, sufficient of the premaxilla and its teeth is present to show its great similarity with that in the holotype, QMF52641 (see Kear 2007). The left maxilla is reasonably well represented and is elongated (reduced to a long point covered by the premaxilla anteriorly in the holotype), deepening along its exposed length before deepening slightly posteriorly (Fig. 3). It is slightly convex laterally and is spooned dorsally to abut and be supported by the anteroventral base of the lateral ethmoid. The bone broadens dorsomedially where it carries a shallow dorsal groove, more defined posteriorly by a dorsolateral flange, apparently to accommodate at least one infraorbital and a supramaxilla. A single row of very small marginal teeth is present, distributed evenly along the bone but absent posteriorly. The teeth are blade-like and spearhead pointed and are slightly angled medially.

Both sides of the lower jaw are preserved with external bone loss in QMF49220 with the left side (seen in Fig. 3) better preserved than the right (Fig. 2). The extreme anterior of the mandible is lacking but the remaining part is clearly similar to that in the holotype. The tooth-bearing dorsal margin is shared by both the coronoid and dentary. The posterolateral end of the mandible is formed by a relatively elongate angular that reaches anteriorly to below the middle of the orbit and extends well behind the level of the groove for the supramaxilla. It deepens and thickens posteriorly and sweeps posterodorsally to form the rounded posterior margin of the lower jaw. Mesially, the posterior of the articular of the right side in QMF49220 appears deep, articulating with the quadrate. A retroarticular is present in a corroded state. The anterior, coronoid part of the dorsal margin of the left mandible is elevated as part of a swollen coronoid plate for a distance of some 50 mm and bears a single, very large, deeply socketed tusk, ovate in section, as well as

three much smaller teeth anteriorly. The tusk crown has lost its enamel; the smaller teeth had a spearhead shaped crown. Posterior to the large tusk, the elevated part of the coronoid is edentate, as is the remainder of the bone except for very fine denticles along the dorsomedial margin, posterior to the diastema. Most of the mandibular marginal teeth are borne on the dentary. Thus the main mandibular teeth as a whole appear only to be a single row. The dentary teeth are of similar size and structure to those anterior to the coronoid tusk. Where seen on the right side of QMF49220, they are very deeply socketed, slightly more than twice as deeply rooted as the crown is exposed. At least 16 dentary teeth are present.

A partial natural mould of the hyomandibular is present on the left side of QMF49220 and is very similar morphologically to that in the holotype but has been rotated posteriorly at about 90° to its original position. Gill arches are incomplete but are largely represented on the right side. Gill rakers are short and relatively robust. One element on the left side is elongated. The left hyoid arch is displaced and the elements are rotated but are too broken and corroded for description.

**Taphonomy.** Preservation of QMF49220 of *A. hurleyi*, differs markedly from that in the holotype, QMF52641, in which much of the rostrodermethmoid and bones behind the front of the orbit are almost completely missing (Kear 2006). It appears that the spine tip in the holotype was lost before fossilisation (or was not collected) probably sank and, because of its weight, partially embedded itself nose-first into the surface sediment. The body of the fish collapsed after death and decay and subsequent loss of the bulk of the back of the skull of the holotype, possibly by water movement, would then have left the preserved part of the skull to be covered and fossilised with the bones immediately anterior to the orbit broken and partially splayed outwards. Isolated pachycormid rostrodermethmoids, including that identified as *A. hurleyi*, are known from near Richmond, NCQ, in the Eromanga Basin (Wretman & Kear 2013) suggesting their loss could occur during predation, fossilisation or collection. Presence

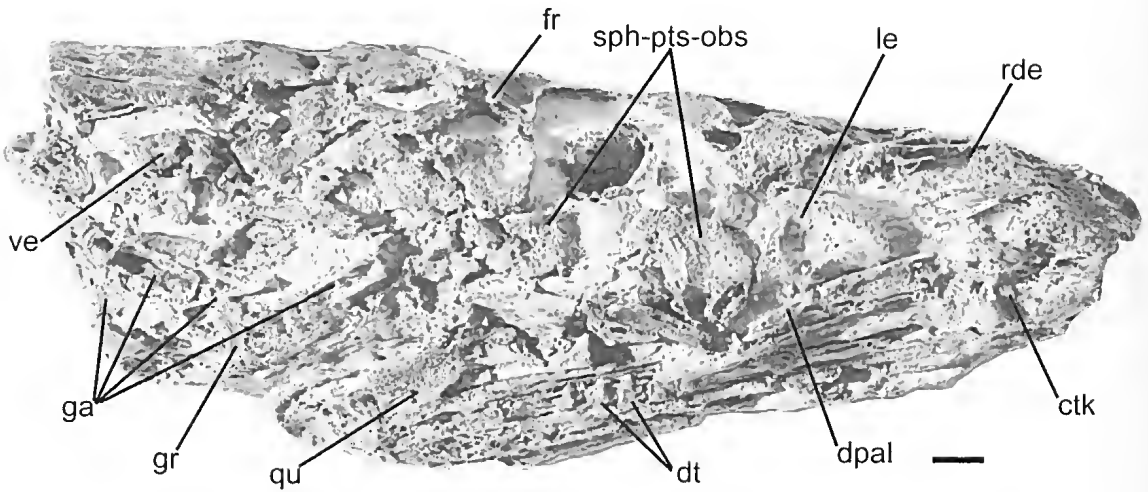


FIG. 2. *Australopachycormus hurleyi* Kear, 2007, specimen QMF49220, oblique view of roof and right side of neurocranium (with some matrix remaining) showing obliquely crushed but compressed mass of broken, disassociated and acid corroded bones; deep, external folds in opercular area associated with possible toughened skin; and almost complete loss of surface bones. Scale bar = 1 cm.

of the holotype's separated hyomandibular, however, precludes a suggestion that loss of posterior skull elements occurred during predation and scavenging was unlikely (see below).

Neurocrania in Eromanga actinopterygians such as the aspidorhynchid *Richmondichthys* (Bartholomai 2004) and the pachyrhizodontid, *Pachyrhizodus marathoneusis* Etheridge Jnr., 1905 (see Bartholomai 2012) were generally preserved as isolated heads (and rare bodies) with one side retaining most of the more delicate dermal bones intact and with little displacement. The other side of the neurocranium (or body) usually suffered loss of surface bones. Schafer (1972) noted that drifting carcasses lose limbs and skulls while drifting and parts can be embedded at different places. It is suggested that the more complete and better preserved side of these fish was that pressed into the surface sediments while the other side was subjected to winnowing and the possibility of scavenger activities before final burial and fossilisation. QMF10913 has the left side elements much more completely preserved, suggesting this was the surface initially buried in the bottom sediments.

Although the left side of the skull in QMF49220 has more complete elements than the remainder of the specimen, the crushing, breaking and disarticulation of the cranial bones within the general skull envelope in QMF49220 is inconsistent with usual sedimentary compaction and fossilisation of Toolebuc fish neurocrania. The bones of the left side show breaks and the outer surfaces that are partially corroded by what appears to be acid etching while in the gut of an animal, conditions that must have been applied before burial. Everhart (2003) similarly records that the surface of bone has the characteristic appearance of being etched by stomach acids, which gives the bone a 'spongy' appearance, clearly distinct from fresh bone and similar to the preservation of bone in QMF49220 (Fig. 2). The mandible in this specimen is broken medially, with the two parts bent apart, with the posterior compressed into a more confined space medial to an unbroken and less robust maxilla (Fig. 3). Similarly, the bones of the hyoid arch are broken and are partially rotated upwards reducing the depth of the skull. Originally near-vertical bones in the head, such as the hyomandibular, have been rotated through 90° and pushed posteriorly,

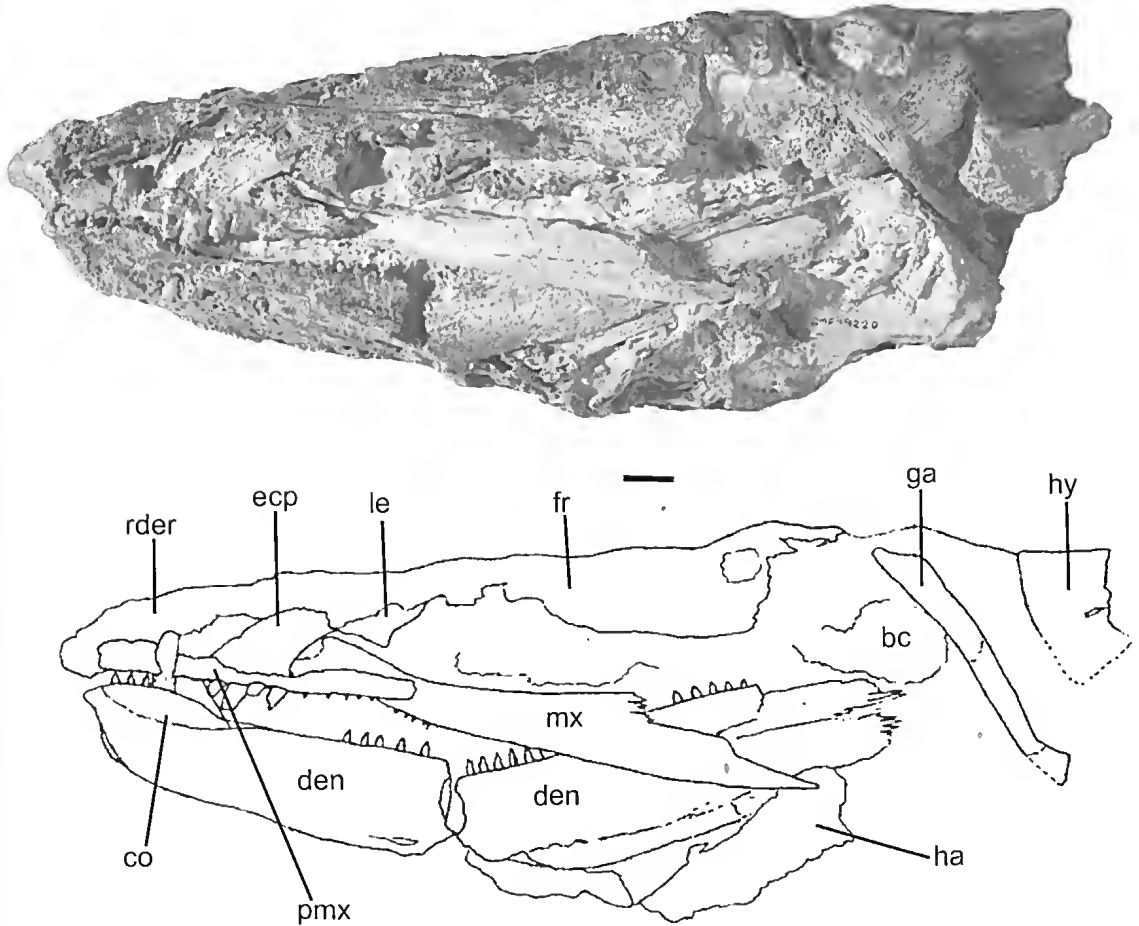


FIG. 3. *Australopachycormus hurleyi* Kear, 2007, specimen QMF49220; left lateral view of skull with some matrix remaining, showing compacted and broken elements and reduced surface corrosion of most bones, together with interpretative drawing showing major bones, including broken mandible inside maxilla, displaced and broken hyoid arch and rotated hyomandibular. Scale bar = 1cm.

again consistent with muscular crushing and compaction of the remains. The majority of the internal bones are preserved as a broken but usually disassociated mash of large and small corroded bony fragments, separated from one another by matrix but contained within a consolidated, compressed and elongated, 'sausage-shaped' mass. Enamel on the larger left coronary and premaxillary teeth has been corroded but this has not usually occurred with regard to the smaller teeth present. Enameloid loss on isolated teeth from the Upper Cretaceous Carlyle Shale of Kansas, USA, was considered a possible result of animal digestion by Shimada

(1997). Dentary and coronoid teeth and bones in QMF49220 shows varying degrees of loss or degradation that are interpreted, herein, as the result of digestive acid etching.

The united sphenotic, pterosphenoid and orbitosphenoid, an unusually robust element in QMF10913, has been broken in two in QMF49220 and the parts separated. Remains of the four epibranchials of the right side in this specimen, however, are not greatly disarticulated and gill rakers are only slightly moved where they are preserved. The upper half of the posterior of the right lateral ethmoid has been lost by

etching (Fig. 4B, cf Fig. 4A). Nearly all bones on the outside of the right side of the skull have been lost. The specimen, has darkened areas at the surface that may represent remains of a toughened skin that incorporate degenerated remnants of dermal bones, a conclusion supported by deep longitudinal surface folds around internal elements, especially below and above the opercular series, consistent with strong muscular crushing. What remains of the frontals is also covered by possible folded, toughened skin. It is considered possible that initial containment in this way was probably responsible for maintaining the mash of broken, partially digested and disassociated neurocranial bones together as a unit, immediately prior to possible regurgitation.

QMF10913 has some features suggesting predation but evidence for possible ingestion of the skull is much less convincing than that for QMF49220. Bones of the right hand side, especially those around the orbit, were disarticulated and moved medially and much of the rostrodermethmoid has been lost. Dermal bone above the left orbit and otic region is still present and does not appear to be strongly corroded. The sclerotic plates (Fig. 1A) and the lateral ethmoids (Fig. 4A for right lateral ethmoid) are virtually unaffected by acid corrosion posteriorly, as is the brain case as originally present in the cast of QMF10913. Extensive surface shedding of bone is associated with the parasphenoid and the right side of the head, consistent with the left side being, in part, buried in sediment and with the right side winnowed before burial and vertically compressed during sediment compaction. No acid etching is evident on dislocated bones medially surrounding the right orbit. Two circular compression fractures are present along the edge of the left dermopterotic, 2.2 cm apart. These oppose a single, similar fracture in the hyomandibular facet and into the post-temporal fossa, midway below the upper fractures, damage that could only occur after tooth slippage up the hyomandibular surface or after dislocation of the articulating head of that bone. Possible, widely-spaced, circular compression fractures (depressions) are also evident in the parasphenoid, anterior and posterior to the ascending wing and

are interpreted as bite marks. The shape of the bite marks suggests that they were caused by conical, somewhat circular teeth.

Numerous large, pelagic, predatory animals co-existed with *A. hurleyi* in the epeiric sea of the Eromanga Basin in the area along its central western rim. Collections made over many years by the late Mr Richard (Dick) Suter, of the Stonehouse Museum, Boulia, record more than 150 specimens of large ichthyosaurs (*Platypterygius*) together with rare plesiosaurs and pliosaurs, including the massive, *Kronosaurus* (Suter, pers. comm.). The degeneration of the skull remains of QMF49220 are not conducive to interpretation by abrasion of gastroliths, although rare plesiosaur skeletons from the area are frequently preserved with them intact (Suter, pers. comm.). Sharks also coexisted with *A. hurleyi*, along with large pelagic actinopterygians such as *Pachyrhizodus* (see Bartholomai 2012) and the ca. 3 m. *Cooyoo*, revised by Lees & Bartholomai (1987) but their teeth could not have been responsible for the circular, widely separated fracturing present in QMF10913.

Ichthyosaurs are statistically the most common of the large reptilian predators in the Toolebuc Formation near Boulia and they had conically-shaped circular teeth. Teeth in the much larger but rarely encountered *Kronosaurus* (also recorded in the Queensland Museum collections) are also conical but are much larger and more separated in adult specimens. Plesiosaur remains are also rare in the Boulia collection. It is thus considered more likely that *P. australis* (reviewed by Zammit 2010), was the predator associated with the additional *A. hurleyi* skulls described herein. Pollard (1968) reported on ichthyosaur gastric contents which were found associated with skeletal remains from the Early Jurassic of Lyme Regis, UK and concluded that they mainly preyed on dibranchiate cephalopods and fish. However, Ball (2002), recorded that in the vomit of predators (thought to be from ichthyosaurs) prey were swallowed whole and the soft tissues in the gut digested, and with hard residues, such as belemnites, regurgitated. Pelagic invertebrate food sources existed in the western part of the Eromanga Basin but are relatively rarely found as fossils compared

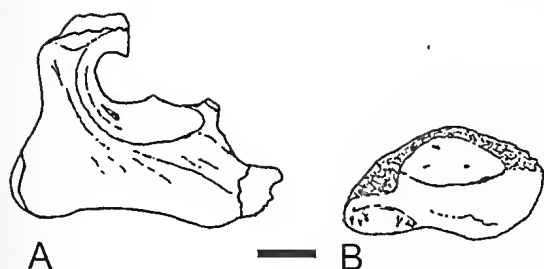


FIG. 4. *Australopachycormus hurleyi* Kear, 2007, drawings of right lateral ethmoids to show possible corrosion. A, lateral view of well preserved, undistorted ethmoid from QMF10913; B, lateral view showing remaining base of the ethmoid from QMF49220, interpreted as the result of corrosion. Scale bar = 1 cm.

with the invertebrate fossil record in the northern part of the Basin (see Cook *et al.* 2013). Food availability may have forced the reptilian fauna of the Toolebuc Formation and Allaru Mudstone to rely more heavily on other vertebrates in the west of the Basin.

Involvement of larger benthic scavengers generally appears unlikely in the reduction and modification of the skulls of *A. hurleyi* or in complete removal of missing individual elements. The fluctuating dysoxic to anoxic bottom waters that prevailed during deposition of the Toolebuc Formation suggest that such conditions would have precluded the general presence of large benthic scavengers. Monospecific benthic communities of the bivalve *lnoceramus* existed within the fluctuating palaeoenvironment (Henderson 2004), suggesting that larger benthic scavengers could exist where more oxygenated and probably isolated microhabitats were present. The scavenging isopod, *Brunnaega*, has been shown by Wilson *et al.* (2011) to be associated with remains of the fossil actinopterygian, *Pachyrhizodus marathonsensis* (Etheridge Jnr. 1905) from the Toolebuc Formation on 'Canary' Station, near Boulia, in the same general part of the Eromanga Basin as that from which *A. hurleyi* has mostly been recorded. The crushing, breaking and disarticulation of the cranial bones within the general skull envelope, especially in QMF49220, is not able to be attributed to small invertebrate scavenging.

The fact that *Australopachycormus* was also a middle-sized predator would not preclude it from being the prey of larger animals. The nature of the preservation discussed above for QMF49220 suggests that this skull was ingested, subjected to digestive stomach acid and compressed before and during digestion by muscular action, and later regurgitated. Regurgitated fossilised remains were termed '*speiballen*' by Schafer (1972), a term usually applied to indigestible stomach contents preserved in mass after regurgitation, including hard parts of small prey, such as belemnites. QMF49220 was not collected in association with other regurgitated and indigestible stomach contents nor was it combined with stomach contents preserved in situ where deposited, nor fossilised within the remains of the predator involved.

The presence of the skull of a single, large fish does not fit comfortably with Schafer's suggested diagnosis for regurgitated remains. Regardless, the characters displayed in QMF49220 indicate that predation, digestion and regurgitation were most likely involved in the history of this particular skull prior to fossilisation. The specimen would most likely have been part of a carcass swallowed whole or in large chunks. No puncturing by teeth of the external bones of the head of this specimen is evident, suggesting that the rather large head of *A. hurleyi* was swallowed without a significant bite by the predator.

## CONCLUSIONS

Additional detail has been provided on the morphology of the skull of the pachycormid, *Australopachycormus hurleyi* Kear, 2007, based on new material collected from the marine Toolebuc Formation of Early Cretaceous (Late Albian) age from near Boulia in central western Queensland, Australia. This augments the description of the species provided by Kear (2007) and that in Wretman & Kear (2013) especially regarding the upper and lower jaws and the orbital region. The new information supports Kear's (2007) conclusions regarding a sister-taxon relationship with the Late Cretaceous, Northern Hemisphere *Protosphyraena*. Although

interpreted as a pelagic predator, it has been shown that *A. hurleyi* was itself prey to larger animals and, at least in one instance, (that of QMF49220) was believed to have been regurgitated after partial digestion, probably by one of the co-existing marine reptiles in the epeiric sea of the Eromanga Basin of central Queensland. Bite damage by an animal like the ichthyosaur, *Platypterygius australis*, on a second specimen of *A. hurleyi* suggests that this ichthyosaur was most likely the predator involved and supports the conclusion that it was also the predator most likely involved with both pachycormids studied in the current work.

## ACKNOWLEDGEMENTS

The author thanks the late Curator of the Stonehouse Museum, Mr Richard Suter, for access to QMF49220, a specimen that was collected by him and for information on other marine vertebrates located and largely prepared by him. Thanks are also offered to Dr Andrew Rozefelds, Head of Geosciences at the Queensland Museum for helpful advice.

## LITERATURE CITED

- Ball, P. 2002. Jurassic vomit comes up at meeting. Nature online, 12th February 2002 doi:10.1038/news020211-3.
- Bartholomai, A. 2004. The large aspidorhynchid fish, *Richmondichthys sweeti* (Etheridge Jnr. & Smith Woodward, 1891) from Albian marine deposits of Queensland. *Memoirs of the Queensland Museum* 49(2): 521–36.
- Bartholomai, A. 2012. The pachyrhizodontid teleosts from the marine Lower Cretaceous (latest mid to late Albian) sediments of the Eromanga Basin. *Memoirs of the Queensland Museum - Nature* 56(1): 119–48.
- Cook, A.G., McKellar, J.L. & Draper, J.J. 2013. Eromanga Basin. In: *Jell, P.A. (Ed) Geology of Queensland*. (Geological Survey of Queensland: Brisbane) 523–33.
- Etheridge, R. Jnr. 1905. Description of the mutilated cranium of a large fish from the Lower Cretaceous of Queensland. *Records of the Australian Museum* 6: 5–8 (<http://dx.doi.org/10.3853/j.0067-1975.6.1905.980>).
- Everhart, M.J. 2003. First records of plesiosaur remains in the lower Smoky Hills Chalk member (Upper Coniacian) of the Niobrara Formation in western Kansas. *Transactions of the Kansas Academy of Sciences* 106(3–4): 139–148 ([http://dx.doi.org/10.1660/0022-8443\(2003\)106\[0139:FROPRI\]2.0.CO;2](http://dx.doi.org/10.1660/0022-8443(2003)106[0139:FROPRI]2.0.CO;2)).
- Henderson, R.A. 2004. A mid-Cretaceous association of shell beds and organic rich shale: bivalve exploitation of a nutrient rich, anoxic sea floor environment. *Palaios* 19: 156–69 ([http://dx.doi.org/10.1669/0883-1351\(2004\)019<0156:AMAO SB>2.0.CO;2](http://dx.doi.org/10.1669/0883-1351(2004)019<0156:AMAO SB>2.0.CO;2)).
- Jell, P.A., Draper, J.J. & McKellar, J.L. 2013. Great Australian Superbasin. Pp. 517. In: *Jell, P.A. (Ed) Geology of Queensland*. (Geological Survey of Queensland: Brisbane).
- Kear, B.P. 2007. First record of a pachycormid fish (Actinopterygii: Pachycormiformes) from the Lower Cretaceous of Australia. *Journal of Vertebrate Paleontology* 27: 1033–38 ([http://dx.doi.org/10.1671/0272-4634\(2007\)27\[1033:FROAPF\]2.0.CO;2](http://dx.doi.org/10.1671/0272-4634(2007)27[1033:FROAPF]2.0.CO;2)).
- Lees, T. & Bartholomai, A. 1987. Study of a Lower Cretaceous actinopterygian (Class Pisces) *Cooyoo australis* from Queensland. *Memoirs of the Queensland Museum* 25: 177–92.
- McCoy, F. 1867. On the occurrence of *Ichthyosaurus* and *Plesiosaurus* in Australia. *Annals and Magazine of Natural History*, Third Series, 19: 355–6.
- Pollard, J.E. 1968. Gastric contents of an ichthyosaur from the Lower Lias of Lyme Regis, Dorset. *Palaeontology* 11(3): 376–88.
- Schafer, W. 1972. *Ecology and paleontology of marine environments*. (Chicago: University of Chicago Press) xiii+568 pp.
- Shimada, K. 1997. Shark tooth-bearing coprolite from the Carlyle Shale (Upper Cretaceous), Ellis County, Kansas. *Transactions of the Kansas Academy of Science* 100(3–4): 133–138 (<http://dx.doi.org/10.2307/3628001>).
- Wilson, G.D.F., Paterson, J.R. & Kear, B.P. 2011. Fossil isopods associated with a fish skeleton from the Lower Cretaceous of Queensland, Australia—direct evidence of a scavenging lifestyle in Mesozoic Cymothoidea. *Palaeontology* 54(5): 1053–68.
- Wretman, L. & Kear, B.P. 2013. Australia's ancient swordfish. *Australian Age of Dinosaurs* 10: 6–7.
- Zammit, M. 2010. A review of Australasian ichthyosaurs. *Alcheringa* 34: 281–92 (<http://dx.doi.org/10.1080/03115511003663939>).

## Appendix

### *Australopachycormus hurleyi* Kear, 2007 (QMF49220)

Total length of preserved elements ..	322.0 mm
Length of preserved neurocranial elements .....	227.0 mm
Posterior depth of preserved skull (including mandible) .....	110.0 mm
Length of mandible .....	235.0 mm
Depth of mandible (mid-mandible) ..	32.2 mm
Depth of mandible (below coronoid fang) .....	27.4 mm
Minimum length of crown of large coronoid fang .....	18.0 mm
Width of crown base of large coronoid fang .....	5.3 mm
Length of exposed crown of anterior coronoid teeth .....	3.6 mm
Maximum exposed length of crown of dentary teeth .....	4.5 mm
Total length of dentary tooth (including root) .....	10.5 mm
Length of premaxilla .....	87.6 mm
Width of largest premaxillary tooth ..	5.5 mm
Maximum length of posterior premaxillary tooth crowns .....	1.2 mm
Maximum length of maxilla .....	135.0 mm
Maximum depth of maxilla .....	20.6 mm
Anterior depth of maxilla .....	10.3 mm
Length of exposed crown of maxillary teeth .....	1.2 mm
Length of exposed crown of largest dermopalatine tooth .....	4.4 mm
Estimated breadth of neurocranial roof across dermosphenotics .....	100.0 mm
Breadth across front of rostrodermethmoids (as preserved) .....	39.2 mm

### *Australopachycormus hurleyi* Kear, 2007 (QMF10913)

Length of orbit .....	65.0 mm
Length of sclerotic plates (external) ..	46.5 mm
Internal opening within sclerotics .....	29.7 mm
Posterior neurocranial breadth .....	93.0 mm
Neurocranial breadth across dermosphenotics .....	93.0 mm
Posterior cranial depth .....	66.9 mm



# **TRACHEAL BOT FLY (*TRACHEOMYIA MACROPI*) IN AN EASTERN GREY KANGAROO (*MACROPUS GIGANTEUS*).**

*Memoirs of the Queensland Museum – Nature*. 59: 256. 2016. The enigmatic bot fly *Tracheomyia macropi* (Froggatt 1913) is the only native species of oestrid fly in Australia and the only extant member of the *Tracheomyia* lineage (Pape 2006). Larvae of this myiasis-causing parasite inhabit the pharynx, trachea, bronchi and bronchioles of kangaroos and wallabies where they feed on mucosal secretions. Little is known about the life-cycle of pupal and adult stages outside the macropod host and few cases have been documented (McCarthy, 1961; Mykytowycz, 1963; Arundel *et al.* 1989; Speare *et al.* 1989; Portas & Spratt 2008). In this study, we report the incidental necropsy findings of a larval infestation of *T. macropi* in an eastern grey kangaroo, *Macropus giganteus* Shaw, 1790 from a wild population in south-east Queensland. This expands the known host and locality records for this parasite as well as confirming its relatively low pathogenicity.

In early spring 2014, there were reports of deaths of approximately 30 eastern grey kangaroos from a high density population in Wacol in Brisbane's western suburbs (27°34'45.4"S, 152°54'53.9"E). Two weak and cachectic eastern grey kangaroos were assessed by a wildlife hospital, and subsequently euthanised and submitted for necropsy. In one individual, a 7.5 kg sub-adult female, there were a total of twelve third-stage instars at the tracheal bifurcation (Fig. 1). The larvae were removed, preserved in 70% ethanol and identified using light microscopy. Voucher specimens were deposited at the Australian National Wildlife Collection, CSIRO Canberra (W/L HC# AR1624) QMN registration T234460.

Macroscopically, the trachea was congested and contained stable foam, but no erosive lesions were observed. Tissues were fixed in 10% neutral buffered formalin, paraffin-embedded, sectioned and stained with haematoxylin and eosin using standard methods. Histopathological examination of the tracheal bifurcation found evidence of mild to moderate, multifocal ulcerative tracheitis with squamous metaplasia and hyperplasia of remnant epithelium in affected areas. A diverse array of ecto- and endoparasites were identified in this animal and the other *M. giganteus* from the same outbreak. In both animals, severe hepatopathy due to infestation with the platyhelminth *Fasciola hepatica* was deemed to be the principal cause of mortality, although polyparasitism and poor nutrition were likely contributors to debility.

The histological findings in this case are similar to those previously described for tracheal bots in other species of macropod (Speare *et al.* 1989; Portas & Spratt 2008). This case concurs with previous studies in which *T. macropi* is generally regarded as an incidental finding rather than a primary pathogen (Portas & Spratt, 2008). Previous reports of *T. macropi* in eastern grey kangaroos are confined to NSW, though they have also been recorded in "Downs and Gidyea country" of central Queensland in either eastern or western grey kangaroos (McCarthy 1961). Other reports specifically mention an absence of infection in grey kangaroos compared to sympatric red kangaroos, *Macropus rufus* (Mykytowycz 1963; Arundel *et al.* 1989). The current case provides confirmation that *M. giganteus* can also be host to *T. macropi* and extends the known distribution of this parasite.



FIG. 1 *Tracheomyia Macropi*, third-stage instars removed from the tracheal bifurcation in *Macropus giganteus* (bar = 1 mm). Variation in colour reflects maturity within the third-stage instar and may partly be an artefact of preservation in ethanol.

## **Acknowledgements**

The authors wish to thank Stephanie Shaw for the submission and field observations. We also acknowledge Ian Beveridge for his technical support.

## **Literature Cited**

- Arundel, J.H., Beveridge, L., & Presidente, P.J. 1989. Parasites and pathological findings in enclosed and free-ranging populations of *Macropus rufus* (Dipodomys) (Marsupialia) at Menindee, New South Wales. *Australian Wildlife Research* 6: 361-379.
- McCarthy, P.H. 1961. Two parasites of marsupials in central Queensland. *Australian Veterinary Journal* 37: 405.
- Mykytowycz, R. 1963. Occurrence of bot-fly larvae *Tracheomyia macropi* Froggatt (Diptera: Oestridae) in wild red kangaroos, *Megalia rufa* (Desmarest). *Proceedings of the Linnean Society of New South Wales* 88: 307-312.
- Portas, T.J. & Spratt, D.M. 2008. Bronchitis associated with *Tracheomyia macropi* in a red necked wallaby (*Macropus rufogriseus*). *Australian Veterinary Journal* 86: 277-278.
- Pape, T. 2006. Phylogeny and evolution of bot flies. Pp. 20-50. In: Colwell, D.D., Hall, M.J.R. & Scholl, P.J. (eds) *The oestrid flies: biology, host-parasite relationships, impact and management*. (CABI Publishing: Oxfordshire).
- Speare, R., Donovan, J.A., Thomas, A.D. & Speare, P.J. 1989. Pp. 705-734. In: Grigg, G., Jarman, P. & Hume, I. (eds) *Diseases of free-ranging Macropodoidae*. (Surrey Beatty & Sons Pty Ltd: New South Wales).
- Leanne Nelson & Anita Gordon. Biosecurity Sciences Laboratory, Health and Food Science Precinct, PO Box 156 Archerfield BC QLD, 4108. Email: leanne.nelson@daf.qld.gov.au. First published online 15 April 2016. <http://dx.doi.org/10.17082/j.2204-1478.59.2016.2016-03>.



# Vale Jeanette Adelaide Covacevich, AM, PSM (1945–2015)

Patrick J. COUPER

Vertebrate Zoology Section, Biodiversity Program, Queensland Museum, South Brisbane, Queensland 4101, Australia.

Judith McKAY

Historian and museum consultant; formerly on the staff of the Queensland Museum.

Citation: Couper, P.J. & McKay, J. 2016. Vale Jeanette Adelaide Covacevich, AM, PSM (1945-2015). *Memoirs of the Queensland Museum - Nature* 59: 257–271. ISSN 2204–1478 (Online), ISSN 0079–8835 (Print). Accepted: 16 February 2016 First published online: 13 April 2016

<http://dx.doi.org/10.1082/j.2204-1478.59.2016.2016-04>

LSID - urn:lsid:zoobank.org:pub:3A7647FE-2B8D-4BD4-B8D8-422F0E61C261

Jeanette Covacevich, who died in Brisbane on 17 September 2015, was one of the Queensland Museum's best known and longest-serving staff members. She will be remembered not only for her professional contribution as a herpetologist and curator but also for her personal qualities. A spirited and adventurous woman, she made a lasting impression on all who knew her, and had an extraordinary capacity for making friendships. Her memorial service, held at the State Library of Queensland a month after her death, was attended by some 350 people and live-streamed to another gathering in Cooktown where she lived in later years.



FIG. 1. Jeanette Covacevich, 1995. Image: Queensland Museum



FIG. 2. Jeanette Covacevich and Charles Tanner, ca 1981, handling dangerously venomous snakes, the Western Taipan, *Oxyurauus microlepidotus* (left) and the Coastal Taipan, *Oxyurauus scutellatus* (right). Image: Charles Tanner collection, courtesy of John Cann.

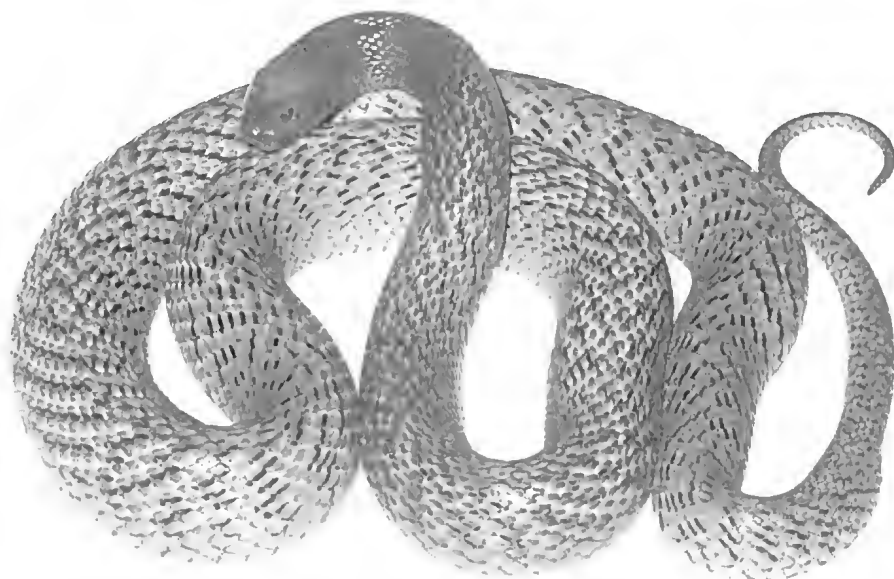


FIG. 3. The Western Taipan, *Oxyurauus microlepidotus*, the world's most venomous land snake. Jeanette Covacevich played a major role in the rediscovery of this species. Image: Queensland Museum.

Jeanette was born in Innisfail, north Queensland on 26 March 1945, the elder of two children of Sir Thomas Covacevich and his wife, Gladys, née Bryant. Sir Thomas, a decorated RAF officer of World War II, was a well-known Cairns solicitor and philanthropist. Jeanette grew up in Cairns and from an early age acquired a taste for outdoor adventure and natural history, interests that persisted throughout her life. She attended Brisbane Girls Grammar School where she excelled at swimming, and went on to study at The University of Queensland as a resident of Women's College. She graduated with a BA in 1967, majoring in Geography and Zoology, and later completed a higher degree in environmental studies at Griffith University (MSc, 1977).

In 1966, Jeanette joined the Queensland Museum in Brisbane as a cadet. She remained with this institution until her retirement in 2002, by which time she had risen through the curatorial ranks to the position of Senior Curator and co-head of the Vertebrate Zoology Section. After retirement, she continued as an Honorary Research Associate until her decline in 2015 due to an inoperable brain tumour. Jeanette's museum career was highly productive with extensive out-reach. She oversaw the growth of the herpetology collections from 7427 specimens in 1966 to 58216 specimens in 2002, wrote two books, edited another five and produced 110 herpetological papers describing 30 new species of reptiles. She was interested in the taxonomy, zoogeography and the conservation of Australo-Papuan reptiles, particularly those from rainforests, deserts and heaths. Her other research interests were diverse and included publications on mammals, Aboriginal trails and medicinal plants, the palm trees of north Queensland, the importance of museum collections and the convict history of North Stradbroke Island.

Jeanette is best known for her work on Queensland snakes and her involvement in the rediscovery of the Western Taipan (*Oxyuranus microlepidotus*). This snake, first described by Frederick McCoy in 1879, was 'lost' to science for almost 100 years, until a specimen was collected in far western Queensland by grazier,

Herb Rabig. Jeanette established the identity of this specimen and undertook fieldwork with her friend the late Charles Tanner to obtain additional specimens. This species was subsequently shown to have the most potent venom of any land snake. The snake, its venom and ecology feature significantly in her many publications. The interwoven Western Taipan / Plague Rat story was told in an exhibit, *Feast & Famine*, when the Queensland Museum relocated to its present South Brisbane site in 1986. The following year she co-edited a best-selling book, *Toxic Plants and Animals*, which was accompanied by a major, live exhibition featuring some of Australia's most venomous creatures.

To many Queenslanders, Jeanette was known as the 'snake lady'. She provided an identification service for government agencies, medical practitioners and members of the public and acted as a consultant to the Poisons Information Centre (based at the former Brisbane Children's Hospital) from 1969, being on call to assist with snake identifications. This service had major implications for the clinical management of snakebite victims and led to improved patient outcomes and significant cost-savings in their treatment. She also served on the Scientific and Clinical Immersions Subcommittee of the Graduate Medical Course at The University of Queensland (1996–2002) and on the Scientific Advisory Committee of Queensland's Environmental Protection Agency (1997–99).

Gregarious and generous, Jeanette gave her time to many organisations. She was president of the Australian Society of Herpetologists (1988–90), secretary of the Stradbroke Island Management Organisation (1975–84), an adviser to the Rainforest Conservation Society of Queensland (1982–98) and a long-time member of both the Queensland Naturalists' Club and the Lyceum Club Brisbane. Her longest association, however, was with the Royal Society of Queensland of which she was secretary (1974–79), councillor (1984–87, 1994–98) and president (1995). Additionally, she co-convened various Royal Society conferences (North Stradbroke Island, 1974; Focus on Stradbroke, 1984; Queensland: the state of science, 1994; The history of natural history in Queensland, 1995 and Exploring our



FIG. 4. Jeanette Covacevich (lower left) participating in fieldwork on Thornton Peak, north-east Queensland, ca 1984. Image: Covacevich family papers and photographs 1909–2014 (ACC 30101), John Oxley Library, Brisbane.



FIG. 5. The Clouded Gecko, *Amalosia jacovae* (Couper, Keim & Hoskin, 2007), named for Jeanette Covacevich to honour her contribution to conservation. Image: Steve K. Wilson

genes and genetic heritage, 1996). Throughout her career, Jeanette championed many conservation causes. She was one of the first to document diminished reptile diversity in

Queensland's Brigalow lands and raised both government and public awareness of the plight of these assailed ecosystems. Her conference presentations carried hard-hitting titles such as 'Is biodiversity maintenance in Queensland's Brigalow Belt just another oxymoron?' Always a polished public speaker, Jeanette once declared that the worst crime one could commit was to be boring; the next-worst was to be long-winded. She was in high demand, even in retirement, and continued to address various clubs and community groups.

Jeanette was honoured with awards which included the St John Priory Vote of Thanks (for voluntary teaching regarding snakes and snakebite over many years); Member in the General Division, Order of Australia, 1995 (for service to science, particularly in the field of herpetology, and to conservation); the Queensland Museum Medal, 2002; the Public Service Medal, 2003 (for outstanding service to the Queensland Museum and to the people of Queensland);

the Queensland Natural History Award, 2003; and the Australian Natural History Medallion, 2007. Her contributions to science are further recognised in the following eponymic species names: *Terriswalkeri* *covacevichae* Jameson, 1994 (an earthworm from the rainforests of north-eastern Queensland); *Zophorame covacevichae* Raven, 1994 (a mygalomorph spider from NEQ); *Pseudophryne covacevichae* Ingram & Corben, 1994 (a broodfrog from NEQ); *Kababina covacevichae* Todd Davies, 1995 (an amphinectid spider from NEQ) and *Oedura* [now *Amalosia*] *jacovae* Couper, Keim & Hoskin, 2007 (a velvet gecko from south-east Queensland). The etymology for the last of these reads: '*jacovae*; for Jeanette Adelaide Covacevich, a former senior curator at the Queensland Museum, for her many contributions to Australian Herpetology. The authors also recognise Jeanette as a prominent figure in Queensland conservation, particularly her efforts to preserve the unique character of North Stradbroke Island where *O. jacovae* sp. nov. occurs in open forest communities.'

In her sporting life Jeanette achieved recognition as an all-round athlete, competing in marathons and triathlons and maintaining her fitness with strenuous swimming and bushwalking. She was always modest about her sporting achievements but her 1987 World Champion title (female age category 40–44) in the Hugall and Hoile World Sprint Triathlon Championship speaks for itself. She was in the habit of celebrating each birthday by swimming the equivalent lengths of an Olympic pool, which ceased only when she was 70 and suffering from her illness.

Following her retirement from the Queensland Museum in 2002, Jeanette moved to Cooktown. There she identified with the local community, even joining the CWA, though drawing a line at dressing up for the town's annual re-enactment of Captain Cook's landing. She was a regular volunteer at Nature's Powerhouse, a museum in Cooktown's Botanic Gardens featuring a natural history exhibit she helped to develop and the botanical paintings of local artist Vera Scarth-Johnson. Jeanette's picturesque property on the Endeavour River became open house for her wide circle of

friends and colleagues. She remained active in the field by assisting her former museum colleagues to undertake fieldwork in the far north and by participating in Australia Zoo's crocodile research trips to Steve Irwin Reserve on Cape York Peninsula. In her later years she also pursued an interest in island history and biogeography, visiting such places as Pitcairn Island, the Chatham Islands, St Helena (in the southern Atlantic) the Marquesas and Vanuatu (Malekula, Maskelynes, Ambrym). She shared her island adventures through eagerly awaited presentations to fellow members of the Queensland Naturalists' Club and the Lyceum Club. As well, she maintained her association with the Queensland Museum, often appearing in the Vertebrate Zoology Lab with a bag full of frozen specimens; snakes, birds and mammals that had been carried down from north Queensland as hand luggage.

Jeanette was supportive of her friends and colleagues and extended a helping hand whenever needed. She was excellent company — cheerful and knowledgeable — and never afraid to speak her mind. Gifted with a wicked sense of humour, she was particularly taken by a transcription error that occurred when one of her hand-written manuscripts was passed to a museum typist, radically changing its meaning. In 1994, she and two male companions witnessed a fight between two male Black Whip Snakes in far north Queensland. She wrote: 'We watched their ritual for close to 45 minutes. They moved, as a pair, about 20 m along the road — all the time twisting, coiling, raising their forebodies both together and separately, and then falling back to begin the sequence anew.' Upon receiving a clean copy of the manuscript she discovered to her delight that an 'm' had been mistaken for a 'w' so that the text now read: 'We matched their ritual for close to 45 minutes...'

Jeanette was a truly unique person who will be missed by many, not least by the writers of this tribute, former museum colleagues whom she so generously mentored.

The following is a summary of Jeanette's research work.

NEW GENERA AND SPECIES  
OF REPTILES DESCRIBED

*Phyllurus caudimaculatus* Covacevich, 1975

A small leaf-tailed gecko, narrowly endemic to eastern Australian rainforest.

*Phyllurus salebrosus* Covacevich, 1975  
(= *Saltuarius salebrosus*)

A large leaf-tailed gecko from rainforest, heaths and brigalow.

*Carlia dogare* Covacevich & Ingram, 1975

A skink confined to Quaternary sandstones near Cooktown, north-eastern Queensland.

*Carlia jarnoldae* Covacevich & Ingram, 1975

A skink from open forests of Cape York Peninsula, south to Charters Towers, north-eastern Queensland.

*Cryptoblepharus fulvi*  
Covacevich & Ingram, 1978

A skink known from a single locality, the black boulders of the Melville Range, Cape York Peninsula, north-eastern Queensland.

*Carlia rinula* Ingram & Covacevich, 1980

A skink confined to vine forests of Cape York Peninsula, north-eastern Queensland.

*Carlia scirtetis* Ingram & Covacevich, 1980  
(= *Liburnasciucus scirtetis*)

A skink known from a single locality, the black boulders of the Trevethan Range, near Cooktown, north-eastern Queensland.

*Eulamprus anplus*  
Covacevich & McDonald, 1980  
(= *Couciinnia anplus*)

A large skink endemic to rainforests in the Mackay-Proserpine area mid-eastern Queensland.

*Eulamprus luteilateralis*  
Covacevich & McDonald, 1980  
(= *Maguella luteilateralis*)

A skink endemic to high altitude rainforests of the Mackay area, of mid-eastern Queensland.

*Leiolopisma jigurru* Covacevich, 1984

A skink known from a single locality, the boulder 'fields' at the summit of Mt Bartle Frere, north-eastern Queensland.

*Lygisaurus roccoco* Ingram & Covacevich, 1988

A skink confined to the limestones in the Chillagoe area, north-eastern Queensland.

*Lygisaurus tauuieri* Ingram & Covacevich, 1988

A skink from the riverine rainforests between the Starcke and Endeavour Rivers, north-eastern Queensland.

*Lygisaurus sesbraui*  
Ingram & Covacevich, 1988

A skink from heaths, and monsoon and open forests of Cape York Peninsula, north-eastern Queensland.

*Carlia rubrigularis*  
Ingram & Covacevich, 1989

A skink confined to the rainforests of the Wet Tropics World Heritage Area (between Cooktown and Townsville, north-eastern Queensland).

*Carlia storri* Ingram & Covacevich, 1989

A skink from Papua New Guinea and Cape York Peninsula, to Townsville, north-eastern Queensland.

*Sulcatideus quadratus* Covacevich, Couper,  
Molnar, Witten & Young, 1990

A fossil dragon from the Riversleigh deposit north of Mt Isa, north-western Queensland.

*Phyllurus isis*

Couper, Covacevich & Moritz, 1993

A leaf-tailed gecko from mid-eastern Queensland.

*Phyllurus ossa*

Couper, Covacevich & Moritz, 1993

A leaf-tailed gecko from mid-eastern Queensland.

*Phyllurus nepthys* Couper, Covacevich & Moritz, 1993

A small leaf-tailed gecko, endemic to the rainforests in the Mackay area, mid-eastern Queensland.

*Saltuarinus occultus* Couper, Covacevich & Moritz, 1993  
(= *Orraya occultus*)

A large leaf-tailed gecko endemic to rainforests of the McIlwraith Range, north-eastern Queensland.

*Naungura spinosa*

Covacevich, Couper & James, 1993

A very distinct (both by genus and species) skink confined to remnants of semi-evergreen vine thicket, near Murgon, south-eastern Queensland.

*Ramphotyphlops silvia*

Ingram & Covacevich, 1993  
(= *Anilius silvia*)

A secretive blind snake from rainforests on Quaternary sands in south-eastern Queensland.

*Ramphotyphlops chamodracæna*  
Ingram & Covacevich, 1993  
(= *Anilius chamodracæna*)

A secretive blind snake from woodlands of western Cape York Peninsula, northern Queensland.

*Carlia parrhasius*

Couper, Covacevich & Lethbridge, 1994  
(= *Lygisaurus parrhasius*)

A skink from a single locality, a sandstone plateau, near west of Iron Range, Cape York Peninsula, far north-eastern Queensland.

*Coggeria naufragus*

Couper, Covacevich, Masterson & Shea, 1996

A burrowing skink from Fraser Island, a World Heritage Site.

*Saltuarinus wyberba*

Couper, Schneider & Covacevich, 1997

A gecko from the Granite Belt, south-eastern Queensland.

*Ramphotyphlops aspina*,  
Couper, Covacevich & Wilson, 1998  
(= *Anilius aspina*)

A poorly known blind snake collected in 'sheep country' of the Barcaldine area, mid-eastern Queensland.

*Ramphotyphlops robertsi*

Couper, Covacevich & Wilson, 1998  
(= *Anilius robertsi*)

A poorly known blind snake from the Cooktown area, north-eastern Queensland.

*Orraya* Couper, Covacevich, Schneider & Hoskin, 2000

A genus to accommodate the leaf-tailed gecko initially described as *Saltuarinus occultus* Couper, Covacevich & Moritz, 1993.

*Phyllurus amnicola* Couper, Hoskin, Schneider & Covacevich, 2000.

A leaf-tailed gecko known from only one locality, Mt Elliot, near Townsville, north-eastern Queensland.

*Phyllurus championae* Couper, Schneider, Hoskin & Covacevich, 2000.

A leaf-tailed gecko, confined to the ranges south-west of Mackay, mid-eastern Queensland.



## BOOKS

- Covacevich, J. 1970. *Snakes of Brisbane*. (Queensland Museum: Brisbane). 30pp.
- Covacevich, J. & Easton, A. *Rats and Mice of Queensland*. (Queensland Museum: Brisbane). 80pp.
- Durbidge, E. & Covacevich, J. 1981. *North Stradbroke Island*. (Stradbroke Island Management Organisation: Brisbane). 168pp.
- Coleman, R., Covacevich, J. & Davie, P. (eds) 1984. *Focus on Stradbroke: New Information on North Stradbroke Island and surrounding areas 1974-1984*. (Boolarong Press, Stradbroke Island Management Organisation: Brisbane). 420pp.
- Covacevich, J., Davie, P. & Pearn, J. (eds) 1987. *Toxic Plants and Animals: A Guide for Australia*. (Queensland Museum: Brisbane). 504pp.
- Pearn, J. & Covacevich, J. (eds) 1988. *Venoms and Victims*. (Amphion Press & Queensland Museum: Brisbane). 136pp.
- Covacevich, J.A. (ed). 1993. *Memoirs of the Queensland Museum* 34(1). (Queensland Museum: Brisbane). 240pp.
- Covacevich, J.A., Pearn, J.H., Case, D., Chapple, I. & Phillips, G. (eds) 1996. *History, Heritage and Health: Proceedings of the Fourth Biennial Conference of the Australian Society of the History of Medicine*. (The Australian Society of the History of Medicine: Brisbane). 439pp.

## HERPETOLOGICAL PAPERS LISTED IN CHRONOLOGICAL ORDER

- Covacevich, J. 1971. Amphibian and Reptile Type-specimens in the Queensland Museum. *Memoirs of the Queensland Museum* 16(1): 49-68.
- Trinca, J.C., Graydon, J.J., Covacevich, J. & Limpus, C. 1971. The Rough-scaled Snake (*Tropidechis carinatus*) a dangerously venomous Australian snake. *Medical Journal of Australia* 2: 801-809.
- Covacevich, J. & Limpus, C. 1972. Observations on community egg-laying by the Yellow-faced Whip Snake, *Demansia psammophis* (Schlegel) 1837 (Squamata Elapidae). *Herpetologica* 28(3): 208-210.
- Covacevich, J. & Limpus, C. 1973. Two large winter aggregations of three species of tree climbing snakes in southeastern Queensland. *Herpetofauna* 6(2): 16-21.
- Covacevich, J. 1974. The status of *Hyla irrorata* De Vis 1884 (Anura : Hylidae). *Memoirs of the Queensland Museum* 17(1): 49-53.
- Covacevich, J. 1974. An unusual aggregation of snakes following major flooding in the Ipswich - Brisbane area, south-eastern Queensland. *Herpetofauna* 7(1): 22-24.

- Covacevich, J. 1975. A review of the genus *Phyllurus* (Lacertilia : Gekkonidae). *Memoirs of the Queensland Museum* 17(2): 293-303.
- Covacevich, J. 1975. Reptiles. Pp. 97-115 In, *The National Estate in the Moreton and Wide Bay-Burnett Regions*. (Queensland Museum, for the Co-ordinator General). 272 pp.
- Covacevich, J. 1975. *Snakes in combat*. *Victorian Naturalist* 92(12): 252-253.
- Covacevich, J. & Archer, M. 1975. The distribution of the Cane Toad, *Bufo marinus*, in Australia and its effects on indigenous vertebrates. *Memoirs of the Queensland Museum* 17(2): 305-310.
- Covacevich, J. & Ingram, G.J. 1975. Three new species of rainbow skinks of the genus *Carlia* from northern Queensland. *Victorian Naturalist* 92: 19-22.
- Covacevich, J. & Ingram, G.J. 1975. The reptiles of North Stradbroke Island. *Proceedings of the Royal Society of Queensland* 86(10): 55-60.
- Covacevich, J. 1976. Recognition of *Paradenansia microlepidotus* (McCoy) a dangerous Australian snake. *Proceedings of the Royal Society of Queensland* 87: 29-32.
- Covacevich, J. & Archer, M. 1976. The Cane Toad in Australia. *Wildlife in Australia* 13(4): 129-132.
- Covacevich, J. & Ingram, G.J. 1978. An undescribed species of rock-dwelling *Cryptoblepharus* (Lacertilia: Scincidae). *Memoirs of the Queensland Museum* 18(2): 151-154.
- Covacevich, J. 1978. Snakes. *Playgroup* 6(6): 13-14.
- Covacevich, J. 1980. Medically significant terrestrial snakes of northern Australia in Child Health Past, Present and Future. *Proceedings of Royal Children's Hospital Academic Week*. Blackall, M.I. & MacDonald H. (eds) (Royal Children's Hospital: Brisbane).
- Covacevich, J. 1980. Australia's most dangerous snakes. *Response*, October 1980.
- Covacevich, J. & Ingram, G. 1980. The endemic frogs and reptiles of Cape York Peninsula. Pp. 49-57 In, *Contemporary Cape York Peninsula*. Stevens, N.C. & Bailey, A. (eds) (Royal Society of Queensland: Brisbane). 100pp.
- Covacevich, J. & McDonald, K.R. 1980. Two new species of skinks from mid-eastern Queensland rainforest. *Memoirs of the Queensland Museum* 20(1): 95-101.
- De Buse, P., Covacevich, J. & Pearn, J. 1980. Report of three cases of snake-bite in Childhood, including a life-threatening case, with recovery in Child Health Past, Present and Future. *Proceedings of Royal Children's Hospital Academic Week*. Blackall, M.I. & MacDonald, H. (eds) (Royal Children's Hospital: Brisbane).



- Ingram, G.J. & Covacevich, J. 1980. Two new lygosomine skinks endemic to Cape York Peninsula. Pp. 45–48 in Contemporary Cape York Peninsula. Stevens, N.C. & Bailey, A. (eds) (Royal Society of Queensland: Brisbane). 100pp.
- Covacevich, J., McDowell, S.B., Tanner, C. & Mengden, G. 1981. The relationship of the Taipan, *Oxyuranus scutellatus* and the Small-scaled Snake *Oxyuranus microlepidotus* (Serpentes: Elapidae). In, Banks, C.B. & Martin, A.A. (eds) *Proceedings of the Melbourne Herpetological Symposium* (Zoological Board of Victoria: Melbourne). 199pp.
- Covacevich, J. 1981. Medically significant terrestrial snakes of northern Australia. Pp. 70–103 In, Pearn, J. (ed) *Animal Toxins and Man* (Division of Health Education and Information: Brisbane). 128pp.
- Ingram, G.J. & Covacevich, J. 1981. Frog and reptile type specimens in the Queensland Museum, with a checklist of frogs and reptiles in Queensland. *Memoirs of the Queensland Museum* 20(2): 291–306.
- Pearn, J. & Covacevich, J. 1981. An atlas of the skin lesions in snake bites. *Medical Journal of Australia* 2: 568.
- Pearn, J. & Covacevich, J. 1981. Skin lesions from bites from Australian snakes. *Australian Journal of Herpetology* 1(2).
- Covacevich, J., Ingram, G.J. & Czechura, G.V. 1982. Rare Frogs and Reptiles of Cape York Peninsula. *Biological Conservation* 22: 283–294.
- Covacevich, J. 1983. Snakes. Pp. 191–216 in Davies, E. (ed.) *Wildlife of the Brisbane Area*. (Brisbane: Jacaranda Wiley). 340pp.
- Covacevich, J., Cannon, L. 1983 In, Scoullar, R. (ed.) *Animals in their environments: a colouring book for children* (Queensland Museum: Brisbane) 24pp.
- Covacevich, J. & Tanner, C. 1983. Come from nowhere .. then just disappear. (*Oxyuranus microlepidotus* and *Rattus villosissimus*). *Australian Natural History* 21(1): 11–14.
- Morrison, J.J., Pearn, J.H., Covacevich, J. & Nixon, J. 1983. identify snakes? *Medical Journal of Australia* 2(2): 67–70.
- Morrison, J.J., Pearn, J.H., Covacevich, J. & Nixon, J. 1983. Can Australians identify snakes? *Medical Journal of Australia* 2(2): 67–70.
- Shine, R. & Covacevich, J. 1983. Ecology of highly venomous snakes: the Australian genus *Oxyuranus* (Elapidae). *Journal of Herpetology* 17(1): 60–69.
- Morrison, J.J., Pearn, J.H., Covacevich, J. & Tanner, C. 1983–1984. Studies on the venom of *Oxyuranus microlepidotus*. *Clinical Toxicology* 21: 273–388.
- Covacevich, J. 1984. Stradbroke Island plants and animals of significance to planners. Pp. 385–391 In, R.J. Coleman, J. Covacevich & P. Davie (eds), *Focus on Stradbroke: New information on North Stradbroke Island and surrounding areas, 1974–1984*. (Boolarong Press, S.I.M.O.: Brisbane). 420pp.
- Covacevich, J. 1984. A biogeographically significant new species of *Leiolopisma* (Scincidae) from northeastern Queensland. *Memoirs of the Queensland Museum* 21(2): 401–411.
- Covacevich, J. 1985. Rainforest and reptiles of Cape York Peninsula. *Wildlife Australia* 22(2): 20–25.
- Czechura, G.V. & Covacevich, J. 1985. Poorly known reptiles in Queensland. Pp. 471–476 In, Grigg, G., Shine, R. & H. Ehmann (eds). *The Biology of Australasian Frogs and Reptiles*. (Surrey Beatty and Sons Pty. Ltd.: Chipping Norton, Sydney). 527pp.
- Patten, B.R., Pear, J.H., De Buse, P., Burke, J. & Covacevich, J. 1985. Prolonged intensive therapy after snake bite. Some lessons from a probable case of envenomation by the Rough-scaled Snake, *Tropidechis* sp. *Medical Journal of Australia* 142: 467–469.
- Covacevich, J. 1986. Aspects of the biogeography of the elapid snakes of northeastern Australia in Longmore, R. (ed.) *Atlas of Elapid Snakes of Australia*. (Australian Government Publishing Service: Canberra).
- Covacevich, J. 1987. Two Taipans! in Covacevich, J., Davie, P. & Pearn, J.H. (eds) *Toxic Plants and Animals: A Guide for Australia*. (Queensland Museum: Brisbane). 502 pp.
- Covacevich, J. 1987. Reptiles of far northern Cape York Peninsula. *Queensland Naturalist* 28(1–4): 22–30.
- Covacevich, J. 1988. Foreword to S.K. Wilson & D.G. Knowles, *Australia's Reptiles: A photographic reference to the terrestrial Reptiles of Australia*. (William Collins: Melbourne). 447pp.
- Covacevich, J. 1988. Australia's most dangerous snakes. Pp. 73–86 In, Pearn, J.H. & Covacevich, J. (eds) *Venoms and Victims* (Queensland Museum: Brisbane). 133pp.
- Covacevich, J., Pearn, J. & White, J. 1988. The world's most venomous snake. Pp.111–120 In, Pearn J.H. & Covacevich, J. (eds) *Venoms and Victims*. (Queensland Museum: Brisbane). 135pp.
- Covacevich, J. 1988. Reptiles. Pp. 265–273 In, Scott, G. (ed) *Lake Broadwater: The natural history of an inland lake and its environs*. (Darling Downs Institute Press: Toowoomba). 344pp.
- Ingram, G.J. & Covacevich, J. 1988. Comments on the proposed suppression for nomenclature of three works by R.W. Wells and C.R. Wellington. *Bulletin of Zoological Nomenclature* 45(1): 52–53.
- Ingram, G.J. & Covacevich, J. 1988. Revision of the genus *Lygisaurus* De Vis (Scincidae: Reptilia). *Memoirs of the Queensland Museum* 25(2): 335–354.

- Ingram, G. & Covacevich, J. 1989. Revision of the genus *Carlia* (Reptilia, Scincidae) in Australia with comments on *Carlia bicarinata* of New Guinea. *Memoirs of the Queensland Museum* 27(2): 443–490.
- Covacevich, J. 1989. Crocodile injuries/Cane Toad poisoning. In, *Preventive First Aid: A Guide to the Reduction of some common preventable injuries*. Pearn, J. & Nixon, J. (eds). (Amphibian Press: Brisbane)
- Covacevich, J. 1990. Phangs and physic: 40,000 years of risky business. Pp. 61–72 In, Pearn, J. & Cobcroft, M. (eds) *Fever and Frontiers* (Amphion Press: Brisbane). 270pp.
- Covacevich, J., Couper, P., Molnar, R.E., Witten, G. & Young, W. 1990. Miocene dragons from Riversleigh: new data on the history of the family Agamidae (Reptilia: Squamata) in Australia. *Memoirs of the Queensland Museum* 29(2):339–360.
- Covacevich, J., Couper, P., McDonald, K. & Trigger, D. 1990. Walunarra, bungarra mali and the gangalidda at Old Doomadgee. *Memoirs of the Queensland Museum* 29(2): 322.
- Covacevich, J.A. & McDonald, K.R. 1993. Distribution and conservation of frogs and reptiles of Queensland rainforests. *Memoirs of the Queensland Museum* 34(1): 189–200.
- Couper, P. & Covacevich, J. 1993. New data on the Australian rainforest leaf-tailed geckos. Pp. 61 in Davies, M. & Norris, R.M. (eds) *Second World Congress of Herpetology*, Adelaide, S.A. 29 December 1993–6 January 1994. (World Congress of Herpetology: Adelaide). 295pp.
- Covacevich, J. & Couper, P. 1993. A new genus and species of skink (*Sphenomorphus* group) from Australia's dry rainforest. Pp. 61 in Davies, M. & Norris, R.M. (eds) *Second World Congress of Herpetology*, Adelaide, S.A. 29 December 1993–6 January 1994. (World Congress of Herpetology: Adelaide). 295pp.
- Pearn, J.H., Covacevich, J.A., Charles, N.T. & Richardson, P. 1993. Snakebite in herpetologists. P. 193 In, Davies, M. & Norris, R.M. (eds) *Second World Congress of Herpetology*, Adelaide, S.A. 29 December 1993–6 January 1994. (World Congress of Herpetology: Adelaide). 295pp.
- Covacevich, J. & Ingram, G.J. 1993. Frogs and reptiles. Pp. 85–86 In, Wadley, D. & King, W. (eds). *Reef, range and red dust. The adventure atlas of Queensland*. (Department of Lands: Brisbane). 244pp.
- Covacevich, J. 1993. Overview of the vertebrate studies. Pp. 21–24 In, (anon.) *Cape York Peninsula Scientific Expedition Wet Season 1992 Report*, Vol. 1. (The Royal Geographical Society of Queensland Inc.: Brisbane). 72pp.
- Ingram, G. J. & Covacevich, J.A. 1993. Two new species of striped Blind Snakes. *Memoirs of the Queensland Museum* 34(1): 181–184.
- Covacevich, J. (1994). Dandarabilla and Gunjiwurr. The discovery of the Taipans -the world's most dangerous snakes in Pearn, J.H. (ed) *Milestones of Australian Medicine*. (Amphion Press: Brisbane).
- Couper, P.J., Covacevich, J.A. & Moritz, C. 1994. Designation of the type species of *Saltuarius*, and other data on the genus. *Memoirs of the Queensland Museum* 35(1): 26.
- Couper, P.J., Covacevich, J.A. & Lethbridge, P.1994. *Carlia parthasius*, a new Queensland skink. *Memoirs of the Queensland Museum* 35(1): 31–33.
- Covacevich, J. 1994. Snakebite, a preventable injury. Abstract. St John Ambulance "Youth in Focus" Seminar Program (26/6/94): 4
- Pearn, J.H., Covacevich, J.A., Charles, N. & Richardson, P. 1994. Snakebite in herpetologists. *The Medical Journal of Australia* 161 5/19 December, 1994:706–708.
- Covacevich, J.A & Couper, P.J. 1994. Type specimens of frog and reptile species, Queensland Museum: recent additions and new information. *Memoirs of the Queensland Museum* 37(1): 69–81.
- Covacevich, J.A., Roberts, L. & McKinna, I. 1994. Male combat in the Black Whip Snake, *Demansia vestigiata*. *Memoirs of the Queensland Museum* 37(1): 52.
- Covacevich, J.A., Pearn, J.H. & Clarkson, J.R. An early Flecker radiograph of *Hydrophis elegans*, and new information on its feeding habits. *Memoirs of the Queensland Museum*. 37(1): 68.
- Covacevich, J.A., Roberts, L., Storch, D.L. & Van Dyck, S. 1994. New *Phascogale tapoatafa* records from Cape York Peninsula, Australia. *Memoirs of the Queensland Museum*. 37(1): 82.
- Covacevich, J. 1995. Review: The Action Plan for Australian Reptiles. *Australian Natural History* Autumn 1995: 72–73.
- Covacevich, J. 1995. The Reptiles of Moreton Bay. In, Pearn, J. (ed) *Characters, coves and cliffs*. (Amphion Press: Brisbane). 139pp.
- Covacevich, J. & Wilson, S. 1995. Land snakes. Pp. 191–216. In, Ryan, M. (ed). *Wildlife of Greater Brisbane* (Queensland Museum, with Environmental Management Branch of Brisbane City Council: Brisbane). 340pp.
- Couper, P.J., Covacevich, J.A. & Wilson, S.K. 1995. Sap feeding by the Australian gecko *Gehyra dubia*. *Memoirs of the Queensland Museum*. 38(2): 396.
- Covacevich, J.A. 1996. Realities in the biodiversity Holy Grail: prospects for reptiles of Queensland's Brigalow Biogeographic Region. (Presidential Address). *Proceedings of the Royal Society of Queensland*. 106(1): 1–9.
- Couper, P.J., Covacevich, J.A., Masterson, S.P. & Shea, G.M. *Coggeria uaufragus* gen. et sp. nov., a sand-swimming skink from Fraser Island,

- Queensland. *Memoirs of the Queensland Museum*. 39(2): 233–241.
- Couper, P.J. & Covacevich, J.A. 1996. A Bandy Bandy with a difference. *Memoirs of the Queensland Museum*. 36(2): 242.
- Covacevich, J.A. and Couper, P.J. 1996. *Aspidites ramsayi* (Boidae) in the Brigalow Biogeographic Region of Queensland: occurrence, conservation status and possible Bilby associations. *Memoirs of the Queensland Museum*. 39(2): 243–246.
- Covacevich, J.A., Couper, P.J. & McDonald, K.R. 1996. *Lerista allanae* (Scincidae: Lygosominae): 60 years from exhibition to extinction? *Memoirs of the Queensland Museum*. 39(2): 247–256.
- Covacevich, J.A., Couper, P.J., Monteith, G., Jago, K., Janetzki, H. and Roberts, L. 1996. Feeding habits of the Ring-tailed Gecko, *Cyrtodactylus louisiadensis*. *Memoirs of the Queensland Museum*. 39(2): 288.
- Covacevich, J.A. & Couper, P.J. 1997. Maida Allan. Pp.29–30 In, McKay, J. (ed.) *Brilliant Careers: Women collectors and illustrators of Queensland*. (Queensland Museum: Brisbane). 80pp.
- Covacevich, J.A., Sutherland, S.K., Coventry, J.A. & Cann, J. 1997. Obituary: Charles Tanner, herpetologists. *Memoirs of the Queensland Museum*. 42(1): 377–78.
- Covacevich, J.A., Couper, P.J. & Roberts, L. 1997. New data on *Lerista ingrami*, a rare skink from southern Cape York Peninsula, Australia. *Memoirs of the Queensland Museum*. 42(1): 24.
- McRae, P.D. & Covacevich, J.A. 1997. Combat and copulation in *Oxyuranus microlepidotus* (Elapidae), the Western Taipan. *Memoirs of the Queensland Museum*. 42(1): 104.
- Couper, P.J., Schneider, C. & Covacevich, J.A. 1997. A new species of *Saltuarius* (Lacertilia: Gekkonidae) from granite-based, open forests of eastern Australia. *Memoirs of the Queensland Museum*. 42(1): 91–96.
- Covacevich, J., Mannion, W. & Irwin, S. 1997. Backyard Wildlife. The Browns at Brookfield. *Wildlife Australia*. 34(2): 32–33.
- Covacevich, J. 1997. Wildlife Questions. *Wildlife Australia*. 34(2): 38.
- Covacevich, J. 1997. Book reviews. A Bedside Nature – Genius and eccentricity in science 1869–1953. *Wildlife Australia*. 34(2): 42.
- Covacevich, J., & Wright, J. 1997. The Golden Geckos, a Brigalow Belt survivor. *Wildlife Australia* Spring 1997 34(3): 10.
- Strimple, P. D. & Covacevich, J. A. 1997. The Taipans of Australia and New Guinea Reptiles. *Guide to keeping reptiles and amphibians*. 5(12): 32–45.
- Covacevich, J. 1998. Wildlife questions. *Wildlife Australia* 35(1): 40–41.
- Covacevich, J. 1997. Herpetological Histories: recent additions to and losses from the southeastern Queensland dossier. Pp. 7–16, in Anonymous, 1997 (released March, 1998). Understanding Forests Seminar, November 2–3, 1996. (Queensland Department of Environment: Brisbane). 117 pp.
- Covacevich, J. & Couper, P. 1998. Comments on the proposed conservation of the specific name of *Varanus teriae* Sprackland, 1991 (Reptilia, Squamata) Case 3043; see BZN 54:100–103, 250–251). *Bulletin of Zoological Nomenclature* 55(1): 37–38.
- Covacevich, J. A. 1998. Messages from the forests – maintaining biodiversity. *Wildlife Australia*. 35(3): 17–20.
- Couper, P. J., Covacevich, J. A., & Wilson, S. K. 1998. Two new species of *Ramphotyphlops* (Squamata: Typhlopidae) from Queensland. *Memoirs of the Queensland Museum* 42(2): 459–464.
- Covacevich, J. A., Couper, P. J. & McDonald, K. R. 1998. Reptile diversity at risk in the Brigalow Belt, Queensland. *Memoirs of the Queensland Museum* 42(2): 475–486.
- Covacevich, J. A. 1998. Snakes with fins? *Wildlife Australia*. 36(3): 39.
- Covacevich, J. A., Van der Duys, E. & Ashdown, R. 1999. Frogs of Queensland. Poster (Queensland Museum: Brisbane).
- Covacevich, J. A. & Couper, P. J. 1999. Preserves of Nature. An argument for museum collections. *Wildlife Australia*. 36(2): 13–18.
- Covacevich, J. A. 2000. Review of Goannas. The biology of varanid lizards. *Wildlife Australia*. 36(4): 46.
- Covacevich, J. A. 2000. Brigalow Belt Blues. *Wildlife Australia*. 36(4): 38.
- Couper, P. J. Schneider, C., Hoskin, C. & Covacevich, J. A. 2000. Australian Leaf – tailed geckos: phylogeny, a new genus, two new species and other new data. *Memoirs of the Queensland Museum*. 45(2): 253–265.
- Covacevich, J. 1999. Dangerous land snakes of Queensland. Inquiry Centre Leaflet Reptiles 1. (Queensland Museum: Brisbane).
- Covacevich, J. 2000. Reptiles & Amphibians of Australia. Review. *Wildlife Australia* 37(2): 35.
- Covacevich, J. 2000. Introduction. Pp. ix–xiii in Ryan, M. & Burwell, C. (eds) *Wildlife of Tropical North Queensland*. (Queensland Museum: Brisbane). 368pp.
- Couper, P., Covacevich, J., Janetzki, H & McDonald, K. 2000. Lizards. Pp. 203–233 In, Ryan, M. & Burwell, C. (eds). *Wildlife of Tropical North Queensland* (Queensland Museum: Brisbane). 368pp.

- Covacevich, J.A., Couper, P.J. & Amey, A.P. 2000. Snakes. Pp. 234–253 *In*, Ryan, M. & Burwell, C. (eds) *Wildlife of Tropical North Queensland* (Queensland Museum: Brisbane) 368pp.
- Covacevich, J.A., Buffett, A.F., Couper, P.J. & Amey, A.P. 2001. Herpetological foreigners on Norfolk Island, an External Territory of Australia. *Memoirs of the Queensland Museum* 46(2): 408.
- Covacevich, J. A., Couper, P. J. & Amey, P. A. 2002. Snakes. [www.qmuseum.qld.gov.au/features/snakes/](http://www.qmuseum.qld.gov.au/features/snakes/) (Queensland Museum: Brisbane).
- Covacevich, J. A. & Couper, P. J. 2002. Dead but not buried: A perspective on museum specimens and the conservation of frogs and reptiles in Queensland. Pp. 112–116 *In*, Franks, J.A., Playford, J & Shapcott, A. (eds) *Landscape Health of Queensland* (The Royal society of Queensland: Brisbane). 112–116.
- Couper, P. J., Covacevich, J. A., Amey, A. P. & Baker, A.M. 2006. The genera of skinks (Family Scincidae) of Australia and its island territories: diversity, distribution and identification. Pp. 367–383 *In*, Merrick, J. R., Archer, M., Hickey, G.M. & Lee, M.S.Y. (eds). *Evolution and Biogeography of Australasian Vertebrates*. (Auscipub Pty Ltd: Sydney). 942 pp.
- Wilson, S., Couper, P., Amey, A. & Covacevich, J. 2007. Land Snakes. Pp. 275–295 *In*, *Wildlife of Greater Brisbane* (2nd Ed). (Queensland Museum: Brisbane).
- Covacevich, J. 2010 Introduction to biodiversity studies at the Steve Irwin Wildlife Reserve, Cape York. *Queensland Naturalist* 48 (1/3): 3–5.
- Lyon, B. J., Couper, P. J., Amey, A., Roberts, L. J. & Covacevich, J. A. 2010. Frogs and Reptiles of the Steve Irwin Wildlife Reserve, Cape York. *The Queensland Naturalist* 48 (1–3) 13–21.
- Couper, P.J. & Covacevich, J. A. 2011. Envenomation by the poorly known elapid Black-striped Snake, *Cryptophis nigrostriatus*. *Queensland Naturalist* 49 (1–3): 21–22.
- Covacevich, J.A., Mulcahy, P.E., Roberts, L.J. & Shorcliff, K. 2012. Terrestrial vertebrates of the Starcke-Dharrba land, Cape York Peninsula. *Queensland Naturalist* 50(1–3): 9–16
- Covacevich, J. 1976. A nest constructed by wild pigs. *Victorian Naturalist* 93(1): 25–27.
- Baverstock, P.R., Hogarth, J.T., Cole, S.T. & Covacevich, J. 1976. Biochemical and karyotypic evidence for the specific status of the rodent *Leggadina lakedownensis* Watts. *Transactions of the Royal Society of South Australia* 100(2): 109–112.
- Covacevich, J. 1978. Museum visitor surveys: their value in Australian Museums. *Kalori* 54: 40–44.
- Covacevich, J.M. & Covacevich, J.A. 1978. Palms of northeastern Australia: I. Species recorded from Iron Range. *Principes* 22(3): 88–93.
- Covacevich, J.M., & Covacevich, J.A. 1980. Palms of north-eastern Australia II: Cooktown area. *Principes* 24(4): 154–61.
- Covacevich, J. 1981. The occurrence of the Nypa Palm, *Nypa fruticans*, in Australia. *Principes* 25(4).
- Covacevich, J. 1983. The Cocos Islands. *Wildlife in Australia* 20(1): 6–9.
- Covacevich, J. 1983. Delicate Mouse, *Pseudomys delicatulus*. P. 406 *In*, Strahan, R. (ed). *The Australian Museum Complete Book of Australian Mammals*. (Angus & Robertson: Sydney). 530pp.
- Covacevich, J. 1983. Lakeland Downs Mouse, *Leggadina lakedownensis*. P. 421 *In*, Strahan, R. (ed). *The Australian Museum Complete Book of Australian Mammals*. (Angus & Robertson: Sydney). 530pp.
- Powell, D. & Covacevich, J. 1983. Lister's Palm (*Arenga listeri*) on Christmas Island: a rare or vulnerable species? *Principes* 27(2): 89–93.
- Covacevich, J., Durbidge, E. & McInnes, J. 1984. Stradbroke in early maps. Ppp.81–99 in Coleman, R.J., Covacevich, J. & Davie, P. (eds). *Focus on Stradbroke Island and surrounding areas, 1974–1984*. (Boolarong Press, S.I.M.O.: Brisbane).
- Davis, G. & Covacevich, J. 1984. Aboriginal Walkway. Mapping a communication trail of the Yidinyji rainforest people of north-eastern Australia. *Wildlife Australia* (Winter): 8–10.
- Covacevich, J. 1985. A review of conservation prospects and problems for reptiles in Queensland. *Proceedings of APESCS 85* (The Scout Association of Australia).
- Covacevich, J., Irvine, A. & Davis, G. 1988. A rainforest pharmacopocia. Five thousand years of effective medicine. Pp. 159–174 *In*, J. Pearn (ed) *Pioneer Medicine in Australia*. (Amphion Press: Brisbane). 324pp.
- Covacevich, J. 1992. Epicentre or Outback? Pp. 3–13. *In*, Pearn, J. (ed). *Health, History and Horizons*. (Amphion Press: Brisbane). 423pp.
- Covacevich, J. & Pearn, J. 1994. Surgeons, sea and shore. European medical explorers and natural history - the first 200 years. Pp. 3–22 *In*, Pearn, J. (ed). *Outback Medicine. Some Vignettes*

## OTHER PAPERS

- Covacevich, J. & Vernon, D.P. 1972. Queensland Hairynosed Wombat, *Lasiorhinus baueri* Longman 1939 in *The Red Data Book* (Morges: Switzerland).
- Covacevich, J. 1973. Vertebrate remains in Haglund-Calley, L. & Quinnell, M.C. A., Shell midden at Cascade Gardens, Broadbeach, south-east Queensland. *Memoirs of the Queensland Museum* 16(3): 399–409.

- of *Pioneering Medicine*. (Amphion Press: University of Queensland, Royal Children's Hospital: Brisbane). 366pp.
- Covacevich, J. 1995. Stradbroke Island. The Convict era of 1825-1853. In, Pearn, J. & Carter, P. (eds) *Islands of Incarceration* (Amphion Press: Brisbane) 122pp.
- Covacevich, J.A., Ogilvie, A. & Walker, F. 1996. 'Stone walls do not a prison make ...'. Portraits of prisoners on North Stradbroke Island, Australia. Pp. 39-45 in Covacevich, J.A., Pearn, J.H., Case, D., Chapple, I. & Phillips, G. (eds) *History, Heritage and Health: Proceedings of the Fourth Biennial Conference of the Australian Society of the History of Medicine*. (Australian Society of the History of Medicine: Brisbane). 439pp.
- Covacevich, J. 2000. Respite for a reef. A Norfolk success story. *Wildlife Australia* Spring 2000: 40-41.
- Covacevich, J.A. 2001. Mine field of emotion. Letter to the Editor. *Wildlife Australia* 38(2): 33.
- Covacevich, J.A. 2002. First formal Australian record of a Tree Kangaroo: Aboriginal, not European. *Aboriginal History*. 26: 220-222.
- Roberts, L. & Covacevich, J. 2010. Orchids of the Steve Irwin Wildlife Reserve, Cape York Peninsula. *Queensland Naturalist* 48 (1/3): 33-35.
- Covacevich, J.A. A naturalist born, made or both? 2013. *Queensland Naturalist* 51 (1/2/3): 3-4.
- Covacevich, J.A. 2014. "He learned to look at nature" Lewis John Roberts, OAM: Bushman and born naturalist. *Queensland Naturalist* 52 (4/5/6): 61-74.
- PAPERS PRESENTED TO NATIONAL & INTERNATIONAL CONFERENCES**
- The Reptiles of Stradbroke Island*. Royal Society of Queensland Conference on North Stradbroke Island, near Brisbane, 15-17 June 1974. (Covacevich, J.).
- Australia's most dangerous snakes*. Centenary International Paediatric Conference, Royal Children's Hospital, Brisbane, 20-25 August 1978. (Covacevich, J.).
- Reports of three cases of snake-bite in childhood, including a life-threatening case, with recovery*. Centenary International Paediatric Conference, Royal Children's Hospital, Brisbane, 20-25 August 1978. (De Buse, P., Pearn, J. & Covacevich, J.).
- Snakebite paralysis*. Australian College of Paediatrics Annual Scientific Meeting; Canberra, 2-4 May 1979. (Patten, B., De Buse, P., Pearn, J., Burke, J., Covacevich, J. & Sutherland, S.).
- The relationship of Oxyuranus microlepidotus (the Western Taipan) and O. scutellatus (the Coastal Taipan)*. The Melbourne Herpetological Symposium of the Australian Society of Herpetologists, 19-21 May 1980, Melbourne. (Covacevich, J., McDowell, S.B., Tanner, C. & Mengden, G.A.).
- The significance of the reptiles of Australia's Cape York Peninsula and their conservation*. 2nd World Wilderness Congress, Cairns, May 1980. (Covacevich, J.).
- Distribution and identification of Australia's dangerously venomous snakes*. Australian College of Physicians Scientific Meeting, Brisbane, September 1980. (Covacevich, J.).
- Snake identification and the suspected snakebite case*. Australian College of Paediatrics Annual Scientific Meeting, Surfers Paradise, 18-20 May 1983. (Morrison, J.J., Pearn, J.H., Nixon, J.J. & Covacevich, J.A.).
- Stradbroke in early maps*. Royal Society of Queensland Symposium on North Stradbroke Island and surrounding areas, 11-12 August 1984. (Covacevich, J., Durbidge, E. & McInnes, J.).
- Plants and animals of Stradbroke of significance to planners*. Royal Society of Queensland Symposium on North Stradbroke Island and surrounding areas, 11-12 August 1984. (Covacevich, J.).
- Review of conservation prospects and problems for Australia's reptiles*. 1st AsiaPacific Environmental Conservation Seminar, Erapah, Brisbane, 21-28 September 1985. (Covacevich, J.).
- The world's most venomous snake*. Australian Bicentennial Medical Congress, Cairns, 27 August - 5 September 1988. (in the Dr Jack Barnes Memorial Symposium of Medical Toxinology). (Covacevich, J.).
- A rainforest pharmacopoeia. Five thousand years of effective medicine*. Australian Bicentennial Medical Congress, Cairns, 27 August - 5 September 1988. (Covacevich, J., Irvine, A. & Davis, G.).
- Australia's Dangerous Snakes*. Australian Bicentennial Conference, North Queensland Medical Conference, Cairns, 27 August - 5 September 1988. (Covacevich, J.).
- Miocene dragons from Riversleigh: new data on the history of the family Agamidae (Reptilia: Squamata) in Australia*. Australian Bicentennial Herpetological Conference, 17-20 August 1988. (Covacevich, J. & Couper, P.).
- Mapping traditional Aboriginal trade routes in the rain forest of north Queensland*. North Queensland Medical Conference, Cairns, 27 August - 5 September 1988. (Covacevich, J.).
- Taipans*. Australian and Pacific Police Medical Officer's Conference, Brisbane, 2 June 1988. (Covacevich, J.).
- Australia's medically significant snakes*. Toxins 89 Conference, Mt Tamborine, 29 September - 1 October 1989. (Pearn, J.H. & Covacevich J.A.).

- Australia's dangerously venomous snakes.* Australian College of Dermatology Conference, Southport, 3 May 1990. (Covacevich, J.).
- Plangs and Physic: 40,000 years of risky business.* North Queensland Medical Conference, Mackay, 1990. (Covacevich, J.).
- Epicentre or Outback? Perspectives on the earliest medical practice in Australia.* North Queensland Medical Congress, Rockhampton, 26 September 1992. (Covacevich, J.).
- Reptiles of Australia's Wet Tropics rainforest* World Wildlife Fund, Wet Tropics Workshop, Cairns, 1-3 August 1992. (Covacevich, J.).
- Report on Queensland's disappearing frogs.* Taxon Advisory Group, International Herpetological Symposium, Miami, U.S.A., 17-21 June 1993. (Covacevich, J.).
- Snakebite first aid and medical treatment - a global perspective,* International Herpetological Symposium, Miami, U.S.A., 17-21. Open forum. June 1993. (Covacevich, J., with Ayerbe, S., Minton, S. & de Silva, A.). *Taxonomic and natural history of Oxyuranus microlepidotus, the world's most dangerous snake.* International Herpetological Symposium, Miami, U.S.A., 17-21 June 1993. (Covacevich, J.).
- Rainforest reptiles of Australia's Wet Tropics.* International Herpetological Symposium, Miami, U.S.A., 17-21 June 1993. (Covacevich, J.).
- Rapt in Reptiles - if not, why not?: taxonomy and nomenclature are far from boring.* Nature Search 2001 Conference, Maroon Dam, Ipswich, 24 October 1993. (Covacevich, J.).
- Australia's Snakes.* International Conference on Toxicology in Clinical Chemistry, Brisbane, 23 November 1993. (Covacevich, J.).
- A new genus and species (Sphenomorphus group) from Australia's dry rain forests.* 2nd World Congress in Herpetology, Adelaide, 29 December 1993-6 January 1994. (Covacevich, J. & Couper, P.).
- New data on Australia's Leaf-tailed Geckos.* 2nd World Congress in Herpetology, Adelaide, 29 December 1993 - 6 January 1994. (Couper, P. & Covacevich, J.).
- Snakebite in herpetologists.* 2nd World Congress in Herpetology, Adelaide, 29 December 1993 - 6 January 1994. (Pearn, J.H., Covacevich, J.A., Charles, N. & Richardson, P.).
- Snakebite, a preventable injury* St John Ambulance Conference "Youth in Focus", Brisbane, 23-24 June 1994. (Covacevich, J.).
- Snakes: friends & foes.* St John Australasia and South East Asia regional seminar International Seminar, Gold Coast/Brisbane, 15-16 October 1994. (Covacevich, J.).
- 'Where have all the flowers gone?...' Declines in vertebrate diversity on the Darling Downs since 1827* Royal Queensland Historical Society Conference, Killarney, 22 October 1994. (Covacevich, J.).
- Surgeons Sea & Shore. Contributions of early medical practitioners to natural history: the first 150 years* North Queensland Medical Conference, Townsville, 24-25 September 1994. (Covacevich, J. & Pearn, J.H.P. - presented by Pearn, JHP).
- The reptiles of Moreton Bay.* Royal Queensland Historical Society Conference, Coochie Mudlo Is. 28 May, 1995 (Covacevich, J.).
- 'Stone walls do not a prison make ...'. Portraits of prisoners on North Stradbroke Island, Australia.* Biennial scientific conference of The Society of the History of Medicine/Mutiny and Medicine, Norfolk Is., 2-9 July, 1995. (Covacevich, J., Ogilvie, A. & Walker, F. - presented by JAC).
- Lerista allanae: 60 years from exhibition to extinction?* 14 October, 1995, 'History of Natural History', Royal Society of Queensland Conference (Covacevich, J., Couper, P. & McDonald, K.).
- Realities in the Biodiversity Holy Grail: prospects for reptiles in Queensland's Brigalow Biogeographic Region.* 18 November, 1995. Presidential Address, The Royal Society of Queensland (Covacevich, J.).
- Is biodiversity maintenance in Queensland's Brigalow Belt just another oxymoron?* 6 February, 1996. Conservation outside nature reserves, a conference to look at nature conservation in landscapes managed primarily for other uses. Sponsored by Australian Nature Conservation Agency, QDOE et al., hosted by Centre for Conservation Biology, The University of Queensland. (Covacevich, J., Couper, P. & McDonald, K.).
- Reptiles of the rainforests of Australia's Wet Tropics: distributions and conservation.* 4 September, 1996. World Heritage Tropical Forests Conference (hosted by the Wet Tropics Management Authority with the Co-operative Research Centre for Tropical Rainforest Ecology and Management) Cairns. (Covacevich, J., Couper, P. & McDonald, K.).
- Reptiles lost and found: a 25 year audit for southeastern Queensland, Australia* 2/11/1996. Forests Conference, Gympie/organised by the Department of Environment, Queensland (Covacevich, J.).
- Reptiles diversity maintenance: lessons from the rainforests and open forests of Australia'. 8 August, 1997. 3rd World Congress in Herpetology, Prague (2-10/8/97) (Covacevich, J.).*
- Preserved to conserve: herpetological collections of the Queensland Museum and biodiversity conservation Landscape Health conference.* Royal Society of Queensland 17/11/2000. (Covacevich, J. & Couper, P.).



## REPORTS

- Covacevich, J. 1974. The frogs and reptiles of the islands of Moreton Bay and of a narrow coastal strip between Noosa and Tweed Heads in Central Management Investigation Queensland - New South Wales border to northern boundary of Noosa Shire. (Co-ordinator General's Department: Brisbane).
- Covacevich, J. 1975. Amphibians and Reptiles of Normanby River Basin, for inclusion in a thesis by Mr J. Harris, Department of Geography, University College, London.
- Covacevich, J. 1976. Amphibians and Reptiles in Fauna of eastern Australian Rainforests I: Preliminary Report on sites surveyed by the Queensland Museum in mid-eastern and north-eastern Queensland. (Queensland Museum: Brisbane).
- Covacevich, J. (ed) 1977. Fauna of Eastern Australian Rainforests II. Preliminary report on site surveyed by the Queensland Museum in southeastern and far north eastern Queensland with additional results from sites surveyed previously in north eastern Queensland. (Queensland Museum: Brisbane).
- Covacevich, J. 1977. Frogs and Reptiles, (in reference above.)
- Covacevich, J. 1978. Design implications for the new Queensland Museum. Extrapolations from the 1977 Visitor Survey. Report to the Trustees, Queensland Museum.
- Martin, J. & Covacevich, J. 1978. Impacts on the vertebrate fauna and landscape of North Stradbroke Island of the proposed road link to the island. Report for the Director, National Parks and Wildlife Service, Brisbane.
- Covacevich, J. & McDonald, K.R. 1984. Frogs and reptiles of eastern Australian rainforests: distribution patterns and conservation, pp.360-383 In, G L Werren & A.P. Kershaw (eds), 'Australian National Rainforest Study Report to the World Wildlife Fund (Australia) Volume 1. Proceedings of a workshop on the past, present and future of Australian rainforests, Griffith University, December 1983'. (Geography Department, Monash University for the Australian Conservation Foundation: Melbourne).
- Covacevich, J. 1985. A review of conservation prospects and problems for reptiles in Queensland. (Proceedings of APECS 85: The Scout Association of Australia).
- Covacevich, J. 1992. Queensland Museum loans for education and public display: an examination of product, pitfalls and prospects of the service. A review. (for the Director, Queensland Museum, 24 December, 1992).
- Covacevich, J.A. & Couper, P.J. 1994. Reptiles of the Wet Tropics Biogeographic Region: Records of the Queensland and Australian Museums, with analysis. Report to the Wet Tropics Management Authority.
- Covacevich, J.A. 1996. Queensland Museum Photographic Section: Review of problems and suggested solutions. Unpublished report to the Director.
- Covacevich, J.A., Couper, P.J. & McDonald, K.R. 1996. Reptiles of Queensland's Brigalow Biogeographic Region: distributions, status, conservation. (Report to ANCA, Canberra).
- Covacevich, J.A., Couper, P.J. & Janetzki, H. 1997. Report on Study Brief 1.5 Biodiversity PNG-Queensland Gas Pipe Line: Reptiles Report (unpublished) prepared for Chevron (South Pacific Chevron Co.) Box 3117, GPO Brisbane 4001, Australia) 132pp.
- Covacevich, J.A. & Couper, P.J. 1998. Frogs and reptiles in Covacevich, J. A. (Compiler). Most significant areas for phylogenetically distinct, relict and/or disjunctly - distributed insect, freshwater fish, frog, reptile, bird and mammal species of south-eastern Queensland. Report prepared The Environment Forest Task force, Environment Australia, GPO Box 787, Canberra ACT 2601.
- Covacevich, J.A., 1999. Reptiles of Timor. Report to Surgeon General J. H. Pearn, Australia Defence Forces for Timor Deployment.

## CITATIONS FOR EPONYMIC SPECIES

- Terriswalkerius covacevichae* Jameson, 1994 - an earthworm from the rainforests of north-eastern Queensland (Mt Fisher). *Memoirs of the Queensland Museum* 37(1), p.162.
- Zophorame covacevichae* Raven, 1994 - a mygalomorph spider from north-eastern Queensland. *Memoirs of the Queensland Museum* 35(2), p.575.
- Pseudophryne covacevichae* Ingram & Corben, 1994 - a frog from near Ravenshoe, north-eastern Queensland. *Memoirs of the Queensland Museum* 37(1), p.267.
- Kababina covacevichae* Todd Davies, 1995 - an amphinectid (spider) from Shipton's Flat, north-eastern Queensland. *Memoirs of the Queensland Museum* 38(2): 463-469, p.467.
- Oedura jacobae* Couper, keim & Hoskin, 2007 - a velvet gecko from south-eastern Queensland. *Zootaxa* 1587: 27- 41.

## ACKNOWLEDGEMENTS

We thank Meg Lloyd for helping to compile the publications list. Bruce Campbell, Anne McClelland and John Pearn for their helpful advice.





# Wenlock and Ludlow (Silurian) rugose corals from the type section of the Jack Formation, Broken River Province, northeast Queensland

T.J. MUNSON

Northern Territory Geological Survey, PO Box 3000, Darwin NT 0801; Email: tim.munson@nt.gov.au

J.S. JELL

School of Earth Sciences, The University of Queensland, St Lucia Qld 4072

Citation: Munson, T.J. & Jell, J.S. 2016. Wenlock and Ludlow (Silurian) rugose corals from the type section of the Jack Formation, Broken River Province, northeast Queensland. *Memoirs of the Queensland Museum – Nature* 59: 273–320. ISSN 2204–1478 (online), ISSN 0079–8835 (Print). Accepted: 6 November 2015. First published online: 13 May 2016.

<http://dx.doi.org/10.1082/j.2204-1478.59.2016.2016-06>

LSID urn:lsid:zoobank.org:pub:72DCFE9C-860A-4649-96F5-B250E7223FE8

## ABSTRACT

The Jack Formation forms part of the Silurian Graveyard Creek Group within the Graveyard Creek Subprovince in northeast Queensland. The formation comprises alternating intervals of carbonate and siliciclastic rocks deposited in a shallow-marine setting. It is very fossiliferous at a number of levels, and contains numerous species of conodonts, rugose and tabulate corals, stromatoporoids, trilobites, brachiopods, crinoids, low-spined gastropods, molluscs, other invertebrates, microvertebrates, and algae. Conodont data indicate that the succession is Wenlock to Ludlow in age at the type section along the Broken River in the Jack Hills Gorge area. Fourteen rugose coral species and one subspecies, referable to eleven genera, are described from the type section of the Jack Formation. New taxa described are *Aphyllum pachystele* sp. nov., *Pycnostylus polyphyllodus* sp. nov., *Multicarinophyllum vepreculatum* sp. nov., *Dokophyllum hilliae* sp. nov., *Vesicospina julli* gen. et sp. nov. and *Ptychophyllum variatum* sp. nov. The rugose coral fauna shows a high degree of endemism with only four species recorded outside the Broken River Province. Within eastern Australia, it is comparable with a Gorstian to early Ludfordian fauna of the Yass district, New South Wales (3 species in common), and 1–2 species are also shared with coral faunas from other Silurian localities in New South Wales, Victoria and Tasmania. At the species level, there is very little in common with overseas faunas. □ Broken River Province, Jack Formation, north Queensland, Silurian, Wenlock, Ludlow, Rugosa, taxonomy, Tryplasmataceae, Cystiphyllidae, Pycnostylidae, Mucophyllidae, Amsdenoididae, Entelophyllidae, Ketophyllidae, Kyphophyllidae, Ptychophyllidae.

The Broken River Province (Arnold & Henderson 1976) is a southwest-trending wedge of Cambrian–Ordovician to Permian rocks, located to the west of Townsville in northeastern Queensland. It can be divided into two subprovinces, each with a different history of sedimentation, igneous activity, and deformation, which are separated by a major dislocation, the Gray Creek Fault (Arnold & Henderson 1976;

Arnold & Fawcckner 1980; Withnall & Lang 1993). Recognition of the two subprovinces is based on the distinct sedimentary and structural histories of the Silurian and Devonian successions, which occupy the greater part of the province. In the more westerly Graveyard Creek Subprovince (Fig. 1), these rocks form a generally shallow-marine sedimentary succession that contains richly fossiliferous intervals and

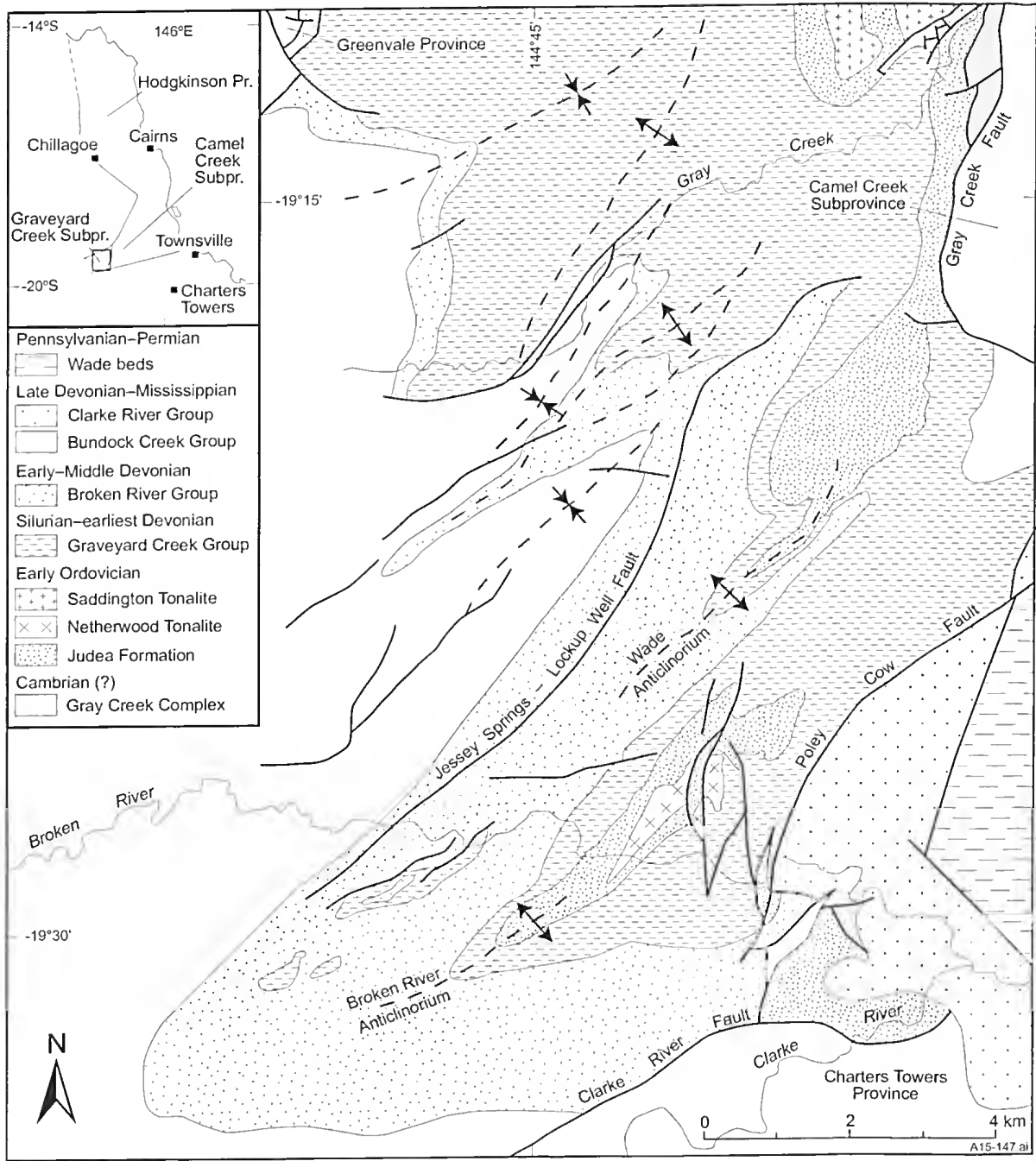


FIG. 1. Simplified solid geology map showing the distribution of the Graveyard Creek Group and the main structural features southwest of the Gray Creek Complex. Cenozoic volcanic and sedimentary covering rocks not shown (redrawn and slightly modified from Henderson & Withnall 2013).

has been deformed by a single phase of upright folding. In the Camel Creek Subprovince to the east, they form a generally deep-marine, turbiditic succession, which is very sparsely fossiliferous and multiply deformed. The Silurian–Devonian successions of the Broken River Province constitute the southern part of the Mossman Orogen (Henderson *et al.* 2013), which also incorporates successions of similar age in the Hodgkinson Province to the north. They unconformably overlie Neoproterozoic–Ordovician rocks assigned to the Thompson Orogen and are unconformably overlain by Upper Devonian–Mississippian rocks of the Bundock and Clarke River basins. A recent summary of the geology of the Broken River Province is in Henderson & Withnall (2013), and the following description is largely derived from this source, except where indicated.

Silurian strata in the Graveyard Creek Subprovince are included within the upper Lower Silurian–middle Lower Devonian Graveyard Creek Group (White 1959a; Withnall *et al.* 1988; Henderson & Withnall 2013). This group is exposed in two main outcrop tracts separated by younger Paleozoic sedimentary rocks and Cenozoic basalt. It unconformably overlies the Lower Ordovician Judea Formation, and is paraconformably overlain by the uppermost Lower to lowermost Upper Devonian Broken River Group (Fig. 1). The Graveyard Creek Group contains siliciclastic and carbonate sedimentary rocks that form a complex facies mosaic ranging in thickness from as little as 150 m to greater than 5000 m. The group has been subdivided into a number of formations; in ascending stratigraphic order, these are the Crooked Creek Conglomerate, Quinton Formation and laterally equivalent Poley Cow Formation, Jack Formation, Ralph Flint Formation and Shield Creek Formation. The geology of these formations was summarised by Henderson & Withnall (2013), who referenced more detailed previous studies. Mapping coordinates use the Universal Transverse Mercator (UTM) grid system.

In the Broken River area, in the south of the Graveyard Creek Subprovince, the Graveyard Creek Group outcrops on both limbs of a large

southwesterly plunging anticline (Fig. 2). It is well exposed along the banks of the Broken River on the western limb of the anticline, where it reaches a maximum thickness of about 1300 m. A thin (30 m) interval of Crooked Creek Conglomerate forms the base of the succession in this area. This is overlain by a 750 m-thick succession of conglomerate, siltstone, and greywacke (Poley Cow Formation), followed by the mixed carbonate–siliciclastic Jack Formation, with a thin interval of Shield Creek Formation on top. North of the Broken River, the Ralph Flint Formation occurs between the Jack and Shield Creek formations, but lenses out just to the north of the river section (Talent *et al.* 2002).

The Jack Formation is richly fossiliferous at various stratigraphic levels, and Munson (1979) provided descriptions of the rugose coral fauna from the type section that are formally described herein.

## JACK FORMATION

The Jack Formation (Withnall & Lang 1993) is restricted to the southern outcrop area of the Graveyard Creek Group. It was originally defined by White (1959a) as the Jack Limestone Member of the Graveyard Creek Formation and was given formation status by Withnall *et al.* (1988). Limestones within the formation outcrop on the limbs and noses of a number of anticlines, including the type area near Jack Hills Gorge and a relatively well studied area to the southeast, near the road crossing of the Broken River (Fig. 2). Further to the southwest of these areas, in the vicinity of the Broken River Anticlinorium, limestones are absent and the formation becomes entirely siliciclastic (Talent *et al.* 2002); the succession in this area is not well studied. The formation overlies the siliciclastic Poley Cow Formation with apparent conformity, but the contact possibly interfingers. It is overlain by thinly bedded shale and fine-grained sandstone with thin interbedded calcarenite of the middle Lochkovian Ralph Flint Formation along a disconformable erosive contact (Talent *et al.* 2002), or where the Ralph Flint Formation is

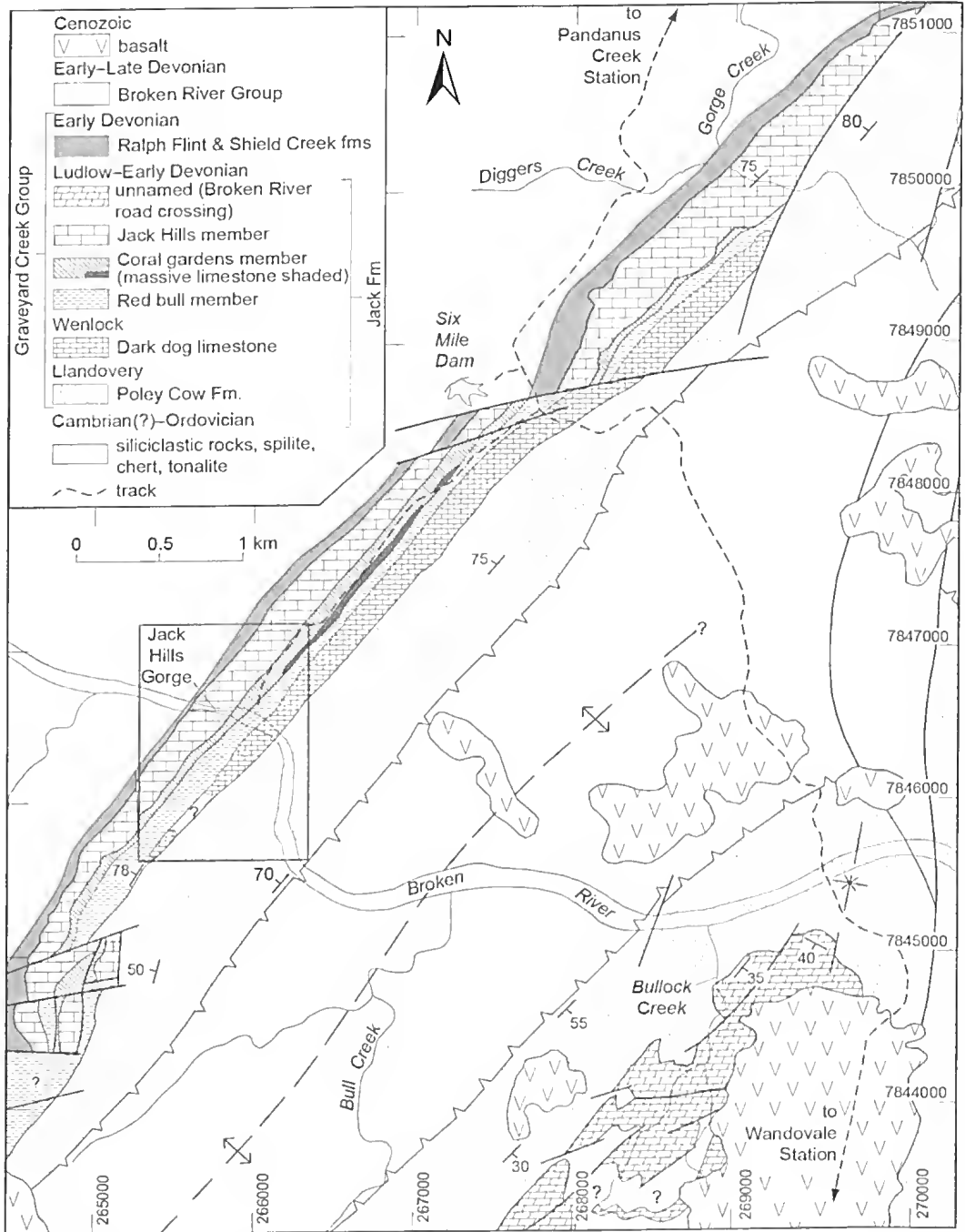


FIG. 2. Solid geology map of the Jack Formation in vicinity of the Broken River, showing the distribution of informal members. Box shows location of Fig. 5.

absent, by the disconformable Lower Devonian Shield Creek Formation. In the north of the Graveyard Creek Subprovince, it is possible that the Ralph Flint Formation might be at least in part a facies equivalent of the Jack Formation, at the level of the Magpie Creek Limestone Member.

**Fossil Assemblages.** The Jack Formation is very fossiliferous and conodonts, rugose and tabulate corals, stromatoporoids, trilobites, brachiopods, crinoids, low-spined gastropods, molluscs, other invertebrates, microvertebrates, and algae are locally abundant and many have been listed or described in previous studies. General summaries of the fossil assemblages with references to previous work and their biostratigraphic and palaeogeographic significance were reported by Jell *et al.* (1993), Talent *et al.* (2002) and Caldon (2003). The Coral gardens member passes through a significant mid-Ludlow global extinction event (Lau Event), the significance of which was discussed in detail by Caldon (2003), Talent *et al.* (2002) and Jeppsson *et al.* (2007, 2012).

Systematic descriptions and biostratigraphic summaries of the conodont faunas include Telford (1972), Simpson (1983 1995a, b, 1998a, 2000), Sloan *et al.* (1995) and Jeppsson *et al.* (2007, 2012). Other microfossils recovered from the formation include foraminifera, algae, sponge spicules, byroniids, and acanthodian and phyllocarid remains (Simpson 1994; Burrow & Simpson 1995).

The macrofossils have been listed in numerous studies, but only a few have been described. Several species of stromatoporoids were described by Webby & Zhen (1997) and a number of species of trilobites from the Coral gardens beds were identified by PA Jell and listed in Savory (1987). Lists of the coral species were included in White & Wyatt (1960), Hill (1965), Arnold & Henderson (1976) and Jell *et al.* (1993). Hill *et al.* (1969) illustrated and tentatively identified corals and other fossils from the type section.

**Succession in Type Section.** The type section is located in the Jack Hills Gorge on the Broken River, from ca. 266160mE 7845450mN (base) to ca. 265560mE 7845680mN (top) within the Clarke

River 1:250 000 (SE55-13) and Burges 1:100 000 (7859) mapsheets. In this area (Fig. 2), the formation forms part of the northwesterly limb of a large, southwesterly plunging anticline. The succession within the type section comprises about 580 m of limestone, sandstone and shale (Withnall 1989; Withnall *et al.* 1993). Thicker limestone lenses tend to be bluff-forming, resulting in a karst topography, whereas siliciclastic intervals and thinner carbonate intervals are more recessive. The succession can be subdivided into four conformable carbonate and siliciclastic intervals that can be mapped for several kilometres along strike on both sides of the river until they are truncated by faults at both ends of the outcrop tract (Munson 1979; Jeppsson *et al.* 2007; Fig. 2).

Jeppsson *et al.* (2007) raised the Jack Formation to group status (and by necessity, Graveyard Creek Group to a supergroup) and considered the four stratigraphic intervals in the type section to be formations within this group; in ascending stratigraphic order, the 'Dark Dog Limestone', 'Red Bull Formation', 'Coral Gardens Formation' and 'Jack Hills Formation'. The 'Coral Gardens Formation' was further subdivided into informal numbered members 1–4, based on data from a detailed traverse along the type section. Jeppsson *et al.*'s nomenclature has not been adopted generally, as the formation names were not formally defined, the 'formations' be recognised only within the vicinity of the Jack Hills, and, with the exception of the 'Jack Hills Formation', recognised geographic names were not used. A broadly defined Jack Formation has therefore been retained in subsequent studies (e.g. see Henderson & Withnall 2013), with its constituent 'formations' being regarded as informal members. This schema is followed herein. A formal revision of the nomenclature, as proposed by Jeppsson *et al.* is beyond the scope of the present study.

**Dark dog limestone.** The Dark dog limestone is ca 100 m thick where it is cut by the river, thickens to a maximum of 120 m further to the northeast, and decreases to 50 m at its southern extremity. This unit consists of generally massive or thickly bedded, partly dolomitised lime mudstone and minor lime wackestone, and extends for about

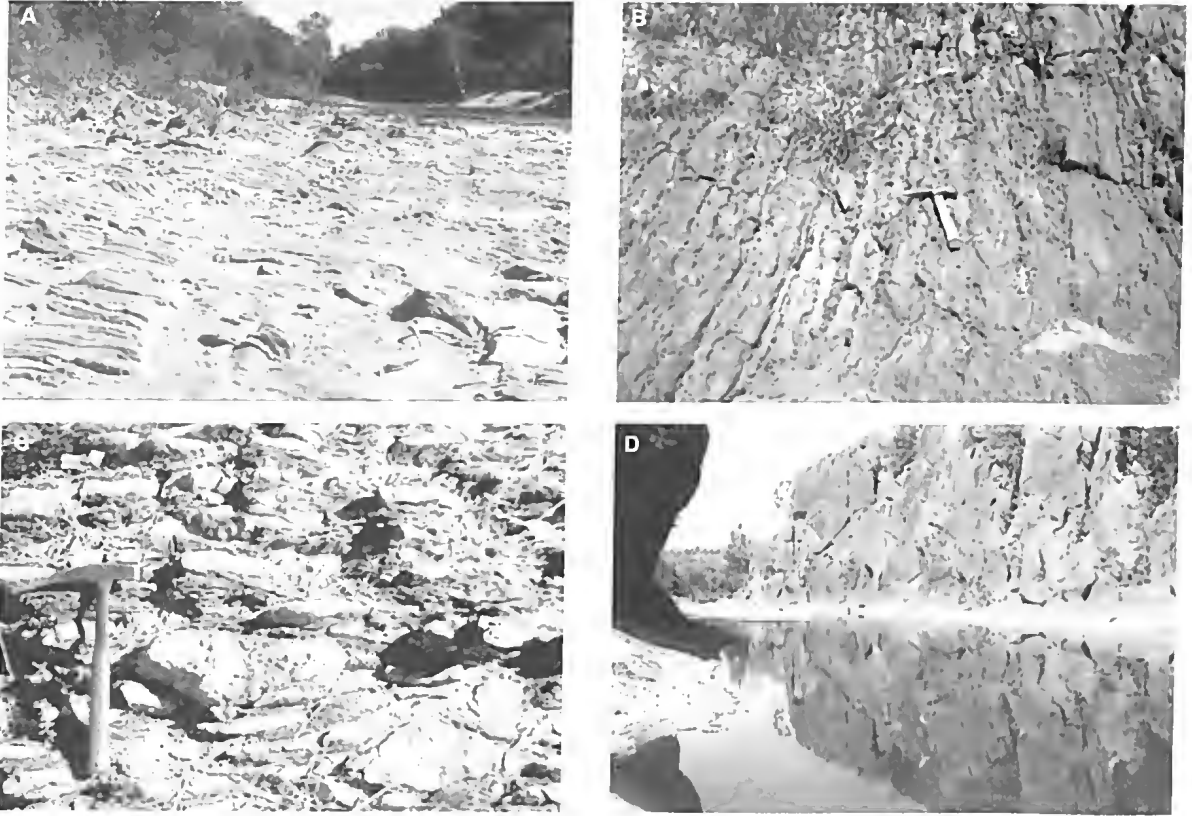


FIG. 3. Jack Formation limestones. A, View northwest (down-dip) of massive to thickly bedded Dark dog limestone exposures in the Broken River, with the Jack Hills Gorge in background. Apparent thin bedding in the image is a solution weathering effect (266100mE 784543mN); B, Thinly bedded fossiliferous limestone at the top of Dark dog limestone on the south bank of Broken River (266010mE 7845460mN); C, Interbedded nodular limestone and shale of the Coral gardens member, showing coral heads in growth position. Corallum of *Entelophyllum patulum yassense* to the right of the hammer; a tabulate coral corallum in the lower right of image (UQL4009); D, Jack Hills Gorge, showing massive bluff-forming limestone of the Jack Hills member. View east from 265520mE 784571mN.

5 km along strike as low-relief strike ridges and rocky pavements, mostly to the northeast of the Broken River (Fig. 3A). Although the bedding in the unit is poorly defined, it is evident through layers rich in skeletal debris, by the orientation parallel to the bedding of elongate fossils, particularly of the rugose coral *Pycnostylus*, and by stromatoporoids in growth position. Thin lenticular interbeds of calcareous siltstone occur at the base and top of the unit and the uppermost 15 m in the Broken River section is well bedded and relatively fossil-rich (Fig. 3B). The member is stylolitic, and towards the top of the unit, microstylolites are common,

forming an irregular network through the limestone; this indicates post-consolidation loss of an unknown thickness of rock.

The lower 50–60 m of the Dark dog limestone is characterised by large bivalve molluscs that reach 20 cm in length and are commonly in growth position. These are observed only in section, and are not readily identifiable; they were referred to the Megalomoidea by Jeppsson *et al.* (2007). Small solitary rugose corals, tabulate corals, small stromatoporoids, pentamerid brachiopods, bryozoans, crinoids, pelecypods, ostracodes and gastropods occur throughout the unit, but are most common in

the upper, more thinly bedded limestones. Withnall *et al.* (1993) also reported the alga *Wetheredella* as oncolites from these beds. Several species of tabulate corals, illustrated by Hill *et al.* (1969), include *Barrandeolites* sp. cf. *bowerbanki* Milne-Edwards & Haime 1851, and species of *Favosites*, *Multisolenia* and *Diplopora*. An unidentified multiserial halysitid is also present at the top of the unit. Stromatoporoids, illustrated by Hill *et al.* (1969) and described by Webby & Zhen (1997) include *Ecclimadictyon* cf. *magnum* Nestor 1976 and an undescribed species of *Simplexodictyon*.

The hard, light to dark grey limestone consists dominantly of micrite, pelmicrite and biomicrite that has been finely recrystallised by aggrading neomorphism. At the top of the unit, the limestone is commonly impure, containing detrital and secondary grains of quartz, and rare feldspar and muscovite. Biogenic allochems within the limestone include corals, disarticulated crinoid ossicles, medium-spined gastropods, brachiopods, and bryozoans.

**Red bull member.** Overlying the basal Dark dog limestone is a 165 m thick, red to purple, deeply weathered recessive succession, consisting of soft, friable conglomerate, fine to coarse micaceous quartz sandstone and siltstone. Exposures are poor and generally confined to gullies and washouts. Coarser lithologies are found towards the base of the unit, which has an overall fining-upward trend. Beds are 15 cm–2 m thick and are commonly normally graded. At the top of the Red bull member (at locality UQL4329; Fig. 4) is an interval of very weathered siltstone and rarer fine sandstone that contains thin fossil-rich layers with fragmented, iron-stained casts and moulds of decalcified brachiopods and trilobites including an ecrinurine (Munson 1979). Concretions and ferruginous staining along joints are common in these beds.

**Coral gardens member.** This is a heterolithic unit consisting of siltstone, thinly interbedded siltstone and limestone, lesser thickly bedded to massive limestone, and minor oolitic and oncolitic limestone. It is ca 80 m thick in the type section of the formation along the Broken River (Jeppsson *et al.* 2007) and has a strike

length of ca 6.5 km (Fig. 2). Exposures are generally recessive and form low pavements of steeply dipping beds, commonly covered by soil or scree, except for a more thickly bedded to massive lime mudstone lens at the base of the unit to the northeast of the type section that tends to be bluff-forming; this lens is about 1700 m in length and reaches a maximum thickness of about 35 m (Fig. 2).

Jeppsson *et al.* (2007) measured a section through this unit along the type section of the Jack Formation, on the banks of the Broken River, which was sampled for conodonts and C, O and Sr isotopes. They recognised and numbered 4 informal 'members'.

The Coral gardens member commences with a few metres of dark grey to grey-brown, calcareous quartz siltstone and fine micaceous sandstone, succeeded by a thick interval of thinly interbedded siltstone and limestone. The contact is transitional, marked by the appearance of infrequent thin lenses of light to dark grey limestone that become more closely spaced over a distance of a few metres up-section. This interval is equivalent to members 1 and 2 of Jeppsson *et al.* (2007).

The thin, lenticular or nodular limestone layers of 'Member 2' of Jeppsson *et al.* (2007) average 4–7 cm, rarely 10 cm or more, in thickness, and are separated by 1–10 cm of siltstone (Fig. 3C). Much of this succession is very fossiliferous, and is characterised by abundant coral heads (Munson 1979; Caldon 2003) and stromatoporoids (Webby & Zhen 1997) in growth position, hence known colloquially as the 'coral gardens'. Commonly, tabulate corals in growth position pass through and interfinger laterally with several layers of siltstone. The siltstones appear to have, partially smothered the corals, which expanded again once they had grown above the sediment–water interface. A similar relationship is found with stromatoporoids, and to a lesser extent with colonial rugosans. Thinning and upturning of sediments against, and depression of sediments beneath coral heads and stromatoporoids were probably caused by post-depositional compaction. The limestone comprises recrystallised impure

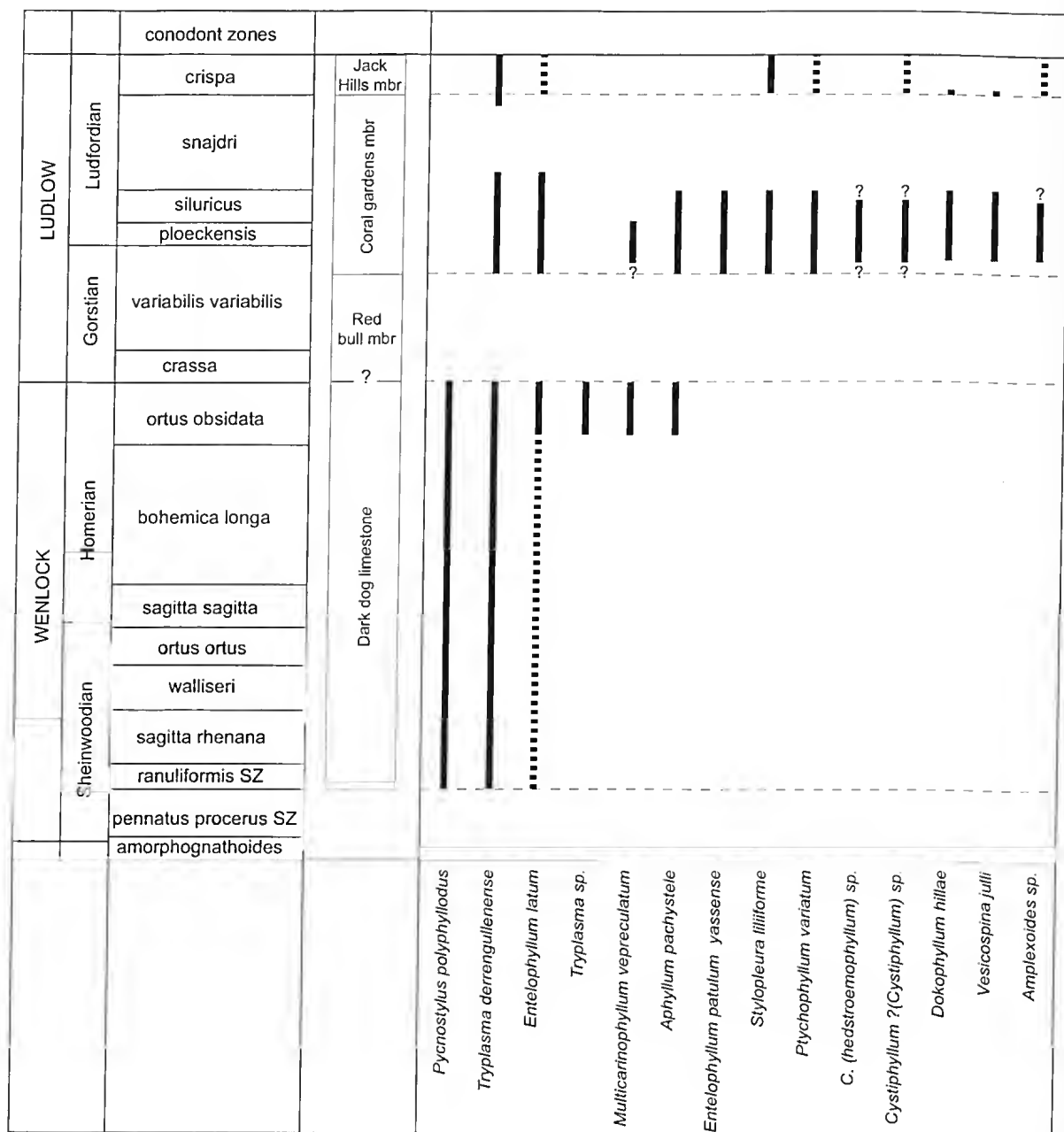


FIG. 4. Biostratigraphic distribution of rugose coral species in the vicinity of the type section of the Jack Formation, incorporating data from all localities (see Appendix 1, Fig. 5). Dashed lines indicate probable *in-situ* occurrence. Conodont zones generated from TSCreator software (<http://www.tcreator.org>), based on geological timescale in Gradstein *et al* (2005). Stratigraphic column not to scale.



micrite and biomicrite, with abundant fine grains of quartz and less common muscovite. Allochems comprise 5–40% of the limestone and in some cases have syntaxial replacement rims; the majority consist of skeletal fragments, mostly less than 5 mm in diameter.

Towards the top of the nodular limestone sequence, siltstone layers become thinner and less abundant, eventually giving way to a more prominently exposed interval of micritic limestone, 8 m thick on the north bank of the river, with 5–10 cm-thick beds that are crudely defined by stylobedding and layers of skeletal debris. This limestone is broadly equivalent to 'Member 3' of Jeppsson *et al.* (2007). It differs petrographically from the underlying unit in having larger more abundant skeletal allochems and fewer siliciclastic grains. Brachiopods, gastropods, crinoids and ostracodes are common, but corals are rare, except as abraded fragments. Jeppsson *et al.* reported abundant cyanobacteria, microproblematica, *Girvanella*, *Sphaerocodium* and *Wetheredella* from this interval.

Above these limestone beds is a ca 30 m-thick succession, equivalent to 'Member 4' of Jeppsson *et al.* (2007), of siltstone and fine sandstone overlain by interbedded limestone and siltstone. The lower interval of grey-brown to red-brown calcareous quartz-mica siltstone and lesser interbedded fine sandstone is 17 m thick on the south bank. It contains abundant fragments of brachiopods, trilobites, crinoids and bryozoans (Caldon 2003) that commonly form nuclei for irregularly shaped macro- and pisooncolites. Rare, abraded, coral debris is also present. Elongate grains and micas are commonly aligned with the bedding. This siltstone contains thin layers rich in trilobites, brachiopods and bivalves (Talent *et al.* 2002). The upper interval comprises thinly interbedded light to dark grey limestone and siltstone, which is 15 m thick on the south bank of the river. Beds are up to and sometimes exceed 20 cm, and the limestone beds become thicker and more evident towards the top. The limestone contains recrystallised ooids, with subordinate micro- and pisooncolites, skeletal fragments, pellets, minor detrital and secondary quartz, and minor detrital muscovite. These are

set in a granular neomorphic spar, which has corroded some ooids. Skeletal allochems include brachiopod, crinoid, bryozoan, and, more rarely, coral debris. Withnall *et al.* (1993) reported the presence of channeling and long-wavelength low-angle cross-beds from this interval.

Solitary and colonial rugose corals are abundant within the Coral gardens member, particularly within the interbedded limestones and siltstones that comprise a large proportion of the unit. Tabulate corals, illustrated by Hill *et al.* (1969), include *Favosites richardsi*? Jones 1937, *Pseudoplasuopora* sp. cf. *heliolitoides* (Lindström 1899), *Heliolites daintreei* Nicholson & Etheridge 1879, (group 4 of Jones & Hill 1940) and species of *Mesofavosites* and *Barrandeolites*?. Stromatoporoids, described by Webby & Zhen (1997), include common occurrences of *Schistodictyon jacksonense* and *Ecclinadictyon microvesiculosum* (Riabinin 1951). Other invertebrates include small brachiopods, medium- and high-spined gastropods, several species of trilobites (including an ecrinurine), bryozoans, crinoids, and rare tentaculitids. The crinoids are typically represented by disarticulated columnals with round or pentapetaloid lumens; several species are present.

*Jack Hills member.* The Jack Hills member is the uppermost carbonate interval of the Jack Formation, and has previously been mapped as the top of the Graveyard Creek Group (White 1965; Arnold & Henderson 1976). It is a thick and extensive, predominantly massive, light to dark grey micritic limestone, with high topographic relief, through which the Broken River has cut a narrow gorge (Fig. 3D). This limestone can be traced along strike for ca 8.5 km (Fig. 2). It is ca 215 m thick on the north bank of the river and reaches a maximum of ca 400 m in thickness in the vicinity of Gorge Creek, northeast of the type section.

Bedding is crudely defined by layers of skeletal material, stromatoporoids in growth position, rare thick pisooncolitic layers, and irregular layers of hard nodular chert and dolomite that are particularly prominent in the top 100 m of the unit. Scattered zones occur where microstylolites are so common that

they form an irregular network through the limestone, similar to those found within the Dark dog limestone.

The basal 20 m of the limestone shows signs of bioturbation and is rich in skeletal debris, particularly brachiopods, corals, bryozoans, medium-spined gastropods and ostracodes. Crinoid stem plates with round lumens are characteristic; small, flat or slightly domed stromatoporoids in growth position and reaching 20–25 cm in length also occur. The succeeding 70–80 m is relatively poor in skeletal fragments, although small crinoid ossicles are relatively common throughout and there are scattered favositids, small stromatoporoids, some thin layers of solitary rugose corals (mainly *Tryplasma*) and pentamerid brachiopods. Stromatoporoids are more common and larger up-section. The limestone is mostly composed of fine, recrystallised micrite, biomicrite, and pelmicrite, except for the topmost 10 m, which is a recrystallised biomicrudite, rich in crinoid ossicles, brachiopod valves, tentaculitids, bryozoans, high- and medium-spined gastropods, and rare corals. This increase in fossil content of the limestone is accompanied by a considerable increase in the size and numbers of stromatoporoids. These are usually strongly domical, rarely laminar or weakly domical, and reach widths greater than 2 m and thicknesses of 50–60 cm.

The top 4–5 m of the biomicrudite are interbedded with a very fine-grained quartz-bearing, micaceous limestone, which continues for another 10 m up-section before the outcrop is concealed by alluvium. Fresh surfaces of the limestone are light grey to grey-green in colour, but weathered surfaces are brown or red-brown. The limestone consists of 10–40% biotite and muscovite in varying proportions, with a large amount of anhedral calcite grains, and minor quartz, set in a fine granular calcite cement. The limestone is poor in fossils, but contains echinoid and brachiopod fragments.

The thickly bedded to massive limestones of the Jack Hills member, are impoverished in rugose corals. Colonial rugosans, other than rare subcompound *Stylopleura liliiforme*

are absent, but uncommon solitary species occur. Tabulates recorded by Hill *et al.* (1969) include *Favosites allani* Jones 1937 and *Heliolites daintreei* Nicholson & Etheridge 1879. There are several species of stromatoporoids, including *Plexodictyon* sp. (Webby & Zhen 1997).

**Environment of deposition.** Fleming in Withnall *et al.* (1988) considered the depositional environment of the Jack Formation in the Broken River area to have been a nearshore shallow-water complex of fans, bars, restricted lagoons, and marine tongues or bays, and this interpretation is generally followed here. Although the environment was conducive to carbonate sedimentation, the presence of interlensed and interbedded siliciclastic intervals within the succession indicates the close proximity of land.

The massive or thickly bedded, bluff-forming limestone intervals within the succession (Dark dog and Jack Hills members, basal Coral gardens member) are carbonate mudbank deposits indicative of generally low-energy, marine conditions. Thin layers of bioclastic debris at various levels within the limestones suggest periodic storm events. Corals, stromatoporoids and algae that occur throughout the succession indicate relatively shallow water depths. This lithofacies probably accumulated in a restricted lagoonal environment. Darker limestones with sparse faunas are probably indicative of relatively anaerobic conditions, whereas lighter-coloured limestones with more abundant faunas and debris layers resulted from more oxygenated and agitated conditions.

Fleming in Withnall *et al.* (1988) interpreted the thick siliciclastic Red bull member as possibly fluvial, at least towards the base, emphasising the presence of red-brown, poorly sorted sandstone, pebbly trough cross-bedded brown sandstone and purplish red beds, and the absence of fossils. The overall fining-upward succession suggests a general deepening of the environment, but the evidence for early fluvial deposition is not conclusive, as the sedimentary structures are also typical of shallow-marine environments, and the red-brown colour is almost certainly

the result of more recent weathering. Sparse brachiopod and trilobite fossils near the top of this unit indicate a marine setting. It is therefore possible that the coarser lower part of the succession was deposited in a relatively high-energy shallow-marine environment, perhaps a nearshore, proximal fan or shoal setting.

Most of the overlying Coral gardens member consists of relatively fine lithologies that were deposited under low to moderate energy conditions, but higher-energy conditions are suggested for the uppermost beds of oolitic limestone and cross-bedded calcarenite. Fleming interpreted the environment of deposition for this heterolithic unit as a shallow to extremely shallow marine bay, bounded by bars and shoreline. The diverse and abundant fauna indicates shallow, clear and warm conditions. The thinly interbedded limestones and siltstones that constitute much of the succession accumulated under fluctuating depositional conditions. Limestone beds were deposited during periods of minimal clastic influx, whereas dilution of carbonates during periods of increased runoff from siliciclastic source areas resulted in the deposition of siltstone and fine sandstone. The nodular structure of many limestone beds is probably the result of differential compaction between the limestone and siltstone so as to form sedimentary boudinage structures. During unconfined compaction, the incompetent siltstone layers move laterally, and pull apart the less competent limestone. Oolitic and oncolitic limestones near the top of the Coral gardens member indicate shallow more energetic conditions. Fleming in Withnall *et al.* (1988) considered these to be marine bar sediments. The cross-bedded calcarenites at the top of the unit were interpreted as carbonate fan or tidal channel deposits in a shoaling environment by Withnall *et al.* (1993) and Talent *et al.* (2002).

Although the shallow marine succession of the Jack Formation was deposited at various water depths, Fleming noted that apparent transgressive-regressive events may not necessarily represent regional relative changes in sea level; for example, the distribution of

facies may have been effected by local patterns of deposition, such as the movement of bars or damming by fans.

**Age of Jack Formation.** Conodonts and macrofossils (Talent *et al.* 2002) indicate that the type section of the Jack Formation in the Jack Hills Gorge area is early Wenlock (Sheinwoodian) to late Ludlow (Ludfordian) in age (Fig. 4), with some intervals more securely dated than others.

A sparse conodont fauna of broad Wenlock age was recovered from the base of the Dark dog limestone near Six-Mile Dam, 3 km northeast of, and along strike from the type section (Simpson 1998a, Fig. 2). The underlying, dominantly siliciclastic succession (Poley Cow Formation and its equivalent, the Quinton Formation) yielded late Llandovery (Telychian) graptolites (*turriculatus* to *greistonensis* zones; Jell *et al.* 1993; Rickards & Jell 2002) and conodonts (Simpson 1999). Jeppsson *et al.* (2007) considered it likely that there was little or no time break between the Poley Cow Formation and the Dark dog limestone, and inferred that the base of the limestone is most probably of early Wenlock age (lower *Kockelella ranuliformis* Zone). They concluded that the base of the Ludlow in the type section is near the base of the Red bull member and that the Dark dog limestone might therefore represent the whole of Wenlock time.

The Coral gardens member includes the *Ancoradella ploeckensis*, *Polygnathoides siluricus*, *Icriodontid* (a portion of which corresponds, at least partly, with the *Icriodus latialata* Zone of Walliser 1964) and *Ozarkodina snajdri* zones (Simpson 1998a; Jeppsson *et al.* 2007). Four new subzones discriminated by Jeppsson *et al.* (2007) are not used herein.

The type section of the Jack Hills member is entirely late Ludlow (*Ozarkodina crispa* Zone) in age (Simpson 1998a, 2000; Talent *et al.* 2002). However, to the southeast of the type area, near the road crossing of the Broken River (Fig. 2), conodonts of the Early Devonian (early Lochkovian) *Icriodus woschmidtii* Zone (equivalent to the *Caudicriodus hesperius* Zone) were recovered (Simpson 1995b, 1998b, 2000), with no obvious break in succession. In

that area, the Jack Formation extends through a generalised Přídolí interval into the Early Devonian. In all other areas, the Jack Formation is no younger than Ludlow, owing to significant erosion of the Jack Formation in those areas prior to deposition of the Ralph Flint Formation (Simpson 1995a, 2000; Talent *et al.* 2002). It is notable that in the vicinity of the road crossing, there is no equivalent of the Dark dog limestone, and the Coral gardens member directly overlies siliciclastic rocks of the Quinton Formation (Simpson 2000). Both the base and top of the formation are therefore demonstrably diachronous between these two areas.

**Rugose Coral Fauna.** Jell (1967) named the rugose coral fauna of the Jack Limestone the *Entelophyllum* fauna as this genus occurs throughout the succession. Fourteen rugose coral species are recognised, but only four have been recorded outside the Broken River Province: *Tryplasma derrengullenense* Etheridge 1907, *Stylopleura liliiforme* (Etheridge 1907), *Entelophyllum patulum yassense* (Etheridge 1892a) and *E. latum* Hill 1940. The fauna includes a new genus, *Vesicospina*, and new species of *Aphyllum*, *Pycnostylus*, *Ptychophyllum*, *Dokophyllum* and *Multicarinophyllum*. This last genus has not previously been recognised from Australia. Other genera present include *Amplexoides*, *Cystiphyllum?* (*Cystiphyllum*) and *Cystiphyllum* (*Hedstroemophyllum*).

The biostratigraphic distribution of rugose coral species from the type section of the formation is shown in Fig. 4. Fossil localities from which the rugose coral fauna was collected are shown in Fig. 5 and listed in Appendix 1. Note that identifications of species from the Dark dog limestone and Jack Hills member are based largely on field observations and are therefore more tentative; specimens from the massive or thickly bedded limestones of these units are difficult to collect without the use of power tools (eg rock saws), which were not available at the time of the original fieldwork in the late 1970s.

There is a weakly defined rugose coral biozonation within the Jack Formation that is likely to have been influenced by facies type

as well as time. Massive to thickly bedded lime mudstones of the basal Dark dog limestone and upper Jack Hills member have relatively low coral diversity (5 and 6 species, respectively) and abundance. This is interpreted as being due to the low-energy deeper water conditions, relatively high turbidity, and mudbank substrates that were less suitable for coral growth. The greatest species diversity (13 rugose species) is in the interbedded limestones and siltstones of the Coral gardens member, where environmental conditions were generally more favourable.

The only species unique to the Dark dog limestone are the relatively common *Pycnostylus polyphyllodus* and a rare unnamed species of *Tryplasma*. Other species from this unit are relatively long-ranging and occur in overlying strata. *Pycnostylus polyphyllodus*, *Tryplasma derrengullenense* and *Entelophyllum latum* occur throughout the unit. In the more thinly bedded limestones at its top in the river section, the fauna includes *Multicarinophyllum vepreculatum* and *Tryplasma pachystele*. However, neither species has been recorded from this unit along strike to the north and south of the Broken River.

Thinly interbedded limestones and siltstones of the Coral gardens member contain the most diverse rugose coral assemblage. Common are *Entelophyllum patulum yassense*, *E. latum*, *Ptychophyllum variatum*, *T. derrengullenense*, and towards the top of the nodular beds, *Dokophyllum hilla* and *Vesicospina julli*. Other species recorded include *Stylopleura liliiforme*, *Cystiphyllum?* (*Cystiphyllum*), *C. (Hedstroemophyllum)* and *Amplexoides*. *M. vepreculatum* and *A. pachystele*, common at the top of the Dark dog limestone, persist into the base of the Coral gardens member, but are rare.

Oncolitic and oolitic limestones at the top of the Coral gardens member have fewer corals and these are generally abraded, reflecting the energetic shifting substrates these probable marine bar sediments. These facies, at the top of the interbedded limestone and siltstone succession, also correspond to the globally recognised Lau extinction event, which is reflected in the conodont assemblages and other faunas (Caldon 2003; Jeppsson *et al.* 2007).

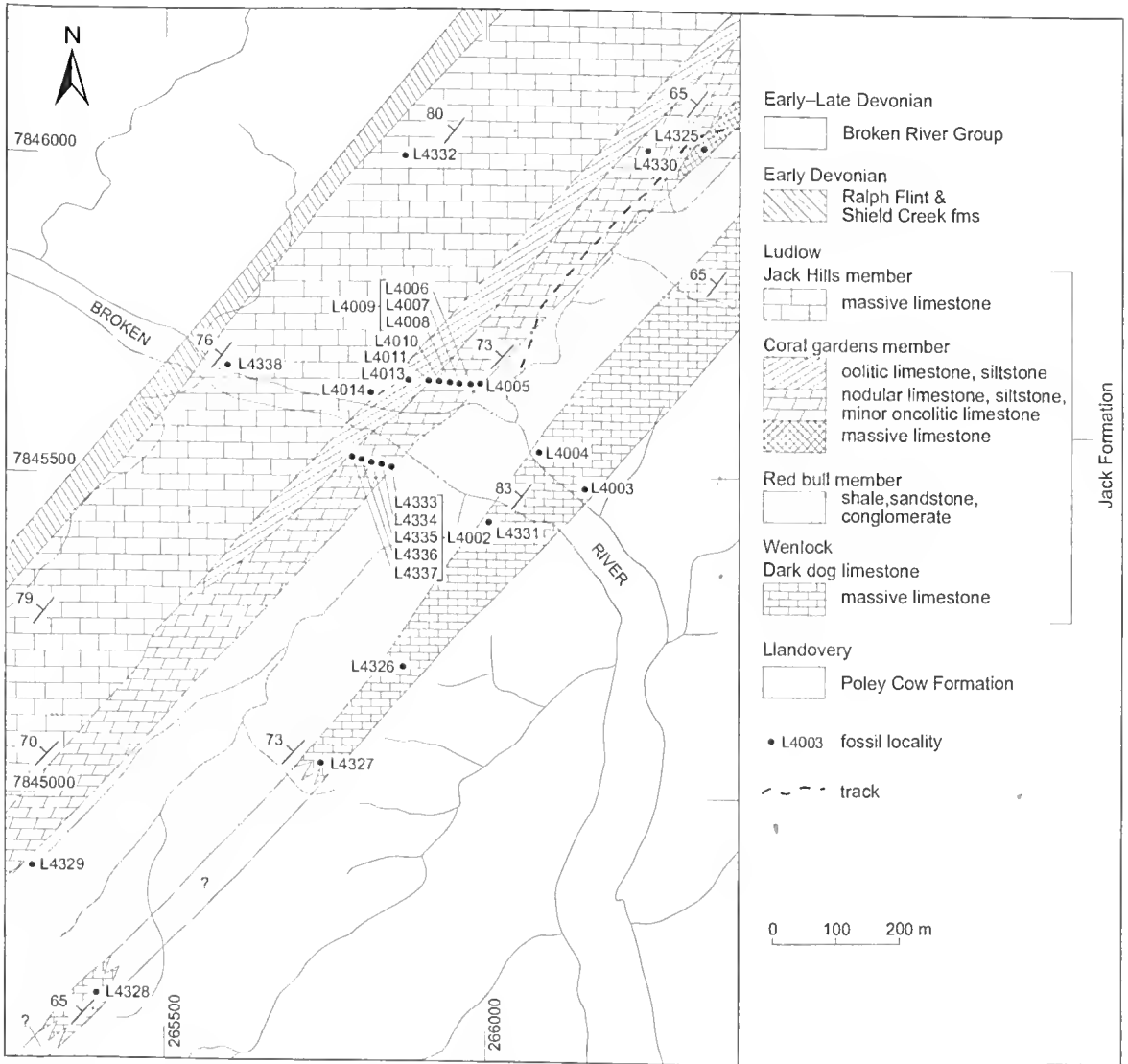


FIG. 5. Solid geology map of the Jack Formation in the vicinity of the type section, showing fossil localities referred to in the text. Localities are listed in Appendix 1.

The uppermost Jack Hills member has an impoverished fauna containing mainly solitary forms, all of which are present in the underlying Coral gardens member. Rare specimens of *V. julli* and *D. hilla* are found at the base of the unit, whereas *Ptychophyllum variatum*, *T. derrengulleuse*, *E. latum*, *Anplexoides*, *C.?* (*Cystiphyllum*) and the sub-compound *S. liliiforme* occur sparsely throughout. It is unclear whether the reduction in rugose coral

diversity and numbers is related to the change in facies from the interbedded limestones and siltstones of the Coral gardens member to the lime mudstones of the Jack Hills member, to the Lau extinction event, or to a combination of these factors.

**Correlation of Entelophyllum Fauna.** Rugose corals from other localities within the Jack Formation are yet to be studied in detail, but

were listed by Arnold & Henderson (1976) from a large exposure of this formation, south of the Broken River, where it is crossed by the Pandanus Creek to Wando Vale homesteads road (Fig. 2). The section in that area is equivalent to just the Coral gardens and Jack Hills members, but as noted above, conodont data indicate that the top of the formation is younger than in the Jack Hills Gorge area, extending into the earliest Devonian (early Lochkovian; Simpson 1995b, 2000). Rugose coral taxa listed by Arnold & Henderson are equivalent to those from the type section and include *Tryplasma*, *Ketophyllum* [= *Dokophyllum hillae*], *Entelophyllum* cf. *yassense*, [= *E. patulum yassense*], ?*Phanlactis* (= *Ptychophyllum variatum*) and ?*Cystiphyllum*. Also listed were the tabulate corals *Heliolites daintreei*, *Favosites* of the *gottilandicus* group and *Pseudoplasmodopora*.

Within eastern Australia, the *Entelophyllum* fauna is most comparable with a coral fauna from the Yass-Bowling district of New South Wales (see Hill 1940; Link & Druce 1972; McLean 1976). The Jack Formation species, *T. derrengullenense*, *S. liliiforme*, and *E. patulum yassense* have all been recorded from the Gorstian to earliest Ludfordian Bowspring Limestone and Hume Limestone members (Silverdale Formation) in the Yass Basin (Thomas & Pogson 2011), and *E. latum* is found in older Wenlock strata at Glenbower to the west (Hill 1940). The genera *Pycnostylus*, *Cystiphyllum* and *Tryplasma* are also common to both the Jack Formation and Yass Basin.

In the Wellington district (central New South Wales) *E. latum* and *T. derrengullenense*? were recorded in probable Ludlow sediments of the Mumbil Group (see Strusz 1961; McLean 1975a; Vandyke & Burnes 1976), and *T. derrengullenense*? ranges into overlying Early Devonian strata, but at that level has probably been reworked from underlying Silurian limestone (D.L. Strusz pers. comm. 2015).

*Stylopleura liliiforme* is known from the Ludlow of Victoria (Chapman 1920), and *E. latum* also occurs in the Wenlock?–Ludlow of Tasmania (Hill 1942a).

Of the other genera of the *Entelophyllum* fauna, *Ptychophyllum* and *C. (Hedstroemophyllum)* occur in the upper Llandoverly Quarry Creek and Rosyth Limestones (New South Wales), and *Dokophyllum* is known from the Rosyth Limestone (as *Ketophyllum*: McLean 1974a, 1975b). Species of *Amplexoides* are until now known only from Llandoverly strata in Australia; two species are present within the late Llandoverly Quinton Formation in the northern Graveyard Creek Subprovince (Munson & Jell 1999) and a single species was recorded from the Panuara area of central NSW (McLean 1985).

Only a few elements of the *Entelophyllum* fauna are sufficiently similar to overseas forms to be of value for international correlation. Faunas from Asia, Europe and North America contain several genera in common with those of the Jack Formation, but the species are generally dissimilar.

*Entelophyllum*, *Tryplasma*, *Ketophyllum* and *C. (Hedstroemophyllum)* are common in Silurian deposits of Asia, and *Stylopleura* is known from the middle Ludlow of the Urals and the Eifelian of Salair (see Pedder 1985). *Ptychophyllum* occurs in the Wenlock of China as *P. "Nanshanophyllum"* (Yu 1956) and *C.?* (*Cystiphyllum*) might be present in Llandoverly deposits of Dolgoy Island and the Siberian Platform as *Cystilasma* Zaprudskaya & Ivanovskiy 1962. *Multicarinophyllum* has been previously recorded from Lower Devonian to Givetian strata of central Asia (Ivanovskiy 1970). Species of *Entelophyllum*, *Dokophyllum*, *Tryplasma*, *Cystiphyllum* (*Cystiphyllum*), and *C. (Hedstroemophyllum)* have all been recorded in the Silurian of Europe, and species of *Pycnostylus*, *Ptychophyllum*, *Tryplasma*, *Entelophyllum*, *Dokophyllum* and *C. (Cystiphyllum)* have been found in the Silurian of North America (see Systematic Palaeontology for more details and references).

At the species level, *Entelophyllum patulum yassense* probably occurs in the Late Silurian of Inner Mongolia (Guo 1978), and *Stylopleura liliiforme* possibly occurs in the Ludlow of Germany as *Amplexus (Coelophyllum) eurycalix* Weissmerel 1894.

## SYSTEMATIC PALAEOONTOLOGY

All fossil specimens are part of the Queensland Museum collection (ex University of Queensland, Department of Earth Sciences), and are prefixed with their original UQF numbers; UQL numbers refer to fossil localities in the Department of Earth Sciences locality catalogue. UQL numbers are listed in Appendix 1, and are shown on Fig. 5. Systematic descriptions are arranged following the suprageneric classification of Hill (1981).

### Class Anthozoa Ehrenberg 1834

#### Subclass Rugosa Milne-Edwards & Haime 1850

#### Order Cystiphyllida Nicholson in Nicholson & Lydekker 1889

#### Family Tryplasmataidae Etheridge 1907

#### Subfamily Tryplasmatinae Etheridge 1907

#### Genus *Tryplasma* Lonsdale 1845.

**Type Species.** *Tryplasma aequabile* Lonsdale 1845: 613–614, 633, pl. A, figs 7, 7a (see Ivanovskiy & Shurygina 1975: 15). Early Devonian or Eifelian, east slope of Ural Mountains, Kavka R. (subsequent designation, Etheridge 1907: 42).

**Diagnosis.** Corallum solitary or with one or more parricidal offsets from calice, but not forming fasciculate coralla; may have epithecal scales; with narrow peripheral stereozone of contiguous laminar bases of commonly short rhabdacanthine, holacanthine, or dimorphacanthine septa, trabeculae free distally; tabulae complete, commonly subhorizontal, some with median notch; dissepiments absent (Hill 1981: F98).

#### *Tryplasma derrengullenense* Etheridge 1907

Fig. 6

*Tryplasma derrengullenense* Etheridge 1907: 88, pl. 22, figs 5–8; Hill 1940: 407, pl. 12, fig. 16.

*Tryplasma derrengullenense*?; Strusz 1961: 345–346, pl. 42, fig. 14, pl. 43, fig. 12.

*Tryplasma* sp. cf. *derrengullenense*; Hill et al. 1969: s.12, pl. S VI, figs 2–3.

**Lectotype** (designated Hill 1940: 407). F9789, Australian Museum, Ludlow, Limestone Creek, near Bowning, Yass Basin, New South Wales. Figured in Etheridge (1907: pl. 22, fig. 8).

**Material.** UQF72681–72683, 72685–72686, 72694 from UQL4002; UQF72684 from UQL4009; UQF72687, 72691–72692 from UQL4336; UQF72688 from UQL4004; UQF72689 from UQL4003; UQF72690, 72693 from UQL4335.

**Diagnosis** (modified from Hill 1940). Small, solitary, trochoid or ceratoid *Tryplasma* with irregular rejuvenescence; calice very deep. Small, fine trabeculae on distal surfaces of tabulae.

**Description.** Solitary, trochoid or ceratoid, with frequent rejuvenescence, succeeding calices not being greater in diameter than the original; resulting in an irregular corallum shape. Epitheca longitudinally ridged. Maximum observed diameter 18 mm, maximum length more than 4.5 cm. Calice very deep, flat-floored, bears numerous spines in vertical series, each series representing a septum. Thin-walled rootlets, 1–2 mm in diameter and lacking transverse partitions, may be developed.

Two orders of septa numbering between 78 and 86 in largest specimens. Septa composed of rhabdacanthine trabeculae directed upwards and inwards at 30–50° from the horizontal, sometimes piercing several tabulae. Major septa up to 3 mm long, minor septa slightly shorter. Small trabeculae, representing axial continuations of septa, borne on distal surfaces of tabulae. Tabulae complete or in some cases incomplete, spaced at 8–12 per cm, flat, rarely flexuous or gently sagging, commonly slightly upturned at periphery of corallite. Peripheral stereozone 1–2 mm-wide, showing indistinct lamination parallel to epitheca.

**Remarks.** Specimens vary in width from 5 to 18 mm, but as septal numbers can be correlated with corallum diameter, they are likely to be conspecific (Fig. 7). Tabulae completeness also varies; UQF72684 has sagging, dominantly incomplete tabulae (Fig. 6B), whereas UQF72686 has complete, planar or slightly flexuous plates (Fig. 6E). Complete and incomplete tabulae may be developed in one corallum, indicating that this variation is intraspecific.



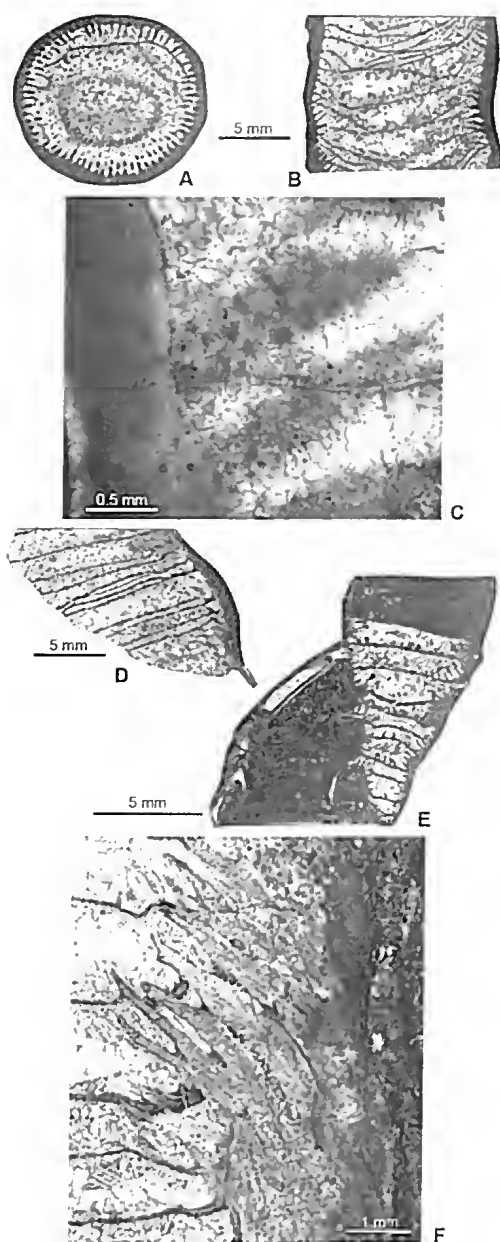


FIG. 6. *Tryplasma derrengullenense* Etheridge 1907. A–C, UQF72684 from UQL4009; A, B, transverse and longitudinal sections; C, portion of B, showing rhabdacanthine septal spines; D, UQF72687 from UQL4336, longitudinal section; E, UQF72686 from UQL4002, longitudinal section, showing rootlets; F, UQF72681 from UQL4002, portion of longitudinal section, showing piercing of tabulae by septal trabeculae.

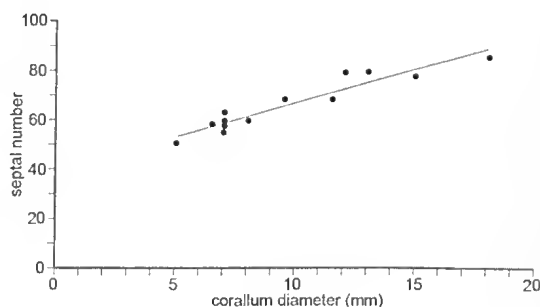


FIG. 7. Linear least squares plot of corallite diameter against septal number (correlation coefficient 0.91) for Jack Formation specimens of *Tryplasma derrengullenense* Etheridge 1907.

*Tryplasma derrengullenense* is distinguished from other species of *Tryplasma* by its size and septal number, and by its tabular trabeculae. Of other Australian species, it most closely resembles *T. columnare* Etheridge 1907, from the Wenlock to Early Devonian of NSW, which has a larger, more regular corallum but fewer septa (60–80 at a diameter of 25 mm).

Strusz (1961) described poorly preserved internal moulds of a solitary coral from the Wellington district (New South Wales) as *T. derrengullenense*?. The specimens were collected from a breccia in the early Lochkovian Cuga Burga Volcanics, and have probably been reworked from underlying Silurian limestone. Minor septa in that species tend to be expressed as rows of holes, whereas the bases of the major septa are continuous, so forming distinct grooves (D.L. Strusz, pers. comm. 2003, 2015). The species was tentatively identified from the size of the corallum, the septal number and by “the depth of the grooves left by the weathering of the septa”. It reaches a larger diameter, and has more septa than other specimens of *T. derrengullenense* (100–120 at the largest diameter of about 25 mm), and is therefore only tentatively included in the synonymy.

**Distribution and Range.** Wenlock and Ludlow of Broken River Province (north Queensland; Fig. 4); Gorstian and earliest Ludfordian of Yass Basin (New South Wales); early Lochkovian (probably reworked Silurian) of Wellington district? (New South Wales).



*Tryplasma* sp.

Fig. 8

**Material.** UQF72702 from UQL4004; the specimen is badly worn.

**Description.** Corallum probably cylindrical, external and calical features unknown. Specimen is 19 mm in diameter and has 58 major and minor septa over an arc of 250°, giving an estimated total of 84. Major septa about 2 mm long, slightly longer than minor septa. Septa embedded in narrow peripheral stereozone (<1 mm wide). Septal trabeculae usually directed upwards and inwards at very low angle (0–10°). Microstructures generally obscured by recrystallisation. Tabulae complete, evenly spaced (5–6 per cm), horizontal or slightly sagging, typically upturned peripherally.

**Remarks.** This species is very similar to Broken River specimens of *T. derrengullenense* Etheridge 1907, but has a slightly larger corallum; slightly smaller, more shallowly inclined septal spines, and lacks tabular trabeculae. Fragments of a coral from the Early? Devonian of the Tamworth district (New South Wales), referred to as *Tryplasma* sp. by Hill (1942b), closely resemble this form, differing only in having slightly more distant tabulae.

**Genus *Aphyllum* Soshkina 1937**

**Type Species.** *Aphyllum sociale* Soshkina 1937: 45–46, pl. 7, figs 1–4. Late Wenlock, west slopes of the Ural Mountains, right bank of Tury River, near Yelkino (by original designation).

**Diagnosis.** Fasciculate, increase lateral or peripheral and pseudoaxial; may have epithecal scales; corallites with acanthine septa and narrow peripheral stereozone of contiguous laminar septal bases from which discrete rhabdacanthine or holacanthine trabeculae are directed inward and commonly upward; tabulae complete, horizontal, in some with median notch, or slightly curved (Hill 1981: F100).

*Aphyllum pachystele* sp. nov.

Fig. 9

"*Tryplasma*" sp. Hill *et al.* 1969: s.12, pl. S VI, fig. 1.

**Etymology.** Greek pachys = thick, stele = pillar, column, referring to the robust corallites of this species.

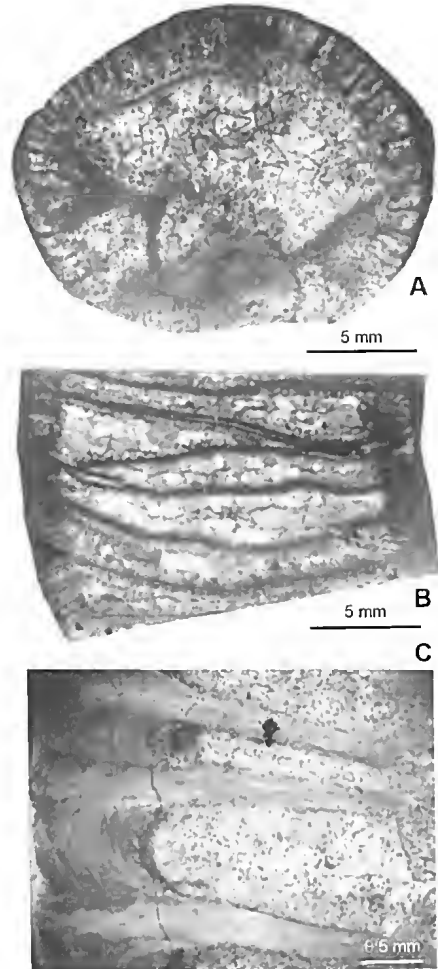


FIG. 8. *Tryplasma* sp., UQF72702 from UQL4004. A, B, transverse and longitudinal sections; C, portion of A, showing microstructures of wall and septa.

**Holotype.** UQF72695 from UQL4004. Late Wenlock, Jack Formation. Graveyard Creek Group, Jack Hills Gorge area, north Queensland.

**Material.** UQF72695–72698, 72700, 72699 (27 serial sections) from UQL4004; UQF72701 from UQL4010.

**Diagnosis.** Large *Aphyllum* with parricidal increase; 110–120 major and minor septa; septal trabeculae rhabdacanthine. Tabulae flat or gently arched. Connecting processes and rootlets common.

**Description.** Corallum large, fasciculate. Corallites cylindrical, straight or slightly curved, separated by up to 2–3 cm. Maximum diameter 25–30 mm,

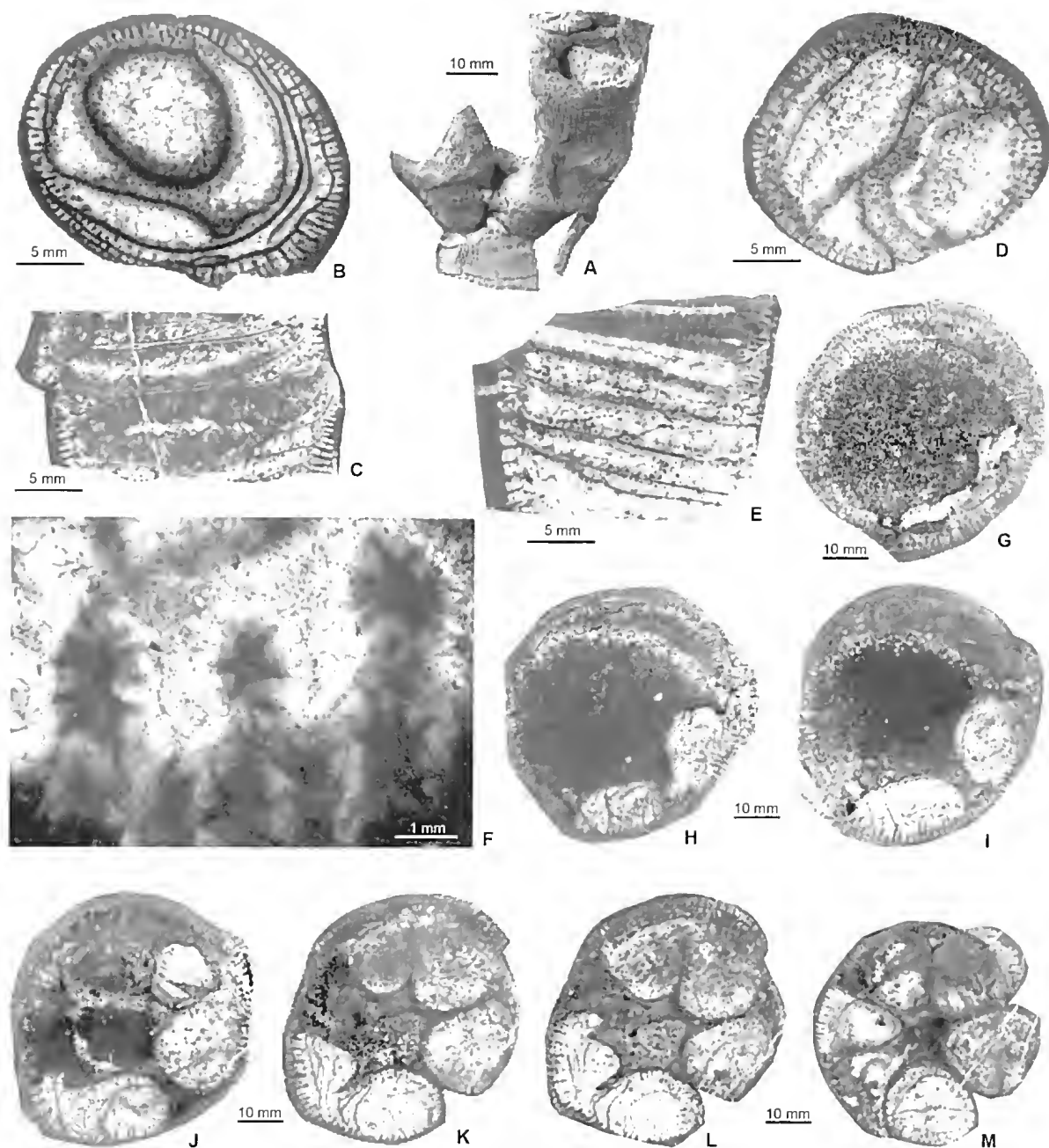


FIG. 9. *Aphyllium pachystele* sp. nov. A-B, UQF72698 from sUQL4004; A, exterior of corallum, showing rootlet and connecting processes; B, transverse section; C, UQF72697 from UQL4004, longitudinal section. D-F, UQF72695, HOLOTYPE from UQL4004; D, E, transverse and longitudinal sections; F, portion of D, showing rhabdacanthine trabeculae; G-M, UQF72699 from UQL4004, selected serial transverse sections showing peripheral increase; distances show cumulative distal growth from first section; G, 0 mm; H, 1 mm; I, 2 mm; J, 3.5 mm; K, 5.5 mm; L, 6.5 mm; M, 10.5 mm.

maximum observed height 8–10 cm. Connecting tubules and small rootlets common, 1–2 mm in diameter, with thin, irregular, transverse partitions. Epitheca longitudinally ridged with faint growth striations.

There are 110–120 rhabdacanthine major and minor septa. Major septa 20–25 mm long; minor septa 0.5–0.6 length of major septa and buried in, or extending just beyond 1 mm-wide peripheral stereozone. Septal trabeculae form discrete spines, directed upwards and inwards at 5–10° from horizontal, spaced vertically at 8–12 per cm. Rhabdacanthine ‘rods’ closely spaced, diverge steeply from trabecular axis in broad curves, their ends are directed almost normally to that axis. Lateral processes have thick walls showing distinct lamination parallel to their exteriors. Connecting tubules are narrow extensions of wall and lumen of one corallite to another, may have irregularly spaced, thin, flexuous transverse partitions.

Tabulae flat or gently sagging, mostly complete, spaced about 4–5 per cm, commonly with upturned edges. Dissepiments absent.

**Increase.** Increase is parricidal. In UQF72699, six offsets are formed at different levels around the periphery of the parent calice, and were examined in 27 serial transverse sections (see Fig. 9G–M). The two lowermost offsets appear as a thin, irregular wall, attached to the axial ends of the major septa on one side of the parent calice (Fig. 9G). Once developed, this wall expands axially into the calice and becomes separated from the major septa. Simultaneously, the midpoint of the wall develops an invagination that enlarges until the two developing corallites are defined (Fig. 9H, I).

Septa of the parent calice that are enclosed by the walls of an early offset are incorporated into the offset’s morphology. Other septa develop as the offset takes shape: firstly, a few stubby, major septa appear at points opposite the axial ends of the major septa of the parent; then additional major septa are inserted and

finally minor septa. Septa then lengthen to differing extents, the major septa reach 1 mm in a corallite of 9 mm diameter. Concurrently, the inner walls of the offset are modified until it assumes a sub-circular shape, and grows free of the parent calice. Daughter corallites formed after the first two offsets display slightly different development. Initially, the wall of the earlier corallite bulges laterally near the calical margin of the parent. This ‘bud’ expands along the periphery of, and incorporates septa from the old calice. An invagination forms and deepens between it and the earlier offset, and development then proceeds as described above (Fig. 9J–M).

During increase, a sub-bilateral symmetry is imposed on the parent corallite; the symmetry plane being between the earliest two and the last two offsets. Offsets to either side of this plane do not necessarily develop in pairs or at the same rate. When all are formed, they are fairly evenly arranged around the old calice.

**Remarks.** A specimen from the “lower part” of the Jack Formation, illustrated by Hill *et al.* (1969) as “*Tryplasma*” sp., has corallites with relatively long major septa (to 3 mm); a wide peripheral stereozone (to nearly 2 mm); and flat or slightly arched tabulae. The specimen otherwise closely resembles the holotype of *A. pachystele*.

The new species is distinguished from other Australian *Aphyllum* by its large robust appearance and numerous septa. *A. lousdalei* (Etheridge 1890), and *A. delicatula* (Etheridge 1907), both from the early to middle Ludlow of New South Wales, and *A. leptostylum* Munson & Jell 1999 from the late Llandovery of the Quinton Formation, Broken River Province, all have much smaller corallites with maximum diameters of 6–8 mm, 3 mm, and 5 mm, respectively. *A. murrayi* (Etheridge 1907) from the Devonian of Victoria also has smaller corallites (ca 12 mm) and fewer septa (about 50) of one order.

**Distribution and Range.** Late Wenlock and Ludfordian of Broken River Province, north Queensland (Fig. 4).

Family Cystiphyllidae Milne-Edwards  
& Haime 1850

Genus *Cystiphyllum* Lonsdale 1839

**Diagnosis.** Solitary, turbinate to cylindrical; major and minor septa long, each represented by trabeculae typically developed only on upper surfaces of successive globose dissepiments and tabellae; sclerocones not strongly developed, thicker and more continuous peripherally than axially; calicular floors inversely conical, inclination of dissepiments and tabellae commonly similar (Hill 1981: F113).

*Cystiphyllum* (*Cystiphyllum*) Lonsdale 1839

**Type Species.** *Cystiphyllum siluriense* Lonsdale 1839: 691, pl. 16, figs 1, 1a, non 2. Middle Silurian, Much Wenlock Limestone Formation, Dudley, Worcestershire, UK.

**Diagnosis.** Axis of sclerocones centric, thickening weak, commonly absent on tabellae; trabeculae grain-like, to moderately long and contiguous, to separate (Hill 1981: F113).

*Cystiphyllum?* (*Cystiphyllum*) sp.  
Fig. 10A, B

**Material.** UQF72632 from UQL4002; the specimen occurs within a corallum of *Eutelophyllum patulum yassense* (Etheridge 1892a), and is almost completely buried in matrix.

**Description.** Small cylindrical corallum, 12 mm in diameter, at least 4 cm high. Calice not preserved, exteriors not visible. Septa absent. Dissepiments small, globose, steeply inclined peripherally, may be shallower adaxially. Axial region 7–8 mm wide, composed of larger, more elongate and globose plates that are sub-horizontally or shallowly based. Towards the margins, these “tabellae” are difficult to distinguish from dissepiments.

**Remarks.** The single specimen was recovered from the Coral gardens member; a number of other specimens probably of this species were identified within the Jack Hills member, but could not be extracted from massive limestones.

Forms that differ from *Cystiphyllum* only in lacking septa have previously been included

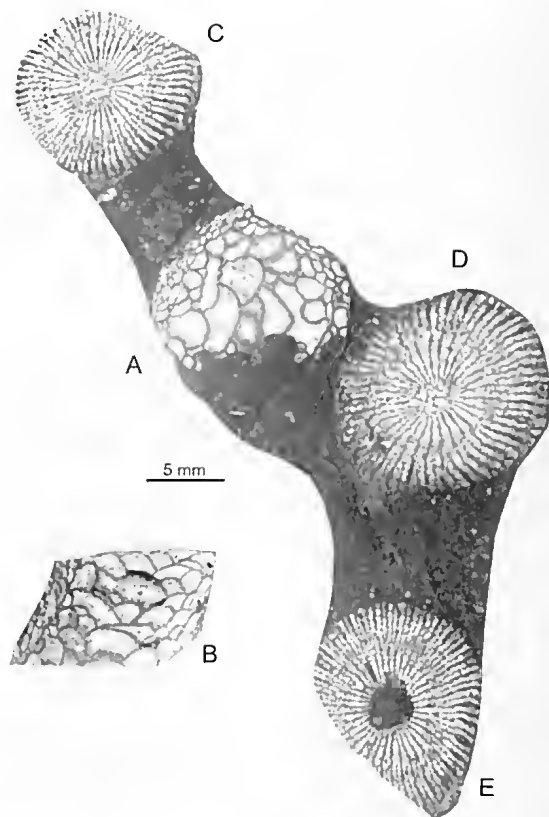


FIG. 10. A–B, *Cystiphyllum?* (*Cystiphyllum*) sp., UQF72632 from UQL4002; A, B, transverse and longitudinal sections; C–E, *Eutelophyllum patulum yassense* (Etheridge 1892a), UQF72631 from UQL4002, transverse sections showing thickened septa.

in *Cystilasma* Zaprudskaya & Ivanovskiy 1962, although Hill (1981) tentatively regarded the two genera as synonymous. Species of *Cystilasma* are known from the Llandovery of Dolgiy Island (Arctic USSR) and the late Llandovery of the Siberian Platform. The type species, *C. sibiricum* Zaprudskaya & Ivanovskiy 1962, differs from the Broken River species in having much coarser dissepiments. If the two forms are congeneric, the range of *Cystilasma* would be extended into the Ludlow [i.e. similar to that of *C. (Cystiphyllum)*], and there would be little biostratigraphic value in separating the two genera. Thus, following Hill (1981), the Broken River form is tentatively included in *C. (Cystiphyllum)*.

*Cystiphyllum?* (*Cystiphyllum*) sp. lacks septal trabeculae, but otherwise closely resembles some New South Wales' specimens of *C. (C.) siluriense cylindricum* Lonsdale 1839, which have small rare septal spines, similar elongated, tabellae-like axial plates and a similar lack of "lamellar sclerenchyme tissue" (McLean 1974b: pl. 1, figs 4, 7). However, other specimens of *C. (C.) s. cylindricum* have numerous long septal spines and greatly thickened horizontal elements (McLean 1974b: text-fig. 3c). There appears to be continuous variation between these two forms.

**Distribution and Range.** Late Gorstian and Ludfordian of Broken River Province, north Queensland (Fig. 4).

### Genus *Cystiphyllum* (*Hedstroemophyllum*) Wedekind 1927

**Type species** (by original designation) *Hedstroemophyllum articulatum* Wedekind 1927: 65, 67, pl. 21, figs 1, 2, pl. 26, figs 6–12. Silurian, middle part of horizon III of Hedström. Northwest coast of the Isle of Gotland, Sweden.

**Diagnosis** (after Hill 1981). Trabeculae long? tufted monacanth, continuous through several successive calicular floors, separate except for their bases in wall or on sclerocones, sclerocones commonly thin especially in axial parts.

**Remarks.** *Cystiphyllum* (*Hedstroemophyllum*) was considered to differ from *Holmophyllum* Wedekind 1927 (type species, *H. holmi* Wedekind 1927, from the Silurian of Gotland) in having monacanthine, as opposed to rhabdacanthine trabeculae; a less sharply marked junction between the tabularium and the dissepimentarium; and inversely concave tabularial floors, with scattered large, convex plates, rather than the flat or concave floors that are common in *Holmophyllum* (Jell & Hill 1970; McLean 1974b). As Jell & Hill pointed out, further study of the Gotland material was needed as Wedekind's original descriptions failed to adequately define (differentiate) the two genera.

*Cystiphyllum* (*Hedstroemophyllum*) differs from *C. (Cystiphyllum)* Lonsdale 1839, principally in

having longer septal spines that penetrate several dissepiment layers (McLean 1974b; Hill 1981).

Australian species of *C. (Hedstroemophyllum)* were discussed by McLean (1974b).

### *Cystiphyllum* (*Hedstroemophyllum*) sp.

Fig. 11

**Material.** UQF72633 from UQL4002; the specimen is worn and partially embedded in matrix.

**Description.** Corallum probably cylindrical or weakly curved, 12 mm in diameter and at least 25 mm high; proximal end and calice missing, exterior not visible.

Septal spines based on wall, dissepiment crests and tabulae. Twenty-one 'rows' of spines over a peripheral arc of 135° give estimated total of 56. Major and minor septa indistinguishable. Septal spines 0.1–0.15 mm thick, directed upwards and inwards at 30–40° from horizontal towards periphery, steep to nearly vertical towards axis; longest spines pierce five tabular plates. In transverse section, they appear as short, radially arranged 'rows' of spines around corallum margin and as small 'dots' in axial region. Partially recrystallised septal spines deeply inset in corallum wall may have dark medial lines, indicating that they were originally monacanthine trabeculae. Corallum wall 0.1–0.2 mm thick, with indistinct lamination parallel to exterior of corallum.

Dissepiments globose or weakly to strongly elongate, steeply inclined inwards at about 60°

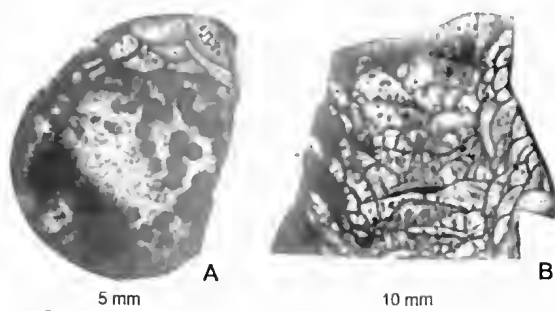


FIG. 11. *Cystiphyllum* (*Hedstroemophyllum*) sp., UQF72633 from UQL4002. A, transverse section; B, longitudinal section.

from the horizontal at periphery. Large, weakly domed tabulae and smaller globose tabellae developed across 6–7 mm wide axial zone.

**Remarks.** The only other described Australian species of *C. (Hedstroemophyllum)* is *C. (H.) crebrum* (McLean 1974b), from the upper Llandovery Quarry Creek and Rosyth Limestones of New South Wales. The north Queensland specimen differs in having slimmer, shorter septal spines that are strongly developed over the axial region and less prominent in the dissepimentarium.

Hill *et al.* (1969) illustrated a fasciculate specimen from the “upper part of the Jack Formation” as “*Hedstroemophyllum*” sp., coralla of which differ from the present specimen in being larger, and in having numerous, strongly radially arranged septal spines, a very wide dissepimentarium and an axial region that lacks well developed spines. That species resembles *C. (H.) nikiforovae* Strelnikov 1971 from the Late Silurian of the Subpolar Urals, but is larger, and has more septa and a wider dissepimentarium. All three forms are known only from single specimens and their relationships are unclear. The species described here could be a juvenile of Hill *et al.*’s specimen.

**Distribution and Range.** Late Gorstian or early Ludfordian of Broken River Province, north Queensland (Fig. 4).

### Order Stauriida Verrill 1865

### Suborder Stauriina Verrill 1865

### Family Pycnostylidae Stumm 1953

### Genus *Pycnostylus* Whiteaves 1884

**Type Species.** *Pycnostylus guelphensis* Whiteaves 1884: 3, pl. i, figs 1–16. Wenlock, Guelph Formation, Ontario, Canada (subsequent designation, Miller 1889: 202).

**Diagnosis.** Fasciculate, increase peripheral, commonly four offsets simulating axial quadripartite increase; corallites with very narrow peripheral stereozone; septa amplexoid, peripheral continuous part very short; no dissepiments; tabulae complete, horizontal (Hill 1981: F140).

**Remarks.** The synonymy, distribution and taxonomic relationships of *Pycnostylus* were discussed by Munson & Jell (1999).

### *Pycnostylus polyphyllodus* sp. nov.

Fig. 12

*Pycnostylus* sp. cf. *guelphensis* Whiteaves 1884; Hill *et al.* 1969: s.12, pl. S VI, fig. 6.

**Etymology.** Greek polys = many, phyllon = leaf, referring to the numerous septa in this species.

**Holotype.** UQF72664 from UQL4004. Late Wenlock, Jack Formation, Graveyard Creek Group, Jack Hills Gorge area, north Queensland.

**Material.** UQF72664–72666, 72668 from UQL4004; UQF72667 from UQL4326.

**Diagnosis.** *Pycnostylus* with small corallites having 80–90 major and minor septa, and thin peripheral stereozone; septal ridges short. Tabulae flat or gently arched, commonly with upturned edges.

**Description.** Fasciculate holotype corallum an irregularly shaped weathered fragment, 10–15 cm in diameter 14 cm high. Corallites in contact, or separated by 2–4 cm, slender, cylindrical, subparallel and slightly flexuous, with diameters averaging 6–7 mm, maximum 8 mm. Epithea longitudinally ridged, with fine transverse growth lines. Calice deep, with flat sides and base.

Two orders of septa radially arranged, number between 80 and 90. Septa thin, amplexoid, extending 1–2 mm towards axis as low ridges on distal surfaces of tabulae. Vertically continuous sections of major septa reach 1 mm in length; minor septa 0.6–0.8 length of major septa. Septal trabeculae fine, closely spaced, directed upwards and inwards at 30–40° from horizontal. Peripheral stereozone up to 0.5 mm thick, axially concave between septa, and indistinctly laminated parallel to corallite exterior.

Tabulae thin, complete, planar or rarely flexuous, slightly arched or horizontal, commonly with upturned edges; spacing 3–6/cm. Increase axial, typically quadripartite.

**Remarks.** *P. polyphyllodus* is distinguished from other Australian species of *Pycnostylus* by its small corallites, numerous septa and thin peripheral

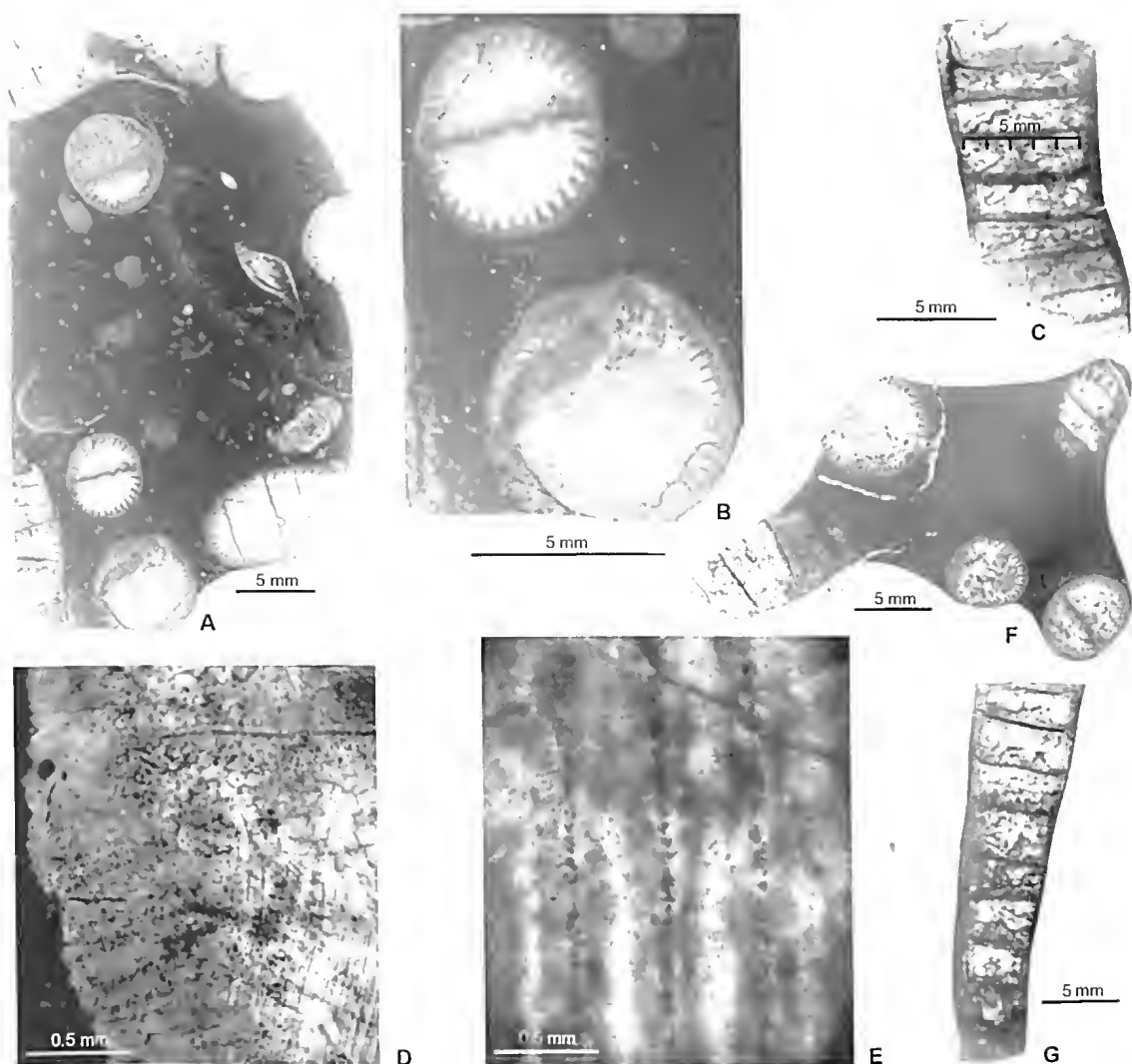


FIG. 12. *Pycnostylus polyphyllodus* sp. nov. A-E, UQF72664, HOLOTYPE, from UQL4004. A, transverse and oblique sections of several corallites; B, enlargement showing two corallites. Note trace of tabula on lower-left corner of lower corallite, showing amplexoid septal ridges; C, longitudinal section; D, portion of C, showing septal trabeculae and thin tabula. E, tangential section through corallite periphery, showing closely spaced trabecular axes. F-G, UQF72665 from UQL4004; F, transverse and oblique sections of several corallites; G, longitudinal section.

stereozone. *P. congregationis* (Etheridge 1907) from the Gorstian to earliest Ludfordian of the Yass Basin has corallites 10–15 mm in diameter with numerous connecting process arranged in tiers. The two orders of septa total between 34 and 36, and extend almost to the axis as low ridges on the distal surfaces of the tabulae (Hill 1940). *P. dendroides* (Etheridge 1907) also from

the early–middle Ludlow of the Yass Basin, has a dendroid corallum, with corallites averaging 12 mm in diameter and expanding to 15 or 20 mm just before increase. Major and minor septa are indistinguishable and number about 55 (Hill 1940). Both of these species are distinct from *P. polyphyllodus*.



The new species most closely resembles the type species, *P. guelphensis* Whiteaves 1884, from the Wenlock of Canada. From Stearn's (1956) description of this species and from examination of a topotype (UQF3458) it differs from *P. polyphyllodus* in having corallites of slightly smaller diameter (5–6 mm); fewer than one-half the number of septa (30–40); and more closely spaced tabulae (ca 14 per cm).

**Distribution and Range.** Wenlock of Broken River Province, north Queensland (Fig. 4).

### Family Amplexidae Chapman 1893

#### Genus *Amplexoides* Wang 1947

**Type Species.** *Amplexoides appendiculatus* Lindström 1883: 63–64, pl. 6, figs 7–8, Wenlock, Chaotien, Sichuan Province, China (by original designation).

**Diagnosis.** Corallum solitary, trochoid to sub-cylindrical, septa amplexoid, longitudinally continuous only in narrow peripheral stereozone, major septa extending adaxially only as long, low ridges developed on upper surfaces of complete, horizontal tabulae that may have downturned edges; minor septa short; no dissepiments (Hill 1981: F146–147).

**Remarks.** The synonymy, distribution and taxonomic relationships of *Amplexoides* were discussed by McLean (1977) and Munson & Jell (1999).

#### *Amplexoides* sp.

Fig. 13

**Material.** UQF72602 from UQL4006; UQF72603 from UQL4002; UQF72604 from UQL4008. All specimens badly worn.

**Description.** Corallum large, probably cylindrical or possibly ceratoid, approaches 3 cm in diameter; most complete specimen (UQF72602) is approximately 8 cm long. Poorly preserved calice of one specimen (UQF72602) appears to be shallow and flat-floored. Neither proximal ends nor epitheca preserved.

Two orders of septa; in UQF72603 105 septa over a peripheral arc of 300° give an estimated total of 126; UQF72602 has 128 septa. Major septa amplexoid, extending at least halfway

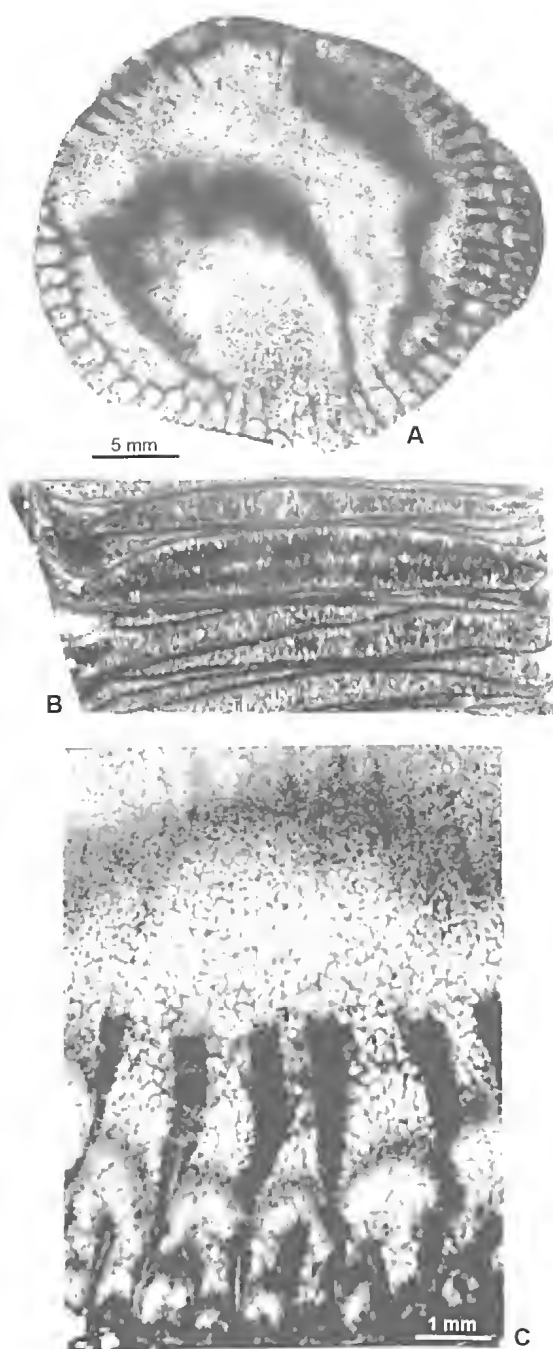


FIG. 13. *Amplexoides* sp., UQF72603 from UQL4002. A, B, transverse and longitudinal sections; C, portion of A showing structure of wall and rhopaloid amplexoid septa.



towards axis as very low ridges over upper surfaces of tabulae. Vertically continuous sections 4–5 mm long, slightly rhopaloid, i.e., axial ends slightly dilated and appear club-shaped in transverse sections. Minor septa 1–1.5 mm long, also slightly rhopaloid, but not amplexoid. Microstructure partly obscured by recrystallisation, particularly in areas of septal dilation. Septal trabeculae, visible only in small region of UQF72602, fine, closely spaced, directed upwards and inwards at low angle (30–40° from the horizontal). Corallite wall is up to 0.5 mm thick, with distinct lamination parallel to exterior of corallum, laminations concave towards interseptal loculi, forming small non-septal bulges similar to those described below in *Multicarinophyllum vepreculatum* sp. nov.

Tabulae mostly complete, flat or slightly domed, with downturned edges; area of downturning appears to be equivalent to zone where major septa are vertically continuous. Tabular spacing unequal; from nearly in contact to 4–5 mm apart. Tabulae finely laminated parallel to their bases.

**Remarks.** This is a large species with numerous septa, distinctive slightly rhopaloid septa and minor septa that are not amplexoid. Insufficient numbers of specimens and the very weathered coralla preclude a precise determination of the species.

*Amplexoides grayense* Munson & Jell 1999, from the upper Llandovery Quinton Formation in the north of the Graveyard Creek Subprovince, can be readily distinguished from this species by its very elongate, slightly smaller corallum (diameter to 23 mm), and fewer septa (maximum 76). *Amplexoides* sp. A, also from the Quinton Formation, is known from a single poorly preserved specimen that is slightly smaller (diameter 25 mm) than *Amplexoides* sp., but has a comparable number of septa (about 110). That species also has shorter amplexoid major septa, and major and minor septa are not dilated at their axial ends.

The only other described species of *Amplexoides* from Australia, *A. gephyra* McLean 1985, from the early Llandovery of New South Wales, has a probable trochoid or ceratoid corallum,

with a diameter of 25–36 mm, similar in size to *Amplexoides* sp., but also has proportionally fewer septa (80–90), and a less regular tabularium.

Etheridge, in Jack & Etheridge (1892b), described and illustrated a single coral fragment, from the Broken River area, as *Amplexus* sp. ind. The precise location of the specimen was not given, and it is of uncertain age; thus limiting its stratigraphic value. The specimen differs from those described above in having fewer septa (ca 30) and an apparently well developed aulos (Etheridge 1892b: pl. 37, fig. 16). Etheridge's description and figures are inadequate for precise identification, but the specimen is possibly referable to the late Paleozoic genus *Amplexocarinia* Soshkina 1928.

**Distribution and Range.** Late Gorstian and Ludfordian of Broken River Province, north Queensland (Fig. 4).

## Suborder Streptelasmatina Wedekind 1927

### Family Mucophyllidae Hill 1940

#### Genus *Stylopleura* Merriam 1973

**Type Species.** *Stylopleura berthiaumi* Merriam 1973: 34–35, pl. 3, figs. 6–20. Late Silurian, Roberts Mountains Formation, Roberts Creek Mountain, Nevada (by original designation).

**Diagnosis.** Fasciculate to sub-compound, with unequal corallites joined by connecting processes that may be hollow; mature calices flaring and trumpet-shaped; wall a narrow peripheral stereozone from which short laminar septa project adaxially as low ridges with little or no distinction between major and minor; tabulae complete, horizontal; no dissepiments; increase marginal, unequal (slightly modified after Hill 1981: F178).

**Remarks.** The synonymy, distribution and taxonomic relationships of *Stylopleura* were discussed by Merriam (1973) and Pedder (1985).

#### *Stylopleura liliiforme* (Etheridge 1907)

Fig. 14

? *Amplexus* (*Coelophyllum*) *eurycalix* Weissmermel 1894: 634, pl. 50, figs 8, 9, pl. 51, fig. 1.

*Tryplasma liliiformis* Etheridge 1907: 95, pl. 14, figs 2, 3, pl. 15, figs 2, 3, 24, pl. 17, figs 7, 8, pl. 24, fig. 1, pl. 25, fig. 8, pl. 27, figs 1, 2.

*Tryplasma liliiformis* Etheridge; Chapman 1920: 184, pl. 17, fig. 3. *Mycophyllum liliiforme* (Etheridge); Hill 1940: 401, pl. 11, figs 18, 19, pl. 12, figs 3–6.

*Mucophyllum liliiforme* (Etheridge); Hill *et al.* 1969: s.12, pl. S VI, figs 4–5.

**Lectotype** (selected Hill 1940: 401). F8892, Australian Museum, Silurian, Barber's Creek, off Derrengullen Creek, Bowring district, New South Wales; illustrated Etheridge 1907: pl. 15, fig. 3.

**Material.** UQF72657, 72662 from UQL4002; UQF72658–72660 from UQL4010; UOF72661 from UQL4332; UQF72663 from UQL4009; UQF60108, replacement slide from specimen illustrated by Hill *et al.* (1969: pl. S VI, figs 4, 5) from the Jack Formation, Jack Hills Gorge.

**Diagnosis** (modified from Hill 1940). Sub-compound *Stylopleura* with turbinate or trochoid stem, and thin, spreading calical rim; with scattered peripheral increase.

**Description.** Corallum large, commonly sub-compound; corallites liliaciform, with proximal trochoid or turbinate stems, and expanding bell-shaped but not everted calical rims, which reach maximum thickness of 3 mm. Offsets arise by peripheral increase from calical rim; 6 are present in UQF72657. Calice deep and flat floored, expands to 7.5 cm in diameter in largest specimen (UQF72657). Stem usually between 20 and 25 mm across; largest reaches 3 cm; longest complete stem measures 2 cm.

Corallite exterior marked by prominent radial lines corresponding to joins between dilated septa, and fine concentric growth lines. Edge of calical rim, where preserved, scalloped, the undulations occurring at septal junctions. Small, 1–2 mm wide rootlets may be developed over stem, and are thick-walled and hollow, commonly with irregularly and distantly spaced transverse partitions, flat or convex towards rootlet tip. No evidence found of an operculum, which Hill (1940) suggested might be present.

About 80 septa, major and minor septa indistinguishable, strongly dilated, laterally in contact except at tabularium, where all taper to abrupt, free spinose ends. Septa appear to continue across tabularium as rows of small fine spines completely buried in tabular thickening or occasionally with free distal ends. Septa may reach 2–3 mm wide at calicular edge in larger specimens. Septal trabeculae rhabdacanthine, typically spaced ca 1 mm apart, their axes directed normally to inner and outer surfaces of corallite wall and calical rim. Rhabdacanthine rods widely spaced, diverge from trabecular

axes in very broad arcs at ca 30° from axis. Dilated septa distinctly laminated parallel to their distal surfaces.

Tabulae complete or less commonly incomplete, flat or gently arched, usually spaced about 6–8 per cm but may be very close together; UQF60108 has 12 over vertical distance of 5 mm. Tabulae usually thin, but may be thickened to as much as 0.5 mm. Thickened tabulae laminated, laminae broadly and shallowly concave distally, appearing to 'lap' onto small tabular trabeculae which are fine and rhabdacanthine. Rootlet walls also laminated, reach a maximum thickness of 0.5 mm. Rootlet partitions much thinner, their laminae continuous with those of walls. Dissepiments absent.

**Remarks.** This species was assigned to *Stylopleura* by Pedder (1985: 588). The Broken River specimens differ from those previously assigned to *S. liliiforme* in possessing tabular trabeculae, and in having undifferentiated major and minor septa; other Australian specimens of the species have major and minor septa that are just distinguishable by length (Etheridge 1907; Hill 1940). All other diagnostic characters of *S. liliiforme* are present in the Broken River specimens.

Variation between specimens is slight, but the calical rim varies from less than 1 mm in UQF72663 to about 3 mm in UQF60108. The wall of the stem is usually thin (>1.5 mm) except in UOF72660, in which it is greatly thickened to 4 mm. However, that specimen, which is partially crushed, has a narrow calical rim (<2 mm) but is otherwise similar to the remaining material. The only other variation of any note between the specimens is in the degree of development of tabular trabeculae; weak in some corallites, relatively strong in others.

**Distribution and Range.** Late Gorstian and Ludfordian of Broken River Province, north Queensland (Fig. 4); Ludfordian of Yass Basin, New South Wales.

### Family Amsdenoididae Hill 1981

#### Genus *Multicarinophyllum* Spasskiy 1965

*Multicarinophyllum* Spasskiy 1965: 24.

*Multicarinophyllum* Spasskiy; Bulvankar *et al.* 1968: 16.

*Multicarinophyllum* Spasskiy; Dubatolov & Spasskiy 1971: 107.

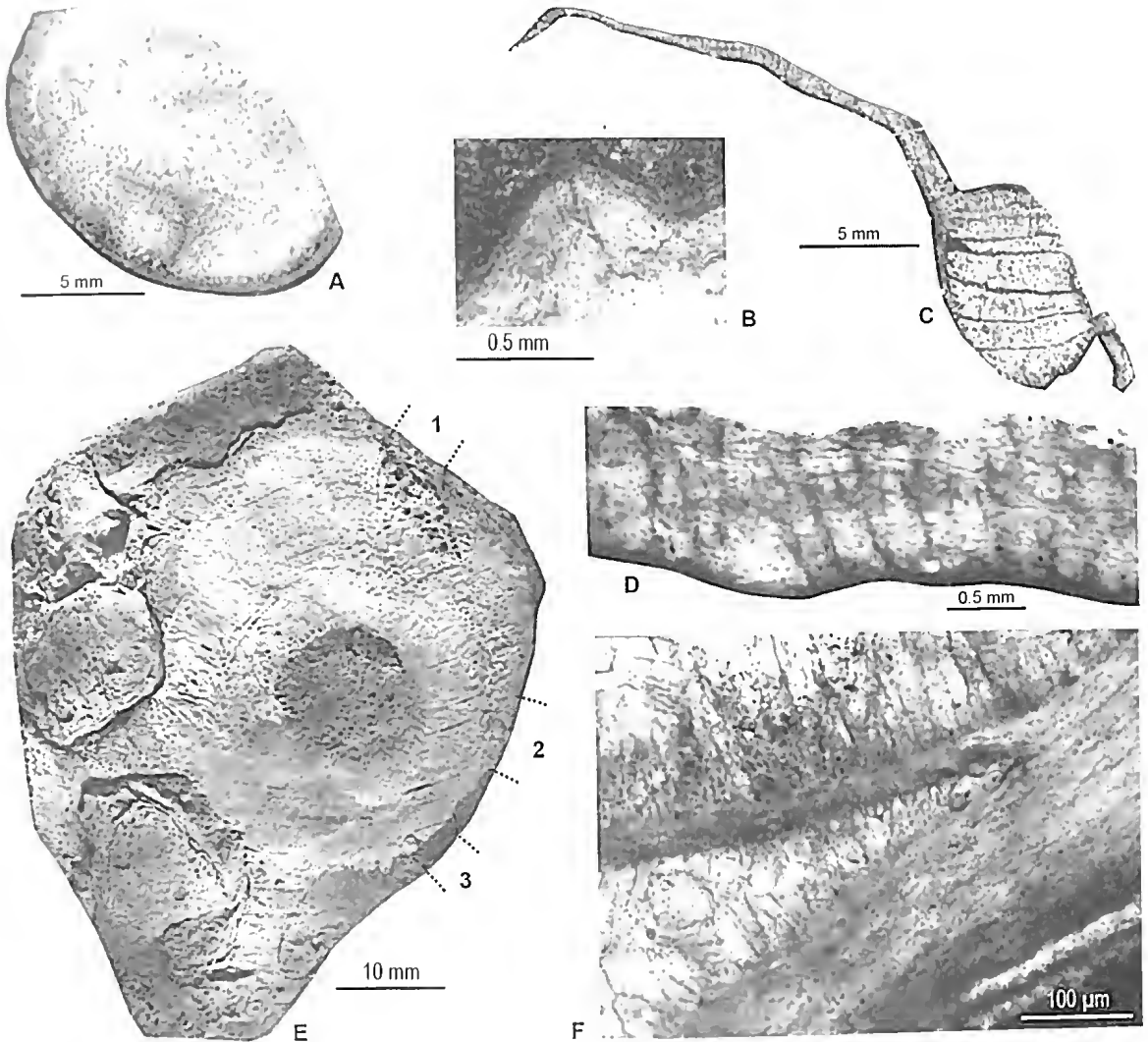


FIG. 14. *Stylopleura liliiforme* (Etheridge 1907). A, UQF72661 from UQL4332, transverse section of stem; B, UQF72658 from UQL4010, portion of transverse section through calice, showing rhabdacanthine septal trabeculae. C-D, UQF72659 from UQL4010; C, longitudinal section, showing stem with rootlet, and wide calice (missing at right); D, portion of C, showing microstructure of calical wall; E, UQF72657 from UQL4002, proximal view (stem missing), showing subcompound corallum; three visible daughter corallites, (left and lower part of figure), and position of three others (not visible in this view) marked 1-3; F, UQF72662 from UQL4002, portion of rootlet showing structure of wall and transverse partition (centre-left).

**Type Species** (by original designation, p.25). *Multicarinoptyllum multicarinatum* Spasskiy 1965: 25, pl. 1, figs 1-2. Eifelian (early Middle Devonian), central Asia.

**Diagnosis** (modified from Dubatolov & Spasskiy 1971). Large ceratoid solitary coral. Epitheca with longitudinal ridges and transverse growth

annulations. Calice moderately deep with sharp edges. Fine, long major septa convolute axially; axial ends may be united. Minor septa 0.25-0.5 length of major septa. All are strongly vepreculate particularly towards the periphery where a stereozone or rare, large dissepiments may be present. Tabulae closely spaced,

incomplete, and usually domed, with many additional plates axially.

**Remarks.** *Amsdenoides* Sutherland 1965, was erected the same year as *Multicarinophyllum* and is a very similar genus. The type species of *Amsdenoides*, *A. acutianmulatum* (Amsden 1949) differs from *M. multicarinatum* in being smaller with fewer septa, in having vepreculae that are developed only on the major septa, and a less complex tabularium with only very sparsely developed tabulae. Kato & Minato (1977) suggested that the two genera might be synonymous, but Hill (1981) tentatively regarded them as distinct. *Amsdenoides* occurs in the Early Silurian (Telychian) of Japan (Kido 2009), Ludlow of North America (Sutherland 1965) and possibly the Early Devonian of north Queensland (Yu & Jell 1990).

The occurrence of vepreculae distinguishes *Multicarinophyllum* from several other genera that would otherwise superficially resemble it. These include *Grewinkia* Dybowski 1873, which also differs in having a less complex axial structure; *Tabnlophyllum* Fenton & Fenton 1924, in which the major septa are withdrawn from the axis and do not form a vortex; *Dinophyllum* Lindström 1882, which also has shorter, almost rudimentary minor septa; and *Zmeinogorskia* Spasskiy (cited Dubatolov & Spasskiy 1971; original reference not quoted), which also has a less complex convoluted zone.

***Multicarinophyllum vepreculatum* sp. nov.**

Fig. 15

*Dinophyllum* sp.; Hill *et al.* 1969: p. s.10, pl. S V, fig. 2.

**Etymology.** Refers to the characteristic vepreculae of this form.

**Holotype.** UQF72613 from UQL4335, Ludfordian, Jack Formation, Graveyard Creek Group, Jack Hills Gorge area, north Queensland.

**Material.** UQF72605–72612, 72614–72615, 72617 from UQL4004; UQF72613 from UQL4335; UQF72616, 72618, 72620 from UQL4002; UQF72619 from UQL4334; UQF53982, from which a thin section was illustrated by Hill *et al.* (1969).

**Diagnosis.** Large, ceratoid or cylindrical *Multicarinophyllum*. Between 47 and 55 weakly or moderately convolute major septa; axial

ends commonly united. All septa vepreculate towards periphery. Cardinal septum short, in open cardinal fossula; alar fossulae weakly developed. Tabulae closely spaced, incomplete, slightly or moderately domed; peripheral plates commonly inclined upwards and outwards. Dissepiments absent.

**Description.** Corallum ceratoid or cylindrical; largest specimen (UQF53982) reaches maximum diameter of ca 40 mm and height of at least 120 mm. Longitudinal ridges corresponding to interseptal loculi, and transverse growth annulations mark epitheca. Calice wide, moderately deep, with flat sides and distally convex base.

Between 47 and 55 major septa usually reach axis where they tend to coalesce, though not all at same point, and are weakly or moderately convolute. Short cardinal septum about twice length of minor septa, and lies in open cardinal fossula that may be slightly expanded axially. Alar fossulae not prominent, usually recognisable by presence of contratingent septa on their counter sides. Minor septa 4–5 mm in length. Both orders of septa thin, with deep keels and slightly dilated peripheral ends. Vepreculae developed on all septa, more numerous towards periphery. Microstructures obscured in most specimens by recrystallisation, but rarely, in longitudinal section, axes of trabeculae appear as dark lines spaced ca 150  $\mu$ m apart, and directed upwards and inwards at between 30° and 40° from the horizontal.

Marginal stereozone variable in thickness, reaches maximum of 3.5 mm across in holotype, and shows distinct lamination roughly parallel to epitheca. In interseptal loculi, laminae bulge axially to form stubby, non-septal projections with irregular medial dark lines; these may be weakly developed or 1–2 mm long. Incomplete tabulae fine, regular, close (as many as 15 per cm in holotype), slightly to moderately domed. Peripheral plates commonly inclined upwards and outwards at low angle. Dissepiments absent.

**Remarks.** Some variation is shown by this species: the marginal stereozone varies in thickness from less than 1 mm to 3.5 mm; the degree of axial convolution of the major septa

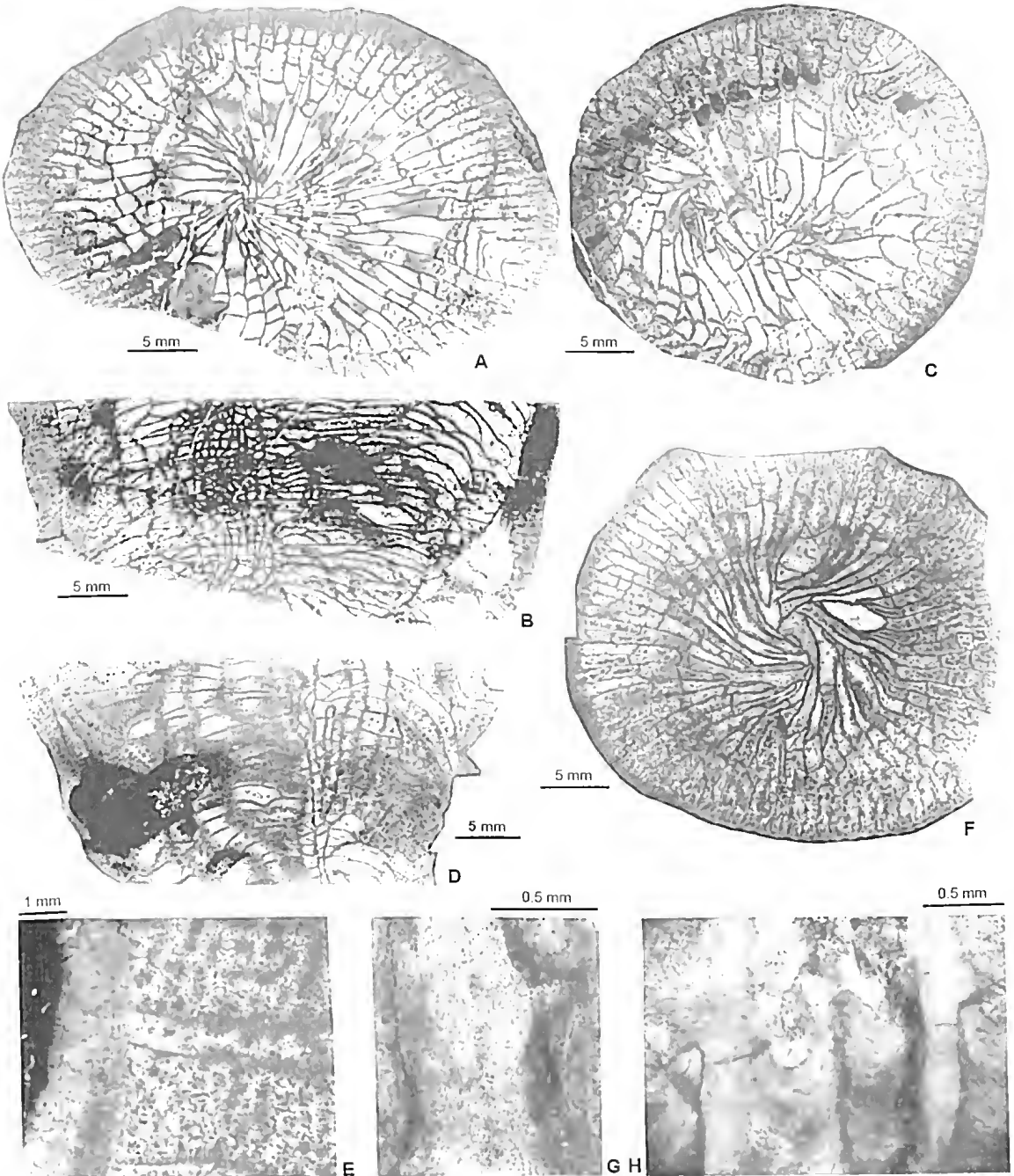


FIG. 15. *Multicarinophyllum vepreculatum* sp. nov. A, B, UQF72613 from UQL4335, HOLOTYPE, transverse and longitudinal sections; C, UQF72606 from UQL4004, transverse section; D, UQF72607 from UQL4004, longitudinal section; E, UQF72615 from UQL4004, portion of longitudinal section showing vepreculae; F-H, UQF72619 from UQL4334; F, transverse section; G, tangential section through periphery of corallum showing axes of septal trabeculae and longitudinal section of veprecula (right); note dark medial line (arrow); H, portion of F showing structure of wall.

may be weak or moderate; vepreculae are more numerous in some specimens than others; the non-septal bulges of the stereozone in the interseptal loculi may be weakly developed or 1–2 mm long. As the variation among specimens appears to be continuous, further subdivision of the taxon is of little value.

All three other recorded species of *Multicarinophyllum* are from central Asia. *M. multitarinatum* Spasskiy 1965, the type species, is closest to *M. vepreculatum*, but can be distinguished by the shape and structure of its tabulae; these are wavy and more complete, and the peripheral plates are inclined upwards and inwards rather than upwards and outwards as in the new species.

*Multicarinophyllum cinctum* Dubatolov & Spasskiy 1971 differs in possessing tabulae with a pronounced medial sag and septa that are dilated towards the periphery, coalescing into a thin stereozone. *M. concavum* Dubatolov & Spasskiy 1971, differs in having large, lonsdaleoid dissepiments which are absent in *M. vepreculatum*. *M. cinctum* and *M. concavum* are also distinguished by having major septa that may be withdrawn from the axis, and are much less convolute.

A poorly preserved species, *Amsdenoides? dubins* Yu & Jell 1990, from the overlying Early Devonian (Lochkovian–Pragian) Shield Creek Formation, is very similar to *M. vepreculatum*, but there are a number of significant differences. *Amsdenoides? dubins* is about one-half the diameter of *M. vepreculatum*, but has a similar number of septa (about 50). All specimens are abraded, so details of the corallum wall and the peripheral ends of septa are poorly known. Septa are dilated peripherally and gradually attenuate towards the axis, whereas those of *M. vepreculatum* are generally thin and are dilated only at their peripheral ends. The major septa in the younger species are commonly slightly withdrawn from the axis, whereas those of *M. vepreculatum* reach the axis and are usually conjoined. The tabulae of *A.? dubins* are sparsely developed, as is typical of *Amsdenoides*,

whereas those of *M. vepreculatum* are regular and close. Although these species are clearly related, these differences are sufficient to distinguish the two forms.

The vepreculae in *M. vepreculatum* appear to be prolongations of lateral, secondary trabeculae given off from the larger primary trabeculae. This is suggested by the presence of rare medial dark lines within vepreculae in tangential section (Fig. 15G) that are interpreted as probable remnant trabecular axes. The vepreculae are thicker than the rods of rhabdacanth, such as those of *Aphyllum pachystele* sp. nov. (Fig. 9F) and are longer and more prominent. They invariably project at right angles to the plane of the septum rather than radially as do the rods of rhabdacanth, and the rhabdacanth also differ in that they are formed entirely of rods; no distinct axial pillar occurs. Spacing is also important. The rods of the rhabdanth are usually closely and uniformly spaced along its length, whereas the vepreculae in *M. vepreculatum* are more widely and irregularly spaced. Rhipidacanth, described by Jell (1969), more closely resemble vepreculae and are compound, consisting of a central primary trabecula from which short secondary trabeculae are given off at regular intervals. They are distinguished from the vepreculae in *M. vepreculatum* by the closer, more regular spacing of the non-spinose secondary trabeculae; these are similar in size to the primary trabecula, whereas vepreculae are smaller.

**Distribution and Range.** Late Wenlock and early Ludfordian of Broken River Province, north Queensland (Fig. 4).

#### Suborder Arachnophyllina Zavoronkova 1972

#### Family Entelophyllidae Hill 1940

#### Genus *Entelophyllum* Wedekind 1927

**Type Species** (designated Lang *et al.* 1940). *Madrepurites articulatus* (Wahlenberg 1821). "Upper Silurian", Gotland.

**Diagnosis** (slightly modified after Jell & Sutherland (1990). Solitary, phaceloid or dendroid



rugosans; septa long, generally radially arranged, counter-cardinal septa rarely distinguishable, smooth or asymmetrically carinate; major septa slightly withdrawn from axis; minor septa contraclined or contratigent in some; tabularium wide, broadly domed commonly with depressed axial area and marginal periaxial trough formed by small subhorizontal or concave tabellae; dissepiments numerous, small, globose with lonsdaleoid dissepiments in some.

**Remarks.** The synonymy, distribution and taxonomic relationships of *Entelophyllum* were fully discussed by Jell & Sutherland (1990). They considered that solitary forms with thickened and carinate septa could possibly be included in *Nanshanophyllum* Yu (1956; type *N. typicum* Yu, Middle Silurian, China) as a subgenus of *Entelophyllum*. However, there does not seem to be any biogeographic or stratigraphic significance for such a division and Jell & Sutherland did not take that step. Solitary forms such as *E. latum* are thus retained within a broader generic concept.

*Entelophyllum patulum*  
(Foerste 1888) comb. nov.

*Cyathophyllum patula* Foerste 1888: 129, pl. 13, figs 9–11.

*Heliophyllum yassense* Etheridge 1892a: 170, pl. 11, fig. 8, pl. 12, figs 1–3.

*Xylodes yassense* (Etheridge); Jones 1936: 56, pl. 7, figs 3, 4 (non fig. 5).

*Entelophyllum yassense* (Etheridge); Hill 1940: 412, pl. 13, figs 11, 12.

*Entelophyllum yassense* var. *patulum* (Foerste); Hill 1940: 413, pl. 13, figs 13 a, b.

*Entelophyllum* sp. cf. *yassense* (Etheridge); Hill *et al.* 1969: s.10, pl. S V, figs 6, 7.

*Entelophyllum yassense yassense* (Etheridge 1892a); McLean 1976: 185–186, pl. 18, figs 8–10, pl. 19, fig. 1, text-fig. 3.

*Entelophyllum yassense patulum* (Foerste); McLean 1976: 186–187, pl. 19, figs 2–6, pl. 20, figs 1–3.

**Diagnosis.** Patellate or fasciculate *Entelophyllum*. Septa carinate and thin, minor septa 0.3–0.5 length of major. Tabularium divided into arched axial series and periaxial concave series; tabulae very closely spaced.

**Remarks.** The species epithet *patulum* predates *yassense* and takes precedence as the specific name (cf. McLean 1976: 185–187). Includes *E. patulum yassense* (*sensu* Etheridge 1892a) as well as the nominate subspecies.

**Distribution and Range.** Ludlow of New South Wales; late Gorstian to early Ludfordian of Broken River Province, north Queensland; Late Silurian (undifferentiated) of Inner Mongolia.

*Entelophyllum patulum yassense*  
(Etheridge 1892a)  
Figs 10 C–E, 16

*Heliophyllum yassense* Etheridge 1892a: 170, pl. 11, fig. 8, pl. 12, figs 1–3.

*Xylodes yassense* (Etheridge); Jones 1936: 56, pl. 7, figs 3, 4 (non fig. 5).

*Entelophyllum yassense* (Etheridge); Hill 1940: 412, pl. 13, figs 11, 12.

*Entelophyllum* sp. cf. *yassense* (Etheridge); Hill *et al.* 1969: s.10, pl. S V, figs 6, 7.

*Entelophyllum yassense yassense* (Etheridge); McLean 1976: 185–186, pl. 18, figs 8–10, pl. 19, fig. 1, text-fig. 3.

**Lectotype** (here designated). F4015, Australian Museum, from the Ludlow of the Yass district, New South Wales, figured by Etheridge (1892a: pl. 12, fig. 3). Jones (1936) indicated that the specimens described by Etheridge were missing, but one slide of the type material had subsequently been found.

**Material.** UQF72621, 72623–72631 from UQL4002; UQF72622, 72634 from UQL4010.

**Diagnosis.** Fasciculate *Entelophyllum patulum*; corallites may be united by lateral expansions; increase non-parricidal. Septa may be dilated in dissepimentarium. Tabularium narrow. Dissepimentarium in two zones; outer of 1–2 series of large rhomboid dissepiments; inner of small globose dissepiments; dissepiments horizontal or shallowly inclined inwards at periphery, more steeply inclined at junction with tabularium.

**Description.** Corallum fasciculate, corallites irregularly spaced; some in contact, others separated by as much as 5 cm (average spacing just less than 1 cm). Corallum expands very rapidly, is usually far wider than high at maturity; largest recorded specimen (*in situ*) had a diameter of 36 cm and a height of 14 cm. Corallites cylindrical or slowly expanding, 8–17 mm in diameter, up to 9 cm high. Calice broad and flat with small axial boss, epitheca shows longitudinal double ridges. Increase peripheral and unequal, larger part of parent corallite being unaffected with continuing growth of parental tabularium.

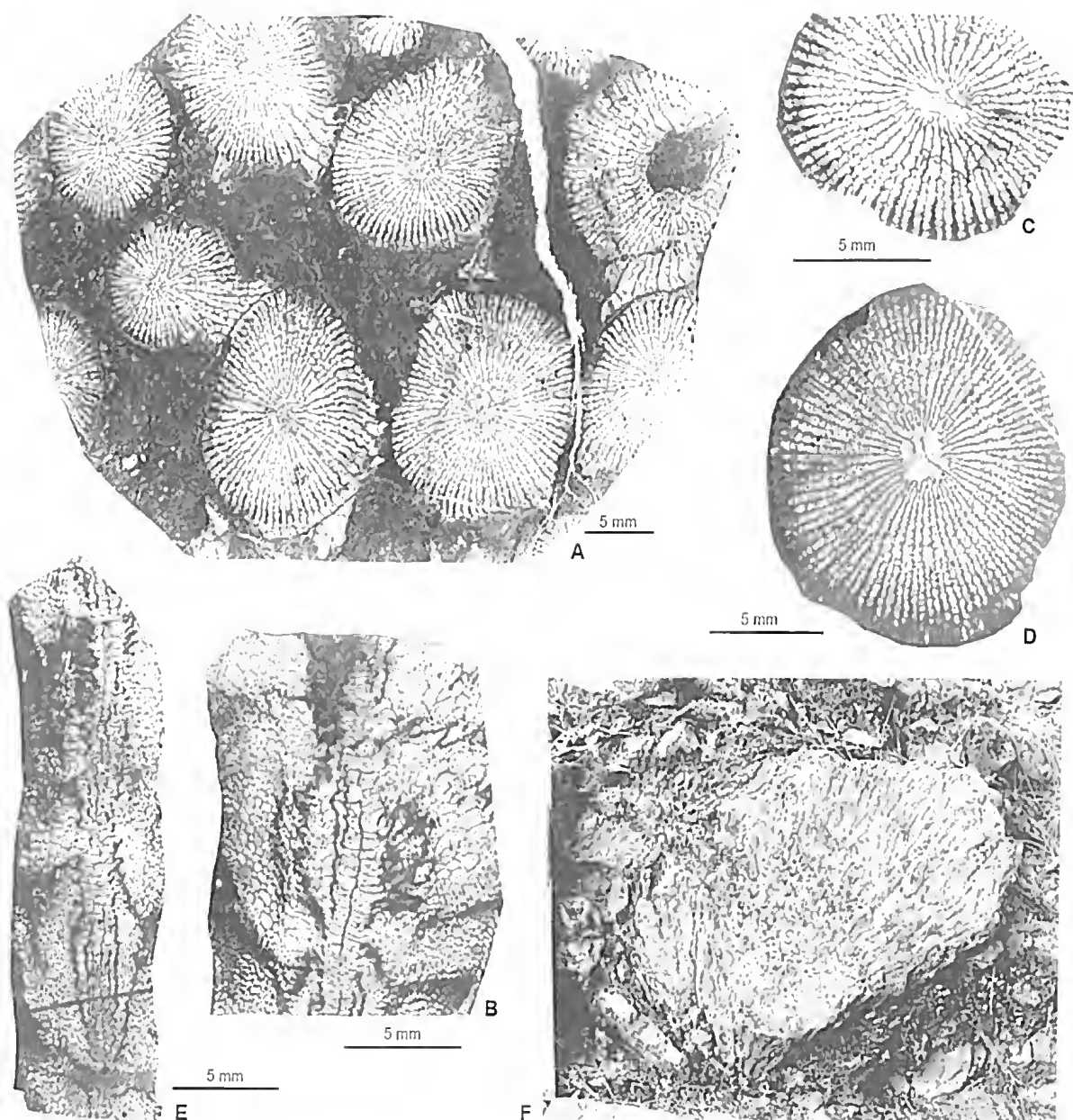


FIG. 16. *Entelophyllum patulum yassense* (Etheridge 1892a). A-B, UQF72624 from UQL4002. A, transverse section showing thin septa and lateral extensions between corallites; B, longitudinal section; C, UQF72629 from UQL4002, transverse section showing dilated carinate septa; D, UQF72622 from UQL4010, transverse section showing dilated carinate septa; E, UQF72625 from UQL4002, longitudinal section; F, exterior of *in-situ* corallum at UQL4009, about 14 cm high.



Two orders of septa number between 70 and 80 in largest corallites. Septa usually attenuate but may be dilated towards corallite periphery. Both orders possess xyloid carinae most prominent in dissepimentarium. Major septa usually slightly withdrawn from axis, leaving small axial space, typically less than 1 mm in diameter, into which longer cardinal and counter septa project. Major septa adjoining cardinal septum may be shortened, or may be slightly curved to outline small fossula. Minor septa usually between 0.3 and 0.5 length of major septa. Septal trabeculae thin, contiguous, and directed normally to upper surfaces of dissepiments. Carinae are lateral outgrowths from trabeculae, are parallel to them, and are irregularly arranged on either side of each septum. Corallite wall very thin, dilated only in vicinity of lateral extensions where it may be as thick as 0.5 mm. Dilated septa show distinct lamination parallel to septa and reach maximum thickness of nearly 0.5 mm.

Lateral extensions may be present between any two corallites. These are irregular prolongations of wall and lumen of one corallite to another and may join corallites for much of their lengths. Only one corallite forms the extension, and its septa and dissepimentarium extend into the process as far as the wall of second corallite, which is greatly dilated in area of contact. Septa within extension usually non-carinate.

Tabularium 0.4–0.5 diameter of corallite, consists of two series of incomplete tabellae: axial series forms loose axial structure with outermost plates globose, innermost flat or sagging; periaxial series of small, slightly sagging plates.

Dissepiments also in two zones: outer of 1–2 series of large rhomboid dissepiments, horizontally based or slightly inclined inwards; inner of smaller globose and more steeply inclined dissepiments. In some cases, a single long, shallow, more gently curved plate may replace several. Dissepiments may be weakly geniculate.

**Remarks.** Variation occurs in respect to corallite size and the amount of dilation of the septa. Corallites with dilated septa tend to have

smaller diameters than those with unthickened septa, but septal numbers correlate well with corallum diameter (Fig. 17), which indicates that this represents intraspecific variation.

The Broken River material differs from previously described specimens of *E. patulum yassense* in possessing septal dilation in some specimens, and in being smaller overall. These differences are considered to be insufficient to recognise at specific rank (see above).

*Entelophyllum patulum patulum* (Foerste 1888) can be distinguished from *E. patulum yassense* by its patellate growth form and more numerous septa.

Guo (1978) illustrated a transverse section of a specimen from the Late Silurian of Inner Mongolia as *Entelophyllum* aff. *yassense* (Etheridge). That specimen closely resembles *E. patulum yassense*, but is not described and is insufficiently illustrated for precise specific identification.

Hill (1940) noted that the overseas species that most closely resemble '*E. yassense*' are possibly the Wenlock and Ludlow *E. articulatum* and *E. pseudoanthum*, from England and the Baltic. These species differ in having parricidal increase, and in lacking an outermost series of rhombic dissepiments. Hill also indicated that the Wenlock, North American *E. rugosum* Smith

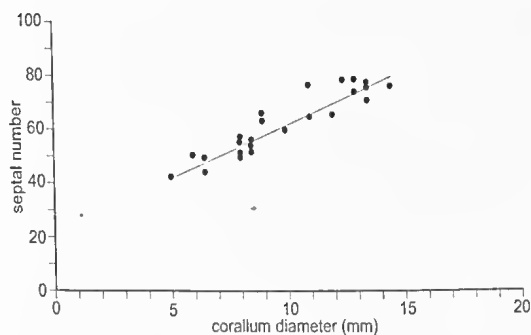


FIG. 17. Linear least squares plot of corallite diameter against septal number (correlation coefficient 0.92) for Jack Formation specimens of *Entelophyllum patulum yassense* (Etheridge 1892a).

1933, had similarities with '*E. yassense*'. McLean (1976), however, suggested that Smith's species was closer to the Soviet genus *Strephophyllum* Lavrusevich 1971, because of its similar flat or sagging tabulae and narrow dissepimentarium. He suggested it may be intermediate between the two genera.

**Distribution and Range.** Late Gorstian to early Ludfordian of Broken River Province, north Queensland (Fig. 4); Ludfordian of New South Wales; Late Silurian (undifferentiated) of Inner Mongolia?

### *Entelophyllum latum* Hill 1940

Fig. 18

*Entelophyllum latum* Hill 1940: 413–414, pl. 13, figs 8–10; Strusz 1961: 338–339, pl. 42, figs 3–5.

*Entelophyllum* sp. Hill 1942a: 4, pl. 2, figs 1 a, b.

**Holotype.** F8973, Australian Museum (collected by AJ Shearsby 1903), from the Wenlock anticline at Glenbowee, between Yass and Canberra, near the Boambolo crossing of the Murrumbidgee River, New South Wales.

**Material.** UQF72635–72639, all from UQL4002.

**Diagnosis** (after Hill 1940). *Entelophyllum* with numerous thin septa, and with axial structure so wide as almost to fill the tabularium.

**Description.** Corallum solitary, cylindrical or broadly trochoid. External characters not observed. Specimens vary from 13 to 22 mm in diameter, with 42 major, and 42 minor septa at a diameter of 17 mm. Septa are attenuate, smooth, or with weakly developed xyloid carinae in dissepimentarium. Major septa generally of unequal length, may unite at their axial ends, but more usually slightly withdrawn from axis leaving axial space 1–2 mm in diameter. A small, weakly developed fossula may be outlined by slightly curved major septa next to cardinal septum. Minor septa 0.3 to 0.5 length of major septa, not quite reaching width of dissepimentarium. Septal trabeculae fine, closely spaced, directed upwards and inwards normally to dissepiments. Carinae unclear in longitudinal section. Apart from no secondary thickening of septa or walls in any observed specimens, microstructure resembles that of *E. patulum yassense* (Etheridge 1892a).

Tabularium of numerous incomplete tabellae forming a wide axial structure separated from

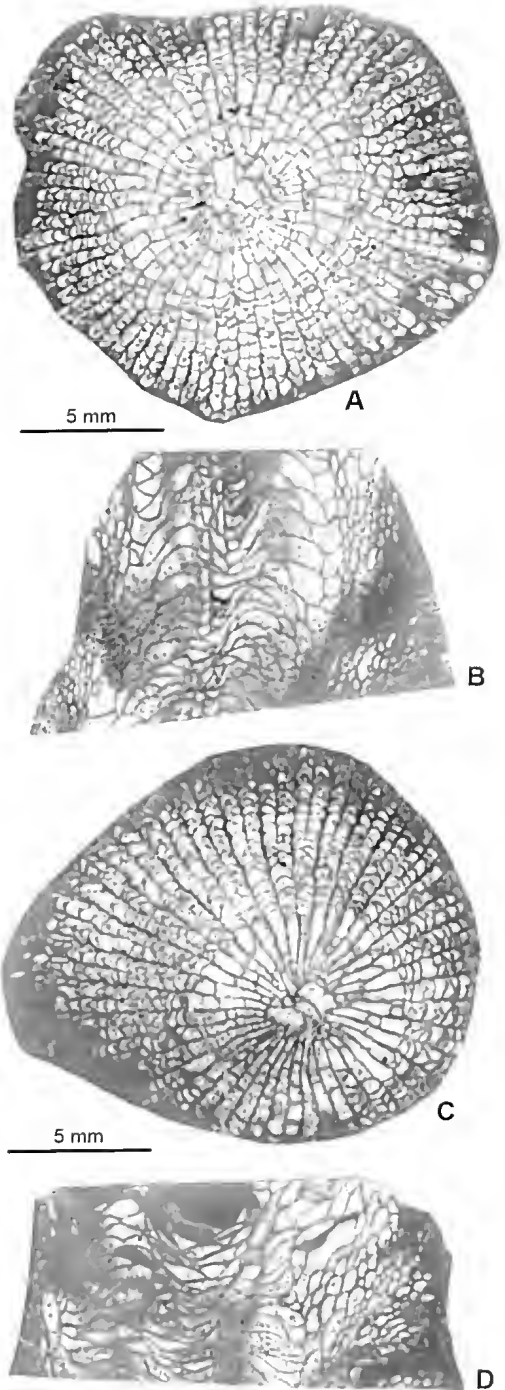


FIG. 18. *Entelophyllum latum* Hill 1940. A, UQF72637 from UQL4002, transverse section; B, UQF72636 from UQL4002, longitudinal section; C, D, UQF72635 from UQL4002, transverse and longitudinal sections.

dissepimentarium by periaxial series of small, flat or slightly sagging tabellae inclined upwards and outwards. Axial structure of central flat or shallowly concave tabellae surrounded by circumferential series of domed, horizontally based tabellae. Dissepiments generally small globose, inclined steeply inwards towards axis. In some cases several may be replaced by a single long shallow tabella.

**Remarks.** Hill (1940) described considerable variation in the development of septal carinae in *E. latum*. The holotype lacks carinae, while three paratypes are carinate, but Hill regarded them all as conspecific. Strusz (1961) described a large specimen of *E. latum*, with carinate septa from the Wellington district, New South Wales, and the Broken River specimens are all weakly carinate, otherwise closely resembling the holotype. They are smaller than Strusz's specimen, which is 40 mm in diameter, but are very close to a Tasmanian specimen described by Hill (1942a) as *Entelophyllum* sp. That specimen was reinterpreted by Strusz as *E. latum*.

Of overseas species, *E. latum* most closely resembles *E. articulatum* Wahlenberg 1821, from the Wenlock and Ludlow of Europe, but differs in having more septa and a wider axial structure (Hill 1940).

**Distribution and Range.** ?Wenlock or Ludlow of Tasmania; Wenlock and Ludfordian of Yass Basin, New South Wales; Wenlock and Ludlow of Broken River Province, north Queensland (Fig. 4); Ludlow (undifferentiated) of Wellington district, New South Wales.

## Suborder Ketophyllina Zhavoronkova 1972

### Family Ketophyllidae Lecompte 1952

#### Genus *Dokophyllum* Wedekind 1927

**Type Species** (by original designation). *Dokophyllum annulatum* Wedekind 1927. Ludlow, Klinteberg Beds, Gotland.

**Diagnosis** (slightly modified after Hill 1981). Solitary, large corallum, septa long, radial, slightly dilated wedgewise in marginarium that is in late stages a lonsdaleoid dissepimentarium with some small concentric or angulate interseptal plates; major septa continue into

tabularium as thin, low ridges on upper surfaces of tabulae; tabulae flat with edges turned down or up, grouped; prominent cardinal tabular fossula, and in some alar fossulae also.

**Remarks.** Discussed (as *Ketophyllum*) in McLean (1974a: 657–659) and in Hill 1981: F219). *Dokophyllum* has page priority over *Ketophyllum* Wedekind 1927.

#### *Dokophyllum hillae* sp. nov.

Fig. 19

*Ketophyllum* sp. cf. *crassiseptatum* Wedekind 1927; Hill *et al.* 1969: s.12, pl. S VI, fig. 8a, b.

**Etymology.** After the Late Professor Dorothy Hill.

**Holotype.** UQF72672 from UQL4010. Ludfordian, Jack Formation, Graveyard Creek Group, Jack Hills Gorge area, north Queensland.

**Material.** UQF72669, 72678 from UQL4334; UQF72670, 72675 from UQL4335; UQF72671, 72674, 72680 from UQL4002; UQF72672–72673, 72676–72677 from UQL4010; UQF72679 from UQL4337.

**Description.** Corallum large, solitary, up to 6.5 cm in diameter and 12 cm in height. Over neanic, turbinate or broadly trochoid stages, epitheca shows longitudinal double ridges, over ephebic, cylindrical stage, septal grooves are weakly developed, and strong transverse wrinkling reflects lonsdaleoid dissepiments. Calice shallow, with flat or gently domed floor. Corallum may show scattered rejuvenescence and rare budding.

Septa amplexoid, extending to axis as low, thin ridges on upper surfaces of tabulae, but otherwise leave axial space up to 1.5 cm across. Major and minor septa not well defined, just distinguishable by length in some specimens (e.g. UQF72677). All are vertically discontinuous, forming septal crests separated by rows of dissepiments, particularly towards periphery where septa may be slightly dilated. Accurate determination of septal number difficult due to irregular septal development; typically 120–135 septa in specimens ca 4 cm in diameter, UQF72672 has 144 septa at diameter of 6.5 cm. Irregular stereozone may be developed in places over dissepimentarium; this is most strongly developed in UQF72672. Septal trabeculae thin, contiguous, directed normal to plates on which

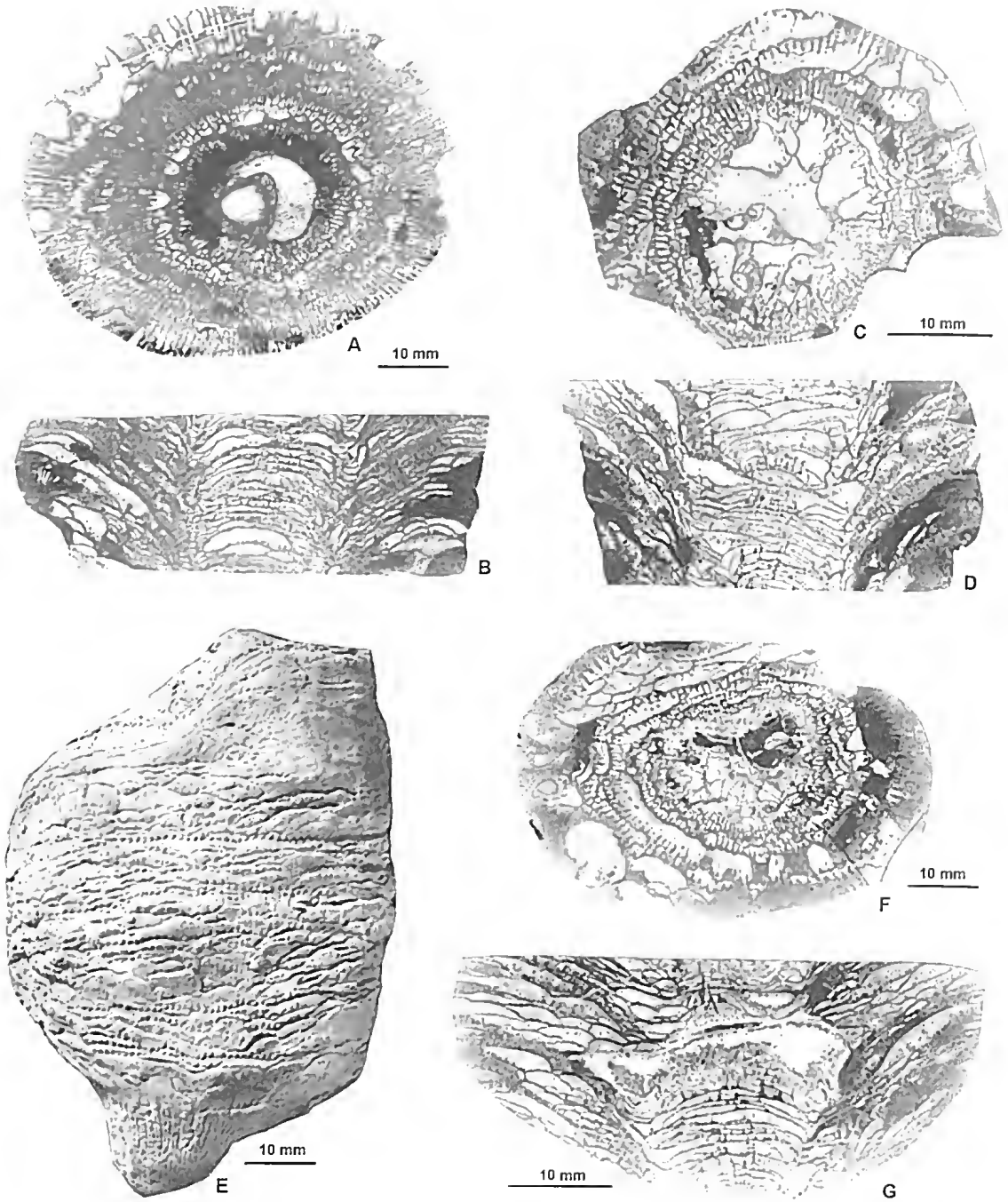


FIG. 19. *Dokophyllum hillae* sp. nov. A, B, UQF72672, HOLOTYPE, from UQL4010, transverse and longitudinal sections; C, D, UQF72677 from UQL4010, transverse and longitudinal sections; E, UQF72679 from UQL4337, exterior; F, G, UQF72673 from UQL4010, transverse and longitudinal sections.

they are based. Peripherally, they may pierce several layers of dissepiments. Between septa, and over dissepimentarium, discontinuous indistinctly laminated stereozone may be developed; these laminae usually concave towards axis in interseptal loculi.

Tabularium generally 0.3–0.5 corallite diameter. Tabulae complete or in some cases incomplete, flat or gently arched, some with upturned edges, commonly occur in groups of 2–6 tabulae. Spacing varies from 10–26 per cm. Slightly thickened tabulae may be developed that show an indistinct lamination parallel to their basal layers. Small shallow tabular fossula may be developed.

Lonsdaleoid dissepiments large (in UQF72673, one intersected 35 septa) very elongate, shallowly inclined inwards, or horizontally based at corallite periphery, but may steepen inwards to about 45° at junction with tabularium. Dissepiments present at all stages of growth, but less common in proximal portions.

**Remarks.** The specimens show substantial variation in septal discontinuity. For example, the transverse section of UQF72672 has relatively few lonsdaleoid dissepiments and septa that are nearly continuous, whereas UQF72673 has numerous dissepiments, and considerably interrupted septa. Longitudinal sections indicate that this variation occurs even within a single corallum; in several specimens (e.g. UQF72672) the number and size of lonsdaleoid dissepiments varies with the particular growth stage of the corallum. The variation is therefore interpreted as intraspecific, rather than reflecting the presence of several coexisting species.

McLean (1974a: 658) remarked that many of the twenty species and varieties of *Dokophyllum* and *Ketophyllum* erected by Wedekind (1927) are synonyms, and that a revision of the genus was needed. However, as a revision of the Gotland species is still pending and as the north Queensland material represents a morphologically distinct taxon that can be largely distinguished from congeneric forms in Gotland, it is appropriate to name the species. *Dokophyllum liillae* shows some resemblance to three of Wedekind's species

from the Wenlock of Gotland. In common with *K. crassiseptatum*, UQF72677 has comparatively short septa that are interrupted close to the periphery (Fig. 19D). However, it lacks the greatly thickened septa of that Gotland species, and the horizontal elements cannot be compared, as Wedekind did not describe or illustrate those of *K. crassiseptatum*. UQF72672 (Fig. 19A) and UQF72676 are closer to *K. bulbosum* Wedekind which has similar long, more complete septa, but these specimens lack the well grouped, commonly sagging tabulae of that form. Wedekind's third species, *K. elegantulum*, closely resembles UQF72673 (Fig. 19F), in its similar strongly discontinuous septa, showing slight wedgewise dilation towards the periphery. *K. elegantulum* also has flatter tabulae showing more clearly defined grouping, and both it and *K. bulbosum* have a much more clearly defined tabular fossula than in the Broken River material.

**Distribution and Range.** Late Gorstian to Ludfordian of Broken River Province, north Queensland (Fig. 4).

## Family Kypophyllidae Wedekind 1927

### Genus *Vesicospina* gen. nov.

**Etymology.** Latin *vesica* = blister, *spina* = thorn, referring to the small trabeculae on the dissepiments.

**Type Species.** *Vesicospina julli* sp. nov. Ludfordian, Jack Formation, Graveyard Creek Group; Jack Hills Gorge area, Broken River Province, north Queensland.

**Diagnosis.** Corallum large, solitary, initially turbinate or broadly trochoid, becoming cylindrical. Calice very deep with axial boss. Septa thin, weakly carinate, interrupted late in ontogeny by peripheral zone of large, lonsdaleoid dissepiments; major septa strongly swirled at axis; minor septa short. Tabularium of complete domed tabulae with axial sag and deep, asymmetric peripheral troughs; peripheral troughs periodically filled by close-set periaxial tabellae. Dissepiments geniculate, shallowly based at periphery but vertical at junction with tabularium; lonsdaleoid dissepiments dominate over small globose interseptal dissepiments; lonsdaleoid dissepiments with small, widely spaced, fine trabeculae directed normal to upper surfaces.

**Remarks.** *Vesicospina* has some characters intermediate to all three subfamilies of the Arachnophyllidae, but has most in common with the Kyphophyllinae and the Ptychophyllinae, each of which contains one genus, *Kyphophyllum* Wedekind 1927, and *Ptychophyllum* Milne-Edwards & Haime 1850, respectively.

The type species of *Ptychophyllum*, *P. stokesi* Milne-Edwards & Haime 1850, from the upper Wenlock-lower Ludlow of Michigan, differs from *Vesicospina* in being patellate with common rejuvenescence; in having major septa that are less convolute axially; a long, narrow cardinal fossula; a less complex tabularium, and septa that may be cavernous over the dissepimentarium. *P. stokesi* also lacks the fine trabeculae over the outer dissepiments which are characteristic of *Vesicospina*, and lacks septal carinae.

*Kyphophyllum lindstromi* Wedekind 1927, from the Silurian of Gotland, the type species of *Kyphophyllum*, differs from *Vesicospina* in having non-convolute, slightly withdrawn major septa, slight peripheral septal dilation, non-carinate septa, no periaxial tabellae in the peripheral troughs of the tabulae, and trabeculae over the outer dissepiments that are aligned with the septa and are in vertical series. The trabeculae of the new genus are widely and more irregularly spaced.

*Kyphophyllum* appears to be closer to *Vesicospina* than does *Ptychophyllum* but it is not congeneric; hence, the new genus is placed in the Kyphophyllinae.

A Western Australian taxon, *Tabulophyllum? lowryi* Hill & Jell 1970, from the Upper Devonian Napier Formation of the Canning Basin shows some resemblance to *Vesicospina*, but differs in having more irregular, less geniculate dissepiments, less prominent minor septa, thicker major septa buttressed by shard-like plates in the dissepimentarium, non-carinate septa, and a less complex tabularium. McLean (1975a: 190) suggested that the Broken River and Western Australian forms might be congeneric, but *T? lowryi* was described from only one specimen, and without further material

its taxonomic position remains unclear. Hill and Jell regarded it as a possible new genus.

A transverse section of a specimen from the Silurian of Gotland, illustrated by Wedekind (1927: pl. 27, fig. 13) as *Kyphophyllum* sp. has strongly swirled major septa, and resembles neanic specimens of *Vesicospina*. It was not described, and is insufficiently illustrated to allow its precise identification.

**Distribution and Range.** Late Gorstian to Ludfordian of north Queensland; Silurian (undifferentiated) of Gotland?; Late Devonian of Western Australia?

### *Vesicospina julli* sp. nov.

Fig. 20

*Pilophyllum* sp.; Hill et al. 1969: s.12, pl. S VI, figs 9a, b.

**Etymology.** After the Late Dr. R.K. Jull.

**Holotype.** UOF72642 from UQL4335. Ludfordian Jack Formation, Graveyard Creek Group, Jack Hills Gorge area, north Queensland.

**Material.** UOF72640, 72643 from UQL4002; UOF72641–72642 from UQL4335; UOF72644–72645 from UQL4010; UOF72646 from UQL4008; UOF72647 from UQL4336.

**Diagnosis.** *Vesicospina* with diameter of 35 mm, height of at least 45 mm and up to 80 septa.

**Description.** Corallum solitary, large; holotype has diameter of 35 mm and height of at least 45 mm. Epithea over neanic, turbinate or broadly trochoid stage has longitudinal double ridges; over cylindrical stage epithea has less well developed septal grooves and strong transverse wrinkles reflecting lonsdaleoid dissepiments. Calice very deep with steep walls, prominent axial boss.

Two orders of attenuate septa number 72–80 in adult specimens. Septa axially smooth, but may possess weak xyloid carinae in dissepimentarium. Peripheral zone of large lonsdaleoid dissepiments interrupts both orders late in ontogeny, but septa may continue over their crests as discontinuous low ridges. Major septa thin, most extend to axis where they are strongly swirled, commonly around small axial space less than 1 mm across. Because of severe crowding in axial vortex some major septa do not extend far into convolute zone and are occasionally even curled back on themselves. Cardinal and counter septa cannot be recognised. Minor septa short, extending just



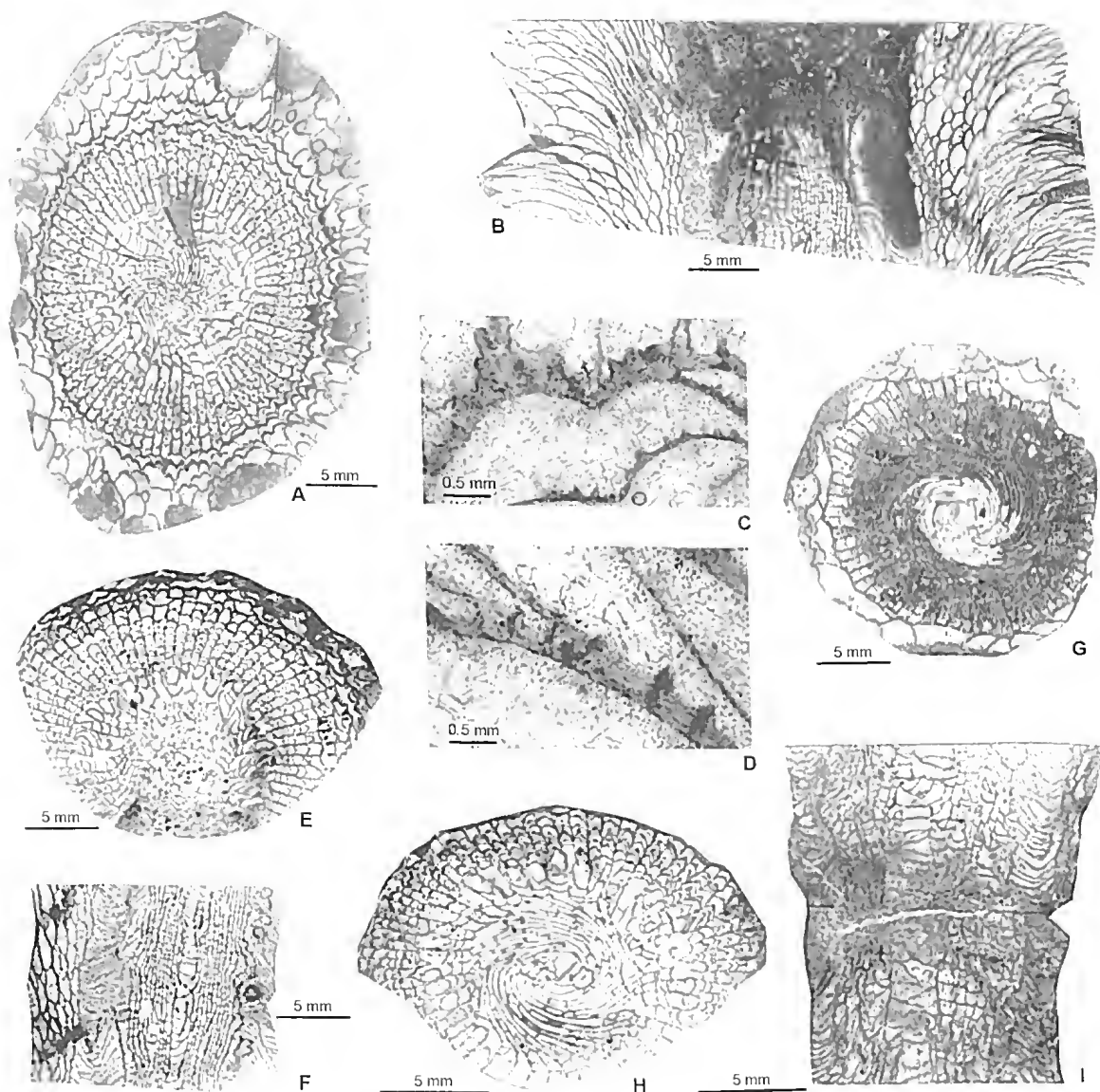


FIG. 20. *Vesicospina julli* gen. et sp. nov. A-D, UQF72642, HOLOTYPE, from UQL4335; A, transverse section; B, longitudinal section through calice showing dissepimentarium; C, portion of A showing small trabeculae on upper surfaces of dissepiments; D, portion of B showing small trabeculae directed normally to dissepiment surfaces; E, F, UQF72644 from UQL4010, transverse and longitudinal sections; G, UQF72643 from UQL4002, transverse section showing weakly carinate septa; H, I, UQF72645 from UQL4010, transverse section of youthful stage, and longitudinal section.

beyond zone of interseptal dissepiments, and not involved in axial convolution. Septal trabeculae thin, contiguous, and directed normally to upper surfaces of dissepiments. Trabecular structure generally masked by recrystallisation.

Large, complete, strongly domed tabulae have axial sag and outer edges upturned to form deep, asymmetric peripheral troughs. Tabulae spaced 20–25 per cm at axis, closer towards the margins. At intervals in corallite growth,



peripheral troughs infilled by small, close-set, slightly sagging tabellae.

Dissepiments geniculate, horizontally based or adaxially inclined to ca 45° at periphery, but steepen inwards to be vertical at junction with tabularium. Large, flatly curved, very elongate lonsdaleoid dissepiments predominate over small, globose interseptal plates. Small, fine, widely spaced trabeculae scattered on, and directed normally to upper surfaces of many lonsdaleoid dissepiments, but very rare on interseptal dissepiments. Peripheral stereozone absent.

**Remarks.** Little intraspecific variation is present. UQF72643 varies from the holotype in having far more septal carinae, and a narrow interseptal dissepimentarium that is only a few series wide; in the holotype it stretches for 0.25 the diameter of the corallum. The holotype varies from the rest of the material in lacking an axial space, although the major septa are strongly swirled and their axial ends are not conjoined.

Hill *et al.* (1969) illustrated a specimen of *V. julli* from the type area, as *Pilophyllum* sp., but that genus possesses a well developed marginal stereozone and a weaker axial vortex (McLean 1975a), and is easily distinguished from *Vesicospina*. In addition to these differences, *Pilophyllum keyserlingi* Wedekind 1927, the type species of *Pilophyllum* from the Ludlow of Gotland, differs from *V. julli* in having slightly withdrawn major septa, a minor septal stereozone developed at the edge of the tabularium, non-geniculate dissepiments, and incomplete domed tabulae that lack peripheral troughs and do not sag axially.

*Ptychophyllum variatum* sp. nov. can be distinguished from neanic specimens of *V. julli* by its weaker axial vortex, more strongly carinate septa, and incomplete, domed tabulae. Mature specimens of *V. julli* are readily distinguished by their peripheral zone of lonsdaleoid dissepiments.

A distinctive feature of this species is the presence of short fine trabeculae on the upper surfaces of many of the plates of the dissepimentarium. They do not appear to be continuations of the existing septa as they are not in vertical series nor are they aligned with the septa. It is possible they are a relict feature inherited from some ancestral species that had

greatly dilated septa, but *V. julli* lacks thickened septa in both the neanic and ephebic stages and the affinities of these tabular trabeculae therefore remain unclear.

**Distribution and Range.** Late Gorstian to Ludfordian of Broken River Province, north Queensland (Fig. 4).

### Suborder Cyathophyllina Nicholson in Nicholson & Lydekker 1889

### Family Ptychophyllidae Dybowski 1873

### Genus *Ptychophyllum* Milne-Edwards & Haime 1850.

**Type Species** (by original designation). *Ptychophyllum stokesi* Milne-Edwards & Haime 1850. Upper Wenlock-lower Ludlow, "Lockport Dolomite", Drummond Island, Lake Huron, Michigan.

**Diagnosis** (slightly modified from Hill 1981). Solitary, ceratoid, turbinate, or patellate; calice with wide, commonly everted platform and broad axial boss in tabularial pit; septa numerous, long, may bear lateral dissepiments; tabularial parts of major septa convolute, unequal, longer reaching axis and shorter confluent with longer; tabular floors domes with edges turned out or up; tabulae incomplete; dissepiments numerous, small, subglobose, interseptal; cardinal fossula long, narrow, inconspicuous, invading tabularium.

**Remarks.** Australian species of *Ptychophyllum* are discussed in McLean (1975b). Smith (1945) added to the original diagnosis of *Ptychophyllum* that the major septa "break up peripherally in such a way that in transverse section they appear to split into component strands." McLean (1975b) described similar cavernous septa in New South Wales specimens of *Ptychophyllum*, and they are also found in the Broken River material. However, cavernous septa may be present or lacking in *Ptychophyllum* even within species, and McLean (1975b) therefore excluded this feature from the generic diagnosis.

### *Ptychophyllum variatum* sp. nov.

Fig. 21

*Phantactis* sp. cf. *shearsbyi* Sussmilch 1914; Hill *et al.* 1969: s.10, pl. S V, figs 1a, b.

**Etymology.** Latin varius = different, variable, referring to the septal variation.

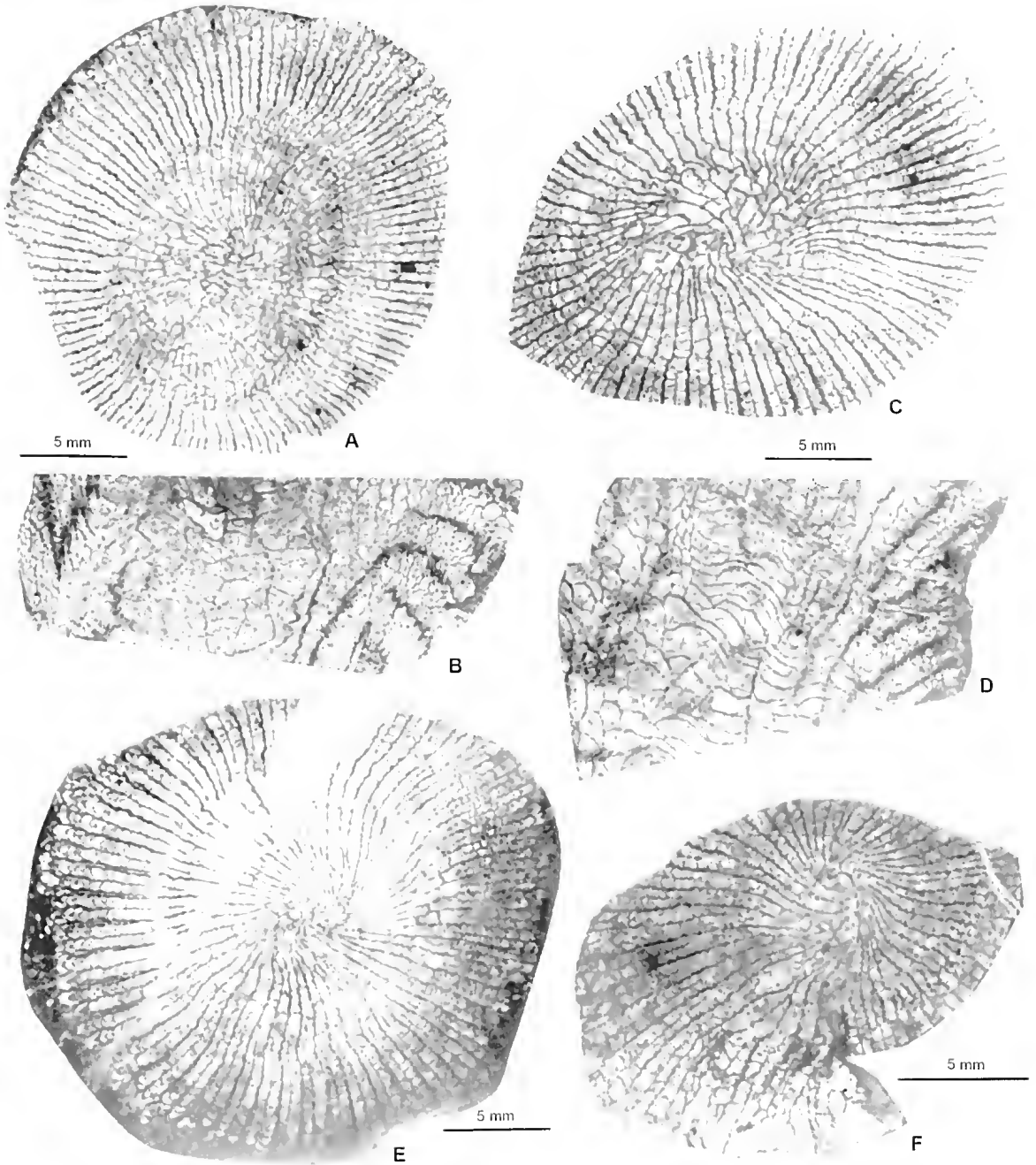


FIG. 21. *Ptychophyllum variatum* sp. nov. A, B, UQF72654, HOLOTYPE, from UQL4002, transverse and longitudinal sections respectively; C-D, UQF72652 from UQL4335. C, transverse section of youthful stage showing fusiform major septa of uneven length; D, longitudinal section; E, UQF72650 from UQL4337, transverse section showing cavernous septa; F, UQF72653 from UQL4336, transverse section showing rejuvenescence.

**Holotype.** UQF72654 from UQL4002. Late Gorstian to Ludfordian, Jack Formation, Graveyard Creek Group, Jack Hills Gorge area, north Queensland.

**Material.** UQF72648 from UQL4010; UQF72649, 72654 from UQL4002; UQF72650, 72656 from UQL4337; UQF72651–72652, 72655 from UQL4335; UQF72653 from UQL4336; UQF60102 from which two thin sections were figured by Hill *et al.* (1969).

**Diagnosis.** Ceratoid *Ptychophyllum* with weak axial vortex and numerous, weakly carinate septa; major septa thickened at periphery and sometimes at axial ends, majority slightly withdrawn from axis in younger stages; minor septa thin. Tabulae domed, but flat or sagging across axial region.

**Description.** Corallum solitary, ceratoid, with infrequent rejuvenescence, reaching diameter of 32 mm and height of 10 cm. Longitudinal ridges and widely spaced growth annulations mark epitheca. Calice wide and deep, small axial boss.

Two orders of weakly carinate xyloid septa number 124 in specimen 29 mm in diameter. Major septa of irregular length in young stages, mostly reach axis in mature stages, gently curved in tabularium. Septa generally thin, may be slightly dilated peripherally and axially. Peripheral thickening fusiform or wedge-shaped. Rarely, septa may be cavernous in dissepimentarium, component strands either reuniting, or turn outwards to become contiguous with dissepiments. Thin minor septa extend to edge of dissepimentarium, and are 0.5–0.6 length of major. Cardinal septum generally slightly elongated, in narrow fossula defined by shorter, slightly curved adjacent major septa. Septal trabeculae directed upwards and inwards normally to upper surfaces of dissepiments. Carinae infrequent, arranged parallel to septal trabeculae. Dilated septa show distinct lamination parallel to septa. Marginal stereozone absent.

Tabularium of small, mainly elongate, incomplete plates forming wide zone 0.4–0.5 corallite diameter. Tabulae domed, but flat or sagging across axial region. Dissepimentarium wide, dissepiments small, globose or slightly elongated, shallowly inclined near corallite

periphery, but steepen axially to almost vertical at junction with tabularium.

**Remarks.** *Ptychophyllum variatum* closely resembles the Middle Silurian, Chinese *Ptychophyllum* (“*Naushanophyllum*”) *typicum* Yu 1956, but the two forms are not easily compared as *P.* (“*N.*”) *typicum* was originally described from only one specimen. *P. variatum* differs in having more numerous septa, thinner minor septa, and in lacking two series of plates in the tabularium.

Of the Australian species of *Ptychophyllum*, *P. variatum* most closely resembles *P. auctum* McLean 1975b, from the Llandoverly of central New South Wales. This species differs in being turbinate or patellate, in having a more prominent axial vortex, fewer septa (60–70 at an average diameter of 20–25 mm), and short, often lonsdaleoid minor septa.

Considerable variation occurs in the character of the septa within this species. The axial vortex may be nearly absent or weak, and is less prominent than those of other Australian species of *Ptychophyllum* (cf. *P. auctum* McLean 1975b). Septal dilation is absent or weak at the axial ends of the major septa, and weak or moderate towards the periphery. Over the dissepimentarium, it may be accompanied by strong zigzagging of the septa, not necessarily accompanied by carinae. Cavernous septa are developed only in some septa of UQF72650 (Fig. 21E), the remaining septa being simple in structure.

Specimens of *Entelophyllum latum* Hill 1940, from the Jack Formation, bear a superficial resemblance to *P. variatum*, but differ in lacking an axial vortex, in having major septa withdrawn from the axis at maturity, shorter minor septa, and less peripheral septal dilation.

**Distribution and Range.** Late Gorstian to Ludfordian of Broken River Province, north Queensland (Fig. 4).

## ACKNOWLEDGEMENTS

The original Honours study was supervised by Prof. J.S. Jell (1978) and during his absence on sabbatical leave in Cambridge, by Prof.

G. Playford (1979). The late Prof. D. Hill FRS provided access to her personal library, and useful advice on taxonomic problems. Prof. J.A. Talent and Assoc. Prof. R. Mawson (School of Earth Sciences, Macquarie University), and the late Dr. M. Wade (Queensland Museum) provided helpful criticism in the field. Mr. R. Banks (University of Queensland) assisted with photography of fossil specimens. Dr. A. Simpson (formerly School of Earth Sciences, Macquarie University) provided advice and information on aspects of the text, in particular on conodont zonations. Comments and suggestions from referees Dr. D.L. Strusz (Research School of Earth Sciences, Australian National University) and Prof. G. Webb (Department of Earth Sciences, University of Queensland) greatly improved the manuscript. The manager and family of Wando Vale Homestead allowed access onto their property, and provided considerable hospitality, which is greatly appreciated. Permission to publish was provided to T.J.M. by Dr. I.R. Scrimgeour (Director, Northern Territory Geological Survey).

#### LITERATURE CITED

- Amsden, T.W. 1949. Stratigraphy and palaeontology of the Brownsport Formation (Silurian) of Western Tennessee. *Bulletin of the Peabody Museum of Natural History* 5: 1-134, pls 1-34.
- Arnold, G.O. & Fawckner, J.F. 1980. The Broken River and Hodgkinson Provinces. Pp. 175-189. In Henderson R.A. & Stephenson P.J. (eds) *The geology and geophysics of northeastern Australia*. (Geological Society of Australia, Queensland Division: Brisbane).
- Arnold, G.O. & Henderson, R.A. 1976. Lower Palaeozoic history of the southwestern Broken River Province, north Queensland. *Journal of the Geological Society of Australia* 23(1): 73-94. <http://dx.doi.org/10.1080/00167617608728922>.
- Bulvankar, E.Z., Gorianov, V.B., Ivanovskiy, A.B., Spasskiy, N.Ya. & Shchukina, V.Ya. 1968. Novye predstaviteli chetyrekhlyuchevykh korallovykh polipov SSSR. Pp. 14-45, pls 3-22. In Markovskiy, B.P. (ed.) *Novye vidy drevnich rasteniy i bespozvochnykh SSSR* 2.
- Burrow, C.J. & Simpson, A.J. 1995. A new ischnacanthid acanthodian from the Late Silurian (Ludlow, plectensis Zone) Jack Formation, north Queensland. *Memoirs of the Queensland Museum*, 38(2): 383-395.
- Caldon, H.-J. 2003. Faunal dynamics of a sequence through the Lau Event in the Broken River region, northeast Australia. BSc Hons thesis, Department of Earth and Planetary Sciences, Macquarie University, Sydney.
- Chapman, E.J. 1893. On the corals and coralliform types of Paleozoic strata. *Transactions of the Royal Society of Canada* 39(4): 39-48.
- Chapman, F. 1920. Palaeozoic fossils of eastern Victoria - Part IV. *Records of the Geological Survey of Victoria* 4: 175-194, pls 16-32.
- Dubatolov, B.N. & Spasskiy, N.Ya. 1971. Devonskie korally Dzhungaro-Balkashskoy provintsii. *Akademiiya Nauk SSSR, Sibirskoe Otdelenie, Institut Geofiziki i Geofiziki, Trudy* 74: 1-132, 41 pls.
- Dybowski, W.N. 1873. Monographie der Zoantharia sclerodermata rugosa aus der Silurformation Estlands, Nord-Livlands und der Insel Gotland. *Archiv für die Naturkunde Livlands, Estlands und Kurlands* 5: 257-414, pls 1-2.
- Ehrenberg, C.G. 1834. Beiträge zur physiologischen Kenntniss der Corallenthiere im Allgemeinen, und besonders des Rothen Meeres, nebst einem Versuche zur physiologischen Systematik derselben. *Abhandlungen der Königlich Akademie der Wissenschaften in Berlin* (1832): 225-380.
- Etheridge, R. Jr 1890. On the occurrence of the genus *Tryplasma* Lonsdale (*Pholidophyllum* Lindström) and another coral apparently referable to *Diphyphyllum* Lonsdale, in the Upper Silurian and Devonian rocks respectively of New South Wales. *Records of the Geological Survey of New South Wales* 2: 15-21, pl. 1.
- Etheridge, R. Jr 1892a. Descriptions of four Madreporaria Rugosa - species of the genera *Phillipsastrea*, *Heliophyllum* and *Cyathophyllum* from the Palaeozoic rocks of New South Wales. *Records of the Geological Survey of New South Wales* 2: 165-174, pls 11, 12.
- Etheridge, R. Jr 1892b. Class Actinozoa. Pp. 50-64, 200-201, pls 1-3, 7, 37, 44. In Jack, R.L. & Etheridge, R. Jr 'The Geology and Palaeontology of Queensland and New Guinea'. *Publications of the Geological Survey of Queensland* 92.
- Etheridge, R., Jr 1907. A monograph of the Silurian and Devonian corals of New South Wales, Part II. The genus *Tryplasma*. *Memoirs of the Geological Survey of New South Wales. Palaeontology* 13: 41-102, pls 10-28.
- Fenton, C.L. & Fenton, M.A. 1924. The stratigraphy and fauna of the Hackberry Stage of the Upper Devonian. *Contributions from the Museum of Paleontology, University of Michigan* 1, 260 p.
- Foerste, A.F. 1888. Notes on Palaeozoic fossils. *Bulletin of the Scientific Laboratories of Denison University* 3: 117-136, pl. 13.
- Gradstein, F.M., Ogg, J.G. & Smith, A.G. 2005. *A Geologic Time Scale 2004*. Cambridge University Press. <http://dx.doi.org/10.1017/CBO9780511536045>

- Guo Shengzhe 1978. Late Silurian tetracorals from northern Bailingmiao of the autonomous region of Inner Mongolia. *Chinese Academy of Geological Sciences, Professional Papers of Stratigraphy and Palaeontology* 6: 50–68, pls 15–20.
- Henderson, R.A., Donchak P.J.T. & Withnall I.W. 2013. Mossman Orogen. Pp. 225–304. In Jell P.A. (ed.) *The Geology of Queensland*. (Geological Survey of Queensland: Brisbane).
- Henderson, R.A. & Withnall I.W. 2013. Broken River Province: Pp. 250–279. In Jell P.A. (ed.) *The Geology of Queensland*. (Geological Survey of Queensland: Brisbane).
- Hill, D. 1940. The Silurian Rugosa of the Yass Bowring District, New South Wales. *Proceedings of the Linnean Society of New South Wales* 65: 388–420, pls 11–13, 4 text-figs.
- Hill, D. 1942a. Some Tasmanian Palaeozoic corals. *Papers and Proceedings of the Royal Society of Tasmania for 1941*: 3–11, pl. 2.
- Hill, D. 1942b. The Devonian rugose corals of the Tamworth district, New South Wales. *Journal and Proceedings of the Royal Society of New South Wales* 76: 142–164, pls 2–4.
- Hill, D. 1965. Determinations of Palaeozoic faunas. In White, D.A. 'The geology of the Georgetown/Clarke River area, Queensland'. Bureau of Mineral Resources, Australia, Bulletin 71: 151, Appendix 2.
- Hill, D. 1981. Coelenterata, Supplement 1, Rugosa and Tabulata. Pp. F1–F762. In Teichert C. (ed.) *Treatise on Invertebrate Paleontology, Part F*, 2 volumes. (Geological Society of America and University of Kansas Press, New York, Lawrence).
- Hill, D. & Jell, J.S. 1970. Devonian corals from the Canning Basin, Western Australia. *Geological Survey of Western Australia, Bulletin* 121: 1–158, 20 pls.
- Hill, D., Playford, G. & Woods, J.T. 1969. Pp. o.2–o.15, pls 0 I–VII, s.2–s.18, pls S I–VIII. In *Ordovician and Silurian fossils of Queensland*. (Queensland Palaeontographical Society, Brisbane).
- Ivanovskiy, A.B. 1970. Stratigraficheskie i paleogeograficheskie kompleksi rugoz na Sibirskoy Platforme. *Akademiya Nauk SSSR, Sibirskoe Otdelenie, Institut Geofiziki i Geofiziki, Trudy* 1970(7): 12–18.
- Ivanovskiy, A.B. & Shurygina, M.V. 1975. Reviziya rugoz Urala. *Akademiya Nauk SSSR, Sibirskoe Otdelenie, Institut Geofiziki i Geofiziki, Trudy* 218: 1–44, 20 pls.
- Jack, R.L. & Etheridge, R. Jr 1892. The geology and palaeontology of Queensland and New Guinea. *Publications of the Geological Survey of Queensland* 92: 768 p., 69 pls.
- Jell, J.S. 1967. Geology and Devonian rugose corals of "Pandanus Creek" North Queensland. Ph.D. thesis, Department of Geology and Mineralogy, University of Queensland, Brisbane.
- Jell, J.S. 1969. Septal microstructure and classification of the Phillipsastracidae. Pp. 50–73, pls 7–8. In Campbell, K.S.W. (ed.) *Stratigraphy and Palaeontology, Essays in honour of Dorothy Hill*. (Australian National University Press: Canberra).
- Jell, J.S. & Hill, D. 1970. The Devonian coral fauna of the Point Hibbs Limestone, Tasmania. *Papers and Proceedings of the Royal Society of Tasmania* 104: 1–16, pls 1–6, text-figs 1–2.
- Jell, J.S. & Sutherland, P.K. 1990. The Silurian rugose coral genus *Entelophyllum* and related genera in northern Europe. *Palaeontology* 33: 769–821.
- Jell, J.S., Simpson, A.J., Mawson, R. & Talent, J.A. 1993. Biostratigraphic summary. pp. 239–245. In Withnall, I.W. & Lang, S.C. (eds) 'Geology of the Broken River Province, north Queensland'. *Queensland Geology*, volume 4.
- Jeppsson, L. & Aldridge, R.J. 2000. Ludlow (Late Silurian) oceanic episodes and events. *Journal of the Geological Society* 157: 1137–1148. <http://dx.doi.org/10.1144/jgs.157.6.1137>
- Jeppsson, L., Talent, J.A., Mawson, R., Simpson, A.J., Andrew, A.W., Calner, M., Whitford, D.J., Trotter, J.A., Sandstrom, O. & Caldon, H.J. 2007. High-resolution Late Silurian correlations between Gotland, Sweden, and the Broken River region, NE Australia: lithologies, conodonts and isotopes. *Palaeogeography, Palaeoclimatology, Palaeoecology* 245: 115–137. <http://dx.doi.org/10.1016/j.palaeo.2006.02.032>
- Jeppsson, L., Talent, J.A., Mawson, R., Andrew A., Corradini C., Simpson, A.J., Wigforss-Lange J. & Schönlaub H.P. 2012. Late Ludfordian correlations and the Lau Event. Pp. 653–675. In Talent J.A. (ed.) *Earth and Life, International Year of Planet Earth*. (Springer Science+Business Media, Netherlands). [http://dx.doi.org/10.1007/978-90-481-3428-1\\_21](http://dx.doi.org/10.1007/978-90-481-3428-1_21)
- Jones, O.A. 1936. On the Silurian corals: *Cyathophyllum shearshyi* and *Heliophyllum yasseuse*. *Memoirs of the Queensland Museum* 11: 53–58, pls 5–7.
1937. The Australian massive species of the coral genus *Favosites*. *Records of the Australian Museum* 20: 79–120, pls 11–16.
- Jones, O.A. & Hill D. 1940. The Heliolitidae of Australia with a discussion of the morphology and systematic position of the family. *Proceedings of the Royal Society of Queensland* 51: 183–215, pls 6–11.
- Kato, M. & Minato, M. 1977. Note on the Occurrence of *Amsdenoides* (Rugosa) from the Japanese Silurian. *Journal of the Faculty of Science, Hokkaido University. Series 4, Geology and Mineralogy* 17(3): 535–539.

- Kido, E. 2009. Silurian Holmophyllidae (Rugosa) from the Gioma Formation of the Kurosegawa Terrane, Southwest Japan. *Paleontological Research* 13(3): 293–306. <http://dx.doi.org/10.2517/1342-8144-13.3.293>
- Lang, W.D., Smith, S.M. & Thomas, H.D. 1940. *Index of Palaeozoic coral genera*. (British Museum (Natural History): London).
- Lavrusevich, A.I. 1971. Rugoznyy rannego silura Zerafshano-Gissarskoy gornoy oblasti. *Trudy Upravleniya Geologii Soveta ministrov Tadzhikskoy SSR, Paleontologiya i Stratigrafiya* 3: 38–136, pls 1–25.
- Lecompte, M. 1952. Madréporaires paléozoïques. Pp. 419–538. In Piveteau J. (ed.) *Traité de Paléontologie 1. Généralités, Protistes, Spongiaires, Céléntères, Bryozoaires*. (Masson et Cie: Paris).
- Lindström, G. 1882. Anteckningar om silurlagren på Carlsoarne. *Öfversigt af Kongliga Vetenskaps-Akademiens Förhandlingar* 39(3): 5–30.
- Lindström, G. 1883. Obersilurische korallen von Tschau-tien im nordöstlichen Theil der Provinz Sz'-Tshwan. Pp. 50–74. In von Richthofen F. (ed.) *Beiträge zur Paläontologie von China 4*. (Dietrich Reimer, Berlin).
- Lindström, G. 1899. Remarks on the Heliolitidae. *Kungliga Svenska Vetenskapsakademiens Handlingar* 32(2): 140 p., 12 pls.
- Link, A.G. & Druce, E.C. 1972. Ludlovian and Gedinian conodont stratigraphy of the Yass Basin, New South Wales. *Bureau of Mineral Resources, Australia, Bulletin* 134, 136p.
- Lonsdale, W. 1839. Corals, graptolites, and nondescripts. Pp. 675–698, pls 15, 15 bis, 16, 16 bis. In Murchison R.I. (ed.) *The Silurian System, parts 1, 2*. (John Murray: London).
- Lonsdale, W. 1845. Description of some characteristic Palaeozoic corals of Russia. Pp. 591–634, pl. A. In Murchison R.I., De Vemeuil E. & Von Keyserling A. (eds) *The geology of Russia in Europe and the Ural Mountains, Volume 1*. (John Murray: London).
- McLean, R.A. 1974a. Chonophyllinid corals from the Silurian of New South Wales. *Palaeontology* 17: 655–668, pls 94–95.
- 1974b. Cystiphyllidae and Goniophyllidae (Rugosa) from the Lower Silurian of New South Wales. *Palaeontographica Abteilung A* 147: 1–38, pls 1–6.
- 1975a. Silurian rugose corals from the Mumbil area, central New South Wales. *Proceedings of the Linnean Society of New South Wales* 99(4): 181–196, pls 8–12.
- 1975b. Lower Silurian rugose corals from central New South Wales. *Journal and Proceedings of the Royal Society of New South Wales* 108: 54–69, pls 1–6.
1976. Genera and stratigraphic distribution of the Silurian and Devonian rugose coral family Cystiphyllidae Edwards and Haime. *Papers of the Geological Survey of Canada* 76-1B: 295–301.
1985. New Early Silurian rugose corals from the Panuara area, central New South Wales. *Alcheringa* 9: 23–34. <http://dx.doi.org/10.1080/03115518508618956>
- Merriam, C.W. 1972. Silurian rugose corals of the Klamath Mountains Region, California. *United States Geological Survey, Professional Paper* 738: 50 p., pls 1–8.
- Merriam, C.W. 1973. Silurian rugose corals of the central and southwest Great Basin. *United States Geological Survey, Professional Paper* 777: 66 p., 16 pls.
- Miller, S.A. 1889. *North American Geology and Palaeontology for the use of amateurs, students, and scientists, 3rd Edition*. (Western Methodist book concern: Cincinnati). <http://dx.doi.org/10.5962/bhl.title.18066> <http://dx.doi.org/10.5962/bhl.title.28778> <http://dx.doi.org/10.5962/bhl.title.40666>
- Milne-Edwards, H. & Haimé, J. 1850. A Monograph of the British Fossil Corals. Part 1. *Palaeontographical Society Monographs* 3: 1–71, 11 pls.
- Milne-Edwards, H. & Haime, J. 1851. Monographie des polypiers fossiles des terrains paléozoïques. *Archives du Museum National d'Histoire Naturelle* 5, 502 p., 20 pls.
- Munson, T.J. 1979. *Geology and Silurian rugose corals of the Jack Hills Gorge area, Broken River Province, North Queensland*. B.Sc. Hons thesis, Department of Geology and Mineralogy, University of Queensland, Brisbane.
- Munson T.J. & Jell J.S. 1999. Llandovery rugose corals from the Quinton Formation, Broken River Province, northeast Queensland. *Association of Australasian Palaeontologists, Memoir* 21: 65 p., 34 figs.
- Nestor, H.A. 1976. *Rannepaleozoiskie stromatoporoidei basseina neki Moiero (sever Sibirskoi platformi)*. (Akademiya Nauk Estonskoi SSR, Institut Geologii, Tallinn).
- Nicholson, B.A. & Etheridge, R. Jr 1879. Descriptions of Palaeozoic corals from Northern Queensland, with observations on the genus *Stenopora*. *Annals and Magazine of Natural History* 4(5): 216–285. <http://dx.doi.org/10.1080/00222937908679819>
- Nicholson, H.A. & Lydekker, R. 1889. *A manual of palaeontology, 3rd Edition, volume 1*. (Wm. Blackwood & Sons: Edinburgh).
- Pedder, A.E.H. 1985. Lower Devonian rugose corals of Lochkovian age from Yukon Territory. In 'Current Research, Part A'. *Geological Survey of Canada, Paper* 85-1A: 587–602.
- Riabinin, V. 1951. Stromatoporoidei estonskoi SSR (Silur i verkhni Ordovika). *Trudy vsesoyuznogo*



- neftyanogo nauchno-issledovatel'skogo geologo-razvedochnogo instituta, novaya seriya 43: 1–68.
- Rickards, R.B. & Jell, J.S. 2002. New graptolite faunas from the Llandoverly, lower Silurian of the Graveyard Creek Subprovince, Broken River region, Queensland, Australia. *Proceedings of the Geologists Association* 113: 111–120. [http://dx.doi.org/10.1016/S0016-7878\(02\)80014-1](http://dx.doi.org/10.1016/S0016-7878(02)80014-1)
- Savory, P.J. 1987. *Geology of the Poley Cow Formation, Broken River area, north Queensland*. B.Sc. Hons thesis, Department of Geology and Mineralogy, University of Queensland, Brisbane.
- Simpson, A.J. 1983. *Silurian to basal Devonian conodont biostratigraphy of the Broken River area, north Queensland*. B.A. Hons thesis, School of Earth Sciences, Macquarie University, Sydney.
1994. Silurian to basal Devonian conodonts and other microfossils from the Graveyard Creek Group, Broken River crossing, north Queensland. *Australasian Palaeontological Convention, 1994, Abstracts and Programme, Macquarie University Centre for Ecostratigraphy and Palaeobiology (MUCEP)*: 88.
- 1995a. Conodont-based ages and stratigraphic relationships of the Siluro–Devonian Graveyard Creek Group. Pp. 71–72. In Brock, G. (ed.) *First Australasian Conodont Symposium (AUSCOS-1) and the Boncot Symposium, Abstracts and Program, volume 1*. Special Publication of the Macquarie University Centre for Ecostratigraphy and Palaeobiology (MUCEP), Sydney.
- 1995b. *Silurian conodont studies in eastern Australia*. Ph.D. thesis, Department of Earth Sciences, University of Queensland: Brisbane.
- 1998a. Lithological sequence and Silurian conodont faunas from the type section of the Jack Formation, north Queensland, Australia. Pp. 103–104. In Bagnoli G. (ed.) *Seventh International Conodont Symposium (ECOS VII)*, 1998, Bologna–Modena, Italia, Abstracts.
- 1998b. Apparatus structure of the latest Silurian to Early Devonian conodont *Icriodus woschmidtii hesperius* Klapper et Murphy, and some comments on phylogeny. In Szaniawski H. (ed.) *Proceedings of the Sixth European Conodont Conference ECOS VI*. *Palaeontologica Polonica* 58: 151–167.
1999. Early Silurian conodonts from the Quinton Formation, northeastern Australia. *Abhandlungen der Geologischen Bundesanstalt (Wien)* 54: 181–199.
2000. Silurian conodonts from the Broken River Crossing, northeastern Australia. *Records of the Western Australian Museum, Supplement* 58: 145–162.
- Sloan, T., Talent, J.A., Mawson, R., Simpson, A.J., Brock, G., Engelbrechtsen, M., Jell, J.S., Aung, A.K., Pfaffenritter, C., Trotter, J. & Withnall, I.W. 1995. Conodont data from Silurian–Middle Devonian carbonate fans, debris flows, allochthonous blocks and adjacent platform margins: Broken River and Camel Creek areas, north Queensland, Australia. *Courier Forschungsinstitut Senckenberg* 182: 77 p.
- Smith, S. 1933. On *Xylodes rugosus* sp. nov., a Niagaran coral. *American Journal of Science* 26: 512–522, pl. i. <http://dx.doi.org/10.2475/ajs.s5-26.155.512>
1945. Upper Devonian corals of the Mackenzie River region, Canada. *Geological Society America, Special Papers* 59: 126 p., 35 pls.
- Soshkina, E.D. 1928. Nizhnepermские (artinskie) кораллы западного склона Северного Урала. *Бюллетен Московского Общества Испытателей Природы, Москва, novaya seriya*, 36, otdel geologii 6(3–4): 339–393.
- Soshkina, E.D. 1937. Кораллы верхнего силура и нижнего девона восточного и западного склонов Урала. *Палеонтологический Институт Труды* 6(4): 1–155, pls 1–21.
- Spasskiy, N.Ya. 1965. Rannedevonskie i eifelskie chetireckluchevie koralli djungarskogo Alatau. *Zapiski Leningradskogo Gornogo Instituta. Leningrad, U.S.S.R.* 49(2): 18–30, pls 1–5, 1 text-fig.
- Stearn, C.W. 1956. Stratigraphy and palaeontology of the Interlake Group and Stonewall Formation of southern Manitoba. *Geological Survey of Canada, Memoir* 281: 162 p. <http://dx.doi.org/10.4095/101508>
- Strelnikov, S.I. 1971. Znachenie rugoz dlya stratigrafii siluriyskikh otlozheniy Pripolyarnogo Urala i Gryady Chernysheva. Pp. 71–88, 141–143, pls 17–22. In Ivanovskiy, A.B. (ed.) *'Rugozы i stromatoporoidei paleozoya SSSR'. Trudy 2. Vsesoyuznogo simpoziuma po izucheniyu iskopaemykh korallov SSSR 2*. (Nauka: Moskva).
- Strusz, D.L. 1961. Lower Palaeozoic corals from New South Wales. *Palaeontology* 4: 334–361, pls. 42–45.
- Stumm, B.C. 1953. Key to the families of the Tetracorallia. Pp. 158–159. In Schrock R.R. & Twenhofel W.H. (eds.) *Principles of invertebrate paleontology, 2nd Edition*. (McGraw Hill: New York).
- Sussmilch, C.A. 1914. *An introduction to the geology of New South Wales*. (Angus & Robertson: Sydney).
- Sutherland P.K. 1965. Rugose corals of the Henryhouse Formation (Silurian) in Oklahoma. *Bulletin of the Oklahoma Geological Survey* 109: 1–92, 34 pls.



- Talent, J.A., Mawson, R., Simpson, A.J. & Brock, G.A. 2002. 'Palaeozoics of NE Queensland: Broken River region: Ordovician–Carboniferous of the Townsville hinterland: Broken River and Camel Creek regions, Burdekin and Clarke River basins'. ICP 2002 field excursion guidebook, special publication 1. (Macquarie University Centre for Ecostratigraphy and Palaeobiology: Sydney).
- Telford, P. 1972. *Lower and Middle Devonian conodont faunas from the Broken River Embayment, North Queensland*. Ph.D. thesis, Department of Geology and Mineralogy, University of Queensland: Brisbane.
- Thomas, O.D. & Pogson, J., 2011. Goulburn, New South Wales, 1:250,000 Geological series explanatory notes. (Geological Survey of New South Wales: Maitland).
- Vandyke, A. & Byrnes, J.G. 1976. Palaeozoic succession beneath the Narragal Limestone, Oakdale Anticline near Mumbil. *Records of the Geological Survey of NSW* 17(2): 123–134.
- Verrill, A.E. 1865. Classification of polyps (Extract condensed from a synopsis of the polypi of the North Pacific Exploring Expedition, under Captains Ringgold and Rogers, U.S.N.). *Essex Institute, Proceedings* 4:145–149.
- Wahlenberg, G. 1821. Petrificata telluris Svecanae examinata. *Nova Acta regiae Societatis Scientiarum Upsaliensis* 8: 1–116.
- Walliser, O.H. 1964. Conodonten des Silurs. *Abhandlungen des Hessischen Landesamtes für Bodenforschung zu Wiesbaden* 41: 1–106, 4 tab., 32 pls.
- Wang, H.C. 1947. New material of Silurian rugose corals from Yunnan. *Geological Survey of China, Bulletin* 27: 171–192, 2 pls.
- Webby, B.D. & Zhen, Y.Y. 1997. Silurian and Devonian clathrodictyids and other stromatoporoids from the Broken River region, north Queensland. *Alcheringa* 21: 1–56. <http://dx.doi.org/10.4095/101508>
- Wedekind, R. 1927. Die Zoantharia Rugosa von Gotland (bes. Nordgotland). Nebst bemerkungen zur Biostratigraphie des Gotlandium. *Sveriges Geologiska Undersökning, series Ca* 19: 94 p., 30 pls.
- Weissermel, W. 1894. Die Korallender Silurgeschiebe Ostpreussens und des östlichen Westpreussens. *Zeitschrift der Deutschen Geologischen Gesellschaft* 46(3): 580–674, pls 47–53, text-figs 1–4.
- White, D.A. 1959a. New names in Queensland stratigraphy, part 2, Clarke River region. *Australasian Oil & Gas Journal* 5(9): 31–36.
- White, D.A. 1965. The geology of the Georgetown/Clarke River area, north Queensland. *Bureau of Mineral Resources, Australia, Bulletin* 71: 165 p.
- White, D.A. & Wyatt, D.H. 1960. Silurian of the upper Burdekin River Valley. In Hill, D. & Denmead, A.K. (eds). 'The geology of Queensland'. *Journal of the Geology Society of Australia* 7: 123–128.
- Whiteaves, I.F. 1884. On some new, imperfectly characterized, or previously unrecorded species of fossils from the Guelph Formation of Ontario. *Geological Survey of Canada, Palaeozoic Fossils* 3(1): 1–43, pls 1–8.
- Withnall, I.W. 1989. Revision of the stratigraphy of the Broken River area, north Queensland – Ordovician and Silurian units. *Queensland Government Mining Journal* 90: 213–218.
- Withnall, I.W., Fielding, C.R., Lang, S.C. & Fleming, P.J.G. 1993. Stratigraphy and sedimentology of the Silurian to Early Devonian Graveyard Creek Group and Shield Creek Formation. Pp. 55–78. In Withnall, I.W. & Lang, S.C. (eds) *Queensland Geology*, volume 4.
- Withnall, I.W. & Lang, S.C. (eds) 1993. 'Geology of the Broken River Province, north Queensland'. *Queensland Geology*, volume 4: 289 p.
- Withnall, I.W., Lang, S.C., Jell, J.S., McLennan, T.P.T., Talent, J.A., Mawson, R., Fleming, P.J.P., Law, S.R., Macanish, J.D., Savory, P., Kay, J.R. & Draper, J.J. 1988. 'Stratigraphy, sedimentology, biostratigraphy and tectonics of the Ordovician to Carboniferous Broken River Province, north Queensland'. *Australian Sedimentologists Group Field Guide Series* 5. (Geological Society of Australia: Sydney).
- Yu Changmin 1956. Some Silurian corals from the Chuichuan Basin, Western Kansu. *Acta Palaeontologica Sinica* 4: 610–620, 2 pls.
- Yu Changmin & Jell, J.S. 1990. Early Devonian rugose coral fauna from the Shield Creek Formation, Broken River Embayment, north Queensland. Pp. 169–209. In Jell P.A. (ed.) 'Devonian and Carboniferous coral studies'. *Memoir of the Association of Australasian Palaeontologists* 10.
- Zaprudskaya, M.A. & Ivanovskiy, A.B. 1962. Dva novykh roda siluriyskikh tsistifillid (Rugosa) s Sibirskoy platformy. *Trudy Vsesoyuznogo Nauchno Issledovatel'skiy Geologorazvedochnyy Neftyanoy Institut (VNIGNI)* 196: 48–58, pls 1, 2.
- Zhavoronkova, R.A. 1972. Opisanie korallov. Pp. 17–55, pls 1–23. In Tyazheva A.P. & Zhavoronkova R.A. (eds) *Korally i brakhiopody pogranichnykh otlozheniy silura i nizhnego devona zapadnogo sklona yuzhnogo Urala*. (Institut Geologii: Moscow).

## APPENDIX 1: FOSSIL LOCALITIES

All localities are from the vicinity of the type section of the Jack Formation in the Jack Hills Gorge area, Broken River Province, north Queensland and are within the Clarke River 1:250,000 (SE55-13) and Burges 1:100,000 (7859) mapsheets. They are listed in numeric order and are mapped in Fig. 5. Grid references refer to the MGA94 datum; bearings refer to true north.

- UQL4002: South bank of Broken River, composite collection from section between UQL4333 and UQL4337. Coral gardens member (ca 265820mE 7845510mN).
- UQL4003: North bank of Broken River, 350 m east of east end of Jack Hills Gorge (UQL4014). Base of Dark dog limestone (266160mE 7845480mN).
- UQL4004: North bank of Broken River, 100 m up-section from UQL4003. Top of Dark dog limestone (266080mE 7845530mN).
- UQL4005: North bank of Broken River, 150 m east of east end of gorge (UQL4014). Base of Coral gardens member (265990mE 7845640mN).
- UQL4006: North bank of Broken River, 16 m up-section from UQL4005. Coral gardens member (265980mE 7845640mN).
- UQL4007: North bank of Broken River, 11 m up-section from UQL4006. Coral gardens member (265960mE 7845640mN).
- UQL4008: North bank of Broken River, 16 m up-section from UQL4007. Coral gardens member (265940mE 7845640mN).
- UQL4009: North bank of Broken River, composite collection from section between UQL4006 and UQL4008. Coral gardens member (ca. 265960mE 7845640mN).
- UQL4010: North bank of Broken River, 13 m up-section from UQL4008. Top of Coral gardens member (265930mE 7845650mN).
- UQL4011: North bank of Broken River, 8 m up-section from UQL4010. Oncolitic limestone at top of Coral gardens member (265910mE 7845650mN).
- UQL4013: North bank of Broken River, 35 m up-section from UQL4011. Micritic limestone at top of Coral gardens member (265880mE 7845650mN).
- UQL4014: North bank of Broken River, at east end of Jack Hills Gorge. Base of Jack Hills member (265820mE 7845630mN).
- UQL4325: Bluff-forming limestone lens at base of Coral gardens member, 500 m bearing 025° from point on north bank of Broken River, 350 m downstream from western end of Jack Hills Gorge (266340mE 7846010mN).
- UQL4326: Bluff-forming limestone lens of Dark dog limestone, 270 m bearing 205° from point on south bank of Broken River, 550 m downstream from west end of Jack Hills Gorge (265870mE 7845200mN).
- UQL4327: Bluff-forming limestone lens of Dark dog limestone, 550 m bearing 205° from point on south bank of Broken River, 550 m downstream from west end of Jack Hills Gorge (265740mE 7845050mN).
- UQL4328: Isolated bluff-forming limestone lens of Dark dog limestone, 1,000 m bearing 205° from point on south bank of Broken River, 550 m downstream from west end of Jack Hills Gorge (265390mE 7844690mN).
- UQL4329: Gully, 900 m bearing 205° from point on south bank of Broken River 350 m downstream from west end of Jack Hills Gorge. Decalcified siltstone in Red bull member (265290mE 7844890mN).
- UQL4330: Hill slope, 500 m bearing 025° from point on north bank of Broken River 300 m downstream from west end of Jack Hills Gorge. Coral gardens member (266260mE 7846010mN).
- UQL4331: Hill slope, 30 m from point on south bank of Broken River 500 m downstream from west end of Jack Hills Gorge. Top of Dark dog limestone (266000mE 7845430mN).
- UQL4332: Hill slope, 450 m bearing 025° from west end of Jack Hills Gorge. Top of Jack Hills member (265870mE 7846000mN).
- UQL4333: South bank of Broken River, 350 m from west end of Jack Hills Gorge. Base of Coral gardens member (265850mE 7845510mN).
- UQL4334: South bank of Broken River, 16 m up-section from UQL4333. Coral gardens member (265840mE 7845520mN).
- UQL4335: South bank of Broken River, 12 m up-section from UQL4334. Coral gardens member (265820mE 7845520mN).
- UQL4336: South bank of Broken River, 17 m up-section from UQL4335. Coral gardens member (265810mE 7845520mN).
- UQL4337: South bank of Broken River, 15 m up-section from UQL4336. Top of Coral gardens member (265790mE 7845530mN).
- UQL4338: North bank of Broken River, at west end of Jack Hills Gorge, Top of Jack Hills member (265600mE 7845670mN).

J2NL C43-C43



## CONTENTS

HITCHCOCK, G., CONATY, S.D., FELL, D.G. GORDON, G., INGRAM, M.S., REIS, T.M., STANTON, D.J. & WIGNESS, J.N. Range extension of the Short-beaked Echidna <i>Tachyglossus aculeatus</i> (Monotremata: Tachyglossidae) and the Northern Brown Bandicoot <i>Isododon macrourus</i> (Marsupialia: peramelidae) in Queensland: Mua (Moa Island), Torres Strait. ....	1
ROSE, H.A., WALKER, J.A. & WOODWARD, J.R. Five new species of soil burrowing cockroaches from Queensland (Blattodea: Blaberidae: Geoscapheinae). ....	11
HURLEY, T. & HURLEY S. In Memorium, Richard 'Dinosaur Dick' Suter (1935–2013). ....	25
TAYLOR, S.M., JOHNSON, J.W. & BENNETT, M.B. Spatial gradient in the distribution of whaler sharks (Carcharhinidae) in Moreton Bay, southeastern Queensland. ....	39
STANISIC, J. <i>Pallidelix simonhudsoni</i> sp. nov.: a new land snail from the central highlands of inland southern Queensland, Australia (Gastropoda: Eupulmonata: Camaenidae) ....	55
BARTHOLOMAI, A. An Early Cretaceous (late Albian) halecomorph (? Ionoscopiformes) fish from the Toolebuc Formation, Eromanga Basin, Queensland ....	61
BAKER, A.M., MUTTON, T.Y., MASON, E.D. & GRAY, E.L. A taxonomic assessment of the Australian Dusky Antechinus Complex: a new species, the Tasman Peninsula Dusky Antechinus ( <i>Antechinus vandycki</i> sp. nov.) and an elevation to species of the Mainland Dusky Antechinus ( <i>Antechinus swainsonii mimetes</i> (Thomas)) ....	75
BAKER, A.M. & VAN DYCK, S. Taxonomy and redescription of the Swamp Antechinus, <i>Antechinus minimus</i> (É. Geoffroy) (Marsupialia: Dasyuridae). ....	127
JAMIESON, B.G.M., MCDONALD, K.R. & JAMES, S. A new species of Diplotrema (Acanthodrilinae, Metagynophora, Crassiclitellata, Oligochaeta) from the Eninasleigh Uplands Bioregion of Queensland ....	171
BARTHOLOMAI, A. Additional chimaeroid specimens from the Early Cretaceous (Late Albian) Toolebuc formation, Queensland, Australia ....	177
CLIFFORD, H.T. & COOK, A.G. A presumed Leichhardt geological specimen in the Queensland Museum ....	186
BISHOP, P.J. A critical re-evaluation of the hindlimb myology of (Aves: Dinornithiformes) ....	187
ROZEFELDS, A.C., WALKER, J., NORRIS, E., WICKS, D. & ILIC, J. A drift log from Cape York Peninsula, Australia identified as <i>Vatica</i> (Dipterocarpaceae), and the use of botanical, zoological, geological and ethnographic data in interpreting the direction of oceanic drift ....	235
BARTHOLOMAI, A. Predation of the Early Cretaceous (Late Albian) pachycormiform, <i>Australopachycormus hurleyi</i> Kear, in Queensland's Eromanga Basin ....	245
COUPER, P.J. & MCKAY, J. Vale Jeanette Adelaide Covacevich, AM, PSM (1945–2015). ....	257
MUNSON, T.J. & JELL, J.S. Wenlock and Ludlow (Silurian) rugose corals from the type section of the Jack Formation, Broken River Province, northeast Queensland. ....	273
<b>NOTES</b>	
MCNAB, A., SANDERS, M. & VANDERDUYS, E. New records of blind snakes resembling the robust blind snake <i>Anilius ligatus</i> (Peters 1879), on Cape York Peninsula. ....	8
SOBBE, I.H. & PRICE, G.J. Confirmation of the presence of the Spotted-tailed Quoll, <i>Dasyurus maculatus</i> (Dasyuridae, Marsupialia) from the Late Pleistocene King Creek Catchment, Darling Downs, Southeastern Queensland, Australia. ....	9
CLIFFORD, H.T., DETTMANN, M.E. & HOCKNULL, S.A. Numerical analysis of the inter-relationships of some extinct and extant taxa of Araucariaceae ....	27
NELSON, L. & GORDON, A. Tracheal bot fly ( <i>Tracheomyia macropi</i> ) in an Eastern grey kangaroo ( <i>Macropus giganteus</i> ) ....	256